



National Library  
of Canada

Bibliothèque nationale  
du Canada

Canadian Theses Service

Service des thèses canadiennes

Ottawa, Canada  
K1A 0N4

## NOTICE

The quality of this microform is heavily dependent upon the quality of the original thesis submitted for microfilming. Every effort has been made to ensure the highest quality of reproduction possible.

If pages are missing, contact the university which granted the degree.

Some pages may have indistinct print especially if the original pages were typed with a poor typewriter ribbon or if the university sent us an inferior photocopy.

Reproduction in full or in part of this microform is governed by the Canadian Copyright Act, R.S.C. 1970, c. C-30, and subsequent amendments.

## AVIS

La qualité de cette microforme dépend grandement de la qualité de la thèse soumise au microfilmage. Nous avons tout fait pour assurer une qualité supérieure de reproduction.

S'il manque des pages, veuillez communiquer avec l'université qui a conféré le grade.

La qualité d'impression de certaines pages peut laisser à désirer, surtout si les pages originales ont été dactylographiées à l'aide d'un ruban usé ou si l'université nous a fait parvenir une photocopie de qualité inférieure.

La reproduction, même partielle, de cette microforme est soumise à la Loi canadienne sur le droit d'auteur, SRC 1970, c. C-30, et ses amendements subséquents.

UNIVERSITY OF ALBERTA

ADFREEZE AND GROUTED PILES IN SALINE PERMAFROST

BY

© KEVIN WILLIAM BIGGAR

A THESIS

SUBMITTED TO THE FACULTY OF GRADUATE STUDIES AND RESEARCH  
IN PARTIAL FULFILLMENT OF THE REQUIREMENTS FOR  
THE DEGREE OF DOCTOR OF PHILOSOPHY

DEPARTMENT OF CIVIL ENGINEERING

EDMONTON, ALBERTA

FALL 1991



National Library  
of Canada

Bibliothèque nationale  
du Canada

Canadian Theses Service    Service des thèses canadiennes

Ottawa, Canada  
K1A 0N4

The author has granted an irrevocable non-exclusive licence allowing the National Library of Canada to reproduce, loan, distribute or sell copies of his/her thesis by any means and in any form or format, making this thesis available to interested persons.

The author retains ownership of the copyright in his/her thesis. Neither the thesis nor substantial extracts from it may be printed or otherwise reproduced without his/her permission.

L'auteur a accordé une licence irrévocable et non exclusive permettant à la Bibliothèque nationale du Canada de reproduire, prêter, distribuer ou vendre des copies de sa thèse de quelque manière et sous quelque forme que ce soit pour mettre des exemplaires de cette thèse à la disposition des personnes intéressées.

L'auteur conserve la propriété du droit d'auteur qui protège sa thèse. Ni la thèse ni des extraits substantiels de celle-ci ne doivent être imprimés ou autrement reproduits sans son autorisation.

ISBN 0-315-69989-2



University of Alberta  
Edmonton

Canada T6G 2G7

Department of Civil Engineering

---

220 Civil/Electrical Engineering Building,  
Telephone (403) 492-4235  
Fax (403) 492-0249

July 15, 1991

Dr. F.S. Chia  
Dean, FGSR  
University of Alberta  
Edmonton, Alberta  
T6G 2E1

Dear Dr. Chia:

Re: Ph.D. Thesis of K.W. Biggar

Dr. Biggar has prepared and is presenting his Ph.D. using the paper format. I am and will be a joint author on various papers which make up this thesis. I hereby give permission to the University of Alberta to reproduce this thesis in the normal manner and to submit it to the National Library for microfilming and archiving.

Should you require any further information please contact me at 492-2059.

Yours sincerely,

D.C. Sego  
Professor of Civil Engineering

DCS/slm

xc: K.W. Biggar



micr.

UNIVERSITY OF ALBERTA  
RELEASE FORM

NAME OF AUTHOR: Kevin William Biggar  
TITLE OF THESIS: Adfreeze and Grouted Piles in Saline Permafrost  
DEGREE: Doctor of Philosophy  
YEAR THIS DEGREE GRANTED: Fall 1991

PERMISSION IS HEREBY GRANTED TO THE UNIVERSITY OF ALBERTA  
LIBRARY TO REPRODUCE SINGLE COPIES OF THIS THESIS AND TO LEND OR  
SELL SUCH COPIES FOR PRIVATE, SCHOLARLY OR SCIENTIFIC RESEARCH  
PURPOSES ONLY.

THE AUTHOR RESERVES OTHER PUBLICATION RIGHTS, AND NEITHER  
THE THESIS NOR EXTENSIVE EXTRACTS FROM IT MAY BE PRINTED OR  
OTHERWISE REPRODUCED WITHOUT THE AUTHOR'S WRITTEN PERMISSION.



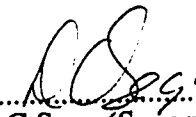
Permanent address:

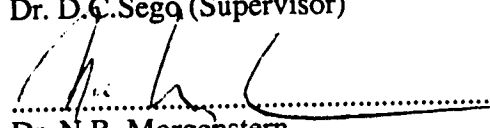
78 Lorraine Crescent  
St Albert, Alberta  
T8N 2R3

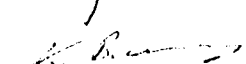
Date: 15 July 1991

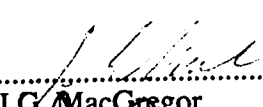
THE UNIVERSITY OF ALBERTA  
FACULTY OF GRADUATE STUDIES AND RESEARCH

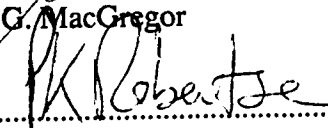
THE UNDERSIGNED CERTIFY THAT THEY HAVE READ, AND  
RECOMMEND TO THE FACULTY OF GRADUATE STUDIES AND RESEARCH  
FOR ACCEPTANCE, A THESIS ENTITLED *ADFREEZE AND GROUTED PILES IN  
SALINE PERMAFROST* SUBMITTED BY *KEVIN WILLIAM BIGGAR* IN PARTIAL  
FULFILLMENT OF THE REQUIREMENTS FOR THE DEGREE OF DOCTOR OF  
PHILOSOPHY.

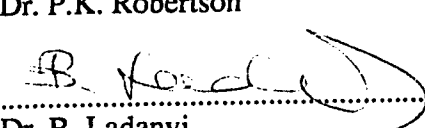
  
.....  
Dr. D.C. Segg (Supervisor)

  
.....  
Dr. N.R. Morgenstern

  
.....  
Dr. K. Barron

  
.....  
Dr. J.G. MacGregor

  
.....  
Dr. P.K. Robertson

  
.....  
Dr. B. Ladanyi  
External Examiner

Date: June 17, 1991

*To my wife, Christine*

*her love and patience made this possible*

## **ABSTRACT**

Solutes present in the pore water of frozen soils are known to reduce the strength of the soil and increase the time dependent deformation under a constant load. Reduced pile capacities in saline permafrost have caused increased pile foundation costs, and little information is available to engineers to use in design for these conditions. This thesis examines the performance of prebored and backfilled piles in saline frozen soils based upon the results of field, and laboratory model pile load tests.

The capacity of piles installed in saline frozen soil is affected by two mechanisms. Firstly the bond between the frozen soil and the pile surface (adfreeze bond) is dramatically weakened by the presence of the solutes. In addition, the saline frozen soil is much more susceptible to time dependent deformation than fresh-water frozen soil. For plain pipe piles installed with a soil-water slurry backfill the reduced adfreeze bond strength governs pile capacities rather than the strength of the saline frozen soil.

To overcome this reduction in adfreeze bond strength and thereby facilitate the mobilization the shear strength of the saline frozen soil surrounding the pile, a number of modifications to the pile surface were tested including sandblasting the pile surface, welding protuberances onto the pile, and the use of a cementitious grout rather than a soil-water slurry as the backfill material.

The use of grouts specially designed to cure in soil at temperatures as cold as  $-10^{\circ}\text{C}$  as a backfill material for prebored piles in saline permafrost provided the greatest pile capacities, alleviates any concern regarding solute diffusion through the backfill which will reduce adfreeze bond strengths with time, and are shown to be an economically viable option for pile foundations in saline permafrost.

## **ACKNOWLEDGEMENTS**

The author would like to sincerely thank Dr. Dave Sego and Dr N.R. Morgenstern for their commitment to the research undertaken. Dr Sego's encouragement, technical guidance, and availability are greatly appreciated. In addition Dr. P.K. Robertson provided valuable discussion and input into the analysis of a number of problems.

The author is grateful to the Department of National Defence who sponsored the first two years of study and graciously permitted a leave of absence for an additional two years to complete the research. They also funded the field test program and permitted the publication of the results.

Financial support provided by the Natural Science and Engineering Research Council, Sika Canada Inc., Lafarge Calcium Aluminates Ltd., the Department of Energy Mines and Resources, the Canadian Circumpolar Institute (formerly the Boreal Institute), and the University of Alberta is gratefully acknowledged.

A large portion of the credit for the timely completion of this research goes to the technical support staff in the Geotechnical Engineering Section, most notably Mr Gerry Cyre and Mrs Christine Hereygers. Their hard work, technical expertise and commitment to excellence payed valuable dividends in both the field and in the laboratory. Without their contributions this research would have not been possible.

The greatest joy of graduate research was the camaraderie developed with fellow graduate students. In addition to the life-long friendships established, the interesting and enlightening discussions provided insight and understanding far greater than the sum of the parts. I am most grateful to all those who freely shared of their experience and knowledge that I may learn and better understand. Over and above all of this, Elisabeth Hivon and Jean Hutchinson deserve special thanks. Their patience, generosity and understanding support was invaluable as I followed in their footsteps, shared their equipment and libraries, and plagued them with questions.

Finally, and most importantly, are the thanks to my family that words cannot express. Their support, encouragement and love helped overcome the most difficult obstacles, those of self-doubt and fatigue.

## TABLE OF CONTENTS

1. INTRODUCTION .....	1
Definition of the problem.....	1
Description of the study .....	2
References.....	4
2. FIELD PILE LOAD TESTS IN SALINE PERMAFROST PART I- TEST PROCEDURES AND RESULTS.....	5
Introduction .....	5
Test program.....	6
Factors affecting pile performance .....	8
Location of the failure surface .....	8
Pile Surface Roughness .....	9
Soil slurry backfill.....	10
Grout as a backfill material.....	11
Impurities in the frozen soil .....	13
Tensile versus compressive loading.....	14
Site conditions .....	15
Location .....	15
Soil conditions.....	15
Pile installation.....	16
Drilling.....	17
Placement.....	17
Pile testing.....	18
Apparatus.....	18
Procedures .....	19
Test results .....	19
Load versus Displacement.....	19
Time dependent deformation in saline permafrost.....	20
Discussion.....	20
Conclusions.....	21
References.....	22
3. FIELD PILE LOAD TESTS IN SALINE PERMAFROST PART II- ANALYSIS OF RESULTS.....	37
Introduction .....	37
Performance of a high alumina cement grout backfill.....	37
General .....	37
Thermal performance .....	38
Grout strength .....	38

Development of load at depth along the pile embedment .....	39
General .....	39
Smooth HSS pile with sand slurry backfill (#11) .....	41
Lugged HSS pile with sand slurry backfill (#12) .....	42
Dywidag bar anchor with grout backfill (#3) .....	44
Time dependent pile displacement.....	46
Comparison with results from others .....	48
Smooth HSS, and plain and sandblasted pipe .....	49
Lugged HSS piles.....	50
Grouted anchors.....	51
Conclusions.....	51
Recommendations for Future Research.....	52
References.....	53
<b>4. THE CURING AND STRENGTH CHARACTERISTICS OF COLD SETTING CIMENT FONDU GROUT.....</b>	<b>67</b>
Introduction .....	67
Prior use of Ciment Fondu in frozen soils .....	68
Testing program and procedure.....	70
General .....	70
Cell description .....	70
Sample preparation.....	72
Compressive strength testing .....	73
Results.....	73
Comparison between the 600 mm cell and the CTBC .....	73
Mix consistency .....	74
Flow cone tests .....	74
Vicat needle tests .....	75
Thermal performance .....	75
Compressive Strengths.....	76
Discussion.....	77
Effect of test cell.....	77
Effect of admixtures.....	77
Effect of cylinder molds .....	78
Application to field operations .....	78
References.....	78
<b>5. STRENGTH AND DEFORMATION BEHAVIOUR OF MODEL ADFREEZE AND GROUTED PILES IN SALINE PERMAFROST.....</b>	<b>90</b>
Introduction .....	90



Pertinent factors affecting pile capacity .....	90
Effect of salinity on soil strength .....	90
Effect of salinity on adfreeze bond strength .....	92
Effect of soil temperature .....	94
Effect of pile surface .....	95
Performance of grout backfill .....	97
Size effects .....	97
Effect of freezeback pressures on adfreeze piles .....	98
Experimental procedure .....	98
Test cell .....	98
Sample preparation .....	99
Loading .....	102
Determination of soil properties .....	103
Results .....	104
General .....	104
Effect of pile size on pile response .....	105
Effect of native soil salinity on pile response .....	106
Effect of backfill material on pile capacity .....	108
Effect of pile surface treatment on pile capacity .....	109
Effect of temperature on pile capacity .....	109
Grout performance .....	111
Lateral pressures due to freezing of the slurry backfill .....	113
Observations of specimen failure modes .....	113
Comparison with results in other studies .....	115
Laboratory test results by others .....	115
Field test results by others .....	116
Comparison with analytical models .....	117
Conclusions .....	119
References .....	120
<b>6. TIME DEPENDENT DISPLACEMENT BEHAVIOUR OF MODEL</b>	
<b>ADFREEZE AND GROUTED PILES IN SALINE FROZEN SOILS .....</b>	<b>148</b>
Introduction .....	148
Experimental procedure .....	148
General .....	148
Loading .....	149
Definitions .....	150
Time dependent displacement of piles in permafrost .....	151
Results .....	152
Displacement versus time behaviour .....	153
Temperature sensitivity of test results .....	154
Grout performance .....	155
Observations of test specimen behaviour .....	155

Analysis of results.....	156
Displacement rate versus applied stress behaviour .....	157
Displacement versus time behaviour .....	158
Pile displacement to the rupture of the adfreeze bond .....	160
Comparison with data from other studies .....	161
Laboratory constant displacement rate test results.....	161
Unconfined constant stress compression test results.....	162
Comparison with pile load tests by others.....	162
Comparison with field test results.....	163
Comparison with pile design guidelines by others .....	164
Migration of solutes into the backfill.....	164
Discussion.....	168
Effect of salinity on pile performance.....	168
Effect of backfill material on pile performance.....	168
Conclusions.....	170
Recommendations for future research .....	170
References.....	171
APPENDIX I TO CHAPTER 6.....	188
7. CONCLUSIONS .....	191
Pile performance in saline permafrost.....	191
Grout as a backfill material.....	193
Recommendations for future research .....	193
References.....	194
APPENDIX A: IQALUIT TEST RESULTS pertinent to CHAPTER 1 .....	196
APPENDIX B: IQALUIT TEST RESULTS pertinent to CHAPTER 2 .....	211
APPENDIX C: GROUT CURING PERFORMANCE FOR VARIOUS MIX DESIGNS .....	219
APPENDIX D: CONSTANT DISPLACEMENT RATE MODEL PILE TEST RESULTS.....	234
APPENDIX E: CONSTANT LOAD MODEL PILE TEST RESULTS.....	277
APPENDIX F: DERIVATION OF FORMULATION FOR TIME DEPENDENT DISPLACEMENT OF PILES .....	336
APPENDIX G: BALLPARK COST ESTIMATE FOR ADFREEZE AND GROUTED PILES.....	340

## LIST OF TABLES

Table	Page
2.1 Summary of pile load tests .....	26
3.1 Iqaluit grout curing temperature details. ....	57
3.2 Corrected shear stresses on strain gauged piles.....	57
3.3 Results of displacement versus time analysis. ....	58
3.4 Comparative test data.....	59
4.1 Results of Lafarge Canada Inc grout testing program.....	80
4.2 Results of Geocon Inc grout testing program.....	81
4.3 Grout mix designs for this study .....	82
4.4 Phase II test results.....	83
4.5 Phase III test results.....	84
5.1 Pile CLA roughness measurements .....	126
5.2 Sample moisture contents, densities and salinities.....	126
5.3 Summary of constant displacement rate test results .....	127
5.4 Effect of salinity on shear stress .....	129
5.5 Laboratory results by others.....	130
5.6 Field results by others.....	131
5.7 Comparisons with suggested adfreeze bond strengths by others .....	132
6.1 Summary of constant load test results.....	174
6.2 Model parameters from minimum displacement rate analysis .....	176
6.3 Regression values of c and D parameters.....	176
6.4 Comparisons of n and B parameters with those from Hivon (1991).....	176

## LIST OF FIGURES

Figure	Page
2.1 Pile capacity in relation to the location of the failure surface .....	27
2.2 Unfrozen water content of various soils. ....	28
2.3 Phase diagram for NaCl. ....	29
2.4 Site map of Iqaluit. ....	30
2.5 Grain size distribution for Iqaluit test site.....	31
2.6 Site temperature profile during installation and testing .....	32
2.7 Salinity and moisture content profile for three different piles .....	32
2.8 Pile configurations used in Iqaluit field test program.....	33
2.9 Pile load test frame .....	34
2.10 Summary of load versus displacement performance for the different pile configurations .....	35
2.11 Typical pile displacement and load versus time .....	35
2.12 Capacities of various pile configurations .....	36
3.1 Location of RTD's to measure grout curing temperatures. ....	60
3.2 Grout curing temperature versus time for sanded grout.....	60
3.3 Typical distribution of load and stress along pile depth.....	61
3.4 Smooth HSS pile-load at depth for various load increments.....	62
3.5 Smooth HSS pile-load at various depths versus time.....	62
3.6 Lugged HSS pile-load at depth for various load increments.....	63
3.7 Lugged HSS pile-load at various depths versus time.....	63
3.8 Dywidag bar-load at depth for various load increments. ....	64
3.9 Typical displacement versus time-measured values and best fit regression line. ....	65
3.10 Values of K parameter versus shear stress for different pile configurations. ....	65
3.11 Displacement versus time-predicted performance and measured values...	66

Figure	Page
4.1 Schematic diagram of 600 mm test cell. ....	85
4.2 Constant Temperature Bath Cell (CTBC).....	86
4.3 Typical temperature versus time in grout and soil during curing of the grout. ....	87
4.4 Grout cylinder compressive strengths for different mix designs.....	88
4.5 Guideline to determine mixed grout temperature.....	89
5.1 Phase diagram for NaCl .....	133
5.2 Schematic diagram of test cell.....	134
5.3 Schematic diagram of cell base plates .....	134
5.4 Grain size distribution of soils used in model pile test program. ....	135
5.5 Load frame for constant displacement rate testing of model piles.....	136
5.6 Typical stress versus displacement behaviour for various pile diameters. ....	137
5.7 Adfreeze bond strength at failure for different pile configurations.....	138
5.8 Typical stress versus normalized pile displacement behaviour.....	139
5.9 Normalized displacement to failure of the adfreeze bond versus unfrozen water content of the native soil. ....	140
5.10 Shear stress at the pile/backfill interface at 1 mm displacement. ....	140
5.11 Comparison of effect of backfill material on pile performance.....	141
5.12 Effect of pile surface treatment on pile behaviour.....	142
5.13 Effect of temperature on pile performance.....	143
5.14 Effect of temperature on mobilized shear stress at 3 mm displacement ....	144
5.15 Typical grout curing temperatures. ....	145
5.16 Comparison of test results from this study with laboratory results by others.....	146
5.17 Comparison of test results with guidelines proposed by Nixon and Neukirchner (1984).....	147
6.1 Constant load test apparatus.....	177

Figure	Page
6.2 Time dependent deformation behaviour in frozen soils. ....	178
6.3 Typical pile behaviour under constant load.....	179
6.4 Typical test result–Test #40-33 .....	180
6.5 Detail of pile deformation at the bottom of the sample for grout backfilled piles.....	181
6.6 Normalized pile displacement rate versus stress for grout and clean sand backfilled model piles .....	182
6.7 Typical log displacement versus log time behaviour for attenuating displacement rate portion of pile displacement.....	183
6.8 Values of time exponent, b, versus applied shear stress.....	184
6.9 Net displacement to adfreeze bond rupture versus adfreeze bond stress.....	185
6.10 Comparison of the results from this study to the results from studies by others. ....	186
6.11 Comparison of results from this study with those reported in Nixon and Neukirchner (1984).....	187
A.1 Field test #5 Smooth HSS pile with sand backfill .....	197
A.2 Field test #7 Smooth HSS pile with sand backfill .....	198
A.3 Field test#11 Smooth HSS pile with sand backfill.....	199
A.4 Field test#15 Plain pipe pile with sand backfill.....	200
A.5 Field test #16 Plain pipe with sand backfill.....	201
A.6 Field test#8 Lugged HSS pile with sand backfill .....	202
A.7 Field test#9 Lugged HSS pile with sand backfill .....	203
A.8 Field test#12 Lugged HSS pile with sand backfill.....	204
A.9 Field test#13 Sandblasted pipe pile with sand backfill .....	205
A.10 Field test#14 Sandblasted pipe pile with sand backfill .....	206
A.11 Field test#2 Dywidag bar with neat Ciment Fondu grout backfill.....	207
A.12 Field test#4 Dywidag bar with neat Ciment Fondu grout backfill.....	208
A.13 Field test#3 Dywidag bar with sanded Ciment Fondu grout backfill .....	209

Figure	Page
A.14 Field test#6 Dywidag bar with sanded Ciment Fondu grout backfill .....	210
B.1 Grout curing temperatures versus time for neat grout backfill .....	212
B.2 Grout curing temperatures versus time for sanded grout backfill.....	213
B.3 Regression analysis of log displacement versus log time for plain pipe piles.....	214
B.4 Regression analysis of log displacement versus log time for smooth HSS piles .....	215
B.5 Regression analysis of log displacement versus log time for lugged HSS piles .....	216
B.6 Regression analysis of log displacement versus log time for sandblasted pipe piles.....	217
B.7 Regression analysis of log displacement versus log time for Dywidag bars .....	218
C.1 Mix I-A grout and soil temperature versus time .....	220
C.2 Mix II-1 grout and soil temperature versus time.....	221
C.3 Mix II-2 grout and soil temperature versus time.....	222
C.4 Mix II-3 grout and soil temperature versus time.....	223
C.5 Mix II-4 grout and soil temperature versus time.....	224
C.6 Mix II-5 grout and soil temperature versus time.....	225
C.7 Mix II-6 grout and soil temperature versus time.....	226
C.8 Mix II-7 grout and soil temperature versus time.....	227
C.9 Mix II-8 grout and soil temperature versus time.....	228
C.10 Mix III-9 grout and soil temperature versus time.....	229
C.11 Mix III-10 grout and soil temperature versus time .....	230
C.12 Mix III-11 grout and soil temperature versus time .....	231
C.13 Mix III-12 grout and soil temperature versus time .....	232
C.14 Repeat of mix II-8 grout and soil temperature versus time.....	233
D.1 Test #4, S = 30 ppt, Backfill = Sand, T = -5° C .....	235

Figure	Page
D.2 Test #5, S = 20 ppt, Backfill = Sand, T = -5° C .....	236
D.3 Test #6, S = 10 ppt, Backfill = Sand, T = -5° C .....	237
D.4 Test #7, S = 0 ppt, Backfill = Sand, T = -5° C, Smooth pipe pile .....	238
D.5 Test #8, S = 0 ppt, Backfill = Sand, T = -5° C.....	239
D.6 Test #9, S = 0 ppt, Backfill = Cuttings, T = -5° C.....	240
D.7 Test #10, S = 10 ppt, Backfill = Cuttings, T = -5° C.....	241
D.8 Test #11, S = 30 ppt, Backfill = Cuttings or ice, T = -5° C.....	242
D.9 Test #12, S = 0 ppt, Backfill = Grout in smooth hole, T = -5° C .....	243
D.10 Test #13, S = 10 ppt, Backfill = Grout in smooth hole, T = -5° C .....	244
D.11 Test #14, S = 20 ppt, Backfill = Grout, T = -5° C.....	245
D.12 Test #15, S = 0 ppt, Backfill = Grout, T = -5° C .....	246
D.13 Test #16, S = 10 ppt, Backfill = Grout, T = -5° C.....	247
D.14 Test #18, S = 0 ppt, Backfill = Sand, T = -5° C .....	248
D.15 Test #23, S = 0 ppt, Backfill = Sand, T = -5° C .....	249
D.16 Test #29, S = 10 ppt, Backfill = Sand, T = -5° C.....	250
D.17 Test #32, S = 10 ppt, Backfill = Sand or Grout, T = -10° C .....	251
D.18 Test #35, S = 30 ppt, Backfill = Grout, T = -10° C .....	252
D.19 Test #37, S = 30 ppt, Backfill = Sand, T = -10° C .....	253
D.20 Test #38, S = 10 ppt, Backfill = Sand, T = -10° C .....	254
D.21 Test #42, S = 30 ppt, Backfill = Grout, T = -10° C .....	255
D.22 Test #43, S = 10 ppt, Backfill = Sand, T = -10° C .....	256
D.23 Test #44, S = 10 ppt, Backfill = Sand, T = -5° C.....	257
D.24 Test #45, S = 10 ppt, Backfill = Grout, T = -5° C.....	258
D.25 Tests with same conditions, S = 0 ppt, T = -5° C, Backfill = Sand.....	259
D.26 Tests with same conditions, S = 10 ppt, T = -5° C, Backfill = Sand .....	260
D.27 Tests with same conditions, T = -10° C .....	261



Figure	Page
D.28 Similar tests in different frames, load versus displacement, $S = 0$ ppt.....	262
D.29 Similar tests in different frames, load versus time, $S = 0$ ppt.....	263
D.30 Similar tests in different frames, load versus displacement, $S = 10$ ppt, ..	264
D.31 Similar tests in different frames, load versus time, $S = 10$ ppt.....	265
D.32 Effect of salinity on sand backfilled piles.....	266
D.33 Effect of salinity on grout backfilled piles.....	267
D.34 Backfill effects on pile performance, $S = 0$ ppt, $T = -5^{\circ} \text{C}$ .....	268
D.35 Backfill effects on pile performance, $S = 10$ ppt, $T = -5^{\circ} \text{C}$ .....	269
D.36 Backfill effects on pile performance, $S = 20$ ppt, $T = -5^{\circ} \text{C}$ .....	270
D.37 Backfill effects on pile performance, $S = 10$ ppt, $T = -10^{\circ} \text{C}$ .....	271
D.38 Backfill effects on pile performance, $S = 30$ ppt, $T = -10^{\circ} \text{C}$ .....	272
D.39 Pipe surface treatment effect on pile performance.....	273
D.40 Temperature effect on sand backfilled pile performance, $S = 10$ ppt.....	274
D.41 Temperature effect on grout backfilled pile performance, $S = 10$ ppt.....	275
D.42 Temperature effect on sand backfilled pile performance, $S = 30$ ppt.....	276
E.1 Constant load test #19-63, $S = 0$ ppt, Backfill = Sand, $\tau = 537$ kPa.....	278
E.2 Constant load test #19-102, $S = 0$ ppt, Backfill = Sand, $\tau = 333, 369,$ 426 kPa.....	279
E.3 Constant load test #20-63, $S = 10$ ppt, Backfill = Sand, $\tau = 290, 357$ kPa.....	280
E.4 Constant load test #21-102, $S = 10$ ppt, Backfill = Sand, $\tau = 195$ kPa.....	281
E.5 Constant load test #22-33, $S = 30$ ppt, Backfill = Sand, $\tau = 147$ kPa.....	282
E.6 Constant load test #22-63, $S = 30$ ppt, Backfill = Sand, $\tau = 164$ kPa.....	283
E.7 Constant load test #22-102, $S = 30$ ppt, Backfill = Sand, $\tau = 124$ kPa.....	284
E.8 Constant load test #24-33, $S = 10$ ppt, Backfill = Sand, $\tau = 362$ kPa.....	285

Figure	Page
E.9 Constant load test #24-63, S = 10 ppt, Backfill = Sand, $\tau = 365$ kPa .....	286
E.10 Constant load test #24-102, S = 10 ppt, Backfill = Sand, $\tau = 356$ kPa.....	287
E.11 Constant load test #25-33, S = 10 ppt, Backfill = Sand, $\tau = 355$ kPa .....	288
E.12 Constant load test #25-63, S = 10 ppt, Backfill = Sand, $\tau = 373$ kPa .....	289
E.13 Constant load test #25-102, S = 10 ppt, Backfill = Sand, $\tau = 359$ kPa.....	290
E.14 Constant load test #26-33, S = 10 ppt, Backfill = Sand, $\tau = 353$ kPa .....	291
E.15 Constant load test #26-63, S = 10 ppt, Backfill = Sand, $\tau = 367$ kPa .....	292
E.16 Constant load test #26-102, S = 10 ppt, Backfill = Sand, $\tau = 355$ kPa.....	293
E.17 Constant load test #27-33, S = 10 ppt, Backfill = Sand, $\tau = 318$ kPa .....	294
E.18 Constant load test #27-63, S = 10 ppt, Backfill = Sand, $\tau = 325$ kPa .....	295
E.19 Constant load test #27-102, S = 10 ppt, Backfill = Sand, $\tau = 307$ kPa....	296
E.20 Constant load test #28-33, S = 10 ppt, Backfill = Sand, $\tau = 312$ kPa .....	297
E.21 Constant load test #28-63, S = 10 ppt, Backfill = Sand, $\tau = 317$ kPa .....	298
E.22 Constant load test #28-102, S = 10 ppt, Backfill = Sand, $\tau = 301$ kPa....	299
E.23 Constant load test #30-63, S = 30 ppt, Backfill = Sand, $\tau = 323$ kPa .....	300
E.24 Constant load test #31-33, S = 10 ppt, Backfill = Grout, $\tau = 365$ kPa ....	301
E.25 Constant load test #31-63, S = 10 ppt, Backfill = Grout, $\tau = 374$ kPa ....	302
E.26 Constant load test #31-102, S = 10 ppt, Backfill = Grout, $\tau = 359$ kPa...	303
E.27 Constant load test #33-33, S = 10 ppt, Backfill = Sand, $\tau = 316$ kPa .....	304
E.28 Constant load test #33-63, S = 10 ppt, Backfill = Sand, $\tau = 325$ kPa .....	305
E.29 Constant load test #33-102, S = 10 ppt, Backfill = Sand, $\tau = 310$ kPa.....	306

E.30	Constant load test #34-33, S = 10 ppt, Backfill = Grout, $\tau = 318$ kPa ....	307
E.31	Constant load test #34-63, S = 10 ppt, Backfill = Grout, $\tau = 322$ kPa ....	308
E.32	Constant load test #34-102, S = 10 ppt, Backfill = Grout, $\tau = 305$ kPa...	309
E.33	Constant load test #36-33, S = 10 ppt, Backfill = Grout, $\tau = 245$ kPa ....	310
E.34	Constant load test #36-63, S = 10 ppt, Backfill = Grout, $\tau = 248$ kPa ....	311
E.35	Constant load test #36-63-2, S = 10 ppt, Backfill = Grout, $\tau = 330$ kPa.....	312
E.36	Constant load test #36-102, S = 10 ppt, Backfill = Grout, $\tau = 495$ kPa...	313
E.37	Constant load test #39-33, S = 10 ppt, Backfill = Sand, $\tau = 252$ kPa ....	314
E.38	Constant load test #39-63, S = 10 ppt, Backfill = Sand, $\tau = 255$ kPa .....	315
E.39	Constant load test #39-102, S = 10 ppt, Backfill = Sand, $\tau = 243$ kPa....	316
E.40	Constant load test #40-33, S = 30 ppt, Backfill = Grout, $\tau = 69$ kPa.....	317
E.41	Constant load test #41-33, S = 30 ppt, Backfill = Grout, $\tau = 97$ kPa.....	318
E.42	Constant load test #41-63, S = 30 ppt, Backfill = Grout, $\tau = 92$ kPa.....	319
E.43	Constant load test #41-102, S = 30 ppt, Backfill = Grout, $\tau = 163$ kPa...	320
E.44	Constant load test #46-33, S = 30 ppt, Backfill = Sand, $\tau = 68$ kPa.....	321
E.45	Constant load test #46-63, S = 30 ppt, Backfill = Sand, $\tau = 66$ kPa.....	322
E.46	Constant load test #46-102, S = 30 ppt, Backfill = Sand, $\tau = 65$ kPa .....	323
E.47	Constant load test #47-33, S = 30 ppt, Backfill = Sand, $\tau = 89$ kPa.....	324
E.48	Constant load test #48-33, S = 0 ppt, Backfill = Sand, $\tau = 211, 316,$ 365 kPa.....	325
E.49a	Constant load test #49-33, S = 10 ppt, Backfill = Sand, $\tau = 130$ kPa.....	326

Figure	Page
E.49b Constant load test #49-33, S = 10 ppt, Backfill = Sand, $\tau = 184$ kPa ....	327
E.50 Constant load test #50-33, S = 30 ppt, Backfill = Sand, $\tau = 95$ kPa.....	328
E.51 Constant load test #50-63, S = 30 ppt, Backfill = Grout, $\tau = 150$ kPa ....	329
E.52 Constant load test #50-102, S = 30 ppt, Backfill = Grout, $\tau = 150$ kPa...	330
E.53 Constant load test #51-33, S = 10 ppt, Backfill = Grout, $\tau = 482$ kPa ....	331
E.54 Constant load test #51-63, S = 10 ppt, Backfill = Sand, $\tau = 186$ kPa ....	332
E.55 Regression analysis for grout backfilled piles.....	333
E.56 Regression analysis for sand backfilled piles .....	334
E.57 Regression analysis, Normalized K versus stress.....	335

## **LIST OF PLATES**

<b>Plate</b>	<b>Page</b>
5.1 Grout surface in roughened hole, 102 mm pile .....	125
5.2 Plane of weakness beyond grout backfill, 33 mm pile .....	125

## LIST OF SYMBOLS

for pile displacement and displacement rate analysis

$P_i$ .....	Pile load at the $i^{\text{th}}$ strain gauge elevation
$\sigma_i$ .....	Axial stress at the $i^{\text{th}}$ strain gauge elevation
$A_x$ .....	Cross sectional area of steel in the pile
$A_s$ .....	Surface area of the pile
$\epsilon_i$ .....	Axial strain measured by the strain gauge at the $i^{\text{th}}$ elevation
$\epsilon_{i0}$ .....	Strain gauge reading prior to loading at the $i^{\text{th}}$ strain gauge elevation
$E$ .....	Youngs modulus
$\tau$ .....	Shear stress along the pile surface
$D$ .....	Pile depth
$d$ .....	Pile diameter
$a$ .....	Pile radius
$u_a$ .....	Pile displacement
$\dot{u}_a$ .....	Pile displacement rate
$n$ .....	Stress exponent for constant pile displacement rate formulation
$B$ .....	Temperature (and salinity) dependent parameter for constant pile displacement rate formulation
$c$ .....	Stress exponent for attenuating pile displacement rate formulation
$D$ .....	Temperature (and salinity) dependent parameter for attenuating pile displacement rate formulation
$t$ .....	Time
$b$ .....	Time exponent for attenuating pile displacement rate formulation

$\tau_a$ .....	Pile adfreeze bond strength
$c_{lt}$ .....	Long term cohesion
$m$ .....	Parameter $\leq 1$ which multiplies the long term cohesion to account for installation and surface effects
$\delta_n$ .....	Normalized pile displacement
$\delta_{nf}$ .....	Normalized pile displacement to failure
$\theta_u$ .....	Unfrozen water content (% vol)

**For solute diffusion analysis**

$D$ .....	Diffusion coefficient
$D_0$ .....	Constant in Arrhenius expression for diffusion
$E$ .....	Activation energy for diffusion
$k$ .....	Boltzman's constant
$T$ .....	Temperature
$f$ .....	Tortuosity factor

## 1. INTRODUCTION

### *Definition of the problem*

Reduced pile capacities in saline permafrost in Canadian Arctic communities has recently been identified as a problem (Hoggan 1983, and 1985, and Nixon 1988) for which there is little information available. Soviet experience (Karpov and Velli 1968, and Velli et al. 1973) generally provides maximum adfreeze bond capacities for different pile materials and various soils, but does not address the issue of time dependent displacement. Nixon and Neukirchner (1984) provide the first design guidelines for piles in saline permafrost considering time dependent displacement, based upon constant stress test results on ice-rich saline silty sand reported by Nixon and Lem (1984). Their formulation was analogous to the constant displacement rate formulation for pile design in ice:

$$\frac{\dot{u}_a}{a} = \frac{\sqrt{3}^{n+1} B \tau^n}{(n-1)} \quad (1.1)$$

developed by Johnston and Ladanyi (1972), Nixon and McRoberts (1976) and Morgenstern et al. (1980), where  $\dot{u}_a$  is the pile displacement rate,  $a$  is the pile radius,  $\tau$  is the applied shear stress,  $n = 3$  is the stress exponent for creep in ice, and  $B$  is a temperature dependent parameter (derivation in Appendix F). Nixon and Neukirchner (1984) proposed that the value of the stress exponent,  $n$ , be maintained equal to 3 as for pile design in ice-rich permafrost, and that the effect of the salinity be encompassed in the  $B$  term. Their formulation showed that pile capacities in saline permafrost may be reduced to as little as 20% of the capacities in ice-rich permafrost, or that the displacement rates may be 10 to 100 times greater than in ice under the same applied stress. Additional work is required in the examination of the behaviour of different saline frozen soils to provide designers with sufficient information to optimize pile design in saline permafrost.

In addition to the reduced strength of saline permafrost, the strength of the bond between the pile and the frozen soil, known as the adfreeze bond, is reduced by the presence of solutes in the pore water. To address this problem Hutchinson (1989)



performed constant load tests on model piles in which the pile surface was in contact with saline frozen silty sand concluding that bond strength values of less than 10 kPa resulted at salinities of 15 ppt. In order to overcome this problem an alternative approach is to design a pile so that the salinity from the native soil does not come in contact with the pile surface. This approach will allow pile design to be based upon the maximum shear strength and time dependent deformation properties of the saline native soil.

This study addresses both the problem of providing a pile configuration which will avoid reductions in adfreeze bond strength due to salinity in the permafrost, and to examine pile performance in different types of saline frozen soil from that presented in Nixon and Neukirchner (1984).

#### *Description of the study*

In 1988 the Department of National Defence was proceeding with the design phase of the Short Range Radar (SRR) program, which included 35 unmanned radar sites spanning the arctic coastline from Alaska to Labrador. Due to the concern over adfreeze and grout bond design values for pile foundations in frozen rock and saline permafrost, the University of Alberta (U of A) was commissioned to conduct field pile load tests in Iqaluit, N.W.T.. The program involved short-term tests of a number of different pile configurations including sand backfilled steel pipe piles, and grout backfilled threaded bar anchors. Chapter 2 presents the results of the test program, comparing the capacities of the different pile configurations. Chapter 3 presents an analysis of the time dependent displacement behaviour of the piles, the development of load along the depth of the piles (based upon the results of strain gauge measurements), and the performance of the cementitious grout backfill material.

The Iqaluit test program showed that a cementitious grout backfill, using Ciment Fondu, provided pile capacities approximately 8 times greater than pipe piles backfilled with a clean sand. There was a concern, however, that the pore water in the grout may be subject to freezing and that the strength of the frozen grout was unknown. In addition

Ciment Fondu hydrates rapidly, and there was concern that the heat generated may cause unacceptable damage to the surrounding permafrost. To address these concerns, a study to develop a grout mix design capable of curing in soil at temperatures as cold as  $-10^{\circ}\text{C}$  using Ciment Fondu was carried out in conjunction with Lafarge Calcium Aluminates, and Sika Canada. Chapter 4 describes the results of the test program and defines the mix design for the grout which was subsequently used extensively in the SRR foundations.

Despite the success of the Iqaluit test program, the saline soil encountered at the site was a dense till, so the strength of the soil was considerably greater than at other saline permafrost sites. Thus there remained the question regarding the performance of different pile configurations in fine-grained saline frozen soil. To examine this problem a model pile load testing program was undertaken. The first phase of the program involved testing different pile configurations in an ice-poor saline silty sand at  $-5^{\circ}\text{C}$  under constant displacement rate conditions. Chapter 5 describes the results of these tests, identifying sandblasted pipe piles with either a clean sand or Ciment Fondu grout backfill as the best configurations.

Due to the extra cost and additional construction control required to install a grout backfill as opposed to a sand slurry backfill, it was desirable to examine if grout backfilled piles provided similar enhancement to load carrying capacity under long-term, constant load conditions which generally govern pile foundation design. To address this problem model piles backfilled with either clean sand or grout were tested under constant load conditions in the same saline silty sand that was used for the constant displacement rate tests. In addition the problem of solute migration through a clean non-saline sand backfill has been addressed. The results from this study are detailed in Chapter 6.

Chapter 7 provides a summary of the major findings of the study and recommendations for future research.

## References

- Hoggan Engineering and Testing (1980) Ltd. 1983. Pile load tests for Kuluak School, Clyde River, N.W.T, Report to Government of the Northwest Territories, Department of Public Works.
- Hoggan Engineering and Testing (1980) Ltd. 1985. Pile load tests, Arctic Bay multi-purpose Hall and School Extension, Report to Government of the Northwest Territories, Department of Public Works.
- Karpov, V., and Velli, Y.Y. 1968. Displacement resistance of frozen saline soils. *Soil Mechanics and Foundation Engineering (English Translation)*, 4 (July/August): 277-279.
- Hutchinson, D.J. 1989. Model pile load tests in frozen saline silty sand. Unpublished MSc Thesis, University of Alberta, Edmonton, Alberta, p. 222.
- Johnston, G.H., and Ladanyi, B. 1972. Field tests on grouted rod anchors in permafrost, *Canadian Geotechnical Journal*, 9: 176-194.
- Morgenstern, N.R., Roggensack, W.D., and Weaver, J.S. 1980. The behavior of friction piles in ice and ice-rich soils. *Canadian Geotechnical Journal*, 17: 405-415.
- Nixon, J.F., and McRoberts, E.C. 1976. A design approach for pile foundations in permafrost. *Canadian Geotechnical Journal*, 13: pp. 40-57.
- Nixon, J.F., and Lem, G. 1984. Creep and strength testing of frozen saline fine-grained soils. *Canadian Geotechnical Journal*, 21: pp. 518-529.
- Nixon, J.F., and Neukirchner, R.J. 1984. Design of vertical and laterally loaded piles in saline permafrost. *Proceedings, 3rd International Specialty Conference on Cold Regions Engineering*, Edmonton, Alberta, Canadian Society of Civil Engineering, 1-6 April, pp. 131-144.
- Nixon, J.F. 1988. Pile load tests in saline permafrost at Clyde River, Northwest Territories. *Canadian Geotechnical Journal*, 25: pp. 24-31.
- Velli, Y.Y., Lenzniiep, and Karpunia, A.A. 1973. Saline permafrost as bearing ground for construction. *Proceedings, 2nd International Conference on Permafrost, USSR Contribution, Yakutsk, USSR*, pp. 545-550.

## **2. FIELD PILE LOAD TESTS IN SALINE PERMAFROST PART I- TEST PROCEDURES AND RESULTS**

### **Introduction**

There is considerable information in the literature dealing with the adfreeze bond capacities between smooth steel and frozen soil for both short-term ultimate capacity and long-term time dependent deformation in both ice-rich and ice-poor soils (Crory 1963; Hutchinson 1989; Ladanyi and Guichaoua 1988; Manikian 1983; Miller and Johnson 1990; Morgenstern et al. 1980; Nixon and McRoberts 1976; Nixon 1988; Parmeswaran 1978a, 1978b; Rowley et al 1973; Vyalov 1959; and Weaver and Morgenstern 1981 to name a few). There is, however, considerably less information dealing with tests on piles which have had their surfaces modified in an attempt to enhance their adfreeze capacity. As emphasized by Bro (1985), a better understanding of frozen ground rheology may improve our understanding of the mechanisms involved in pile behaviour which may improve the prediction of their capacity. Little gain in capacity can be expected using current configurations (i.e. smooth pipe with a frozen soil slurry backfill) so that increased capacities require reconfiguration of the piles using different geometries and installation procedures.

A recently recognized complication in pile design in permafrost is the effect of saline pore water in the permafrost on the response of the piles. Nixon and Lem (1984) state that salinities which have been observed in situ may increase pile deformation rates by 10 to 100 times. Nixon (1988) suggested that a native saline soil slurry backfill material used in field pile load tests in saline permafrost may have contributed to reductions in pile capacity of between 50 to 65% from the capacities expected from previous design experience. Saline permafrost is encountered in coastal areas or areas which were previously inundated by ocean water. This includes areas of shallow water where permafrost exists and inland areas of low elevation which have been subject to isostatic uplift above sea level (Nixon and Lem 1984; and Hivon 1991).

A field pile load test program was conducted in saline permafrost and seasonally frozen rock to examine the effect of modifications to the pile surface and the backfill material and to compare their performance to piles installed using current practice. The results from the tests in rock are contained in a paper by Biggar and Sego (1989). This paper will focus on the pile tests conducted in saline permafrost.

#### *Test program*

The Department of National Defence (DND) is currently proceeding with the installation of the North Warning System (NWS) to replace the aging Distant Early Warning (DEW) Line System. This includes 35 unmanned Short Range Radar (SRR) sites spanning the arctic coastline from Alaska to Labrador that encounter foundation conditions varying from ice rich fine-grained soils to bedrock.

Due to the concern over the adfreeze and grout bond design values for the foundations of the SRR sites, the University of Alberta (U of A) was commissioned by 1 Construction Engineering Unit (1 CEU) to conduct field pile load tests on steel piles in saline permafrost and frozen rock. Planning began 9 May 1988 and deployment was to occur as quickly as possible. Installation commenced on 26 June and was completed by 6 July. Testing began on 2 September and was completed by 14 September.

The conditions required for the test program are outlined below:

1. The piles in saline permafrost were to be installed in soils with salinities of about 20 parts per thousand (ppt), ground temperatures between  $-5^{\circ}\text{C}$  and  $-10^{\circ}\text{C}$  during installation and approximately  $-4^{\circ}\text{C}$  during load testing of the piles.
2. The piles grouted into rock were to be installed when the temperature in the rock mass was  $-5^{\circ}\text{C}$  or colder and then load tested when the temperature was warmer than  $0^{\circ}\text{C}$ .

The rationale for these conditions was to attempt to duplicate the worst case conditions anticipated at a number of the SRR sites; i.e., installation of the piles in the coldest anticipated ground conditions (particularly when grouted piles were used) and testing of the piles when they were subject to the warmest anticipated conditions. The site chosen for the

testing was Iqaluit, NWT as both rock and saline permafrost were present and the infrastructure was locally available to support the test program (as lead time for deployment was minimal). There was also considerable local experience in the piling techniques to be employed, information regarding local ground temperature, salinity, and soil conditions was readily obtainable, and a test site was available.

Pullout tests were conducted on piles with various surface modifications and various backfills in both saline permafrost and frozen rock. The test piles were to be 100 mm diameter pipes installed into prebored 165 mm holes. The configuration is represented schematically in Figure 2.1. The hole size of 165 mm was governed by the capability of a down hole hammer mounted on an airtrack drill which would be used on most of the remote sites to prebore the pile holes. The tests were to be conducted as pull-out tests because the piles beneath the radar towers could be subjected to either tension or compression during high winds, and the tensile capacity of the pile was judged to be critical. The results of the field test study included:

1. Installation methodology,
2. Grout mix and curing performance,
3. Pile load versus displacement performance,
4. Pile displacement versus time performance, and
5. Distribution of load with depth along the piles.

For the purpose of this paper creep refers to deformation of a material (ice, frozen soil or grout) subject to a constant stress. When referring to creep of permafrost it will be assumed that no volume change due to consolidation occurs. Time dependent deformation will refer to the displacement with time of a pile subject to a constant load.

Pile failure will be defined as any one of the following:

1. Continued time dependent deformation at a rate exceeding 0.25 mm/hr (0.01"/hr);
2. Accelerating time dependent deformation; or

3. A brittle failure resulting in a dramatic reduction in pile capacity.

### **Factors affecting pile performance**

The adfreeze bond strength of a pile in permafrost is influenced by the pile material and geometry, the method of installation (driven or prebored backfilled), the backfill material, the rheology of the frozen ground and the method of load application. The influence of the pile material and geometry is a function of the pile modulus, the roughness of the material or any surface preparation such as paint, lugs, creosote or sandblasting, and the size and shape of the pile. The effect of the backfill material depends on the material that is used, such as a slurry of the native soil cuttings or an imported material such as sand or a grout. The rheology of the frozen ground is influenced by strain rate, soil temperature, soil type, ice content (density), and any impurities in the soil-ice matrix such as naturally occurring saline pore fluid. The load geometry and the method of loading (static, cyclic, tensile or compressive) will also affect the pile capacity.

Of the above factors those with the greatest influence on pile capacity are the strain (or loading) rate applied to the soil, the temperature of the surrounding soil, and impurities in the soil-ice matrix. However for a given soil type and ground temperature regime the factors which may be adjusted to optimize the pile capacity are those influenced by the pile material and geometry and the backfill material. The factors relevant to this study are discussed below.

#### ***Location of the failure surface***

A common practice for piling in permafrost is to use plain pipe coated with a black lacquer for protection during transportation placed in a prebored hole with a soil slurry backfill in the annulus between the pipe and the borehole wall as shown in Figure 2.1. In ice-poor soils the strength of this configuration is generally governed by the strength of the adfreeze bond between the pipe and the slurry backfill (Weaver and Morgenstern 1981). If modifications can be made to this configuration to force the failure surface to occur at the interface between the backfill and the borehole wall, the surface area carrying the load will

increase and the capacity of the pile will be governed by the shear strength of the interface between the backfill and the native soil.

#### *Pile Surface Roughness*

When the pile surface is roughened there will be a concomitant increase in the pile capacity. Long (1973) discusses the use of piles with rings or helix-type protuberances to mobilize the shear strength of the soil rather than relying on the adfreeze bond along the surface of a smooth pile. Thomas and Luscher (1980) describe the use of a corrugator that is drawn up the inside of the pipe pile, after the backfill is installed but before it freezes, which produces a series of corrugations along the pile embedment length. The enhanced capacities of such piles was examined in field load tests reported in Luscher et al. (1985) and Black and Thomas (1980). Long (1978) states that tests on piles which were corrugated along their length "showed compressive failure at the corrugations". Work by Andersland and Alwahhaab (1983) showed that the introduction of lugs onto a steel rod embedded in frozen sand greatly increased the pullout capacity of the rod. Sego and Smith (1989) observed an increase of 100% in adfreeze resistance for model piles in a sand slurry backfill when the surface of the pile was sandblasted to remove the black lacquer coating and to roughen the pile surface. Ladanyi and Guichaoua (1985) showed increases in model pile capacities of approximately four times when the pile surface was corrugated along its length. Direct shear tests between saline ice and steel plates reported by Berenger et al. (1985) showed that corroded steel plates had adfreeze bond strengths approximately 5 times greater than those of clean steel plates.

Model sandblasted steel piles installed in ice had their adfreeze bond strength reduced by 50% when they were painted with Inertia 160 marine coating (Frederking and Karri 1983). Parmeswaran (1978a) showed that painting of sandblasted steel piles, installed in frozen sand, reduced the adfreeze bond capacity by an average of 13%, and that creosote treatment of BC timber fir piles reduced the adfreeze bond capacity by an average of 55%. From direct shear tests with saline ice Berenger et al. (1985) report reductions of



approximately 80% in the adfreeze bond strength for clean steel plates compared to corroded steel plates.

In ice-poor soils where the pile adfreeze bond strength may govern rather than the time dependent deformation (Weaver and Morgenstern 1981), increases in pile capacity may be realized by roughening the interface between the pile and the backfill. Conversely one must be aware that many coatings on the surface of the pile will cause a reduction of the adfreeze bond strength between the pile and the backfill.

### *Soil slurry backfill*

Soil slurry backfills may be divided into two general categories: slurries of native soil cuttings and of imported soil. Backfilling with slurries of native soil cuttings has been commonly practiced but it is recognized that there are problems with this method of installation.

In fresh-water permafrost an increase of fines content in the cuttings results in an increase in unfrozen water (Anderson and Morgenstern 1973) as shown in Figure 2.2. This will result in reduced soil strength, particularly with respect to long-term loading. Consequently the use of native soil cuttings where there are considerable fines in the soil is seldom recommended for adfreeze piles unless the loads on the piles are very small, or clean sand is either unavailable or uneconomical to transport to the site.

The use of a properly placed clean granular (sand) backfill (as opposed to backfilling with native soil cuttings) can result in an increased pile capacity for a number of reasons. Firstly the adfreeze strength of the slurry itself will be increased. Secondly the shear strength of the slurry may be greater, and ice content less, than that of the surrounding native soil. Consequently, for long-term time dependent deformation considerations the failure surface will be located at the backfill/native soil interface. Thirdly there will be little or no strength reduction due to unfrozen water in a clean sand slurry backfill, as would occur in a backfill containing fines. Finally, using imported clean granular material will ensure that no salinity is introduced into backfill by the soil fraction.

Crory (1963) noted that clay-water slurries were difficult to mix, and had adfreeze bond strengths approaching that of ice. Silt water slurries displayed bond strengths nearly double that of the clay water slurries, and the bond strengths of sand slurries were approximately 50% greater than for silt. Sego and Smith (1989) report similar short-term adfreeze strengths on model piles using backfills of either imported clean sand or silty sand drill cuttings in soil at temperatures of  $-5^{\circ}\text{C}$ . The pile capacity with a pure ice backfill was approximately 60% of the capacity in clean sand. A backfill slurry of saline silty sand drill cuttings gave a capacity of approximately 50% of the clean sand backfill.

Nixon (1988) suggests that there is little to be gained using soil or water of zero salinity in the slurry backfill in saline soils, as salt diffusion on a local scale would likely equalize the salinity in the backfill after a relatively short time period. This is appropriate if there are fines in the backfill slurry which result in unfrozen water. Murrmann (1973) reports data on the self-diffusion coefficient of the sodium ion in a frozen silty clay ranging from  $1 \times 10^{-7}$  to  $5 \times 10^{-7} \text{ cm}^2 \text{ s}^{-1}$ , which is about a factor of 10 less than those reported for unfrozen bentonite. However if a clean granular backfill is used resulting in no continuous unfrozen water in the pore space (Hivon 1991), then the diffusion of solute ions will be considerably reduced. This is an area which requires further quantitative assessment and research.

#### *Grout as a backfill material*

The use of cementitious grouts as a backfill material for piles in cold permafrost is in its infancy. This is due to the problems associated with developing a grout which will cure adequately in a sub-zero environment without adversely affecting the surrounding native soil. Weaver (1979) points out that in order for a grout to be used successfully for piling in permafrost it must be able to cure at temperatures below  $0^{\circ}\text{C}$ , the mixing water must not freeze prior to curing, it must develop adequate compressive strength, the heat of hydration must not cause excessive thermal disturbance to the surrounding permafrost, it must be

stable to repeated freeze-thaw cycles, and an adequate bond strength to the piling material must develop.

The two principal advantages of using a grout backfill compared to a soil slurry backfill are that the cementitious bond between the grout and the pile is strong, and that the grout is much less susceptible to creep than a soil slurry backfill. For a properly cured grout the capacity of the bond between the pile and the grout (typically greater than 1500 kPa, Biggar and Sego in press b [Chapter 5]) will exceed that at the grout/native soil interface. Therefore the pile capacity will be governed by the shear strength at the grout/native soil interface, which fully mobilizes the shear strength of the native soil, beyond which no increase can be realized for a given pile geometry.

The problems associated with using a grout backfill are the development of a grout which will perform adequately in the sub-zero environment, the associated costs of purchasing, transporting and placing the grout, and the difficulties in handling and mixing the grout to ensure quality construction in the adverse environment.

There are essentially four ways to ensure that the grout will cure adequately in a sub-zero environment: 1) the temperature (T) of the grout may be artificially maintained above 0°C using external heat sources (this method is expensive and impractical for sub-surface grouting in frozen soils), 2) cements with rapid rates of hydration (evolving heat at a high rate) may be utilized to maintain the grout temperature above 0°C as it cures, 3) admixtures may be added to the cement to depress the freezing point of the mixing water and accelerate the curing time, and 4) grouts with very low water contents may be used which set rapidly.

High alumina cements (such as Ciment Fondu) are utilized in grouts so that their high heats of hydration prevent freezing of the mix water during curing of the grout. Utilizing admixtures the grout may be designed to provide optimum workability and thermal performance in the field (Biggar and Sego 1990). The use of these grouts is reported by

Johnston and Ladanyi (1972) in warm permafrost ( $T > -1^{\circ}\text{C}$ ) and by Kast and Skermer (1986) and Biggar and Sego (1989) in frozen rock and soil at temperatures as cold as  $-7^{\circ}\text{C}$ .

Weaver (1979) discusses the use of gypsum-based cement grout which uses salts to depress the freezing point of the mixing water. Salt diffusion from the grout into the surrounding soil resulted in a thawed annulus of soil adjacent to the grout at temperatures warmer than  $-4^{\circ}\text{C}$ . At colder temperatures ( $T < -6^{\circ}\text{C}$ ) Cunningham et al. (1972) report an adequate bond between soil and gypsum based cement used to install oil well casing. Gypsum based grouts, or any other grouts with freezing point depressants which may diffuse into the surrounding soil, must be used with care in frozen soils since such impurities may cause a rapid decrease in the shear strength of the frozen soil (Sego et al 1982; Nixon and Lem 1984; and Hivon 1991).

Biggar and Sego (1989) report successful use of Type 30 Portland cement with admixtures in rock at temperatures of  $-5^{\circ}\text{C}$ . Ballivy et al. (1990) describe grout mix designs using Type 30 Portland cement and various admixtures to depress the freezing point of the mix water for use in rock anchors at temperatures as cold as  $-12^{\circ}\text{C}$ . Considerable advances have been made recently with antifreeze admixtures with Portland cement for concreting at temperatures below freezing (Korhonen 1990), and this technology may be applicable to the design of grouts for piling in permafrost soils.

Geocon Inc. (1988) has reported success using a magnesium phosphate based grout which has a low water-cement ratio and which sets quickly, before the sensible heat of the grout can be lost to the surrounding frozen soil.

#### *Impurities in the frozen soil*

Recent studies have found naturally occurring frozen soils with salts in the pore water. Gregerson et al. (1983) describe marine saline permafrost in Spitzbergen. Hivon (1991) provides a comprehensive discussion on the distribution of saline permafrost in the Canadian Arctic. The distribution of saline permafrost in the Soviet Union is reported in Dubikov et al. (1988). The effect of salinity on reducing the strength and increasing the

creep of frozen soils is examined in studies by Sego et al. (1982), Ogata et al. (1983), Nixon and Lem (1984), Pharr and Merwin (1985), and Hivon (1991).

Nixon and Lem (1984) discuss how the reduced frozen soil strength is a result of two phenomena. Firstly the freezing point of the water is depressed. At a salt concentration of 30 ppt the freezing point of brine is  $-1.8^{\circ}\text{C}$ , thus the thermal analysis in design is essentially 'axis translated' by approximately  $2^{\circ}\text{C}$ . Secondly, and potentially more serious, is the increase in unfrozen water within the soil. Ice crystals are generally formed of fresh water which excludes impurities such as salt ions from the pure crystalline ice structure into the remaining unfrozen water contained in the soil. Consequently the pore fluid of the frozen saline soil is formed of ice crystals comprised of nearly fresh water surrounded by zones of salt ion enriched unfrozen water. As the temperature decreases, increasing amounts of salt ions are excluded into the remaining brine solution further depressing its freezing point. This process continues until the pore solution becomes a matrix of ice and salt ions with no liquid brine at the eutectic temperature, which for a sodium chloride solution is  $-21.3^{\circ}\text{C}$  (Ogata et al. (1983)). This is illustrated in the phase diagram for an NaCl solution shown at Figure 2.3.

#### *Tensile versus compressive loading*

The reduction in pile capacity under tensile loading versus compressive loading is discussed in Janbu (1976), Frederking and Karri (1983), and Fellenius and Samson (1976). Fellenius and Samson (1976) present a comparison of uplift tests to compression tests for piles in unfrozen marine clay illustrating downward shaft resistances 50% to 100% greater than upward shaft resistances. Tests on model PVC piles embedded in an ice sheet by Frederking and Karri (1983) show similar results. The authors' qualitative analysis of this phenomena suggested that the difference is due in part to changes in lateral effective pressure on the pile shaft as a result of decreased pile diameter under tensile loading compared to compressive loading. Janbu (1976) on the other hand provides a quantitative solution for piles in thawed soils based on pile roughness and lateral earth pressures. Thus

although it is difficult to quantify, it may be expected that the adfreeze shaft resistance of a pile in tension will be lower (approximately one-half) than that in compression.

## **Site conditions**

### *Location*

The saline permafrost site was within the municipality of Iqaluit in a vacant lot south east of the Hudson Bay store approximately 100 m from the high tide line. The site is shown on the maps in Figure 2.4.

### *Soil conditions*

The soil at the test site consisted of a dense grey clayey, gravelly sand till with some cobbles overlain by up to 2 m of clean reddish-brown gravelly sand with cobbles. The grain size distribution of the native soil is shown in Figure 2.5. The depth to permafrost was approximately 1.5 m during the installation in July 1988 and 2 m during the testing in August 1988. Ground temperatures at the depths of embedment during installation were  $-6^{\circ} \pm 0.5^{\circ}$  C and during load testing were  $-5^{\circ} \pm 1.0^{\circ}$  C. The ground temperature profile at the site during installation and testing is shown in Figure 2.6. Also included in Figure 6 is the depth range of effective pile embedment. Soil moisture contents over the embedded portion varied from 6.5% to 9.5% with bulk densities of the frozen soil between 2.27 and 2.36 Mg/m<sup>3</sup>. Salinities were determined by extracting pore water from grab samples and using an AO Model 10419 Hand Refractometer to measure the salinity of the fluid extract. The values of salinity obtained ranged from 15 to 24 ppt. Soil ice classification from a core sample was Nbn, well bonded pore ice with no visible ice lensing or crystals. The salinity and moisture content profiles are presented in Figure 2.7. Unconfined compression tests were conducted on core samples obtained using a CRREL core barrel. At a strain rate of 0.8%/hr and a temperature of  $-5^{\circ}$ C the shear strengths were between 500 and 600 kPa.

## **Pile installation**

### *Pile configurations*

One of the objectives of the project was to examine the additional capacity gained by incorporating certain modifications to the pile surface and backfill materials. The pile and backfill configurations tested are shown schematically in Figure 2.8. In an effort to limit the portion of the pile which carried the applied load to a region of nearly constant temperature, a bond breaker consisting of layers of grease and tape was used on the upper 4 m of each pile. A total of 14 pile load tests were performed.

Both hollow structural steel (HSS) and schedule 40 pipe, and Dywidag threaded bars were used. Modifications to the HSS piles included welding rebar bracelets on the lower 1 m of the pile (lugged HSS) and cleaning the pile with a solvent to remove any oil or grease from the surface (smooth HSS). Pipe piles identical to those currently used in the region, with a black laquer paint coating, were installed both untreated (plain pipe) and with the embedded portion sandblasted (sandblasted pipe). Pile surface roughness profiles including center line average (CLA) roughness measurements were obtained using a Taylor Hobson 'Talysurf 4' surface measuring instrument. The pile CLA roughnesses for the sand blasted pipe piles were 6.10 to 8.60  $\mu\text{m}$ , and for the smooth HSS piles were between 0.28 to 0.46  $\mu\text{m}$ . The smooth HSS piles were backfilled with Silica Sil #8 sand. The grain size distribution for the silica #8 sand is shown on Figure 5. The remainder of the piles were backfilled with a local well graded clean sand screened through a 6 mm mesh and tested to ensure that it had no salinity. Dywidag bars were grouted into the permafrost using both a neat and a sanded Ciment Fondu grout to make anchors.

To examine the development of load with depth strain gauges were attached to one of each of the smooth HSS, lugged HSS and Dywidag bar piles. On the HSS piles at each elevation three weldable uniaxial strain gauges were placed 120° radially apart in order to account for any differential axial straining. On the Dywidag bars bondable uniaxial strain gauges were mounted 180° apart on the flat sides of the bar. The strain gauges were

mounted with one set immediately above the effective embedded portion of the pile to examine the effectiveness of the bond breaker. The remaining strain gauges were placed along the effective embedment portion of the pile to examine the measured load distribution with depth.

### *Drilling*

All of the project drilling was carried out using a Joy Airtrac drill model RAM along with a Halco Rotary Mission downhole hammer. Core samples were taken with a 100 mm CRREL core barrel modified to fit the airtrack drill.

To prevent the ingress of water into the hole, a 165 mm hole was drilled to the permafrost table then a 200 mm diameter pipe casing was driven around the hole approximately 0.3 m into the permafrost. A pile hole was then drilled down through the casing to a depth of 7.5 m (approximately 1.0 m deeper than the pile length) to allow cuttings and or sloughed material to rest beneath the pile, thereby ensuring that no saline soil would be in contact with the pile when it was installed. In practice this would not be the normal method of pile installation, but rather the pile would be driven well into the bottom of the hole by the downhole hammer to seat it. This would necessitate however that the lower 0.5-1 m of the pile be designed with a reduced strength when calculating the adfreeze load capacity of the pile.

### *Placement*

Piles backfilled with sand were lowered and suspended in place using the drill rig then the sand backfill was placed. This ensured that the embedded portion of the pile was in contact with a clean sand slurry backfill and no strength loss would be attributed to salinity in the backfill from native soil cuttings. The sand was poured down the annulus between the pipe and the hole wall, then washed down with clean non saline water. Approximately 20 liters of sand were poured followed by 4-5 liters of water. This process was continued until the annulus was filled. This procedure was used to avoid bridging of a



premixed soil slurry in the narrow annulus. The center of the pile was then filled with dry sand to hasten freeze-back of the slurry backfill.

For the grouted piles the grout was poured into the hole using a large funnel (allowing free fall) then the pile was lowered into place using the drill rig. The depth of the grout was measured after the pile was placed.

The neat grout mix used Ciment Fondu, water and a sulphonated naphthelene formaldehyde condensate water reducing admixture (superplasticizer (SPN)). The water:cement ratio was 0.35:1, by weight, and the SPN was added at 0.75% by weight of cement. The sanded grout mix used a water:cement:sand ratio of 0.35:1:0.45, by weight, and SPN was added at 0.75% by weight of cement. Silica Sand, Sil #8 sand was used in the sanded grout mix.

## **Pile testing**

### *Apparatus*

Piles were loaded in tension (pullout tests) using a center-pull hydraulic jack resting on top of a reaction frame. A length of Dywidag bar, which was coupled to the pipe piles using a threaded connector, passed up through the center of the jack and was secured with a plate and a nut. The loading frame apparatus is shown schematically in Figure 2.9.

Load was measured both directly using a load cell in series with the jack, and indirectly via a pressure transducer on the hydraulic fluid line between the pump and the jack. The output from these devices were manually recorded using a strain indicator display. Spherical seats were used beneath the load cells and if necessary beneath the jack to maintain the alignment of the loading system and the pile. Strain gauge output was also manually recorded using the strain indicator display.

Pile displacement was measured using two dial gauges with 0.025 mm (0.001") divisions mounted on a separate frame at right angles to the loading frame, supported approximately 1.5 m on either side of the pile. A survey level accurate to 0.01 mm was

used to check the pile displacement and to monitor the dial gauge support frame for movements.

### *Procedures*

The piles were loaded incrementally with the subsequent load increment being applied once the displacement rate of the pile decreased to less than 0.25 mm/hr (.01"/hr). Applied loads were maintained within 1% of the desired load by a person monitoring the load cell output and operating the hydraulic hand pump. The load was maintained until the pile displaced at least 15 mm unless an accelerating displacement rate or brittle failure was observed.

Outputs from the load cell, pressure transducer, and dial gauges were recorded every 10 minutes unless the load was maintained for extended periods, then the time interval between readings was increased. Generally load increments were applied every 30 minutes until the applied load reached approximately 80% of the failure load. Strain gauge readings (if applicable) were taken immediately before the next load increment was applied, though frequently more often in order to examine the load redistribution along the pile with time under a constant applied load.

### **Test results**

#### *Load versus Displacement*

A summary plot of typical load versus displacement response for the different pile configurations is shown in Figure 2.10. Pertinent details of the test results are tabulated in Table 1. A summary of the applied loads at failure are summarized in Figure 2.11.

It can be seen in Figure 2.10 that the load versus displacement behaviour was essentially linear to approximately 80 to 90% of the failure load. Post failure behaviour can be generally grouped into two categories: plastic or strain weakening. The grouted anchors and the lugged piles failed plastically, whereas the smooth (or plain) and sandblasted piles failed in a strain weakening manner.

### *Time dependent deformation in saline permafrost*

A typical plot of displacement versus time is shown at Figure 2.12. For applied loads less than 80% to 90% of the failure load generally the displacement rate for each load increment attenuated to a value less than the allowable 0.25 mm/hr within 30 minutes. As the failure load was subsequently approached, load increments had to be maintained for longer time intervals due to increased rates of displacement. At the failure load, generally the deformation rate attenuated for one or two readings then (slowly) increased. The time to the onset of an accelerating displacement rate or reduction in pile capacity varied for each test.

An anomaly to the above behavior was observed for the lugged piles. At the failure load the deformation rate remained relatively constant, exceeding the allowable rate. With increasing loads (up to twice the defined failure load) the deformation rate increased incrementally but remained constant at each load increment.

### **Discussion**

A comparison of the short-term capacity of the different pile configurations is shown best in Figure 2.11. The smooth (and plain) piles consistently had the lowest capacity. The lugged piles carried approximately twice the load of the plain piles. The increased capacity realized by sandblasting the piles was approximately four times that of the plain steel piles. The use of a grout backfill resulted in an increased load carrying capacity of approximately 8-10 times that of the plain piles.

The difference between plastic and strain weakening failure modes is a result of the rough (or irregular) failure surface developed by the grouted anchors and lugged piles, forcing shear failure within the frozen backfill. The failure of the smooth and sandblasted piles occurred when the adfreeze bond failed along the planar surface of the pile resulting in a strain weakening failure mode.

It is believed that the effect of changing the backfill from a sand slurry to a grout was that of shifting the failure surface from the pile/backfill interface outward to the

backfill/native soil interface, increasing the surface area over which the load was resisted and fully mobilizing the shear strength of the native soil. As there was no discernible difference in capacity between the threaded bar anchors backfilled with either neat or sanded grout, the strength of the grout adjacent to the soil did not likely govern the pile capacity. Further the average shear stress at the bar/grout interface did not exceed 1750 kPa, which is considerably lower than interfacial shear strengths of approximately 2800 kPa determined from tests conducted at a nearby site in rock reported in Biggar and Sego (1989). These results support the assertion that the ultimate capacity of the anchors were governed by the shear strength of the frozen native soil, rather than the shear strength of the grout. There exists a possibility that yield of the bar may have governed the pile capacity, but a more detailed analysis of this mechanism is contained in Part II of this paper.

As there was no measurable difference in the capacity between the anchors in which the neat and the sanded Cement Fondu grouts were used, it is suggested that the use of the sanded grout would be preferable to the neat grout. There would be less thermal disturbance to the surrounding permafrost, and likely a lower cost due to the reduced cement content.

## **Conclusions**

1. Considerable gains in short-term pullout capacity of piles in saline permafrost were realized by modifying the pile surfaces and/or backfill materials. In a frozen sand backfill, welding four 12 mm rebar bracelets over the lower meter of the pile doubled the capacity of plain piles. Sandblasting the pile surface gave a fourfold increase in capacity. Using a grout backfill increased the load carrying capacity to nearly 10 times that of smooth piles.
2. Grout backfill was successfully used in permafrost soil in which the temperatures were  $-5.5^{\circ} \pm 1^{\circ} \text{ C}$  without preheating the prebored hole.

3. The testing methodology used in these tests worked well to determine the load carrying capacities for the piles, and negated end bearing effects. The load frame was portable and could be manhandled around the site by two or three people.
4. The failure loads and mechanisms observed in the tests were consistent and reproducible. It is believed that the results are reliable for the conditions encountered.

## References

- Andersland, O.B., and Alwahhaab, M.R. 1983. Lug behavior for model steel piles in frozen sand. Proceedings, 4th International Conference on Permafrost, Fairbanks, Alaska, USA. pp. 16-21.
- Anderson, D.M. and Morgenstern, N.R. 1973. Physics, chemistry and mechanics of frozen ground: a review. Proceedings, 2nd International Conference on Permafrost, North American Contribution, Yakutsk, USSR, pp. 257-288.
- Ballivy, G., Benmokrane, B. Hernandez, P., and Aitcin, P.C. 1990. Injection d'ancrages dans le roc gelé du grand Nord à l'aide d'un coulis à base de ciment Portland. Proceedings, 5th Canadian Permafrost Conference. Quebec City, Quebec, pp. 357-364.
- Berenger, D.M., Edwards, R.Y., and Nadreau, J.P. 1985. Preliminary assessment of the adhesion shear strength of ice-steel and ice-frozen sand binds. Arctic Petroleum Operators' Association, Research Project Report 85-1, p. 55.
- Biggar, K.W. and Sego, D.C. 1989. Field load testing of various pile configurations in saline permafrost and seasonally frozen rock. 42nd Canadian Geotechnical Conference, October 25-27, Winnipeg, pp. 304-312.
- Biggar, K.W., and Sego, D.C. 1990. The curing and strength characteristics of cold setting Ciment Fondu grout. Proceedings, 5th Canadian Permafrost Conference. Quebec City, Quebec, pp. 349-355.
- Biggar, K.W. and Sego, D.C. in press a. [Chapter 3] Field pile load tests in saline permafrost, Part II, Analysis of results.
- Biggar, K.W. and Sego, D.C. in press b. [Chapter 5] Strength and deformation behaviour of model adfreeze and grouted piles in saline permafrost.
- Biggar, K.W. and Sego, D.C. in press c. [Chapter 6] Time dependent displacement behaviour of model adfreeze and grouted piles in saline permafrost.
- Black, W.T. and Thomas, H.P. 1979. Prototype pile tests in permafrost soils. in Pipelines in Adverse Environments: A State of the Art, Proceedings of the ASCE Pipeline Division Specialty Conference, New Orleans, Louisiana, V. 1, pp. 372-383.
- Bro, A. 1985. Research challenges in frozen ground pile design. Proceedings, Arctic '85: Civil Engineering in the Arctic Offshore, San Francisco, California, ASCE, 25027 March, pp. 1196-1205.

- Crory, F.E. 1963. Pile foundations in permafrost. Proceedings, 1st International Conference on Permafrost, Lafayette, Indiana, USA. pp. 467-476.
- Cunningham, W.C., Fehrenbach, J.R., and Maier, L.F. 1972. Arctic cements and cementing, *Journal of Canadian Petroleum Technology*, Oct.-Dec., pp. 49-55.
- Dubikov, G.I. et al. 1988. Pore solutions of frozen ground and its properties. Proceedings, 5th International Conference on Permafrost, Trondheim, Norway, pp. 333-338.
- Fellenius, B.H., and Samson, L. 1976. Testing of drivability of concrete piles and disturbance to sensitive clay. *Canadian Geotechnical Journal*, 13: 139-160.
- Frederking, R., and Karri, J. 1983. Effects of pile material and loading state on adhesive strength of piles in ice. *Canadian Geotechnical Journal*, 20: 673-680.
- Geocon Inc. 1988. Grout testing arctic grout pile. Report submitted to UMA Engineering Ltd, August 26, 1988, p. 23.
- Gregersen, O., Phukan, A., and Johansen, T. 1983. Engineering properties and foundation design alternatives in marine Svea clay, Svalbard. Proceedings, 4th International Conference on Permafrost, Fairbanks Alaska, USA, pp. 384-279.
- Hivon, E.G. 1991. Behaviour of saline frozen soils. Unpublished Ph. D. Thesis, University of Alberta, Edmonton, Alberta, p. 435.
- Hutchinson, D.J. 1989. Model pile load tests in frozen saline silty sand. Unpublished MSc Thesis, University of Alberta, Edmonton, Alberta, p. 222.
- Janbu, N. 1976. Static bearing capacity of friction piles. Proceedings VI European Conference on Soil Mechanics and Foundation Engineering, Vol. 1.2, pp. 479-488.
- Johnston, G.H., and Ladanyi, B. 1972. Field tests on grouted rod anchors in permafrost, *Canadian Geotechnical Journal*, 9: 176-194.
- Kast, G. and Skermer, N. 1986. DEW Line anchors in permafrost. *Geotechnical News*, 4 (4): 30-34.
- Korhonen, C.J. 1990. Antifreeze admixtures for cold regions concreting, A literature review. CRREL Special Report 90-32. p. 14.
- Ladanyi, B., and Guichaoua, A. 1985. Bearing capacity and settlement of shaped piles in permafrost. Proceedings, XI International Conference on Soil Mechanics and Foundation Engineering, San Francisco, USA, pp. 1421-1427.
- Long, E.L. 1973. Designing friction piles for increased stability at lower installed cost in permafrost. Proceedings, 2nd International Conference on Permafrost, North American Contribution, Yakutsk, USSR, pp. 693-698.
- Long, E.L. 1978. Permafrost Foundation Designs. Proceedings: Cold Regions Specialty Conference, Anchorage, Alaska, ASCE, 17-19 May, pp. 973-987.

- Luscher, U., Black, W.T. and McPhail, J.F. 1983. Results of load tests on temperature-controlled piles in permafrost. Proceedings, 4th International Conference on Permafrost, Fairbanks, Alaska, USA, pp. 756-761.
- Manikian, V. 1983 Pile driving and load tests in permafrost for the Kuparuk pipeline system. Proceedings, 4th International Conference on Permafrost, Fairbanks Alaska, USA, pp. 804-810.
- Miller, D.L. and Johnson, L.A. 1990. Pile settlement in saline permafrost: a case history. Proceedings, 5th Canadian Permafrost Conference. Quebec City, Quebec, pp. 371-378.
- Morgenstern, N.R., Roggensack, W.D., and Weaver, J.S. 1980. The behavior of friction piles in ice and ice-rich soils. Canadian Geotechnical Journal, 17: 405-415.
- Murrmann, R.P. 1973. Ionic mobility in permafrost. Proceedings, 2nd International Conference on Permafrost, North American Contribution, Yakutsk, USSR, pp 352-359.
- Nixon, J.F. 1988. Pile load tests in saline permafrost at Clyde River, Northwest Territories, Canadian Geotechnical Journal, 25: 24-31.
- Nixon, J.F., and Lem, G. 1984. Creep and strength testing of frozen saline fine-grained soils. Canadian Geotechnical Journal, 21: 518-529 .
- Nixon, J.F., and McRoberts, E.C. 1976. A design approach for pile foundations in permafrost. Canadian Geotechnical Journal, 13: 40-57.
- Ogata, N., Masayuki, Y., and Tetsuyuki, K. 1983. Effects of salt concentration on strength and creep behaviour of artificially frozen soils. Cold Regions Science and Technology, 8: 139-153.
- Parneswaran, V.R. 1978a. Adfreeze strength of frozen sand to model piles. Canadian Geotechnical Journal, 15: 494-500.
- Parneswaran, V.R. 1978b. Creep of model piles in frozen soil. Canadian Geotechnical Journal, 16: 69-77.
- Pharr, G.M. and Merwin, J.E. 1985. Effects of brine content on the strength of frozen Ottawa sand. Cold Regions Science and Technology, 11: 205-212.
- Rowley, R.K., Watson, H.W., and Ladanyi, B. 1973. Vertical and lateral pile load tests in permafrost. Proceedings, 2nd International Conference on Permafrost, North American Contribution, Yakutsk, USSR, pp. 712-721.
- Sego, D.C., Schultz, T., and Banasch, R. 1982. Strength and deformation behavior of frozen saline sand. Third International Symposium on Ground Freezing, Hanover, New Hampshire, pp. 11-19.
- Sego, D.C. and Smith, L.B. 1989. The effect of backfill properties and surface treatment on the capacity of adfreeze pipe piles. Canadian Geotechnical Journal, 26: 718-725.

- Thomas, H.P. and Luscher, U. 1980. Improvement of bearing capacity of piles by corrugations. CRREL Special Report 80-40, pp. 229-234.
- Vyalov, S.S. 1959. Rheological properties and bearing capacity of frozen soils. Translation 74, U.S. Army CRREL, translated in 1965, p 219.
- Weaver, J.S. 1979. Pile foundations in permafrost. Unpublished Ph. D. Thesis, University of Alberta, Edmonton, Alberta, p. 224.
- Weaver, J.S., and Morgenstern, N.R. 1981. Pile design in permafrost. Canadian Geotechnical Journal, 18: 357-370.



**TABLE 2.1**  
Summary of pile load test data

PILE TYPE	#	APPLIED LOAD		FAILURE STRESS*		DISPL AT FAILURE (mm)	AVG TEMP (°C)	FAILURE MODE / COMMENTS
		at Failure (kN)	Prior to Failure (kN)	Pile/ Backfill (kPa)	Backfill/ Native Soil (kPa)			
PLAIN PIPE	15	80	75	90	62	3.2	?	Accelerating displacement rate 30 min after failure load applied. Dramatic reduction in capacity 60 min after failure load applied.
	16	80	40	67	46	1.9	?	Accelerating displacement rate 40 min after failure load applied. Dramatic reduction in capacity 170 min after failure load applied.
SMOOTH HSS PIPE	7	100	50	111	77	4.1	-5.0	Accelerating displacement rate 60 min after failure load applied.
	5	80	50	67	46	14.3	-4.3	Accelerating displacement rate 100 min after failure load applied.
Strain gauged	11	70 to 80	60	78-89	54-62	2.27 at end of 70 kN	-4.8	Pile displacement rate of approx 0.46 mm/hr @ 70 kN for 1 hr. Accelerating displacement rate 20 min after 80 kN load applied.
LUGGED HSS PIPE	9	300	260	334	231	6.4	-5.5	Accelerating displacement rate 50 min after failure load applied.
	8	120	100	134	93	11.6 at end of 120 kN	-5.5	Observed constant displacement rate of approx .38 mm/hr for 15 hrs at 120 kN, after which the test was terminated.
Strain gauged	12	150	100	167	116	1.41 at end of 100 kN 9.92 at end of 150 kN	-4.8	At 150 kN the displacement rate exceeded the allowable rate. Observed increasing, constant displacement rates with increasing loads up to the max applied load of 290 kN.
SANDBLASTED PIPE	14	250	230	278	193	4.6	-4.6	Accelerating displacement rate 50 min after failure load applied. Brittle failure 180 min after failure load applied.
	13	290	270	323	224	5.7	-5.2	Accelerating displacement rate 20 min after failure load applied. Brittle failure 105 min after failure load applied.
DYWIDAG BAR IN NEAT GROUT	4	600	580	1719	463	11.9	-5.0	Displacement rate had only dropped to 0.39 mm/hr at 580 kN. Pile unable to maintain 600 kN load.
	2	575	555	1647	443	12.5	-4.5	Catastrophic failure due to welding of lugs onto bar.
DYWIDAG IN SANDED GROUT	6	580	560	1641	448	19.1	-5.4	Pile stable at 560 kN, unable to maintain 580 kN.
	3	593	576	1699	458	14.9	-4.5	Pile was stable at 576 kN but unable to maintain 593 kN.

\*Failure Stress calculated as the load applied by the jack distributed divided by the 2.5 m embedded portion of the pile.

Actual stresses measured by strain gauges differed depending on pile configuration, see Part II for details.

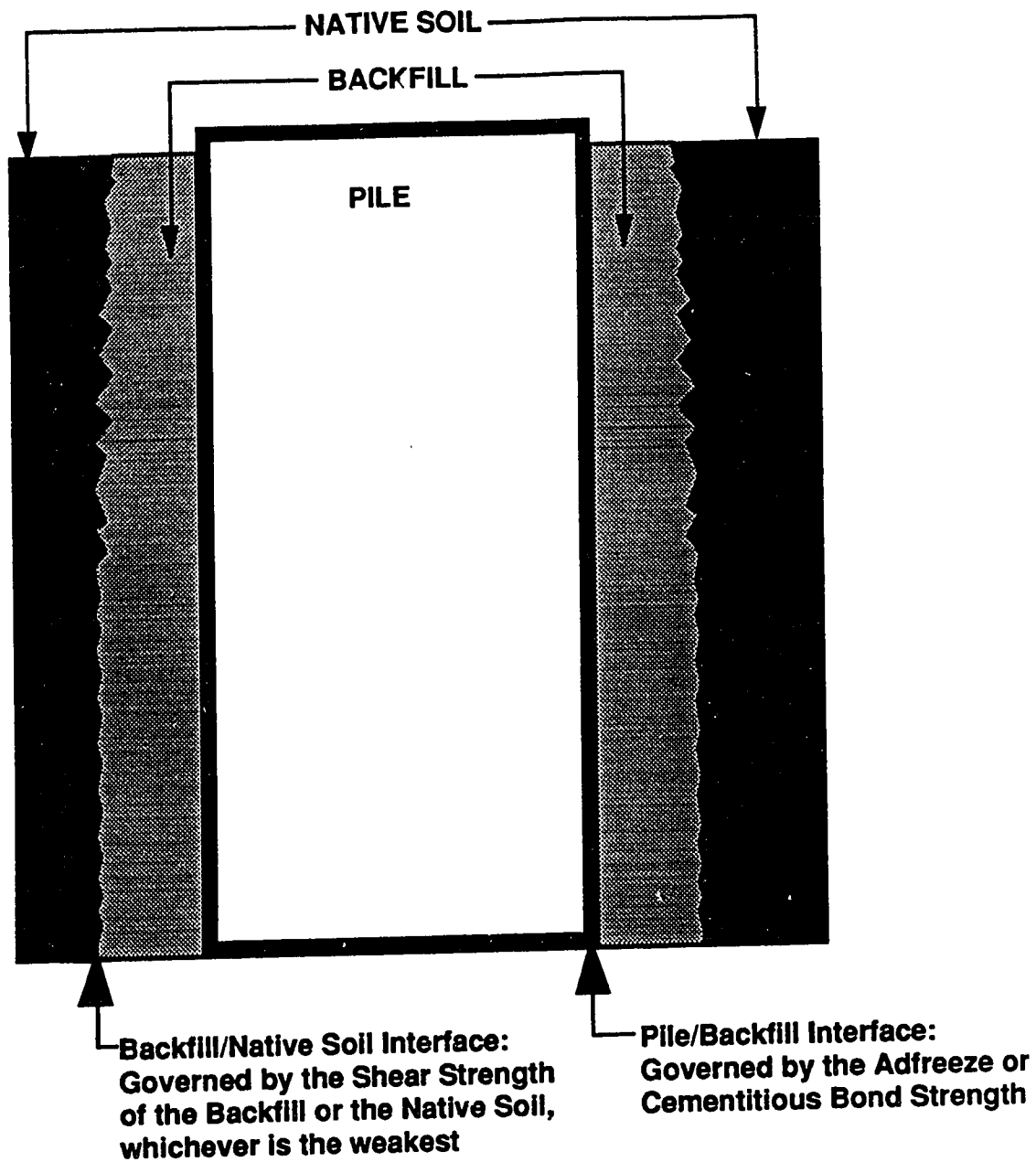


Figure 2.1: Pile Capacity in Relation to the Location of the Failure Interface

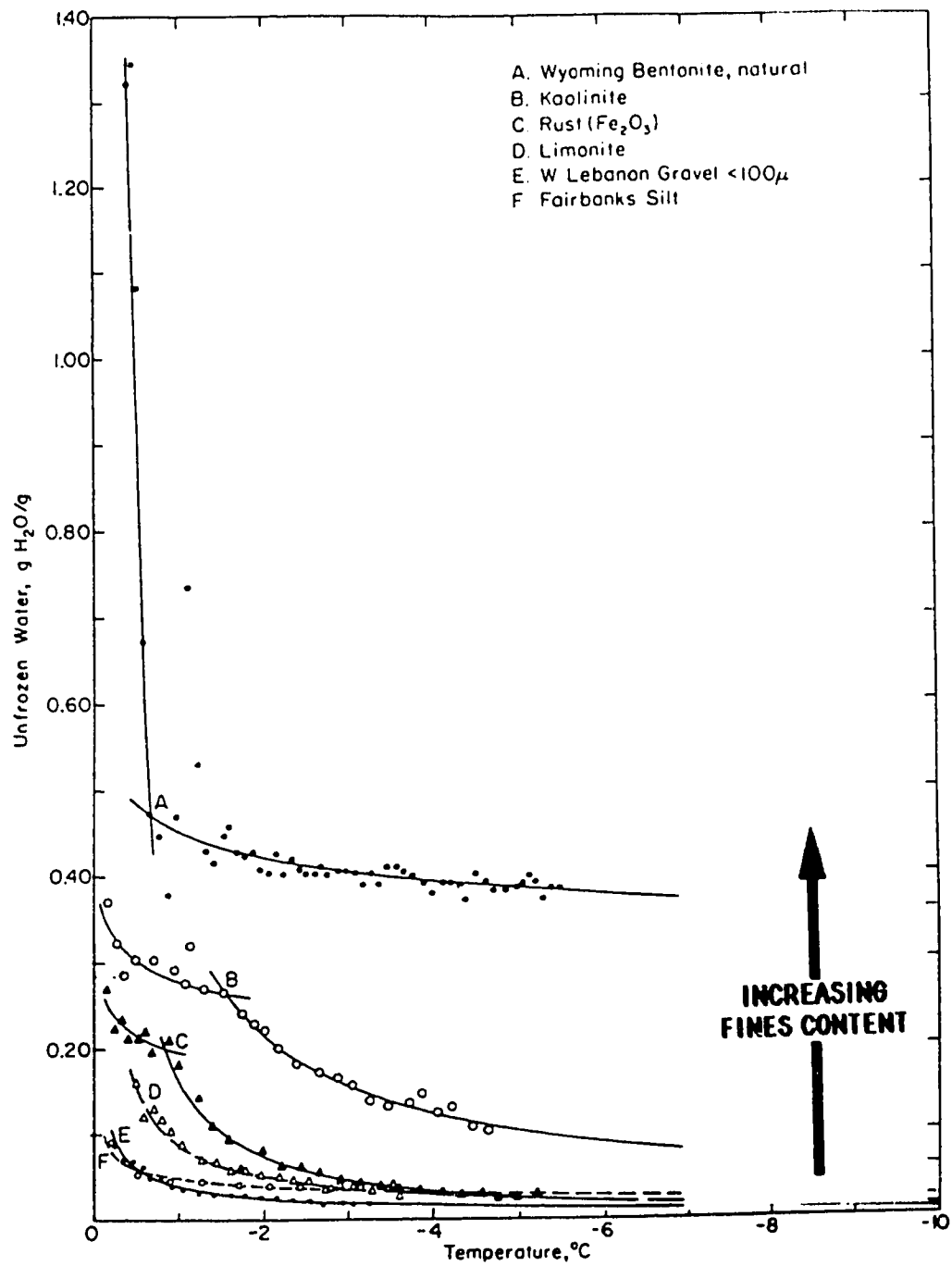


Figure 2.2 Unfrozen water content of various soils.  
(Modified from Anderson and Morgenstern 1973)

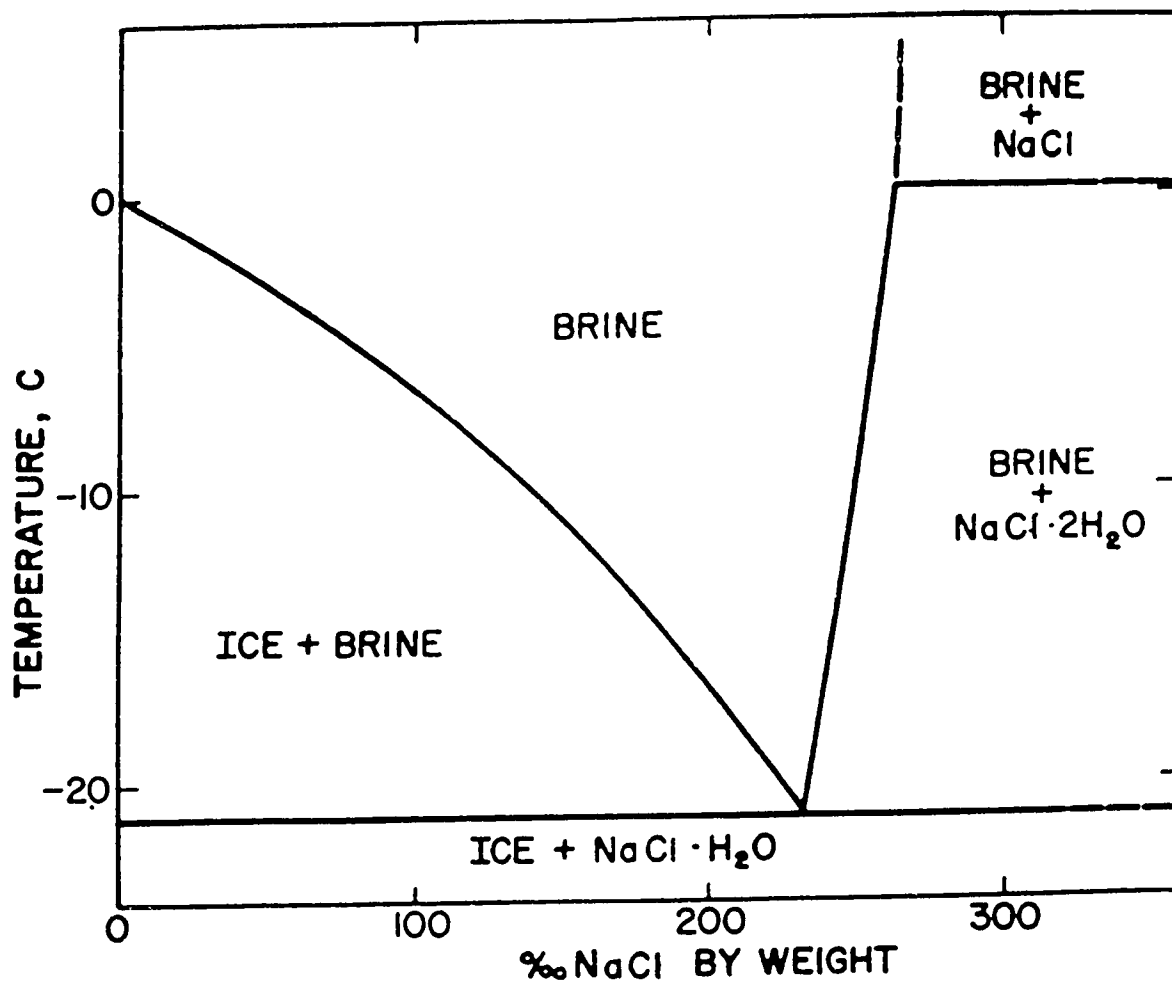


Figure 2.3 Phase diagram for NaCl.

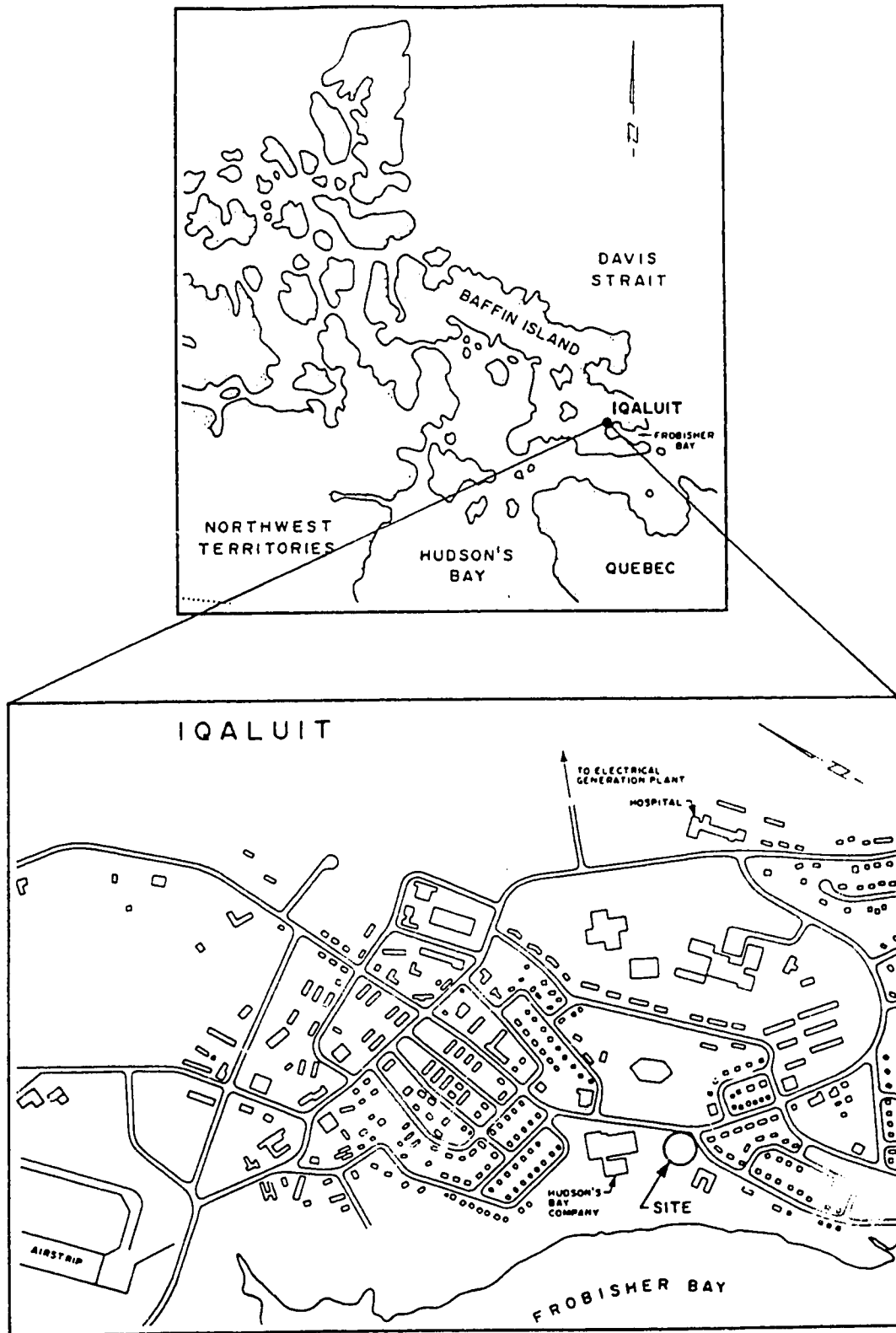


Figure 2.4 Site map of Iqaluit.

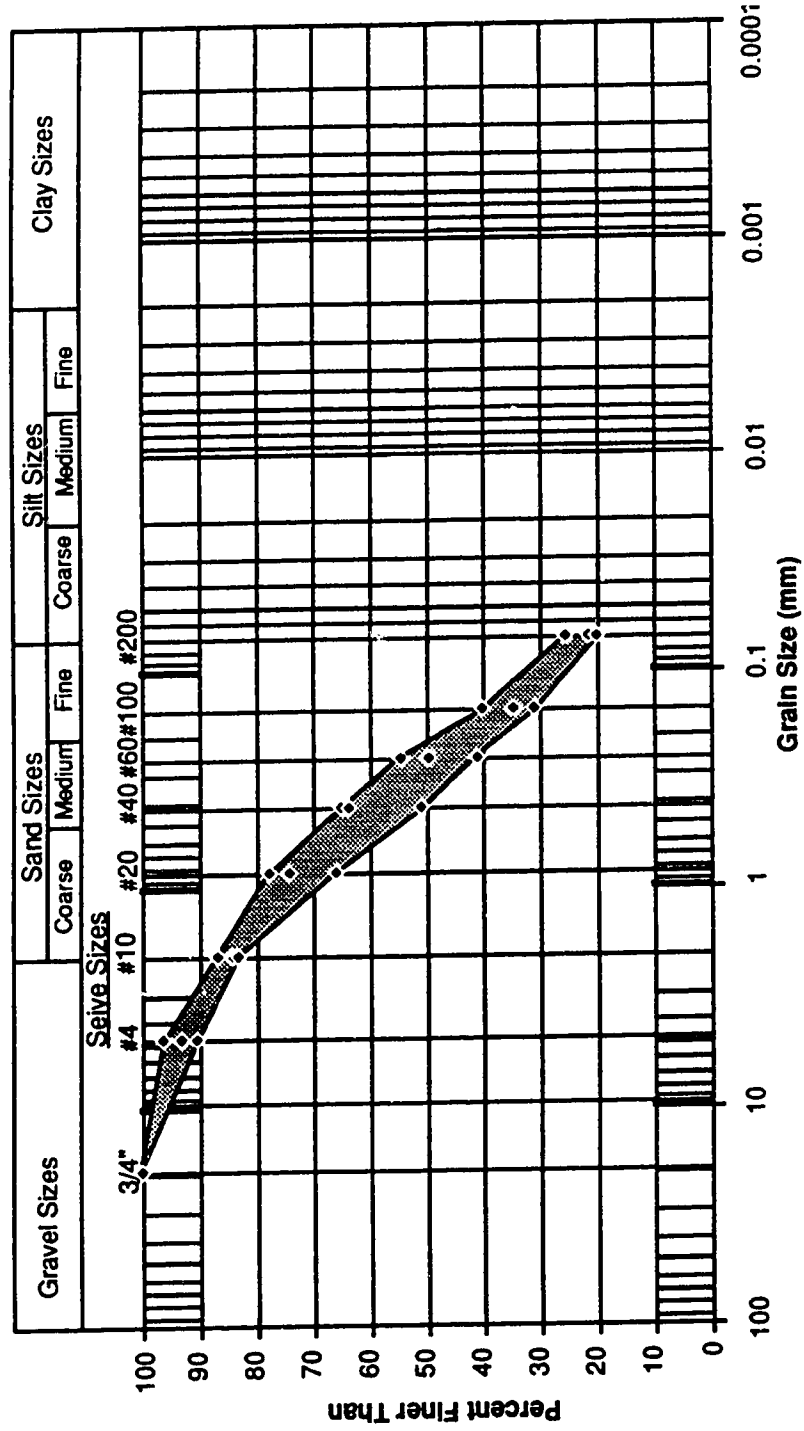


Figure 2.5: Grain Size distribution for Iqaluit Test Site

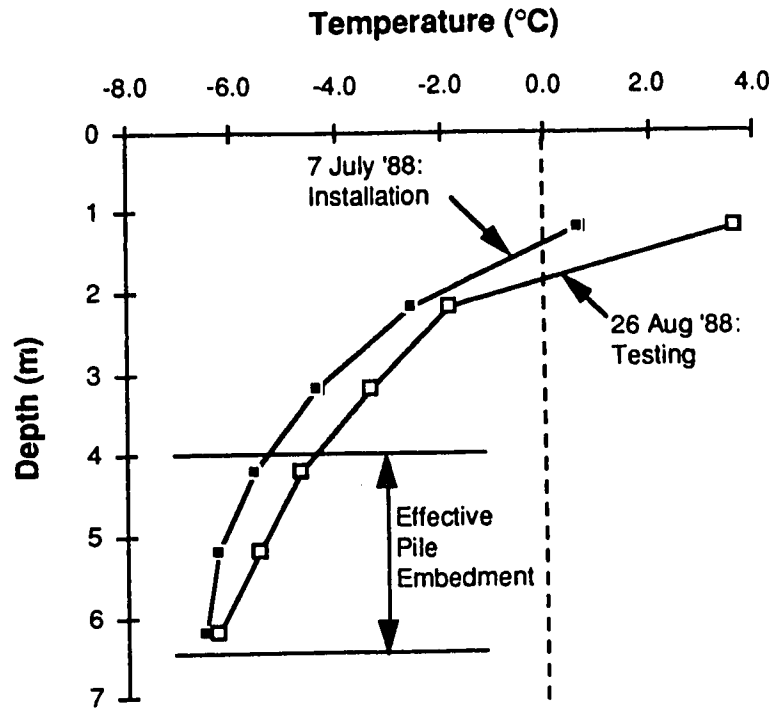


Figure 2.6: Site Temperature Profile During Installation and Testing

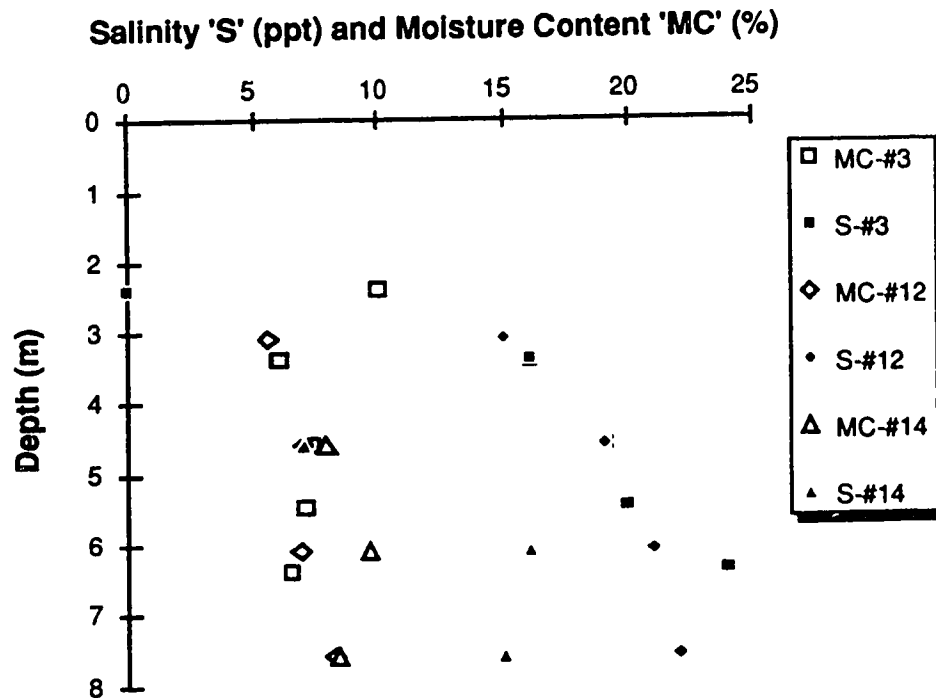
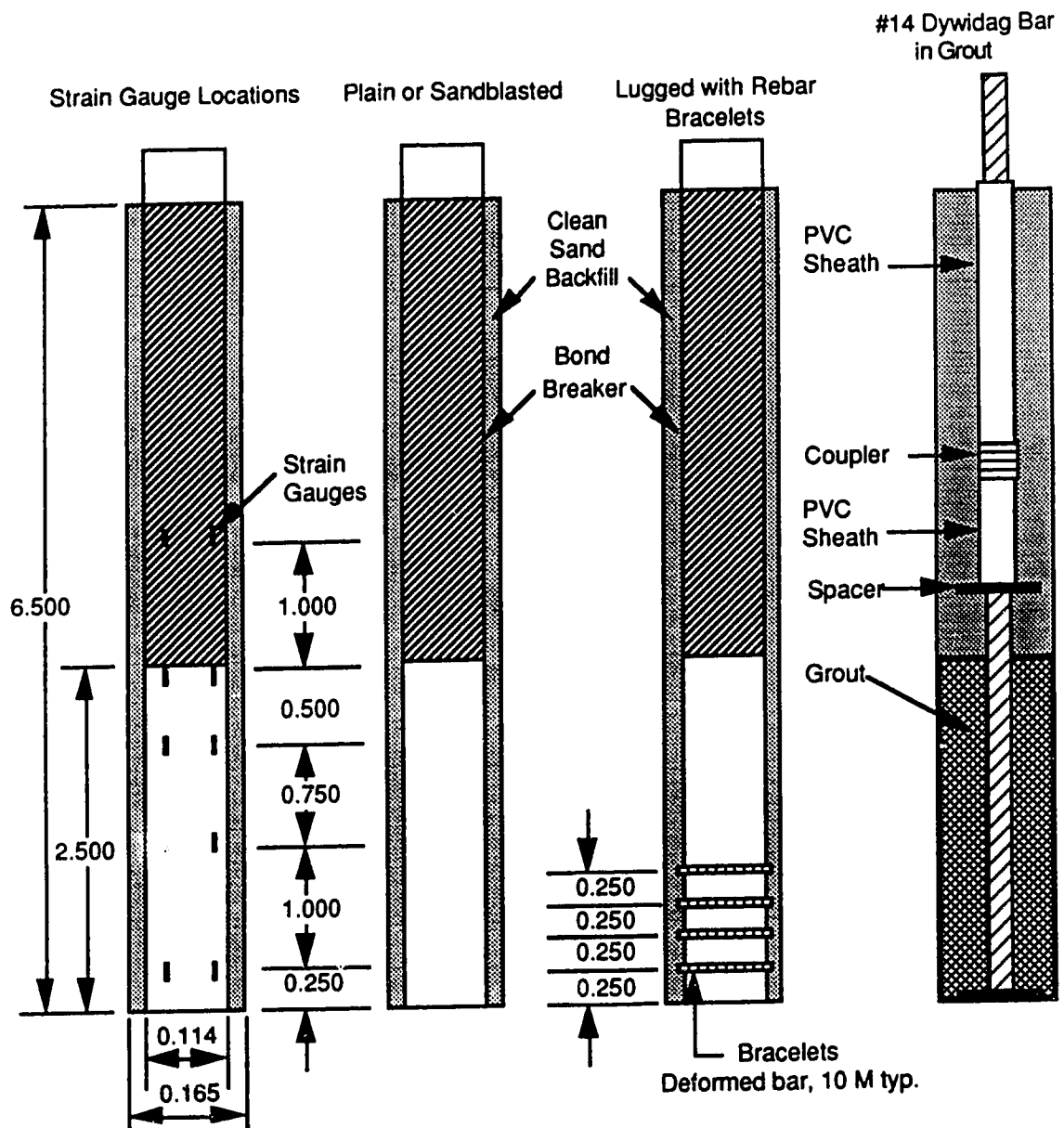


Figure 2.7: Salinity and Moisture Content Profiles for Three Different Piles



#### NUMBERS AND TYPES OF PILES

Smooth Hollow Structural Steel (HSS)----	3 (1 strain gauged)
Lugged Hollow Structural Steel (HSS)----	3 (1 strain gauged)
Dywidag bar in grout-----	4 2 in neat grout
	2 in sanded grout (1 strain gauged)
Sandblasted Pipe-----	2
Plain Pipe-----	2

Figure 2.8: Pile configurations used in Iqaluit field test program



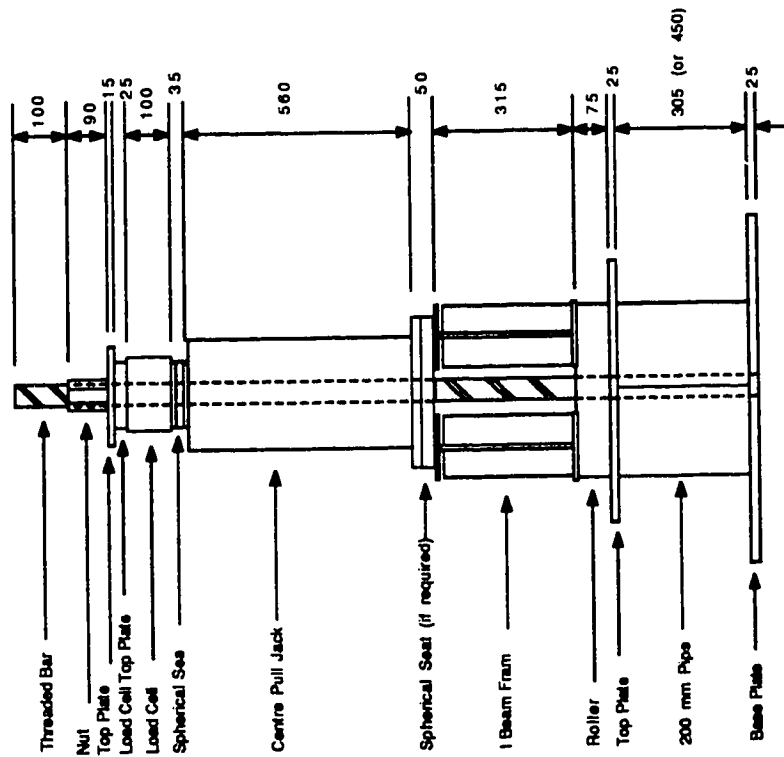
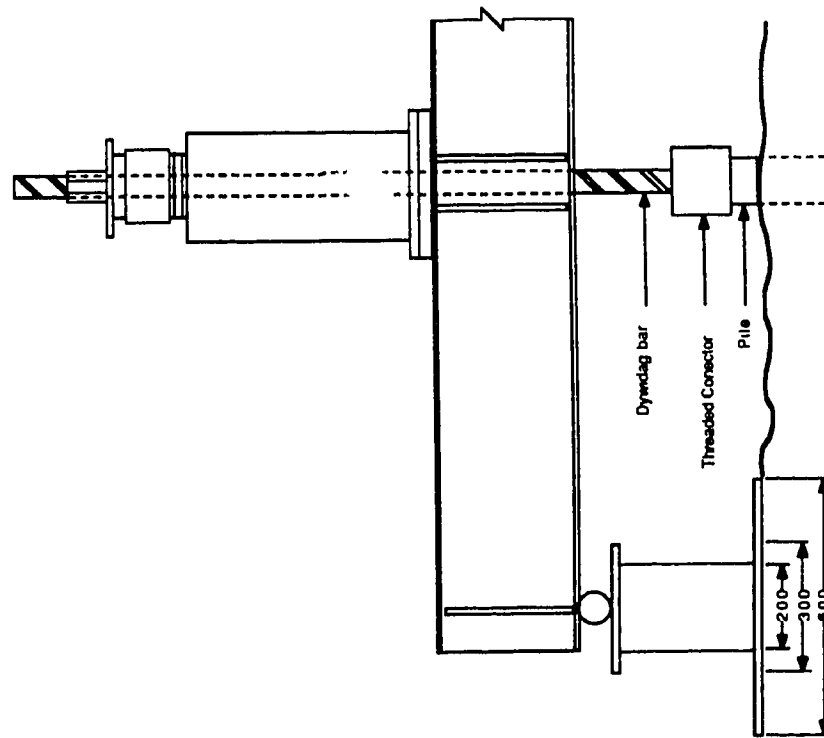


Figure 2.9: Pile Load Test Frame

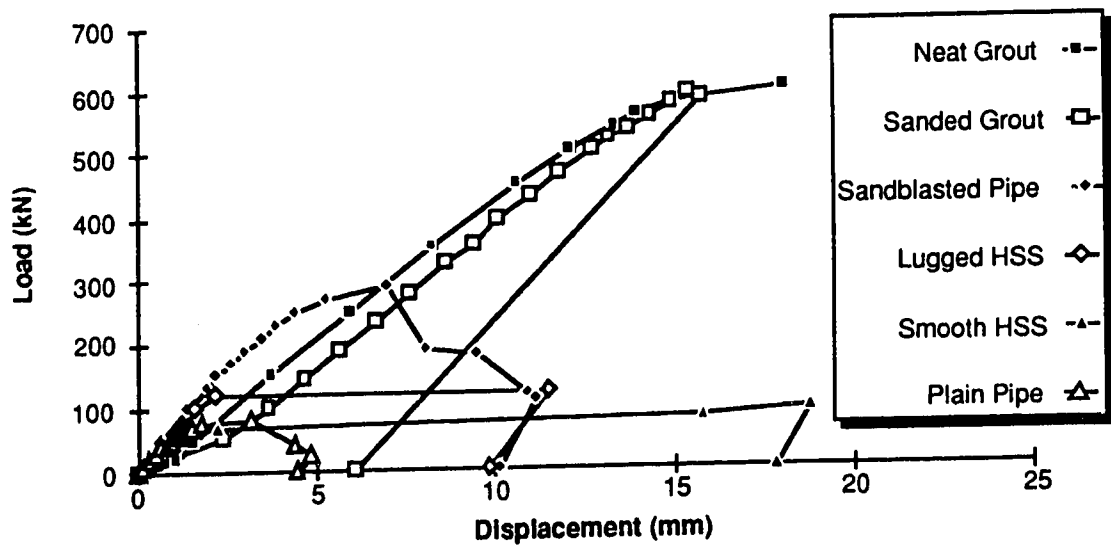


Figure 2.10: Summary of Load versus Displacement Performance for the Different Pile Configurations

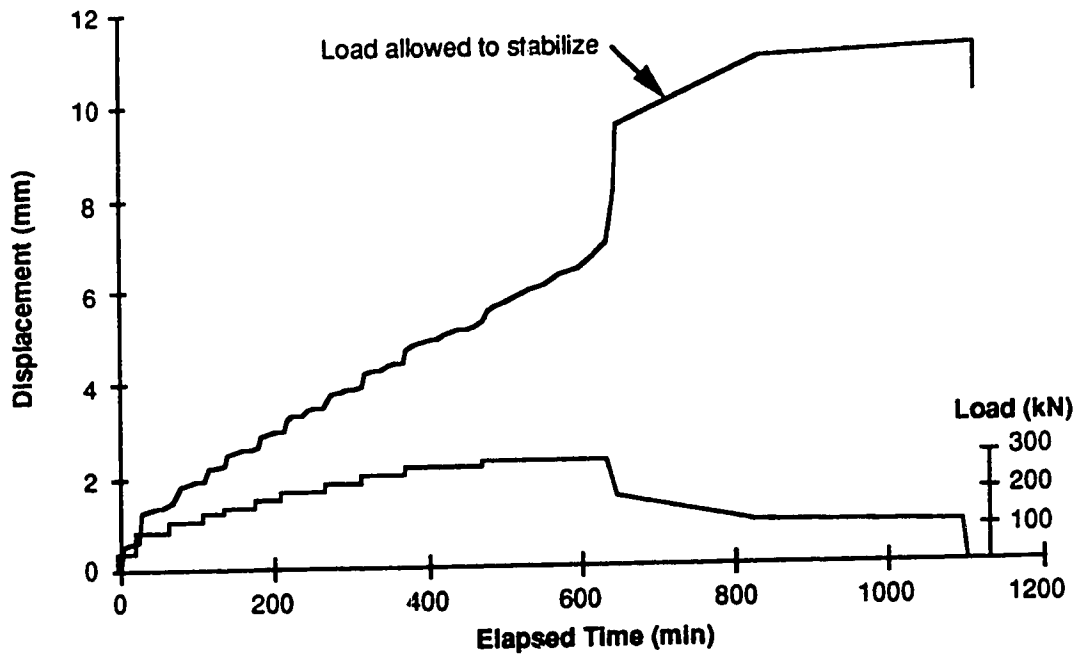


Figure 2.11: Typical Pile Displacement and Load versus Time (Pile #13)

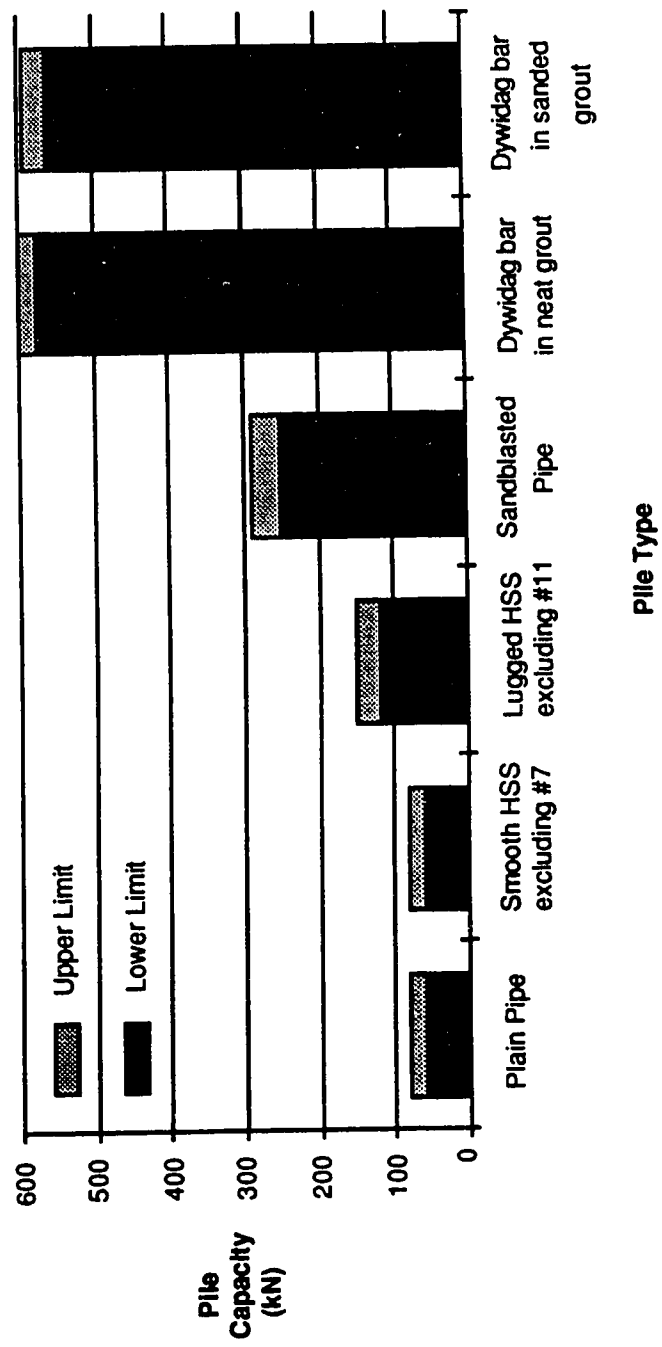


Figure 2.12: Capacities of Various Pile Configurations

### **3. FIELD PILE LOAD TESTS IN SALINE PERMAFROST PART II- ANALYSIS OF RESULTS**

#### **Introduction**

A field pile test program was conducted in Iqaluit, N.W.T. in 1988 by the University of Alberta (U of A) for the Department of National Defence (DND) to examine the performance of different pile configurations in saline permafrost and frozen rock, for foundation design guidance in the construction of the Short Range Radar (SRR) sites. The preliminary presentation of the load versus displacement results in both the saline permafrost and rock were presented in Biggar and Sego (1989). A more detailed discussion of the factors influencing the performance of the piles, and a review of the site conditions, installation and testing procedures, and the load versus displacement results are contained in Part I of this paper (Biggar and Sego in press a) [Chapter 2].

The intent of this paper is to provide additional test results data, and a detailed analysis thereof, pertaining to:

1. the performance of the grout which was used as a backfill material,
2. the development of load along the embedment of the piles as determined from strain gauges mounted along the pile length, and
3. the time dependent displacement behaviour of the piles, and

#### **Performance of a high alumina cement grout backfill**

##### *General*

A high alumina cement (Ciment Fondu) based grout was used as a backfill material for four anchors, two each with a neat grout (cement and water only) and a sanded grout (cement, sand, and water). The respective mix designs, by weight, were a water:cement ratio of 0.35:1.0, and a sand:water:cement ratio of 0.45:0.35:1.0. A powdered sulphonated naphthelene formaldehyde condensate superplasticizer was utilized, in a proportion of 0.75% by weight of cement, to make the grout less viscous in order to ease placement. However it also had the effect of retarding the set time. The grout temperature was typically 25° to 30° C when it was placed. Anchor installation was accomplished by

first pouring the grout into the hole to the desired depth, then lowering the Dywidag bar into the grout and aligning the bar with the assistance of the drill rig.

#### *Thermal performance*

Resistance temperatures devices (RTD's) were placed in the grout as close to the borehole wall as possible to measure the temperature of the grout as it cured, as shown in Figure 3.1. A typical plot of temperature versus time is shown in Figure 3.2 [Plots for all tests are contained in Appendix B]. Generally the temperature of the grout decreased for approximately 4 hours then, as the grout hydrated, heat was generated and the temperature of the grout increased. Hydration was complete after approximately 8 hours and the temperature of the grout decreased until it stabilized at the temperature of the surrounding native soil, approximately 60 hours after placement. Curing of the grout was essentially complete after the temperature peaked, approximately 8 hours after mixing. Pertinent details of each test are contained in Table 3.1.

The minimum temperatures listed in Table 3.1 show that except in test #4 the grout adjacent to the native soil was subjected to sub-zero temperatures during the initial 10 hours, which would result in freezing of the mix water before curing of the grout was complete. As discussed in Biggar and Sego (1990) this results in a weaker grout, though its strength likely exceeded that of the surrounding permafrost.

The measured temperatures in pile #4 show that considerably greater amounts of heat were generated by the additional cement in the mix when a neat grout was used. Thus the use of neat grout in a 165 mm diameter hole in ice-rich or warm permafrost ( $T > -2^{\circ}\text{C}$ ) may result in excessive thermal disturbance to the surrounding native soil. In the ice-poor till in which this test was conducted, however, no undesirable effects were observed.

#### *Grout strength*

Laboratory tests conducted with Dywidag bars embedded in properly cured Cement Fondu grout (Kast and Skermer 1986, and Biggar and Sego in press b, [Chapter 5]) indicate that the bond strength between the grout and the bar ranges between 4 and 7 MPa.

Load tests were conducted approximately 6 weeks after pile installation so the grout strength was fully developed. An average bond strength of 2.8 MPa was obtained in a pullout test of a Dywidag bar grouted into rock at a nearby site in this test program (Biggar and Sego 1989), however the localized stress where the bar entered the grout may have been considerably greater. RTD readings from the tests in rock indicated that some of the grout adjacent to the rock may have been subject to freezing, but the grout adjacent to the bar is believed not to have frozen. Inspection of the anchors in rock was not possible so this could not be confirmed.

The compressive strength of Ciment Fondu grout in which the mix water has been subject to freezing during curing, when tested at temperatures above 0° C, is lower than for grout which has not experienced any freezing (Biggar and Sego 1990). No strength data is available, however, for grout which is maintained at sub-zero temperatures. The pile load tests conducted in this program indicate that the shear strength of the grout (in which the water was subject to freezing) exceeded the shear strength of the native soil (500 to 600 kPa), but since the actual failure surface along the embedded portion of the pile could not be examined this cannot be proven categorically.

### **Development of load at depth along the pile embedment**

#### *General*

The development of load along the length of the pile was calculated from elastic analysis using the strain gauge data and the relationship:

$$P_i = \sigma_i A_x = (\epsilon_i - \epsilon_{io}) E A_x \quad (3.1)$$

where  $P_i$  denotes the load at the  $i^{\text{th}}$  strain gauge elevation,  $\sigma$  the axial stress,  $A_x$  denotes the cross sectional area of steel in the pile,  $\epsilon$  the axial strain (measured) with the subscript 'o' denoting the strain gauge reading immediately prior to loading, and  $E$  is Young's Modulus for the pile material. The calculated shear stress over a portion of the pile was simply the change in the calculated load divided by the pile surface area between strain gauges at different elevations, expressed as:

$$\tau = \frac{\partial P}{\partial A_s} = \frac{(P_i - P_{i+1})}{\pi d (D_{i+1} - D_i)} \quad (3.2)$$

where  $A_s$  denotes the surface area of the pile,  $D$  the depth as a positive value, and  $d$  the pile diameter. Hence a linear load distribution indicates a uniform stress distribution, and a non-linear load distribution indicates a non-uniform stress distribution.

Redistribution of stress with time along the pile embedment in frozen soil is discussed in detail by Johnston and Ladanyi (1972), Nixon and McRoberts (1976), Weaver (1979), and Theriault and Ladanyi (1988). Generally uniform stress conditions will be experienced with short rigid piles during short time intervals. For longer rigid piles at relatively high loads or for more compressible piles (ie. timber) the stress distribution will be non-uniform initially, tending to become uniform as time progresses, examples of which are illustrated in Dipasquale et al. (1983) and Zhigul'skiy (1966). Long piles at relatively low loads may never redistribute the stresses to the lower regions of the pile. The above is illustrated in Figure 3.3, from Linnel and Lobacz (1980).

The development and redistribution of load at depth for each of the pile configurations tested during the 1988 Iqaluit field program is discussed below. The term effective embedment refers to the portion of the pile below a depth of 4.0 m, which did not have any bond breaker material applied to the pile surface. The term applied load refers to the load applied at the top of the pile by the jack as measured by the load cell.

The calculation of shear stresses from the strain gauge data was complicated by two phenomena. The strain gauge cables were fastened to the pile surface, hence the surface area of the pile carrying the load was reduced by an amount equivalent to the area covered by the cables. Values of calculated shear stresses which have included a correction for this reduced surface area are listed in Table 3.2. Further, the HSS piles were installed with the bottom end open and the pile center was backfilled with dry sand. It is reasonable to assume that water from the slurry in the annulus between the pile and the native soil seeped into the centre of the pile although the actual height of rise of this water is unknown. Thus

there would be a nominal force resisting the uplift force on the pile base equal to the lesser value of:

1. the area of the frozen soil in contact with the pile surface inside the pipe multiplied by the adfreeze bond strength; or
2. the cross-sectional area of the inside of the pile multiplied by the short-term tensile strength of the backfill material.

Analysis indicates that the maximum value of this force will be approximately 6 kN, beyond which the tensile strength of the backfill will be exceeded and the bond would rupture.

#### *Smooth HSS pile with sand slurry backfill (#11)*

Smooth HSS pipe with a sand backfill is similar to the pile configuration used for most adfreeze piles installed in permafrost. The load distribution along the pile embedment is shown in Figure 3.4. Little load was carried over the upper 3 m of the pile; a result of an active layer depth of approximately 1.5 m, warm soil temperatures from 1.5 to 3 m, and the bond breaker material applied to the pile surface. At small applied loads, a considerable portion of the load was resisted between 3 and 4 m even though the bond breaker had been installed along this portion. As the applied load increased, the resistance over this region decreased relative to the load carried over the effective embedment of the pile. The load versus depth relationship from 4 to 5.25 m was nearly linear indicating a uniform stress distribution along this region of the pile. The decrease in the slope of the load versus depth relationship between 5.25 and 6.5 m, at the bottom of the pile, suggests an increase in stress along this portion. Such behaviour is unlikely, and may be attributed to the effect of frozen material in the center of the pile as previously discussed. At applied loads of 70 and 80 kN there were anomalous strain gauge readings suggesting either strain gauge malfunction or localized failure of the adfreeze bond along the pile.

A linear least squares regression was performed on the load versus depth data for the portion of the pile between 4 and 5.25 m to estimate the in-situ uniform adfreeze shear



stresses on the pile. Shear stresses calculated by dividing the load applied at the top of the pile over the effective embedment of the pile are approximately 25% greater than shear stresses calculated from the strain gauge data (Table 3.2). Assuming that similar behaviour occurred for all smooth HSS and plain pipe piles, the *mobilized* adfreeze bond stresses at failure were approximately 50 to 70 kPa for smooth HSS and plain pipe piles.

The redistribution of load with time along the pile embedment is shown in Figure 3.5. Although the response measured by the strain gauges is not ideal, certain trends may be observed. At a depth of 3 m where the bond breaker was applied there is little variation in the measured load with time. The measured load at the top of the effective embedment at a depth of 4.0 m, however, decreases as time progresses under the higher applied load increments. Conversely at a depth of 5.25 m a slight increase in the measured load is evident under the 80 kN load increment. Despite the small changes in measured load with time, the load distribution at the end of each load increment is nearly linear between the depths of 4 to 5.25 m as shown in Figure 3.4. At the failure load of 80 kN, the load measured at the 4.0 and 4.5 m depths converge to the same value indicating a failure of the adfreeze bond along this region of the pile.

The results from the strain gauges mounted at the 6.25 m depth are curious. It is uncertain whether the decrease in measured load is due to failure of the anchoring effect of frozen soil inside the pile as discussed above, a malfunction of the strain gauges, or a combination of the two.

#### *Lugged HSS pile with sand slurry backfill (#12)*

The load distribution along the embedment section of the pile, shown in Figure 3.6, is nearly linear for applied loads of 50 and 100 kN indicating a nearly uniform stress distribution, with provisions as noted previously for measured loads at 3 and 6.25 m. At the failure load of 150 kN the adfreeze bond stresses along the effective embedment of the pile above the lugs were approximately 50 kPa, shown in Table 3.2. After a short period of

time the bond failed and the entire load was carried by the lugged portion of the pile, shown in Figure 3.6.

The load measured just below the lugs, at 6.25 m, was 30 kN at an applied load of 100 kN. Assuming a downward acting force on the bottom of the pile of 6 kN caused by the frozen soil inside the pile as detailed previously, it follows that the bond stresses along the lower 0.25 m of the pile were 468 kPa. Such a large adfreeze bond strength is unlikely based upon the test results, hence either all three strain gauges at that depth had malfunctioned or the mechanism of load transfer at the bottom of the pile is much more complex than assumed in this analysis.

The load carried by the lugs on the pile can be considered as an equivalent stress carried over the 1 m portion onto which they were installed, or as a load per lug. According to the strain gauge data the load carried by the lugged portion of the pile was approximately 60 kN under an applied load of 100 kN, and approximately 120 kN under the failure load of 150 kN. In terms of an equivalent stress, the pile was stable at an equivalent stress of 60 kPa and failed at an equivalent stress of 120 kPa. Alternatively, in terms of a load per lug, the pile was stable at 15 kN per lug and failed at 30 kN per lug. Since the displacement rate of the pile only slightly exceeded the allowable rate at an applied load of 150 kN, it is reasonable to assume that the equivalent strength of the lugged portion pile was approximately 100 kPa, or 25 kN per lug.

A reduction in load with time at a depth of 4.0 m, and a gain in load with time at 5.25 m is shown in Figure 3.7. The magnitude of the change in load was greater for the lugged pile than for the smooth HSS pile, due in part to the higher applied loads. The loads measured between 4.0 and 5.25 m converge to the same value at 360 minutes indicating that the adfreeze bond had completely failed at this time. The anomalously low value of load at 4.0 m depth beyond this time is assumed to be equipment error. As mentioned above, the results from the strain gauges at a depth of 6.25 m are unusual and no explanation has been determined for this behaviour.

### *Dywidag bar anchor with grout backfill (#3)*

The load distribution along the embedded section of the Dywidag bar embedded in grout is shown in Figure 3.8 . Two major differences in behaviour, compared to the pipe piles, are evident: the load versus depth relationship was non-linear at all loads, and the applied loads were much greater. Strain gauge output was only recorded at the end of each load increment, so no data is available regarding the redistribution of load with time along the bar.

The parabolic shape of the load versus depth relationship indicates a non-uniform shear stress distribution. Such a load distribution is common for Dywidag bars grouted into soil (Gaffran 1989; and Kast 1991) and is similar to that observed for deformed bars in concrete (Comite Euro-International du Beton 1982). The difference in the load versus depth distribution between the smooth piles and the Dywidag bar is a result of the radial stresses induced in the grout by the deformations on the surface of the bar as the anchor was loaded.

At an applied load of 575 kN (the load increment prior to failure), based upon the strain gauge data, the calculated average shear stress over the portion of the bar between the depths of 4.0 and 5.0 m was 559 kPa at the grout/native soil interface and 1921 kPa at the bar/grout interface. This compares to average stresses over the entire 2.5 m effective embedment of 417 kPa and 1430 kPa respectively. Examination of the strength of the different components of the anchor system shows:

1. unconfined compression tests conducted on core samples from the Iqaluit site tested at a strain rate of 0.8 %/hr and a temperature of -5° C gave shear strengths of 500 to 600 kPa,
2. the strength of the bond between the grout and the bar exceeded 2800 kPa at failure for tests of Dywidag bars grouted into rock at a nearby site (Biggar and Sego 1989), and
3. the yield strength of #14 Dywidag bars is 600 kN.

The results in Table 2.1 of Part I (Biggar and Sego in press a) [Chapter 2] show that all anchors were at or near their yield capacity, and the results from the strain gauged bar shows that the native soil was at or near failure in shear. The results from tests #3, #4 and #6 in which the anchors were unable to sustain the final load increment indicate that possibly the bars had also reached their yield point. Failure of the bars at loads less than 600 kN may have resulted if the anchors which were not vertically aligned when they were installed (ie. bending was also induced). It is possible, however, that for the grouted bars with failure loads less than 600 kN, the failure mechanism involved was one of shear failure of the native soil at the grout/native soil interface along the upper portion of the anchor, and the progression of this failure along the length of the pile. In this case the shear strength of the native soil was not fully developed along the entire length of the pile due to the non-uniform stress distribution. Because the failure surface was not examined it is not possible to ascertain which of the above failure mechanisms was invoked.

Due to the magnitude of the calculated load at the deepest strain gauges it again appears that there is an increase in shear stresses over the bottom 0.5 m of the pile. Such behaviour is unlikely hence the actual mechanism for the development of shear stress distribution at the base of the anchor is likely more complex than simply the shearing of concentric cylinders. Detailed analysis of such a mechanism is beyond the scope of this paper.

In summary, the adfreeze bond strength along the effective embedment of untreated piles was observed, from the strain gauge results, to be approximately 50 to 70 kPa, or 25% less than that calculated using the load applied at the top of the pile. The lugged piles carried the load along the lugged portion of the piles after the adfreeze bond along the upper portion of the piles was exceeded (at approximately 50 kPa). The equivalent strength along the lugged portion of the pile was approximately 100 kPa, or 25 kN/lug. The stress distribution along the effective embedment of the grouted anchors was non-uniform, and the failure mechanism was either one of yield of the bar or shear failure of the native soil.

commencing at the top of the effective embedment and progressing downwards. The calculated stresses at the bottom of the piles and anchor suggest that the localized load transfer mechanism was more complex than the shearing of concentric cylinders, however more research is necessary to better define the actual process involved. Finally at loads less than the failure load there was little redistribution of load along the depth of the pile with time, thus for practical purposes the stress distribution for smooth HSS piles was uniform at the end of each load increment. At the failure load, redistribution of load was observed, leading to the progressive failure of the adfreeze bond.

### **Time dependent pile displacement**

The time dependent displacement of the different pile configurations has been analysed based on the following assumptions:

1. uniform stress distribution along the pile, and
2. the response of the pile at a given load increment is independent of previous load increments.

The first assumption has been shown to be valid for Smooth HSS piles and for lugged piles at loads less than 100 kN. Because the sandblasted piles had a planar surface similar to the Smooth HSS piles it is reasonable to assume that this assumption also applies to them. The first assumption has been shown to be invalid for grouted piles, and lugged piles at loads in excess of 150 kN.

The second assumption relates to the concept of hereditary creep in frozen soils, proposed in Ladanyi (1972), which is valid for non-strain strengthening materials. The unconfined compression tests on the Iqaluit core samples showed the frozen soil was non-strain strengthening hence the assumption of hereditary creep is reasonable.

An equation proposed for the primary creep of piles in ice-poor soils by Weaver and Morgenstern (1981), based on earlier work by Vyalov (1959), Sayles (1968), Sayles and Haines (1974), and Johnston and Ladanyi (1972) [see Appendix F], is expressed as:

$$\frac{u_a}{a} = \frac{3^{(c+1)/2} D \tau^c t^b}{c-1} \quad (3.3)$$

where  $u_a$  = pile displacement

$a$  = pile radius

$D$  = experimentally determined temperature dependent coefficient

$\tau$  = applied shear stress

$t$  = elapsed time

$c$  = experimentally determined stress exponent

$b$  = experimentally determined time exponent

For the conditions of constant temperature, stress and pile diameter, (3.3) reduces to:

$$u_a = K t^b \quad (3.4)$$

where

$$K = \frac{3^{(c+1)/2} a D \tau^c}{(c-1)} \quad (3.5)$$

The parameters  $K$  and  $b$  may be determined for each load increment by plotting the pile displacement versus time using logarithmic coordinates. Using the average value of  $b$  for a particular pile type and a least squares fit to the recorded data, the respective value of  $K$  for each load increment may be calculated. The recalculated values of  $K$  may then be plotted against the shear stress on logarithmic coordinates and the stress exponent,  $c$ , can be obtained. Substituting the value of  $c$  into (3.5) the respective value of  $D$  may be calculated. A typical example of this technique is shown in Figures 3.9 and 3.10.

The above procedure was applied to the results from the smooth HSS, lugged HSS, plain pipe, and sandblasted piles [shown in Appendix B]. Due to a scarcity of data for the smooth HSS and plain pipe piles, the results from the failure load increments were used, including only the values which represented an attenuating displacement rate. The calculated values of  $K$  and  $b$  for the tests are contained in Table 3.3. The initial values of  $b$  obtained from each load increment for the different pile configurations suggest that  $b$  is

independent of the applied stress level but does depend on the pile surface conditions. The calculated pile displacement versus time based on the average  $b$  and recalculated  $K$  values is compared to the measured data in Figure 3.11a, 3.11b, and 3.11c for the Smooth HSS, Plain Pipe and Sandblasted Pipe piles respectively.

The values of  $c$  and  $D$  for the smooth HSS and plain pipe piles are not useful because of the lack of data at loads less than the failure load. In addition, for the Smooth HSS pile, there is a poor fit of the data to a linear least squares regression ( $R^2 = 0.535$ ), and the calculated value of  $c$ , based on the three available data points, is less than unity, which is precluded by the formulation in equation (3.3).

The non-uniform shear stress distribution over the effective embedment of the grouted anchors negates the use of the above procedure to analyse the displacement versus time behaviour. Redistribution of stress along the length of the pile with time results in greater displacement rates than those applicable for uniform stress conditions, which may be observed in the results presented in Black and Thomas (1979). This is further illustrated by applying the relationship expressed in equation (3.3) to the data from the grouted anchors; the values of  $K$  and  $b$  are listed in Table 3.3. As the applied load was increased the stress distribution became more uniform, shown in Figure 3.8, and the value of  $b$  decreased. Lower values of  $b$  (for more uniform stress conditions) will result in lower displacement rates and smaller displacements, as expected. The values of  $b$  at the highest load increments (hence the most uniform shear stress conditions) are approximately  $1/3$  as large as the values for the sandblasted piles. This suggests that after uniform stress conditions are attained for grouted anchors, the time dependent displacements will be smaller, and the displacement rates will be less than for sandblasted piles.

### **Comparison with results from others**

A summary of published comparative pile load test data has been compiled in Table 3.4, listing both field and laboratory test data for each different pile configuration. It is

apparent that there are considerable data available for piles with untreated surfaces but very little for the other configurations.

It must be noted that pile capacities in permafrost are also affected by relative strains between the pile and the frozen soil (Sanger 1969). Field pile load tests, however, generally only record pile head displacements, and detailed analysis is necessary to attempt to determine relative strains between the soil and the pile at depth. The following discussion deals only with adfreeze bond resistance or native soil shear strengths and does not attempt to concurrently analyse pile displacements.

*Smooth HSS, and plain and sandblasted pipe*

To enable the adfreeze bond strength values from tension tests to be comparable with compression test results it is reasonable to suggest that the values from the tension tests should be increased by 50% to 100%, as discussed in Part I (Biggar and Sego in press a) [Chapter 2]. Adjusting the values for the untreated piles in this study in such a manner gives adfreeze bond values of approximately 100 to 150 kPa. Considering that the tests represent short term capacity, they are in reasonable agreement with the other field tests conducted in saline permafrost which were loaded for longer time intervals (Hoggan 1985; Nixon 1988; and Miller and Johnson 1990). The adfreeze bond strength results in saline permafrost are considerably lower than those reported in non-saline permafrost (Crory 1963; and Manikan, 1983).

No information was available dealing specifically with field load testing of sandblasted piles. Laboratory constant displacement rate tests on sandblasted piles have resulted in adfreeze bond strengths of 700 to 900 kPa in non-saline frozen sand (Parmeswaran, 1978, Sego and Smith, 1989, and Biggar and Sego, in press b [Chapter 5]), 670 kPa in a saline native soil with a clean sand backfill, and 390 kPa with a saline (10 ppt) silty sand backfill (Biggar and Sego in press b [Chapter 5]). Constant load tests on sandblasted model piles in contact with saline soil resulted in adfreeze bond strengths of from 7 to 70 kPa at salinities of 15 and 5 ppt respectively (Hutchinson 1989).



The weak adfreeze bond strengths for sandblasted piles reported in Hutchinson (1989) suggest that there was no solute in contact with the piles in the present study. The results from Parmeswaran (1978), Sego and Smith (1989) and Biggar and Sego (in press b) [Chapter 5], however, suggest that the adfreeze strengths for the sandblasted piles were less than may be expected in a non-saline soil. This discrepancy may possibly be explained by the dependence of bond strength on relative strains between the pile and the soil, and that there were increased strains in the soil surrounding the pile during the field tests due to the salinity of the native soil.

#### *Lugged HSS piles*

Field test data for piles with protuberances on their surface is limited to those performed by the Alyeska Pipeline Co. presented in Black and Thomas (1979), Luscher et al. (1983), and Ulrich et al. (1986), however the protuberances were over a much longer length of the pile, the load increment durations were 72 hrs, and they were compression tests performed in warmer, non-saline permafrost ( $-0.3^{\circ}\text{C}$ ). General comments on the performance of piles with protuberances are contained in Long (1973 and 1978). Thus direct comparison of the results from this study to other field test results is not possible. The general observations by these authors of shear failure occurring in the backfill material (or in the a weaker native soil) thereby providing pile load carrying capacity exceeding that governed by the adfreeze bond strength of the pile were also observed in the present study.

Laboratory tests on model piles with lugs, in frozen sand, conducted at displacement rates of 0.25 mm/hr, are reported in Andersland and Alwahhaab (1983). Enhanced load carrying capacities were observed with the introduction of lugs, and increased lug heights resulted in increased capacities, for lug heights between 1.59 and 4.76 mm. Interpolation from their results suggest that one 4.8 mm high lug in a non-saline sand at a temperature of  $-5.0^{\circ}\text{C}$  would have a capacity of approximately 13 kN. The values determined in this test program of approximately 25 kN/lug for a 12 mm high lug are in general agreement with their observations. A fourfold increase in the capacity of aluminum model piles, when the

piles were corrugated along their length, are reported in Ladanyi and Guichaoua (1985). Maximum shear stresses of approximately 250 kPa were observed for piles under constant load in a non-saline sand. For comparison purposes it is difficult to compensate for differences in scale, soil and pile physical properties, and load application, however the results from this study do show similar trends.

#### *Grouted anchors*

Detailed performance records of anchors grouted into permafrost are limited to those reported in Johnston and Ladanyi (1972), however soil temperatures in their tests were approximately  $-0.5^{\circ}\text{C}$ . General comments about anchors grouted into frozen rock are contained in Kast and Skermer (1986), however no anchors were loaded to failure as the capacity of the anchors exceeded the yield strength of the steel bars. A fourfold increase in ultimate adfreeze strength of cast-in-place concrete piles over slurry backfilled concrete piles in warm permafrost ( $-0.5^{\circ}\text{C}$ ) are reported by the Research group on pile foundations, People's Republic of China (1978), however details are lacking. No laboratory test results of grouted piles in frozen soil were found in the literature.

Although no quantitative comparisons are available, excavation of some anchors was undertaken in the study by Johnston and Ladanyi (1972). The surface of the grout was observed to be corrugated, following the contours left by the auger during drilling. The deformations in the surrounding soil consisted of a highly sheared thin zone immediately adjacent to the anchor associated with slip at the interface during failure, and an outer zone of uniform shear strain which decreased rapidly with distance from the anchor. Similar performance of the anchors in this study is expected.

#### **Conclusions**

The cement grout which was used as a backfill material for 48 mm diameter Dywidag bars in a 165 mm diameter hole provided sufficient strength to yield the steel bar (600 kN) and possibly caused shear failure within the native soil. The neat grout, however, resulted in considerably higher temperatures during curing. Consequently it is recommended that

for similar installation conditions a sanded grout be utilized as it generates less heat during curing (hence less thermal disturbance to the surrounding permafrost), and less cement is required resulting in a less expensive mix.

The results from the strain gauge data showed a nearly uniform distribution of stress at the end of each load increment for the smooth HSS pile. The results also showed that the mobilized adfreeze shear stress was approximately 75% of the stress calculated by simply dividing the load applied at the top of the pile by the effective embedment area of the pile. The stress distribution was non-uniform for the lugged HSS pile at loads in excess of 100 kN, and for all load increments on the grouted anchor. This emphasizes that it is unconservative to expect to fully mobilize the shear strength of the soil along the entire pile length because a progressive failure will occur where failure of the soil at the upper regions of the pile occurs before the maximum stress is developed along the lower regions of the pile.

The initial time dependent deformation of the piles which had no protuberances on their surface can be described by a power law in the form:

$$u_a = K t^b$$

It is not possible to determine if the relationship will provide adequate results for long-term deformations since no long term load tests were conducted.

### **Recommendations for Future Research**

There is still concern regarding the strength of grout in which the water has been subject to freezing during curing, and which remains frozen in the permafrost. One solution to the problem is to develop a grout, using suitable cement and admixtures, which will prevent the mix water from freezing. This is an expensive solution which requires careful control during mixing and installation, but one which has been recently addressed on several fronts (Biggar and Sego 1990; Ballivy et al. 1990; and Korhonen 1990). For piles and anchors grouted into permafrost *soils* it is possible that the strength of grout which has been subject to freezing exceeds that of the surrounding native soil such that the failure will

still occur in the soil. The strength of grouts whose water has been subject to freezing, and which remain frozen, should be investigated to resolve a controversial construction problem and possibly result in less expensive grout mix designs.

The results from the strain gauge data indicate that the stress distribution at the base of the pile is more complex than generally assumed in design and analysis, and that enhanced load carrying capacity is evident. If this is the case, marginal gains in pile capacity may be possible if the mechanism is better defined.

Long term load tests of piles in saline ice-poor permafrost will determine if a power law similar to the one proposed in this paper (for an attenuating pile displacement rate) is appropriate to estimate long-term deformations or whether a constant displacement rate formulation (Nixon 1988) is more suitable.

The issue of when it is economical to use grout backfilled piles in saline permafrost should be addressed. This includes the problems of solute migration into the slurry backfill, the long-term load carrying capacity of slurry backfilled piles in saline permafrost compared to grout backfilled piles, and the economics of purchasing, transporting and placing the grout.

## **References**

- Andersland, O.B., and Alwahhaab, M.R. 1983. Lug behavior for model steel piles in frozen sand. Proceedings, 4th International Conference on Permafrost, Fairbanks Alaska, USA. pp. 16-21.
- Biggar, K.W. and Sego, D.C. 1989. Field load testing of various pile configurations in saline permafrost and seasonally frozen rock. 42nd Canadian Geotechnical Conference, October 25-27, Winnipeg, pp. 304-312.
- Biggar, K.W., and Sego, D.C. 1990. The curing and strength characteristics of cold setting Cement Fondu grout. Proceedings, 5th Canadian Permafrost Conference. Quebec City, Quebec, pp. 349-355.
- Biggar, K.W. and Sego, D.C. in press a. [Chapter 2] Field pile load tests in saline permafrost, Part I, Procedures and results.
- Biggar, K.W. and Sego, D.C. in press b. [Chapter 5] Strength and deformation behaviour of model adfreeze and grouted piles in saline permafrost.

- Biggar, K.W. and Sego, D.C. in press c. [Chapter 6] Time dependent displacement behaviour of model adfreeze and grouted piles in saline permafrost.
- Black, W.T., and Thomas, H.P. 1979. Prototype pile tests in permafrost soils. in *Pipelines in Adverse Environments: A State of the Art*, Proceedings of the ASCE Pipeline Division Specialty Conference, New Orleans, Louisiana, 1. pp. 372-383.
- Comite Euro-International du Beton. 1982. Bond action and bond behaviour of reinforcement: State-of-the-art. Information Bulletin No 151, Contribution to the 22 Session Pienièrre du C.E.B., Munich, West Germany, pp. 20-49.
- Crory, F.E. 1963. Pile foundations in permafrost. Proceedings, 1st International Conference on Permafrost, Lafayette, Indiana, USA. pp. 467-476.
- DiPasquale, L., Gerlek, E., and Phukan, A. 1983. Design and construction of pile foundations in Yukon Kuskokwin Delta, Alaska. Proceedings, 4th International Conference on Permafrost, Fairbanks Alaska, USA, pp. 238-243
- Gaffran, P. 1989. Monitoring of anchored sheet pile walls. Unpublished MSc Thesis, University of Alberta, p. 514.
- Hivon, E.G. 1991. Behaviour of saline frozen soils. Unpublished Ph. D. thesis, University of Alberta, Edmonton, Alberta. p. 435.
- Hoggan Engineering and Testing (1980) Ltd. 1985. Pile load tests, Arctic Bay multi-purpose Hall and School Extension, Report to Government of the North West Territories, Department of Public Works.
- Hutchinson, D.J. 1989. Model pile load tests in frozen saline silty sand. Unpublished M.Sc. Thesis, University of Alberta, Edmonton, Alberta, p. 222.
- Johnston, G.H., and Ladanyi, B. 1972. Field tests on grouted rod anchors in permafrost, *Canadian Geotechnical Journal*. 9: 176-194.
- Karpov, V., and Velli, Y. 1968. Displacement resistance of frozen saline soils. *Soil Mechanics and Foundation Engineering (English Translation)*, 4 (July/August): 277-388.
- Kast, G. and Skermer, N. 1986. DEW Line anchors in permafrost. *Geotechnical News*, 4 (4): 30-34.
- Kast, G. 1991. Personal Communication. Vice President Western Division, Dywidag Systems International Canada Ltd (DSI).
- Ladanyi, B. 1972. An engineering theory of creep in frozen soils. *Canadian Geotechnical Journal*, 9: (1): 63-80.
- Ladanyi, B., and Guichaoua, A. 1985. Bearing capacity and settlement of shaped piles in permafrost. Proceedings, XI International Conference on Soil Mechanics and Foundation Engineering, San Francisco, USA, pp. 1421-1427.
- Linnell, K.A., and Lobacz, E.F. 1980. Design and construction of foundations in areas of deep seasonal frost and permafrost. US Army Cold Regions Research and Engineering Lab, Hanover, New, Hampshire, Special Report 80-34, p. 320.

- Long, E.L. 1973. Designing friction piles for increased stability at lower installed cost in permafrost. Proceedings, 2nd International Conference on Permafrost, North American Contribution, Yakutsk, USSR, pp. 693-698.
- Long, E.L. 1978. Permafrost Foundation Designs. Proceedings: Cold Regions Specialty Conference, Anchorage, Alaska, American Society of Civil Engineering, 17-19 May. 11, pp. 973-987
- Luscher, U., Black, W.T., and McPhail, J.F. 1983. Results of load tests on temperature-controlled piles in permafrost, Proceedings, 4th International Conference on Permafrost, Fairbanks Alaska, USA, pp. 756-761.
- Manikian, V. 1983 Pile driving and load tests in permafrost for the Kuparuk pipeline system. Proceedings, 4th International Conference on Permafrost, Fairbanks Alaska, USA, pp. 804-810.
- Miller, D.L. and Johnson, L.A. 1990. Pile settlement in saline permafrost: a case history. Proceedings, 5th Canadian Permafrost Conference. Quebec City, Quebec. pp. 371-378.
- Nixon, J.F., and McRoberts, E.C. 1976. A design approach for pile foundations in permafrost. Canadian Geotechnical Journal, 13: 40-57.
- Nixon, J.F. 1988. Pile load tests in saline permafrost at Clyde River, Northwest Territories, Canadian Geotechnical Journal, 25: 24-31.
- Parneswaran, V.R. 1978. Adfreeze strength of frozen sand to model piles. Canadian Geotechnical Journal, 15: 494-500.
- Research Group on Pile Foundations in Permafrost, Research Institute of Ministry of Railways, The People's Republic of China. 1978. Testing of pile foundations in permafrost areas. Proceedings, 3rd International Conference on Permafrost, Edmonton, Alberta, Canada., 1. pp. 179-185.
- Sanger, F.J. 1969. Foundations of structures in cold regions. US Army Cold Regions Research and Engineering Laboratory, Hanover, New Hampshire, Monograph III-C4, p. 93.
- Sayles, F.H. 1968. Creep of frozen sands. US Army Cold Regions Research and Engineering Laboratory, Hanover, New Hampshire, Technical Report 190, p. 54.
- Sayles, F.H. and Haines, D. 1974. Creep of frozen silt and clay. US Army Cold Regions Research and Engineering Laboratory, Hanover, New Hampshire, Technical Report 252, p. 51.
- Sego, D.C. and Smith, L.B. 1989. The effect of backfill properties and surface treatment on the capacity of adfreeze pipe piles. Canadian Geotechnical Journal, 26: 718-725.
- Theriault, A. and Ladanyi, B. 1988. Behaviour of long piles in permafrost. Proceedings, 5th International Conference on Permafrost, Trondheim, Norway. pp. 1175-1180.

- Thomas, H.P., and Luscher, U. 1980. Improvement of bearing capacity of piles by corrugations. US Army Cold Regions Research and Engineering Laboratory, Hanover, New Hampshire, Special Report 80-40, pp. 229-234.
- Ulrich, U., Black, W.T., and McPhail, J.F. 1986. Results of load tests on temperature-controlled piles in permafrost. Proceedings, 4th International Conference on Cold Regions Engineering, TCCRE, ASCE, Anchorage, Alaska, USA, pp. 756-761.
- Vyalov, S.S. 1959. Rheological properties and bearing capacity of frozen soils. Translation 74, U.S. Army US Army Cold Regions Research and Engineering Laboratory, Hanover, New Hampshire, translated in 1965, p. 219.
- Weaver, J.S. 1979. Pile foundations in permafrost. Unpublished Ph. D. thesis, University of Alberta, Edmonton, Alberta, p. 224.
- Weaver, J.S., and Morgenstern, N.R. 1981. Pile design in permafrost. Canadian Geotechnical Journal, **18**: 357-370.
- Zhigul'skiy, A.A. 1966. Experimental investigation of the state of stress and strain in the soil around a pile. Proceedings, 8th Conference on Geocryology, Yakutsk, USSR, Part 5, pp. 211-223.

**TABLE 3.1**  
**Iqaluit grout curing temperature details**

Pile #	Grout Type	Minimum Temperature (°C)	Time to Min Temp (hrs)	Maximum Temperature (°C)	Time to Max Temp (hrs)	Comments
2	Neat	-1.2	5.0	6.9	11.3	1.0% SPN [1]
3	Sanded	-0.8	3.2	14.1	7.7	0.75% SPN
4	Neat	2.4	1.8	36.4	5.3	0.75% SPN
6	Sanded	-1.1	4	7.0	9.9	0.75% SPN

Note 1. Poor seal at bottom of casing allowed material to slough into the hole during grout placement

**TABLE 3.2**  
**Corrected shear stresses on strain gauged piles**

Assuming a uniform stress distribution between 4.0 and 5.25 m depth, and performing a linear least squares regression on the calculated load versus depth data.

	Applied Load (kN)	Slope ( $\Delta P/\Delta L$ )	Stress [1] (kPa)	Stress [2] (kPa)	Stress [3] (kPa)
Smooth HSS 1-11	50	9.449	26	29	56
	60	16.05	45	49	67
	70	19.85	55	60	78
Lagged HSS 1-12	50	7.453	21	23	56
	100	14.45	40	44	112
	150 [4]	16.69	47	51	168

Notes: [1] Calculated as: Slope + ( $\pi d$ ).  
 [2] Corrected for pile surface area covered by cables (weighted average of 8%).  
 [3] Average stress using applied load over embedment length.  
 [4] Used data from second time increment only as data at subsequent increments had anomalous values.



TABLE 3.3

Results of displacement versus time analysis

Test #	Pile Type	Load (kN) Failure Applied	Measured Values		R for b	Average b	Recalc K (mm min <sup>-b</sup> )	Estimated Shear Stress* (kPa)	c	Calculated Values	
			K (mm min <sup>-t</sup> )	b						D (mm min <sup>-b</sup> kPa <sup>-c</sup> )	R for c
7	Smooth HSS	100	0.845	0.167	0.976	0.140	0.923	84	0.581	0.0742	0.535
11	Smooth HSS	70	0.646	0.128	0.973	0.140	0.644	50			
		70	0.980	0.124	0.936	0.140	0.931	59			
			Average = 0.1399								
15	Plain Pipe	80	1.52	0.0449	0.940	0.0573	1.49	63			
		80	1.69	0.0634	0.906	0.0573	1.78	67	1.07	0.0189	0.981
16	Plain Pipe	60	0.741	0.0635	0.904	0.0573	0.823	34			
			Average = 0.05727								
13	Sandblasted Pipe	290	2.26	0.0374	0.994	0.0491	2.22	142			
		210	2.93	0.0393	0.991	0.0491	2.88	176			
		250	3.86	0.0327	0.973	0.0491	3.70	209			
		270	4.28	0.0379	0.981	0.0491	4.17	226	1.51	0.00116	0.952
14	Sandblasted Pipe	250	1.85	0.0751	0.991	0.0491	2.06	151			
		210	2.45	0.0640	0.928	0.0491	2.64	176			
		230	3.07	0.0574	0.946	0.0491	3.21	193			
			Average = 0.04912								
12	Lugged HSS	150	0.551	0.189	0.978						
4	Neat Grout	620	4.97	0.0472	0.993						
		350	6.83	0.0450	0.997						
		450	9.57	0.0252	0.991						
		540	12.2	0.0176	0.962						
		580	13.9	0.0162	0.950						
6	Sanded Grout	57	6.18	0.0505	0.962						
		350	8.56	0.0392	0.992						
		450	10.7	0.0356	0.997						
		500	12.6	0.0228	0.993						
		540	14.0	0.0174	0.959						

\* Estimated Shear stress calculated as:

$$\frac{0.75 \times \text{Applied Load}}{\text{Effective Embedment Area}}$$

TABLE 3.4  
Comparative test data

Author(s)	Native Soil [1] Material S (ppt)	Backfill [1] Material S (ppt)	Pile Surface [2] Surface [2]	Temp (°C)	Failure Stress (kPa)	Failure Time (mins)	Load or Displ Rate	Load Type [3]	Comments
<b>SMOOTH PILE SURFACE</b>									
Field Test Results									
Croxy (1983)	7	07	SM	-3.3	325		45 kN/day	C	
Croxy (1983)	?	07	SP	-2.2	-385		45 kN/day	C	
Maniklan (1983)	SM [5]	0	Un	-6.0	815	197	-3 kPa/min	T	
Hoggan (1985)	DS & S [4]	10-30	Un	-5	90		33 kN/day	C	
Miller et al. (1984)	SM	20-80	Un	-4	30-50		Const Load	C	Note 9
Hixon (1988)	SM	15-30	Un	-6	80		Const Load	C	
This study	SW [6]	15-25	SP	-4.8	50-70 [7]	20-60 [8]	>25 mm/hr	T	
This study	SW [6]	15-25	SP	-5.2	323	20-50 [6]	>25 mm/hr	T	
Laboratory Test Results									
Ladanyi and Guichas (1985)	SP	0	Un Al	-5.0	429	?	0.62 mm/min	C	
Ladanyi and Guichas (1985)	SP	0	Un Al	-5.0	62	7200	Const Load	C	
Parmerman (1976)	SP	0	Sb	-8.0	800	185	.005 mm/min	C	
Parmerman (1978)	SP	0	Sb & P	-8.0	677	110	.005 mm/min	C	
Karpov and Vall (1988)	CL	10	Wood & Concrete	-4.5	640	?	150 kPa/min	C	Short-term
Sego and Smith (1988)	CL	10	Concrete	-4.5	170	?	Incremental	C	Long term
Sego and Smith (1988)	SM	10	Un	-5.0	386	120	.008 mm/min	C	
Sego and Smith (1988)	SM	10	Un	-5.0	180	182	.008 mm/min	C	
Sego and Smith (1988)	SM	0	Sb	-5.0	733	378	.008 mm/min	C	
Hutchinson (1989)	SM	0	Sb	-5.0	193	-14000	Const Load	C	
Hutchinson (1989)	SM	5	Sb	-5.0	71	100	Const Load	C	
Hutchinson (1989)	SM	15	Sb	-5.0	7.5	250	.008 mm/min	C	
Bigger and Sego (in press)	SM	0	Sb	-5.0	887	180	.008 mm/min	C	
Bigger and Sego (in press)	SM	10	Sb	-5.0	670	180	.008 mm/min	C	
Bigger and Sego (in press)	SM	10	Sb	-5.0	128	55	.008 mm/min	C	
Bigger and Sego (in press)	SM	30	Sb	-5.0	6	155	.008 mm/min	C	
Field Test Results									
Lueker et al (1983)	ML [5]	0	Cor	-0.3	200-275+	?	89 kN / 3 day	C	
Lueker et al (1983)	CL	0	Cor	-0.3	120	?	89 kN / 3 day	C	
This study	SW [6]	15-25	Lugged	-5.0	120		>25 mm/hr	T	Excessive displacement rate
Laboratory Test Results									
Anderson and Alshabab (1983)	SP	0	1 Lug	-5.0	13 kN/avg		.25 mm/hr	T	Note 10.
Ladanyi and Guichas (1985)	SP	0	Cor Al	-5.0	-250		Const Load	C	Min rate 0.004 mm/hr
Ladanyi and Guichas (1985)	SP	0	Cor Al	-5.0	1700	-170	0.3 mm/min	C	
Grouted Anchors									
Field Test Results									
Johnson and Ladanyi (1972)	CL [5]	0	Re bar	-0.5	249	<120	Const Load	T	Gilliam results.
Johnson and Ladanyi (1972)	CL [5]	0	Re bar	-0.5	118	-75000	Const Load	T	Gilliam results.
This study	SW [6]	15-25	Dywidag	-5.0	560		>25 mm/hr	T	Unable to maintain last load increment

Notes: 1. Based on Unified Soil Classification system,  $S_u$  = salinity.  
2. Pile surface treatment: Sb = sandblasted, Un = untreated, P = painted, Al = aluminum, Cor = corrugated.  
3. Compression = C; Tension = T.  
4. Dolomitic Shale and Slate, fractured with ice.  
5. Ice-rich.  
6. Dense clayey, gravelly sand with some cobbles, moisture content 6.5% to 9.5%.  
7. Adjusted based on strain gauge results. Range of results from 4 tests.  
8. Time to failure for last increment only.  
9. Excessive settlement of pile foundation in summer.  
10. For 4.8 mm lug, estimated based on data presented in paper.

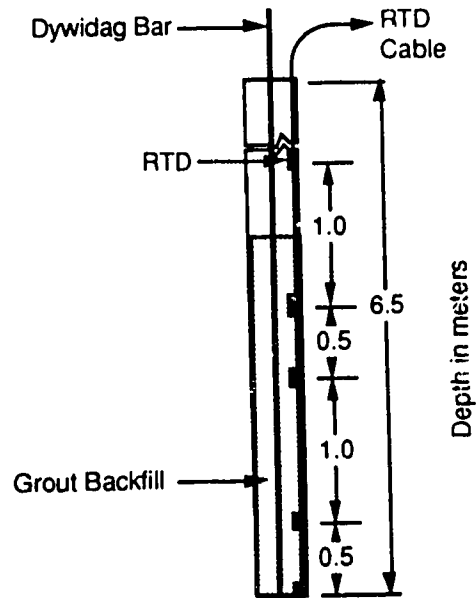


Figure 3.1: Location of RTD's to Measure Grout Curing Temperatures

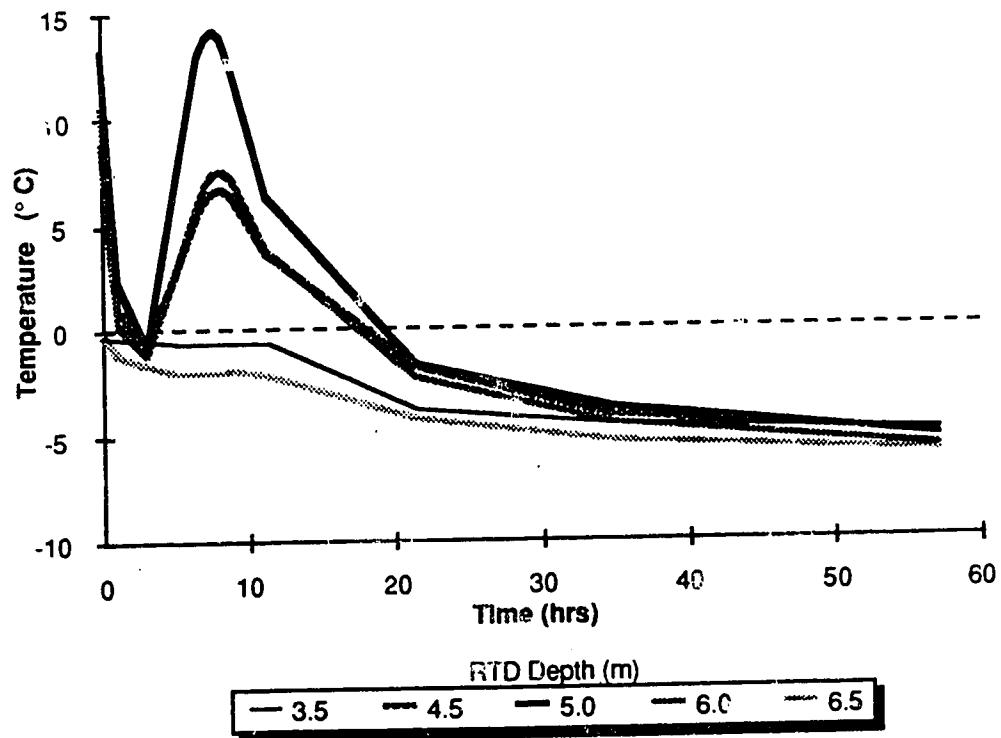


Figure 3.2: Temperature versus Time for Sanded Grout

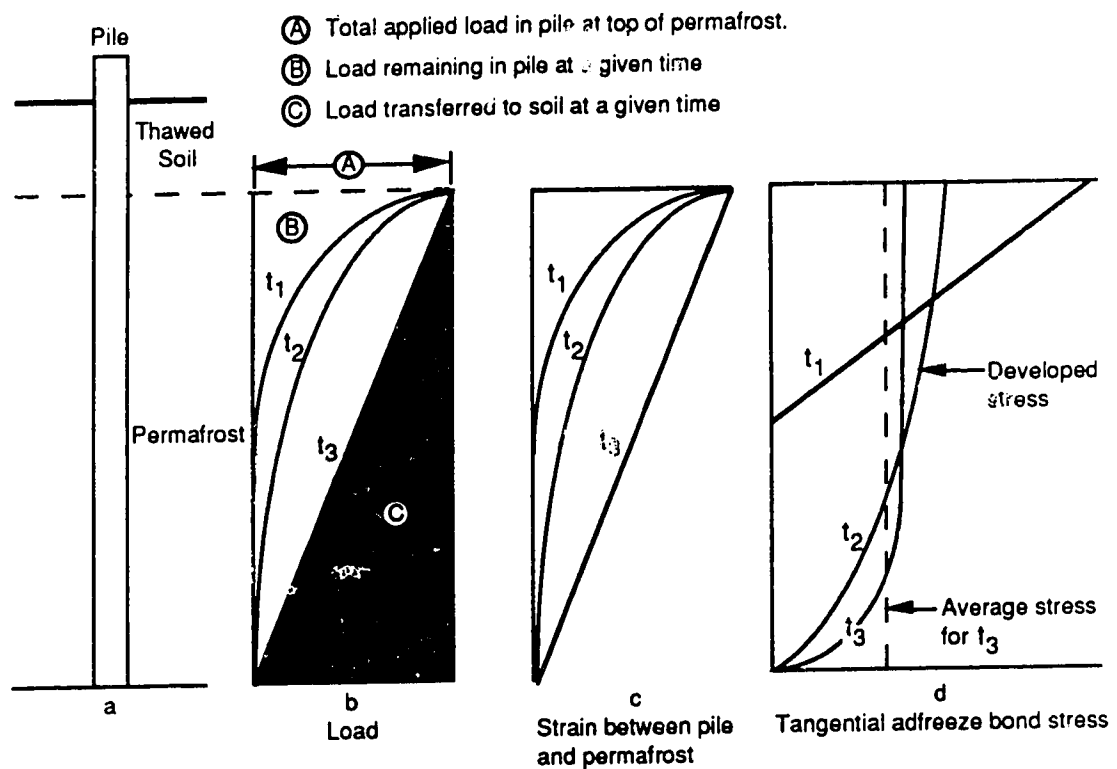


Figure 3.3 Typical distribution of load and stress along pile depth.  
(Modified from Linnel and Lobacz 1980)

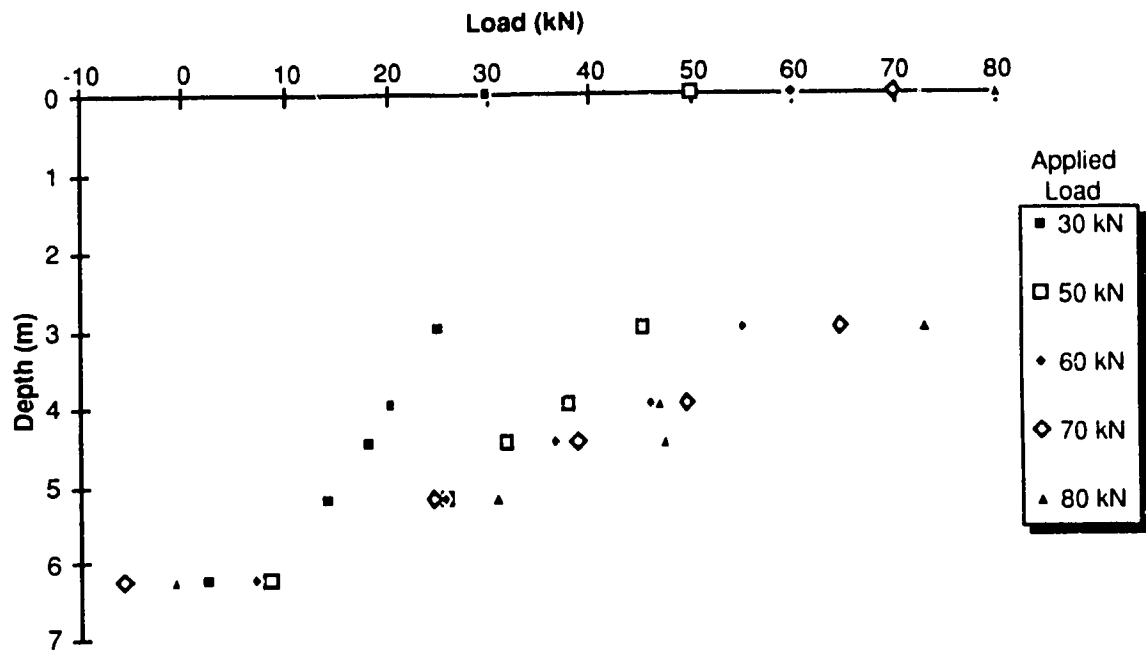


Figure 3.4: Smooth HSS Pile -Load at Depth for various load increments

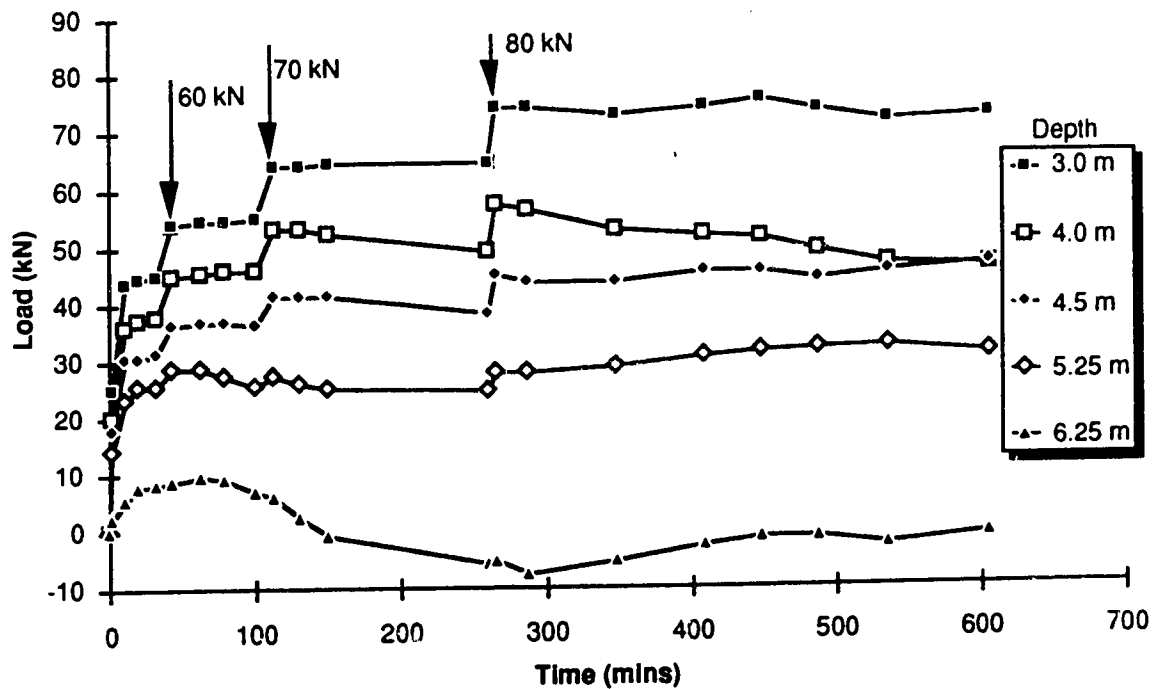


Figure 3.5: Smooth HSS Pile -Load at various Depths versus Time

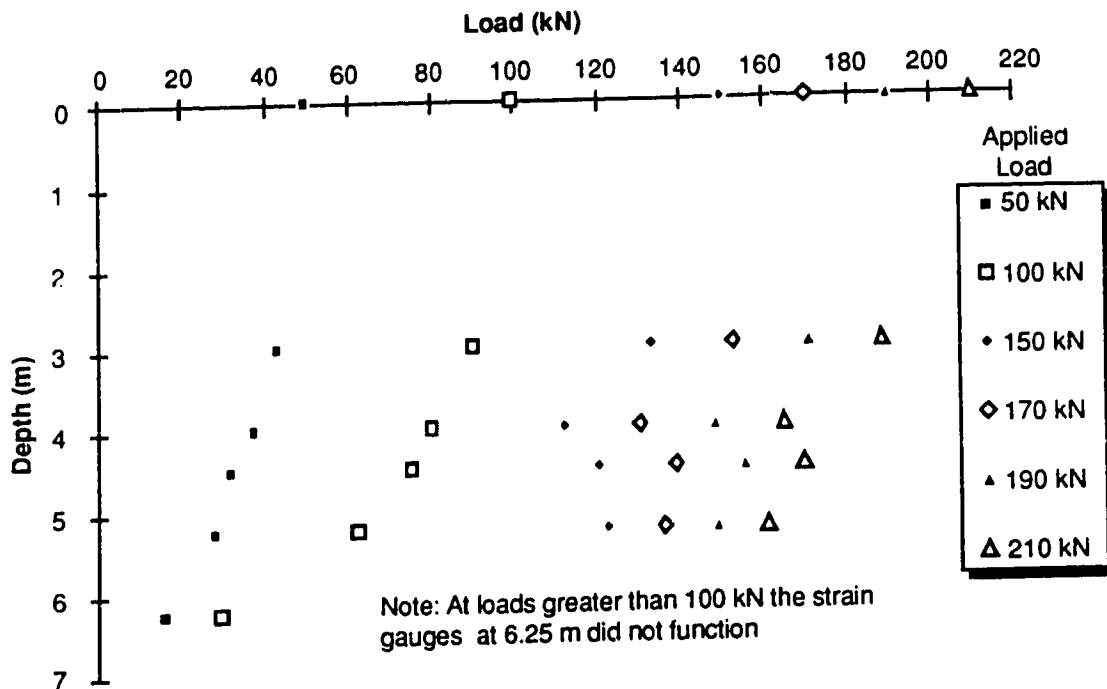


Figure 3.6: Lugged HSS Pile -Load at Depth for various load increments

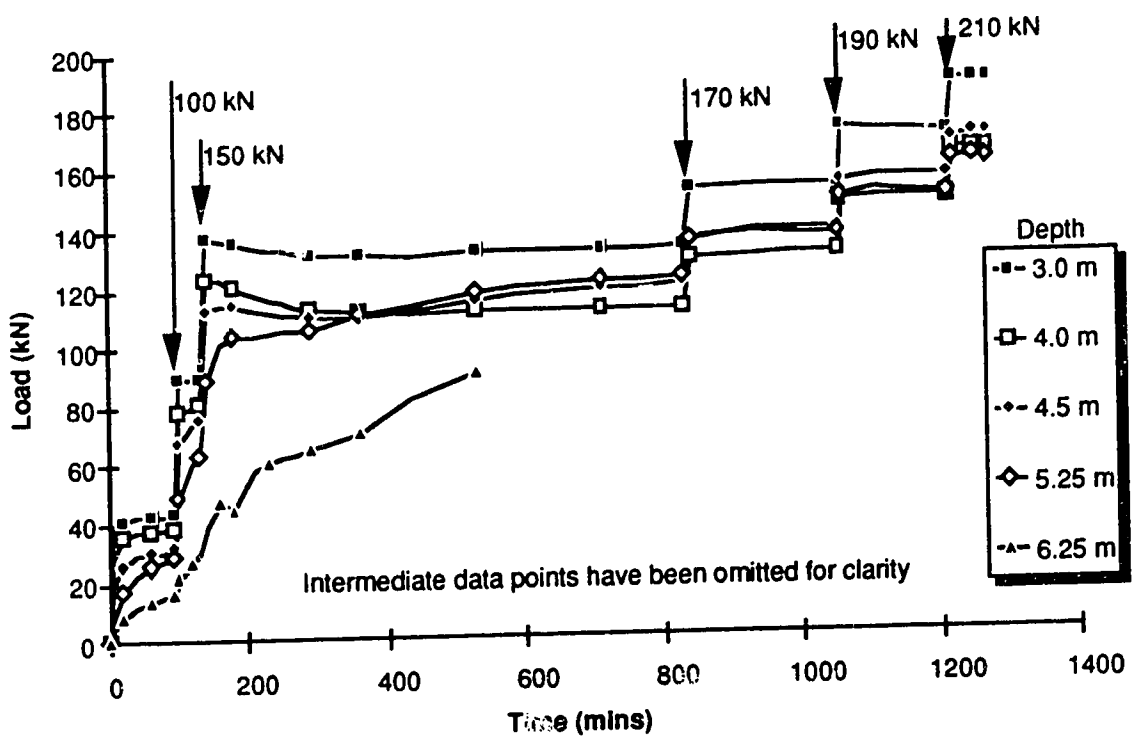


Figure 3.7: Lugged HSS Pile -Load at various Depths versus Time

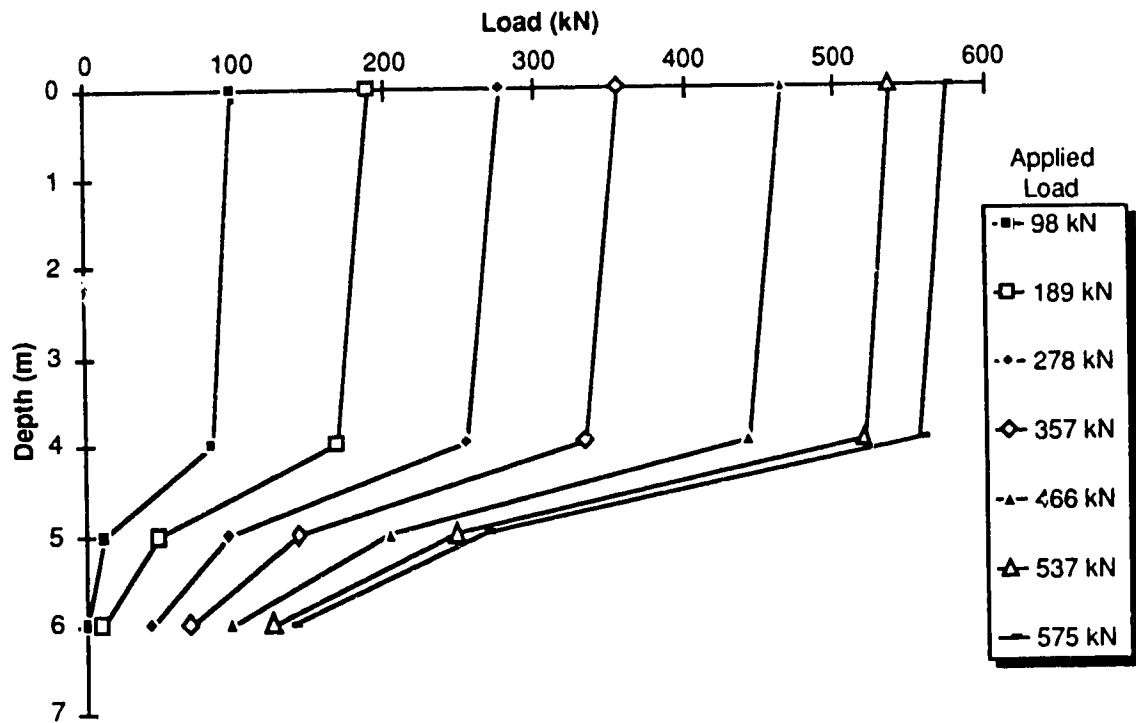


Figure 3.8: Dywidag bar -Load at Depth for various load increments

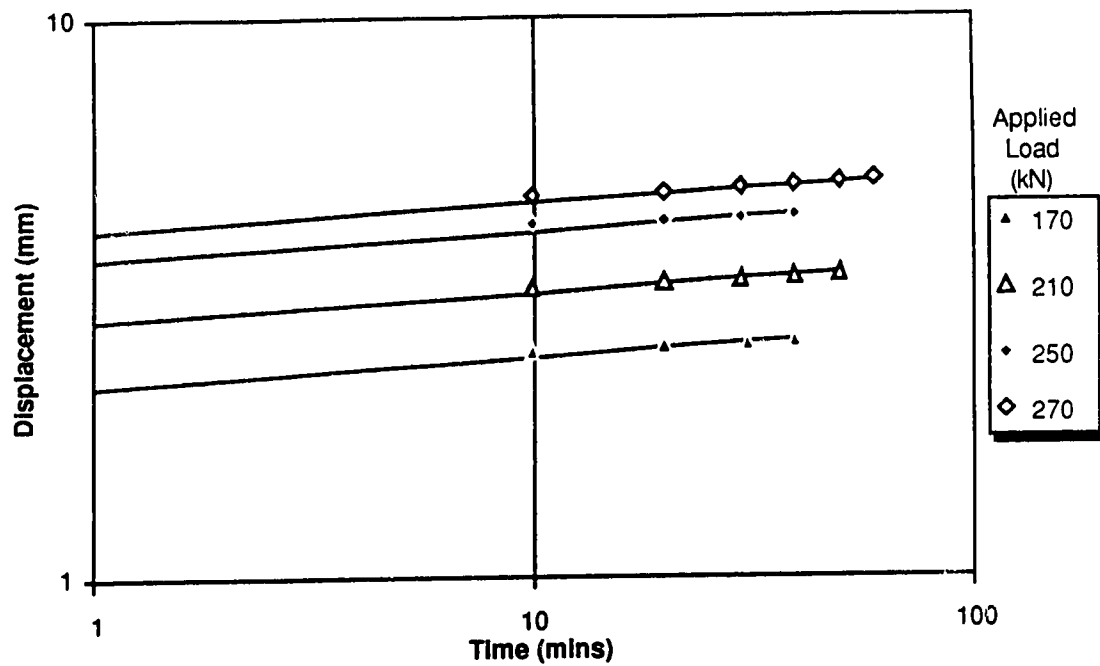


Figure 3.9: Typical Displacement versus Time - Measured values and best fit regression line

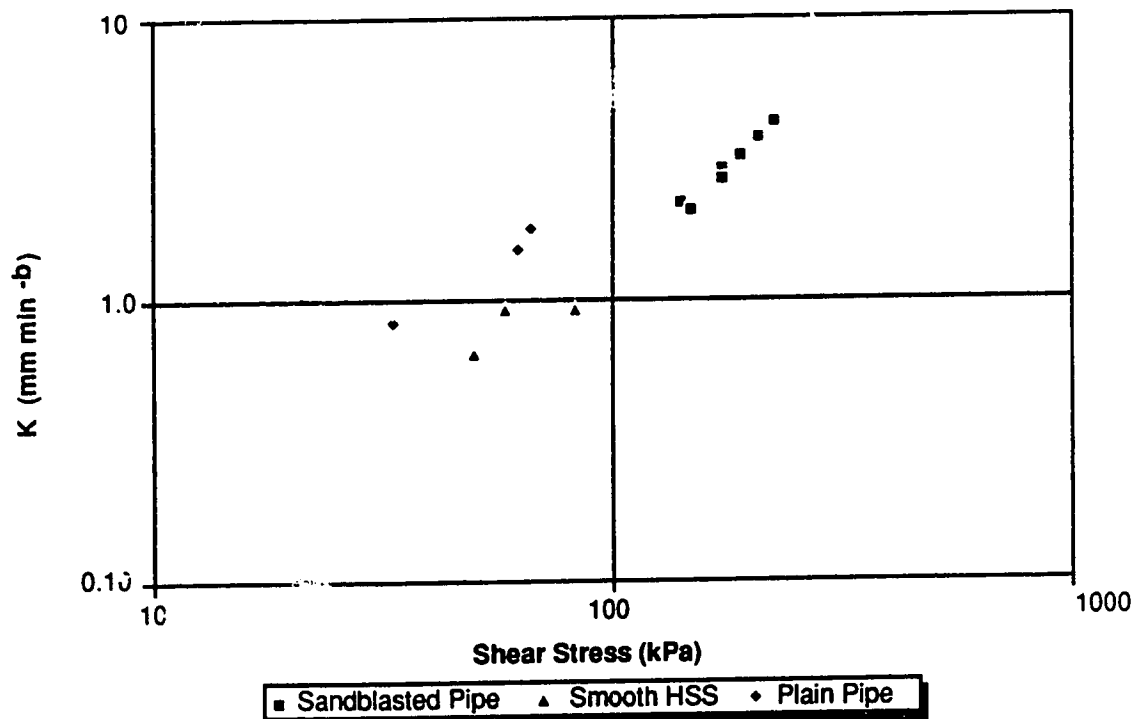


Figure 3.10: Values of K parameter versus Shear stress for different pile configurations



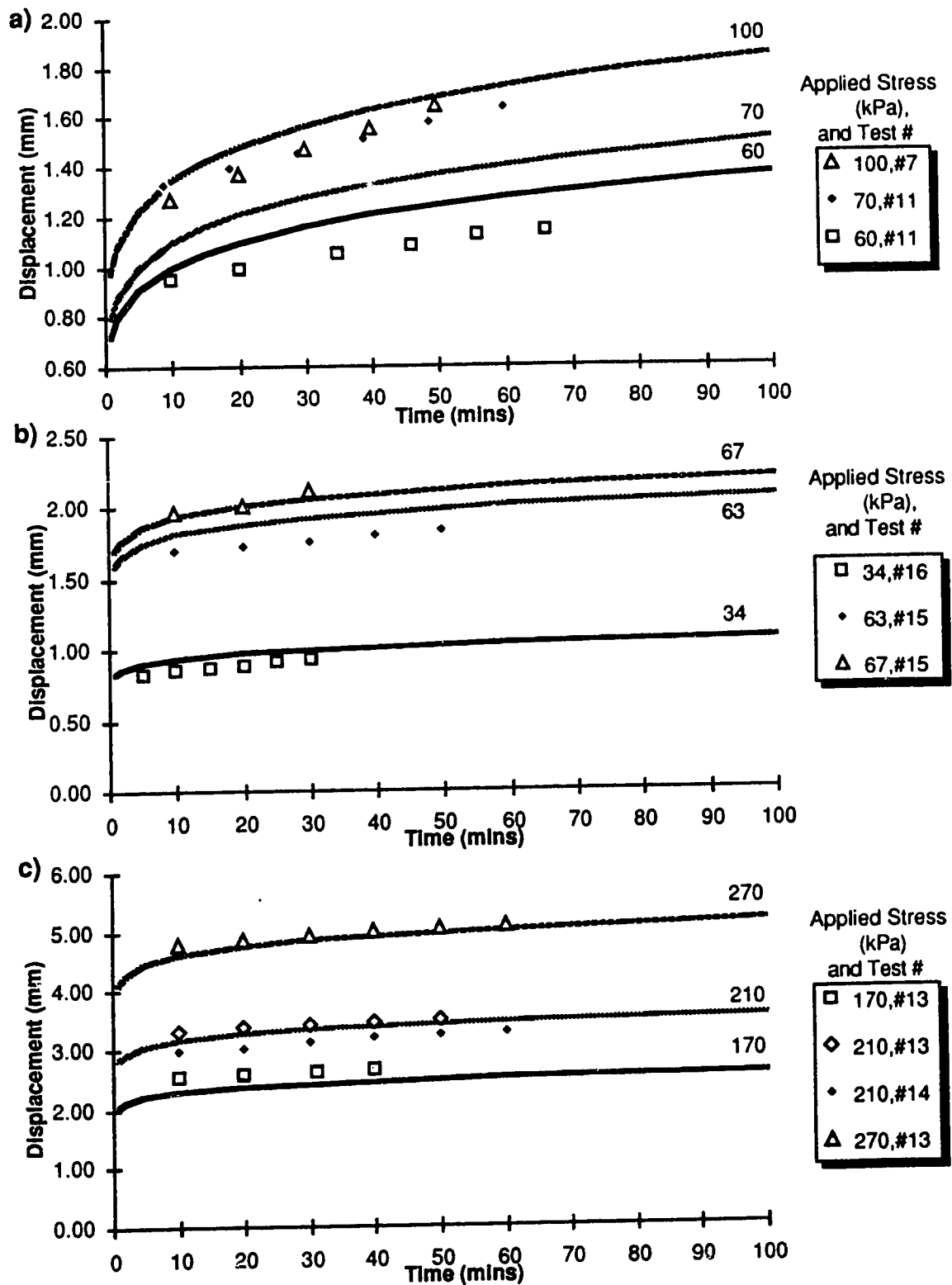


Figure 3.11: Displacement versus time—Predicted performance and measured values  
a)Smooth HSS b)Plain Pipe c)Sandblasted Pipe

#### 4. THE CURING AND STRENGTH CHARACTERISTICS OF COLD SETTING CIMENT FONDU GROUT<sup>1</sup>

##### Introduction

The Department of National Defence (DND) is currently proceeding with the construction of the North Warning System (NWS) to replace the aging DEW (Distant Early Warning) Line System. The NWS includes 35 unmanned Short Range Radar (SRR) sites which span the Canadian arctic coastline from Alaska to Labrador. These sites encounter foundation conditions varying from ice-rich fine-grained soils to bedrock. The SRR facility foundation design was to be based on 100 mm pipe piles installed in 165 mm prebored holes. The hole size of 165 mm was governed by the capability of an airtrack drill which would be used on most of the remote sites to prebore the pile holes. One of the options which was examined was that of using a grout backfill which was capable of curing with the surrounding soil as cold as -10° C.

The use of cementitious grouts as a backfill material for piles in permafrost is in its infancy. This is due to the problems associated with developing a grout which will cure adequately in a sub-zero environment without adversely affecting the surrounding native soil. Weaver (1979) points out that in order for a grout to be used successfully for piling in permafrost it must be able to set at temperatures below 0° C, the mixing water must not freeze prior to curing, it must develop adequate compressive strength, the heat of hydration must not cause excessive thermal disturbance to the surrounding permafrost, it must be stable to repeated freeze-thaw cycles, and an adequate bond strength to the piling material must develop.

The two principal advantages of using a grout backfill compared to a soil slurry backfill are the strong cementitious bond between the grout and the pile, and that the grout is not susceptible to time dependent deformation. For a properly cured grout the capacity of

---

<sup>1</sup> A version of this chapter has been published.

Biggar, K.W. and Sego, D.C. 1990. The curing and strength characteristics of cold setting Ciment Fondu grout. Proceedings, 5th Canadian Permafrost Conference. Quebec city, Quebec. pp.349-356

the bond between the pile and the grout will exceed that at the grout/native soil interface. Therefore the pile capacity will be governed by the shear strength at the grout/native soil interface, which fully mobilizes the shear strength of the native soil, beyond which no increase can be realized for a given pile geometry.

The problems associated with using a grout backfill are the development a grout which will perform adequately in the subzero environment, the associated costs of purchasing, transporting and placing the grout, and the difficulties in handling and mixing the grout to ensure quality construction in the adverse environment.

There are essentially four ways to ensure that the grout will cure adequately in a sub-zero environment: 1) the temperature of the grout may be artificially maintained above  $0^{\circ}\text{C}$  using external heat sources (this method is expensive and impractical for sub-surface cementing in frozen soils), 2) cements with rapid rates of hydration (evolving heat at a high rate) may be utilized to maintain the grout temperature above  $0^{\circ}\text{C}$  as it cures, 3) admixtures may be used to depress the freezing point of the mixing water and accelerate the curing time, and 4) grouts with very low water contents may be used which set rapidly.

High alumina cements (such as Ciment Fondu) may be utilized in grouts so that their high heats of hydration prevent freezing of the mix water during curing of the grout. Johnston and Ladanyi (1972) report successful use of Ciment Fondu in warm permafrost ( $T > -1^{\circ}\text{C}$ ). Biggar and Sego (1989) report successful use of Ciment Fondu grout in soil and rock at temperatures of  $-5^{\circ}$  to  $-7^{\circ}\text{C}$ .

#### **Prior use of Ciment Fondu in frozen soils**

The earliest work which deals with the use of Ciment Fondu in sub-zero environments was conducted by Morris, Stude and Cameron (1971). Laboratory tests performed to simulate the cementing of oil well pipe casing in Arctic conditions showed that in a soil at  $-10^{\circ}\text{C}$ , a grout slurry at  $+5^{\circ}\text{C}$  (either Neat Ciment Fondu and Ciment Fondu mixed 50/50 with Fly Ash) maintained slurry temperatures high enough for the grout to set providing adequate bonding of the pipe into frozen soil.

Subsequent work reported by Cunningham, Fehrenbach and Maier (1977) examined the freeze-thaw stability of both Neat Ciment Fondu and Ciment Fondu mixed 50/50 with Fly Ash. They observed that Neat Ciment Fondu grout cubes were stable for temperature cycles varying between  $-12^{\circ}\text{C}$  and  $+18^{\circ}\text{C}$ , however they deteriorated markedly when the temperature was cycled between  $-10^{\circ}\text{C}$  and  $+70^{\circ}\text{C}$ .

More recent work has been performed as a result of the SRR foundation design. Lafarge (1988a) reports the results of compression tests on 100 mm by 200 mm grout cylinders cast in metal molds embedded in a 20 l pail of dry sand kept in a cold room at a temperature of approximately  $-8^{\circ}\text{C}$ . A summary of their test results are shown in Table 4.1. Further laboratory tests performed by Master Builders, reported in Geocon (1988), used a larger (600 mm by 600 mm) mold of fine sand with a moisture content of 18%. Due to the larger size of the mold and the presence of water in the soil, it acted as a more efficient heat sink than that used by Lafarge. Cylinders of neat Ciment Fondu (cement and water only) and sanded Ciment Fondu grout were cast in these molds, grout and soil temperatures were monitored, and compression tests were performed on the cylinders. The mix designs and compressive strengths are shown in Table 4.2. The outer annulus of the grout cylinders were observed to have a different structure than the rest of the cylinder, and this effect was more pronounced in the sanded grout. The different structure at the outer annulus of the grout cylinder was reported to be fractured, with the extreme outer edges crumbling and flakey. It was suggested that this different structure was a result of freezing water at the outer portion of the cylinder before the grout cured.

In an effort to overcome this problem, Lafarge (1988b) performed subsequent tests in which an accelerator was added to the sanded Ciment Fondu grout mix causing the grout to become exothermic more quickly. They observed that the peak temperature of the grout occurred approximately 2.5 hours after the grout was mixed as opposed to the usual 4 to 6 hours for an unaccelerated mix. The accelerated grout mix cylinders still had an outer annulus with a different structure but the thickness of this annulus was much diminished

from an unaccelerated mix. The work performed at the University of Alberta, reported herein, is an extension of the work performed by Geocon and Lafarge described above.

## **Testing program and procedure**

### *General*

This research program involved the testing of different grout mixes prepared using differing amounts of admixtures while maintaining the cement: sand: water ratio the same. The objective was to produce a mix which would cure adequately at temperatures of  $-10^{\circ}\text{C}$  yet be workable enough for field placement around piles. Cylinders of grout were cast in a frozen soil mold maintained at  $-10^{\circ}\text{C}$ . Temperatures of the grout and surrounding soil were monitored during the first 24 hours of the curing. Subsequently compressive strengths of the cylinders were measured at regular time intervals. In addition, strength tests were performed on cubes which were cast and cured at room temperature. Flow cone and vicat needle tests were conducted to assess grout workability.

The test program consisted of three phases:

- I. The first phase involved comparing the performance of a 600 mm diameter soil mold (which has been used on tests conducted previously by Geocon 1988, and Lafarge 1988b) and a constant temperature bath cell (CTBC) to determine if the CTBC would provide comparable curing conditions,
- II. The second phase involved varying the admixture proportions in the grout mix to produce an optimum mix design which would cure completely at  $-10^{\circ}\text{C}$  while providing adequate workability, and
- III. The third phase involved utilizing the optimum mix design and varying the environmental conditions under which it was produced and cured.

### *Cell description*

A schematic diagram of the 600 mm mold which was used is shown in Figure 4.1. The bottom portion of a 200 litre drum was used, into which a 50 mm thick layer of Styrofoam was placed in the bottom. On top of the insulation a 300 mm thick by 600 mm

diameter soil 'donut' surrounded a steel pipe 160 mm in diameter by 300 mm long by 3 mm thick into which the 150 mm diameter grout cylinder mold could be placed. A 50 mm layer of Styrofoam was placed directly on top of the soil after the grout cylinder was installed. Resistance Temperature Devices (RTD's) were placed in the soil at distances of 25, 50, and 100 mm from the edge of the grout cylinder. The small annular space between the cylinder mold and the steel pipe was filled with antifreeze to provide adequate thermal contact between the grout cylinder and the soil.

A schematic diagram of the CTBC is shown in Figure 4.2. It consisted of a 300 mm thick by 300 mm diameter soil 'donut' surrounding a steel pipe as with the 600 mm mold. The soil 'donut' was surrounded by a bath of antifreeze which contained copper tube coils through which glycol maintained at  $-10^{\circ}\text{C}$  was circulated. A 50 mm layer of Styrofoam was placed beneath the soil and grout cylinder and directly on top of the cell. RTD's were placed in the soil at distances of 25 and 50 mm from the edge of the grout cylinder, one was placed in the fluid bath of the cell, and others were placed in the grout cylinder, in center and near the edge. The small annular space between the cylinder mold and the pipe was filled with antifreeze to provide adequate thermal contact between the grout and the soil. The soil masses had a moisture contents of approximately 15% and dry densities of between 1650 and 1850  $\text{kg/m}^3$ .

The operation of the CTBC will be described in more detail. By maintaining a nearly constant temperature 75 mm from the edge of the grout cylinder, a steep temperature gradient is maintained in the frozen soil and a large heat sink is more closely modelled than by using the 600 mm soil cell, which has its outer surface exposed to the ambient temperature in the cold room. Studies of data from models similar to the 600 mm drum indicate that the temperature of the entire soil mass surrounding the grout cylinder may increase such that the temperature at the outer edge of the soil cell rises above the initial soil temperature (Geocon 1988). The air in the cold room is a poor heat conductor, consequently field conditions are poorly modelled. Thus the CTBC more closely represents

field conditions. In any case, the temperature conditions in the CTBC will be more severe than in the 600 mm cell so if the grout performs adequately in the CTBC it will certainly perform adequately in the 600 mm cell, and should perform adequately under field conditions.

#### *Sample preparation*

The mix designs of the grouts tested are shown in Table 4.3. The cement: sand: water ratio was maintained constant and only the proportion of the admixtures was changed. Only one accelerator (lithium carbonate) and one superplasticizer (SPN) (Sulphonated Naphthelene Formaldehyde Condensate) were used.

Phase I: A spatula mixer was utilized for this small batch size. Twenty kg of cement were added to the water over the first minute of mixing and the sand was added over the second minute; the grout was mixed for a total of four minutes. The temperatures of the components was  $21^{\circ} \pm 1^{\circ} \text{ C}$  prior to mixing. The cylinders were prepared and placed within 20 minutes of starting the mixing.

Phase II: The mixes used 50 kg of cement ( $0.042 \text{ m}^3$ ) and proportionate amounts of the other components. All components of the mix were maintained at a temperature of  $21^{\circ} \pm 1^{\circ} \text{ C}$  prior to batching. The batch size provided enough grout for six cylinders, the cubes, the flow cone test, and the vicat needle test. The grout was mixed in a  $0.10 \text{ m}^3$  mortar mixer. The cement was added to the water over the first minute and the sand was added over the second minute of batching. The grout was allowed to mix for approximately 1 minute at which time the admixtures were added. The grout was mixed for a total of 4 to 5 minutes. The flow cone test was carried out immediately after the mixing stopped and then the cylinders were cast and placed in the test cells. The grout was poured directly from the mixer into the cylinders. Generally the cylinders were in the cold room within 10 minutes of mixing and in the cells within 20 minutes. The cubes were cast immediately after the flow cone test was completed.

**Phase III:** The mixing of the grout in this phase of testing differed from the previous phases in that all of the dry components were blended together initially, then added to the water. The mix time remained the same (4 minutes), as did the sample preparation and testing procedure. The aim of the initial test was to compare the workability and curing temperatures of the optimum grout mix design in which the dry components were preblended to the results of the tests in which the dry components were individually added, under the initial environmental conditions (20° C grout cured at -10° C). Tests were then conducted with the preblended grout mix to examine its performance when its temperature was colder (13° C) when it was placed and cured at -10° C, and for 20° C grout cured in soil at warmer temperatures (-5° C and +1° C).

#### *Compressive strength testing*

Constant rate of loading compression tests were conducted on 50 mm cubes cured in a moisture room at 20° C, after 6 and 24 hours which provided an index strength for the grout cured under normal conditions. Constant rate of loading compression tests were conducted on the cylinders cured at sub-zero temperatures at 12 hours, and 24 hours, 7 days and 28 days. Prior to compression testing, the cylinders were kept at room temperature until the temperature at the center of the cylinder was above 0° C (approximately 6 hours) to ensure that ice bonding did not contribute to the measured strength.

## **Results**

### *Comparison between the 600 mm cell and the CTBC*

The results from Mix I-A showed that temperatures at the outer edges of the cylinders in both cells reached 0° C for approximately 3.5 hours. Figure 4.3 shows some of the temperature versus time curves for the grout and soil. The maximum temperature at the centre of the grout cylinder in the CTBC reached a maximum of only 10.3° C compared to 15.0° C in the 600 mm cell. The soil temperatures in the CTBC can be seen to be consistently lower than in the 600 mm cell. Subsequent tests duplicated this observed



behaviour, which supports the previous contention that the CTBC provided a more severe (colder) curing environment.

After curing for 24 hours in the cells the cylinders were removed from the soil molds and were sawn in half crosswise. Both cylinders had an outer annulus, approximately 20 mm thick with an unusual structure. This structure was needle-like but was not flakey nor could it easily be scraped away with a knife. The inner portion of the cylinder had cured properly, and appeared to be unconverted, as it was greyish in colour as opposed to the characteristic brown seen in converted Ciment Fondu (the conversion of high alumina cements is discussed subsequently).

#### *Mix consistency*

All mixes were thixotropic (with and without the SPN). Mix II-3 which had the greatest proportion of accelerator set so quickly, however, that it was difficult to properly fill the six cylinder molds. The remaining mixes had to be stirred briefly after 3 cylinders had been cast in order to pour the grout for the final 3 cylinders.

In phase III the preblending of the admixtures into the cement and sand appeared to enhance the performance of the admixtures. Initially the mix was less viscous than the mixes in phase II. However the material began to set at an earlier time and hardened more quickly. The cold grout mix (13° C) was less workable than the warm grout (20° C) initially, though there was no effect on the vicat needle test results.

#### *Flow cone tests*

The tests were conducted in accordance with CSA A23.2-1B. The results are contained in Table 4.4. In phase II there was some difficulty experienced in the first few mixes as blockages occurred or the mix was too stiff. Generally flow cone times varied between 24 and 35 seconds, with Mixes II-5 and II-6 giving the shortest times (ie. the least viscous). The preblended mixes had considerably shorter times, except for the grout prepared at 13° C.

### *Vicat needle tests*

The tests were conducted in accordance with CSA CAN3-A5-M77. In phase II the time from the start of set to complete hardening was approximately 1 hour, though in some cases it was as little as 30 minutes (Table 4.4). This is noteworthy when compared to the results from phase III.

In phase III generally the time to complete set was slightly less than in phase II (100 versus 120 minutes), but the time interval from the start of hardening to complete set was considerably less, dropping from 60 minutes in phase II to 15 minutes for the preblended mixes in phase III. In other words the preblended grout started to harden later but the rate of hardening was much faster.

### *Thermal performance*

A summary of the maximum and minimum temperatures for the samples is contained in Table 4.4. After Mix II-3 was completed it was realized that the use of cardboard cylinder molds was inappropriate. These molds provided an insulating layer around the grout, consequently the measured grout temperatures were too high. Subsequently metal cylinder molds were used which allowed the heat to be conducted out of the grout much more efficiently, resulting in lower grout temperatures during curing. No measurable difference in cylinder compressive strength resulted from the higher temperatures caused by the cardboard cylinder molds.

The grout cylinders in Mix II-8 had an outer annulus approximately 12 mm thick with the same structure as that observed on the cylinders of Mix II-1. This was observed on cylinders from both the 600 mm cell and the CTBC. This phenomena was not observed in Mix II-4 which had the same admixture quantities. Consequently this mix was re-tested and the results of Mix II-8 were confirmed. In no other cases was there any structural change observed at the outer edges of the grout when an accelerator was used in a 20° C mix. The grout mixed at 13° C and cured at -10° C (III-10) had an outer annulus 2 to 3 mm thick with the needle like structure. The thickness of this layer approached 20 mm at the

bottom of the cylinder. Although the outer RTD did not indicate temperatures below 0° C it is believed that at the temperature at the outer edge of the cylinder was at 0° C for a short period of time.

In phase II there were no cases in which the measured soil temperature rose above 0° C 25 mm from the edge of the grout cylinder. Similar maximum and minimum temperatures, and respective times, were observed in the 20° C grout cured at -10° C for the preblended (phase III) and the unblended (phase II) grout mixes.

For the warmer soil conditions (-5° C) in Mix III-11 the temperatures in the grout were only slightly higher than in Mix III-9 where the soil temperature was -10° C. The soil temperature rose above 0° C at a distance of 25 mm from the grout cylinder but not at 50 mm. With soil temperatures above 0° C in Mix III-12, the grout and soil temperatures were considerably higher than in previous mixes, as no energy was required to overcome the latent heat in the ice.

### *Compressive Strengths*

The cylinder compressive strengths up to 7 days were  $33 \pm 3$  MPa for phases I and II tests except Mix II-1 (Table 4.4). Mix II-3 had lower values than the rest but this may have been due to difficulty in casting the cylinders as the grout set so quickly. Cylinder compressive strengths at 1, 7, and 28 days are shown in Figure 4.4

The compressive strengths of the cubes varied significantly. Six hour strengths varied between 27 and 49 MPa and 24 hour strengths between 36 and 59 MPa. Generally the lower the accelerator content, the higher the strength.

In phase III the strengths of the mixes in which the grout was placed at a temperature of 20° C are similar to those in phase II. The compressive strengths were lower for the mix which was placed at a temperature of 13° C (#10), a result of the weaker grout structure at the outer edge of the cylinder.

High alumina cement (HAC) undergoes a change in the crystal structure of the hydrate with time when maintained at mild temperatures (20° C) (Neville 1975). This

process is called conversion, and results in a decrease in strength with time for concretes made with HAC. There was some concern regarding whether or not the grout strength would diminish if the Ciment Fondu underwent conversion at some later time. To the author's knowledge no research has been conducted regarding the time for conversion of Ciment Fondu grouts maintained in a freezing environment. One cylinder from this testing program (Mix III-11) was immersed in a 60° C water bath for 14 days after it had been cured for 28 days at -10° C. Subsequent analysis (Lafarge 1989) indicated that the grout was 68% converted prior to immersion in the water bath and 93% converted afterwards. The compressive strength of the cylinder was 40 MPa, which was within 10% of the mean of the compressive strengths of the other cylinders of that test batch.

## **Discussion**

### *Effect of test cell*

The CTBC provided a more severe thermal regime than the 600 mm mold by maintaining a steeper temperature gradient in the soil adjacent to the grout cylinder. It is believed that this cell more closely models field conditions.

### *Effect of admixtures*

The water reducing admixture (SPN) which was used provided a more fluid mix and enhanced workability. It also retarded the set time. The lithium carbonate accelerator reduced the time interval for the grout to become exothermic preventing the temperature of the grout at the outer edge of the cylinder from dropping below 0° C, thus preventing the mix water from freezing before the grout set.

The optimum mix design for the given conditions involved testing with only one type of each of the two admixtures. No attempts were made to test other SPN or accelerating admixtures.

The reduced set time of the preblended mix is believed to be a result of the SPN dispersing in the cement more thoroughly thus allowing the accelerator to interact more efficiently, in addition to a longer period of time in which both the admixtures were in

contact during mixing. The reason that the cold grout mix (Mix III-10) was less workable initially may be due to the fact that the lithium carbonate accelerator dissolves better in cold water than in warm water allowing it to initiate setting more quickly.

#### *Effect of cylinder molds*

The use of cardboard cylinder molds was found to be inappropriate for thermal testing of the grout as the cardboard acted as an insulative layer around the grout. This resulted in grout temperatures being excessively high and not representative of what would occur in-situ. The use of metal cylinder molds better simulates field thermal conditions as heat is more efficiently conducted into the soil. The compressive strength of the grout was not affected by the type of mold used.

#### *Application to field operations*

The grout mix which was designed and tested was intended to cure without freezing at soil temperatures as cold as  $-10^{\circ}\text{C}$ , which was expected to be the most severe conditions encountered in the SRR pile foundations. The fluidity of the mix is intended to simplify grout placement in the field. With a preblended grout, field preparation of the mix requires only that the proper amount of water be added and that the mixing time be adequate. The temperature of the grout prior to placement is important and will require that the materials must be heated during severe weather conditions. Figure 4.5 contains a guide for the required mix water temperature based upon the temperature of the dry components of the optimum mix design. The temperature of the mixing equipment and environmental conditions will affect the final grout temperature so adjustment will be required on site to ensure that the temperature of the mixed grout during placement is correct.

#### **References**

- Biggar, K.W. and Sego, D.C. 1989. Field load testing of various pile configurations is saline permafrost and seasonally frozen rock. Proceedings, 42nd Canadian Geotechnical Conference, October 25-27, Winnipeg, pp. 304-312.
- C.S.A. STANDARD A23. 2-1B. Viscosity, bleeding expansion and compressive strength of flowable grout.

- C.S.A. STANDARD CAN 3-A5-M77 7.4.2. determination of normal consistency.
- Cunningham, W.C., Fehrenbach, J.R. and Maier, L.F. 1972. Arctic cements and cementing, *Journal of Canadian Petroleum Technology*, Oct.-Dec, pp. 49-55.
- Geocon Inc. 1988. Grout testing arctic grout pile. Report submitted to UMA Engineering Ltd. Aug. 26, p. 23.
- Johnston, G.H. and Ladanyi, B. 1972. Field tests on grouted rod anchors in permafrost. *Canadian Geotechnical Journal*, 9: pp. 176-194.
- Lafarge Canada Inc. 1988a. Internal report: Cold weather environment Fondur testing. June 27, 1988, p. 8.
- Lafarge Canada Inc. 1988b. Project #12300 Ciment Fondur grout frozen annulus problem investigation. Report submitted to Geocon Inc., October 5, 1988, p. 19.
- Lafarge Coppee Recherche. 1989. Internal report: Research program on the curing and strength characteristics of cold setting Ciment Fondur grout. p. 4.
- Morris, E.F., Stude, D.L. and Cameron, R.C. 1971. Evaluation of cement systems for permafrost. *Journal of Canadian Petroleum Technology*, January-March, 1971, pp. 19-22.
- Neville, A.M. 1975. **High alumina cement concrete**. John Wiley and Sons, p. 201.
- Weaver, J.S. 1979. Pile foundations in permafrost. Unpublished Ph. D. Thesis, University of Alberta, Edmonton, Alberta, p. 224.

**TABLE 4.1****Strength of Ciment Fondu grout cured at sub-zero temperatures  
Results of study by Lafarge Canada Inc**

<b>Mix</b>	<b>1</b>	<b>2</b>	<b>3</b>	<b>4</b>
Fondu (kg)	1000	1200	1200	1000
Sand (kg)	0	543	543	900
Protard (ml) [1]	0	1500	0	0
S.P.N. (ml) [2]	0	5000	5000	4150
Water/Cement	0.35	0.35	0.35	0.35
<b>Performance</b>				
Curing temp (°C)	-10	-10	-8 to -3	-5 to -8
Peak grout temp (°C)	+35	No peak	+28	+22
Compressive Strength @ 7 da	37.8	0 [3]	52	57

- Notes: 1. Protard is a chemical admixture to retard the set of cement.  
2. S.P.N. is an abbreviation for superplasticizer, used to enhance grout workability. The brand of S.P.N. was not specified.  
3. The grout mix water froze and the grout did not cure.

**TABLE 4.2**

**Performance of Grouts cured at sub-zero temperatures  
Results of study by Geocon Inc.**

<b>Mix</b>	<b>Set 45</b>	<b>Set 45</b>	<b>Set 45</b>	<b>Set 45</b>	<b>Ciment Fondu</b>	<b>Ciment Fondu</b>
Cement (kg)	46.1	45.5	46.4	45.9	47.3	68.2
Water (kg)	3.4	3.3	3.5	3.4	16.5	23.9
Sand (kg)	0	0	0	0	20.9	0
SPDA (kg) [1]	0	0	0	0	0.354	0.510
Water/Cement	0.073	0.073	0.074	0.074	0.35	0.35
Mix time (min)	2	2	2	2	2.5	3
<b>Temperatures (°C)</b>						
Cement	23	-8	-8	-4	25	26
Water	24	22	1	46	28	28
Mixed grout	27	8	4	13	25	26
<b>Performance</b>						
Flow Table %	106	80	88	96	—	—
(15 drops)						
Flow cone (sec)	—	—	—	—	35	21
Set (min)	20	105	—	—	360+	360+
Comp Strength (MPa)	13.5	—	29.0	28.1	6.6	23.0
Time of test (hrs)	2	—	24	24	24	24
<b>Curing data</b>						
Soil mold (°C)	-10	-9	-9	-9	-9	-9
Max temp in grout						
cylinder (°C)	80	11	6	7	33	16
Time to max temp (min)	2 min	10 min	4 min	4 min	10 hrs	9 hrs
Time for edge of cylinder	190	45	70	144	132	195
to reach 0° C (min)						

Notes: 1. SPDA is a type of superplasticizer, the report did not detail any specifics.



**TABLE 4.3****Grout mix designs used in this study**

Mix #	Ciment Fondu (kg)	Sand (1) (kg)	Water (kg)	Accelerator (2) (g/%)	SPN (3) (g/%)
Phase I					
I-A	20	8.9	7.0	0	150/0.75
Phase II					
II-1	40	17.9	14.0	0	300/0.75
II-2	50	22.6	17.5	2.5/.005	0
II-3	50	22.6	17.5	7.5/.015	375/0.75
II-4	50	22.6	17.5	2.5/.005	375/0.75
II-5	50	22.6	17.5	5.0/.010	375/0.75
II-6	50	22.6	17.5	5.0/.010	375/0.75
II-7	50	22.6	17.5	2.5/.005	0
II-8	50	22.6	17.5	2.5/.005	375/0.75
Phase III					
III-9	50	22.6	17.5	5.0/.010	375/0.75
III-10	50	22.6	17.5	5.0/.010	375/0.75
III-11	50	22.6	17.5	5.0/.010	375/0.75
III-12	50	22.6	17.5	5.0/.010	375/0.75

- Notes:
- 1) SIL SILICA, Silica sand, grade Sil-7.
  - 2) Lithium carbonate accelerator.
  - 3) Sulphonated naphthelene fromaldehyde condensate water reducing admixture (superplasticizer).

**TABLE 5.4**  
**Phase II test results**

MIX	Min Temp (°C) @ time (hrs) (edge of cylinder)	Max Temp (°C) @ time (hrs) (centre of cyl)	Compressive Strengths (MPa)		Flow Cone (sec)	Vicat Needle (mins)	COMMENTS
			Cubes	Cylinders			
			6 / 24 hr	12 hr / 24 hr / 7da / 28 da			
II-1	0° @ 2.5<5.5	12° @ 11.5 hrs	--- / 59.1	---- / 10.2 / 9.9 / 12.1	--	--	Sample had different structure 20 mm thick at outer edge (likely frozen).
II-2	11° @ 1.0 hr	57° @ 3.0 hrs	35 / 52.7	36.8 / 32.9 / 32.6 / 38.3	35 (NOTE 1)	100<135	Cardboard molds used on cylinders for temp measurement.
II-3	16° @ 1 hr (NOTE 3)	34° @ 3 hr (NOTE 3)	26.6 / 36.0	29.0 / 29.6 / 38.3 / 34.5	too stiff	too stiff	Cardboard molds used on cylinders for temp measurement.
II-4	4° @ 1.5 hr	32° @ 4 hrs	31.2 / 50.4	31.0 / 34.8 / 36.5 / 37.0	53.4 (NOTE 2)	145<175	
II-5	2.3° @ 1.5 hr (NOTE 3)	25° @ 4.0 hrs (NOTE 3)	35.2 / 42.9	30.4 / 31.2 / 30.7 / 34.3	26.8	120	Cold room cooling unit froze-up so had to defrost during test, thus temperatures are high.
II-6	0.4° @ 1.5 hrs	20° @ 3.5 hrs (NOTE 4)	---- / 46.5	34.2 / 36.4 / 34.2 / 40.6	24.1	120	
II-7	1.2° @ 1.6 hrs	14° @ 4.4 hrs	49.3 / ---	34.8 / 33.7 / 33.2 / 33.8	31.9 (NOTE 2)	90<105	without SPN not as good a mix; more lumps, and cement sticking to paddles.
II-8	0.5° @ 1.8 hrs (NOTE 3)	11° @ 6.3 hrs (NOTE 3)	27.4 / 51.4	----- / 32.1 / 36.3 / 39.5	33.5	169	failure of constant temp bath, so temps in lab cell were too high. 12 mm outer layer had different structure observed (frozen).

**NOTES:**

- 1) Flow stopped at 35 seconds but the cone did not empty, estimate 50 - 75 mm left in bottom.
- 2) Cone had to be manually shaken to complete flow as grout would completely not drain.
- 3) Temperatures are from the cylinder in the 600 mm cell due to problems with CTBC.
- 4) RTD only 38 mm from cell edge instead of 75 mm.

**TABLE 5.5**  
**Phase III test results**

MIX	Conditions T <sub>g</sub> = T <sub>grout</sub> T <sub>s</sub> = T <sub>soil</sub>	Min Temp (°C) @ time (hrs) (edge of cylinder)	Max Temp (°C) @ time (hrs) (centre of cyl)	Compressive Strengths (MPa)		Flow Cone (sec)	Vicat Needle (mins)	COMMENTS
				Cubes	Cylinders			
				6 / 24 hr	12 hr / 24 hr / 7 da / 28 da			
III-9	T <sub>g</sub> = 20°C T <sub>s</sub> = -10°C	3.9° @ 1.3 hrs (NOTE 2)	25° @ 3.3 hrs (NOTE 2)	28.0 / 42.2	31.8 / 33.7 / 37.2 / 36.7	15.0	84 < t < 104	Pump breakdown on bath #1 CTBC temps too high.
III-10	T <sub>g</sub> = 13°C T <sub>s</sub> = -10°C	1.2° @ 1.0 hrs	15° @ 3.9 hrs	37.1 / 51.3	---- / 28.0 / 25.8 / 36.0	25.8	95 < t < 115	3 mm thick outer layer with different structure observed (likely frozen)
III-11	T <sub>g</sub> = 20°C T <sub>s</sub> = -5°C	3.2° @ 1.0 hrs	25° @ 3.3 hrs	41.2 / 49.3	34.5 / 36.3 / 38.9 / 40.0 (NOTE 4)	27.7 (NOTE 1)	97 < t < 112	28 day cylinder cured in water @ 60°C from 28-42 days
III-12	T <sub>g</sub> = 20°C T <sub>s</sub> = +1°C	16° @ 1.3 hrs (NOTE 3)	60° @ 2.8 hrs (NOTE 3)	31.2 / 35.8	37.8 / 30.9 / 33.7 / 27.3 (NOTE 4)	16.6	90 < t < 110	

**NOTES:**

- 1) Appeared to be small blockage at throat of cone.
- 2) Temperatures from 600 mm cell as pump failure resulted in high temperatures in the other cell.
- 3) Edge temperatures are for the constant temp bath cell, centre temperatures are for the 600 mm cell.
- 4) Compression test for 7 day strength done on different loading machine than other tests.



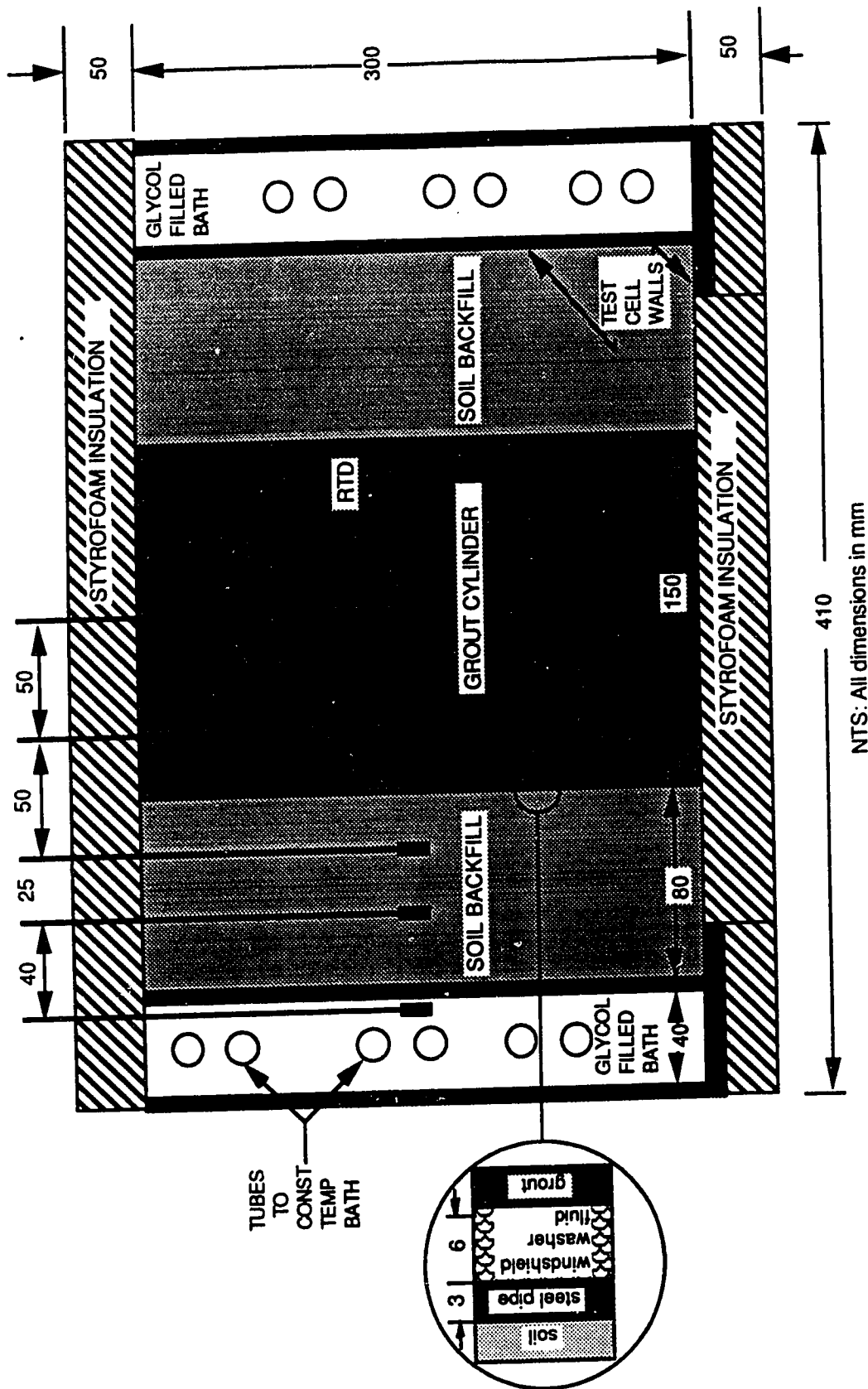


Figure 4.2: Constant temperature bath cell (CTBC)

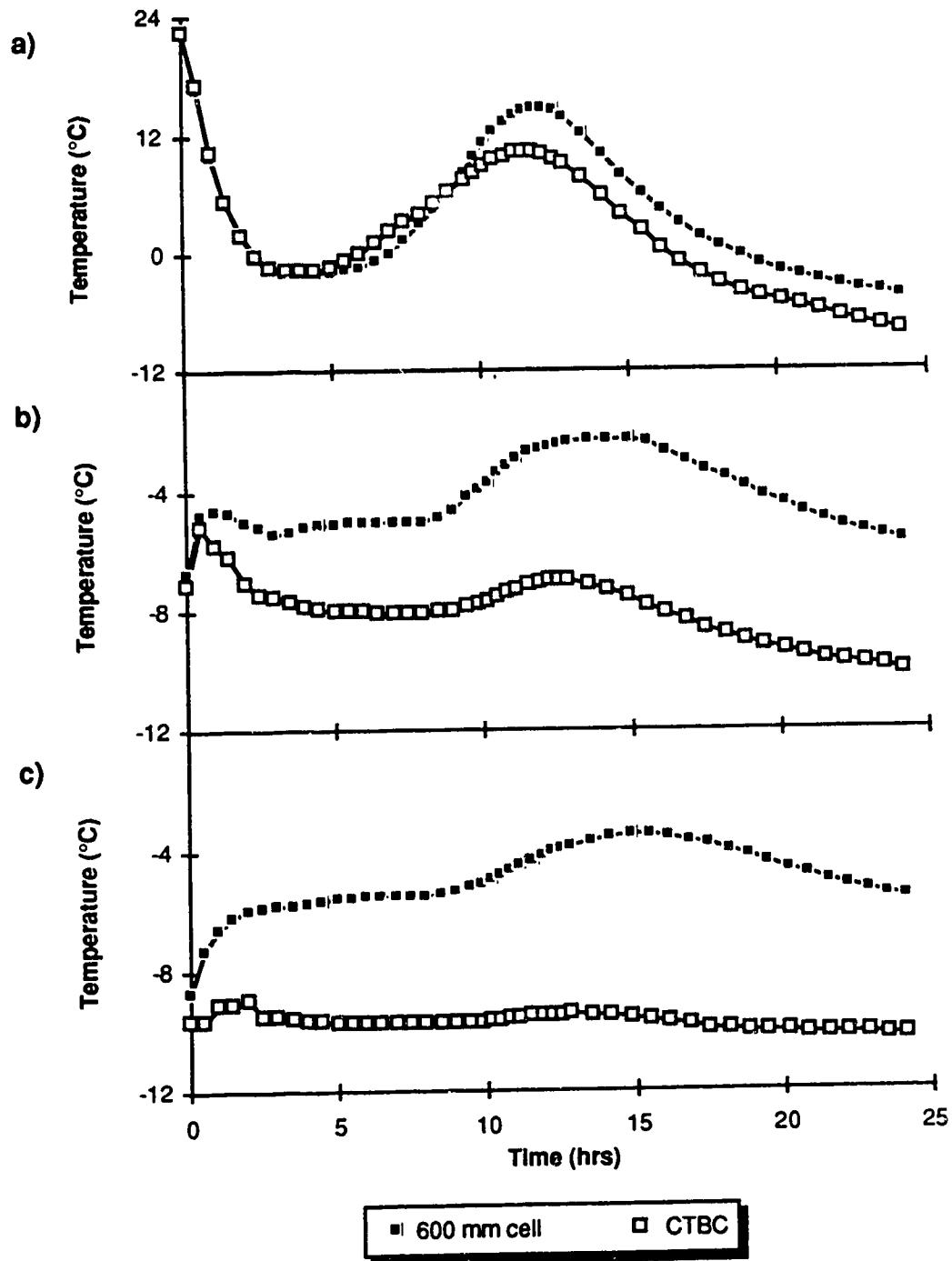


Figure 4.3: Comparison of the temperatures in two the different cells during curing of grout, Mix I-A  
a) center of grout cylinder  
b) in soil 25 mm from grout cylinder edge  
c) 100 mm from grout cylinder edge (600 mm cell) and in bath (CTBC)

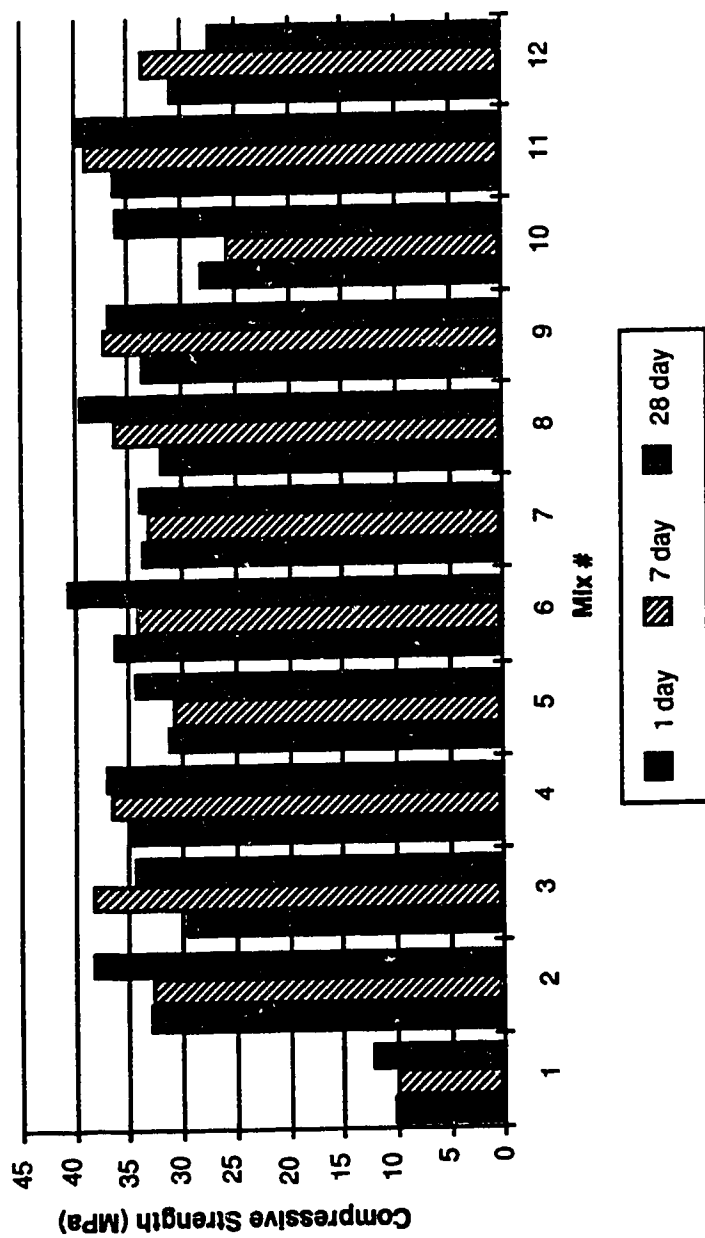


Figure 4.4 Cylinder compressive strengths for different mix designs

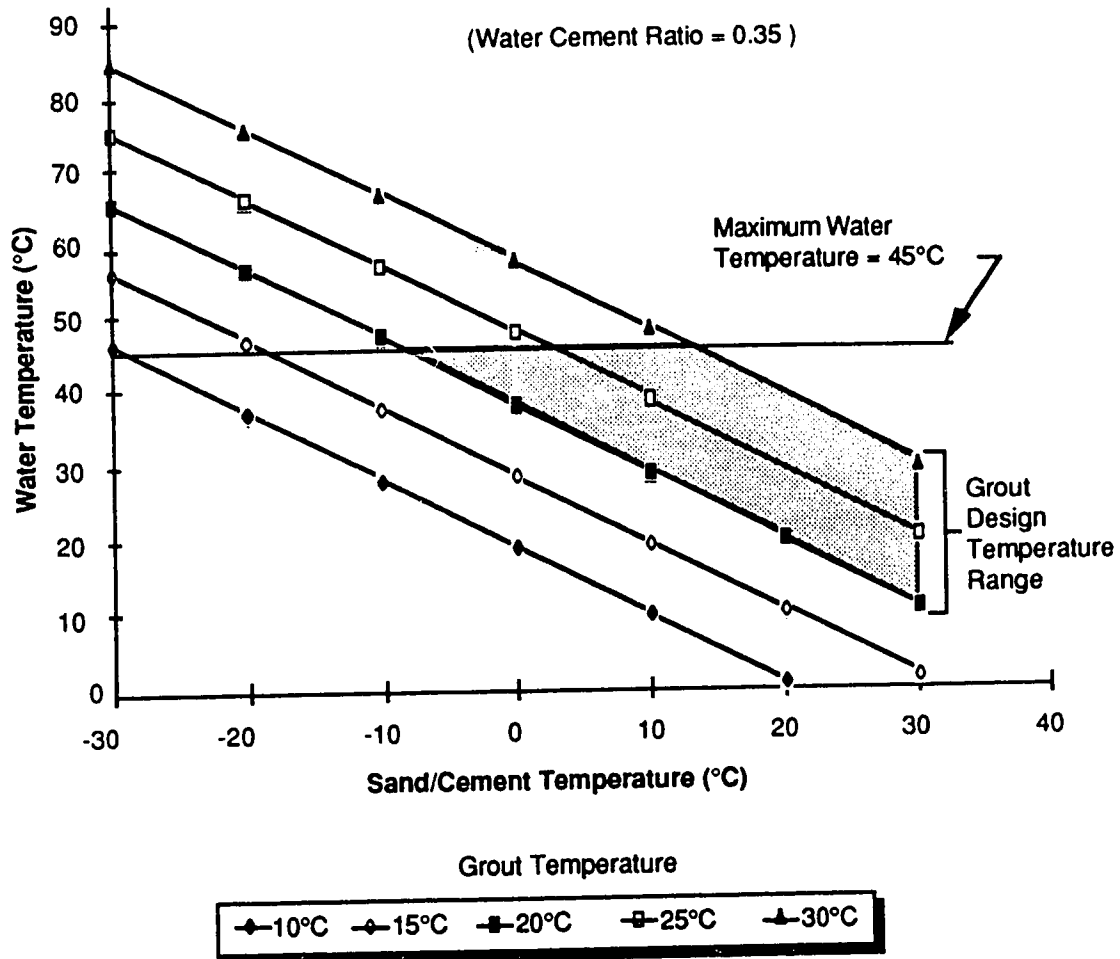


Figure 4.5: Guideline to determine mixed grout temperature for specified water and dry component temperatures



## **5. STRENGTH AND DEFORMATION BEHAVIOUR OF MODEL ADFREEZE AND GROUTED PILES IN SALINE PERMAFROST**

### **Introduction**

The presence of dissolved solutes in the pore water of permafrost is known to reduce its strength and increase its time dependent deformation under a constant stress. In addition the bond formed between piles and the frozen soil, known as the adfreeze bond, is dramatically reduced in the presence of saline pore fluid. These phenomena have caused a number of foundation problems in Arctic communities because the distribution and mechanical properties of saline permafrost are poorly understood.

Field load tests of piles with different surfacetreatments and backfills in a dense saline till conducted for the Short Range Radar program for the Department of National Defence showed significant increases in the short-term load carrying capacities when a cementitious grout was used as a backfill material, rather than a sand slurry. Sand blasting of the pile surface to remove the coating applied during manufacturing of the pipe was also shown to increase pile capacities significantly (Biggar and Sego 1989) [Chapter 2].

In an attempt to better define the effects of soil salinity, and pile surface and backfill modification on pile performance, a model pile testing program was conducted at the University of Alberta. This paper reviews the factors pertinent to pile design and testing in saline frozen soils, and describes the results of constant displacement rate tests on model piles. A companion paper describes the results of a constant load testing program on model piles in saline frozen soils. By analysing the effects of soil salinity and pile configuration on the pile response, optimum design configurations for different soil conditions were examined.

### **Pertinent factors affecting pile capacity**

#### *Effect of salinity on soil strength*

Unfrozen water occurs in the void space of fine grained soils at temperatures colder than 0° C due to the adsorbed water surrounding the individual soil particles (Anderson and

Morgenstern 1973). It has become recognized that permafrost in some locations contain salts in the pore water which increases the unfrozen water content (Karpov and Velli 1968; Tsytoich et al. 1973; Gregerson et al. 1983; Nixon and Lem 1984; and Hivon 1991). The effect of dissolved solutes in the pore water on the strength and deformation behaviour of the frozen soil has only recently been studied.

Early reports of the effect of salinity on the behaviour of permafrost were published based upon Soviet experience. Tsytoich et al. (1973) proposed a classification system, and discussed the physical and mechanical properties of remoulded saline soil samples. Soil strengths were defined in terms of equivalent cohesion, determined from ball indenter tests<sup>2</sup>. They reported the greatest strength reductions were observed in sandy soils at low salt concentrations while less marked reductions in strength were observed for soils with appreciable fines content since increases in solute concentration reduced the ice-cement strength more acutely than the cohesion. Velli et al. (1973) discuss the effects of saline permafrost on foundation performance at various locations in the USSR, and review laboratory results pertaining to soil freezing point depression, settlement, and strength.

Unconfined compressive strength and deformation behaviour of frozen saline sand were appreciably influenced by increased saline pore fluid concentration in a study by Sego et al. (1982), resulting in weaker and more compliant performance. Work by Ogata et al. (1983) corroborated these observations and went on to relate the compressive strength of three different saline frozen sands to the percentage of unfrozen water. This relationship was supported by the work of Nixon and Pharr (1984) for Prudhoe Bay gravels and Pharr and Merwin (1985) for Ottawa sand.

For cohesive soils Ogata et al. (1983) observed that the relationship between unfrozen water content and unconfined compressive strength was valid for individual soil types but could not be applied to unify the behaviour of different soil specimens. A

---

<sup>2</sup>Discussed in Chapter III of Tsytoich (1975).

relationship developed between the thickness of the unfrozen film and the unconfined compressive strength was more universally applicable.

Creep strains in alluvial sand observed by Ogata et al.(1983) increased dramatically with increasing salinity from 0 to 10 ppt. In fine-grained saline soil Nixon and Lem (1984) showed that increases in uniaxial strain rates of 10 to 100 times may occur for salinities near that of sea water at temperatures applicable in foundation engineering.

In summary, at a specified temperature the unfrozen water in the pore space of frozen soils increases with the addition of dissolved solutes. The greatest strength reduction is observed in cohesionless soils at low values of salinities ( $S < 10$  ppt) due to the loss of cohesion between the ice and the soil grains. Strength reduction is less pronounced and more gradual in cohesive soils where unfrozen water is already present in the form of adsorbed water. Time dependent soil deformation under constant stress is increased many times by the presence of solutes in the pore fluid. Thus piles installed in saline frozen soils will have considerably reduced load carrying capacity due to the susceptibility of the surrounding soil to time dependent deformation.

#### *Effect of salinity on adfreeze bond strength*

Berenger et al. (1985) examined the effect of temperature, salinity and surface area on the adfreeze bond strength of ice to clean and corroded steel plate using constant displacement rate loading. Multiple linear regression indicated that the bond strength was most greatly affected by the temperature and secondly by the salinity. The adfreeze bond strength of saline ice to steel (Makkonen and Lehmus 1987) decreased rapidly at salinities less than 10 ppt after which it became nearly constant at approximately 10% of the strength for fresh water ice. This reduction in strength was attributed to the formation of a liquid film at the ice/steel interface thereby reducing the effective contact area.

Based on the results of laboratory model pile tests, direct shear tests, and field pile load tests Karpov and Velli (1968) recommended that the adfreeze bond strength specified for non-saline soils be reduced by 50%, 75% and 90% for soils with a salinities of 5, 10,

and 15 ppt respectively. Results of field pile load tests in saline suglinok soils (clayey silt,  $PI \approx 17\%$ ) and silts with salinities of up to 15 ppt at temperatures between  $-1^{\circ}$  to  $-5.5^{\circ}$  C are described by Velli et al. (1973). Bond strengths were reduced by approximately one-half for soil salinities of 5 ppt and by two-thirds at 11 ppt. At salinities of 15 ppt no ice bonding was observed at a temperature of  $-4.5^{\circ}$  C. The greatest reduction in bond strength was observed at low values of salinity.

Time dependent deformation of piles in saline soils has been examined by Nixon (1988), Hutchinson (1989), and Miller and Johnson (1990). Results of field pile load tests at Clyde River, analysed by Nixon (1988), indicated that steel pipe piles backfilled with a soil-slurry of saline *native* soil cuttings (salinities of 10 to 20 ppt) had capacities of approximately two thirds that expected for adfreeze piles with a fresh water soil slurry backfill. Observed pile settlement rates were more than ten times greater than the normal allowable rates and approximately equal to rates expected for soil with salinities of approximately 35 ppt, based on previously conducted tests on saline soil and theoretical considerations. Hutchinson (1989) performed constant load tests on model piles in a silty sand at various salinities and temperatures. Reductions in pile capacity were approximately 60% and 85% at soil salinities of 5 and 10 ppt respectively at temperatures of  $-5^{\circ}$  and  $-10^{\circ}$  C. Miller and Johnson (1990) document a case history of excessive pile foundation settlement rates in permafrost with salinities as high as 60 ppt in Barrow, Alaska. Excessive pile settlements were arrested by placing insulation on the ground surface to reduce the warming effect of increased temperatures during the summer on the soil surrounding the piles.

In summary the strength of the bond between frozen soils and the steel pile surface is dramatically reduced by the presence of dissolved solutes in the soil pore water. It appears that a film of unfrozen water may form at the interface reducing the effective frozen bond area and/or reducing the strength of the ice which has bonded. Pile load carrying

capacities are reduced by at least 50% at salinities as low as 5 ppt, by 60% to 75% at 10 ppt, and by as much as 90% at 15 ppt.

#### *Effect of soil temperature*

It is well documented that reduction of the temperature of a frozen soil increases the strength and decreases the time dependent deformation when all other variables are maintained constant (Vyalov 1959; Sayles 1968; Sayles and Haines 1974; and Parmeswaran 1980) due to the reduction of unfrozen water and the increased cohesion of the ice. Although many authors have used the theory of rate processes to describe time dependent deformation in ice and frozen soil, Mellor (1979) points out that this relationship in ice is highly non-linear at temperatures warmer than  $-10^{\circ}\text{C}$ , which is the range most applicable to foundation engineering. Hence the activation energy must be expressed as a function of temperature. Another relationship which has received wide application is based on work done by Vyalov (1959) which relates strain to temperature ( $T+1$ ) as a simple power law (Sayles 1968; Nixon and McRoberts 1976; Morgenstern et al. 1980; and Sego and Morgenstern 1983).

The relationship between unfrozen water and temperature in saline soils and ice is described in detail in Ogata et al. (1983) and Hivon and Sego (1990). Generally, ice crystals are formed of fresh water excluding impurities, such as salt ions, from the pure crystalline ice structure into the remaining unfrozen water. As the temperature decreases, the salt ions are excluded into the remaining unfrozen brine solution further depressing its freezing point. This process continues until the pore solution becomes a matrix of ice crystals and salt ions with no liquid brine at the eutectic temperature, which for a sodium chloride solution is  $-21.3^{\circ}\text{C}$ . This relationship is illustrated in the phase diagram for an NaCl solution shown in Figure 5.1.

The strength and deformation behaviour of piles is significantly affected by the temperature of the surrounding soil. At temperatures near the freezing point of the pore water, adfreeze bonds are weak and the soil is highly susceptible to time dependent

deformation. A summary of the variation of adfreeze bond strength with changes in temperature in non-saline frozen materials is reported in Weaver and Morgenstern (1981), and in saline permafrost reported in Velli et al. (1973). The effect of temperature on the time dependent deformation of piles in non-saline soils is shown in Weaver and Morgenstern (1981), and in saline soils in Nixon and Neukirchner (1984).

#### *Effect of pile surface*

The effect of pile surface roughness on the strength of the adfreeze bond has been studied by many authors.

Velli et al. (1973) suggest that the adfreeze bond strength specified in the Soviet codes be multiplied by 1.0 for rough concrete and wooden surfaces and by 0.75 for metal piles. Weaver and Morgenstern (1981) recommended that the adfreeze bond strength be related to the long-term cohesion through a coefficient 'm' by the expression:

$$\tau_a = m c_{lt} \quad (5.1)$$

where  $\tau_a$  is the adfreeze bond strength and  $c_{lt}$  is the long-term cohesion. The recommended values of 'm' are 1.0 for corrugated steel pipe, 0.7 for untreated wood, and 0.6 for steel and concrete.

The results of constant displacement rate model pile tests conducted by Parmeswaran (1978) showed the highest bond strengths measured were for untreated wood, followed by concrete ( $\approx 55\%$ ), and sandblasted steel ( $\approx 50\%$ ). When pile surfaces were sandblasted, Sego and Smith (1989) observed an increase in the adfreeze bond strength of approximately 100% for model piles in sand, and Biggar and Sego (1989) observed an increase of more than 300% during field pile load tests.

The use of lugs or corrugations on pile surfaces in field tests has been reported by Long (1978), Thomas and Luscher (1980), and Biggar and Sego (1989). Andersland and Alwahhaab (1983) examined the effect of lugs on model piles. Generally the failure mechanism becomes one of crushing or compressive failure of the frozen soil ahead of the

lug as the pile displaces. Hence the pile capacity is dependent on the shear strength of the backfill rather than the adfreeze bond strength between the pile and the backfill.

Berenger et al. (1985) observed that the adfreeze bond strength of saline ice to corroded steel plates was markedly higher (5 to 10 times) than that observed with smooth plates. Saeki et. al. (1986) relate the adfreeze bond strength of sea ice to various materials to the ratio of the mean wave height of the surface irregularities, showing an increase in strength with increasing wave height. Weaver and Morgenstern (1980) suggest that for smooth surfaces (average asperity height (CLA)= 0.0025 mm), air is trapped between the pile material and the ice reducing the effective contact area and inhibiting mobilization of the shear strength of the ice. A rougher plate surface (CLA=0.125 mm) resulted in an increase in bond strength to ice of approximately 3.5 times. Tests of the smooth plates with frozen sand and frozen silt resulted in greater adhesive shear strength than that of ice. Makkonen and Lehmus (1987) suggest that the adfreeze bond of saline ice to various materials was affected by the porosity at the surface of contact. Their results indicated that a liquid brine film formed at the interface between the ice and the material is absorbed by more porous material (such as rough concrete or chloride-polymer paint), whereas it is retained at the interface for plain steel. This retention of the liquid film resulted in greatly reduced adfreeze bond strengths.

Reductions in bond strengths of 50% between ice and sandblasted steel model pipe piles were observed by Frederking and Karri (1983) when Inertia 160 marine coating was applied. Parmeswaran (1978) observed reductions of approximately 55% in bond strengths between Ottawa and B.C. fir when creosote preservative was applied to the wood.

Thus in ice poor soils where adfreeze bond strengths may govern design rather than the time dependent deformation (Weaver and Morgenstern 1981), increases in pile capacity may be realized by roughening the interface between the pile and the backfill. Conversely any coating on the pile surface may reduce the adfreeze bond capacity.

### *Performance of grout backfill*

The implications of using a grout as a backfill material for piling in permafrost are discussed in detail in Biggar and Sego (1990) [Chapter 4], Sego and Biggar (1990), and Biggar et al. (1991). Details of the thermal performance of the grout mix design used in this study are contained in Biggar and Sego (1990) [Chapter 4].

Briefly, it is essential that the grout form an adequate bond to the pile surface and develop a shear strength exceeding that of the *native* soil such that shear failure occurs within the *native* soil, beyond which no increase in pile load carrying capacity is possible. Further, the thermal performance of the grout must not cause detrimental effects to the surrounding frozen *native* soil.

### *Size effects*

Vyalov (1959) examined "conditions for similarity" for piles of various dimensions by performing pull-out tests on wooden model piles with various length/diameter ( $l/d$ ) ratios. Experimental results showed that as pile diameter increased, failure stresses decreased, even when the  $l/d$  ratios were maintained constant. Increasing the pile diameter by a factor of 4 decreased bond strength by a factor of approximately 1.8. The reduced strength approached an asymptotic value at pile diameters of approximately 150 to 180 mm. A mathematical expression was developed for the similarity of visco-plastic flow for the axi-symmetrical situation, but the determination of the parameters was too complex to be of practical use. It was suggested that with an accumulation of experimental data it would eventually be possible to develop conversion factors to extrapolate laboratory results to full-scale pile design.

Nixon and McRoberts (1976) developed an expression for pile displacement velocity based upon work by Johnston and Ladanyi (1972). The formulation assumes that the constitutive behaviour of the soil may be described by a simple power law, that the pile displaces at a constant rate (secondary creep), and that the deformation of the frozen ground around the pile shaft is idealized as shearing of concentric cylinders. Their relationship



supports Vyalov's observations, indicating that doubling the pile diameter would reduce allowable shaft stress by approximately 30%. Frederking (1979) and Saeki et.al. (1986) also report a reduction in adfreeze bond strength with increasing pile diameter in tests of piles frozen into an ice sheet.

Thus it may be expected that the results of tests on model piles in this study will show reductions in load carrying capacity as the pile diameter increases. If this phenomena is observed, corrections must to be made to extrapolate the model test results to field conditions.

#### *Effect of freezeback pressures on adfreeze piles*

The solution of borehole relaxation to relieve pressures generated during freezeback of a slurry backfill have been investigated by Weaver (1979) and Ladanyi (1979, and 1988). The results of the two authors vary considerably. The solution by Ladanyi (1988) using a "Modified Reference Stress Method" suggests that lateral pressures in ice and Ottawa sand should relax rapidly, falling to less than 1% after one day. The solution by Weaver (1979) on the other hand suggests that in Hanover silt at temperatures of  $-1^{\circ}\text{C}$  radial stresses will dissipate after approximately 500 hours, but at  $-5^{\circ}\text{C}$  approximately 40 days are required. Due to the the uncertainties surrounding the development and dissipation of lateral pressures due to the freezing of the slurry backfill, efforts must be made to measure directly their magnitude and effect on the tests conducted in the test program.

### **Experimental procedure**

#### *Test cell*

A schematic diagram of the test cell is shown in Figure 5.2. The cell consisted of a bucket with two concentric chambers. The *native* soil sample was placed in the inner chamber and ethelene glycol was placed in the outer chamber. Ethelene glycol from a constant temperature bath was circulated through copper coils located in the outer chamber in order to maintain the soil mass at a constant temperature (within  $\pm 0.2^{\circ}\text{C}$ ). During consolidation and freezing of the *native* soil an aluminum baseplate was inserted and

clamped into the bottom of the cell. During load testing a PVC baseplate replaced the aluminum baseplate in the bottom of the cell, and a 50 mm thick STYROFOAM cap was placed on top of the soil to further reduce the effects of cold room temperature fluctuations on the sample.

To facilitate the testing of three different size piles, PVC baseplates with three different sized holes were used, as shown in Figure 5.3. The hole in the baseplate was slightly larger in diameter than the hole cored into the soil to allow failure to occur at either the pile/backfill or the backfill/*native* soil interface. When the backfill material was placed into the sample, the hole in the baseplate was filled with a removable plug. A circular recessed notch was machined into the centre of the removable plug to ensure that the pile was installed in the center of the soil mass and to maintain it in position during the placement of the backfill.

#### *Sample preparation*

The *native* soil used in these experiments was identical to that used in a previous model pile study (Hutchinson 1989) and in a study on the uniaxial strength of saline soils (Hivon 1991) conducted at the University of Alberta (U of A). The particle size distribution (shown in Figure 5.4) was designed to be similar to silty sands observed in a number of Arctic communities.

Equal portions by weight of a dried locally obtained mortar sand and Devon silt were placed alternately in 20 litre pails. A specified volume of pure Sodium Chloride (NaCl) brine solution was added as the soil was placed in the pails, the mixture was covered and left to soak for a minimum of 24 hours. After soaking, the soil was mixed in a 0.057 m<sup>3</sup> concrete mixer for approximately 30 minutes then passed through a 6 mm sieve before being placed into the test cell in preparation for consolidation.

To enhance drainage during consolidation, prior to placing the soil in the cell, a perforated PVC tube 25 mm in diameter wrapped in filter paper was placed vertically in the centre of the cell, and filter paper was placed on the bottom and around the perimeter of the

cell. The soil was placed to a height of approximately 275 mm, covered with two layers of filter paper, and a 25 mm thick layer of well graded gravelly sand was placed on top of the filter paper to provide a free draining upper surface and a stable base for the top loading cap. The soil was consolidated under a stress of 80 kPa in a room maintained at a temperature of approximately  $+4^{\circ}\text{C}$  for a period of time sufficient to ensure at least 95% consolidation (a minimum of 24 hrs). The load was applied via an air actuated Bellofram to a 25 mm thick aluminum loading cap which fit closely inside the test cell. Consolidated sample heights were typically  $245 \pm 5$  mm.

Immediately after consolidation the upper sand layer was removed and the cell was placed onto a freezing plate. Liquid Nitrogen was circulated through the freezing plate and the sample was frozen from the bottom up in approximately six hours. When freezing was complete a thin layer of distilled water was sprayed onto the sample top surface to prevent sublimation of the sample moisture, the sample was placed in a cold room at  $-25^{\circ}\text{C}$  and remained there until it was cored for the placement of a model pile.

Piles with either untreated or sandblasted surfaces were used in the testing program. The pile surface profiles and centre line average (CLA) roughness measurements were obtained using a Taylor Hobson 'Talysurf 4' surface measuring instrument. The pile centre line average roughnesses are tabulated in Table 5.1. The untreated piles were seamless C1020 steel pipe with a wall thickness of 6.3 mm, and were used in the condition in which they were received from the manufacturer. The sandblasted piles had their surface prepared by sandblasting in a Clemo mini hone dry blast cabinet using quartz sand. The sandblasting initially stripped away the surface treatment on the piles and roughened the surface to a nearly uniform finish. Subsequently the sandblasting removed any oxidation from the previous test and provided a similar surface texture throughout the study.

To test piles of three different diameters with the same test specimen, the smaller piles were overcored with a larger core barrel. Pile diameters were  $2/3$  of the hole diameter, thus piles 33, 63, and 100 mm in diameter were placed in 52, 102, and 152 mm diameter

holes respectively. The 52 mm holes were cored with a diamond core barrel (similar to those used to core concrete) using chilled, extra dry air as a flushing fluid. Liquid Nitrogen was sprayed on the soil ahead of the core barrel to keep the test specimen frozen thereby inhibiting the warmed cuttings from clogging around the core barrel, freezing the barrel into the test specimen. The 102 and 152 mm holes were cored using a CRREL core barrel; a flighted core barrel mounted on a gas powered earth auger. The hole walls were subsequently wire brushed to remove any of the finer soil which became smeared on the hole wall. When a grout backfill was used the hole wall was usually notched (with a chisel and hammer), thereby more closely simulating anticipated field conditions of a rough hole wall. A photograph the grout surface after testing (Plate 1) illustrates the result. Notching the hole wall was deemed necessary after preliminary tests indicated that a plane of weakness developed along the smooth interface between the soil and the grout created by the laboratory coring method used, and such conditions would not likely occur during field placement conditions. Notching was not deemed necessary when a soil slurry backfill was used, as there there was no evidence of a weak interface between the backfill and the *native* soil.

Four different backfill materials were used:

1. a slurry of a clean sand (Sil #7) and distilled water;
2. a slurry of cuttings of the *native* soil;
3. ice; and
4. a cementitious grout based on high alumina cement.

The temperatures of the pile and backfill were 20°C when they were placed, with the exception of *native* soil cuttings and ice which were placed at temperatures of approximately +4° C. The temperature of the test specimen was maintained constant (-5° C) while the backfill was freezing (or curing) by using a constant temperature bath as described above. The soil slurries were placed only in the annulus between the pile and the hole wall. The grout, however, was also placed inside the centre of the pile due to the

requirement to provide a sufficient thermal mass (of grout) to ensure proper curing of the grout between the pile and the *native* soil. The thermal performance of the grout is discussed later.

The clean sand backfill was placed at a moisture content of 19% and tamped in layers approximately 50 mm thick using a 6 mm diameter steel rod. The grout was poured into the hole firstly, then the pile was lowered into the grout and aligned into the centering notch in the base plate. The *native* soil slurries (cuttings) consisted of material which remained after the test specimen had been prepared, and was maintained in a moisture room until required. The slurry of cuttings was placed in the same method as the sand slurry. The ice backfill consisted of chilled distilled water which was poured into the annulus after the pile had been installed.

#### *Loading*

The apparatus consists of a hydraulic jack mounted onto a load frame. The jack was connected to a Jeffery Pump which was adjusted to provide a jack ram displacement rate of  $12 \pm 0.2$  mm/day. Two loading frames were used. For lower loads during the initial portion of the program a frame consisting of reinforced 150 mm wide channels welded to form a hollow rectangle was used. The jack was suspended from the top member of the frame and pushed downward directly onto the pile, while the test cell remained stationary. For later tests and higher applied loads a much stiffer frame was used in which the jack was mounted onto the bottom plate of the frame, as shown in Figure 5.5. Thus the test cell rested on the jack and was displaced upward at a constant velocity while the top of the pile remained stationary.

Loads were recorded using load cells with an error of less than 0.25%. A 19 mm diameter ball bearing was placed between the load cell and the pile load cap to ensure axial load application to the load cell. Displacements were monitored using 24 volt Direct Current Differential Transducers (DCDTs) with 50 or 100 mm of travel, capable of recording displacements with an accuracy exceeding 0.02 mm. The DCDT body was mounted to a

magnetic base and the tip of the core rested on an 'L' bracket which was securely clamped to either the pile or the jack ram. Temperatures were measured using Resistance Temperature Devices (RTDs) which were calibrated at 0.0° C in a distilled water ice bath. Recorded temperatures were accurate to  $\pm 0.1^{\circ}$  C. Strains were recorded (when applicable) using bondable strain gauges capable of recording strains with an accuracy of  $1 \times 10^{-6}$  mm/mm. A Fluke 2240 data acquisition system connected to an Operand XT computer recorded the output from the transducers measuring loads, displacements, temperatures and strains (if required). Output from the electronic transducers were recorded at 5 minute intervals onto floppy disks for subsequent analysis.

#### *Determination of soil properties*

After the largest pile had been tested the *native* soil mass was removed from the test cell and wedges of the sample were cut from the frozen soil mass using a gas powered cutoff saw with a fibre masonry blade. From this large wedge smaller specimens, approximately 30 mm cubed, were cut from the centre of the sample using a table mounted cut-off saw with a diamond blade. Sample density was determined in accordance with ASTM Standard D 1188-83, using a paraffin-coating technique for the frozen samples, and averaging the measurements from two samples. Salinities of the specimens were measured on both the unconsolidated (mixed) and consolidated (frozen) *native* soil. Salinity specimens were double-bagged in plastic bags and maintained in a moisture room at  $+4^{\circ}$  C until tested. The saline solution was extracted from the specimen using a specially designed press and collected with a syringe. The syringe was placed with the needle pointing upwards to allow any suspended soil particles to settle, after which a few drops of solution were placed on an AO Model 10419 Hand Refractometer which enabled direct reading of the salinity to  $\pm 1$  ppt. The measured sample densities and salinities are listed in Table 5.2.

## Results

### General

The test results were analysed in terms of shear stress at the pipe pile surface,  $\tau$ , versus the measured displacement,  $\delta$ . Twenty two test specimens, each with piles of three different diameters were used to examine the effects of soil salinity, pile surface, backfill material, and temperature on the strength and deformation behaviour of model piles. The test results are summarized in Table 5.3 [and are plotted in Appendix D] where the test number indicates firstly the specimen number followed by the pile diameter. Reference to the test salinity in the following paragraphs refers to the salinity of the *native* soil only, unless otherwise stated.

The plots of  $\tau$  versus  $\delta$  generally show an initial linear portion, which is believed to describe the behaviour during which the ice matrix within the *native* soil was intact, followed by a curvilinear portion which describes the behaviour after the ice matrix was ruptured and the resistance of the soil matrix became mobilized. In some tests the adfreeze bond between the pile and the backfill material failed resulting in a dramatic reduction in pile capacity to a residual value. In the remaining tests the  $\tau$  versus  $\delta$  behaviour was strain strengthening until the termination of the test. Generally, the tests were terminated after approximately 8 mm of displacement, which was the limit of the Jeffery pump.

To examine the reproducibility of test results nine replicated tests were conducted with various salinities, temperatures and backfills [presented in Appendix D]. With the exception of one test at 10 ppt salinity and  $-5^{\circ}\text{C}$  (#44-102), the loads at failure were within 3% to 15% and in all instances the  $\tau$ - $\delta$  response was similar. Hence the experimental procedure provided reproducible results.

The performance of the two different loading frames was compared for 5 tests, all with sand backfill, at a nominal temperature of  $-5^{\circ}\text{C}$  with salinities of 0 or 10 ppt. The  $\tau$ - $\delta$  response of the tests were similar, however the smaller frame applied load to the pile at a rate approximately 1/2 of that applied by the large frame. This slower loading rate did not

appear to significantly affect the test results. The post peak–strength behaviour in the two frames differed in that tests conducted in the large frame experienced little post peak–strength displacement and the load decreased gradually to a residual value, whereas tests conducted in the small frame exhibited greater displacements and a greater reduction in pile capacity due to the release of the strain energy stored within the smaller frame.

The test program examined the effects of:

1. pile size;
2. *native* soil salinity;
3. backfill material;
4. pile surface treatment; and
5. *native* soil temperature.

#### *Effect of pile size on pile response*

For the 21 test specimens examined, excluding a few tests which encountered equipment difficulties, as the pile diameter increased greater displacements were required to mobilize a specified shear stress, as illustrated in Figure 5.6. Test results did not however consistently show a reduction in adfreeze bond strength,  $\tau_a$ , between the sand backfill and the pile with increasing pile diameter. Figure 5.7 shows that although in some instances  $\tau_{a33} > \tau_{a63} > \tau_{a102}$ , in other instances  $\tau_{a33} \approx \tau_{a63} > \tau_{a102}$ , and usually  $\tau_{a33}$  and  $\tau_{a63}$  were within 10% of their respective mean values.

As suggested in Nixon and McRoberts (1976) the pile displacements were normalized to the pile radius and the stress versus normalized displacement,  $\tau$ - $\delta_n$ , behaviour was examined. It should be noted that for this analysis the radius of the structural member (i.e. the pile) was used, not that of the hole. A typical plot illustrating the results for a sand backfilled pile is shown in Figure 5.8a. The results of this analysis for sand backfilled piles, summarized in Figure 5.9, revealed that as the unfrozen water content of the *native* soil,  $\theta_u$  (from Hivon 1991) increased, the normalized displacement to failure,  $\delta_{nf}$ , increased. The best fit linear least squares regression relationship defined from these



results may be expressed as:

$$\delta_{nf} = -0.0601 + 0.0276 \theta_u \quad (5.2)$$

within the limits of the unfrozen water in the soils tested, where  $\delta_{nf}$  is in units of (mm/mm) and  $\theta_u$  is in units of (% vol.). The scatter in the values of  $\delta_{nf}$  increased at higher values of  $\theta_u$  however. Thus although the above relationship may be proposed as a general guideline for limiting displacements to failure, the scatter of  $\delta_{nf}$  at higher values of  $\theta_u$  suggest that the relationship be used with caution.

The response of grout backfilled piles differed significantly. The cementitious bond between the grout and the pile did not fully develop for some of the 33 mm piles (as discussed later) thus the piles failed in a brittle manner. The failure of the grout/pile bond occurred at greater normalized displacements than for comparable piles backfilled with sand as shown in Figure 5.8a. Generally the normalized displacements may be described by:

$$\delta_{ngrout} = \alpha \delta_{nsand} \quad (5.3)$$

where  $\alpha \approx 3$  for specimens with salinities of both 0 and 10 ppt at  $-5^\circ \text{C}$ .

The  $\tau$ - $\delta_n$  relationship for piles which displayed strain strengthening behaviour was similar for all pile sizes in tests conducted at  $-10^\circ \text{C}$  as shown in Figure 5.8b. The response of tests conducted at  $-5^\circ \text{C}$  however were similar only over the initial linear portion of the plot as shown in Figure 5.8c. At the onset of non-linear behaviour generally  $\tau_{33} > \tau_{63} > \tau_{102}$  at the same value of  $\delta_n$ . Thus the examination of the behaviour of grout backfilled piles in terms of normalized displacements was of limited value during this test program.

#### *Effect of native soil salinity on pile response*

Because some piles failed in a brittle manner at small displacements and others behaved in a strain strengthening manner, in order to evaluate the effect of *native* soil salinity on pile capacity, the values of  $\tau$  at 1 mm displacement are tabulated in Table 5.4 and shown graphically in Figure 5.10.

Sand backfilled piles in *native* soil with salinities of 0 and 10 ppt failed when the adfreeze bond strength of the pile was exceeded, whereas the shear strength of the *native*

soil at salinities of 20 and 30 ppt was so low that the adfreeze bond capacity was never achieved. Reductions in capacity of 25% to 55%, 80%, and 95% were observed at 1 mm displacement when the *native* soil salinity was increased to 10, 20, and 30 ppt respectively (shown in Table 5.4). Reduced capacities at specified values of displacement were also observed when stress was plotted against normalized displacement, though the reductions were less pronounced.

The reduction in the adfreeze bond strength ( $\tau_a$  in Figure 5.7) observed when the *native* soil salinity was increased from 0 to 10 ppt is believed to be a consequence of a reduced local displacement rate at the pile/backfill interface due to the additional displacement which occurred in the *native* soil rather than due to salt migration into the backfill. This is supported by salinity measurements conducted on samples of the sand backfill 3 mm from the *native* soil, and at the pile/backfill interface, which did not reveal any measurable salinity within the backfill.

In summary, for conditions when the pile surface was not in contact with saline soil, increases in the salinity of the *native* soil is shown to dramatically reduce its shear strength resulting in concomitant decreases in pile capacity. At salinities of up to 10 ppt however, the capacity of sand backfilled piles was still governed by adfreeze bond capacities.

The strength values presented in Figure 5.10 for piles backfilled with grout are similar to those for piles backfilled with sand with two notable exceptions. The capacity of the 33 mm diameter pile at 0 ppt is considerably greater for the grouted pile than that for the sand backfilled pile. This is because the sand backfilled pile actually failed at a displacement of 0.7 mm, whereas the pile backfilled with grout failed at a displacement of 1 mm. In addition the hole for the grouted pile was enlarged to 60 mm from 52 mm due to difficulties during sample preparation. Accounting for these two factors the comparable shear stress for the grouted pile at 0.7 mm displacement would be 1036 kPa, which compares more favourably to the value of 888 kPa obtained for the sand backfilled pile. The capacity of the

33 mm diameter grouted pile at 20 ppt is considerably less than may be expected because of a smooth hole wall adjacent to the grout (discussed in the next section).

*Effect of backfill material on pile capacity*

Four different backfill configurations were tested with *native* soil salinities of 0 and 10 ppt at -5° C:

1. Sil #7 sand slurry;
2. Ciment Fondu based grout with a roughened hole wall;
3. Ciment Fondu based grout with a smooth hole wall; and
4. a slurry of *native* soil cuttings.

During the testing program the pile behaviour when a grout backfill was initially used was weaker than expected. It was discovered that this behaviour was a result of a weak grout/*native* soil interface caused when the cored hole was left with a smooth wall. As a result the hole wall was roughened for all subsequent tests using grout backfill to more closely simulate anticipated field conditions, as detailed in the procedure portion of the paper. Subsequent reference to these two different backfill configurations will be as "smooth grout" and "rough grout" backfill.

Typical  $\tau$ - $\delta$  behaviour for the four different backfills in *native* soil with salinities of 0 and 10 ppt is presented in Figure 5.11a and b. The response of a pile with a rough grout backfill is seen to be nearly identical to that with a sand backfill until the adfreeze bond fails for the sand backfilled piles. The response of the piles with a smooth grout backfill was more compliant and developed approximately 20% less resistance. The reduction in capacity when cuttings were used as a backfill material was approximately 50% at 0 ppt and more than 80% at 10 ppt. The response when cuttings of 30 ppt were used is shown in Figure 5.11b. The backfill was predominantly unfrozen and unconsolidated at a temperature of -5° C resulting in a measured resistance of only 6 kPa.

A more detailed investigation was carried out for sand and rough grout backfilled piles only. In some instances the sand backfilled piles appeared to develop more resistance

at a specified displacement, however in these tests the temperature of the sand backfilled specimens were colder by 0.3° C or more. When the specimen temperatures were within  $\pm 0.1^{\circ}\text{C}$  the behaviour of the sand and rough grout backfilled piles was nearly identical until the adfreeze bond of the sand backfilled piles failed. The  $\tau$ - $\delta$  performance of sand and rough grout backfilled model piles tested under constant displacement rate conditions was then, for practical purposes, identical until the adfreeze bond of the sand backfilled pile failed, at which time the capacity of the rough grout backfilled piles was governed by the shear strength of the surrounding soil.

In summary, clean sand and rough grout backfilled piles behaved in a similar manner until the adfreeze bond failed for the sand backfilled piles. The use of silty sand (cuttings) backfill resulted in reduced pile capacity due to the unfrozen water in the backfill. This effect was dramatic at a backfill salinity of only 10 ppt, and when the salinity rose to 30 ppt the backfill was essentially unfrozen.

#### *Effect of pile surface treatment on pile capacity*

Tests on untreated model pipe piles were conducted only at a temperature of  $-5^{\circ}\text{C}$  in a *native* soil with no salinity (Test #7). The adfreeze bond strengths of the untreated piles are listed in Table 5.3 and shown graphically in Figure 5.7. Typical  $\tau$ - $\delta$  response is compared to a that of a sandblasted pile in Figure 5.12. Generally the capacities of the untreated piles were 35% to 45% of that resisted by the sandblasted piles.

Table 5.1 shows that there was marginal difference in surface CLA roughness between the sandblasted and untreated piles. Thus it may be assumed that the reduction in capacity observed for the untreated piles is due not so much to surface roughness effects but rather to the surface treatment processes which the pipe underwent during manufacturing.

#### *Effect of temperature on pile capacity*

A small number of tests were conducted at a temperature of  $-10^{\circ}\text{C}$  with grout and sand backfill in *native* soil with salinities of 10 and 30 ppt to examine the effect of

temperature on the response of piles in saline soils. In addition, equipment difficulties experienced during testing at  $-5^{\circ}\text{C}$  resulted in a small number of tests being conducted at temperatures between  $-6^{\circ}$  and  $-7^{\circ}\text{C}$ .

The effect of the temperature variation on  $\tau_a$  for sand backfilled piles is illustrated in Figure 5.7. At salinities of 10 ppt  $\tau_a$  increased by approximately 80% when the temperature was reduced from  $-5^{\circ}$  to  $-10^{\circ}\text{C}$ . An increase in  $\tau_a$  of approximately 15% was observed in test #29-102 when the temperature was reduced from  $-5^{\circ}$  to  $-6^{\circ}\text{C}$ .

The  $\tau$ - $\delta$  response for sand and grout backfilled piles at different temperatures is shown in Figure 5.13a and b respectively. The results of tests performed at  $-5^{\circ}\text{C}$  with no salinity are included for comparison because the unfrozen water content in the *native* soil under these conditions is similar to that at  $-10^{\circ}\text{C}$  and 10 ppt salinity, (Figure 5.9). The response of sand backfilled piles at  $-5^{\circ}\text{C}$  became strain strengthening at stresses of approximately 400 kPa, whereas at  $-10^{\circ}\text{C}$  the response was nearly linear until failure at 1266 kPa. The response of the piles in soils with similar unfrozen water contents is similar until the adfreeze bond was exceeded (at  $-5^{\circ}\text{C}$ ). Thus the effect of the lower temperatures on sand backfilled piles is seen to both increase the adfreeze bond strength between the backfill and the pile, and to reduce the deformations in the surrounding *native* soil mass.

Grout backfilled piles in *native* soil with salinities of 10 ppt tested at a temperature of  $-10^{\circ}\text{C}$  showed an increase in capacity of approximately 70% to 100% at displacements in excess of 1 mm. These piles also displayed similar behaviour for tests conducted with *native* soils of similar unfrozen water contents as discussed above.

The sand backfilled piles in *native* soil with salinities of 30 ppt in test #4 showed reductions in strength of approximately 90% at  $-5.2^{\circ}$ , 75% at  $-6.5^{\circ}$  and 70% at  $-7^{\circ}\text{C}$  compared to those observed at  $-10.3^{\circ}\text{C}$ . Because of the temperature variations experienced during test #4 (nominally  $-5^{\circ}\text{C}$ ), and the difference in pile diameters which were used for this comparison, these results are only offered as general observations.

Based upon the above discussion, Figure 5.14 shows the observed trend in pile capacity as a function of temperature for 63 mm model piles in saline soils. Stresses shown in the figure were obtained at an arbitrarily chosen pile displacement of 3 mm, and are the stresses at the backfill/*native* soil interface. In addition the values of stress obtained from 102 mm pile tests are included, and were adjusted (multiplied by 1.2) to account for the lower values of stress at a given displacement (as shown in Figure 5.6). It is emphasized that these data only reflect mobilized shear stress at 3 mm displacement for the test conditions encountered, and a simplified adjustment has been made to correct for pile diameter differences. Insufficient data are available to formulate a mathematical relationship defining the dependence of strength on temperature.

#### *Grout performance*

The curing performance of the grout differed depending on the pile size, resulting in two different types of pile behaviour. In the instances when the pore water in the grout was subjected to freezing, a different structure was observed in the grout matrix than was evident when no freezing took place. The properly cured grout was homogeneous, well bonded with no structural flaws. The grout which had been subject to freezing appeared to have a platey structure, though it was still strongly bonded and could not be separated or scraped with a knife. The results of compression tests on cylinders of grout which had been subject to such freezing conditions is discussed in Biggar and Sego (1990) [Chapter 4].

For the 33 mm diameter piles the pore water in the grout adjacent to the pile surface was subject to freezing as the grout cured so the full potential of the grout/steel bond was not realized. A typical grout curing temperature with time relationship for these conditions is shown in Figure 5.15a. To attempt to overcome this problem a neat grout (using only cement and water) was used rather than a sanded grout for the 33 mm diameter piles, however even this modification did not resolve the problem. Thus in certain circumstances as discussed above the bond between the grout and the pile failed.

The grout at the surface of the 63 and 102 mm diameter piles cured without experiencing freezing of the pore water so a stronger bond was developed. In no instances did the bond between the pile and the grout fail for these tests at shear stresses as high as 1500 kPa. The grout adjacent to the *native* soil was subject to freezing however, with observed thicknesses of 6 to 15 mm for the 63 mm piles and 0 to 3 mm for the 102 mm piles. Typical grout curing temperatures for a 102 mm pile are shown in Figure 5.15b. Failure of 63 and 102 mm piles with a grout backfill always occurred in the *native* soil. In no instances was shearing observed through grout which had been subject to freezing, at shear stresses of up to 900 kPa at the grout/ *native* soil interface.

One test (#23-63) was conducted to examine the strength of properly cured grout surrounding a #14 Dywidag threaded bar. The Dywidag bar had a nominal diameter of 48 mm, was installed in a 102 mm hole and a neat grout was used. The threaded bar was loaded in compression and a base plate with a 65 mm diameter hole was used to ensure that the failure surface occurred in the grout and not in the surrounding soil. The grout adjacent to the threaded bar was properly cured, and the grout failed by shearing at the outer edge of the threaded bar at a shear stress of approximately 4000 kPa.

Another noteworthy observation was that the grout "plug" in the centre of the 63 and 102 mm piles was usually easily removed after the test was completed. It appeared that the grout in the centre of the piles was subject to sufficient shrinkage that no bond was developed between the grout and the inside of the pipe. This was not the case however for properly cured grout on the outer portion of the pile where bond strengths as high 1500 kPa were observed without failure. It was also observed that the grout in the centre of the pile was brownish in color indicating that the grout had converted. The grout on the outside of the pile was greyish in color indicating that the grout had not converted.<sup>2</sup>

---

<sup>2</sup> Details on conversion of High Alumina Cements may be found in Neville (1975), and Biggar and Sego (1989).

### *Lateral pressures due to freezing of the slurry backfill*

As mentioned previously it is known that considerable lateral pressures may be generated along a pile due to the 9% increase in the volume of the water in the slurry backfill during freezing. To investigate the development (and dissipation) of such lateral stresses, strain gauges were installed to measure radial strains at midheight on the test cell wall for tests #18, 23, and 29 and on the pile for test #29. The measured radial strains were observed to be extremely sensitive to temperature variation due to the thermal expansion (contraction) of the cell and pile. As a consequence the data obtained during the placement and freezing of the backfill (when there was a considerable temperature variation in the sample) provided inconsistent results. When the sample temperature had stabilized approximately 8 hours after the backfill had been placed however, no significant change in the strains were observed for a duration of up to 3 days, indicating that no significant dissipation of lateral stresses had occurred.

After the soil slurry backfill had frozen, a layer of ice was observed on the top of the backfill indicating that water had been ejected from the backfill during freezing. This phenomena would negate or at least reduce any buildup of lateral pressure. Further, as discussed previously the stress-displacement behaviour of the grout and sand backfilled piles under the same conditions was nearly identical until the adfreeze bond between the pile and the frozen slurry failed. Assuming that the grout did not expand as it cured and thus no additional lateral stresses were generated, it follows that no significant lateral stresses were developed when the sand slurry backfill froze.

Thus although it was not possible to measure lateral stresses generated during slurry freezeback, based upon the above observations it is postulated that if such stresses developed, they were of insufficient magnitude to affect the test results.

### *Observations of specimen failure modes*

A number of observations were made regarding the modes of failure of the different pile configurations which are worthy of further comment. Firstly when failure occurred in



the *native* soil, a plug of soil was observed to have been pushed out of the bottom of the sample that was exactly the same diameter as the hole in the base plate, which exceeded the diameter of the predrilled borehole. The actual deformation of the *native* soil within the soil mass could not however be discerned.

Test #16-33 was conducted using a base plate with a 165 mm diameter hole. The soil mass at the bottom of the cell in this instance was observed to deform in a manner similar to a circular plate with a point load in the centre. After the 33 mm pile was overcored with the 102 mm core barrel and allowed to dry, a definite plane of weakness was observed at a distance of approximately 6 mm from the outside edge of the grout, shown in Plate 2. In subsequent tests on 102 mm piles using a grout backfill, after the soil mass had been removed from the cell and allowed to dry on completion of the test, a vertical crack was observed at a distance of 1 to 3 mm from the outer edge of the grout. The development of such a plane was not observed when a sand slurry backfill had been used.

The above suggests that when a grout backfill was used, the failure surface in the *native* soil occurred on a cylindrical surface at or slightly beyond the outer edge of the grout lugs notched into the *native* soil. Extrapolating this to field pile installations, it follows that the diameter of the failure surface will be slightly larger than the drill bit size due to the whip of the bit as it rotates. Considering a bit with a diameter of 165 mm, the diameter of the hole may be approximately 180 mm thus the failure surface may be at diameter of approximately 185 mm. This would result in an increased capacity of approximately 12%. It is not suggested that this additional capacity be included in design calculations, however it is noteworthy that there is an inherent additional safety factor included when a grout backfill is used.

In a number of instances when the failure occurred in the *native* soil using the 63 and 102 mm piles, a series of concentric cracks were observed on the top of the soil mass surrounding the pile. The specimen from test #12 was closely examined after it had been removed from the cell and allowed to dry, and some of the cracks had progressed

completely through the soil. This observation is in agreement with accepted design practice which is based upon the assumption of the shearing of concentric cylinders in the soil mass surrounding the pile.

### **Comparison with results in other studies**

#### *Laboratory test results by others*

There is a scarcity of data available in the literature which may be directly compared with the results from this test program. A summary of comparable test results is contained in Table 5.5, and is shown graphically in Figure 5.16.

The most comparable tests are reported in Sego and Smith (1989), which were essentially the precursors to this study. The tests provided an opening in the cell baseplate larger than the cored hole to permit failure at the weakest interface, although they were conducted using a different test cell and smaller loading frame. The small differences in adfreeze bond strength is likely due to the differences in times to failure associated with the different test cell and loading frame. The smaller value obtained by Sego and Smith (1989) using cuttings with no salinity are due to the difference in the pile surfaces. Hence the results from this test program agree very well with those presented in Sego and Smith (1989).

In constant load tests reported by Hutchinson (1989) the pile surface was in direct contact with the saline soil hence may be compared with the tests in this program when cuttings were used as a backfill material. Her results emphasize that pile capacity is considerably less when the pile surface is in direct contact with saline soil, and long-term constant load conditions are considered.

The tests conducted in this study with no salinity only may be compared with the data presented by Parmeswaran (1978), although the differences in the test cell configurations may have an indeterminate effect on the results. Piles with sandblasted surfaces in the two studies had similar bond strengths. Considerable difference exists however in the strengths observed for piles which were painted or untreated. This is likely

because the piles used by Parmeswaran (1978) had been sandblasted then painted with a red oxide primer, whereas those used by Sego and Smith (1989) and in this study were installed in the condition in which they were received from the manufacturer.

Tests conducted by the Department of National Defence, 1 Construction Engineering Unit (1 CEU) (1987) utilized a concrete cylinder 305 mm high, 305 mm in diameter at a temperature of  $-10^{\circ}\text{C}$  with a 150 mm hole cored into the centre. A 114 mm OD pipe was centered in the hole and grout at room temperature was placed into either only the annulus between the pipe and the hole wall or into both the centre of the pipe and the annulus. Their results provide an estimate of the bond strength between a sanded Cement Fondu grout and smooth pipe. No admixtures were utilized to enhance the curing of the grout in cold temperatures hence there was an indeterminate amount of freezing of the pore water in the grout before curing was complete. The 74% increase in bond strength which was observed when grout was placed in the center of the pile emphasizes the importance of this practice to enhance the curing of the grout. In this study the upper limit of bond strength between the grout and pile was not determined however comparison with the results from 1 CEU (1987) supports values in excess of 1000 kPa.

#### *Field test results by others*

Although there is little comparative laboratory test data available, it was even more difficult to obtain field test results to which the results from this study may be reasonably compared as very few test programs examined similar variables or were conducted at constant loading or displacement rates. Table 5.5 contains the results from comparable field tests reported by Biggar and Sego (1988) and Manikian (1983). Constant load tests in saline permafrost reported by Nixon (1988), and Hoggan (1985) result in much lower pile capacities, similar to the laboratory results reported by Hutchinson (1988) discussed above.

The results reported by Biggar and Sego (1989) examine the effect of pile surface finish on pile capacity however the piles were loaded incrementally in tension. The reported values of adfreeze bond strength are approximately 50% lower than those obtained in this

study however the relative increase in adfreeze bond strength for sandblasted piles is similar in both studies. The lower bond strength values reported in Biggar and Sego (1989) may be attributed in part to the fact that pile load tests in tension generally result in strengths of 1/3 to 1/2 those obtained in compression (Fellenius and Sampson 1976; Frederking and Karri 1983; and Janbu 1976). Any further difference is likely due to the fact that laboratory load tests generally result in higher strengths than field tests.

The results reported by Manikian (1983) contain one test (#9) in which a 457 mm diameter pipe pile installed into a 610 mm diameter hole with a sand slurry backfill in an ice rich non-saline permafrost at a temperature of  $-6^{\circ}\text{C}$  was loaded in tension at a constant rate. The higher adfreeze bond strength observed was likely due in part to the faster loading rate, and possibly the surface of the pile used in the test was rougher than that used in the other tests listed in Table 5.5.

Constant load tests on anchors installed into warm ice-rich non-saline permafrost using a Ciment Fondu based grout reported by Johnson and Ladanyi (1972) provide insight into the performance of the grout and the associated failure mechanisms observed in the permafrost. Although the authors do not comment on the texture of the grout matrix specifically, they do note that "the surface of the grout in contact with the soil was quite firm and not flakey or powdery". They also comment that the surface of the grout was corrugated following the contours left by the auger. The deformations in the surrounding soil consisted of a thin zone of high shear strain immediately adjacent to the anchor associated with slip at the interface during failure, and an outer zone of uniform shear strain which decreased rapidly with distance from the anchor. Their observations concur with the results for grouted piles tested in this laboratory test program.

#### *Comparison with analytical models*

Design guidelines for predicting pile capacity emphasize that both the strength of the adfreeze bond and the time dependent deformation must be examined as either condition may govern. The results from this study are compared with guidelines in the literature in

both respects, although it is noted that the displacement rates used in this test greatly exceed those applicable in design.

Adfreeze bond strength design values for similar conditions were obtained from Johnston (1981), Linnel and Lobacz (1980), Tsytoich (1975), and Weaver and Morgenstern (1981). The results from this study are compared with these values in Table 5.7. The sustained bond strength values obtained from the references are seen to be approximately 50% of the ultimate, or short-term strengths. The results from this study for untreated pipe piles are similar to the ultimate strength values found in the literature, as would be expected. It follows that the test results from this study suggest that long term (sustained) adfreeze bond strength for sandblasted piles with a sand backfill will be approximately 400 kPa at  $-5^{\circ}\text{C}$  and 650 kPa at  $-10^{\circ}\text{C}$ .

The design guidelines proposed by Nixon and Neukirchner (1984) for piles in saline fine-grained ice-rich soils are compared with the results from this program in Figure 5.17. The highest and lowest normalized (to the hole radius) pile displacement rates from this study are for the 33 and 102 mm diameter piles respectively. The results plotted for the tests in *native* soil with salinity of 30 ppt at  $-5^{\circ}\text{C}$  are for piles with a clean sand slurry backfill whereas the remaining data are for piles which were backfilled with grout. The calculated stress values are the maximum values obtained at the interface between the backfill and the *native* soil. The strain strengthening behaviour exhibited in this study and the high values of the normalized velocities renders such a comparison rather tenuous, however some conclusions may be drawn. The shear stress values obtained in this study in *native* soil with salinities of 30 ppt are approximately 10 to 35% less than the proposed design values at  $-5^{\circ}\text{C}$ , and 45 to 65% less than proposed design values at  $-10^{\circ}\text{C}$ . Further the line for  $-5^{\circ}\text{C}$  and 35 ppt from Nixon and Neukirchner (1984) passes between the results from this study for salinities of 10 and 20 ppt at  $-5^{\circ}\text{C}$ . The above observations concur with those in Nixon (1988), and Miller and Johnson (1990) which show field pile performance where load carrying capacities were lower than those proposed in Nixon and

Neukirchner (1984). The above suggests that the design guidelines in Nixon and Neukirchner (1984) may be unconservative, however additional constant load testing is necessary to verify this observation.

## Conclusions

The effect of salinity and temperature are interrelated as they both influence the unfrozen water content of the frozen soil, and it is this unfrozen water which affects the behaviour of the soil (Ogata et al. 1983, and Hivon 1991). The results from this study showed that when the adfreeze bond strength did not govern the pile capacity, the pile behaviour was similar for tests in which the unfrozen water content of the *native* soil was similar.

The effect of salinity on pile capacity was shown to be twofold; it dramatically reduces the adfreeze bond strength at low values of salinity, and it also reduces the strength of the *native* soil. Salinity in the silty sand (cuttings) backfill was shown to reduce adfreeze bond strengths by approximately 80% and 99% for salinities of 10 and 30 ppt. Tests conducted with different *native* soil salinities at the same temperature showed reductions in mobilized shear stress (at a specified displacement) of 25% to 50%, 80%, and 95% when the *native* soil salinity was increased to 10, 20, and 30 ppt respectively.

A small number of tests conducted at a temperature of  $-10^{\circ}\text{C}$  showed increases in pile capacity of 70% to 100% compared with capacities measured at a temperature of  $-5^{\circ}\text{C}$ . Increased adfreeze bond strengths for sand backfilled piles and increases in mobilized shear stress (at specified values of displacement) for all piles were observed when the temperature decreased.

The use of a cementitious grout backfill designed to cure in frozen soil resulted in considerable gains in pile load carrying capacity in soils with low salinities, where the capacity of sand backfilled piles was limited by the strength of the adfreeze bond. The shear stress versus displacement behaviour of piles backfilled with clean sand and grout was similar *prior* to failure of the adfreeze bond however. The use of silty sand (cuttings) as a

backfill material resulted in adfreeze bond strengths approximately 50% lower than those observed using a clean sand backfill. Sandblasting the surface of the pipe was shown to increase adfreeze bond strength 2 to 3 times compared with that obtained when the pipe was installed as received from the manufacturer.

Failure of the bond between the grout backfill and the steel pile occurred when the mix water had been subject to freezing (for the 33 mm piles), illustrated the importance of proper mix design and installation for grout backfilled piles. When the grout adjacent to the pipe had properly cured however, maximum bond stresses of 1500 kPa at the pile/grout interface were obtained without failure at this interface. The shear strength of the grout at the grout/*native* soil always exceeded the shear strength of the soil, even when freezing of the mix water had occurred, and shear stresses of 900 kPa at the grout/*native* soil interface were observed without failure within the grout.

The results from the constant displacement rate tests on model piles of various configurations in saline frozen silty sand showed maximum pile capacities were obtained using a grout backfill, followed by sandblasted pipe piles with a clean sand backfill. The use of untreated pipe or silty sand (cuttings) backfill gave inferior pile capacities. Dramatic reductions in adfreeze bond strength were observed when the backfill contained saline pore fluid, resulting in the lowest pile capacities.

There remains the question regarding the long-term performance of piles in saline ice-poor permafrost. The increased short-term pile capacity realized when grout is used as a backfill material may be of little consequence if the behaviour is similar to that of sand backfilled piles at stresses common in foundation design. The companion paper examines this problem using constant load tests at a temperature of  $-5^{\circ}\text{C}$ .

## References

- 1 Construction Engineering Unit 1987. SRR model pile load tests report No 87-CEU-19. p. 71.

- Andersland, O.B., and Alwahhaab, M.R. 1983. Lug behavior for model steel piles in frozen sand. Proceedings, 4th International Conference on Permafrost, Fairbanks Alaska, USA, pp. 16-21.
- Andersland, O.B., and Anderson, D.M. 1978. **Geotechnical engineering for cold regions**. McGraw-Hill Inc., p. 566.
- Anderson, D.M. and Morgenstern, N.R. 1973. Physics, chemistry and mechanics of frozen ground: a review. Proceedings, 2nd International Conference on Permafrost, North American Contribution, Yakutsk, USSR, pp. 257-288.
- Berenger, D.M., Edwards, R.Y., and Nadreau, J.P. 1985. Preliminary assessment of the adhesion shear strength of ice-steel and ice-frozen sand binds. Arctic Petroleum Operators' Association, Research Project Report 85-1, p. 55.
- Biggar, K.W. and Sego, D.C. 1989. Field load testing of various pile configurations in saline permafrost and seasonally frozen rock. Proceedings, 42nd Canadian Geotechnical Conference, October 25-27, Winnipeg, pp. 304-312.
- Biggar, K.W., and Sego, D.C. 1990. The curing and strength characteristics of cold setting Ciment Fondu grout. Proceedings, 5th Canadian Permafrost Conference. Quebec City, Quebec, pp. 349-355.
- Biggar, K.W. and Sego, D.C. In press a. [Chapter 2] Field pile load tests in saline permafrost, Part I, Test procedures and results.
- Biggar, K.W. and Sego, D.C. In press b. [Chapter 3] Field pile load tests in saline permafrost, Part II, Analysis of results.
- Biggar, K.W. and Sego, D.C. In press c. [Chapter 6] Time dependent displacement behaviour of model adfreeze and grouted piles in saline permafrost.
- Biggar, K.W., Sego, D.C., and Noel, M. 1991. Laboratory and field performance of a Ciment Fondu based grout in frozen soil. Proceedings of the 45th Canadian Geotechnical Conference, Calgary, Alberta, Canada.
- Fellenius, B.H., and Samson, L. 1976. Testing of drivability of concrete piles and disturbance to sensitive clay. Canadian Geotechnical Journal, 13: pp 139-160.
- Frederking, R.M.W., and Karri, J. 1983. Effects of pile material and loading state on adhesive strength of piles in ice. Canadian Geotechnical Journal, 20: pp 673-680.
- Frederking, R.M.W. 1979. Laboratory tests on downdrag loads developed by floating ice covers on vertical piles. Proceedings, 5th International Conference on Port and Ocean Engineering under Arctic Conditions, NGI, Trondheim, Norway, Vol II, pp. 1097-1110.
- Gregersen, O., Phukan, A., and Johansen, T. 1983. Engineering properties and foundation design alternatives in marine Svea clay, Svalbard. Proceedings, 4th International Conference on Permafrost, Fairbanks Alaska, USA, pp. 384-279.
- Hivon, E.G. 1991. Behaviour of saline frozen soils. Unpublished Ph D. Thesis, University of Alberta, Edmonton, Alberta, p. 435.



- Hivon, E.G. and Sego, D.C. 1990. Determination of the unfrozen water content in saline permafrost using time domain reflectometry (TDR). Proceedings, 5th Canadian Permafrost Conference, June 6-8 1990, Quebec City, Quebec, pp. 257-262.
- Hoggan Engineering and Testing (1980) Ltd. 1985. Pile load tests, Arctic Bay multi-purpose hall and school extension, report submitted to the Department of Public Works, Government of the Northwest Territories.
- Hutchinson, D.J. 1989. Model pile load tests in frozen saline silty sand. Unpublished MSc Thesis, University of Alberta, Edmonton, Alberta, p. 222.
- Janbu, N. 1976. Static bearing capacity of friction piles. Proceedings, 6th European Conference on Soil Mechanics and Foundation Engineering, 1.2: pp. 479-488.
- Johnston, G.H. ed 1981. **Permafrost Engineering Design and Construction**. John Wiley and Sons, p. 483.
- Johnston, G.H., and Ladanyi, B. 1972. Field tests on grouted rod anchors in permafrost. Canadian Geotechnical Journal, 9: pp. 176-194.
- Karpov, V., and Velli, Y. 1968. Displacement resistance of frozen saline soils. Soil Mechanics and Foundation Engineering (English Translation), 4(July/August): pp.277-279.
- Ladanyi, B. 1979. Borehole relaxation test as a means for determining the creep properties of ice covers. Proceedings, 5th International Conference on Port and Ocean Engineering under Arctic Conditions, NGI, Trondheim, Norway, pp. 757-770.
- Ladanyi, B. 1988. Short- and long-term behavior of axially loaded bored piles in permafrost. Deep Foundations on Bored and Auger Piles, Van Impe (ed.) Balkema, Rotterdam, pp. 121-130.
- Linnell, K.A., and Lobacz, E.F. 1980. Design and construction of foundations in areas of deep seasonal frost and permafrost. US Army Cold Regions Research and Engineering Lab, Hanover, New, Hampshire. Special Report 80-34, p. 320.
- Long, E.L. 1978. Permafrost foundation designs. Proceedings, Cold Regions Specialty Conference, Anchorage, Alaska, American Society of Civil Engineering, 17-19 May, pp. 973-987.
- Makkonen, L., and Lehmus, E. 1987. Studies on adhesion strength of saline ice. Proceedings, 9th International Conference on Port and Ocean Engineering under Arctic Conditions, Fairbanks, Alaska, pp. 45-55.
- Manikian, V. 1983 Pile driving and load tests in permafrost for the Kuparuk pipeline system. Proceedings, 4th International Conference on Permafrost, Fairbanks Alaska, USA, pp. 804-810.
- Mellor, M. 1979. Mechanical properties of polycrystalline ice. International Union of Theoretical and Applied Mechanics symposium, Physics and mechanics of ice, Copenhagen, Aug 6-9, pp. 217-245.

- Miller, D.L. and Johnson, L.A. 1990. Pile settlement in saline permafrost: a case history. *Proceedings, 5th Canadian Permafrost Conference*. Quebec City, Quebec, pp. 371-378.
- Morgenstern, N.R., Roggensack, W.D., and Weaver, J.S. 1980. The behavior of friction piles in ice and ice-rich soils. *Canadian Geotechnical Journal*, **17**: pp. 405-415.
- Neville, A.M. 1975. **High Alumina Cement Concrete**. John Wiley and Sons, p. 201.
- Nixon, J.F. 1988. Pile load tests in saline permafrost at Clyde River, Northwest Territories, *Canadian Geotechnical Journal*, **25**: pp. 24-31.
- Nixon, J.F., and Lem, G. 1984. Creep and strength testing of frozen saline fine-grained soils. *Canadian Geotechnical Journal*, **21**: pp. 518-529.
- Nixon, J.F., and McRoberts, E.C. 1976. A design approach for pile foundations in permafrost. *Canadian Geotechnical Journal*, **13**: pp. 40-57.
- Nixon, J.F., and Neukirchner, R.J. 1984. Design of vertical and laterally loaded piles in saline permafrost. *Proceedings, 3rd International Specialty Conference on Cold Regions Engineering*, Edmonton, Alberta, Canadian Society of Civil Engineering, 1-6 April, pp. 131-144.
- Nixon, M.S. and Pharr, G.M. 1984. The effects of temperature, stress and salinity on the creep of frozen soil. *Transactions of the ASME Journal of Energy Resources Technology*, **106**: pp. 344-348.
- Ogata, N., Yasuda, M. and Kataoka, T. 1983. Effects of salt concentration on strength and creep behaviour of artificially frozen soils. *Cold Regions Science and Technology*, **8**: pp 139-153.
- Parmeswaran, V.R. 1978. Adfreeze strength of frozen sand to model piles. *Canadian Geotechnical Journal*, **15**: pp. 494-500.
- Parmeswaran, V.R. 1980. Deformation and strength of frozen sand, *Canadian Geotechnical Journal*, **17**: pp. 74-88.
- Pharr, G.M. and Merwin, J.E. 1985. Effects of brine content on the strength of frozen Ottawa sand. *Cold Regions Science and Technology*, **11**: pp 205-212.
- Saeki, H., Ono, T., Takeuchi, T., Kanie, S., and Nakazawa, N. 1986. Ice forces due to changes in water level and adfreeze bond strength between sea ice and various materials. *Fifth Offshore Mechanics and Arctic Engineering Conference*, Vol IV, pp. 534-540.
- Sayles, F.H. 1968. Creep of frozen sands. US Army Cold Regions Research and Engineering Lab, Hanover, New, Hampshire, Technical Report 190, p. 54.
- Sayles, F.H., and Haines, D. 1974. Creep of frozen silt and clay. US Army Cold Regions Research and Engineering Lab, Hanover, New, Hampshire, Technical Report 252, p. 51.

- Sego, D.C., Schultz, T., and Banasch, R. 1982. Strength and deformation behavior of frozen saline sand. Proceedings, 3rd International Symposium on Ground Freezing, Hanover, New Hampshire, pp. 11-19.
- Sego, D.C., and Morgenstern, N.R. 1983. Deformation of ice under low stresses. Canadian Geotechnical Journal. 20: pp 587-602.
- Sego, D.C. and Smith, L.B. 1989. The effect of backfill properties and surface treatment on the capacity of adfreeze pipe piles. Canadian Geotechnical Journal, 26: pp. 718-725.
- Sego, D.C. and Biggar, K.W. 1990. Grouts for use in permafrost regions. Geotechnical News, 8 (3): pp. 33-34.
- Thomas, H.P., and Luscher, U. 1980. Improvement of bearing capacity of piles by corrugations. US Army Cold Regions Research and Engineering Lab, Hanover, New, Hampshire, Special Report 80-40, pp. 229-234.
- Tsytoich, N.A. 1975. The mechanics of frozen ground. McGraw-Hill, New York, p. 426.
- Tsytoich, N.A., Kronik, Y.A., Markin, K.F., Aksenov, V.I., and Samuel'son, M.V. 1973. Physical and mechanical properties of saline soils. Proceedings, 2nd International Conference on Permafrost, USSR Contribution, Yakutsk, USSR, pp. 238-247.
- Velli, Y.Y., Lenzniep, and Karpunia, A.A. 1973. Saline permafrost as bearing ground for construction. Proceedings, 2nd International Conference on Permafrost, USSR Contribution, Yakutsk, USSR, pp. 545-550.
- Vyalov, S.S. 1959. Rheological properties and bearing capacity of frozen soils. Translation 74, US Army Cold Regions Research and Engineering Lab, Hanover, New, Hampshire, translated in 1965, p 219.
- Weaver, J.S. 1979. Pile foundations in permafrost. Unpublished Ph D. Thesis, University of Alberta, Edmonton, Alberta, p. 224.
- Weaver, J.S., and Morgenstern, N.R. 1981. Pile design in permafrost. Canadian Geotechnical Journal, 18: pp. 357-370.

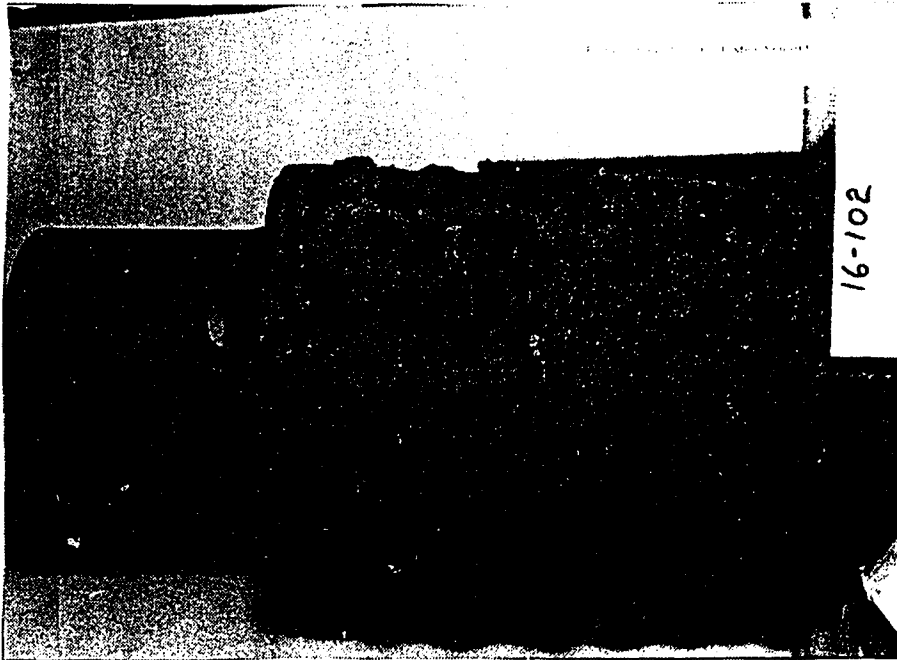


Plate 1: Grout surface in roughened hole,  
102 mm pile

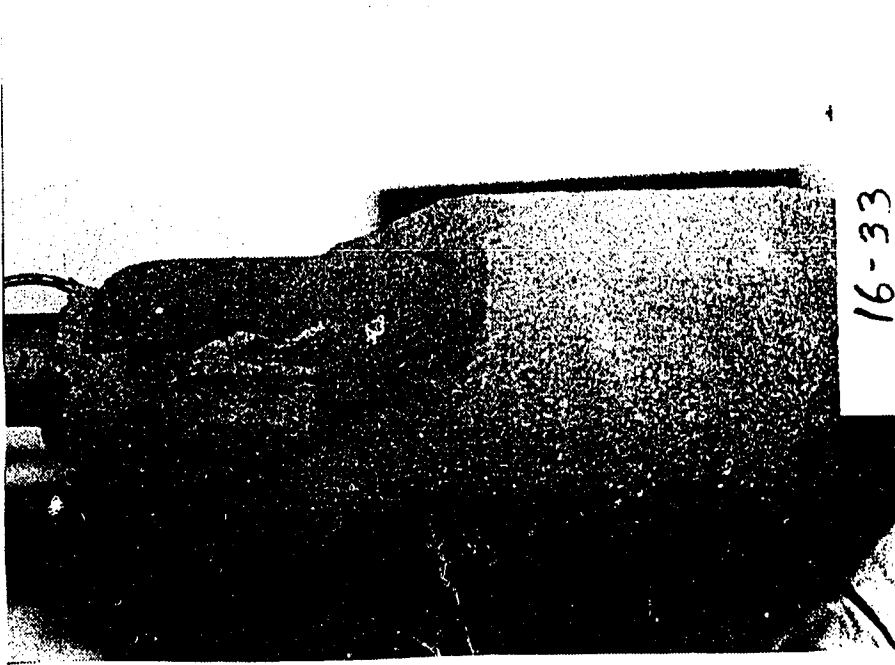


Plate 2: Plane of weakness beyond grout backfill  
33 mm pile

**TABLE 5.1**

**Pile Center Line Average (CLA) Roughness (x 10<sup>-6</sup> in)**

Pile Roughness  
(Average of 3 readings along pile surface)

Diameter (mm)	Untreated Pipe	Sandblasted Pipe
33	61	73
63	36	56
102	30	65

**TABLE 5.2**

**Sample Moisture Contents, Densities and Salinities**

Test#	Backfill	SALINITY			M.C. and DENSITY			
		Nominal	Measured Mixed	Frozen	Native soil M.C.	Dry Density	102 mm Backfill M.C.	Dry Density
					(%)	(kg/m <sup>3</sup> )	(%)	(kg/m <sup>3</sup> )
4	Sand	30	30	27	17.9	1.78	18.5	1.65
5	Sand	20	20	20	17.2	1.76	19.6	1.67
6	Sand	10	10	10	17.8	1.78	19.7	1.65
7	Sand	0	0	0	Not Done			
8	Sand	0	0	0	17.2	1.74	17.9	1.60
9	Cuttings	0	0	0	18.5	1.70	20.7	1.63
10	Cuttings	10	9	9	18.5	1.71	29.9	1.39
11	Cut's/Ice	30	28	25-30	19.6	1.68	N/A	N/A
12	Grout	0	0	0	18.6	1.69	N/A	N/A
13	Grout	10	9	9	17.5	1.73	N/A	N/A
14	Grout	20	17	18	17.3	1.74	N/A	N/A
15	Grout	0	0	0	19.0	1.70	N/A	N/A
16	Grout	10	10	Not Done	19.2	1.70	N/A	N/A
18	Sand	0	0	0	19.9	1.68	17.5	1.60
23	Sand	0	0	0	19.5	1.68	Not Done —	
24	Sand	10	9	9	19.4	1.69	17.8	1.65
25	Sand	10	9.5	10	18.8	1.71	Not Done —	
26	Sand	10	10	11	18.7	1.70	Not Done —	
29	Sand	10	10	Not Done	17.7	1.76	17.9	1.66
32	Grout	10	12	12	16.6	1.77	N/A	N/A
35	Grout	30	30	29	17.0	1.77	N/A	N/A
37	Sand	10	9	Not Done	Not Done			
38	Sand	10	9	10	Not Done			
42	Grout	30	32	29	19.0	1.71	N/A	N/A
43	Sand	10	10	9	17.8	1.76	17.8	1.63
44	Sand	10	9	8	18.1	1.74	18.0	1.64
45	Grout	10	10	9	17.5	1.75	N/A	N/A

TABLE 5.3  
Summary of Test Results

Test #	Salinity (ppt)	Backfill Type (Note 4)	Test Temperature (°C)	Failure Surface (Note 5)	Maximum Load (kN)	Time to Max Load (mins)	Displacement at Max Load		Embedment Length (mm)	Max Stress		COMMENTS
							Measured (mm)	Corrected (mm) (Note 6)		Pile (kPa)	N.S. (kPa)	
4-33	30	Sand	-5.2 ± 0.1	N.S.	2.9	N/A	7.1		250	112	71	Jack displacement used.
4-63	30	Sand	-6.0 to -6.6	N.S.	15.7	N/A	6.8		250	317	196	
4-102	30	Sand	-5.4 to -7.0	N.S.	24.9	N/A	9.8		250	311	209	
5-33	20	Sand	-5.1 ± 0.1	N.S.	10.8	N/A	6.5		250	417	264	
5-63	20	Sand	-6.5 to -6.9	Pile	41.0	1100	6.8		250	829	512	Equipment failure caused rapid temp incr at test start.
5-102	20	Sand	-5.4 ± 0.1	N.S.	45.6	N/A	12.0		250	569	382	
6-33	10	Sand	-3.5 to -5.5	Pile	20.0	475	2.8		250	772	490	
6-63	10	Sand	-5.0 to -4.0	Pile	39.4	675	6.5		250	796	492	
6-102	10	Sand	-5.1 ± 0.1	Pile	56.7	805	4.0		250	708	475	
7-33	0	Sand	-5.5 to -5.2	Pile	10.1	100	0.1		250	390	247	
7-63	0	Sand	-5.6 to -3.8	Pile	9.0	95	0.2		250	182	112	
7-102	0	Sand	-5.0 to -5.7	Pile	17.7	155	0.2		250	221	148	
8-33	0	Sand	-5.5 to -5.8	Pile	30.5	235	0.6		255	1154	732	
8-63	0	Sand	-5.7 ± 0.1	Pile	56.8	615	3.1		255	1125	695	
8-102	0	Sand	-6.3 to -5.8	Pile	53.3	395	1.2		245	679	456	Virtually unfrozen cuttings. Note 1. Pile was overloaded during set-up. Note 1, Note 2. Note 2. Note 2. Note 2. Note 2. Slow displacement rate (9.8 mm/da) Note 2. Note 3. Used large base plate ring. Note 3 Excessive displ of soil mass from 33 mm test.
9-33	0	Cuttings	-5.6 ± 0.1	Pile	15.1	215	0.7		250	583	370	
9-63	0	Cuttings	-5.6 ± 0.1	Pile	26.0	230	0.7		250	525	325	
9-102	0	Cuttings	-5.4 to -5.0	Pile	38.9	345	1.2		250	486	326	
10-33	10	Cuttings	-5.1 ± 0.1	Pile	3.4	55	0.2		260	126	80	
10-63	10	Cuttings	-5.4 ± 0.1	Pile	7.8	110	0.4		260	152	94	
10-102	10	Cuttings	-5.1 to -5.4	Pile	7.1	140	0.3		260	85	57	
11-33	30	Cuttings	-5.4 ± 0.1	Pile	0.2	155	1.4		250	6	4	
11-63	30	Ice	-4.9 to -5.5	N.S.	10.1	N/A	6.0		240	213	131	
11-102	30	Ice	-5.5 to -6.9	Pile	6.0	195	0.7		250	75	50	
12-33	0	Grout	-5.6 ± 0.1	Pile	29.3	325	0.6	0.3	250	1130	717	Used large base plate ring. Note 3 Excessive displ of soil mass from 33 mm test.
12-63	0	Grout	-5.2 to -5.6	N.S.	52.0	N/A	5.7	5.2	257	1022	631	
12-102	0	Grout	-4.5 to -4.9	N.S.	45.6	N/A	3.3	2.8	250	569	382	
13-33	10	Grout	-4.8 to -5.2	Pile	18.1	615	4.3	4.1	250	698	443	
13-63	10	Grout	-5.1 ± 0.1	N.S.	42.0	N/A	7.1	6.7	250	849	524	
13-102	10	Grout	-5.1 to -5.5	N.S.	78.0	N/A	5.0	4.2	250	974	653	
14-33	20	Grout	-5.6 to -5.3	N.S.	4.2	N/A	8.0	7.9	255	159	101	
14-63	20	Grout	-5.3 ± 0.1	N.S.	17.0	N/A	6.8	6.6	255	337	208	
14-102	20	Grout	-5.2 ± 0.1	N.S.	30.1	N/A	6.6	6.3	255	368	247	
15-33	0	N Grout	-4.9 ± 0.1	Pile	34.6	195	1.0	0.6	250	1335	734	
15-63	0	Grout	-5.3 to -5.0	N.S.	74.1	N/A	6.7	5.9	250	1498	925	Used large base plate ring. Note 3 Excessive displ of soil mass from 33 mm test.
15-102	0	Grout	-5.4 ± 0.1	N.S.	86.9	N/A	7.7	6.7	250	1085	728	
16-33	10	N Grout	-5.2 ± 0.1		17.4	N/A	8.9	8.7	250	671	426	
16-63	10	Grout	NOT DONE									
16-102	10	Grout	-5.2 to -4.9	N.S.	68.3	N/A	8.5	7.8	250	853	572	
18-33	0-SG	Sand	-5.1 ± 0.1	Pile	22.8	160	0.8	0.5	248	887	563	

**TABLE 5.3**  
**Summary of Test Results**

Test #	Salinity (ppt)	Backfill Type (Note 4)	Test Temperature (°C)	Failure Surface (Note 5)	Maximum Load (kN)	Time to Max Load (mins)	Displacement at Max Load		Embedment Length (mm)	Max Stress		COMMENTS
							Measured (mm)	Corrected (mm) (Note 6)		Pile (kPa)	N.S. (kPa)	
18- 63	0-SG	Sand	-5.1 ± 0.1	Pile	52.8	215	1.3	0.8	248	1076	664	
18- 102	0-SG	Sand	-5.2 ± 0.1	Pile	65.6	280	1.2	0.5	235	871	585	Note 3.
23- 33	0-SG	Sand	-4.9 to -5.2	Pile	22.1	170	0.6	0.3	235	907	576	Note 1.
23- 63	0-SG	N. Grout	-5.1 ± 0.1	Bar	149.3	335	1.9		235	4213		Used small base plate ring to force failure in grout.
23- 102	0-SG	Sand	-5.3 to -4.7	Pile	57.3	285	1.5	0.9	235	761	511	Defrost produced low peak load.
28- 33	10-SG	Sand	-5.3 to -7.6	Pile	21.0	275	0.7	0.4	250	810	514	Rapid temperature drop at start of test.
28- 63	10-SG	Sand	-5.1 ± 0.1	Pile	39.4	705	4.7	4.3	250	796	492	
28- 102	10-SG	Sand	-5.6 to -6.2	Pile	75.6	655	4.0	3.2	250	944	633	Note 1.
32- 33	10	Sand	-10.3 ± 0.1	Pile	30.6	190	1.0	0.7	250	1181	749	
32- 63	10	Grout	-9.8 to -10.4	N.S.	69.1	N/A	7.7	7.0	250	1397	863	
32- 102	10	Grout	-10.3 ± 0.1	N.S.	100.0	N/A	7.0	5.6	250	1248	838	
35- 33	30	N. Grout	-10.2 to -8.1	N.S.	17.5	N/A	3.8	3.6	250	675	428	Cooling unit failure at 4 mm displacement.
35- 63	30	Grout	-9.8 ± 0.1	N.S.	45.2	N/A	4.1	3.6	250	913	564	
35- 102	30	Grout	-10.2 to -9.8	N.S.	59.0	N/A	5.6	5.0	250	724	486	Note 1.
37- 33	30	Sand	-10.4 ± 0.1	Pile	23.1	640	4.1	3.8	250	891	566	
37- 63	30	Sand	-10.2 ± 0.1	N.S.	47.4	N/A	7.0	6.5	250	958	592	
37- 102	30	Sand	-10.4 ± 0.1	N.S.	65.4	N/A	6.0	5.4	250	816	548	
38- 33	10	Sand	-10.0 to -10.3	Pile	36.8	245	0.8	0.4	235	1510	959	Note 1.
38- 63	10	Sand	-10.4 ± 0.1	Pile	64.0	395	2.0	1.4	235	1376	850	Note 1.
38- 102	10	Sand	-10.3 ± 0.1	Pile	104.1	490	3.1	1.6	235	1382	928	
42- 33	30	N. Grout	-10.8 ± 0.1	N.S.	18.9	N/A	4.8	4.6	255	715	454	
42- 63	30	Grout	-9.9 ± 0.1	N.S.	33.6	N/A	7.3	6.9	250	679	419	
42- 102	30	Grout	-10.1 ± 0.1	N.S.	56.9	N/A	8.6	8.0	255	696	467	Note 3.
43- 33	10	Sand	-10.4 ± 0.1	Pile	32.8	240	1.2	0.8	250	1266	803	
43- 63	10	Sand	-10.4 ± 0.1	Pile	60.1	330	1.1	0.5	250	1215	750	Base plug not removed prior to loading.
43- 102	10	Sand	-10.3 ± 0.1	Pile	87.7	545	2.9	1.9	250	1095	735	
44- 33	10	Sand	-5.3 ± 0.1	Pile	18.0	180	1.2	1.0	259	670	425	
44- 63	10	Sand	-5.3 ± 0.1	Pile	34.2	500	3.4	3.0	259	667	412	
44- 102	10	Sand	-5.2 ± 0.1	Pile	40.4	360	2.5	2.1	259	487	327	
45- 33	10	N. Grout	-5.4 ± 0.1	Pile	24.7	625	4.0	3.7	250	953	605	
45- 63	10	Grout	-5.2 ± 0.1	N.S.	43.7	N/A	7.5	7.1	250	883	545	
45- 102	10	Grout	-5.2 ± 0.1	N.S.	55.3	N/A	6.9	6.4	250	690	463	

- Notes:
1. A slow initial displacement rate resulted from air being trapped in the hydraulic lines.
  2. The hole wall was left as originally cored thus it was smooth and straight.
  3. Problems with the jack LVDT's necessitated using the nominal jack displacement instead of measured displacement.
  4. N Grout denotes where a neat grout was used.
  5. N.S. denotes where failure occurred in the Native soil.
  6. Corrected displacement = jack displacement - displacement of the top of the pile
  7. S.G. denotes tests in which strain gauges were utilized.

**TABLE 5.4**

**Effect of *Native* Soil Salinity on Mobilized Shear Stress  
at 1 mm Displacement**

Salinity	Sand Backfilled Piles				Grout Backfilled Piles		
	0 ppt	10 ppt	20 ppt	30 ppt	0 ppt	10 ppt	20 ppt
Pile Diameter	Mobilized Shear Stress at the pile/backfill interface						
33 mm	888	652	180	41	1328	562	60
63 mm	940	427			966	475	137
102 mm	643	335	110		606	299	119
	Mobilized Shear Stress at the backfill/ <i>native</i> soil interface						
33 mm	564	414	140	26	843	357	38
63 mm	581	264			597	293	85
102 mm	431	225	74		407	201	80



**TABLE 5.5**  
**Laboratory Comparative Test Data**

Author(s)	Native Soil [6]		Backfill [6]		Pile [7]	$\phi$ (mm)	T (C)	t <sup>f</sup> (mins)	U <sup>f</sup> (mm)	U/t <sup>f</sup> (mm/min)	Nom Rate (mm/min)	T <sup>f</sup> (kPa)	Comments
	Material	S (ppt)	Material	S (ppt)									
Parneswaran '78	SP	0	SP	0	Sb	76	-6.0	185	0.925	0.005	0.005	806	Note 1.
Sego and Smith '89 This Study	SP	0	SP	0	Sb	76	-6.0	20.4	1.02	0.050	0.05	1181	Note 1.
	SM	0	SP	0	Sb	33	-5.3	378	2.48	0.007	0.008	733	
	SM	0	SP	0	Sb	33	-5.1	160	0.8	0.005	0.008	887	
	SM	0	SP	0	Sb	63	-5.1	215	1.3	0.006	0.008	1076	
	SP	0	SP	0	Sb & P	76	-6.0	110	0.55	0.005	0.005	677	Note 1.
Parneswaran '78	SP	0	SP	0	Sb & P	76	-6.0	12.2	0.61	0.050	0.05	1026	Note 1.
Sego and Smith '89 This Study	SM	0	SP	0	P	33	-4.8	162	0.77	0.005	0.008	357	
	SM	0	SP	0	Un	33	-5.3	100	0.1	0.001	0.008	390	
	SM	10	SP	0	Sb	33	-5.1	594	5.33	0.009	0.008	581	
Sego and Smith '89 This Study	SM	10	SP	0	Sb	33	-5.3	180	1.2	0.007	0.008	670	
	SM	0	SM	0	P	33	-6.4	120	0.67	0.006	0.008	360	
	SM	0	SM	0	Sb	33	-5.6	215	0.7	0.003	0.008	583	
Sego and Smith '89 Hutchinson '89 This Study	SM	10	SM	10	P	33	-4.8	162	0.98	0.006	0.008	190	
	SM	10	SM	10	Sb	33	-5	25	0.4	0.008	0.008	36	Note 2.
	SM	10	SM	10	Sb	33	-5.1	55	0.2	0.004	0.008	126	
1 CEU This Study	Concrete	N/A	Grout	N/A	Un	114	-2.5	18	0.38	0.021	5 kN/min	610	Note 3. Note 4.
	Concrete	N/A	Grout	N/A	Un	114	-2.6	35	1.02	0.029	5 kN/min	1064	Note 3. Note 5.
	SM	0	Grout	N/A	Sb	102	-5.4	None	N/A	N/A	0.008	>1085	Note 5.

Notes: 1. Actual pile displacement rate may be an order of magnitude smaller than the nominal machine rate stated.

2. Constant load test

3. Grout mix did not include admixtures to enhance curing performance in cold temperatures.

4. Grout placed in annulus between pile and hole wall only.

5. Grout placed in pipe centre as well as annulus.

6. SM denotes silty sand, Sp denotes clean uniform sand

7. Pile surface treatment: Sb denotes sandblasted, Un denotes untreated, P denotes painted.

**TABLE 5.6**  
**Field Comparative Test Data**

Author(s)	Native Soil [4]		Backfill [4]		Pile [5]	Ø (mm)	T (°C)	tf (mins)	Nom Rate	Tf (kPa)	Load Type (2)	Comments
	Material	S (ppt)	Material	S (ppt)								
<b>Smooth Pile Surface</b> Hoggan (1985) Miller et. al. (1990) Biggar and Sego (1989) Manikian (1983) This Study	DS & S [6]	10-30	SP	0?	Un	114	~ -5		33 kN/day	75-110	C	Note 9.
	SM	20-60	SM	0	Un	457	~ -4		Const	30-50	C	
	SW [7]	15-25	SP	0	Un	114	-4.8	20-60 [3]	N/A	60-90 [1]	T	
	SM [8]	0	SP	0	Un	457	-6.0	197	3 kPa/min	615	T	
	SM	0	SP	0	Un	102	-5.5	155	1.4 kPa/min	221	C	
<b>Biggar and Sego (1989)</b> This Study	SW [7]	15-25	SP	0	Sb	114	-5.2	20-50 [3]	N/A	323	T	
	SM	10	SP	0	Sb	102	-5.1	805	0.008	796	C	

Notes: 1. Results of 4 tests.

2. Compression = C, Tension = T.

3. Time to failure for last increment only.

4. SM denotes silty sand, SP denotes clean uniform sand.

5. Pile surface treatment: Sb denotes sandblasted, Un denotes untreated.

6. Dolomitic Shale and Slate, fissured with ice.

7. Dense clayey, gravelly sand with some cobbles, moisture content 6.5% to 9.5%.

8. Ice-rich silty sand.

9. Excessive settlement of pile foundation in summer.

**TABLE 5.7**

**Comparison of Results to Suggested Adfreeze Bond Strengths  
between Steel and Slurry Backfill, by Various Authors**

Author(s)	Backfill Material	Temp (° C)	Shear Strength (kPa)	
			Ultimate	Sustained
Johnston (1981)	ice-rich clays or silts	-5°	275	145
Linnel and Lobacz (1980)	Sand	-4°	390	280
Tsytovich (1975)	Sand M.C. = 18%	-5°	398	
Weaver and Morgenstern (1981)	Sand	-5°		294
This study: untreated steel	Sand M.C. = 18%	-5°	220 - 390	
This study: sandblasted steel	Sand M.C. = 18%	-5°	760 - 1100	
This study: sandblasted steel	Sand M.C. = 18%	-10°	1240 - 1380	

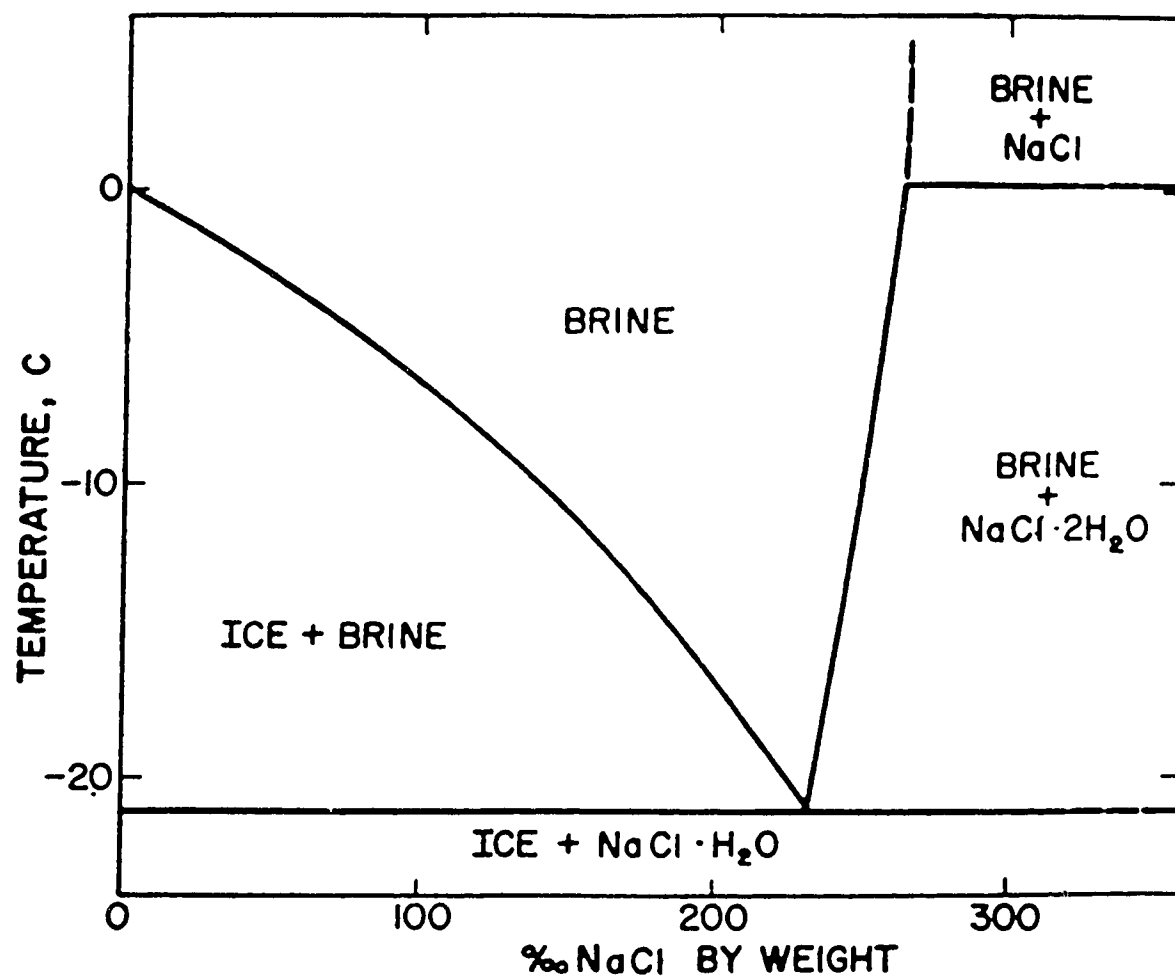


Figure 5.1 Phase diagram for NaCl

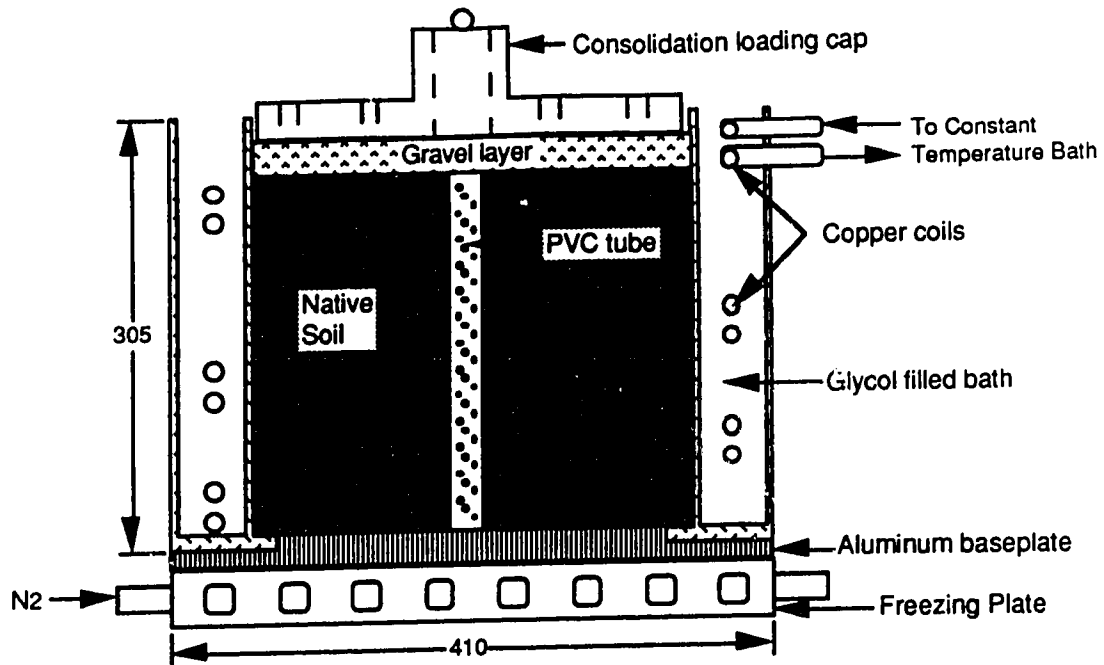


Figure 5.2: Test cell

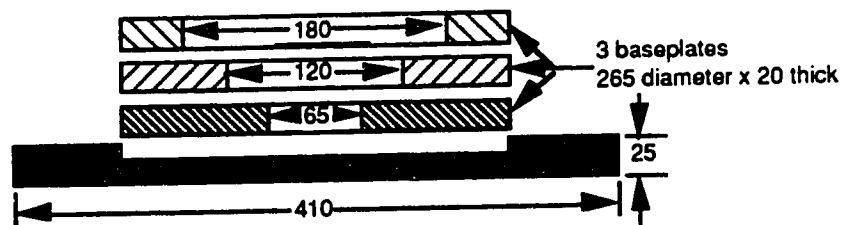


Figure 5.3: Test cell PVC base plates, for loading piles of 3 different diameters

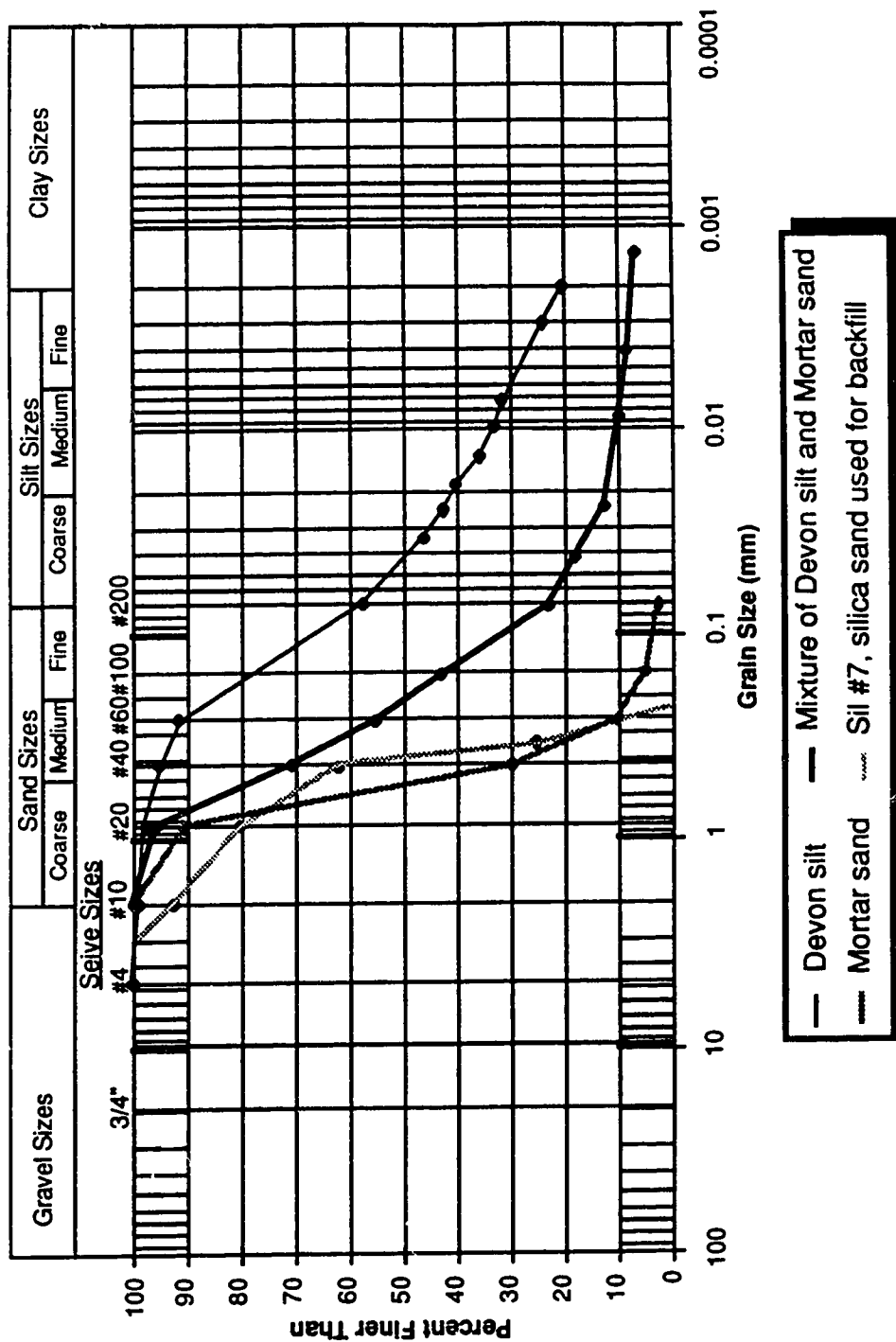


Figure 5.4: Grain size distribution of soils used in the test program

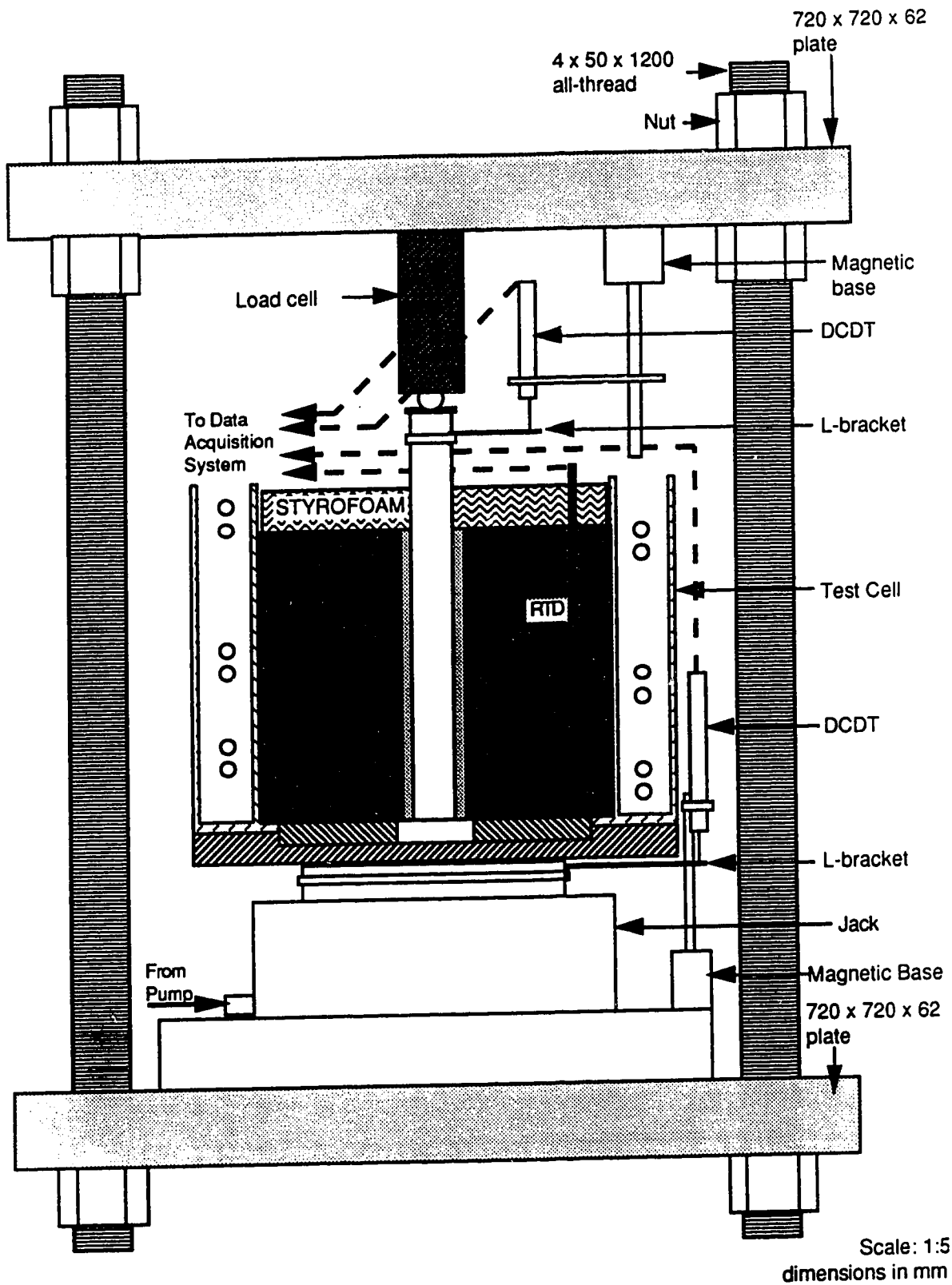


Figure 5.5: Load frame for constant displacement rate testing of model piles

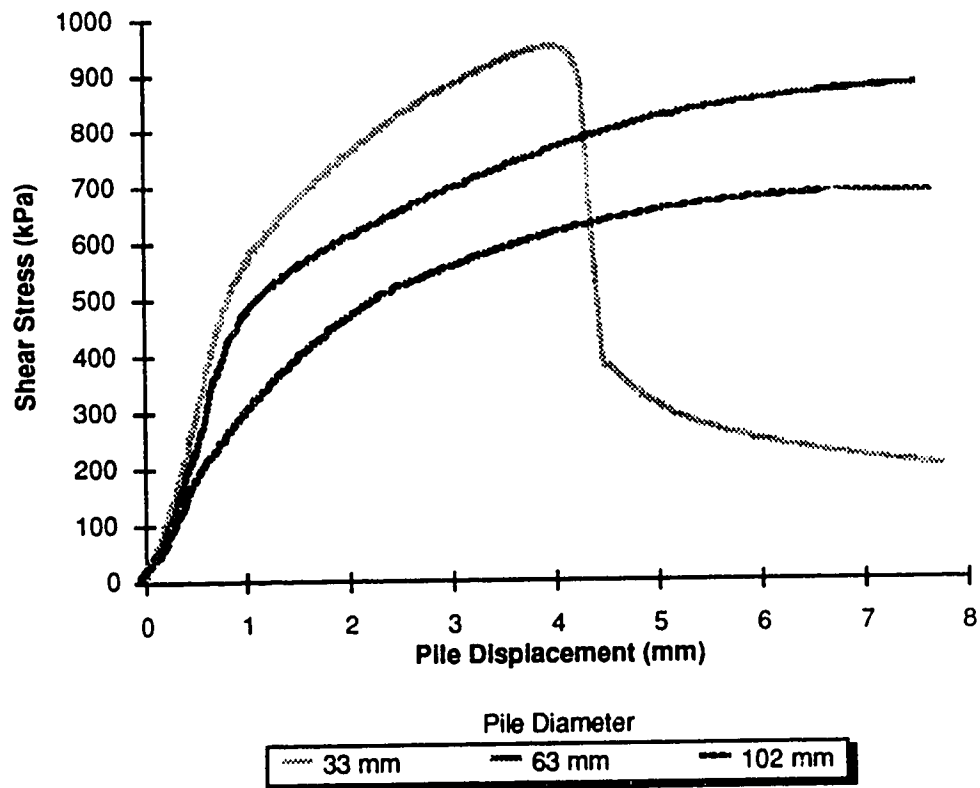


Figure 5.6: Typical stress versus displacement behaviour of model piles in saline frozen silty sand, from test #45:  $S = 10$  ppt,  $T = -5^{\circ}\text{C}$ , Backfill = grout.



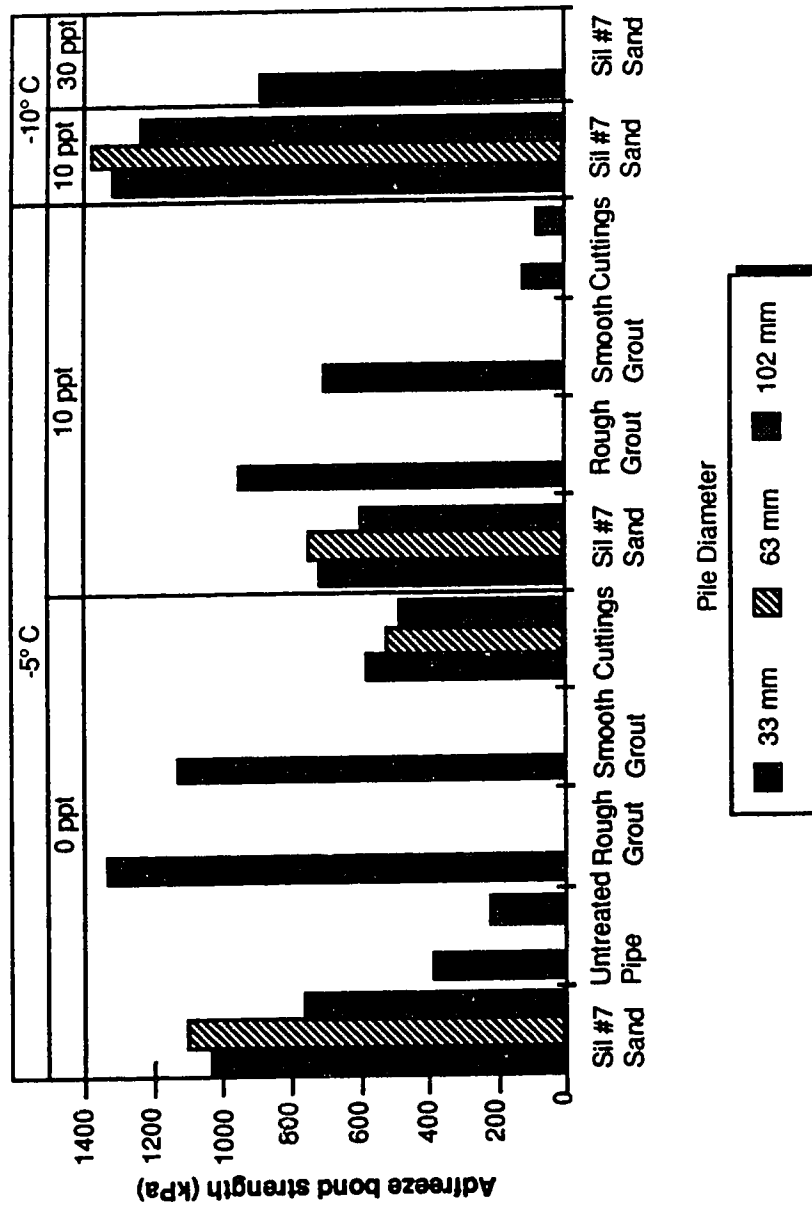


Figure 5.7: Adfreeze bond strength at failure for different pile configurations

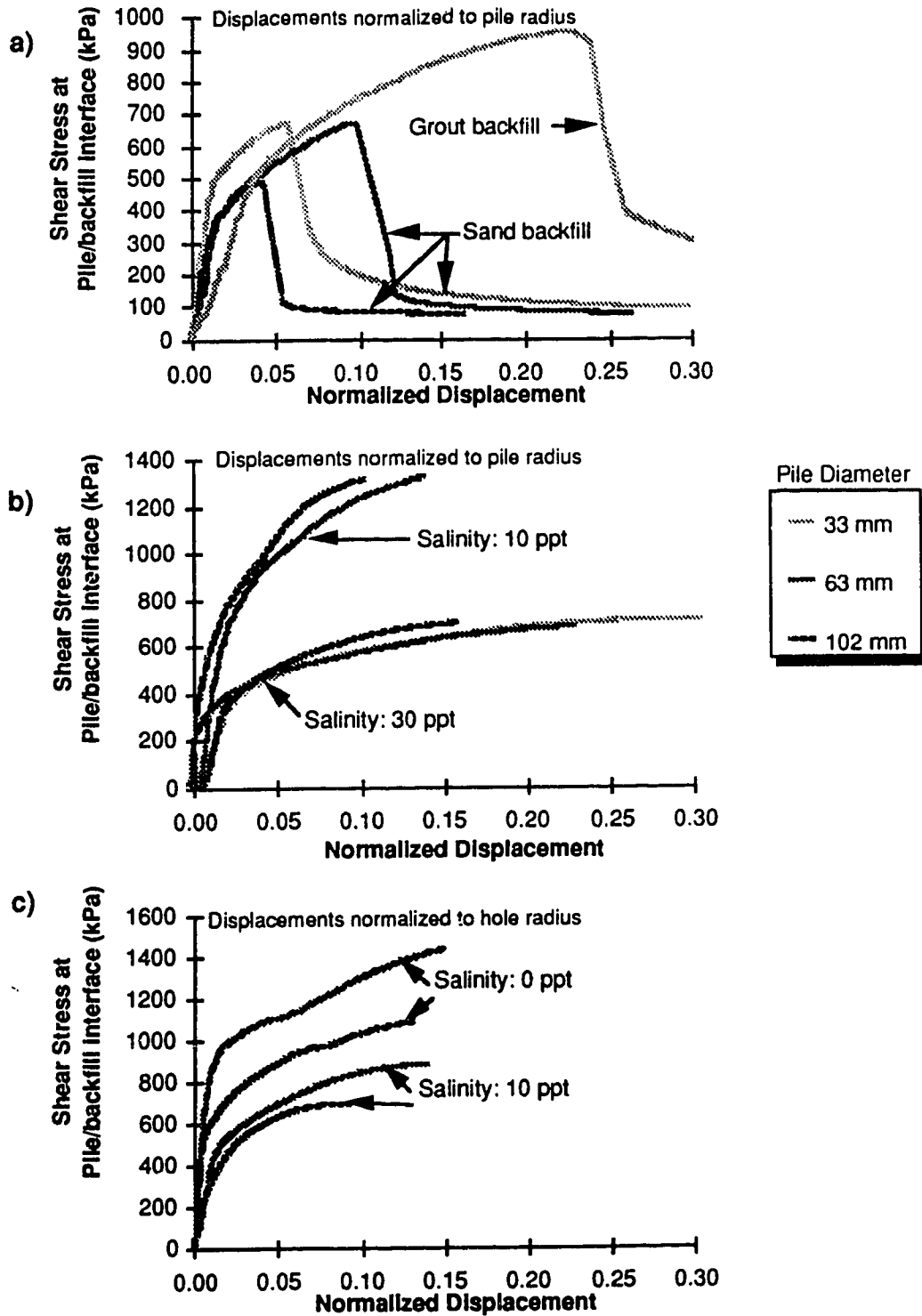


Figure 5.8: Typical stress versus normalized pile displacement behaviour

- a) brittle failure,  $T = -5^{\circ}\text{C}$
- b) grout backfilled piles,  $T = -10^{\circ}\text{C}$
- c) grout backfilled piles,  $T = -5^{\circ}\text{C}$

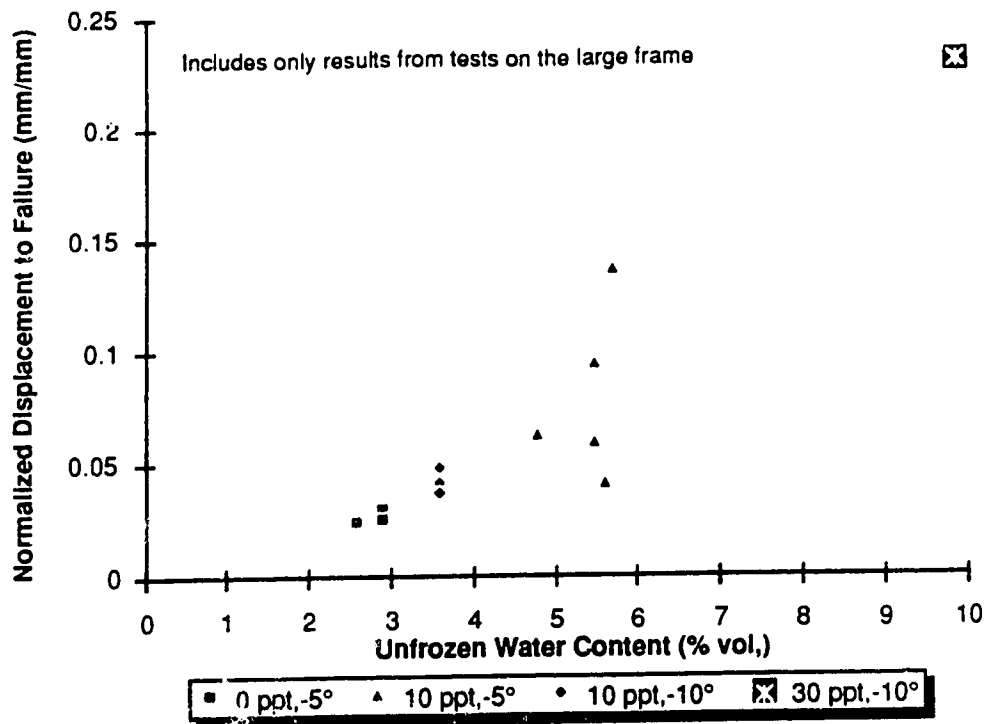


Figure 5.9: Normalized displacement to failure of the adfreeze bond versus unfrozen water content of the *native* soil

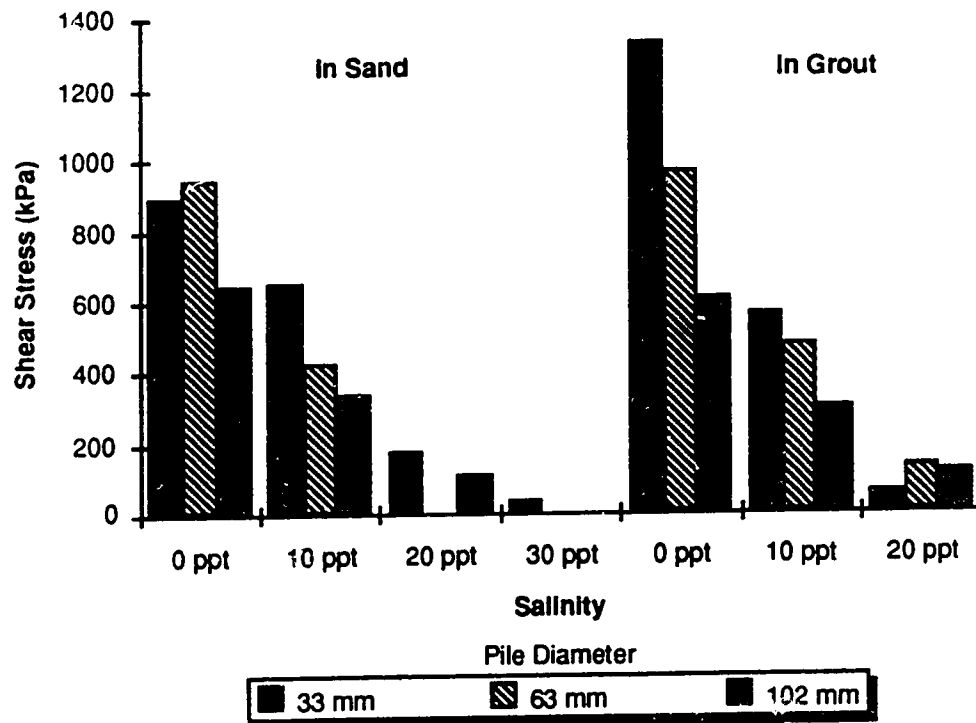


Figure 5.10: Shear stress at the pile/backfill interface at 1 mm displacement

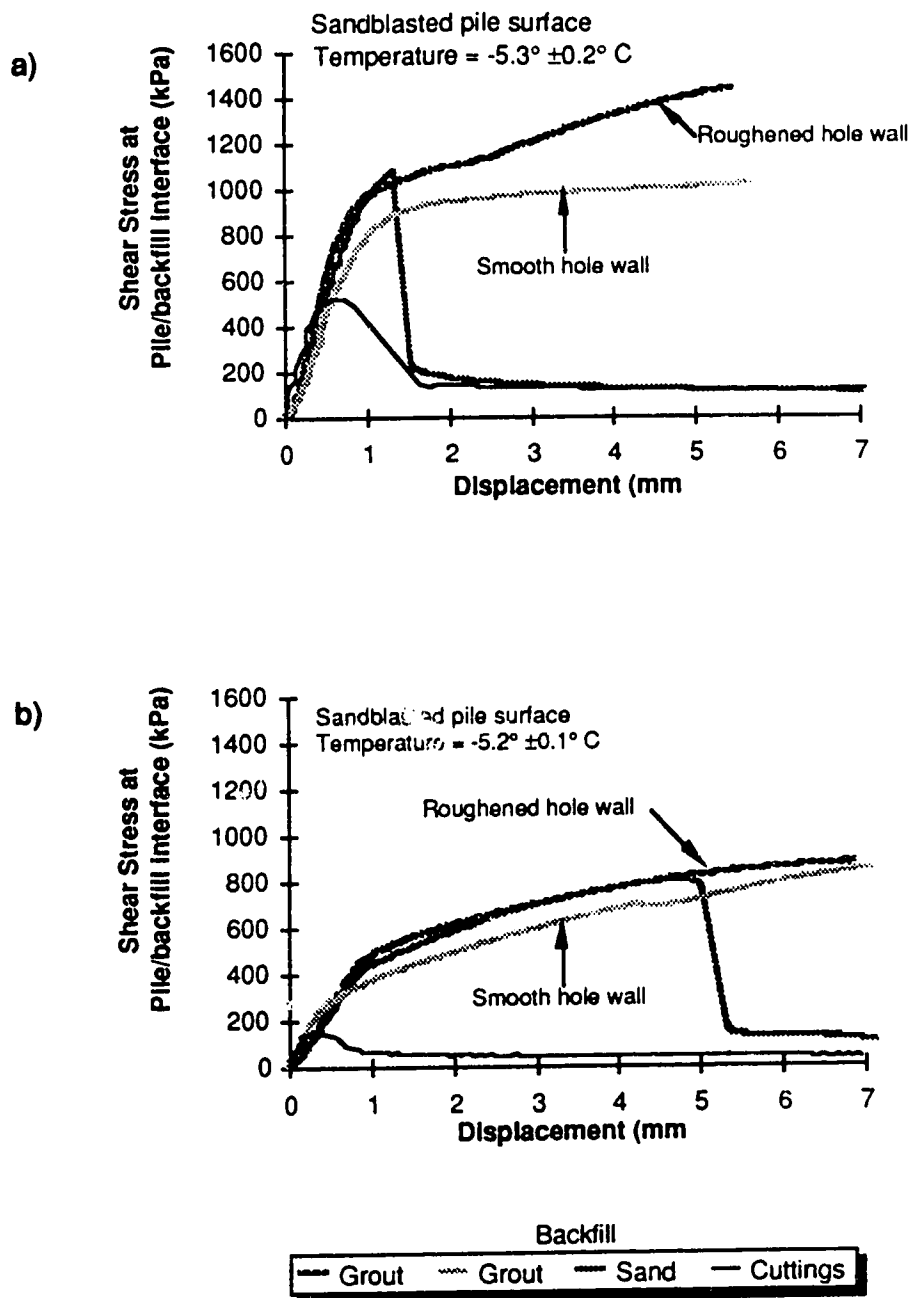


Figure 5.11. Comparison of effect of backfill material on pile performance

a)  $S = 0 \text{ ppt}$

b)  $S = 10 \text{ ppt}$

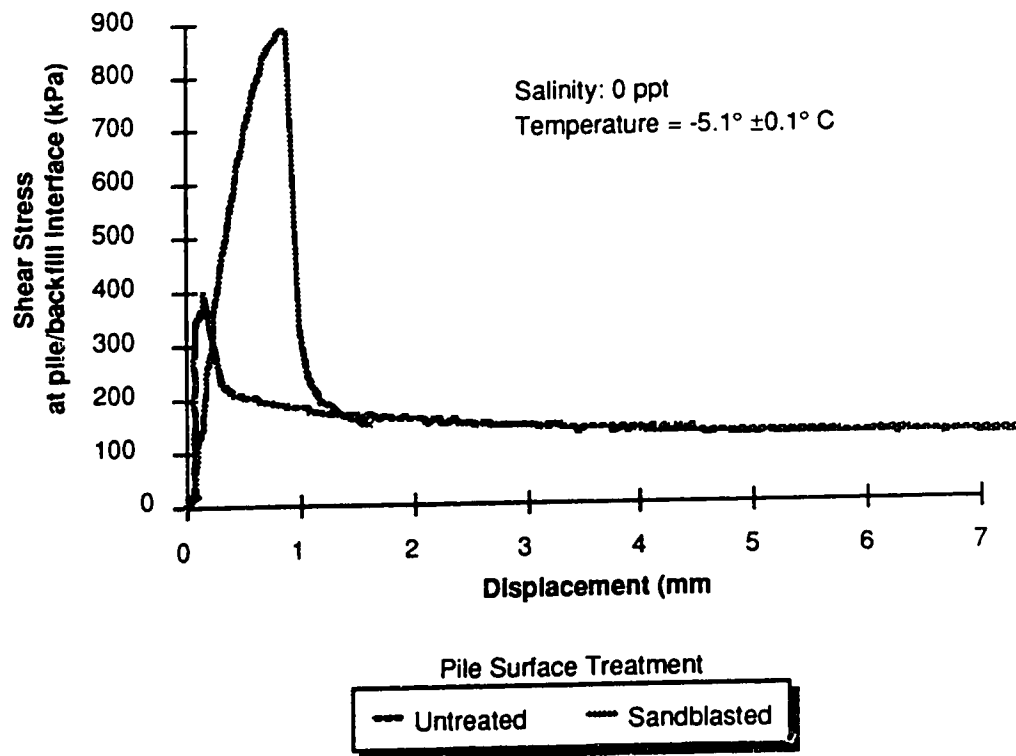


Figure 5.12: Effect of pile surface treatment on pile behaviour

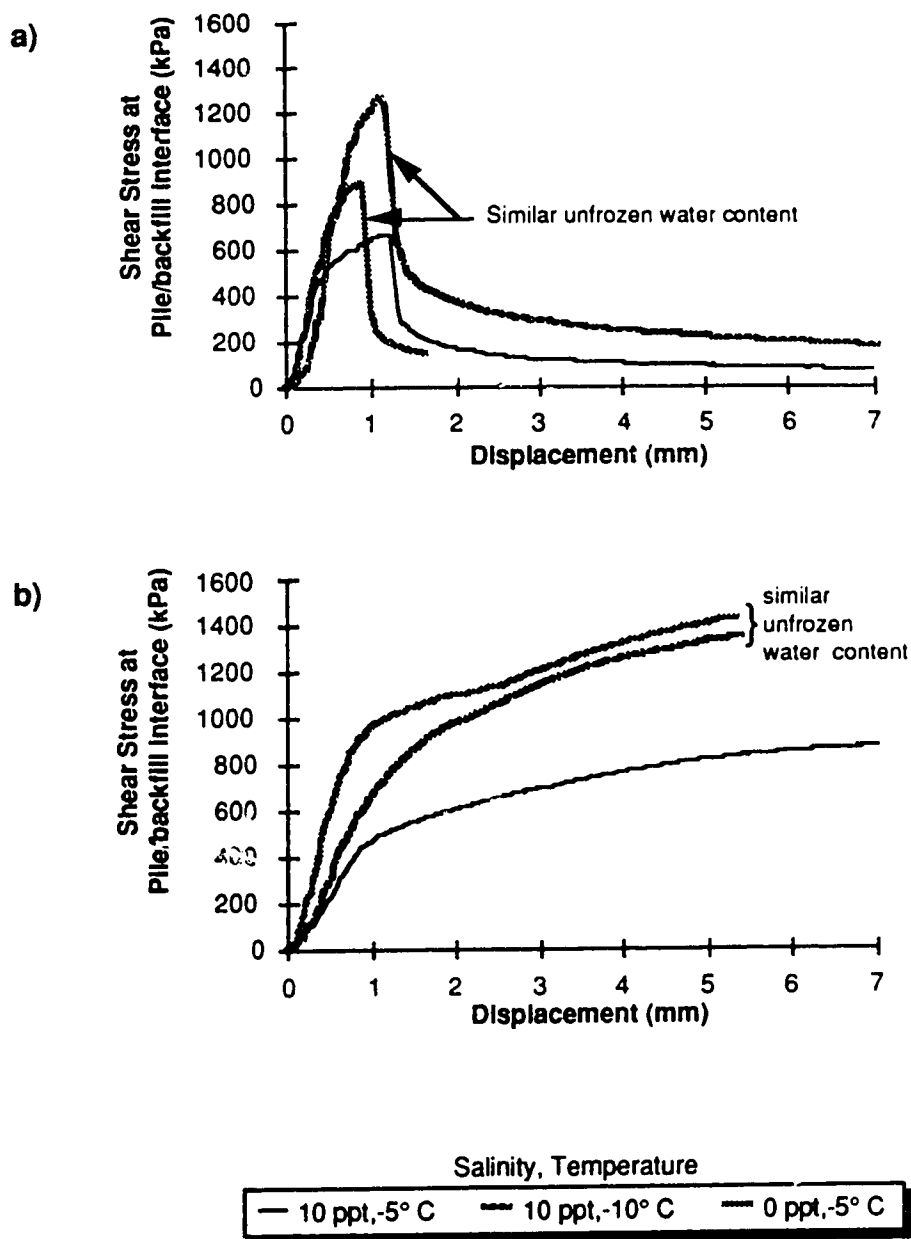
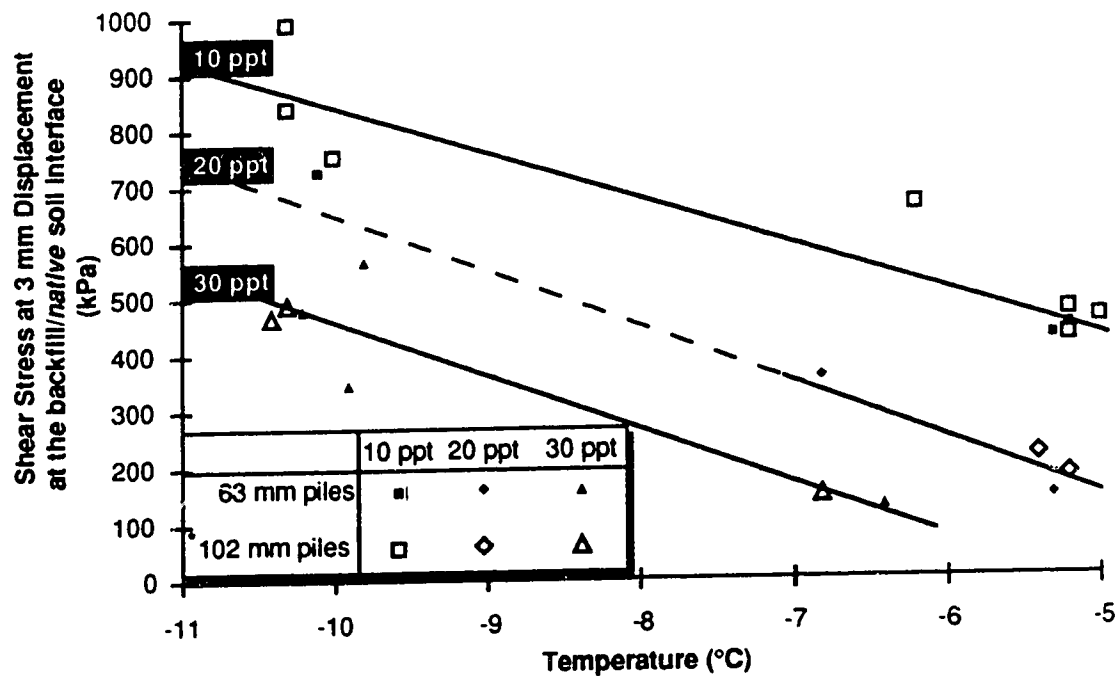


Figure 5.13: Effect of temperature on pile performance  
a) Sand backfill, 33 mm diameter pile  
b) Grout backfill, 50 mm pile



\*NOTE: Stresses for 102 mm piles were multiplied by 1.2 to adjust for observed reductions in mobilized shear stress with increasing pile diameter.

Figure 5.14: Effect of temperature on mobilized shear stress at 3 mm displacement

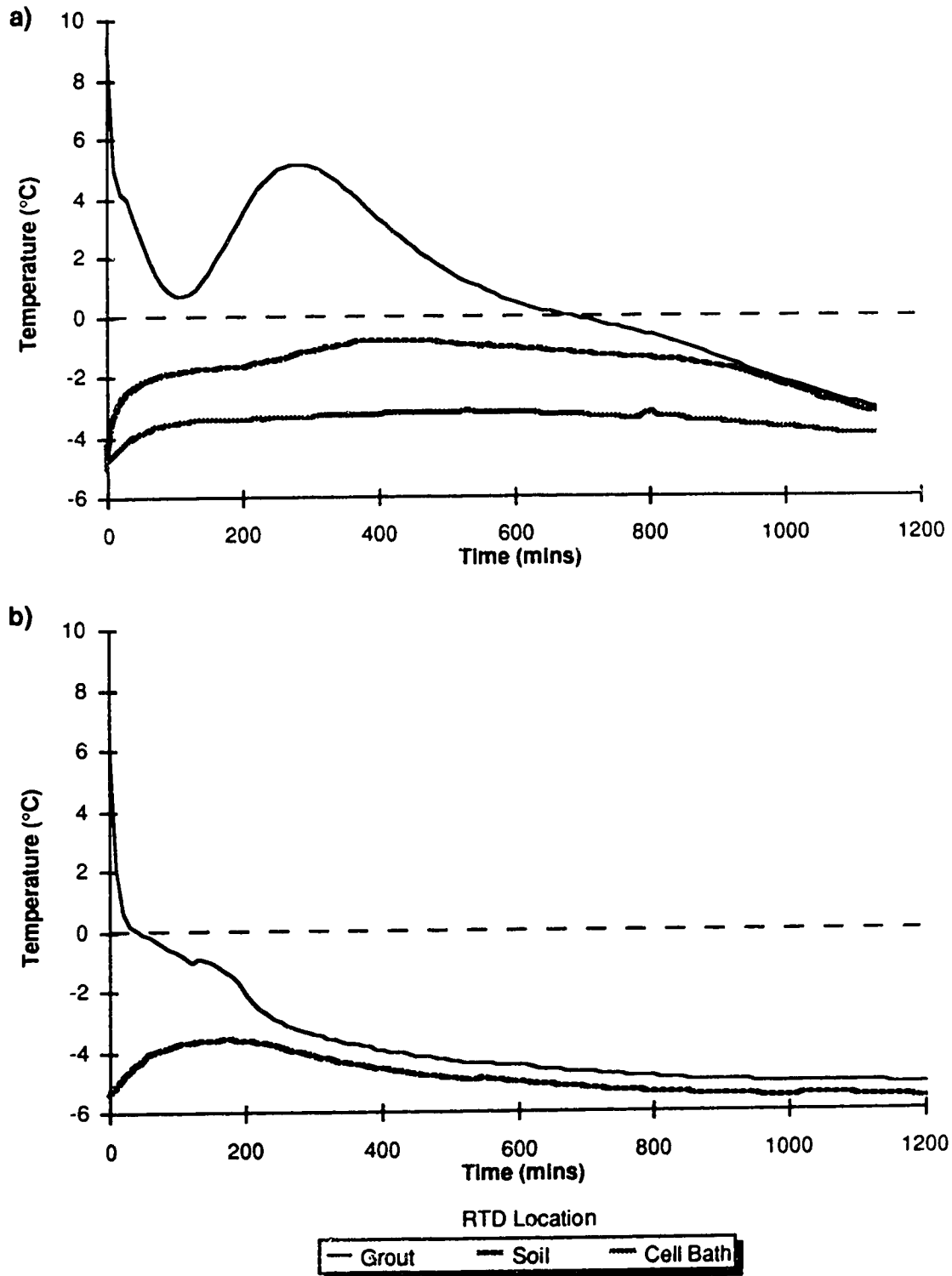
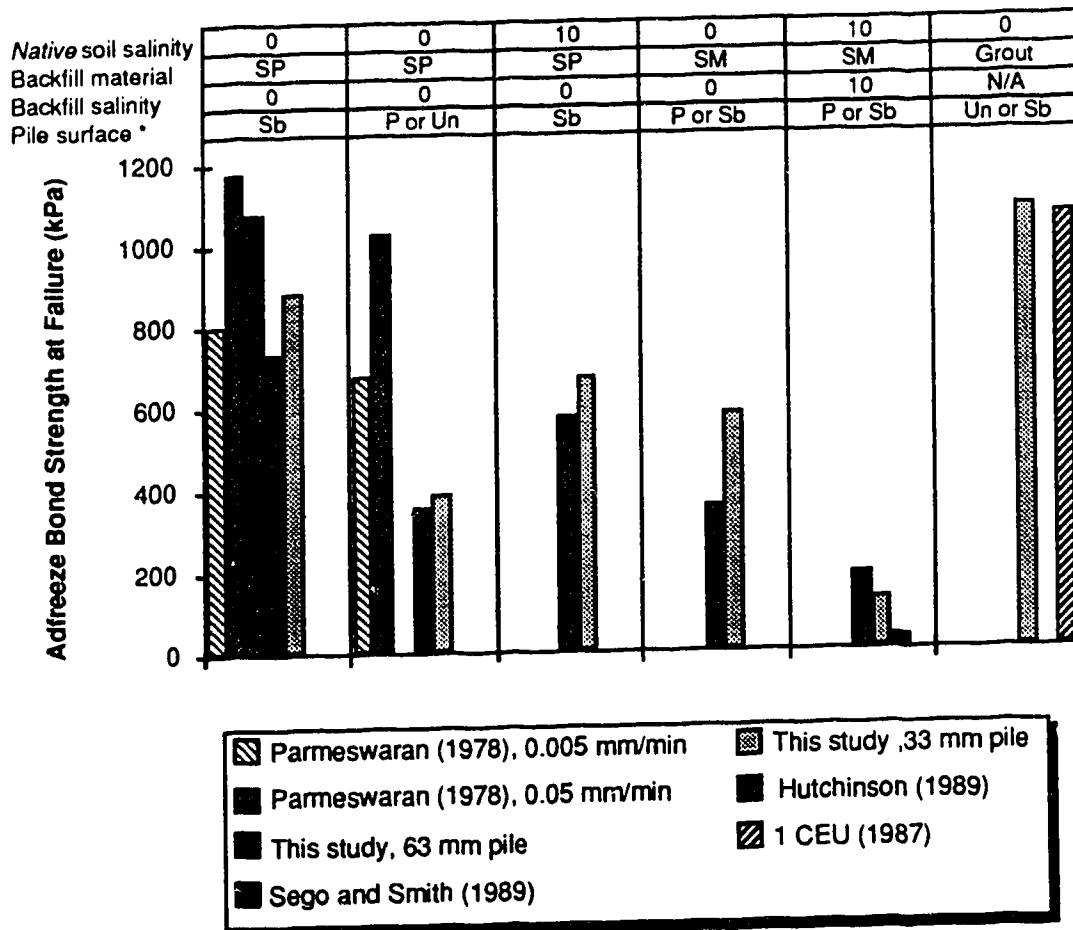


Figure 5.15: Grout curing temperatures  
a) 102 mm pile  
b) 33 mm pile





\*Note: Pile surfaces:  
 Sb denotes sandblasted steel pipe  
 Un denotes untreated steel pipe  
 P denotes painted steel pipe

Figure 5.16: Comparison of test results from this study with laboratory results by others.

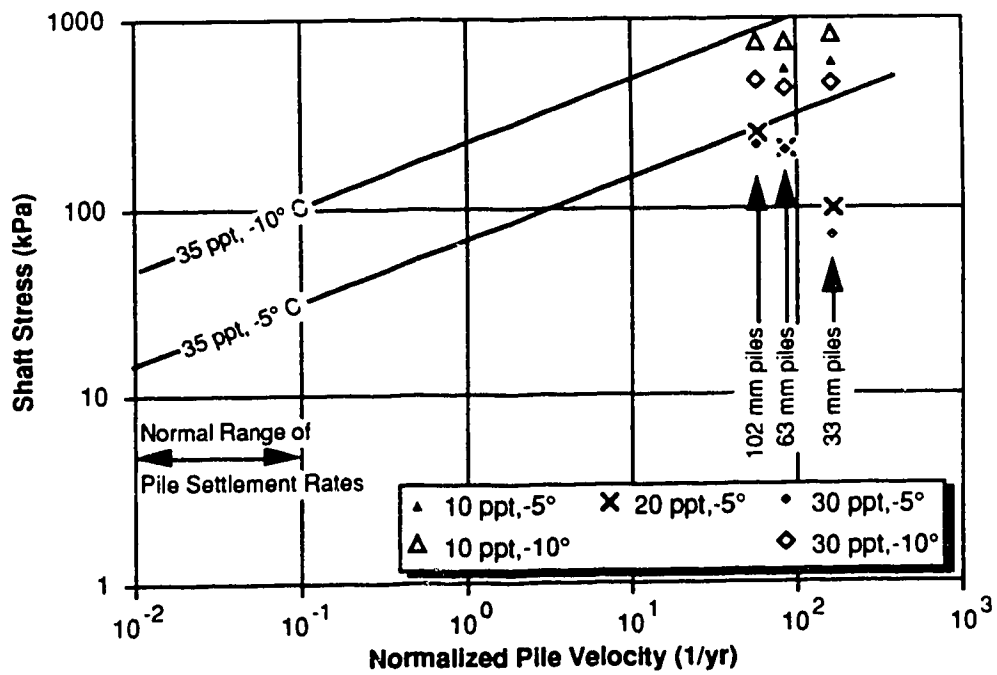


Figure 5.17: Comparison of test results with guidelines proposed by Nixon and Neukirchner (1984)

## **6. TIME DEPENDENT DISPLACEMENT BEHAVIOUR OF MODEL ADFREEZE AND GROUTED PILES IN SALINE FROZEN SOILS**

### **Introduction**

Part I [Chapter 5] examined the performance of a number of different model pile/backfill configurations in saline frozen silty sand under constant displacement rate loading conditions. Sandblasted pipe piles with clean sand or grout backfill were observed to undergo similar stress-displacement behaviour although the capacity of the clean sand backfilled piles was limited by the strength of the adfreeze bond whereas the grout backfilled piles behaved in a strain strengthening manner. Untreated pipe piles with a clean sand backfill, and the use of silty sand cuttings as a backfill material was observed to provide inferior pile load carrying capacity.

The use of a grout as a backfill material is more expensive and requires greater construction control than use of a sand backfill, so a study was undertaken to determine whether the enhanced load carrying capacity of grout backfilled piles observed in short-term tests was also applicable under long-term, constant load conditions. The study examined the performance of model sandblasted pipe piles with grout and sand backfill in frozen silty sand at salinities of 0, 10, and 30 ppt. The objective was to examine pile performance in soil at salinities in which either adfreeze bond strength or time dependent deformation govern the pile capacity, thereby providing guidance on which pile configuration provides optimum performance in the various *native* soil conditions.

### **Experimental procedure**

#### *General*

The test cell, pile material, and sample preparation for the constant load tests was identical to that used for the constant displacement rate tests discussed in Part I [Chapter 5] so will not be discussed further. Only one soil temperature was examined ( $-5^{\circ}\text{C}$ ), and all piles had their surface sandblasted prior to installation. The variables examined in this program were limited to the *native* soil salinity, and the backfill material. Pile performance

under constant load with a saline backfill material was reported in Hutchinson (1989), thus only clean sand and grout backfill materials were examined in this study.

After the piles were placed and backfilled in the test specimen, it was left for a minimum of 24 hours to allow the backfill to freeze (or cure, for grouts). The test cells were then moved into the test frame, connected to a constant temperature bath and the soil temperature was allowed to stabilize for a further 24 hours.

### *Loading*

The loading frame, shown schematically in Figure 6.1, consisted of reinforced 150 mm wide channels on the top and bottom separated by four 25 mm all-thread rods. The height of the frame was adjusted via nuts on the all-thread rods to facilitate different load cell heights. A second type of frame was also used which had 150 mm channels for the vertical members instead of threaded rods. Load was applied to the cell via a Bellofram or a jack (further referred to simply as jacks) using compressed air controlled by a pressure regulator. Loads less than 25 kN were applied using building compressed air (up to 875 kPa) and the Belloframs. Larger loads (up to 56 kN) were applied using bottled compressed extra dry air and jacks capable of sustaining air pressures up to 7000 kPa. Each loading system was capable of maintaining the load within 1% of the desired level.

An initial small load ( $<0.2$  kN) was applied to ensure alignment of the loading apparatus and the pile, and to ensure that the output from the Direct Current Differential Transducer (DCDT) was within its linear range. After the transducers' initial output was recorded by the data acquisition system (within 30 sec), the load was applied at a rate of approximately 8.0 kN/min using the Belloframs. Larger loads (using the jacks) were applied at a rate of approximately 13.0 kN/min. Thus load application was generally complete within 5 minutes at the highest loads, and typically within 2 minutes.

Loads were measured using load cells of various capacities between 22.2 kN and 133 kN which were calibrated to within 0.25 %. A 19 mm steel ball bearing was installed between the load cell and the pile cap to ensure axial load application on the load cell.

Displacements were measured using 24 volt DCDTs with 50 or 100 mm of travel, capable of recording displacements with an accuracy exceeding 0.02 mm. The DCDT body was held in a bracket secured to the jack ram and the core rested on the test cell, thus the displacement of the of the jack ram was measured. Temperatures were measured using Resistance Temperature Devices (RTDs) as detailed in Part I.

Output from the transducers were recorded using a Fluke Helios data acquisition system (which transformed the analog signal to a digital signal) connected to an Operand XT computer. Data files were compiled using the program Labtech Notebook, © Laboratory Technologies Corporation, which allowed the sampling intervals, output display and data file organization to be specified. Sampling intervals were set at 30 seconds when the load was initially applied, reduced to 2 then 5 minutes until approximately 100 minutes has expired, afterwhich sampling intervals were maintained at 10 minutes for the remainder of the test. Preliminary data reduction and analysis was accomplished using Lotus 123, © Lotus Development Corporation. Final data reduction was accomplished using Microsoft Excel, © Microsoft Corporation. Regression analysis was accomplished using Cricket Graph, © Cricket Software, Inc.

## Definitions

The expressions creep, and time-dependent deformation or displacement are often used interchangeably without regard to the mechanisms involved. Strictly speaking, creep refers to time-dependent deformation of a material under constant stress with no change in volume. Volume change during constant stress unconfined compression tests on the *native* soil used for this test program was observed by Hivon (1991), however it was noted that the volume change was not related to the creep phenomenon (in the ice matrix) itself but rather due to rearrangement within the soil matrix. Further, in frozen saline soils the time-dependent deformation behaviour may be affected by consolidation due to higher unfrozen water contents (Domaschuk et al. 1983; Nixon and Lem 1984). In order to avoid such ambiguity in this paper, the expression "time-dependent deformation" will be used to refer

to soil deformation behaviour under constant stress, and 'time-dependent displacement' will refer to the displacement behaviour of piles under constant load.

Time-dependent deformation in soils may be described in four stages:

1. an instantaneous strain;
2. a period of decelerating strain rate, often called primary creep;
3. a period of constant strain rate, often called secondary creep; and
4. a period of accelerating strain rate, often called tertiary creep.

To confirm that a constant strain rate has been achieved it is most useful to plot the data with the logarithm of strain rate as the ordinate (y) axis versus the logarithm of time as the abscissa (x) axis (Morgenstern et al. 1980). The four stages of time dependent deformation and the relationship between strain rate and time are shown schematically in Figure 6.2.

#### **Time dependent displacement of piles in permafrost**

A general expression for the time-dependent displacement of piles in permafrost based on the work of Ladanyi (1972), Ladanyi and Johnston (1974), Nixon and McRoberts (1976) and Weaver and Morgenstern (1981) may be written as:

$$u_a = \frac{\sqrt{3}^{(c+1)} D \tau^c a F(t)}{(c-1)} \quad (6.1)$$

where  $u_a$  is the displacement at the pile radius  $r = a$ ,  $c > 1$  is the creep exponent for stress which is generally accepted to be independent of temperature and stress level for stresses in the region of interest in foundation engineering,  $D$  is a temperature and material dependent variable,  $\tau$  is the applied shear stress, and  $F(t)$  is a function of time [derivation in Appendix F]. The expression is based upon the assumptions of simple shear, plane strain conditions, an incompressible von Mises material and a weightless soil. The temperature dependence of the expression embodied in the term,  $D$ , may be formulated in a number of ways (Ladanyi 1972), however one commonly used expression based on the work by Vyalov (1962) is formulated as (Weaver and Morgenstern 1981):

$$D = \left[ \frac{1}{w (\theta + 1)^k} \right]^c \quad (6.2)$$

where  $k$  is a material dependent constant  $\approx 1$  over limited temperature intervals for many soil materials,  $\theta$  is the absolute value in  $^{\circ}\text{C}$  of the temperature below  $0^{\circ}\text{C}$ , and  $w$  is an experimentally determined parameter.

For the conditions of constant displacement rate which may be encountered in ice and ice-rich permafrost (Nixon and McRoberts 1976; and Morgenstern et al. 1980)  $F(t) = t^1$ , and equation (6.1) simplifies to:

$$\dot{u}_a = \frac{u_a}{t} = \frac{\sqrt{3}^{(n+1)} B \tau^n a}{(n-1)} \quad (6.3)$$

where  $u_a$  is the constant displacement rate of the pile. The values of  $n = 3$ , and  $B(T)$  for ice may be used as detailed in Morgenstern et al. (1980).

For an attenuating pile displacement rate, which may be expected in ice-poor frozen soils, a commonly used expression is a simple power law of time,  $F(t) = t^b$  (Weaver and Morgenstern 1981; and Ladanyi and Guichaoua 1985). Hence the expression for pile displacement becomes:

$$u_a = \frac{\sqrt{3}^{(c+1)} D \tau^c a t^b}{(c-1)} \quad (6.4)$$

The value of  $b$  represents the slope of the line obtained from a plot of the pile displacement versus time in logarithmic coordinates. The value of  $c$  may be subsequently calculated as the slope of the line obtained from a plot of  $u_a / a t^b$  at a given time versus the applied shear stress,  $\tau$ , in logarithmic coordinates.

## Results

A total of 65 constant load model pile tests were conducted in a saline silty sand maintained at a temperature of  $-5^{\circ}\text{C}$ , using sandblasted pipe piles with either a clean sand or a cementitious cold temperature grout as a backfill material. *Native* soil salinities of 0, 10 and 30 ppt were used, and test durations varied from instantaneous failure to as long as 76

days without failure. Five of the tests had loads applied incrementally after the pile displacement rate reached zero or continued at a constant rate for an extended period of time. The remaining tests had only one load increment applied. A summary of the test results is contained in Table 6.1. More detailed presentation of individual test results may be found in Biggar (1991) [Appendix E].

#### *Displacement versus time behaviour*

Two types of failure behaviour were observed during the test program, shown in Figure 6.3a. For the sand backfilled piles at higher stresses and in *native* soil at salinities of 0 and 10 ppt, after an initial period of attenuating displacement rate, a brief period of accelerating displacement rate was observed followed by brittle rupture of the adfreeze bond (Line 1). Grouted piles at intermediate and high stresses, and most sand backfilled piles in *native* soil with salinities of 20 and 30 ppt failed with an accelerating displacement rate without brittle rupture of the bond between the pile and the backfill (Line 2). At the lowest stresses tested in the saline soils, no failure was observed, and the piles continued to displace at either a constant or decelerating rate until the test was terminated after 41 to 76 days.

In order to determine the time to failure (defined as the onset of an accelerating displacement rate) the test results were plotted with the displacement rate versus time in log-log coordinates, illustrated in Figure 6.3b. The minimum displacement rate is easily defined in this manner, however some judgement and a close examination of the test data is required to determine the time of failure, particularly at long times (i.e. greater than 100 hrs). Due to the small displacement rates experienced at failure (.01 to .0001 mm/hr), and the effect on the testing apparatus of temperature fluctuations in the cold room of 1° to 2° C, minimum displacement rates may only be defined to an accuracy to 2 significant figures.

Pile stresses listed in Table 6.1 are shown at both the pile/backfill and the backfill/*native* soil interface, reflecting the adfreeze (or cementitious) bond stresses and *native* soil shear stresses respectively. The tabulated stresses are those applied at the start of



the test based upon the measured sample height and the borehole diameter. Because the applied load remained constant, the applied shear stress increased as the pile displaced. Shear stresses remained within 1% of the original applied stress at displacements of up to 2.5 mm, and within 2% at 5 mm displacement. With few exceptions, net pile displacements to failure (total displacements - elastic displacements) were typically less than 6 mm, hence applied stresses were maintained within 3% of the tabulated stresses throughout the test.

#### *Temperature sensitivity of test results*

Periodic problems with constant temperature baths or cold room compressors caused cold room and/or test specimen temperature fluctuations. Although only one nominal test temperature was examined, the temperature fluctuations due to equipment malfunctions emphasized the temperature sensitivity of pile behaviour, particularly at a salinity of 30 ppt. Periods of accelerating displacement rate due to intervals of increased sample temperature are illustrated in Figure 6.4, from tests #40-33 and #34-63. The temperature fluctuations shown in Figure 6.4b were due to a cold room compressor malfunctions during which the room temperature warmed to approximately -1° C where as the *native* soil temperature measured by the RTD increased by only 0.4° and 0.7° C for the respective tests. Thus although the temperature at the grout/*native* soil interface is unknown, the increase was likely less than 1° C. The dramatic effect of this temperature increase on the increased pile displacement rate is shown in Figure 6.4a and 6.4c. At a salinity of 30 ppt the effect is far more pronounced than at 10 ppt. This example serves to reinforce the requirement to maintain the ground thermal regime as cold as possible to limit pile settlement in saline soils. Successful reduction of pile settlements in saline permafrost by installing insulation on the soil surface to reduce permafrost temperatures is discussed in Miller and Johnson (1990).

### *Grout performance*

The thermal and curing performance of the grout used in this study was identical to that used in the constant displacement rate tests discussed in Part I [Chapter 5]. In no instances did failure occur at the interface between the pile and the grout backfill during the constant load tests. Maximum observed shear stresses at the pile/grout interface were 694 kPa in test #36-102. For tests in which the grout at the pile interface had not properly cured (for 33 mm piles, as discussed in Part I [Chapter 5]) maximum shear stresses at the pile/grout interface of 575 kPa were observed in test #31-33. From the results in Part I, short term bond strengths of 1500 kPa were observed. The above bond stress values are the maximum encountered in this program without failure; ultimate bond stresses are greater. Shearing failure or creep within the grout was not observed in any instances in this test program; failure always occurred within the *native* soil. For grout backfilled piles the maximum shearing stress observed at the grout/*native* soil interface was 466 kPa, in test #36-102.

### *Observations of test specimen behaviour*

In all grout backfilled pile tests a plug of soil with a diameter equal to the inside diameter of the baseplate was pushed out of the bottom of the sample, as illustrated in Figure 6.5. The grout backfill remained intact with no signs of deformation or deterioration. Sand backfilled piles in *native* soil with a salinity of 30 ppt generally behaved in the same manner, except tests #22-33 and #30-33 which failed immediately after the full load was applied. Again there did not appear to be any deformation in the backfill material, but as no mechanism was in place to measure backfill deformations specifically, only visual observations were made when the test was completed. Tests conducted with sand backfilled piles in *native* soil with a salinity of 10 ppt behaved in a similar manner until the rupture of the adfreeze bond, i.e. the *native* soil was pushed out of the bottom of the sample along the inside edge of the base plate. Displacements to failure for these tests

varied, but typically 2 to 5 mm of soil was displaced out of the bottom of the test specimen before the adfreeze bond ruptured.

Sand backfill adjacent to the *native* soil from tests #21-33 and #22-33 was analysed for salinity upon completion of the test; no measurable salinity was evident. Although this procedure was not performed on all sand backfilled piles, the results indicate that the sand backfill installation procedure was adequate to prevent solute migration into the backfill, which would have resulted in deterioration of the strengths of the backfill and adfreeze bond.

### **Analysis of results**

Friction pile design in non-saline cold ( $T < -1^{\circ}\text{C}$ ) permafrost can generally be divided into two categories: pile design for ice-rich or for ice-poor soils (Weaver and Morgenstern 1981). Pile design in ice-rich permafrost is usually governed by long-term settlement due to the time dependent deformations of the soil resulting from creep in the ice matrix. Design based upon constant deformation rates in ice (Ladanyi 1972; Nixon and McRoberts 1976; and Morgenstern et al. 1980) provide an upper limit for the pile displacements. Pile load carrying capacity in ice-poor soils may be governed by either the adfreeze bond capacity or by time dependent deformations of the frozen soil, depending on the pile configuration and on the *native* soil properties. Time dependent deformations in ice-poor soil may be formulated in terms of a simple power law of time (equation 6.4) (Vyalov 1962; Ladanyi and Johnson 1974; and Weaver and Morgenstern 1981).

Pile time dependent deformation in saline ice-rich permafrost has been addressed by Nixon and Neukirchner (1984) based upon the results of creep tests on ice-rich saline frozen soils performed by Nixon and Lem (1984). A constant displacement rate formulation (equation 6.3) was proposed which maintained the stress exponent used for design in ice ( $n = 3$ ), and adjusted the value of the temperature dependent variable,  $B$ , as a function of salinity and temperature.

Because the *native* soil used in this study was an ice-poor saline soil, the results from the tests were analysed both in terms of constant and attenuating displacement rates to determine which mechanism would be most applicable in design. The behaviour was examined in terms of the relationship between the applied shear stress at the backfill/*native* soil interface and the minimum pile displacement rate (normalized to the hole radius), and in terms of the pile displacement versus time behaviour. In addition the pile time dependent displacement developed prior to the rupture of the adfreeze bond was analysed.

#### *Displacement rate versus applied stress behaviour*

The relationship between minimum pile displacement rate (normalized to the hole radius) and applied shear stress at the backfill/*native* soil interface is shown in a log-log relationship in Figure 6.6 for *native* soil salinities of 10 and 30 ppt with both grout and sand backfilled piles. At the higher stresses for a particular pile-soil configuration, the minimum displacement rate represented the point of inflection in the displacement-time curve where the displacement rate changed from an attenuating to an accelerating rate, as discussed previously and shown in Figure 6.2. At intermediate stresses there was a short duration of constant displacement rate followed by an accelerating rate. At the lowest stresses no failure was observed although the pile continued to displace at a constant, albeit very slow rate. In none of the tests in which a saline *native* soil was used did the pile displacement rate stop completely. However the pile displacement rate did stop in two of the tests in which a non-saline *native* soil was used.

Although there is a moderate amount of scatter in the results shown in Figure 6.6 certain trends are apparent. Using the relationship defined in equation (6.3), a least squares fit to the data resulted in the parameters  $n$  and  $B$  shown in Table 6.2. The results from the grout backfilled piles show a decrease in the stress exponent,  $n$ , from 9.5 to 6.1 when the salinity of the *native* soil increased from 10 to 30 ppt. In the *native* soil with a salinity of 30 ppt both the grout and the sand backfilled piles behaved in a similar manner (i.e. the  $n$

values are nearly the same) but the grouted piles had approximately twice the capacity of the sand backfilled piles at a given displacement rate (i.e. the B values differ).

The scatter in the results for the sand backfilled piles in a *native* soil with 10 ppt salinity at shear stresses in excess of 350 kPa were due to the rupture of the adfreeze bond. Unfortunately time constraints did not permit sufficient tests to be conducted at lower stresses in order to better define the stress exponent,  $n$ , for this configuration. The line defined from the results of the grout backfilled pile tests however, provides a reasonable fit to the data at the higher stresses for the sand backfilled piles.

#### *Displacement versus time behaviour*

As discussed previously and expressed in equation (6.4) an attenuating pile displacement rate may be defined by a simple power law of time. For the attenuating portion of the pile displacement rate, the displacement of the piles was plotted versus time on log-log coordinates as shown in Figure 6.7. The displacement of the pile is then defined by the expression:

$$u_a = K t^b \quad (6.5)$$

where the slope of the resulting line defines the time exponent,  $b$ , and the intercept at 1 hour defines the constant,  $K$ . Relating equation (6.5) to equation (6.4) the parameter  $K$  is then defined as:

$$K = \frac{\sqrt{3}^{(c+1)} D \tau^c a}{(c-1)} \quad (6.6)$$

By plotting the values of  $K$  versus the applied shear stress the stress exponent,  $c$ , and the parameter  $D$  may be obtained.

The values of  $b$  for different backfills and *native* soil salinities are plotted versus the stress at the backfill/*native* soil interface in Figure 6.8. It is generally accepted that the time exponent is constant over a limited stress range, and the results of this study agree with this concept. The mean values of  $b$ , denoted as  $\bar{b}$ , for the grouted piles was 0.28. In the *native* soil 10 ppt salinity  $\bar{b}_{g10} = 0.26$ , and for the *native* soil with 30 ppt  $\bar{b}_{g30} = 0.30$ .

The values of  $b$  obtained from the sand backfilled piles were different for the tests conducted at the two different salinities. In *native* soil with a salinity of 30 ppt the values of  $b$  were similar to those obtained for the grouted piles, and a value of  $\bar{b}_{s30} = 0.37$  was obtained. Although there was considerable scatter in the values of  $b$  for the sand backfilled piles in *native* soil with a salinity of 10 ppt, Figure 6.8 shows that they were noticeably lower, with a value of  $\bar{b}_{s10} = 0.135$ . This lower value of  $b$  indicates that sand backfilled piles would undergo less time dependent displacement over a long period of time, which is unlikely. The lower  $b$  value is likely due in part to the fact that a different strain pattern developed around the sand backfilled piles in *native* soil with salinity of 10 ppt, than in the other configurations. The grout backfill behaves as a rigid body relative to the more deformable frozen saline soil, hence all of the shear strain occurs within the *native* soil. For the sand backfilled piles in the *native* soil with a salinity of 30 ppt, the backfill material was also considerably stronger than the *native* soil thus the mode of deformation was similar to that of the grout backfilled piles. For the sand backfilled piles in *native* soil with a salinity of 10 ppt, however, the backfill material was subject to greater shear strains than in the other pile configurations, hence the shear strains at the interface between the backfill and the *native* soil were less. A more detailed analysis of this behaviour is beyond the scope of this paper.

The value of the  $K$  parameter is affected by the initial displacement of the pile as well as by the value of the time exponent,  $b$ . The magnitude of the initial measured displacement (of the jack ram) in the tests varied appreciably because of the different loading frame configurations used (three different types of jacks and two different types of frames) in order to provide a sufficient load capacity for the larger diameter piles. Due to these effects, analysis of the  $K$  versus  $\tau$  relationship (to determine the stress exponent,  $c$  in equations (6.4) and (6.6)) for piles in *native* soil with a salinity of 10 ppt, was unsuccessful. The tests on the piles in *native* soil with a salinity of 30 ppt were carried out

using a single frame configuration, and sufficient data was available to estimate the magnitude of  $c$ , as discussed below.

Some test results indicated that either excessive or too little initial displacement occurred due to load cap and/or LVDT seating errors. Further, three different pile diameters were used hence for piles of different sizes initial elastic deformations varied at similar applied stress levels. In order to account for these effects, spurious values of  $K$  were deleted from the analysis and the remaining values of  $K$  were normalized to the pile radius. [Details of the procedure are contained in Appendix E]. The values of the normalized  $K$  parameter,  $K_n$ , were plotted against soil shear stress at the backfill/*native* soil interface in log-log coordinates, and a linear least squares regression provided an estimate of the parameters  $c$  and  $D$ , presented in Table 6.3. It is emphasized that these values are specific to the test apparatus used, and were determined by normalizing the  $K$  parameter to the pile radius.

The parameters obtained from the attenuating pile displacement rate analysis are only valid for short-term displacements in saline frozen soils, as the test results from this study indicate that a constant displacement rate will eventually be achieved. Substituting the parameters  $b$ ,  $c$ , and  $D$  in Table 6.3 into equation (6.4) for a grout backfilled pile in a *native* soil with a salinity of 30 ppt at an applied shear stress of 100 kPa and a temperature of  $-5^{\circ}$  C, a normalized displacement of approximately 0.018 is obtained at 100,000 hrs (approximately 11 years). The constant displacement rate analysis described previously results in a normalized displacement of 15.4 under the same conditions. An attenuating displacement rate formulation based on short-term results is inappropriate to calculate long-term displacements for the conditions tested, and will result in unconservative pile settlement estimates.

#### *Pile displacement to the rupture of the adfreeze bond*

Considerable difficulty was experienced carrying out the tests on the sand backfilled piles in *native* soil with a salinity of 10 ppt. At adfreeze bond stresses in excess of 360 kPa

(approximately 50% of the constant displacement rate test adfreeze bond capacity detailed in Part I [Chapter 5]), pile failure occurred due to rupture of the adfreeze bond rather than failure of the *native* soil. Due to time constraints only two tests were conducted at stresses less than 350 kPa (#49-33 and #51-63). These piles were loaded in 100 kPa increments to a maximum of 300 kPa. At the time of writing neither test has failed after 30 days, and less than 1.0 mm of accumulated time dependent displacement.

An analysis of the adfreeze bond rupture data was performed to determine if there existed a limiting deformation to the rupture of the adfreeze bond. No single value of displacement to failure was observed either directly or by normalizing the displacement to the pile radius. The net displacement to failure (equal to the total displacement - elastic displacement) versus stress at the pile/backfill interface is shown in Figure 6.9. Generally displacements to rupture of the adfreeze bond were in excess of 2 mm however three tests failed at smaller displacements. A general trend is observed indicating that the displacement to failure decreased with decreasing stress, however the scatter in the data is sufficient to question this relationship. Based upon the results of tests #49-33 and #51-63, it may be safely stated that failure has not been observed for time dependent displacements less than 1 mm.

### **Comparison with data from other studies**

#### ***Laboratory constant displacement rate test results***

Limited comparison may be made between the constant load test results of this study and the constant displacement rate (CDR) tests described in Part I [Chapter 5] due to differences in the failure mechanisms observed. Strain strengthening behaviour (without failure in the *native* soil) was observed during the CDR tests for all grout backfilled piles, and for sand backfilled piles in *native* soil with a salinity of 30 ppt. Net displacements to failure for the grout backfilled piles in the constant load tests varied between 2.8 mm and 9.4 mm, hence choosing a representative pile displacement at which to compare CDR and constant load test results is impractical.



The results from the CDR tests for sand backfilled piles in *native* soil with a salinity of 10 ppt are plotted in Figure 6.6, as the failure mechanism was the same for both sets of tests, i.e. rupture of the adfreeze bond. The CDR test results are bounded rather well by the line described by the grout backfilled piles in the *native* soil with 10 ppt salinity, which also bounds the highest values from the constant load tests using sand backfilled piles.

#### *Unconfined constant stress compression test results*

Unconfined constant stress compression tests on three different saline ice-poor frozen soils are reported in Hivon (1991) for salinities of 0, 5, 10, and 30 ppt at a temperature of  $-7^{\circ}\text{C}$ . In a silty sand and a fine silty sand it was observed that value of  $n$  decreased as the salinity increased, suggesting that as salinity increased beyond 30 ppt, the value of  $n$  may approach that of ice. For the soil identical to the one used in this study, at salinities of 10 and 30 ppt, the values of  $n$  were determined to be 11 and 4.9 respectively. These values compare favourable to the values of 9.5 and 6.1 obtained in this study. In order to compare the  $B$  values from the two studies, the shear stresses were normalized to 500 kPa ( $\sigma_1 = 1000\text{ kPa}$ ) and displacement rates were calculated in units of  $\text{hr}^{-1}$ . The values of  $n$  and  $B$  calculated at salinities of 10 and 30 ppt from the two studies are shown in Table 6.4. Considering that the values of  $B$  vary by several orders of magnitudes for small changes in salinities and temperature, the results are encouraging.

#### *Comparison with pile load tests by others*

Constant load tests on model piles are reported by Parmeswaran (1978) and Hutchinson (1989). Concrete and steel H-section piles in non-saline frozen Ottawa sand are reported in Parmeswaran (1978) and sandblasted pipe piles in contact with saline silty sand are reported by Hutchinson (1989). Results from these two studies are displayed in Figure 6.10 along with the regression lines obtained in this study.

The upper values of adfreeze bond strengths for the piles in a clean sand backfill in this study are in close agreement with the line presented in Parmeswaran (1978). There are however a number of results from this study which fall considerably below the line as well,

suggesting that the saline *native* soil had an adverse affect on the adfreeze bond strength although no saline pore fluid was in contact with the pile. This observation is supported by the results reported in Part I [Chapter 5] which showed a reduction in adfreeze bond strength when the salinity of the *native* soil changed from 0 to 10 ppt.

The results from Hutchinson (1989) illustrates the dramatic reduction in pile load carrying capacity when the pile surface is in contact with saline pore fluid. At a *native* soil salinity of 10 ppt a reduction in capacity of approximately an order of magnitude is seen when the pipe is in contact with the saline soil compared with the results of either grout or clean sand backfilled piles in the same soil. The data from Hutchinson (1989) also indicate that the  $n$  value decreases with increasing salinity.

#### *Comparison with field test results*

Data from field performance of piles in saline permafrost are also presented in Figure 6.10. Miller and Johnson (1990) provide a valuable case study on the performance a steel pipe pile foundation in permafrost with salinities typically between 30 to 40 ppt, and as high as 60 ppt, in Barrow, Alaska. Pipe piles 457 mm in diameter were installed in 610 mm diameter holes and backfilled with a clean sand-water slurry. Soil temperatures varied between approximately  $-2^{\circ}$  and  $-8^{\circ}$  C over the pile embedment during the summer months when excessive displacement occurred. The normalized pile displacement rate versus shear stress results presented in the paper are shown in Figure 6.10, and are in close agreement with the results from this study.

A field pile load test program in permafrost with salinities of between approximately 10 and 35 ppt conducted in Clyde River, NWT is reported by Nixon (1988). Pipe piles 140 mm in diameter were installed in 175 mm diameter holes and backfilled with saline silty sand cuttings from the site. Ground temperatures during the test program varied from approximately  $-2^{\circ}$  to  $-9^{\circ}$  C along the embedment of the pile. The results are seen to correlate well with the data from this study at salinities of 10 ppt. However comparison with the results from Hutchinson (1989), in which saline silty sand was also in contact with the pile

surface, show reasonable correlation for salinities of 5 to 10 ppt. Considering that the salinity of the *native* soil cuttings used as the backfill material from the Clyde River tests would have been diluted when water was added to prepare the slurry, the comparison is reasonable.

#### *Comparison with pile design guidelines by others*

The results from this study are compared with those published by Nixon and Neukirchner (1984) in Figure 6.11. The considerable difference in the results is attributable to the difference in soil grain size and ice content. The silty sand data from Nixon and Lem (1984) used in the study by Nixon and Neukirchner (1984) had a approximately 45% fines and distinct ice lenses, although the sample moisture and densities are similar to those in this study. At a specified displacement rate, reductions in strength of approximately 50% were observed in this study as *native* soil salinities were increased from 10 to 30 ppt. This compares to similar strength reductions presented in Nixon and Neukirchner (1984) as salinities increased from 0 to 35 ppt. Further, as mentioned in Nixon and Neukirchner (1984), at the same stress level, increases in pile displacement rates of at least 100 times may be expected as salinities increase from 10 to 30 ppt.

#### **Migration of solutes into the backfill**

The migration of solutes from the native soil through the slurry backfill to the pile surface will dramatically reduce the adfreeze bond capacity between the backfill and the pile, and will increase the time dependent deformation of the slurry backfill. In order to determine the likely extent of solute migration through slurry backfills, the mechanisms of water redistribution during freezing and solute diffusion in ice and frozen soil must be examined.

The redistribution of solutes in freezing soils has been addressed in Sheeran and Yong (1975), Hallet (1976), Kay and Groeneveldt (1983), Kay and Perfect (1988), Baker and Osterkamp (1988) and Romanov (1989). Generally it was found that solutes were not rejected forward of the freezing front on a macro scale. Rather the freezing front 'jumped'

over solute enriched zones immediately ahead of the freezing front (where the freezing temperature had been depressed) leaving layers of solute enriched soil between layers of solute-poor soil. Thus although concentration of solutes ahead of the freezing front was observed on a micro scale, the salinity of the soil on a macro scale was not affected. Romanov (1989) did observe limited solute rejection at the slowest freezing rates (17.6 mm/day), and at the highest concentrations (1.0 mol /litre, 28 ppt), but for most tests there was little or no change in the overall soil salinity. Solute enrichment in the unfrozen soil forward of the freezing front was observed by Kay and Groeneveldt (1983) in field tests. This was attributed, however, to convective transport of solutes arising from water migration from the unfrozen soil into the freezing zone, rather than rejection of solutes from the freezing soil.

The implications of these observations on slurry backfilled piles in saline permafrost are twofold. Firstly the convective transport of solutes to the freezing front may have an adverse affect on pile performance if the piles are installed without being warmed in the winter. The cold pile wall will cause the migration of water to its surface. This will not only have the effect of forming a layer of ice at the pile surface (Weaver and Morgenstern, 1981), but may also result in the convective transport to the pile surface of solutes which have been dissolved into the slurry from the native soil, resulting in a weakened adfreeze bond. Secondly, if a non-saline clean sand slurry is used for a backfill material and it is carefully placed to avoid washing saline cuttings into the backfill, a small amount of solute may be dissolved at the interface between the backfill and the native soil. At the high freezing rates experienced in the backfill slurry (in cold permafrost) this solute will not be rejected towards the pile, rather it will be trapped near the interface between the backfill and the native soil when the freezing front jumps over the brine enriched zone.

Having reviewed the migration of solutes during the freezing of the backfill, the next issue to examine is that of diffusion of the solute through the frozen backfill with time.

Diffusion may be defined in terms of the diffusion coefficient 'D', expressed by the Arrhenius relation as (Glen 1974):

$$D = D_0 e^{(-E/kT)} \quad (6.6)$$

where D is the diffusion coefficient ( $\text{m}^2 \text{sec}^{-1}$ ),  $D_0$  is a constant for a particular solute ( $\text{m}^2 \text{sec}^{-1}$ ), E is the activation energy for diffusion (eV), k is Boltzman's constant ( $8.617 \times 10^{-5} \text{ eV/K}$ ), and T is the temperature (K).

Increased ionic diffusion rates with increased unfrozen water contents in frozen silt and clay are reported in Murrmann (1973). Measurements of diffusion coefficients, D, for sodium ions in silt and clay were between  $0.5$  to  $9 \times 10^{-11} \text{ m}^2 \text{sec}^{-1}$  over the temperature range of  $-1^\circ$  to  $-15^\circ \text{ C}$ . These values are only about ten times smaller than those expected in the unfrozen soil at  $25^\circ \text{ C}$ . The values of D for diffusion of NaCl in ice (at a concentration of 0.1 ppt) are approximately  $6 \times 10^{-13} \text{ m}^2 \text{sec}^{-1}$  at  $-15^\circ \text{ C}$  (Barnaal and Slotfeldt-Ellingsen 1983). The diffusion rates of different solutes (NaCl, HCl, and  $\text{HNO}_3$ ) in ice is largely independent of the solute type, except for HF which has a higher value of D of approximately  $6 \times 10^{-11} \text{ m}^2 \text{sec}^{-1}$  at  $-15^\circ \text{ C}$  (Barnaal and Slotfeldt-Ellingsen 1983; and Haltenc and Klinger 1969). By comparison the value of D for self-diffusion in ice at  $-10^\circ \text{ C}$  is considerably smaller, approximately  $4 \times 10^{-16} \text{ m}^2 \text{sec}^{-1}$  (Glen 1974).

When oil slurry backfill contains fines, the resulting unfrozen water will provide a preferred path for diffusion. Considering a 114 mm pile in a 165 mm hole, backfilled with a Barrow silt at  $-5^\circ \text{ C}$  (Murrmann 1973), in a native soil with a salinity (NaCl) of 30 ppt, the salinity at the pile would reach 6 ppt after 0.12 years (20% equalization or  $T_{20}$ ), and 27 ppt (90% equalization or  $T_{90}$ ) after 3.17 years (calculations contained in Appendix I). Diffusion of solute ions through ice at this temperature however would be an order of magnitude slower, giving a time to  $T_{20}$  of between 0.76 and 1.1 years and to  $T_{90}$  of between 20 and 30 years.

It can be argued that a frozen clean sand slurry (with no fines) has no unfrozen water (Hivon 1991; Gilpin 1980; and Hoekstra 1969). Ice diffusion in this case will be reduced compared with that for ice, due to the increased length of the diffusion path. This effect may be expressed by multiplying the diffusion constant by a tortuosity factor 'f', typical values of which lie between 0.01 and 0.8 (Daniel and Shackelford 1988). For a dense clean sand backfill values of f between 0.04 and 0.8 result in times to attain 20% equalization of salinity at the pile surface between 0.95 and 27 years and 90% equalization between 25 and 710 years respectively. Thus conservative values of f suggest that salinity at the pile surface may reach levels detrimental to foundation stability within the lifetime of the structure.

In addition to the considerable variation in the values of f, there are two further difficulties with the above calculations for diffusion of ions through a frozen clean sand. The first relates to the values of D, which were measured for concentrations of 0.1 ppt (Barnaal and Slotfeildt-Ellingsen 1983). At higher salinities, bubbles of concentrated brine form in the ice matrix and the diffusion rate of these bubbles is unknown, particularly through a frozen soil matrix. The second difficulty relates to the possibility of saline material from the hole wall being mixed into the backfill as it is placed, which will result in unfrozen water in the backfill potentially providing preferred paths of diffusion. If the backfill installation method is carefully designed and monitored this limitation may be overcome, and the engineer may design based upon the above discussion. Otherwise, it is conservative to assume that the salinity in the backfill will equalize with the surrounding soil, and design for a saline backfill material.

In summary then, a preliminary analysis based upon information available in the literature suggests that even if care is taken in the placement of the slurry backfill such that no native saline material is washed into backfill (ie. the slurry is tremmied into place), there are no fines in the backfill, and the pile is vibrated in order to densify the backfill after it is placed, that solute migration through the backfill to the pile surface may still be a concern

during the expected lifetime of a structure. For a native soil salinity of 30 ppt, 20% equalization at the pile surface would result in salinities of 6 ppt which are sufficient to cause considerable loss in adfreeze bond capacity. Thus it is recommended that pile design with a soil slurry backfill be based upon adfreeze bond strength values for a saline backfill material.

## **Discussion**

### *Effect of salinity on pile performance*

The dramatic reduction in pile load carrying capacity due to time dependent displacement in ice-rich saline permafrost presented in Nixon and Neukirchner (1984) has been shown to be as severe in ice-poor saline frozen soil. The values of the parameters  $n$  and  $B$  in equation (6.3) for ice-poor saline soils are shown to differ from those presented by Nixon and Neukirchner (1984), and the results of Hutchinson (1989), Hivon (1991), and from this study indicate that the value of  $n$  decreases with increasing salinity.

The results from Nixon (1988), and Hutchinson (1989) illustrate the dramatic reduction in adfreeze bond strength that results when saline pore fluid comes into contact with the pipe pile surface. Examination of the problem of solute migration from a saline native soil through a clean sand backfill to the pile surface suggests that for the design life of most structures, particularly in soils with salinities in excess of approximately 10 ppt, degradation of the adfreeze bond is possible, even with the most carefully placed sand slurry backfills. The lack of quantitative data pertaining to solute diffusion through frozen porous media render physical confirmation impossible at this time.

### *Effect of backfill material on pile performance*

Although grout backfilled piles have been shown to have superior load carrying capacities in short-term tests (Biggar and Sego 1989; and Part I of this paper [Chapter 5]) the question remained whether or not a grout backfill would provide increased capacity in the long-term, when time dependent displacements would likely govern. Grout backfilled piles in this study were shown to have greater load carrying capacity than sand backfilled

piles under constant load in a *native* soil with a salinity of 30 ppt, in which time dependent displacement governed pile performance. The time dependent displacement behaviour of the two different configurations was similar, as indicated by the similar  $n$  values, however at a specified displacement rate the grout backfilled piles had approximately twice the load carrying capacity of the sand backfilled piles. In *native* soil with a salinity of 10 ppt, adfreeze bond capacities of the sandblasted pipe piles governed pile capacity over most of the range of displacement rates tested.

The above discussion does not include the aspect of degradation of the strength of the frozen sand slurry backfill, and reduction of the adfreeze bond strength, due to the diffusion of solutes from the native soil through the backfill. If pile capacities are designed accounting for these detrimental effects, the capacity of grout backfilled piles in saline native soil may be an order of magnitude greater than sand slurry backfilled piles, as shown by the comparison between the results from Hutchinson (1989) and this study for silty sand with a salinity of 10 ppt.

The ultimate decision of which type of pile configuration to recommend will also be affected by the economics of purchasing, transporting and installing a grout backfill. A ballpark estimate has been drafted to compare the costs of grout and soil slurry backfilled piles based upon a common pile configuration [contained in Appendix G]. Costing data is based upon recent experience in piling operations in the Canadian Arctic, and grout and shipping costs are effective June 1991. The data indicate that in highly saline permafrost ( $S \geq 10$  ppt) grout backfilled piles will provide the most economical foundations, and that in low or non-saline permafrost it may still provide a more economical foundation than slurry backfilled piles.

The grout utilized in this study is satisfactory for pipe piles installed in holes up to approximately 200 mm in diameter in permafrost with temperatures between approximately  $-3^{\circ}$  and  $-10^{\circ}$  C. However for larger diameter piles excessive thermal disturbance to the permafrost may result from the additional heat generated by an increased volume of grout.



The technology of grout mix designs which are capable of curing at temperatures colder than 0° C are advancing rapidly, some of which are discussed in Biggar and Sego (1990). However, as discussed in Weaver (1979) and Biggar and Sego (1990), care must be exercised to ensure that the grout does not introduce solutes (used to depress the freezing point of the mix water) into the permafrost thereby dramatically reducing the strength of the surrounding native frozen soil at the interface.

## **Conclusions**

Time dependent displacement of piles in ice-poor frozen saline silty sand was found to be adequately described by a simple power law of time for short term displacements, however for long-term displacements a constant displacement rate formulation as shown in equation (6.3) was found to be more appropriate. Values of  $n$  were shown to decrease with increasing salinities, and the calculated values of  $n$  and  $B$  from this study were found to correlate well with values obtained in an independent study of the same soil in unconfined constant stress compression tests (Hivon 1991).

Piles backfilled with a cementitious grout were found to have approximately twice the load carrying capacity as piles backfilled with a clean sand slurry when all other conditions were the same.

Comparison of the test results from this study with other laboratory test results and to field pile performance in saline permafrost showed good agreement.

## **Recommendations for future research**

The effect of temperature on the time dependent displacement of piles in ice-poor saline permafrost has not been addressed. Based upon the results of this study it is recommended that if such a study is conducted in the future, that a grout backfill be used as it ensures that mobilization of the native soil strength will be examined rather than adfreeze bond effects.

The encouraging correlation between the results in this study and those reported in Hivon (1991) suggest that the time dependent deformation parameters obtained for the two

other saline soils reported in that study may be used to predict pile performance in saline sand and fine silty sand at temperatures of  $-5^{\circ}$  to  $-7^{\circ}$  C.

## References

- Baker, G.C., and Osterkamp, T.E. 1988. Salt redistribution during lab freezing of saline sand columns. Proceedings, 5th International Symposium on Ground Freezing, Nottingham, UK, pp. 29 - 33.
- Barnaal, D., and Slotfeildt-Ellingsen, D. 1983. Pulsed nuclear magnetic resonance studies of doped ice Ih. *Journal of Physical Chemistry*. **87**: 4321-4325.
- Barnaal, D 1991. Personal Communication. Professor, Physics Department, Luther College, Decorah, Iowa.
- Biggar, K.W. and Sego, D.C. 1989. Field load testing of various pile configurations in saline permafrost and seasonally frozen rock. Proceedings, 42nd Canadian Geotechnical Conference, October 25-27, Winnipeg, pp. 304-312.
- Biggar, K.W. and Sego, D.C. 1990. The curing and strength characteristics of cold setting Cement Fondu grout. Proceedings, 5th Canadian Permafrost Conference. Quebec City, Quebec, pp. 349-355.
- Biggar, K.W. and Sego, D.C. In press a [Chapter 2]. Field pile load tests in saline permafrost, Part I, Test procedures and results.
- Biggar, K.W. and Sego, D.C. In press b [Chapter 3]. Field pile load tests in saline permafrost, Part II, Analysis of results.
- Biggar, K.W. and Sego, D.C. In press c [Chapter 5]. Strength and deformation behaviour of model adfreeze and grouted piles in saline permafrost.
- Biggar, K.W. and Sego, D.C. In press d [Chapter 6]. Time dependent displacement behaviour of model adfreeze and grouted piles in saline permafrost.
- Daniel, D.E. and Shackelford, C.D. 1988. Disposal barriers that release contaminants only by molecular diffusion. *Nuclear and Chemical Waste Management*, **8**: 229-305.
- Domaschuk, K.L., Man, C.S., Shields, D.H. and Yong, E. 1983. Creep behaviour of frozen saline silt under isotropic compression. Proceedings, 4th International Conference on Permafrost, Fairbanks Alaska, USA., pp 238-243.
- Gilpin, R.R. 1980. A model for the prediction of ice lensing and frost heave in soils. *Water Resources Research*, **16**: 918-930.
- Glen, J.W. 1974. The physics of ice. US Army Cold Regions Research and Engineering Laboratory, Hanover, New Hampshire, monograph II-C2a, p. 81.
- Hallet, B. 1978. Solute redistribution in freezing soils. Proceedings, 3rd International Conference on Permafrost, Edmonton, Alberta, Canada., **1**. pp. 85-91.

- Haltenorth, H., and Klinger, J. 1969. **Physics of ice**. N. Riehl, B. Bullemer, and H. Englehardt, Ed., Plenum, New York.
- Hivon, E.G. 1991. Behaviour of saline frozen soils. Unpublished Ph D. Thesis, University of Alberta, Edmonton, Alberta, p. 435.
- Hoekstra, P. 1969. The physics and chemistry of frozen soils. Highway Research Board Special Report 103, pp. 78-90.
- Hutchinson, D.J. 1989. Model pile load tests in frozen saline silty sand. Unpublished MSc Thesis, University of Alberta, Edmonton, Alberta, p. 222.
- Kay, B.D. and Perfect, E. 1988. State of the art: Heat and mass transfer in freezing soils. Proceedings, 5th International Symposium on Ground Freezing, Nottingham, UK, pp. 3- 21.
- Kay, B.D. and Groenevelt, P.H. 1983. The redistribution of solutes in freezing soil: exclusion of solutes. Proceedings, 4th International Conference on Permafrost, Fairbanks Alaska, USA, pp. 584-588.
- Ladanyi, B. 1972. An engineering theory of creep in frozen soils. Canadian Geotechnical Journal, 9(1): pp. 63-80.
- Ladanyi, B. and Johnston, G.H. 1974. Behaviour of circular footings and plate anchors embedded in permafrost. Canadian Geotechnical Journal: 11: 531-553.
- Ladanyi, B. and Guichaoua, A. 1985. Bearing capacity and settlement of shaped piles in permafrost. Proceedings, XI International Conference on Soil Mechanics and Foundation Engineering, San Francisco, California, USA, pp 1421-1427.
- Miller, D.L. and Johnson, L.A. 1990. Pile settlement in saline permafrost: a case history. Proceedings, 5th Canadian Permafrost Conference. Quebec City, Quebec, pp. 371-378.
- Morgenstern, N.R., Roggensack, W.D., and Weaver, J.S. 1980. The behavior of friction piles in ice and ice-rich soils. Canadian Geotechnical Journal, 17: 405-415.
- Murrmann, R.P. 1973. Ionic mobility in permafrost. Proceedings, 2nd International Conference on Permafrost, North American Contribution, Yakutsk, USSR, pp. 352-359.
- Nixon, J.F., and McRoberts, E.C. 1976. A design approach for pile foundations in permafrost. Canadian Geotechnical Journal, 13: pp. 40-57.
- Nixon, J.F., and Lem, G. 1984. Creep and strength testing of frozen saline fine-grained soils. Canadian Geotechnical Journal, 21: pp. 518-529.
- Nixon, J.F., and Neukirchner, R.J. 1984. Design of vertical and laterally loaded piles in saline permafrost. Proceedings, 3rd International Specialty Conference on Cold Regions Engineering, Edmonton, Alberta, Canadian Society of Civil Engineering, 1-6 April, pp. 131-144.

- Nixon, J.F. 1988. Pile load tests in saline permafrost at Clyde River, Northwest Territories. *Canadian Geotechnical Journal*, **25**: pp. 24-31.
- Parneswaran, V.R. 1978. Creep of model piles in frozen soil. *Canadian Geotechnical Journal*, **16**: pp. 69-77.
- Romanov, V.P. et al. 1989. Migration of salts in freezing soils. *Soviet Engineering Geology*, No2: 44-51.
- Sheeran, D.E., and Yong, R.N. 1975. Water and salt distribution in freezing soils. *Proceedings, 1st Conference on Soil-Water problems in Cold Regions*, Calgary, Alberta, Canada, pp. 58-69.
- Vyalov, S.S. 1962. Strength and creep of frozen soils and calculations in ice-soil retaining structures. (Russian, translated in 1965) US Army Cold Regions Research and Engineering Laboratory, Army Translation No. 74, Hanover, New Hampshire, p. 219.
- Weaver, J.S. 1979. Pile foundations in permafrost. Unpublished Ph D. Thesis, University of Alberta, Edmonton, Alberta, p. 224.
- Weaver, J.S., and Morgenstern, N.R. 1981. Pile design in permafrost. *Canadian Geotechnical Journal*, **18**: pp. 357-370.

TABLE 6.1

Summary of Test Results											
Test #	Pile Diameter (mm)	Native Soil Properties	Backfill Material	Stress Pile/Backfill (kPa)	Stress Backfill/Soil (kPa)	Min Normalized Displ Rate Pile/Backfill (1/hr)	Backfill/Soil (1/hr)	Time to Failure (min)	Instantaneous (mm)	Measured Displacement To failure (mm)	Test Temp (°C)
36	33	8	Grout	386	245	-4.6	-4.8	>105,000	0.1	<1.4	-5.2
36	63	8	Grout	402	248	-4.5	-4.7	>59,000	0.5	<3.4	-5.3
34	102	9	Grout	454	305	-2.9	-3.1	3000	3.4	12.8	-5.5
34	33	9	Grout	502	318	-3.9	-4.1	60000	0.2	3.8	-5.1
34	63	9	Grout	521	322	-3.9	-4.1	44700	1.6	6.5	-5.1
36	63	8	Grout	534	330	-3.9	-4.1	12000	3.4	5.2	-5.3
31	102	9	Grout	534	359	-4.7	-4.9	>65,000 NO FAILURE, const displ rate @ t=9500 m			-5.2
31	33	9	Grout	575	365	-3.5	-3.7	9500	0.4	3.2	-5.1
31	63	9	Grout	606	374	-2.8	-3.0	2800	2.0	7.9	-5.0
51	33	10	Ongoing	760	482	-2.3	-2.5	1267	0.5	4.9	-5.3
36	102	8	Grout	738	495	-2.4	-2.6	1600	5.2	17.5	-5.3
40	33	28	Grout	108	69	-4.1	-4.3	>110,000	1.5	<8	-5.3
41	63	28	Grout	150	92	-3.9	-4.1		0.7	No failure to 15 mm displ.	-5.3
41	33	28	Grout	152	97	-2.9	-3.1	3700	3.1	10.2	-5.1
50	102	26	Grout	223	150	-2.7	-2.9	2000	0.7	9.1	-5.2
50	63	26	Grout	244	150	-2.6	-2.8	1500	?	6.9	-5.5
41	102	28	Grout	243	163	-3.5	-3.7	6700	0.3	5.4	-5.4
48	33	0	Sand	332	211	No Time Dependent Displacement			1.8	<1.9	-5.4
48	33	0	Sand	498	316	-5.6	-5.8	>16000	Incremental	<2.1	-5.4
19	102	0	Sand	496	333	-5.1	-5.3	>6700	2.6	<3.3	RTD Failure
48	33	0	Sand	575	365	-5.3	-5.5	~25000	Incremental	2.1	-5.5
19	102	0	Sand	550	369	-4.9	-5.1	>13000	Incremental	<3.9	RTD Failure
19	102	0	Sand	635	426	-3.8	-4.0	8700	Incremental	4.3	RTD Failure
19	33	0	Sand	799	507	IMMEDIATE FAILURE					
49	33	10	Sand	205	130	-5.6	-5.8	> 67000	0.6	<0.9	-5.3
49	33	10	Sand	289	184	-4.6	-4.8	>30000	Incremental	<1.2	-5.4
51	63	10	Sand	301	186	-5.0	-5.2	> 50000	Incremental	<1.2	-4.9
39	102	10	Sand	362	243	-3.0	-3.2	800	2.9	4.4	-5.3
39	33	10	Sand	398	252	-3.1	-3.3	1400	0.5	1.6	-5.2
39	63	10	Sand	412	255	-2.7	-2.9	330	1.8	2.6	-5.1
28	102	10	Sand	449	301	-2.8	-3.0	500	3.4	6.1	-5.0
27	102	9	Sand	458	307	-3.1	-3.3	900	3.4	5.8	-5.1
33	102	10	Sand	462	310	-3.2	-3.4	1600	3.3	6.0	-5.2
28	33	10	Sand	492	312	-3.9	-4.1	8500	1.4	3.6	-5.2
33	33	10	Sand	498	316	-2.7	-2.9	480	0.3	1.9	-5.0
28	63	10	Sand	513	317	-2.4	-2.6	300	?	2.5	-4.9

**TABLE 6.1**  
**Summary of Test Results**

Test #	Pile Diameter (mm)	Native Salinity (ppt)	M.C. (%)	Soil Properties Density ((kg/cu m))	Backfill Material	Stress Pile/Backfill (kPa)	Stress Backfill/Soil (kPa)	Min Pile/Backfill (1/hr)	Normalized Backfill/Soil (1/hr)	Time to Failure (min)	Instantaneous Displacement (mm)	Measured Displacement To failure (mm)	To bond rupture (mm)	Test Temp (°C)
27	33	9	19.1	1.70	Sand	502	318	-2.9	-3.1	1100	0.6	2.6	2.9	-5.1
27	63	9	19.1	1.70	Sand	525	325	-3.9	-4.1	5600	2.2	5.6	6.4	-5.2
33	63	10	18.3	1.73	Sand	525	325	-3.1	-3.3	1300	2.0	4.8	5.4	-5.0
25	33	10	18.8	1.71	Sand	548	348	-4.1	-4.3	9500	?	2.1	2.8	-5.3
25	102	10	18.8	1.71	Sand	524	351	-2.9	-3.1	750	5.3	8.0	8.3	-5.2
26	33	11	18.7	1.70	Sand	556	353	-3.4	-3.6	4000	0.8	4.4	5.1	-5.0
26	102	11	18.7	1.70	Sand	529	355	-3.7	-3.9	6000	3.7	8.8	10.3	-5.2
24	102	9	19.4	1.69	Sand	531	356	-3.0	-3.2	950	3.1	6.1	7.6	-5.4
20	63	10	19.2	1.70	Sand	578	357	-3.3	-3.5	2300	Incremental	8.4	11.0	-5.2
20	63	10	19.2	1.70	Sand	469	290	-4.1	-4.3	>25000	1.1	6.8	None	-5.1
24	33	9	19.4	1.69	Sand	571	362	-3.2	-3.4	3000	?	2.7	3.1	-5.3
24	63	9	19.4	1.69	Sand	590	365	-2.8	-3.0	1800	3.0	7.8	8.7	-5.0
25	63	10	18.8	1.71	Sand	592	366	-3.0	-3.2	500	0.3	1.0	1.2	-4.9
26	63	11	18.7	1.70	Sand	594	367	-2.7	-2.9	600	2.8	5.8	6.5	-5.2
21	102	18	19.2	1.70	Sand	291	195	-1.7	-1.9	8900				
21	33	18	19.2	1.70	Sand	309	196							
21	63	18	19.2	1.70	Sand	465	287							
46	102	27	19.6	1.69	Sand	98	65	-3.6	-3.8	9051	0.8	6.3		-5.1
46	63	27	19.6	1.69	Sand	108	66	-3.4	-3.6	9100	0.5	5.7		-5.3
46	33	27	19.6	1.69	Sand	107	68	-2.9	-3.1	8000	1.1	6.1		-5.2
47	33	29	18.2	1.73	Sand	141	89	-3.5	-3.7	10000	0.2	4.6	7.0	-5.2
50	33	26	16.7	1.75	Sand	150	95	-2.4	-2.6	2400	0.3	6.2		-5.4
22	63	28	18.3	1.72	Sand	164	101	-2.4	-2.6	1790	0.7	8.4		-5.1
22	102	28	18.3	1.72	Sand	185	124	-2.5	-2.7	1500	1.3	9.7		-5.1
22	33	28	18.3	1.72	Sand	231	147	-0.9	-1.1	120	1.2	7.9		
30	33	30	18.4	1.73	Sand	502	318			20	2.2	10.3		RTD Failure
30	63	30	18.4	1.73	Sand	523	323	-0.2	-0.4					-5.3

**TABLE 6.2****Model parameters from minimum displacement rate analysis**

Salinity-Backfill	n	B (yr <sup>-1</sup> kPa <sup>-n</sup> )
10—Grout	9.5	5.12 x 10 <sup>-26</sup>
30—Grout	6.1	1.07 x 10 <sup>-13</sup>
30—Sand	5.9	3.94 x 10 <sup>-12</sup>

**TABLE 6.3****Regression values of c and D parameters**

Salinity-Backfill	c	D (mm hr <sup>-b</sup> kPa <sup>-c</sup> )
30—Sand	1.45	7.08 x 10 <sup>-2</sup>
30—Grout	1.50	2.10 x 10 <sup>-3</sup>

**TABLE 6.4****Comparison of n and B parameters to those in Hivon (1991)  
(for shear stresses normalized to 500 kPa)**

Salinity (ppt)	Hivon (1991)		This study (grouted piles)	
	n	B (hr <sup>-1</sup> kPa <sup>-n</sup> )	n	B (hr <sup>-1</sup> kPa <sup>-n</sup> )
10	11	0.00010	9.5	0.00027
30	4.9	0.50	6.1	0.28

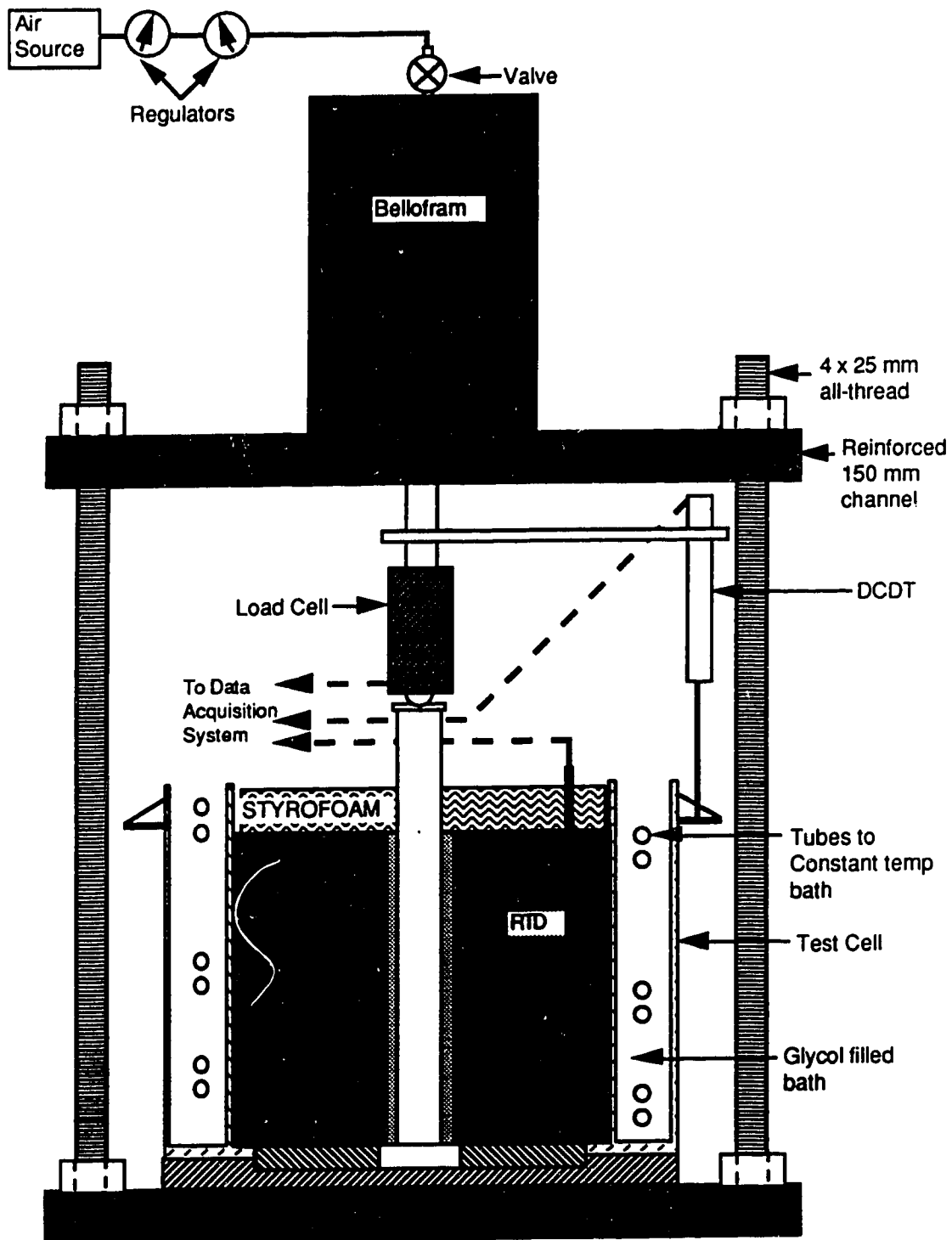


Figure 6.1: Constant load test apparatus



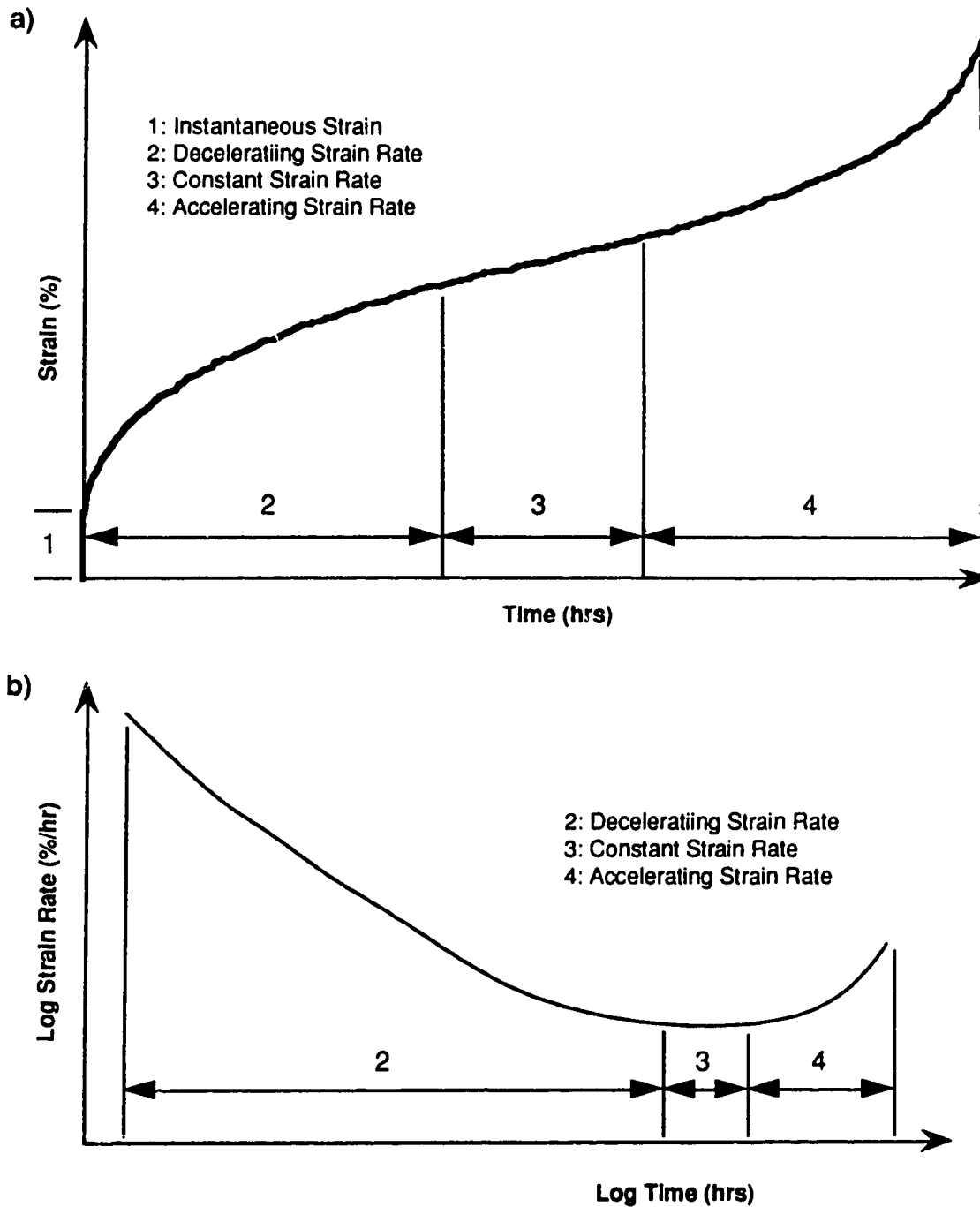
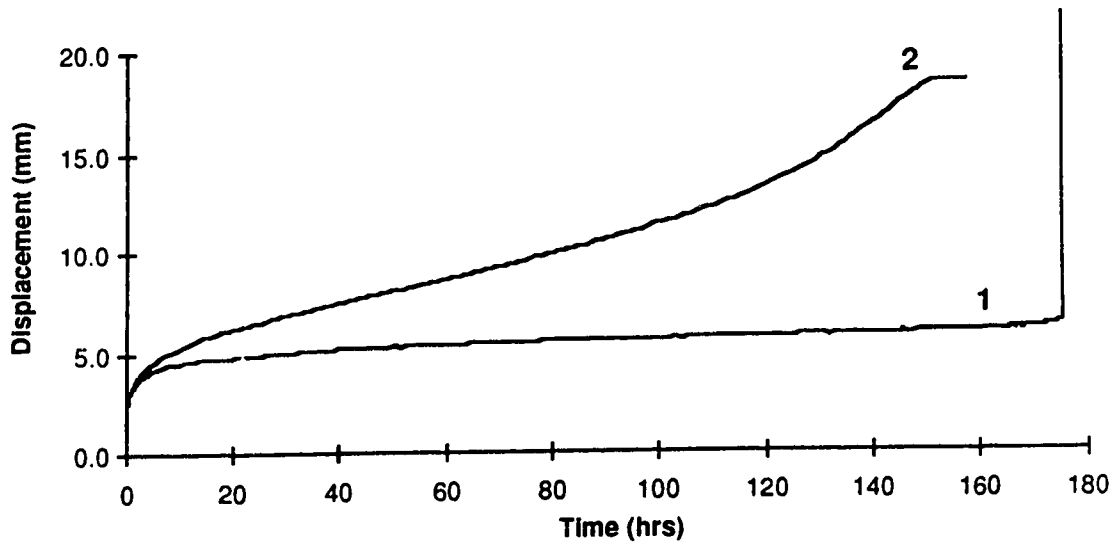
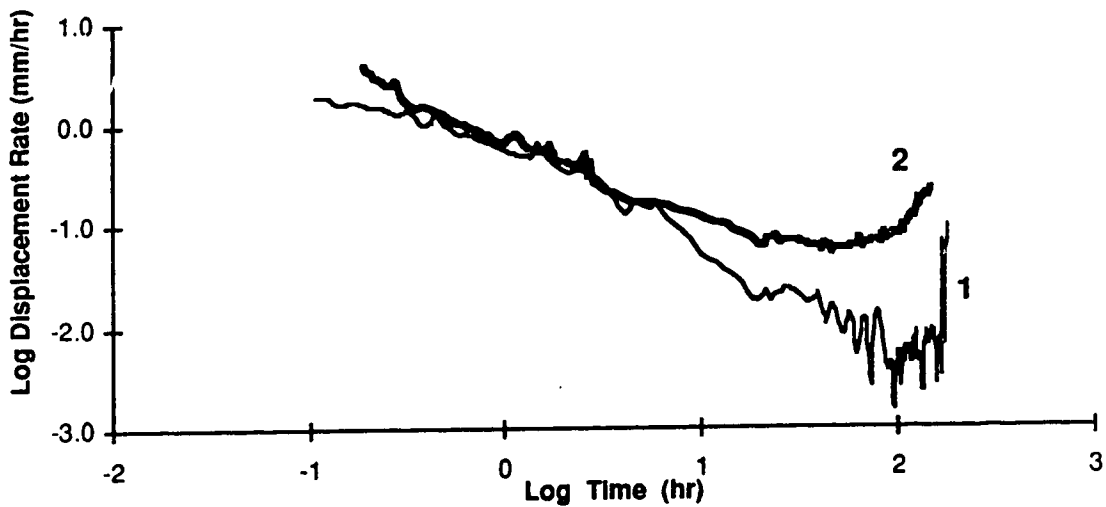


Figure 6.2: Time dependent deformation behaviour in frozen soils  
a) Strain versus time  
b) Log strain rate versus log time

a)



b)



- 1: Sand backfilled pile in native soil with a salinity of 10 ppt (test #27-63)  
2: Grout backfilled pile in native soil with a salinity of 10 ppt (test #31-63)

Figure 6.3: Typical pile behaviour up to failure  
a) displacement versus time  
b) log displacement rate versus log time

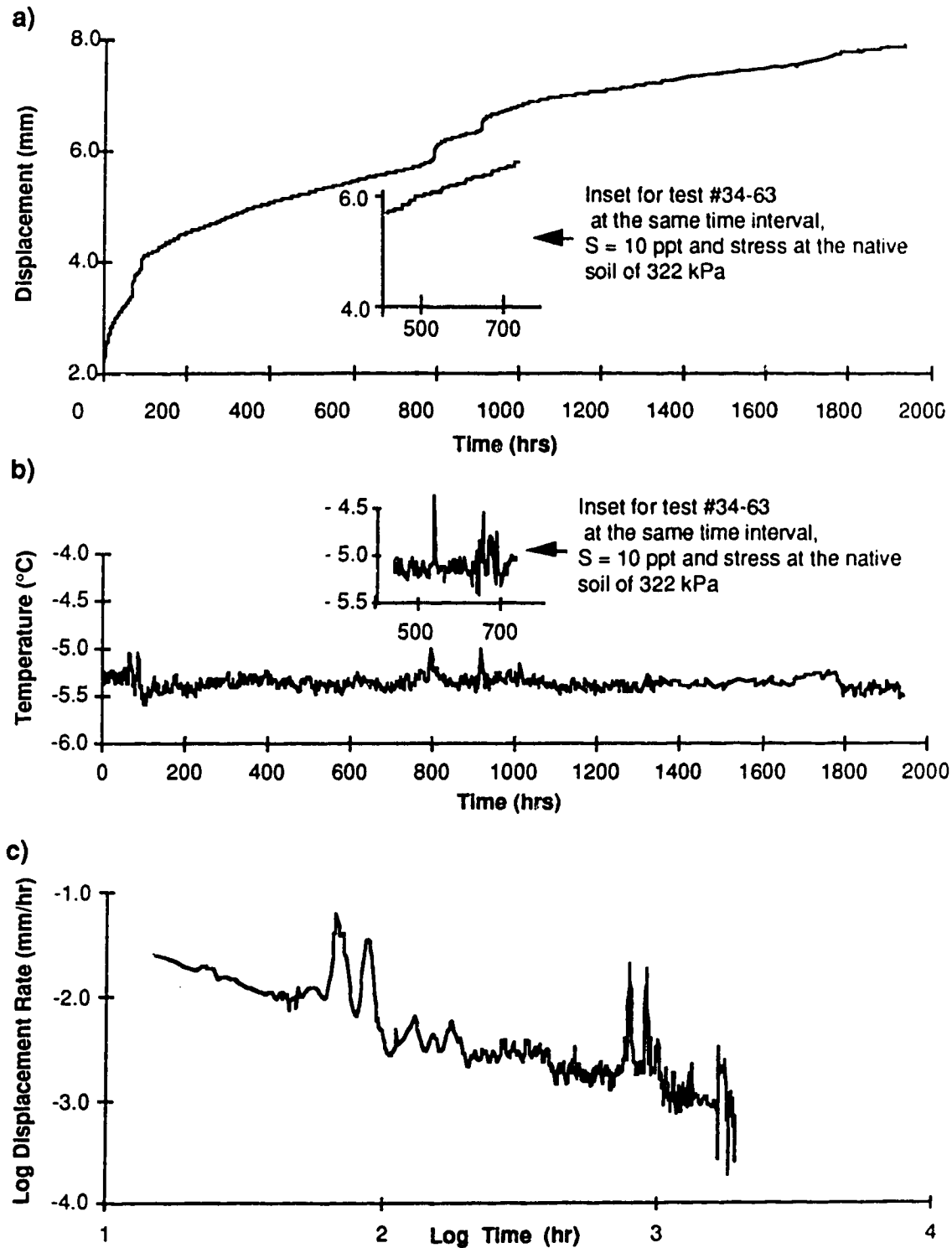


Figure 6.4: Test #40-33, 30 ppt, Sand backfill, 69 kPa

- a) displacement vs time
- b) soil temperature vs time
- c) log displacement rate vs log time

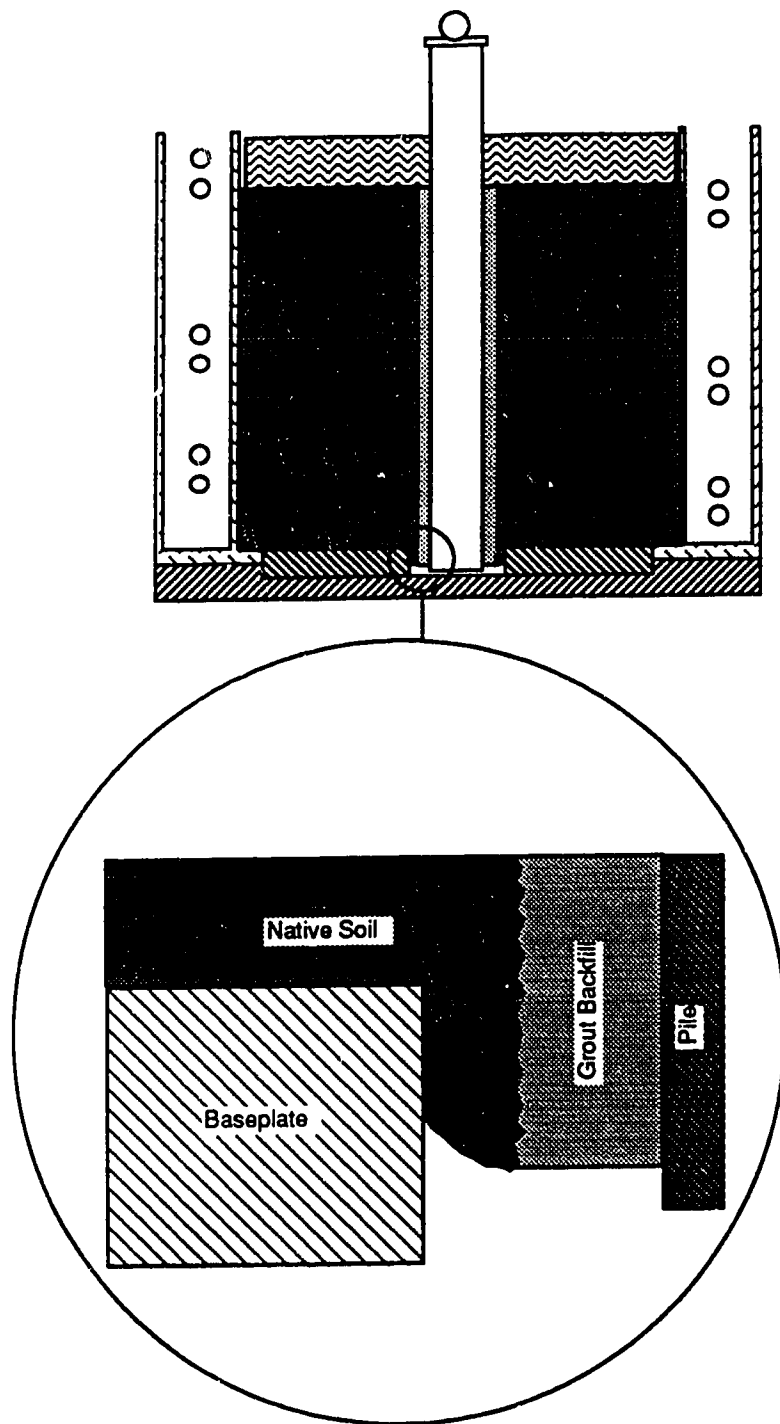


Figure 6.5: Detail of mode of pile deformation for grout backfilled piles

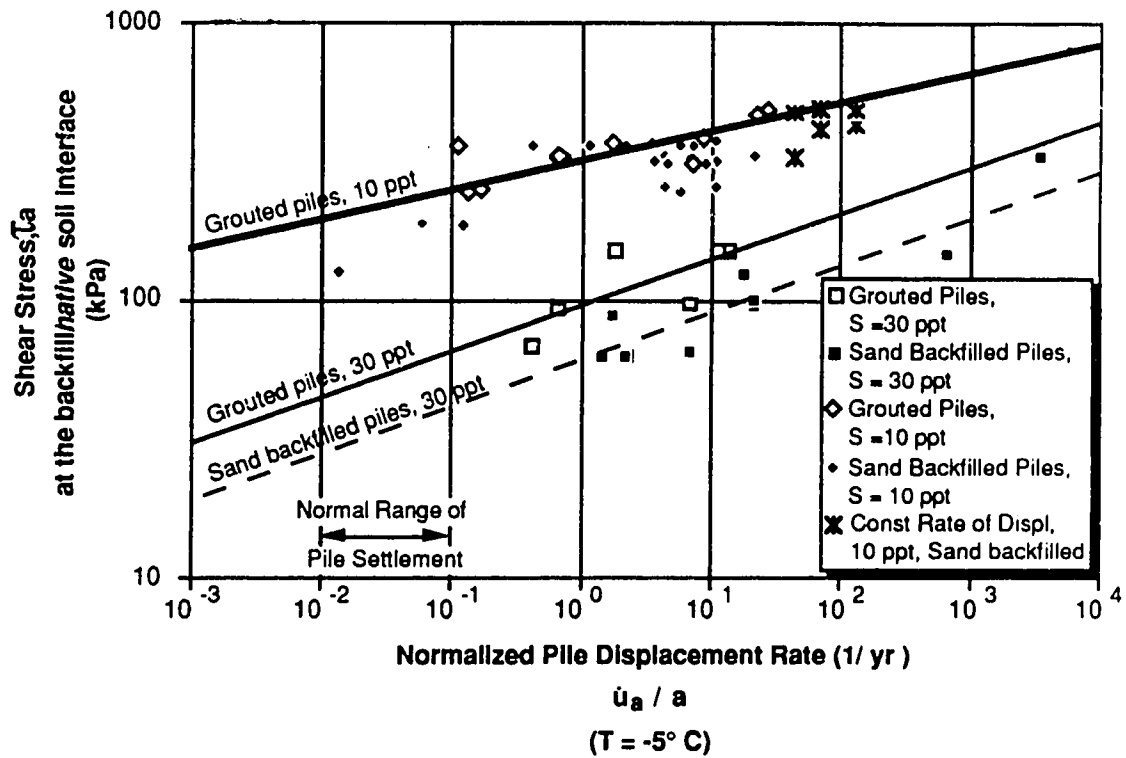
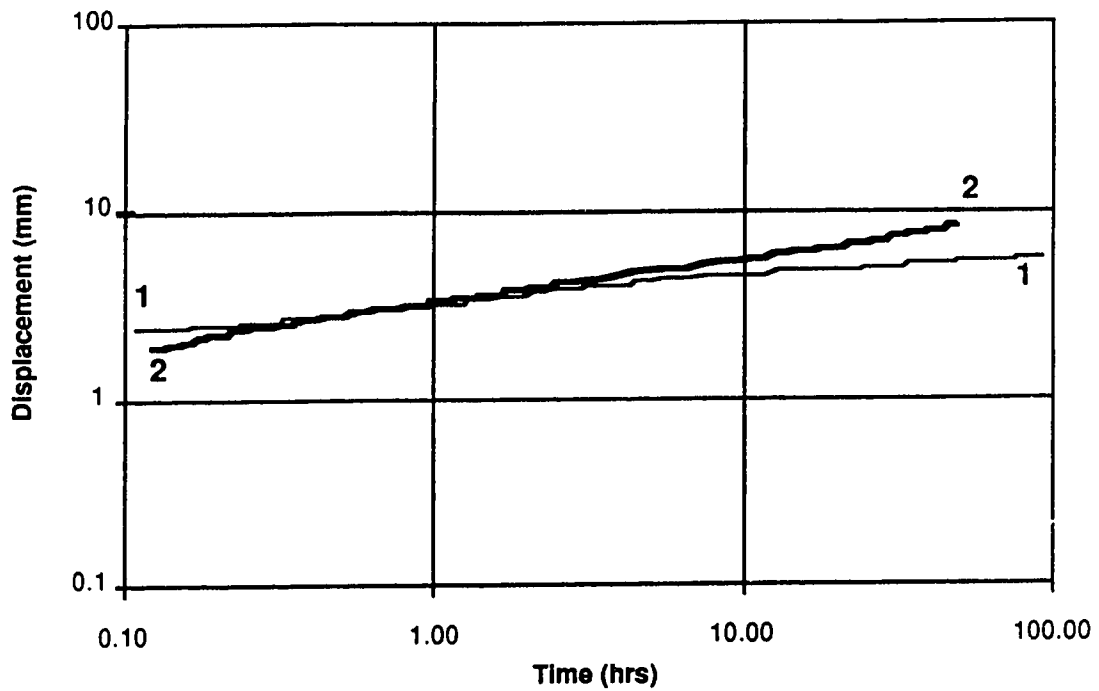


Figure 6.6: Pile displacement rate normalized to the hole radius versus shear stress at the backfill/*native* soil interface for grout and clean sand backfilled model piles in silty sand at salinities of 10 and 30 ppt.



1-1: Sand backfilled pile in native soil with a salinity of 10 ppt (#27-63)  
2-2: Grout backfilled pile in native soil with a salinity of 10 ppt (#31-63)

Figure 6.7: Typical log displacement versus log time behaviour for attenuating displacement rate portion of pile displacement.

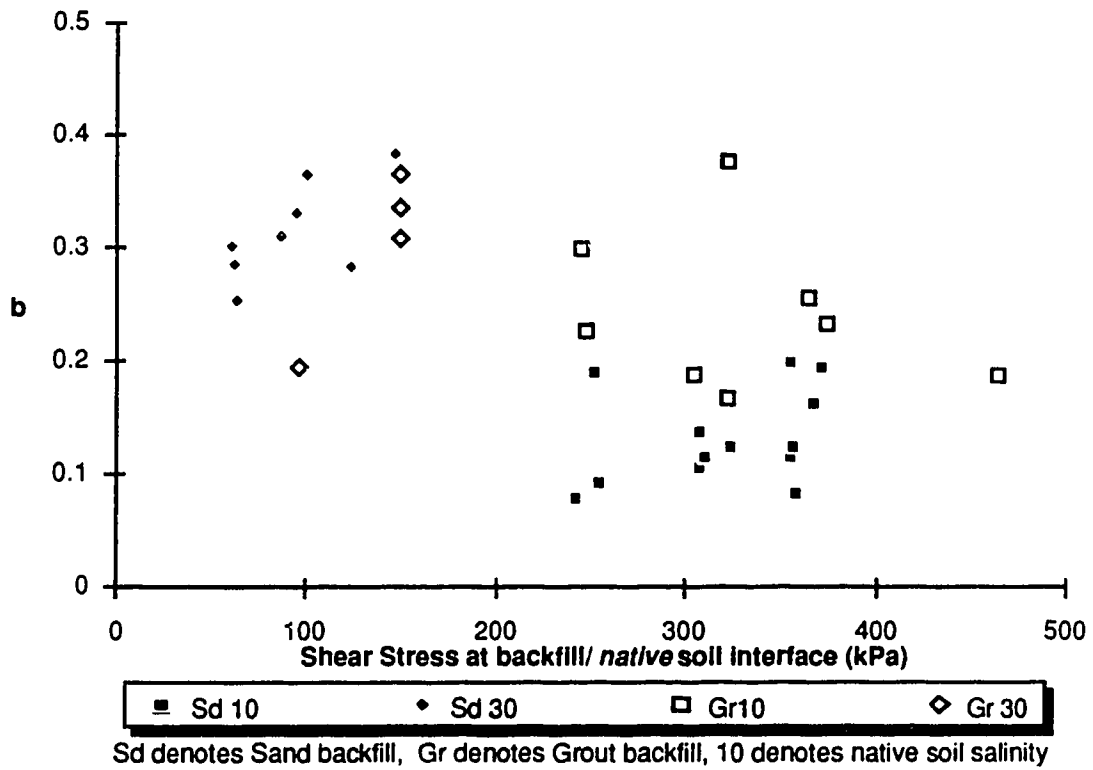


Figure 6.8: Values of time exponent,  $b$ , versus applied shear stress at backfill/native soil interface

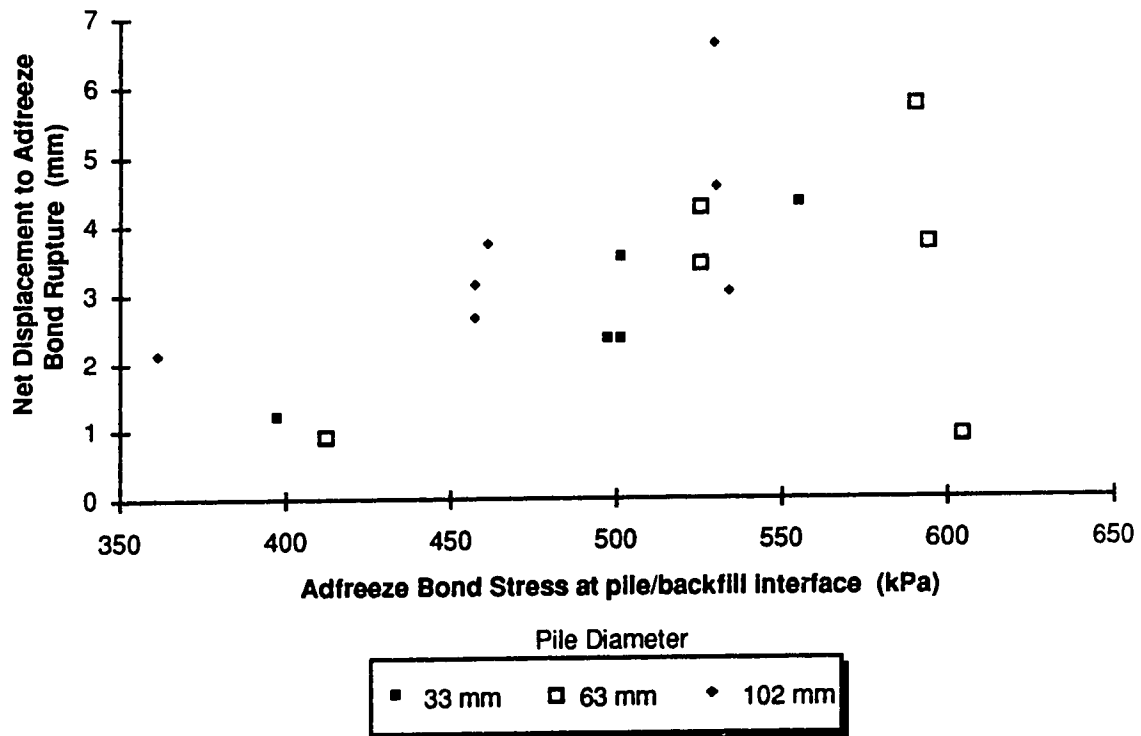


Figure 6.9: Net pile displacement to adfreeze bond rupture versus adfreeze bond stress at the pile/backfill interface



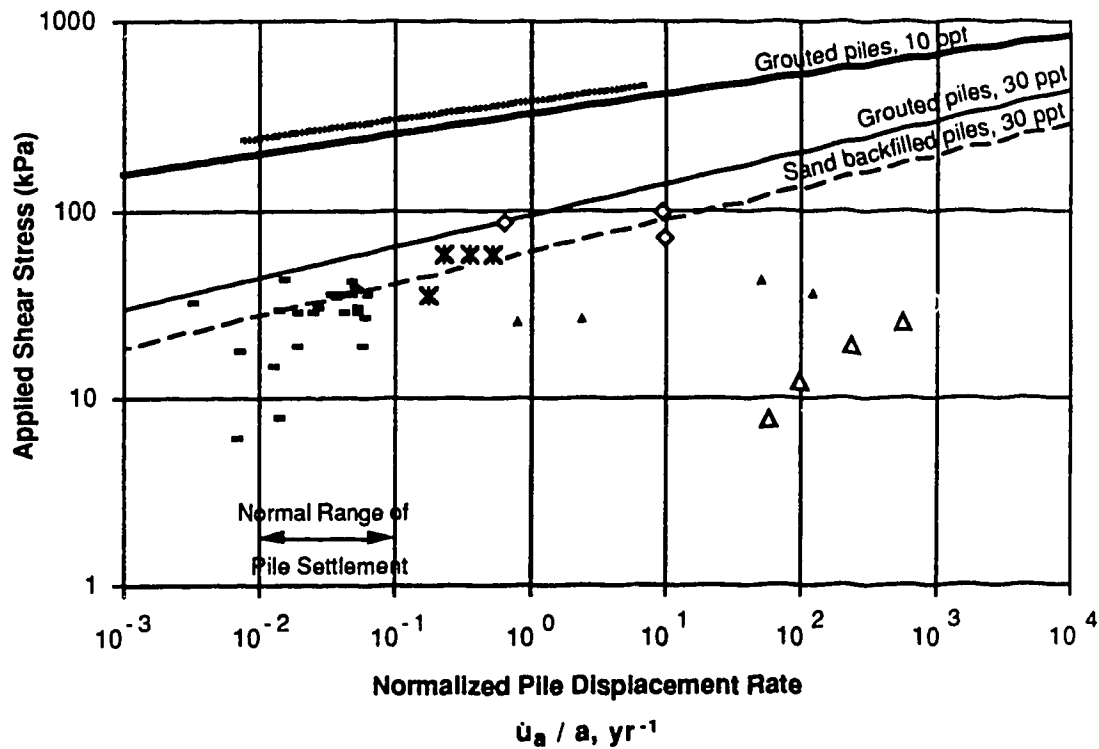


Figure 6.10: Comparison of the results from this study with results from studies by others.

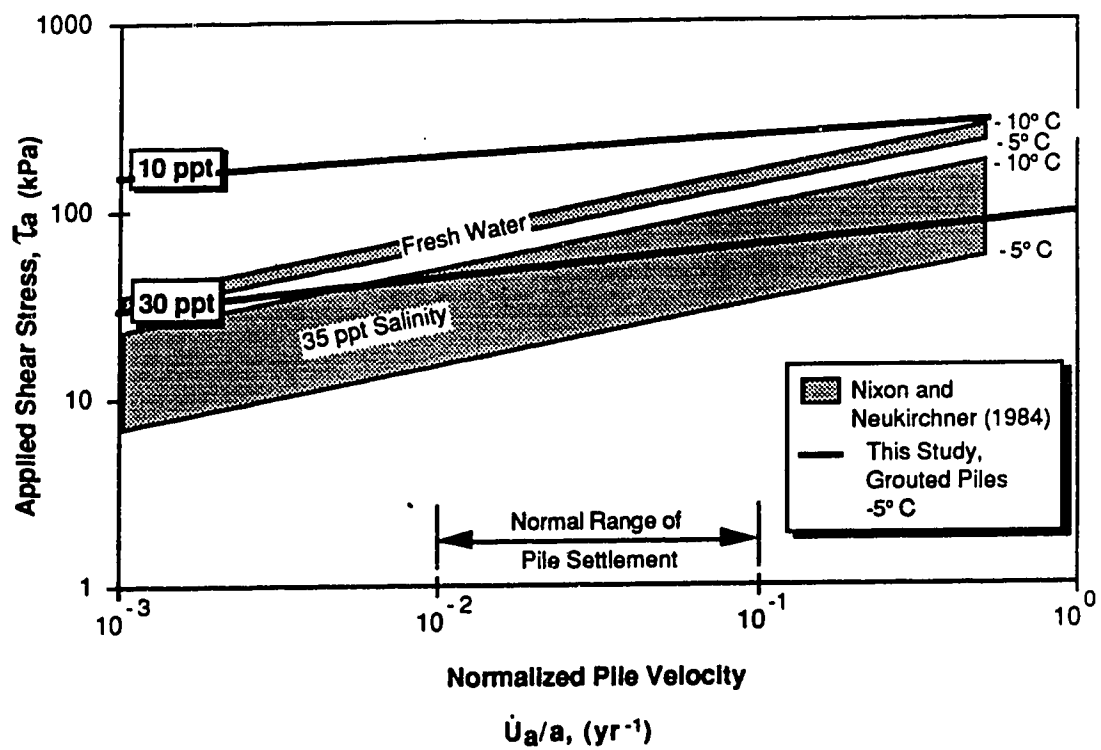


Figure 6.11: Comparison of results from this study to those reported in Nixon and Neukirchner (1984)

## APPENDIX I TO CHAPTER 6

### DIFFUSION OF SOLUTES IN ICE AND FROZEN SOIL

The Arrhenius relation for the diffusion constant 'D' may be expressed as (Glen 1974):

$$D = D_0 e^{(-E/kT)} \quad (1)$$

where D = diffusion constant ( $\text{m}^2/\text{sec}$ )

$D_0$  = constant ( $\text{m}^2/\text{sec}$ )

E = activation energy for diffusion (eV)

k = Boltzman's constant ( $\text{J} / ^\circ\text{K}$ ) =  $1.36 \times 10^{-23}$

T = temperature (K)

To convert k into units of eV:  $1 \text{ J} = 6.242 \times 10^{18} \text{ eV}$

thus

$$k = 8.62 \times 10^{-5} (\text{eV} / \text{K})$$

#### Self diffusion of water molecules through the ice lattice

Values of E are stated to be between 0.63 and 0.68 eV (Glen 1974). The values of  $D_0$  are stated to be  $10.97 \times 10^{-4}$  (calculated) and  $9.13 \times 10^{-4} \text{ m}^2/\text{sec}$  (experimentally) (Glen 1974). Using these values of E and  $D_0$ , the range of values for D are calculated below:

T ( $^\circ\text{C}$ )	$D_0$	for E = 0.63	for E = 0.68
-10	$9.13 \times 10^{-4}$	$7.72 \times 10^{-16}$	$0.850 \times 10^{-16}$
-10	$10.67 \times 10^{-4}$	$9.02 \times 10^{-16}$	$0.993 \times 10^{-16}$
-5	$9.13 \times 10^{-4}$	$13.0 \times 10^{-16}$	$1.49 \times 10^{-16}$
-5	$10.67 \times 10^{-4}$	$15.2 \times 10^{-16}$	$1.74 \times 10^{-16}$

thus at  $-10^\circ\text{C}$ ,  $0.850 < D < 9.02 \times 10^{-16} \text{ m}^2/\text{sec}$ ; and

at  $-5^\circ\text{C}$ ,  $1.49 < D < 15.2 \times 10^{-16} \text{ m}^2/\text{sec}$ .

#### Diffusion of ions in ice

At T =  $-10^\circ\text{C}$  for HF:  $D \approx 1 \times 10^{-11} \text{ m}^2/\text{sec}$  (Haltenorth and Klinger 1969)

At T =  $-5^\circ\text{C}$  for HF:  $D \approx 6 \times 10^{-11} \text{ m}^2/\text{sec}$

for NaCl,  $\text{HNO}_3$ , and HCl  $D \approx 4 \times 10^{-13} \text{ m}^2/\text{sec}$

(Barnall and Slotfeldt-Ellingsen 1983)

### Calculation of $D_0$ for NaCl:

Exact values of  $E$  are not available. From Figure 2 of Barnall and Slotfeldt-Ellingsen (1983) a value of  $E = 0.266$  is obtained for NMR T1. It is reasonable to assume that the value of  $E$  for diffusion is similar (Barnaal 1991), hence reasonable limits may be as  $0.2 < E < 0.4$  (eV). Thus the calculated values of  $D_0$  for NaCl in ice are:

T (° C)	D	for E = 0.2	for E = 0.4
-15	$4.00 \times 10^{-13}$	$3.23 \times 10^{-9}$	$2.61 \times 10^{-5}$

Thus using [1] and solving for  $D$  at  $-5^\circ \text{C}$

T (° C)	for E = 0.2	for E = 0.4
-5	$5.60 \times 10^{-13}$	$7.83 \times 10^{-13}$

The second law of diffusion, which expresses the change in concentration with time, has the same form as that for one-dimensional consolidation:

for diffusion

$$\frac{dc}{dt} = D \left( \frac{dc}{dx} \right)^2$$

for consolidation

$$\frac{du}{dt} = C_v \left( \frac{du}{dx} \right)^2 \quad (2)$$

where

$c$  = concentration

$x$  = distance

$t$  = time

$D$  = diffusion constant

$u$  = pore pressure

$x$  = distance

$t$  = time

$C_v$  = coefficient of consolidation

Using this analogy to one-dimensional consolidation:

$$T = \frac{C_v t}{H^2} \quad (3)$$

where  $t$  = time

$H$  = distance to the measured pore pressure

$T$  = non dimensional time factor

Substituting  $D$  for  $C_v$  and solving for  $t$ :

$$t = \frac{H^2 T}{D} \quad (4)$$

Solving for 20% and 90% equalization across a 25 mm thick annulus of ice:

equalization (%)	20	20	90	90
T	0.03	0.03	0.8	0.8
D (m <sup>2</sup> /sec)	5.60 x 10 <sup>-13</sup>	7.83 x 10 <sup>-13</sup>	5.60 x 10 <sup>-13</sup>	7.83 x 10 <sup>-13</sup>
t (yrs)	1.06	0.760	28.3	20.3

#### Diffusion of ions in frozen soils

The diffusion constant for Na<sup>+</sup> ions in Wyoming bentonite, Fairbanks silt, and Barrow silt has been measured for temperatures between -1° and -15° C by Murrmann (1973). Tabulated below are calculations for diffusion of ions through a 25 mm thick annulus of soil slurry at a temperature of -5° C surrounding a pile:

	bentonite	silt	bentonite	silt
equalization (%)	20	20	90	90
T	0.03	0.03	0.8	0.8
D (m <sup>2</sup> /sec)	4.00 x 10 <sup>-11</sup>	5.00 x 10 <sup>-12</sup>	4.00 x 10 <sup>-11</sup>	5.00 x 10 <sup>-12</sup>
t (yrs)	0.0142	0.119	0.396	3.17

In a frozen clean slurry with no unfrozen water the diffusion of ions through the frozen sand slurry backfill may be calculated by multiplying the diffusion constant for ice by a tortuosity factor 'f', thus the expression for diffusion (4) becomes:

$$t = \frac{H^2 T}{f D} \quad (5)$$

Representative values of f for a sand backfill lie between 0.04 and 0.8 (Daniel and Shackelford 1988). Using these values, the upper and lower limits on the time required for 20% and 90% equalization of solute diffusion through a 25 mm thick sand slurry annulus are calculated below:

equalization (%)	20	20	90	90
T	0.03	0.03	0.8	0.8
f	0.04	0.8	0.04	0.8
D (m <sup>2</sup> /sec)	5.60 x 10 <sup>-13</sup>	7.83 x 10 <sup>-13</sup>	5.60 x 10 <sup>-13</sup>	7.83 x 10 <sup>-13</sup>
t (yrs)	27	.95	710	25

## **7. CONCLUSIONS**

### **Pile performance in saline permafrost**

It has been shown that reduced capacities of piles in saline permafrost results from a number of phenomena. The most dramatic effect is the reduction of adfreeze bond strength due to the presence of dissolved solutes in the pore fluid of the permafrost. The results from Hutchinson (1989), Sego and Smith (1989) and Chapter 5 have shown reductions in capacity of 80% may be anticipated at salinities of only 10 ppt. Reduced adfreeze bond strengths were also observed when a clean sand backfill was used in a saline soil (Chapter 5) which suggests that the additional displacement of the pile due to the weaker saline native soil causes degradation of the adfreeze bond. Finally the reduced strength of the saline native soil results in increased time dependent displacement of the piles.

The temperature sensitivity of saline soils discussed in Chapter 5 emphasizes the necessity of maintaining or improving the cold thermal regime in saline soils. Measures such as the installation of insulation on the ground surface to reduce temperature increases in the summer months were successfully implemented in Barrow, Alaska to limit pile settlement (Miller and Johnson 1990). The use of active or passive refrigeration systems for piles is also a possible solution depending on the local conditions and the economics of the situation.

Preliminary tests under constant displacement rate conditions indicated that for the soil tested, when salinities exceeded 10 ppt a clean sand backfill performed as well as a grout backfill because failure occurred in the native soil at loads less than the maximum adfreeze bond capacity. The results of the constant load tests reported in Chapter 6, however, indicated that grout backfilled piles had approximately twice the capacity of sand backfilled piles under long-term conditions. In addition subsequent analysis of the diffusion of solutes through a clean sand backfill suggest that even if the backfill is carefully placed to prevent contamination by solutes from the native soil, within the lifetime

of most structures solute diffusion through the backfill to the pile surface will occur. This necessitates that design be based on the worst case conditions of a saline backfill in contact with the pile surface.

Long-term time dependent displacement of piles in saline soils is best expressed in terms of a constant displacement rate, described by a simple power law of stress as:

$$\dot{u}_a = \frac{u_a}{t} = \frac{\sqrt{3}^{(n+1)} B \tau^n a}{(n-1)} \quad (7.1)$$

(derivation contained in Appendix F). Nixon and Neukirchner (1984) proposed that the value of the stress exponent,  $n$ , be maintained equal to 3 as for pile design in ice-rich permafrost, and that the effect of salinity be encompassed in the  $B$  term. Work by Hutchinson (1989), Hivon (1991) and this study (Chapter 6) indicate that the value of  $n$  decreases with increasing salinity in ice-poor saline soils. Unconfined constant stress compression tests (Hivon 1991) conducted on the same saline silty sand as the model pile tests in this study resulted in similar values of  $n$  and  $B$ . This suggests that the creep parameters,  $n$  and  $B$ , obtained for two other saline soils tested by Hivon (1991) (mortar sand and fine saline sand) may be used to predict pile performance in those saline soils as well.

Attenuating displacement rate analysis using a simple power law of time expressed as:

$$u_a = \frac{\sqrt{3}^{(c+1)} D \tau^c a t^b}{(c-1)} \quad (7.2)$$

provided a reasonable fit to the short-term field data obtained in Iqaluit and the initial displacement data obtained from the constant load tests reported in Chapter 6. It appears that this formulation is inappropriate to predict long-term pile displacement, however, as model piles in saline soils tested in this study eventually displaced at a constant rather than an attenuating rate. This guideline cannot be stated with certainty due to the lack of long-term field pile displacement data, however design based upon constant displacement rate

behaviour will provide a conservative estimate of pile capacity whereas the attenuating displacement rate formulation may be unconservative.

### **Grout as a backfill material**

It is apparent that grout backfilled piles provide the greatest potential for increased pile capacities in saline permafrost. Grout backfill does not suffer from degraded strength nor reduced bond strengths to the pile, in saline soil, so design may be based on the shear strength and deformation properties of the native soil at the interface between the grout and the soil.

The successful use of grout backfill for prebored piles in permafrost has potential for other applications as well. The use of grout backfilled piles has shown the greatest increases in pile capacities for short-term loading conditions (Chapter 2 and 5). Although these conditions seldomly govern pile design in permafrost, in the particular instance of the SRR tower foundations they were deemed to provide the best solution. In addition as permafrost regions are developed for their vast natural resource potential, foundations for large structures will be required. The use of cast in place piles using cold temperature curing grouts may provide a viable option for these conditions. Finally in non-saline ice-poor permafrost, adfreeze bond strengths may govern pile capacities rather than time dependent displacement (Weaver and Morgenstern 1981). Grout backfilled piles will provide increased pile capacities under such conditions as well. In ice-rich non-saline permafrost in which time-dependent displacement of the piles will govern pile capacity, soil slurry backfilled piles will likely provide the most economical pile foundation.

### **Recommendations for future research**

Although considerable data have become available on the time dependent deformation of saline soils at one temperature (Hivon 1991), more work is needed to better define the strength and deformation behaviour dependence of various saline soils at different temperatures. Dramatic increases in pile displacement rate in soils with salinities of



30 ppt were observed for piles under constant load when changes in temperature were less than 0.5° C.

The behaviour of saline frozen soils has been shown to be related to the unfrozen water content which is affected by both salinity and temperature (Ogata et al. 1983; Hivon 1991, and Chapter 5). Time-domain reflectometry has become a practical method of determining unfrozen water contents (Hivon and Sego 1990), and if this technology can be packaged into a unit which may be used for *in-situ* testing it will be a valuable tool for pile design in saline permafrost.

Long-term field pile performance of grout and sand backfilled piles in saline soil is needed to confirm if a constant displacement rate formulation is appropriate for design in ice-poor saline soils, or if the pile displacements will eventually attenuate. Such tests will also quantify the increased capacity provided by grout backfilled piles under field conditions.

There are a number of commercially available grouts which have the potential of being used successfully as a backfill material in frozen soils. There is no comparative data available to the designer to determine which grout is most suitable for a particular situation. For example the grout developed in this study (Chapter 4) is not suitable for use in warm permafrost, and due to increased generation of heat with increased volumes of cement, its use in prebored holes should be limited to holes with diameters less than approximately 200 mm. It may, however, be suitable to backfill an annulus between large precast piles and permafrost if the annulus is 100 to 150 mm wide.

## References

- Biggar, K.W., and Sego, D.C. 1990. The curing and strength characteristics of cold setting Ciment Fondu grout. Proceedings, 5th Canadian Permafrost Conference. Quebec city, Quebec, pp. 349-355.
- Biggar, K.W. and Sego, D.C. In press a. [Chapter 2] Field pile load tests in saline permafrost, Part I, Test procedures and results.
- Biggar, K.W. and Sego, D.C. In press b. [Chapter 3] Field pile load tests in saline permafrost, Part II, Analysis of results.

- Biggar, K.W. and Sego, D.C. In press c. [Chapter 5] Strength and deformation behaviour of model adfreeze and grouted piles in saline permafrost.
- Biggar, K.W. and Sego, D.C. In press d. [Chapter 6] Time dependent displacement behaviour of model adfreeze and grouted piles in saline permafrost.
- Hivon, E.G. and Sego, D.C. 1990. Determination of the unfrozen water content in saline permafrost using time domain reflectometry (TDR). Proceedings, 5th Canadian Permafrost Conference. Quebec city, Quebec, pp. 257-262.
- Hivon, E.G. 1991. Behaviour of saline frozen soils. Unpublished Ph. D. Thesis, University of Alberta, Edmonton, Alberta, p. 435.
- Hutchinson, D.J. 1989. Model pile load tests in frozen saline silty sand. Unpublished M.Sc. Thesis, University of Alberta, Edmonton, Alberta, p. 222.
- Miller, D.L. and Johnson, L.A. 1990. Pile settlement in saline permafrost: a case history. Proceedings, 5th Canadian Permafrost Conference. Quebec City, Quebec, pp. 371-378.
- Morgenstern, N.R., Roggensack, W.D., and Weaver, J.S. 1980. The behavior of friction piles in ice and ice-rich soils. Canadian Geotechnical Journal, 17: 405-415.
- Nixon, J.F., and Neukirchner, R.J. 1984. Design of vertical and laterally loaded piles in saline permafrost. Proceedings, 3rd International Specialty Conference on Cold Regions Engineering, Edmonton, Alberta, Canadian Society of Civil Engineering, 1-6 April, pp. 131-144.
- Ogata, N., Yasuda, M. and Kataoka, T. 1983. Effects of salt concentration on strength and creep behaviour of artificially frozen soils. Cold Regions Science and Technology, 8: pp 139-153.
- Sego, D.C. and Smith, L.B. 1989. The effect of backfill properties and surface treatment on the capacity of adfreeze pipe piles. Canadian Geotechnical Journal, 26: pp. 718-725.
- Weaver, J.S., and Morgenstern, N.R. 1981. Pile design in permafrost. Canadian Geotechnical Journal, 18: pp. 357-370.

**APPENDIX A**  
**IQALUIT TEST RESULTS**  
**pertinent to**  
**CHAPTER 1**  
Load versus displacement  
and  
Displacement versus time

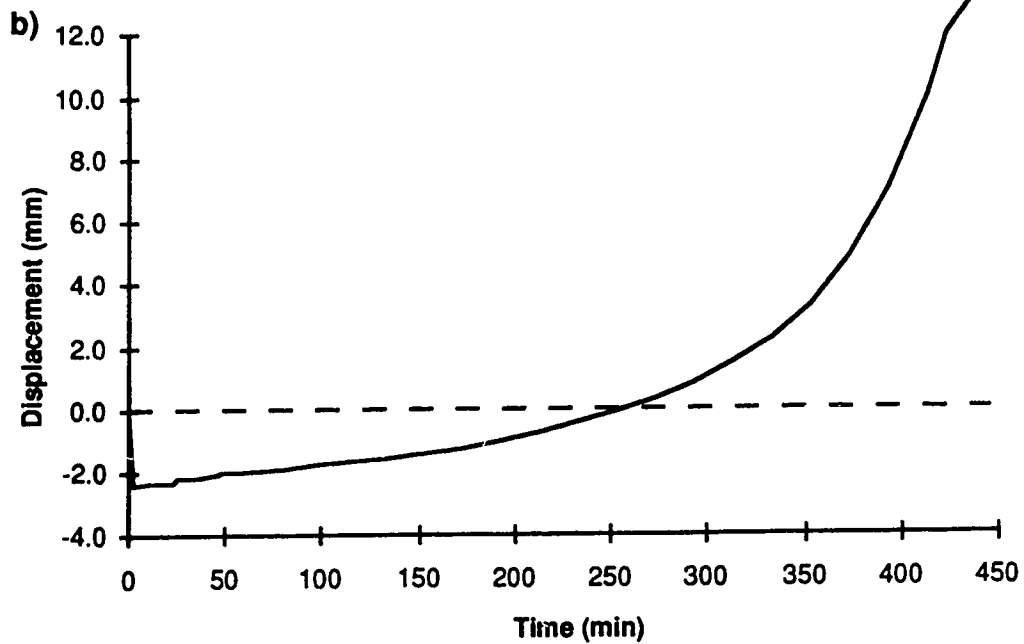
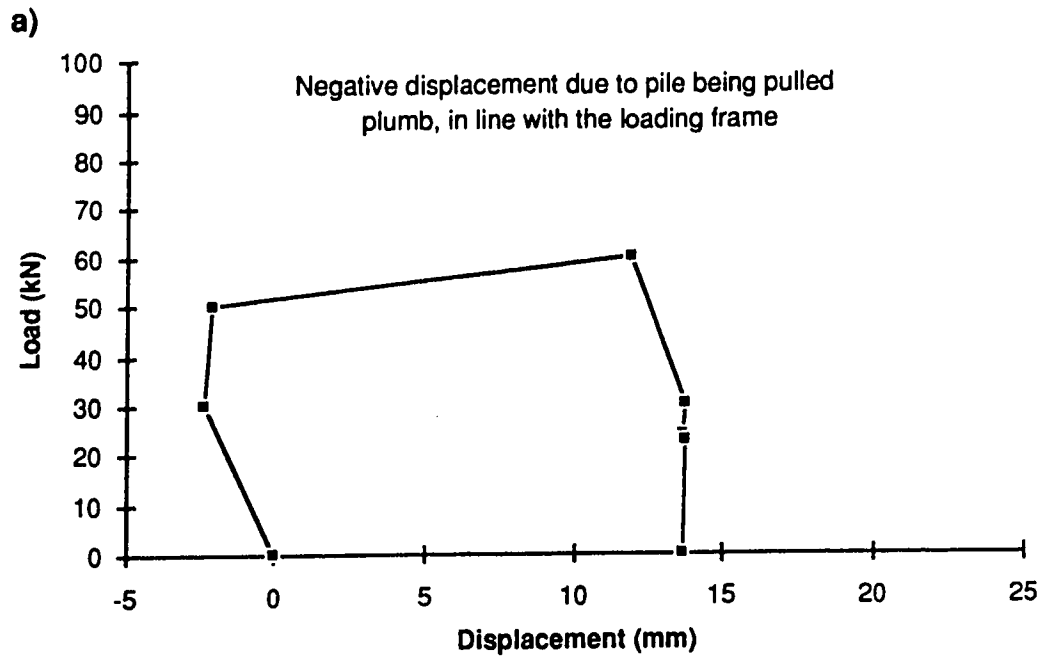


Figure A.1: Test #5—Smooth HSS pile with sand backfill  
 a) Load versus displacement  
 b) Displacement versus time

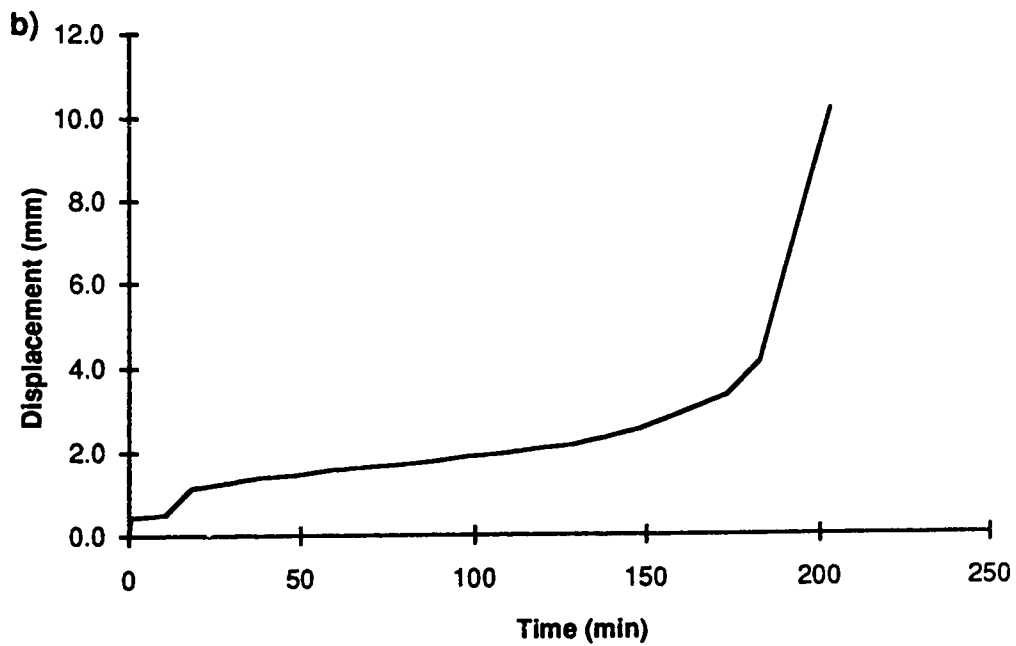
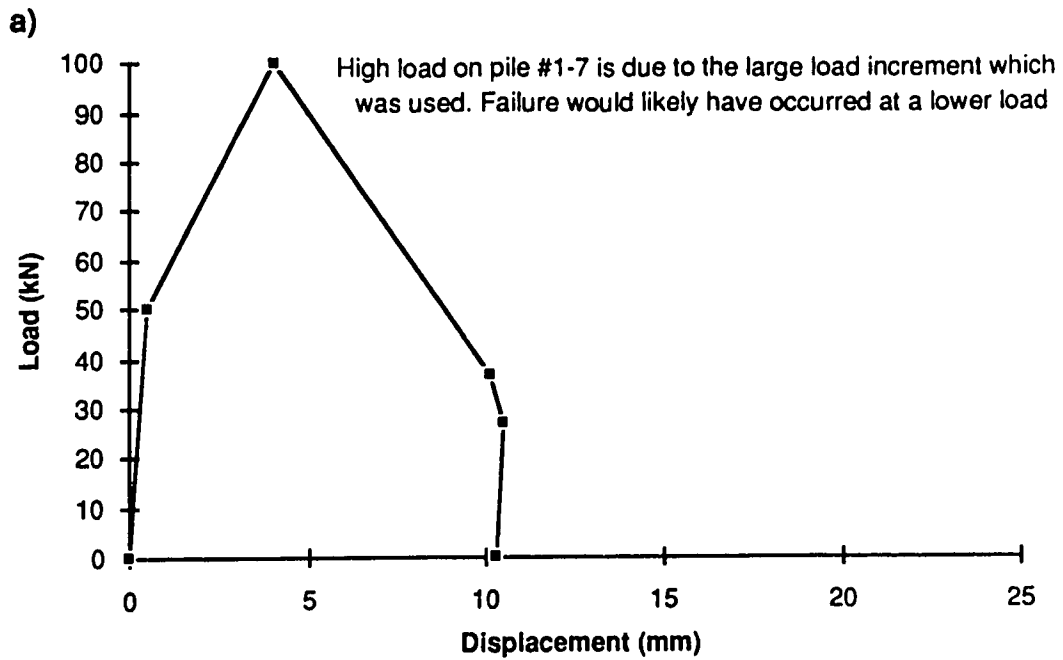


Figure A.2: Test #7–Smooth HSS pile with sand backfill  
a) Load versus displacement  
b) Displacement versus time

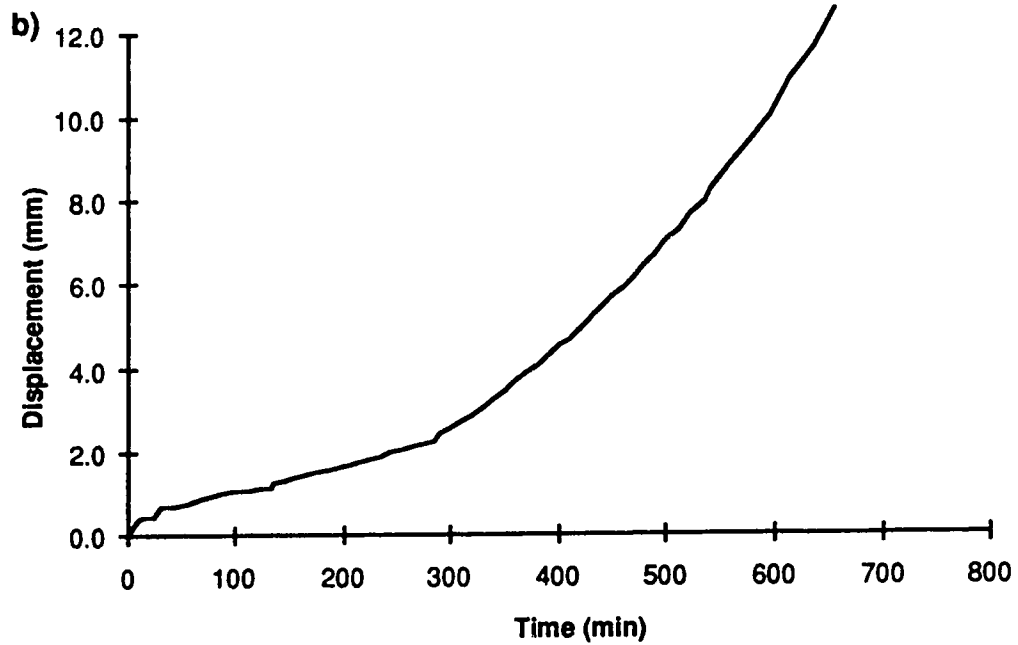
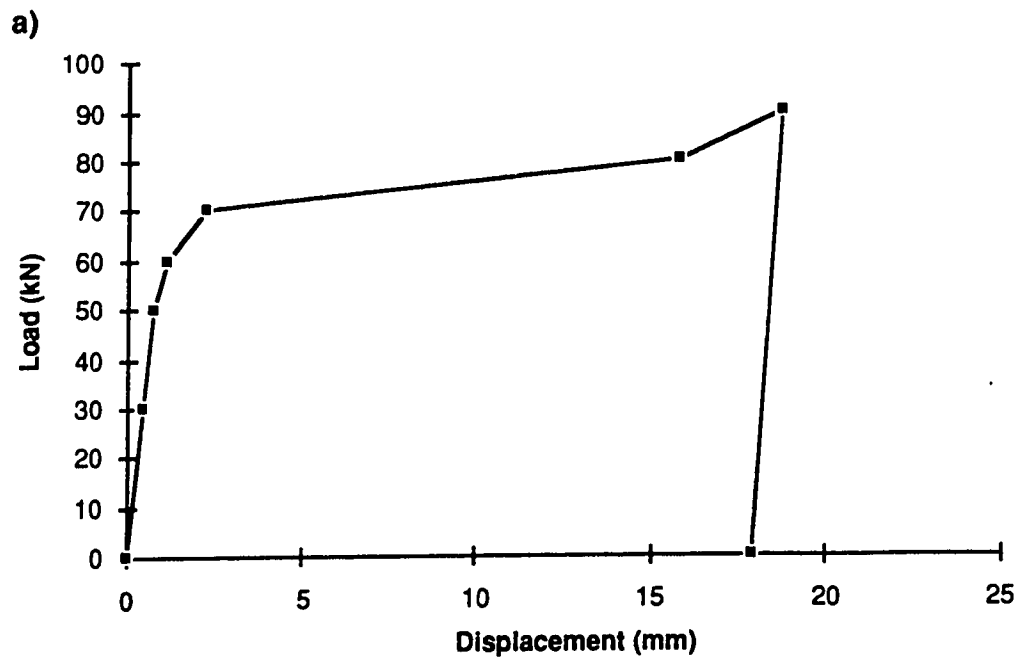


Figure A.3: Test #11—Smooth HSS pile with sand backfill  
a) Load versus displacement  
b) Displacement versus time

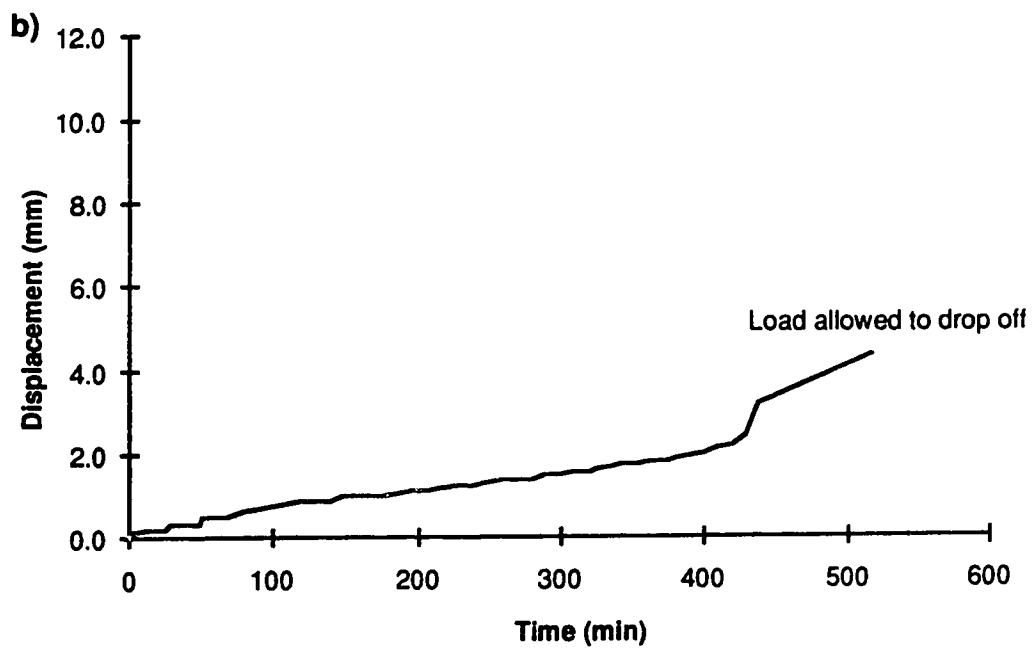
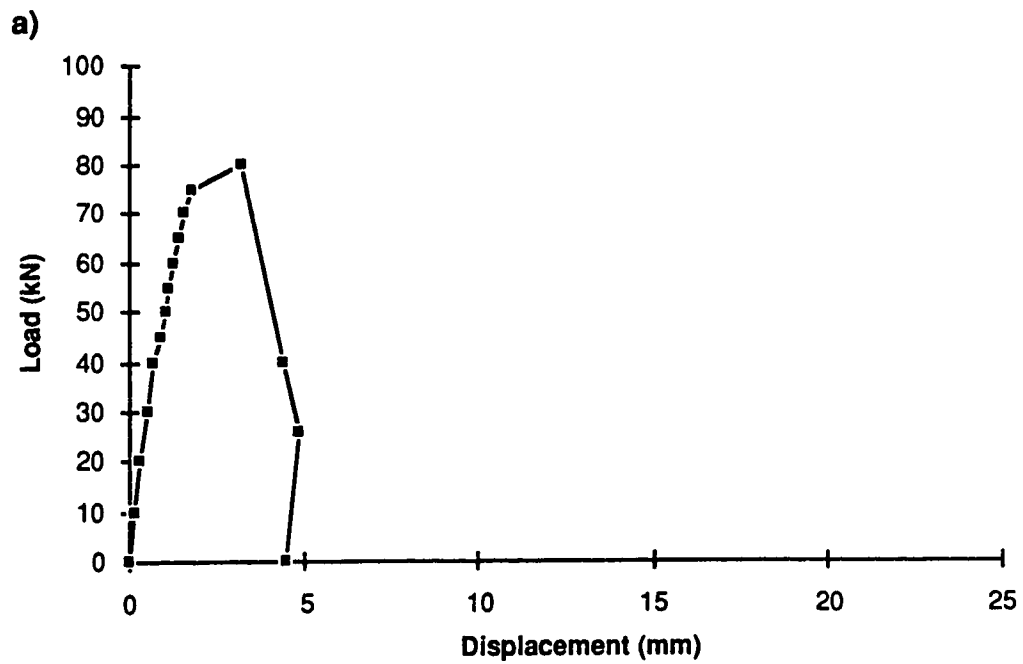


Figure A.4: Test #15—Plain pipe pile with sand backfill  
a) Load versus displacement  
b) Displacement versus time

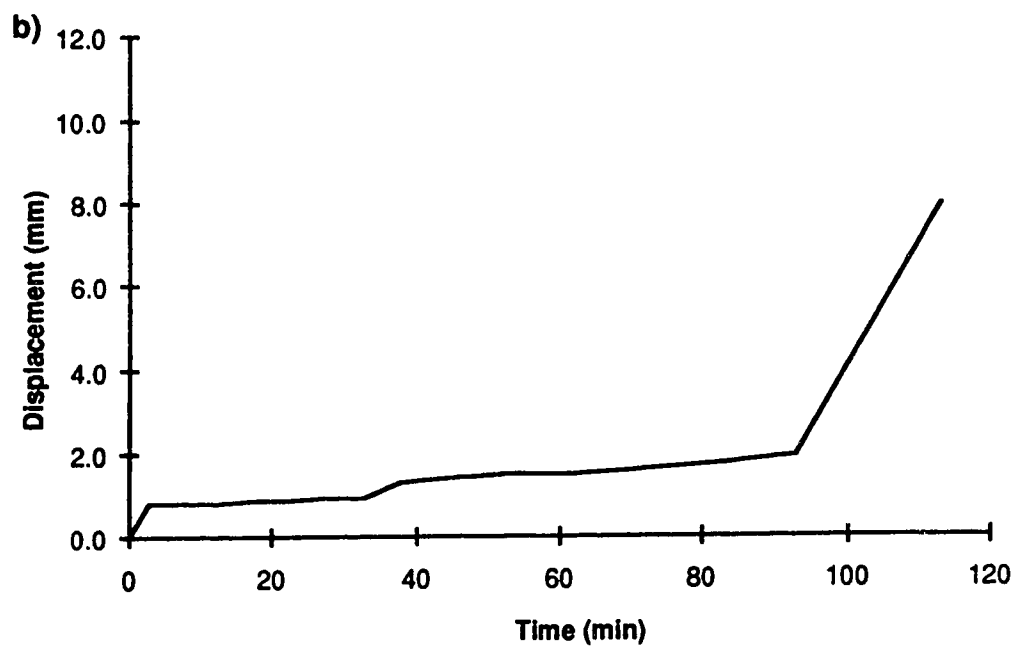
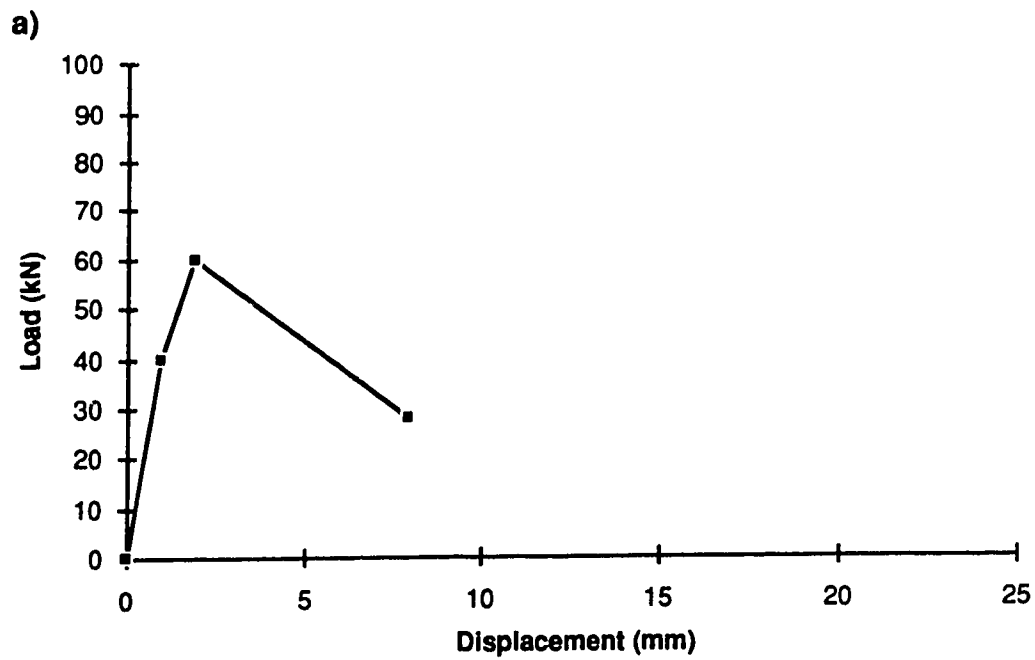


Figure A.5: Test #16—Plain pipe with sand backfill  
a) Load versus displacement  
b) Displacement versus time



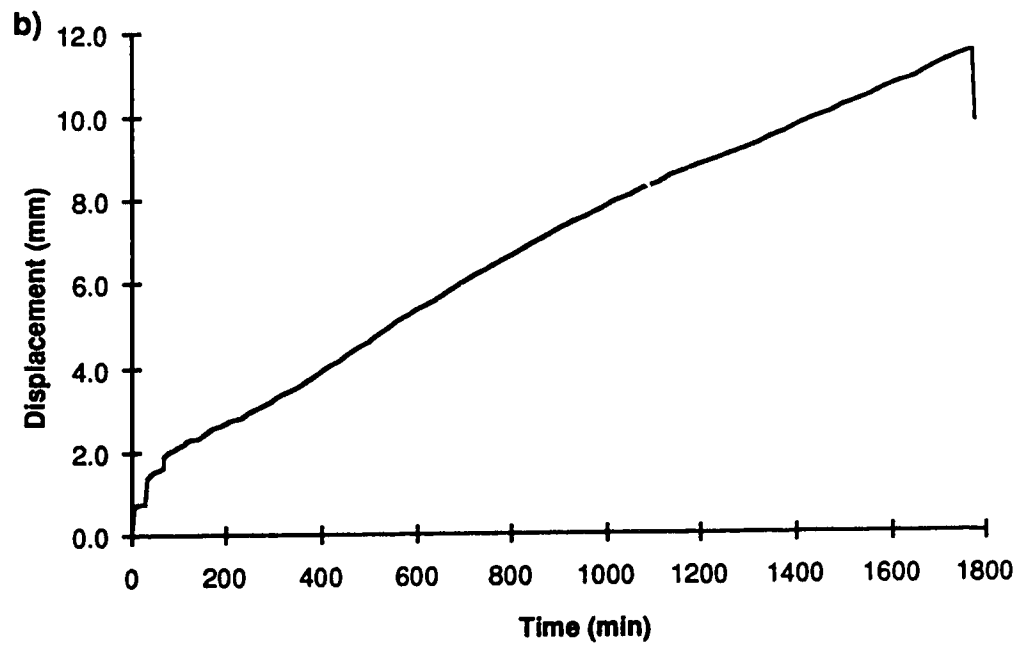
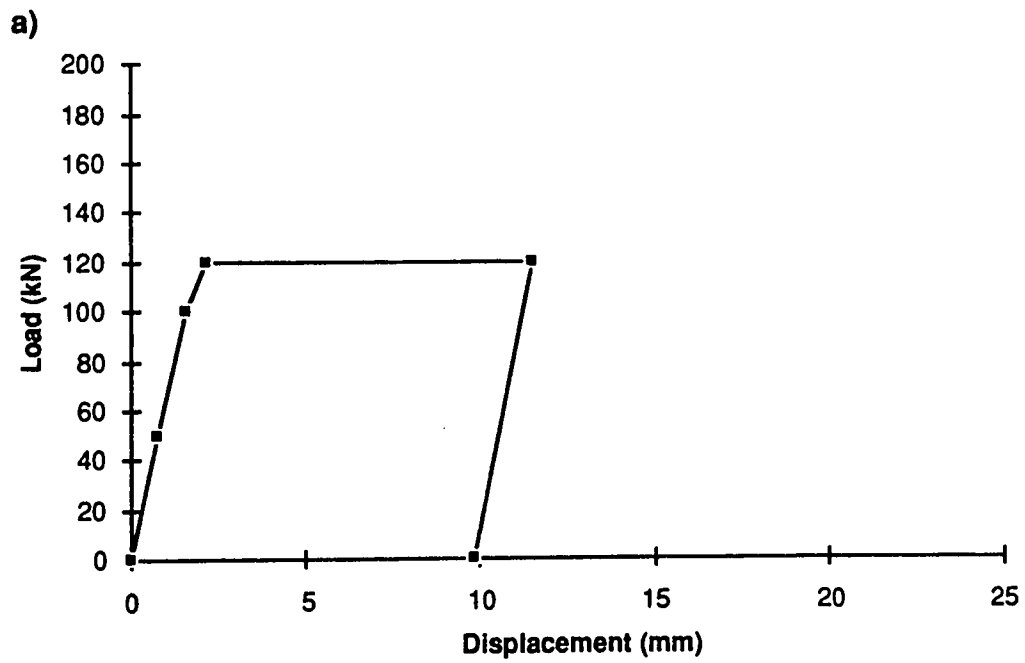


Figure A.6: Test #8—Lugged HSS pile with sand backfill  
a) Load versus displacement  
b) Displacement versus time

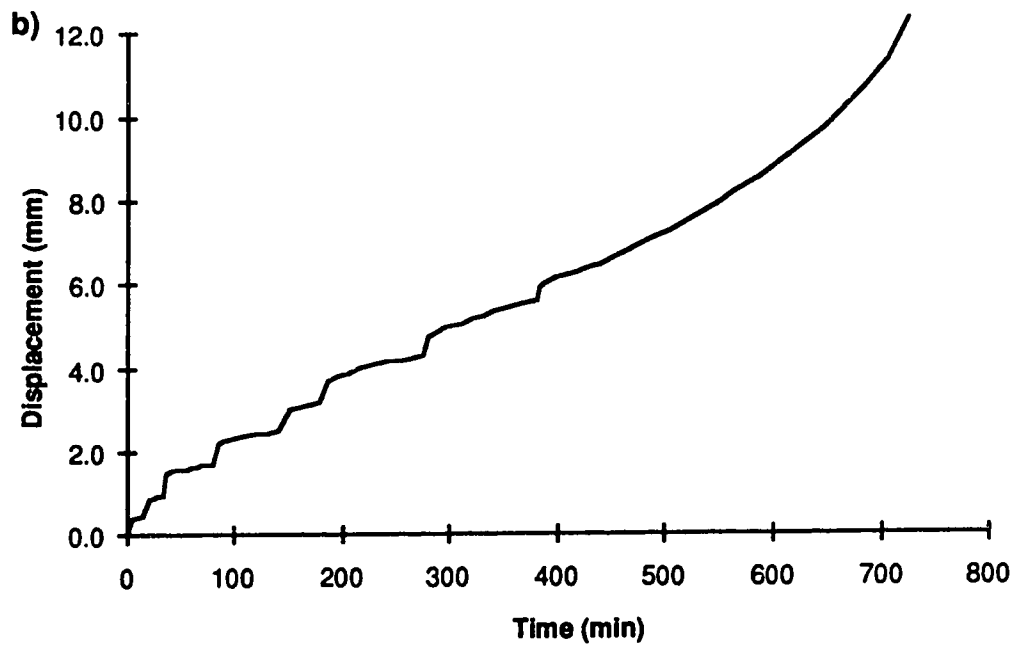
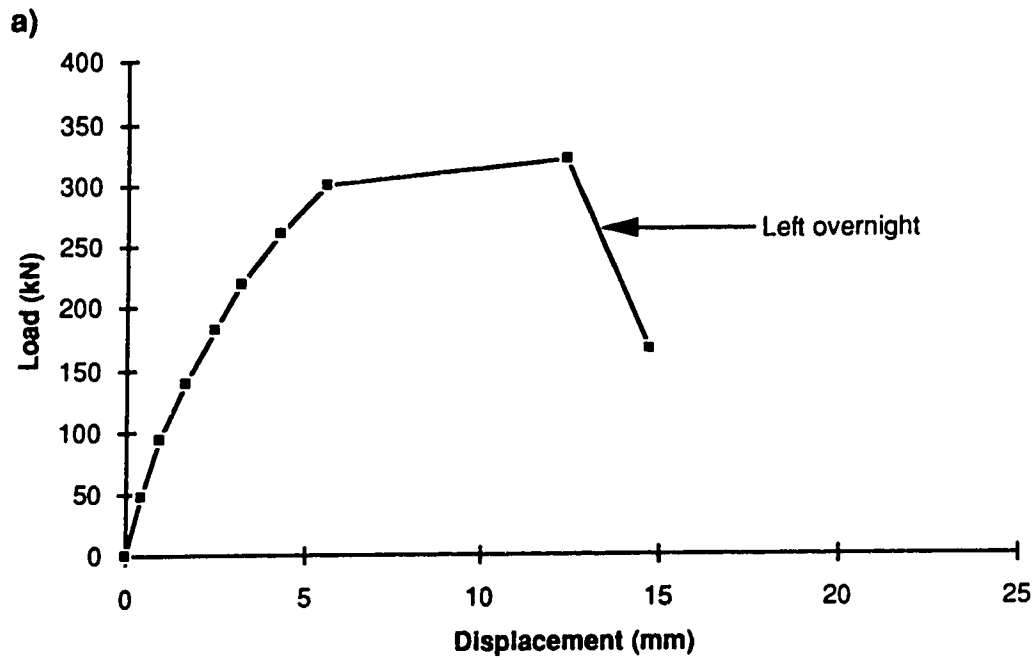


Figure A.7: Test #9—Lugged HSS pile with sand backfill  
a) Load versus displacement  
b) Displacement versus time

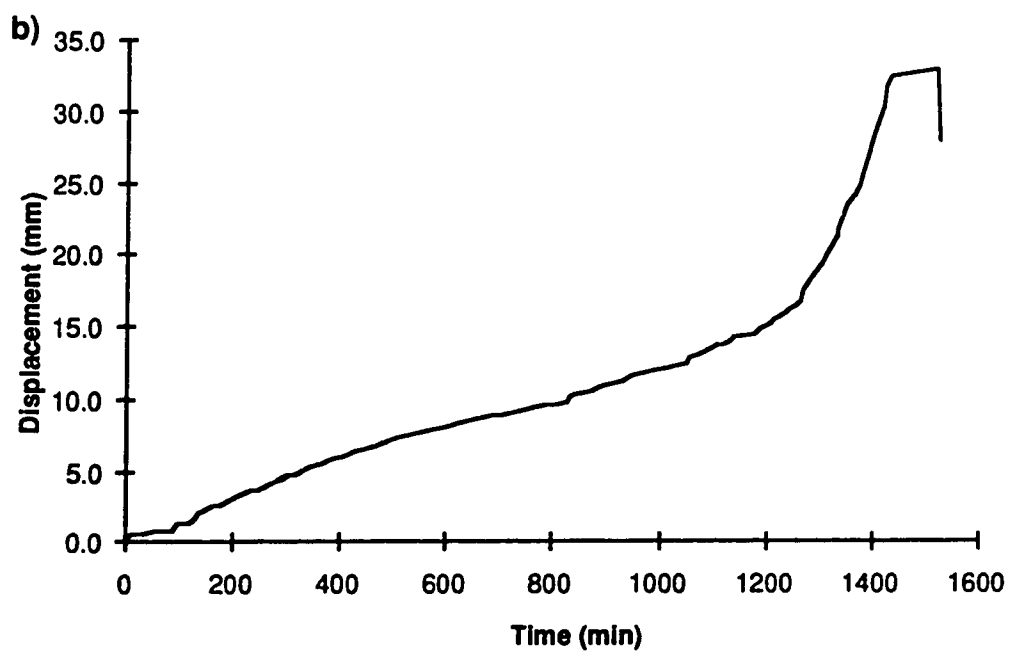
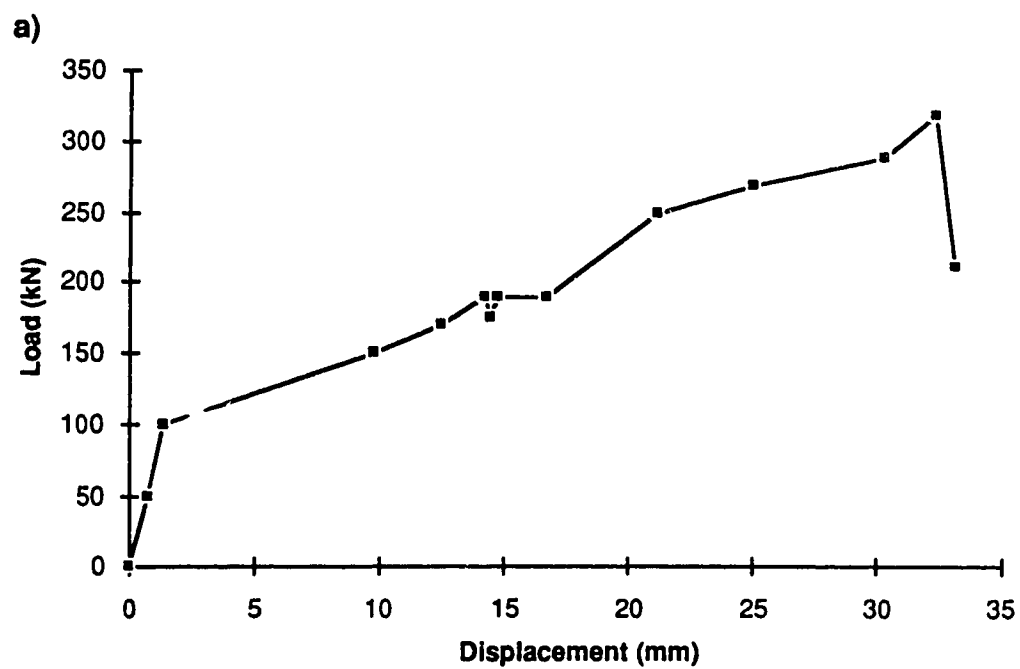


Figure A.8: Test #12–Lugged HSS pile with sand backfill  
a) Load versus displacement  
b) Displacement versus time

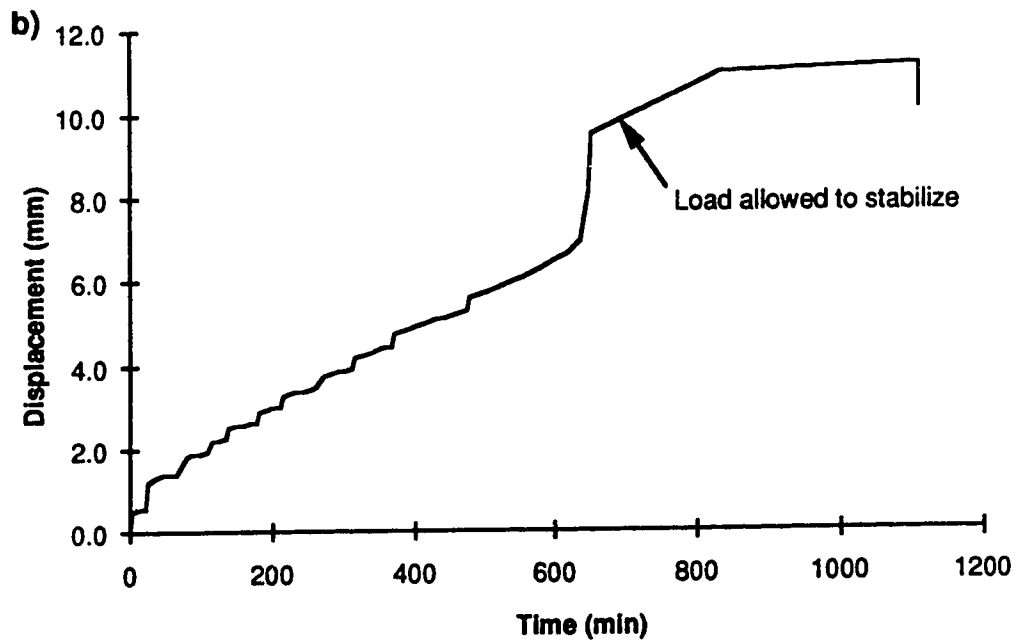
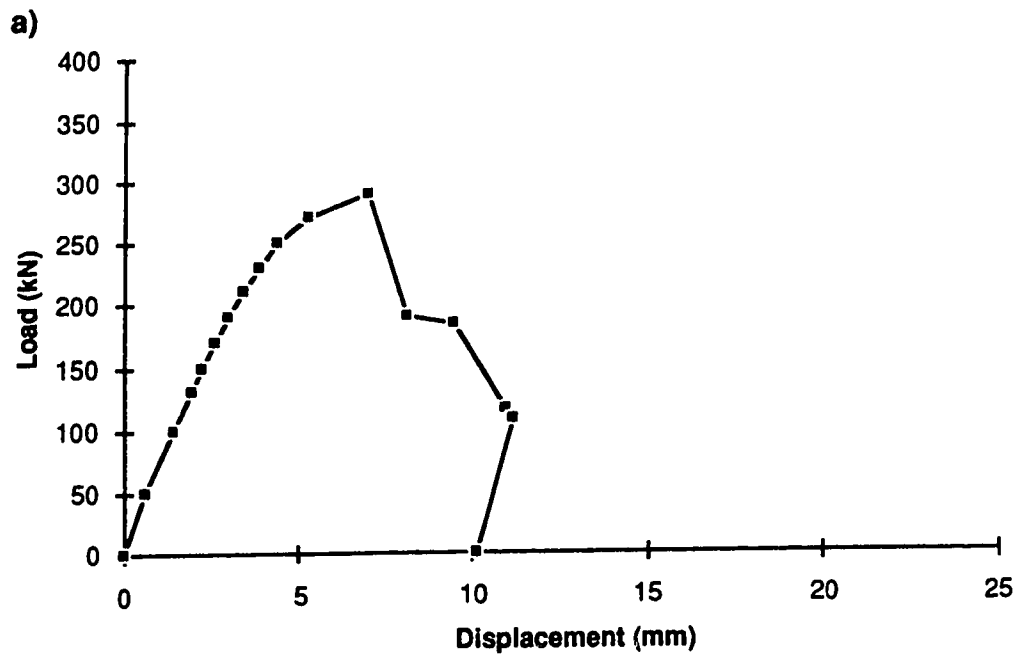


Figure A.9: Test #13—Sandblasted pipe pile with sand backfill  
a) Load versus displacement  
b) Displacement versus time

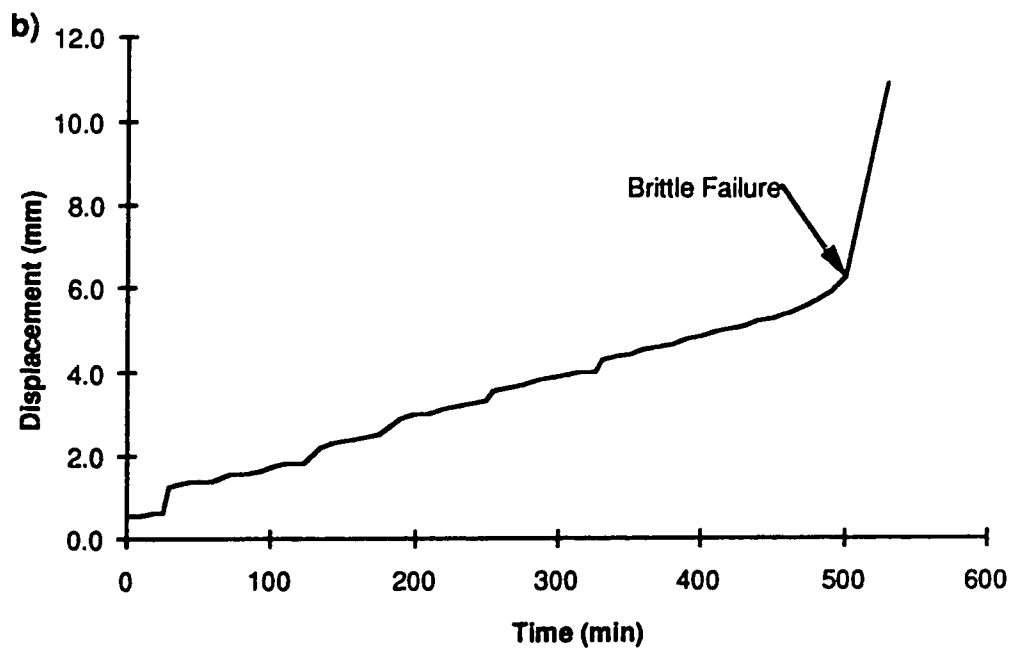
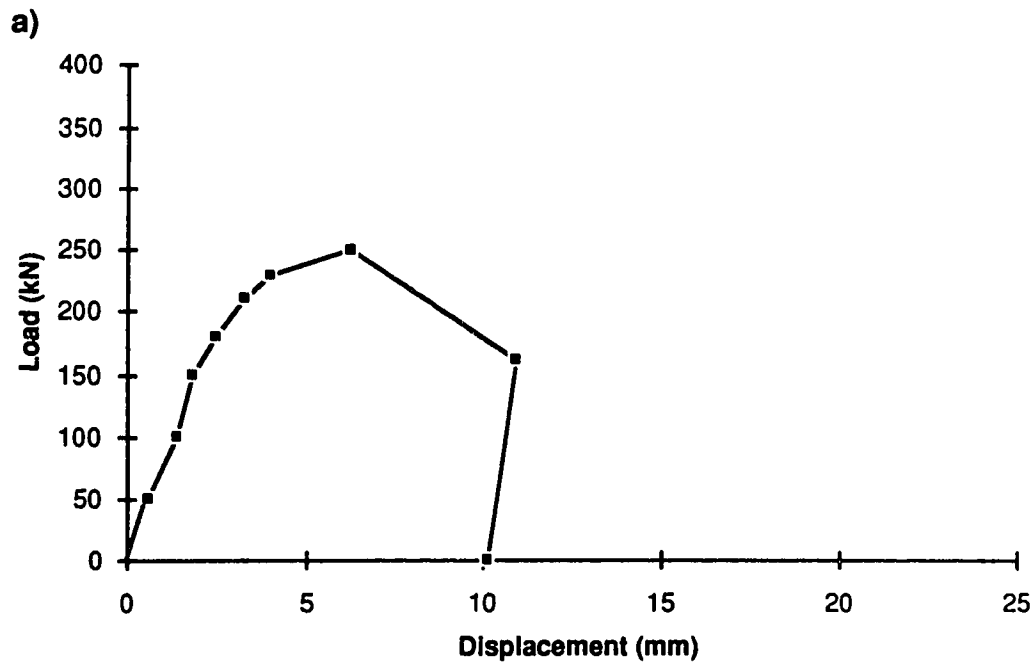


Figure A.10: Test #14—Sandblasted pipe pile with sand backfill  
a) Load versus displacement  
b) Displacement versus time

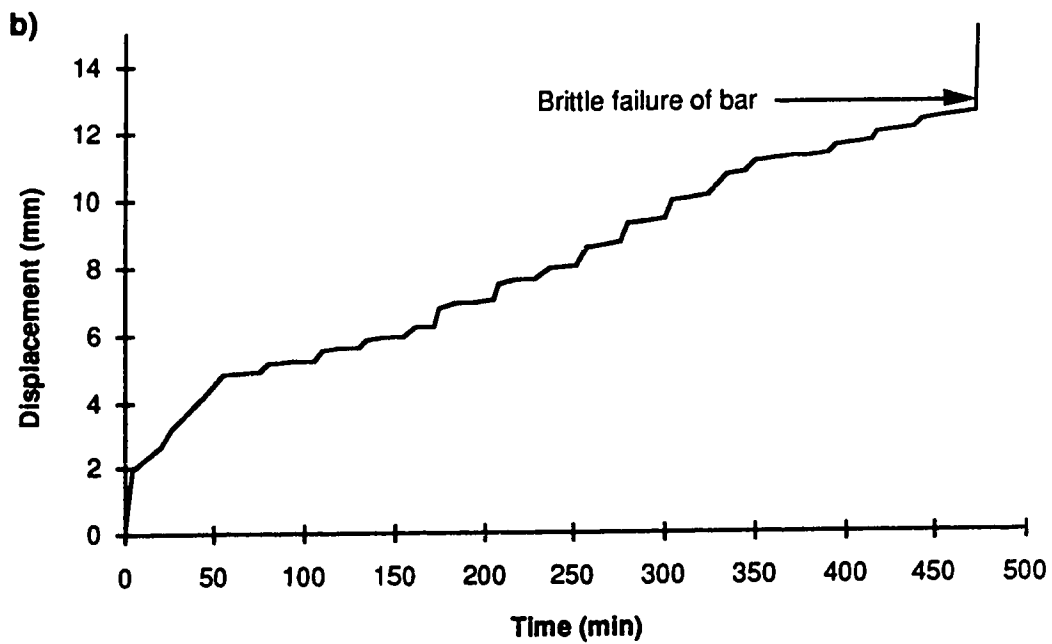
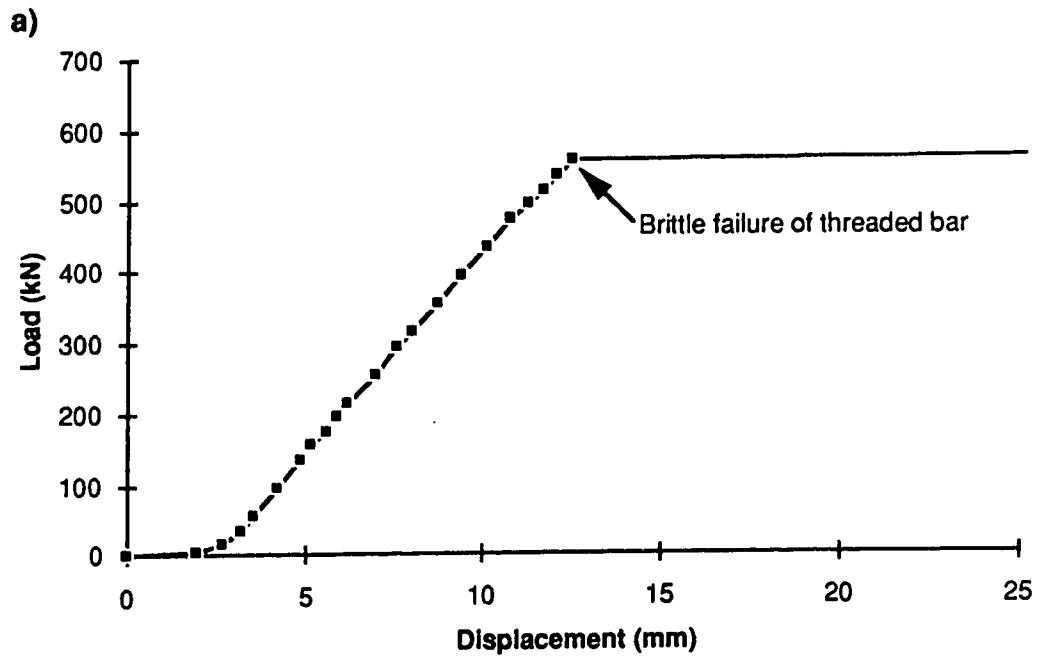


Figure A.11: Test #2–Dywidag bar with neat Ciment Fondu grout backfill  
a) Load versus displacement  
b) Displacement versus time

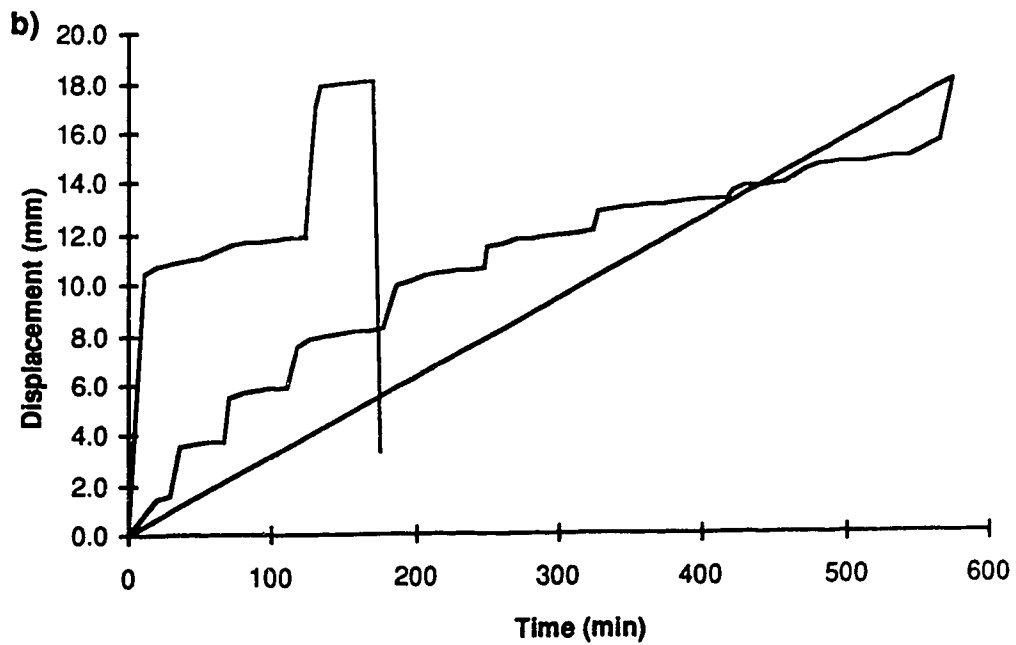
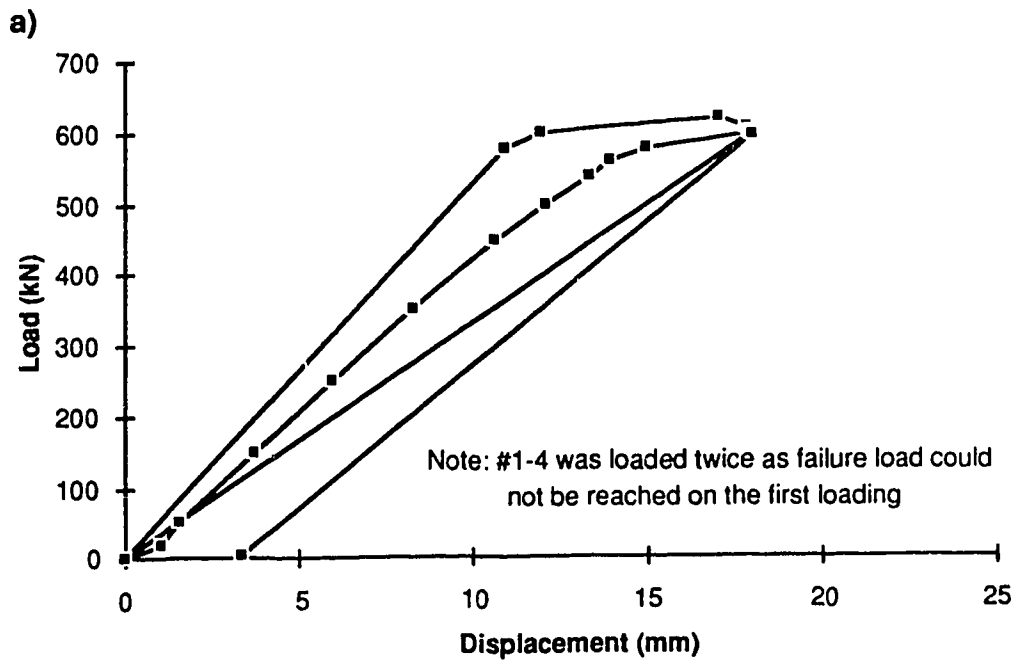


Figure A.12: Test #4—Dywidag bar with neat Cement Fondu grout backfill  
a) Load versus displacement  
b) Displacement versus time

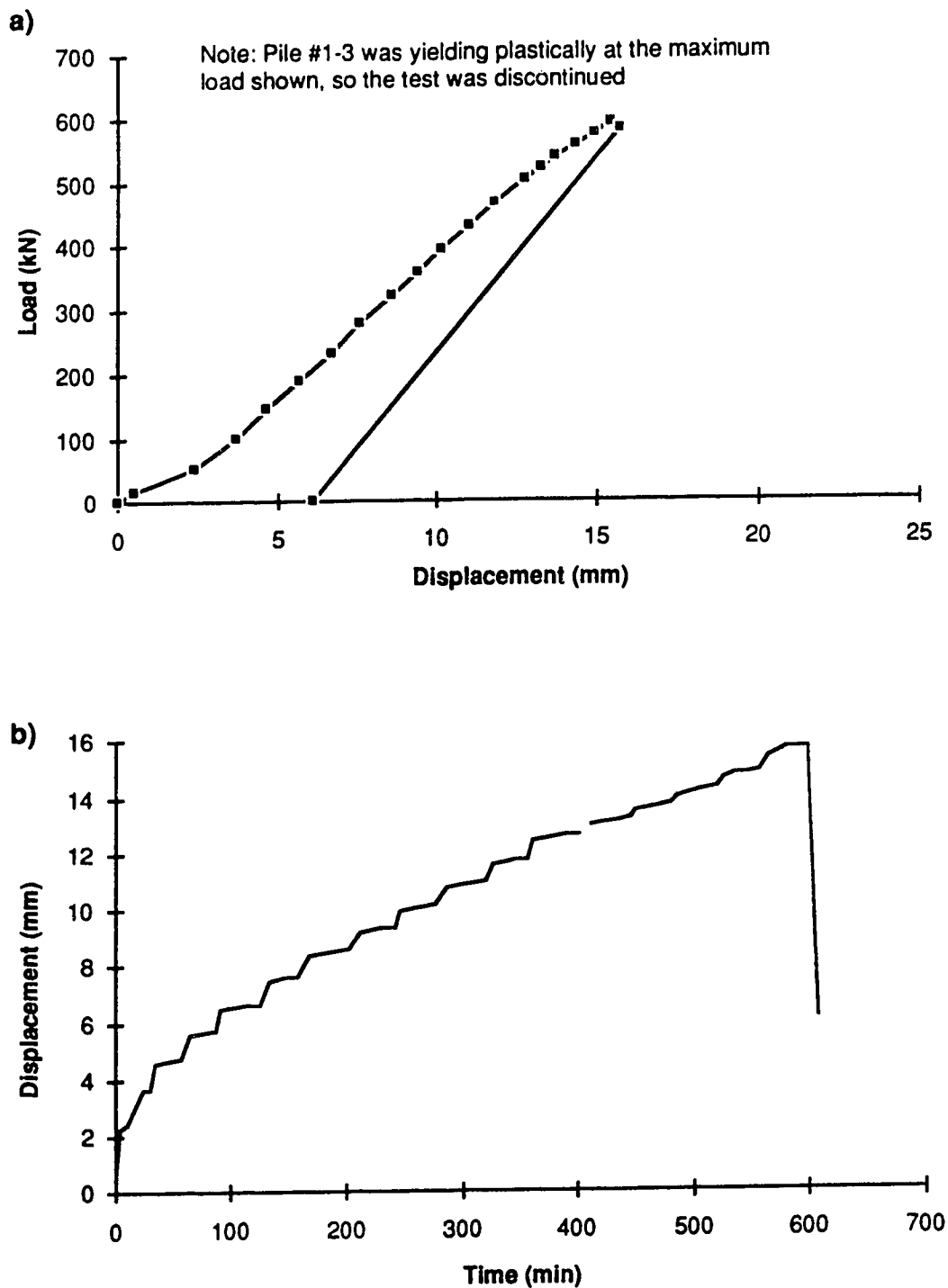


Figure A.13: Test #3—Dywidag bar with sanded Cement Fondu grout backfill  
a) Load versus displacement  
b) Displacement versus time



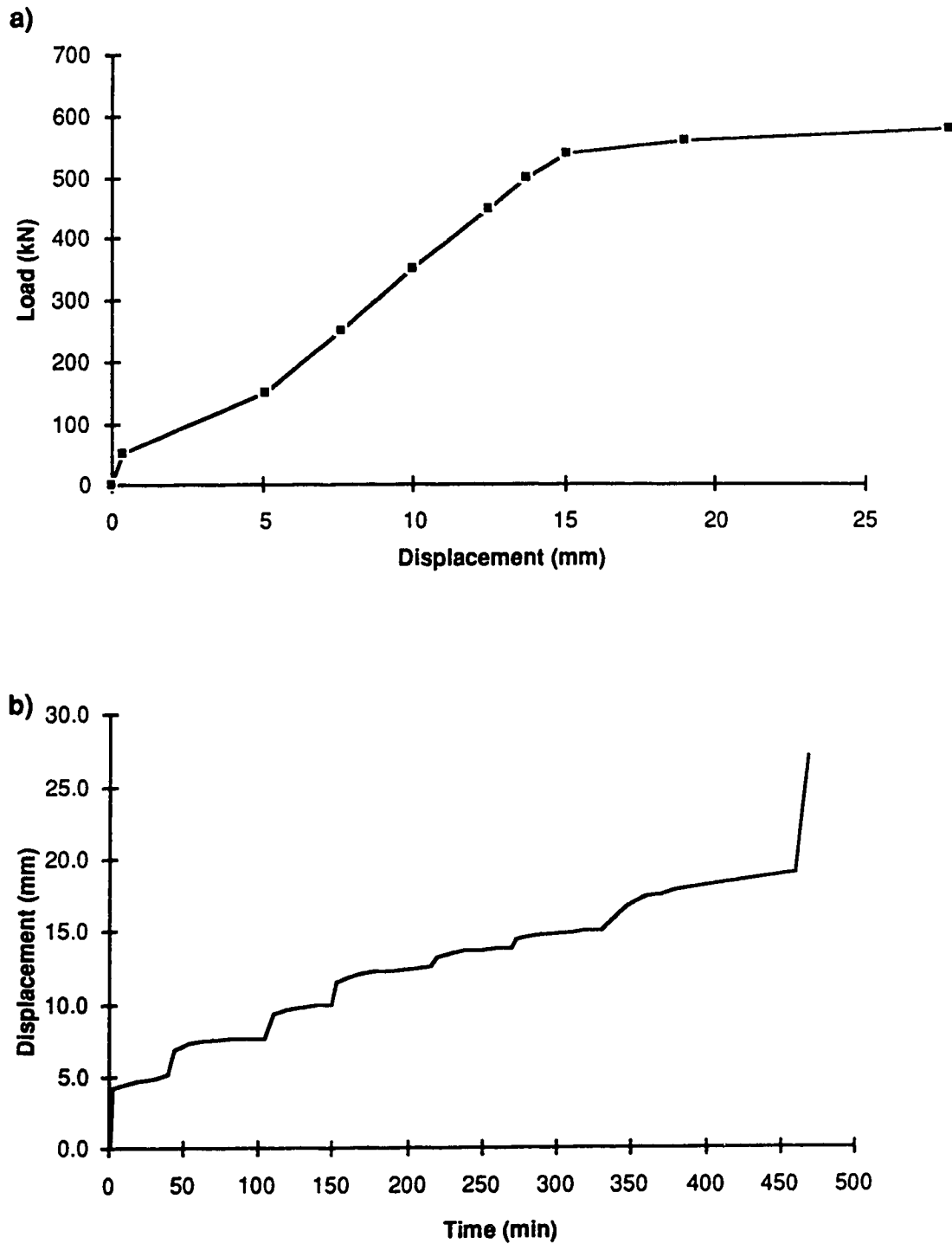


Figure A.14: Test #6—Dywidag bar with sanded Ciment Fondu grout backfill  
a) Load versus displacement  
b) Displacement versus time

**APPENDIX B**  
**IQALUIT TEST RESULTS**  
**pertinent to**  
**CHAPTER 2**

Grout curing temperatures  
and  
Log displacement versus log time

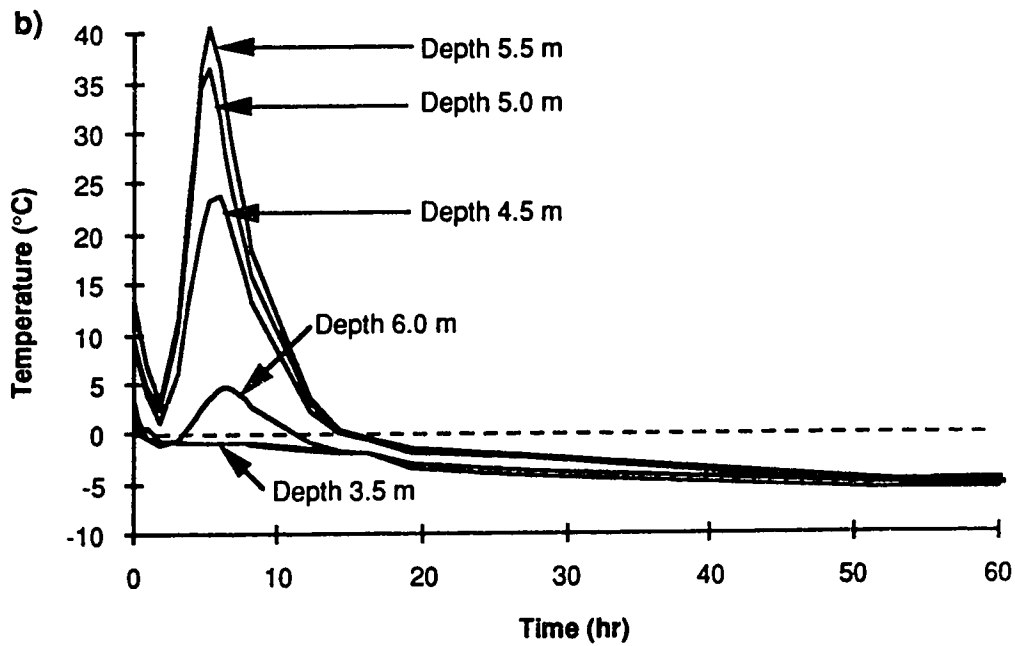
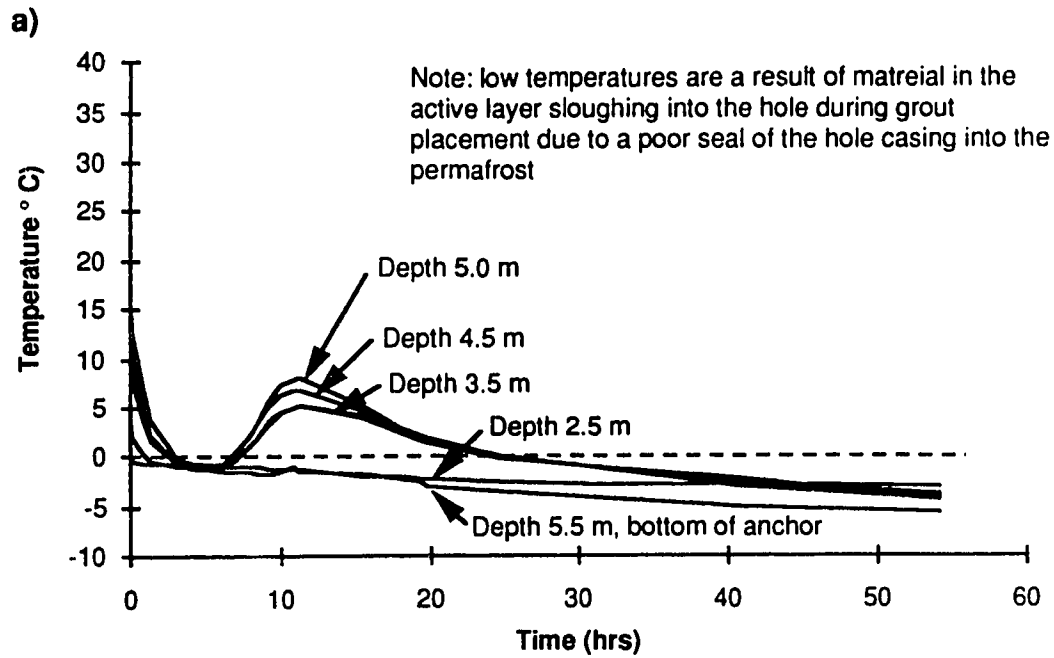


Figure B.1: Grout curing temperatures versus time for neat grout backfill  
a) Pile #2  
b) Pile #4

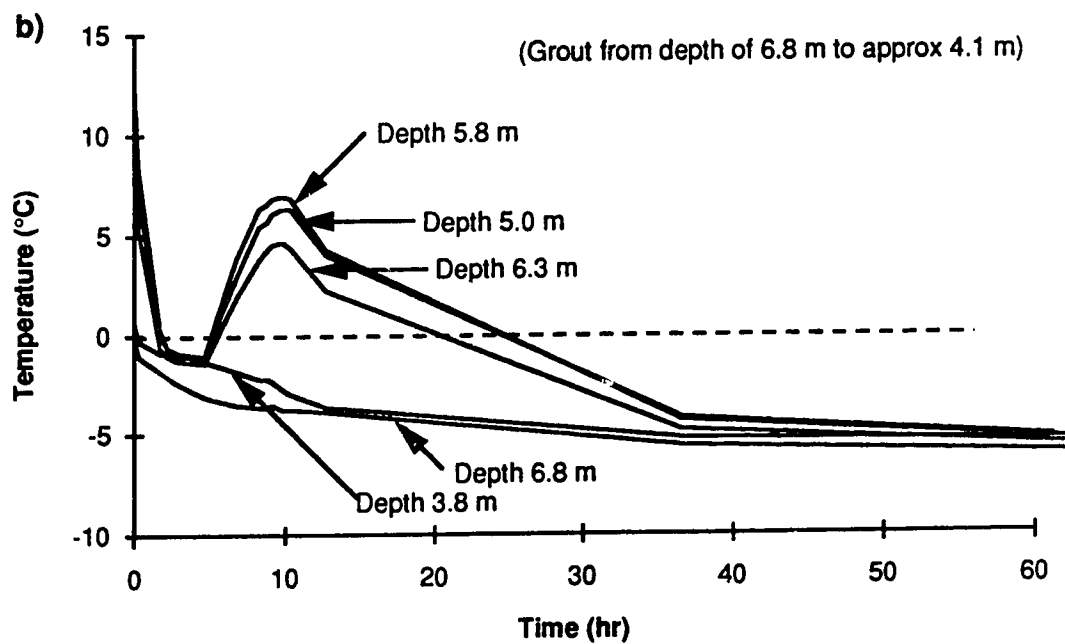
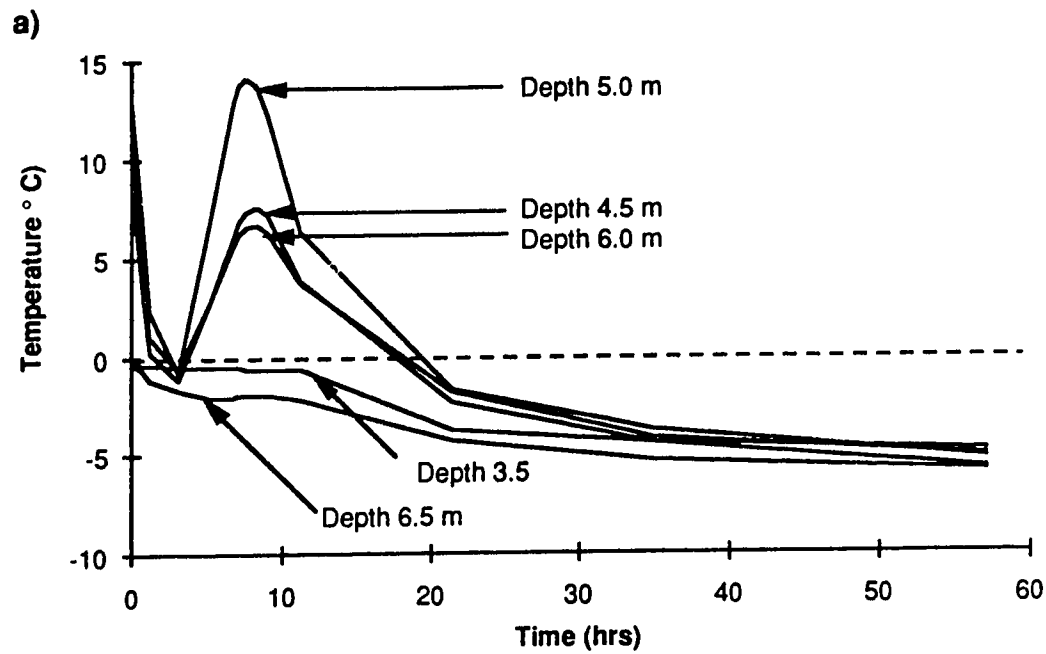


Figure B.2: Grout curing temperatures versus time for sanded grout backfill

a) Pile #3

b) Pile #6

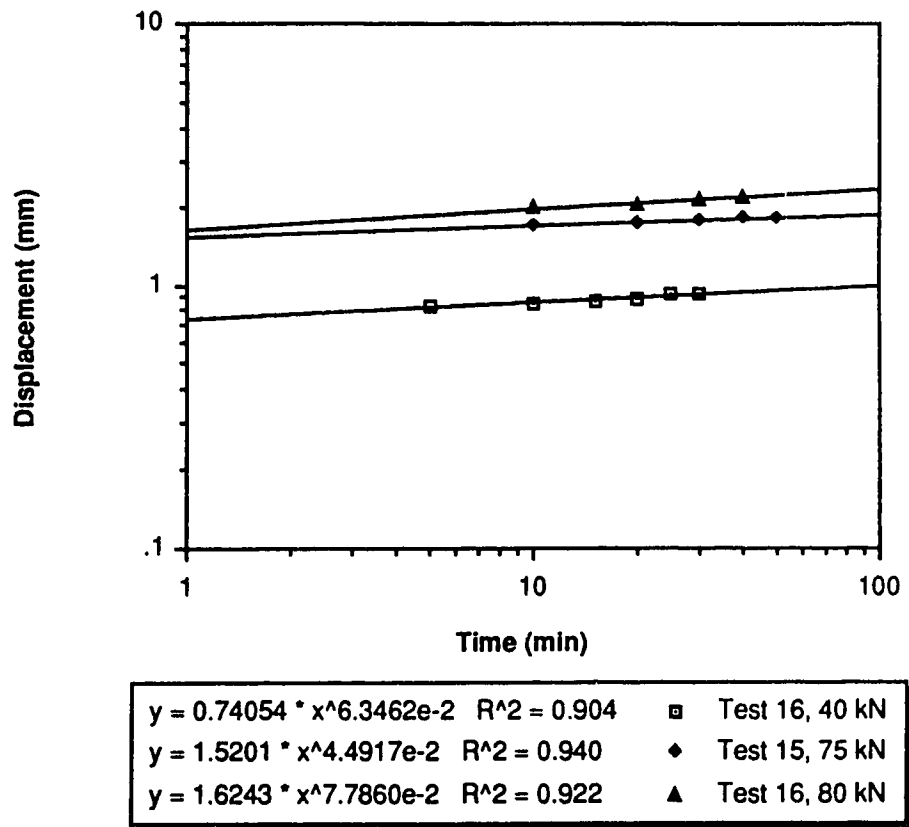


Figure B.3: Regression analysis of log displacement versus log time for plain pipe piles

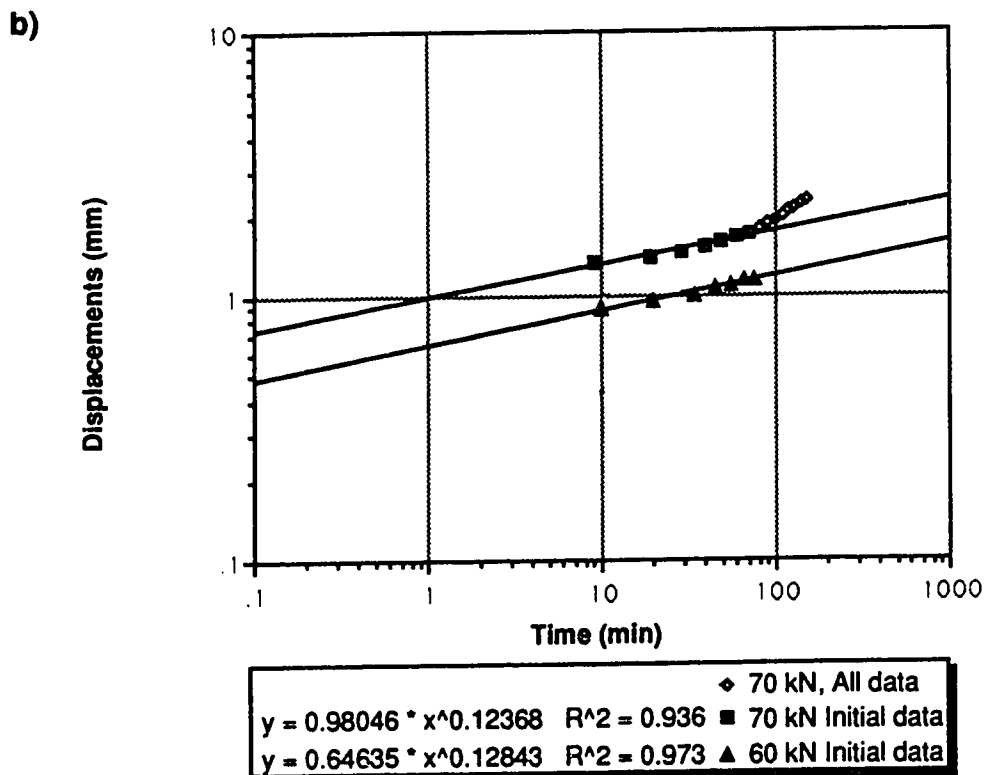
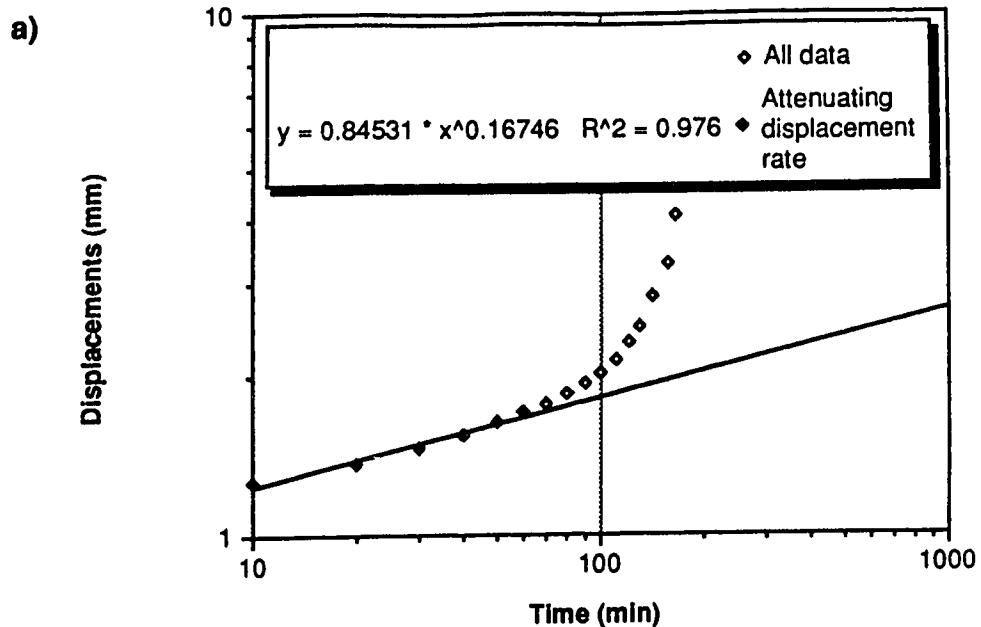


Figure B.4: Regression analysis of log displacement versus log time for smooth HSS piles  
 a) test #7  
 b) test #11

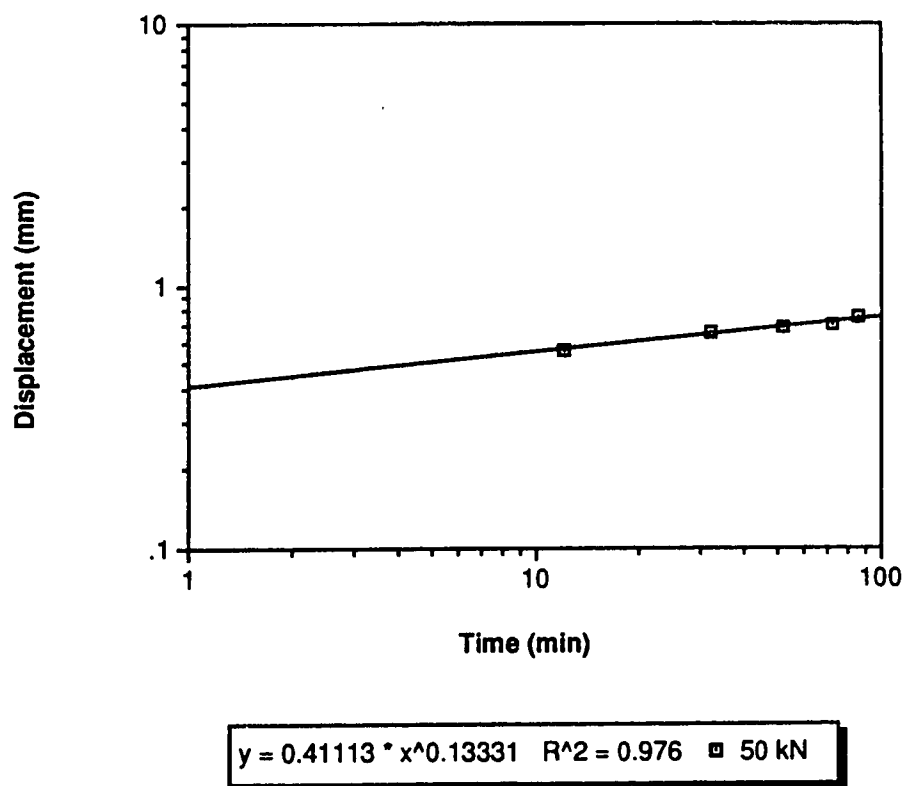


Figure B.5: Regression analysis of log displacement versus log time for lugged HSS piles

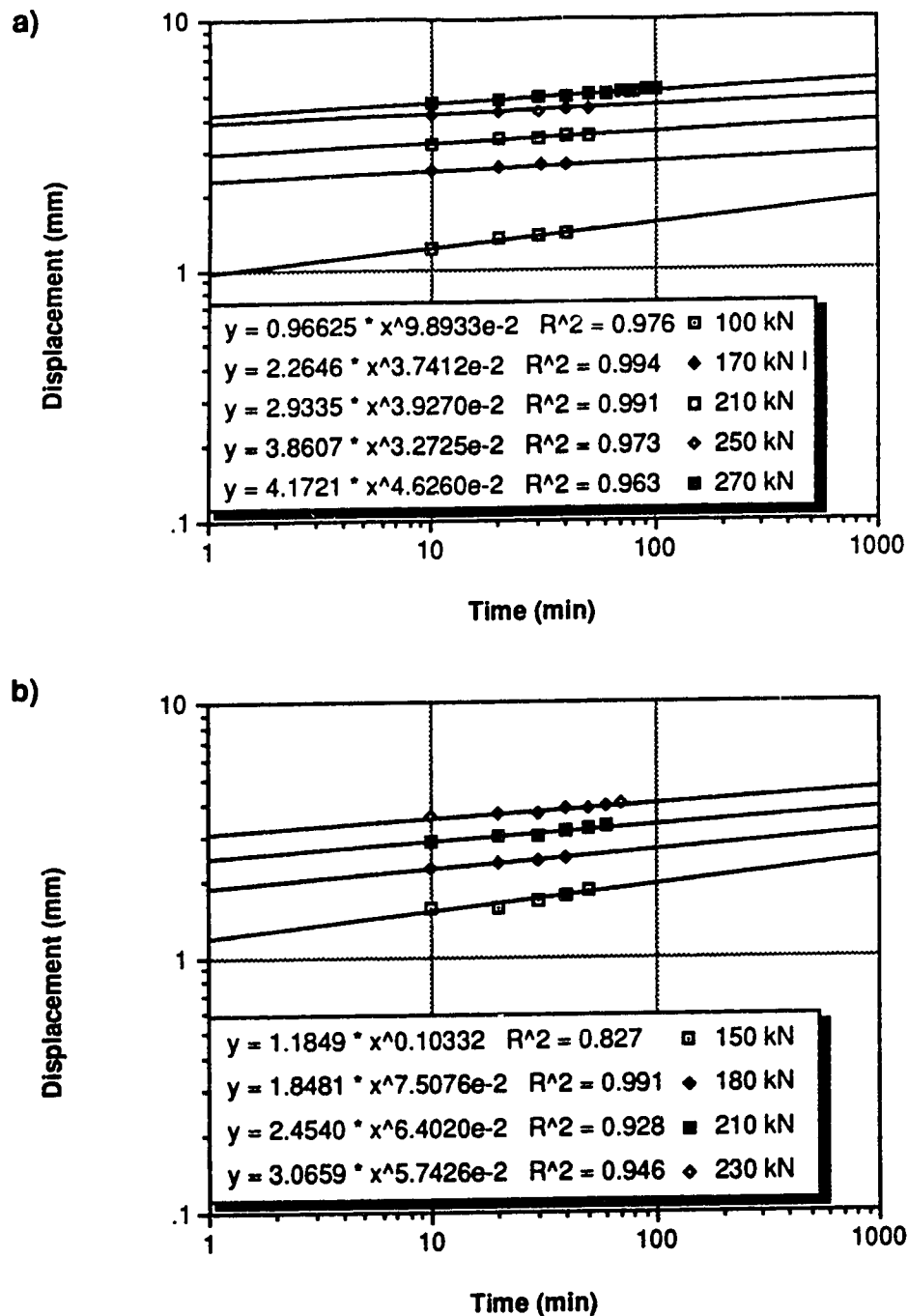


Figure B.6: Regression analysis of log displacement versus log time for sandblasted pipe piles  
 a) test #13  
 b) test #14



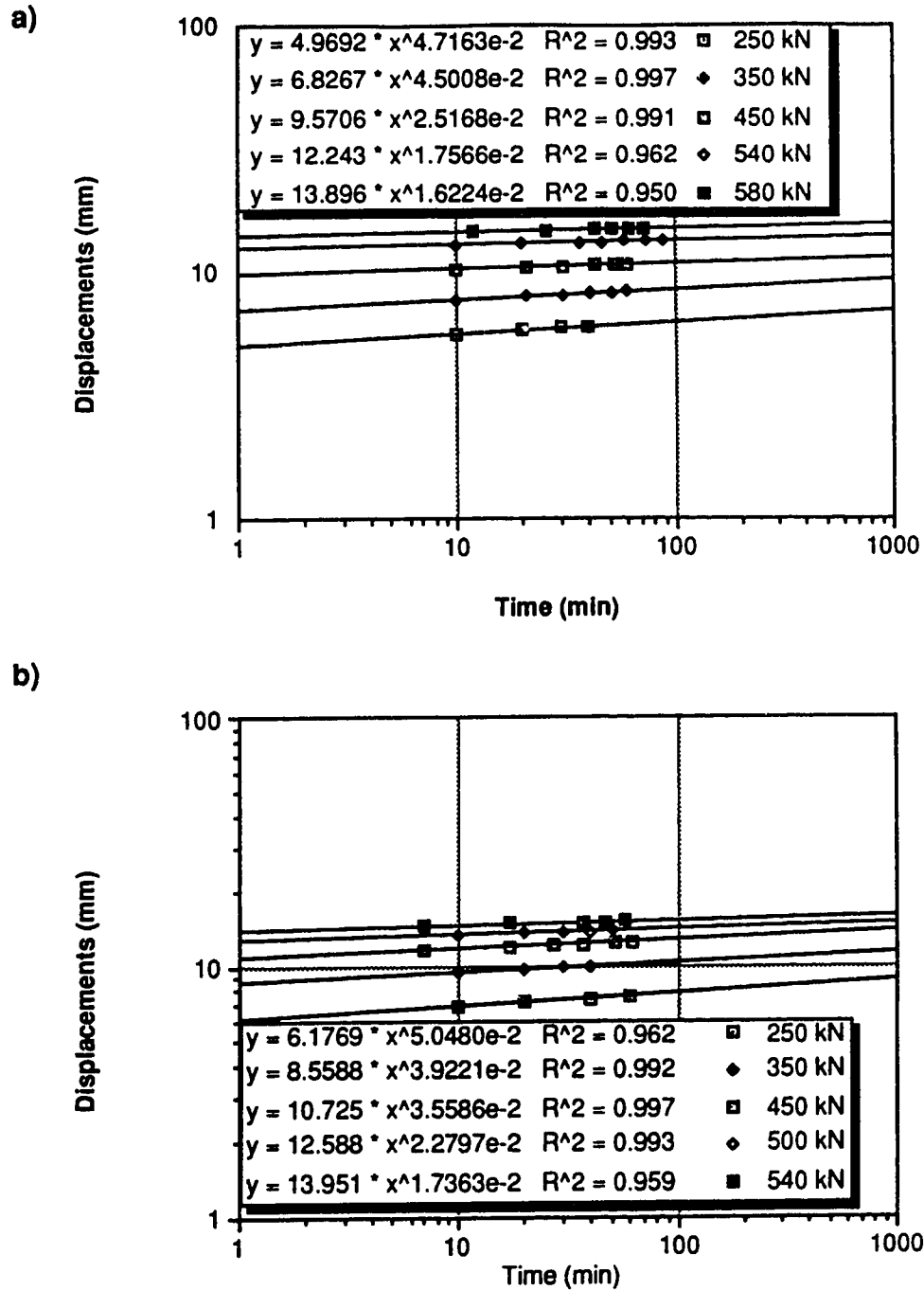


Figure B.7: Regression analysis of log displacement versus log time for  
sanded grout backfilled Dywidag bars

a) test #4

b) test #6

**APPENDIX C**  
**GROUT CURING PERFORMANCE**  
**FOR VARIOUS MIX DESIGNS**

Grout and soil temperature versus time

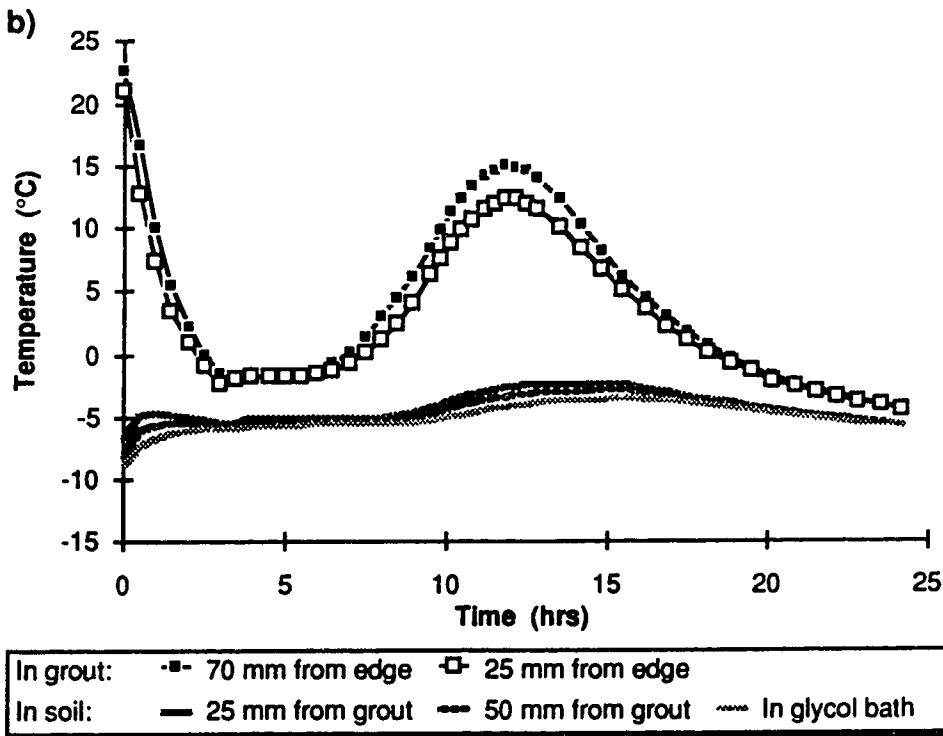
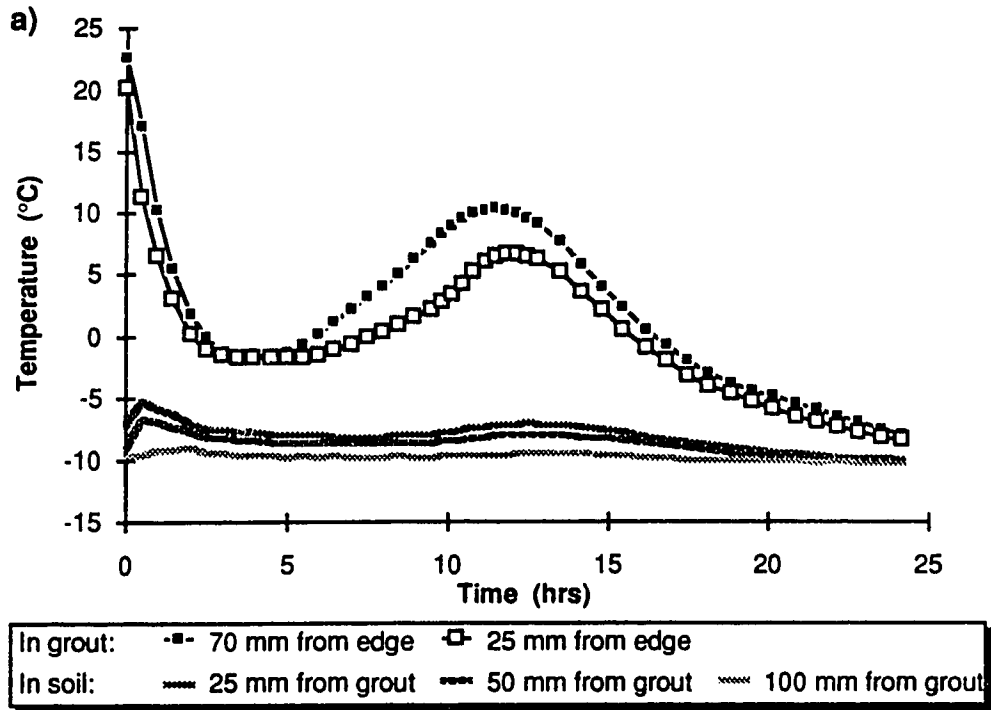


Figure C.1: Mix I-A, grout and soil temperature versus time  
a) 600 mm cell  
b) Constant temperature bath cell (CTBC)

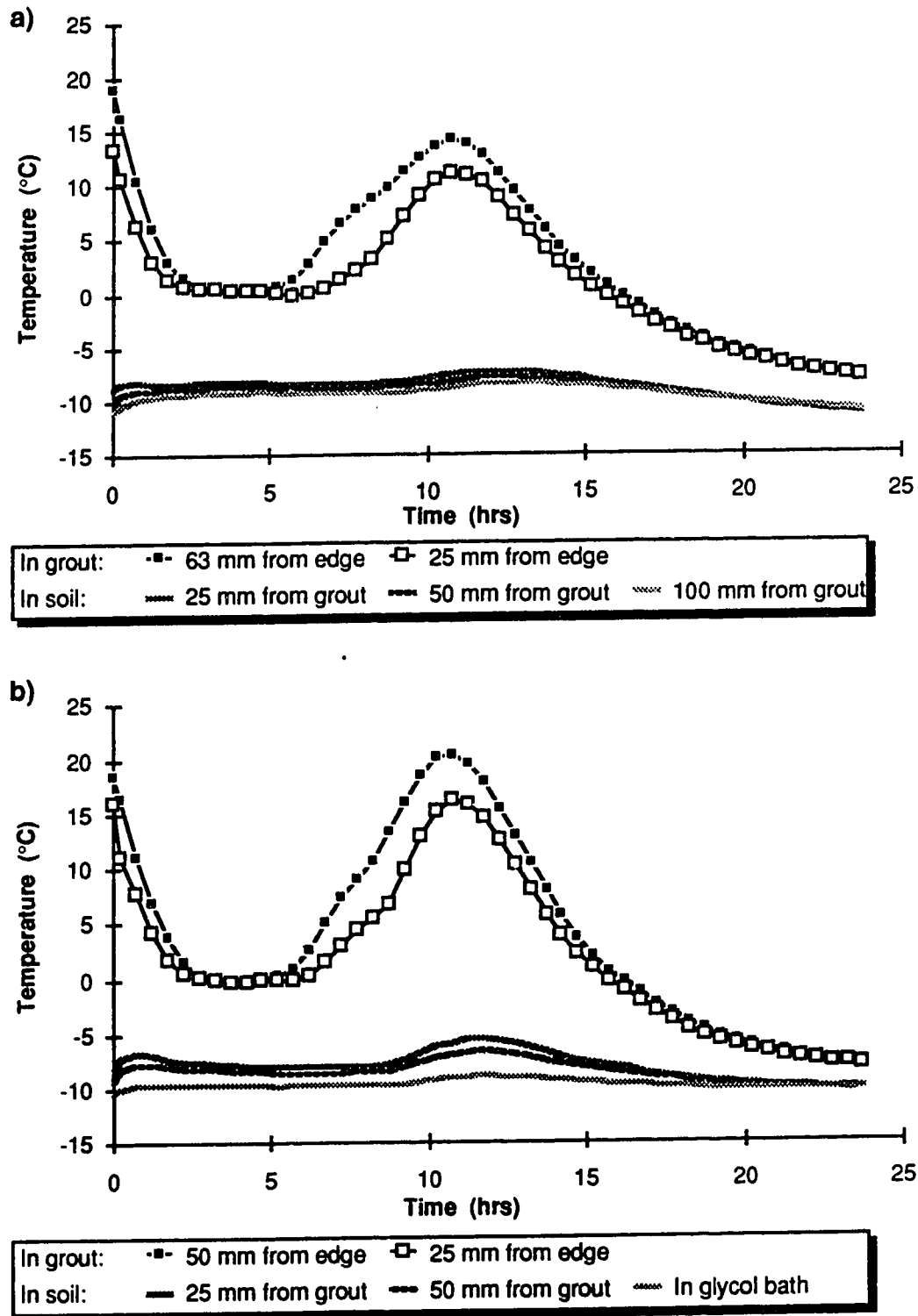
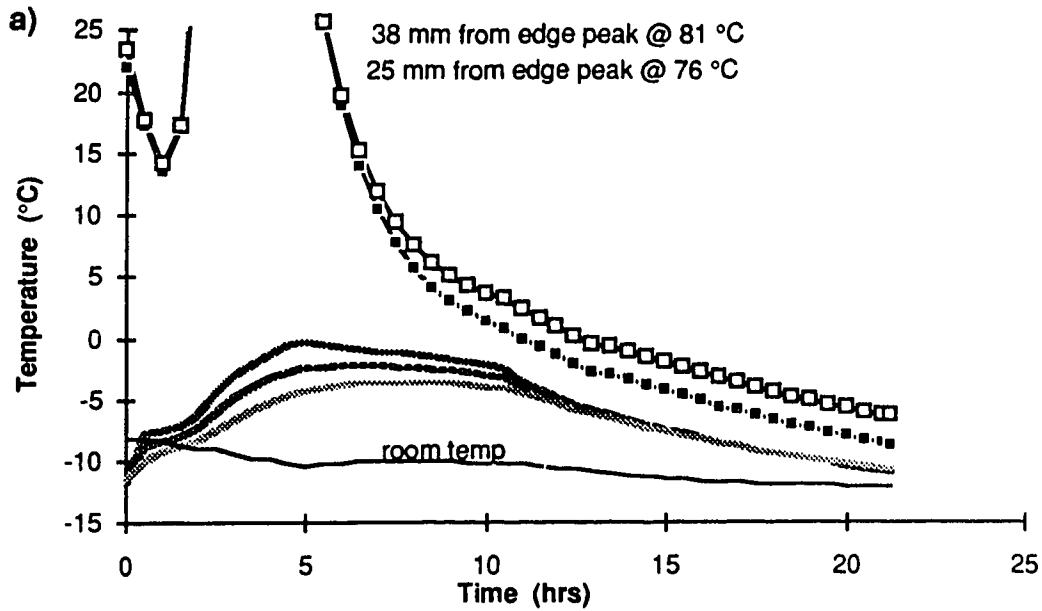
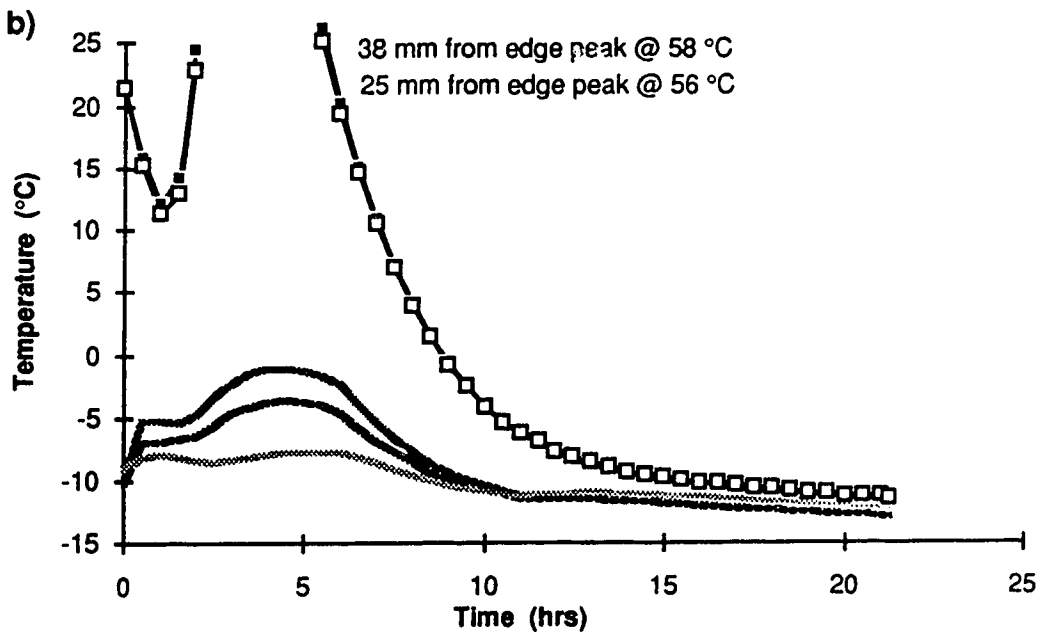


Figure C.2: Mix II-1, grout and soil temperature versus time  
a) 600 mm cell  
b) Constant temperature bath cell (CTBC)



In grout:    -■- 38 mm from edge    -□- 25 mm from edge  
In soil:    - - - 25 mm from grout    - - - 50 mm from grout    - - - 100 mm from grout



In grout:    -■- 38 mm from edge    -□- 25 mm from edge  
In soil:    - - - 25 mm from grout    - - - 50 mm from grout    - - - In glycol bath

Figure C.3: Mix II-2, grout and soil temperature versus time  
a) 600 mm cell  
b) Constant temperature bath cell (CTBC)

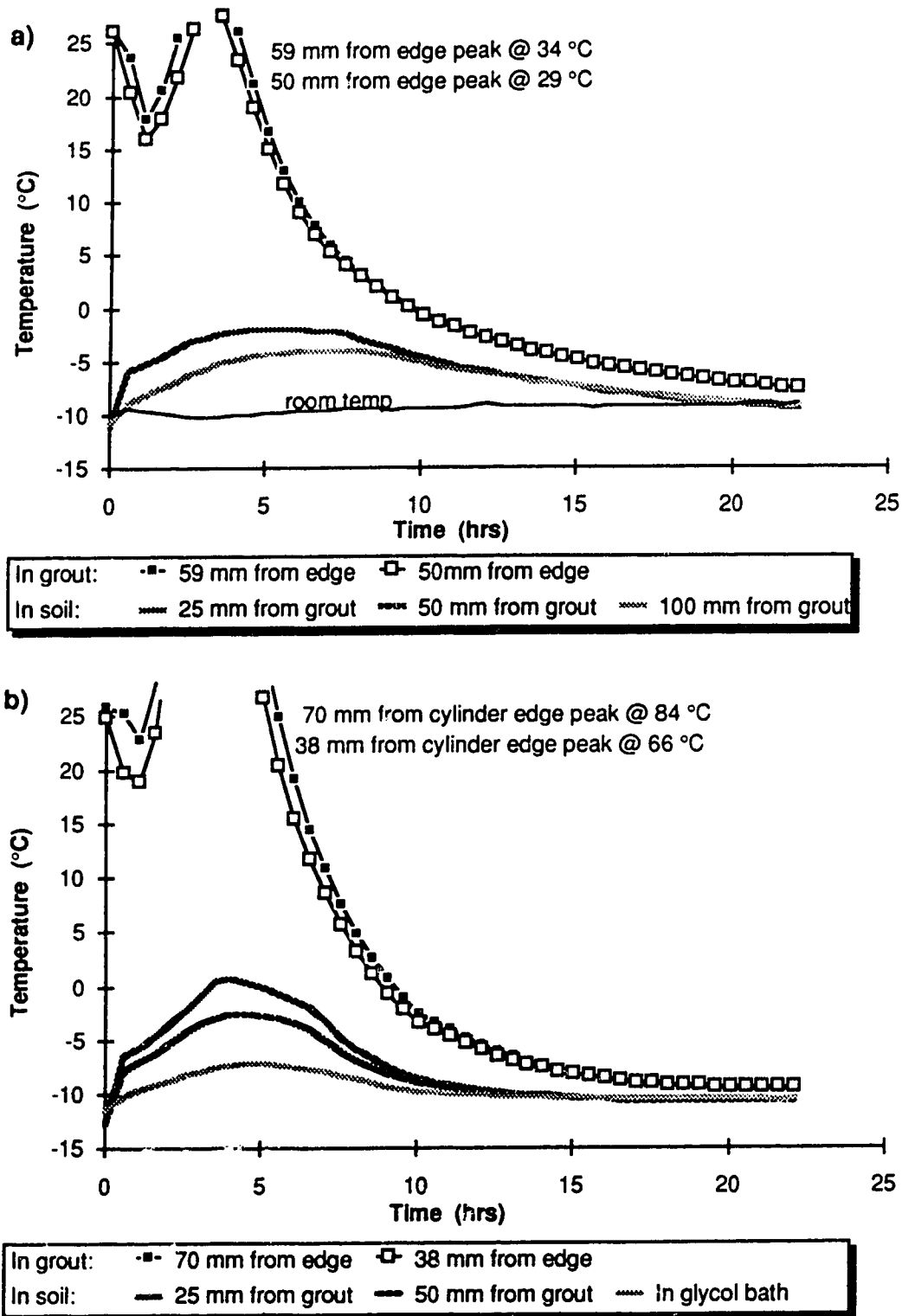
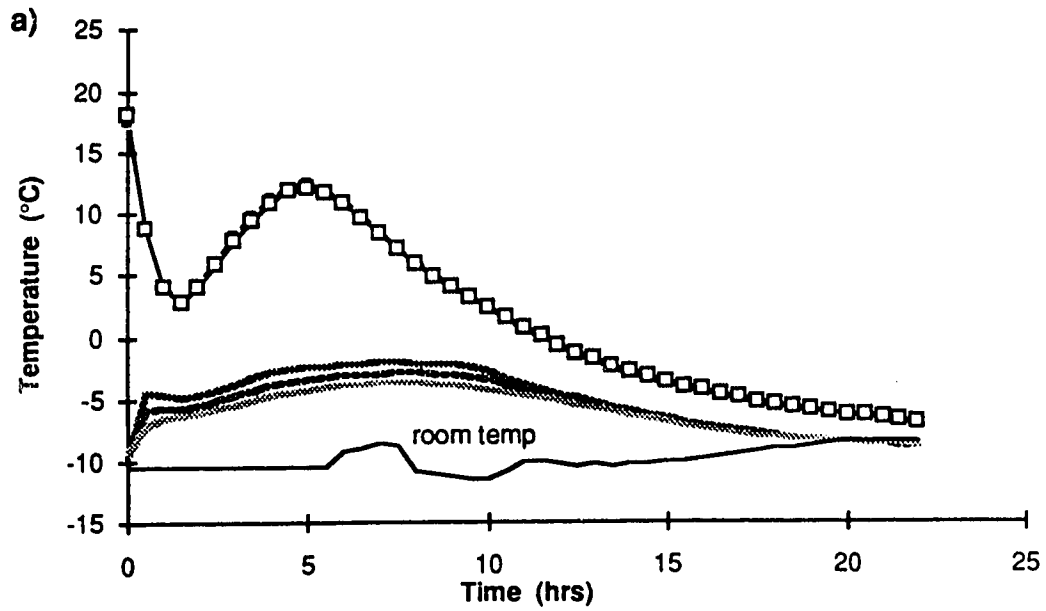
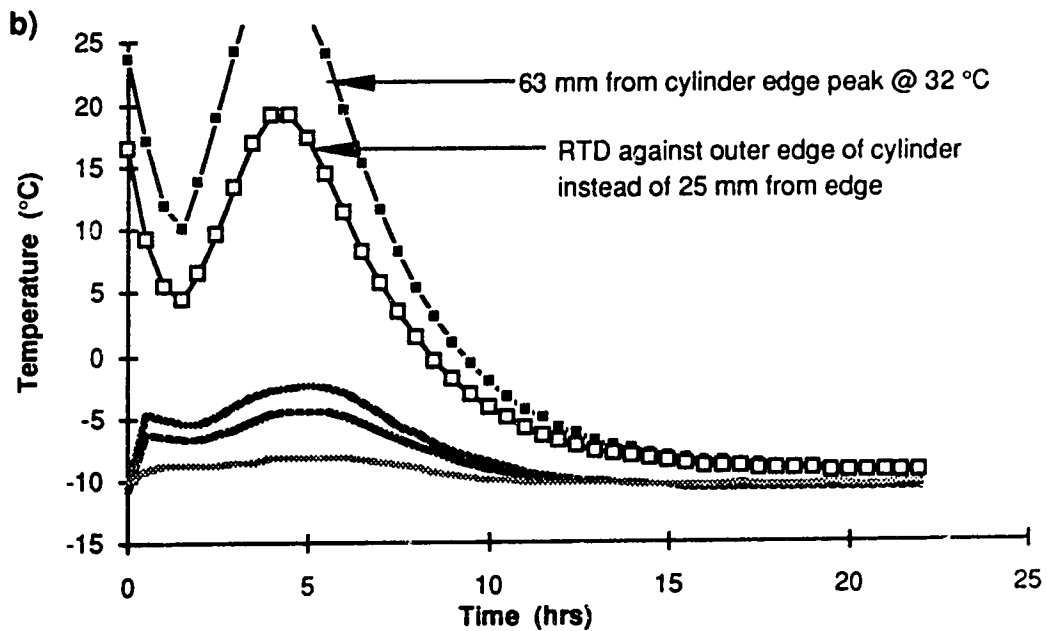


Figure C.4: Mix II-3, grout and soil temperature versus time  
a) 600 mm cell  
b) Constant temperature bath cell (CTBC)



In grout:    -■- 30 mm from edge    -□- 25 mm from edge  
 In soil:    -...- 25 mm from grout    -...- 50 mm from grout    -...- 100 mm from grout



In grout:    -■- 63 mm from edge    -□- 0 mm from edge  
 In soil:    -...- 25 mm from grout    -...- 50 mm from grout    -...- In glycol bath

Figure C.5: Mix II-4, grout and soil temperature versus time  
 a) 600 mm cell  
 b) Constant temperature bath cell (CTBC)

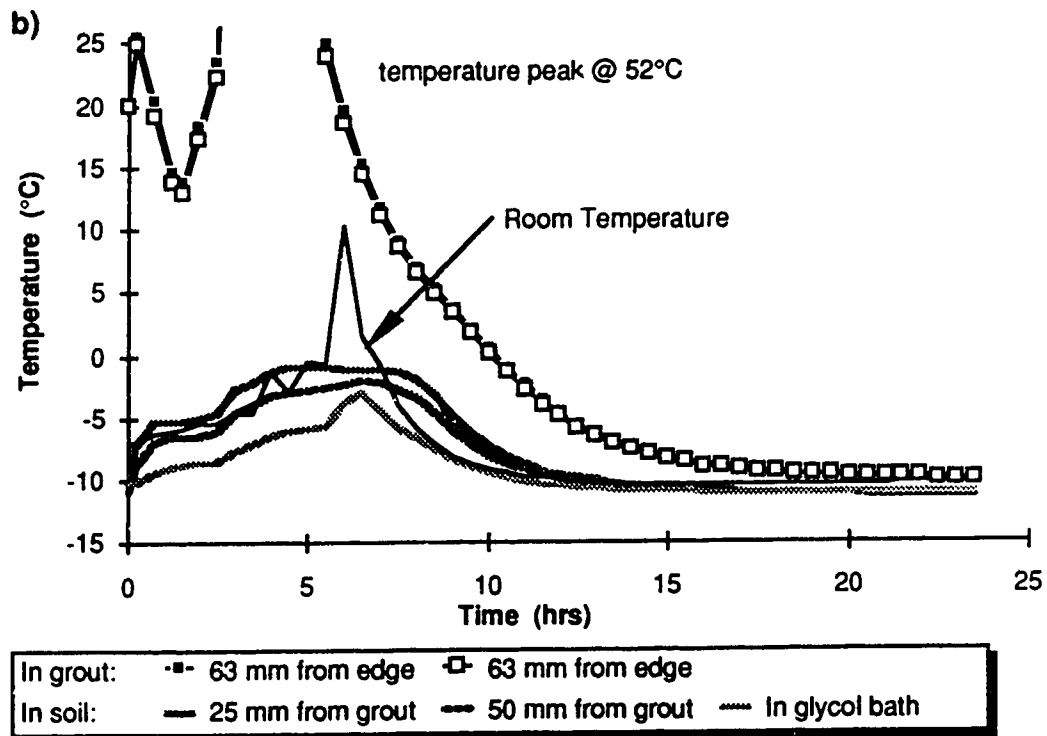
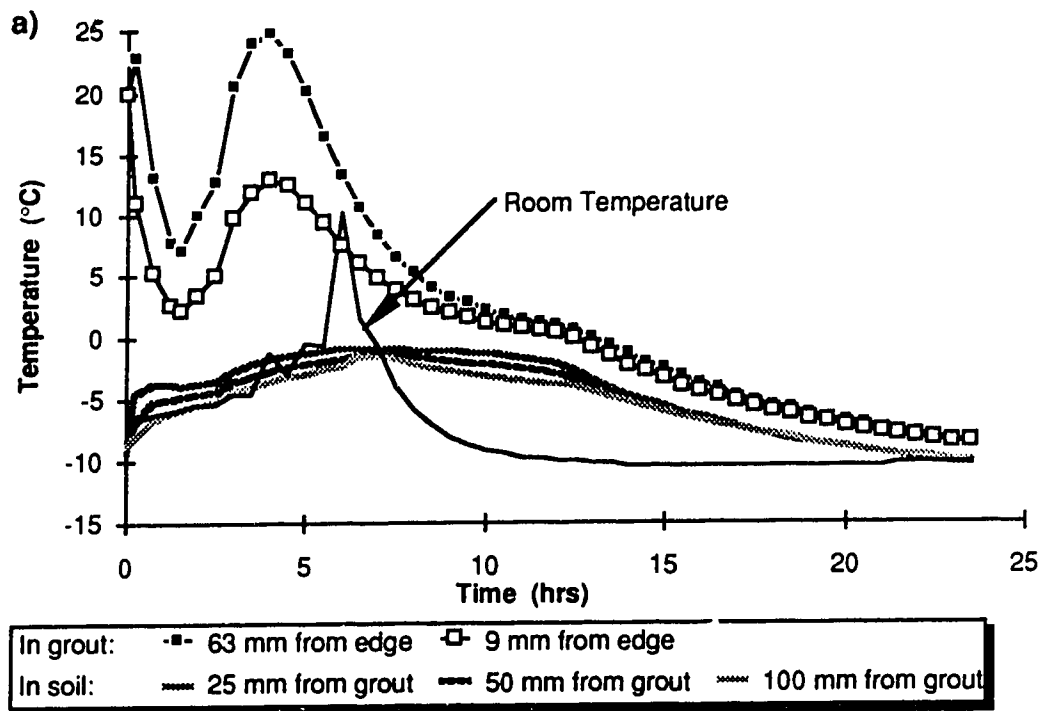


Figure C.6: Mix II-5, grout and soil temperature versus time  
a) 600 mm cell  
b) Constant temperature bath cell (CTBC)



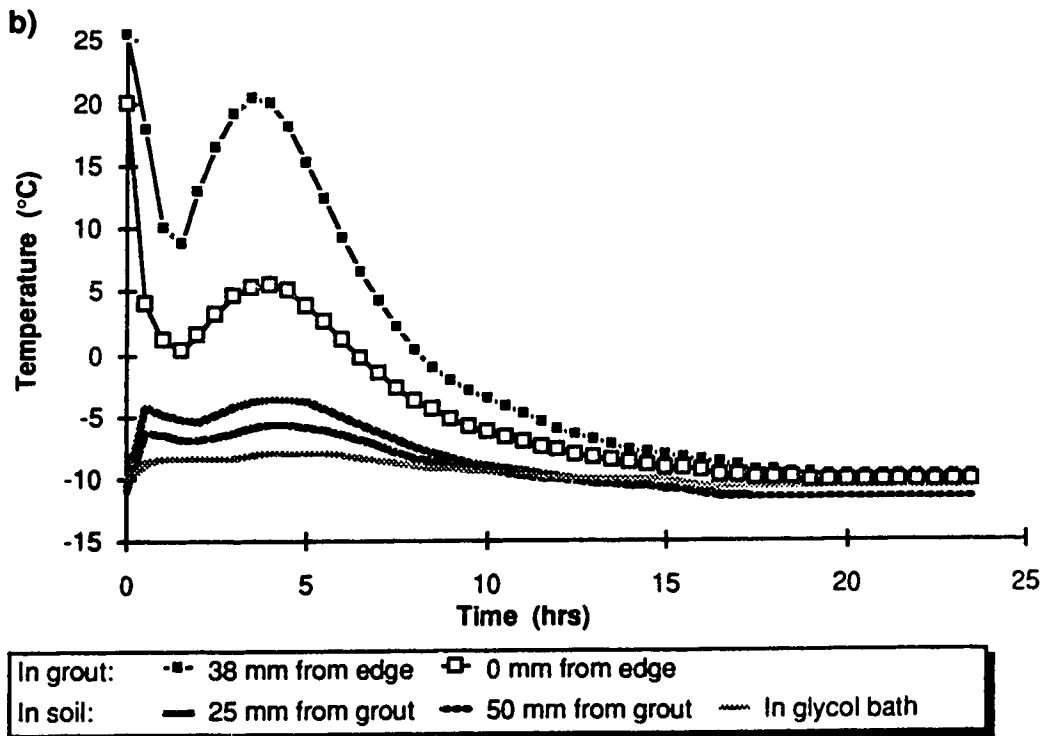
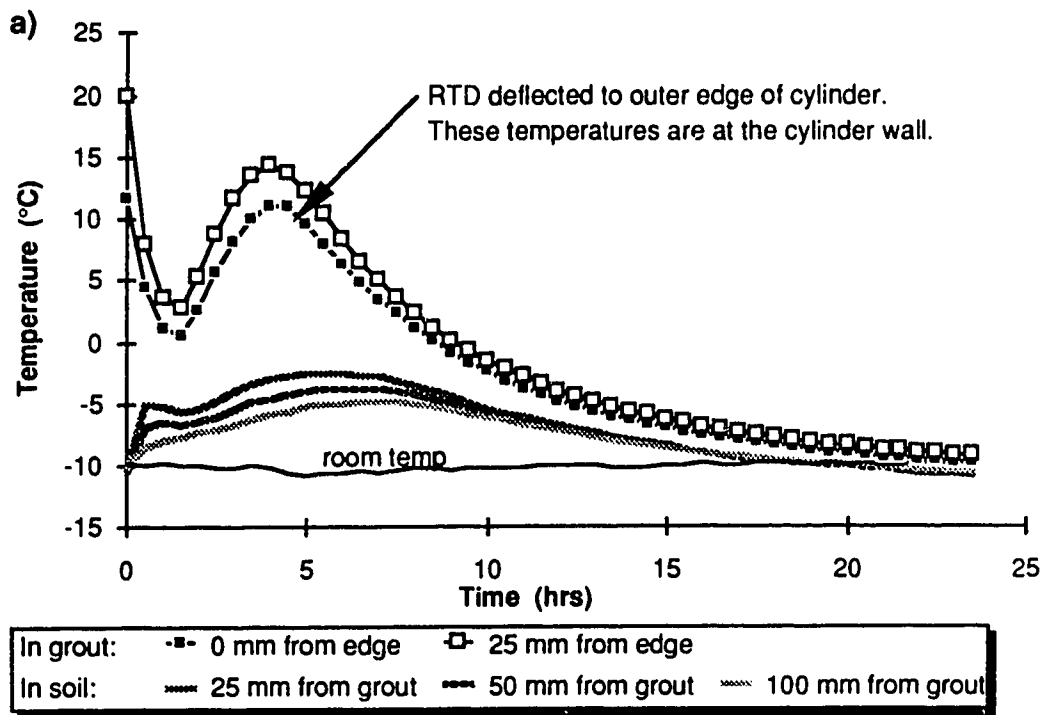


Figure C.7: Mix II-6, grout and soil temperature versus time  
a) 600 mm cell  
b) Constant temperature bath cell (CTBC)

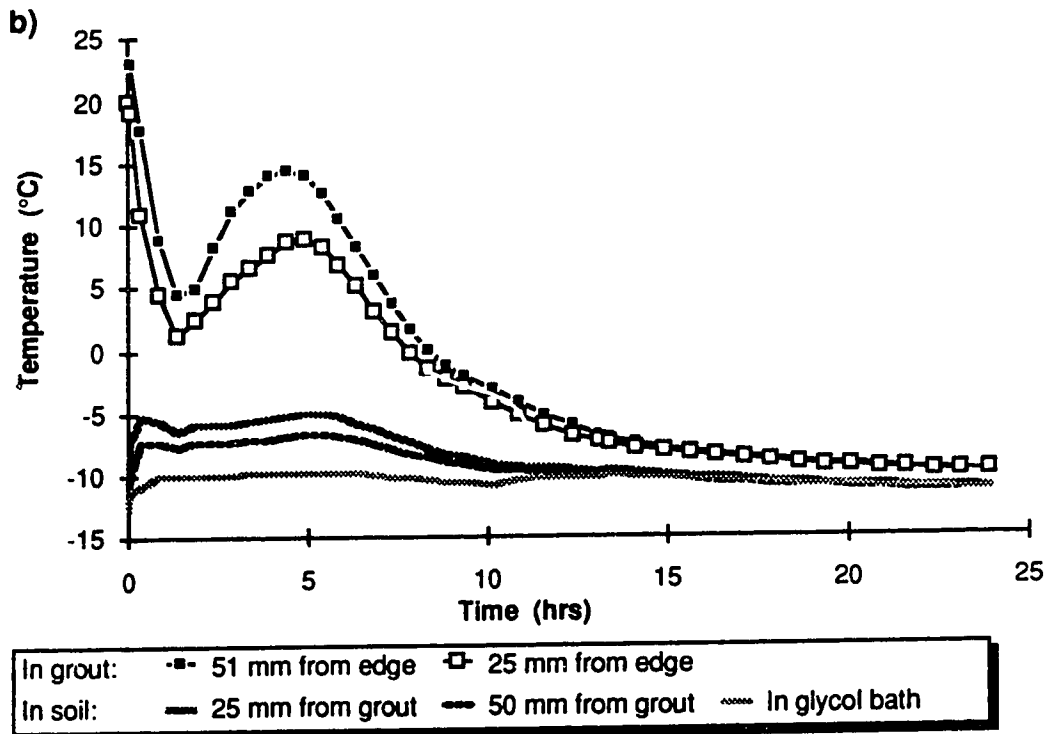
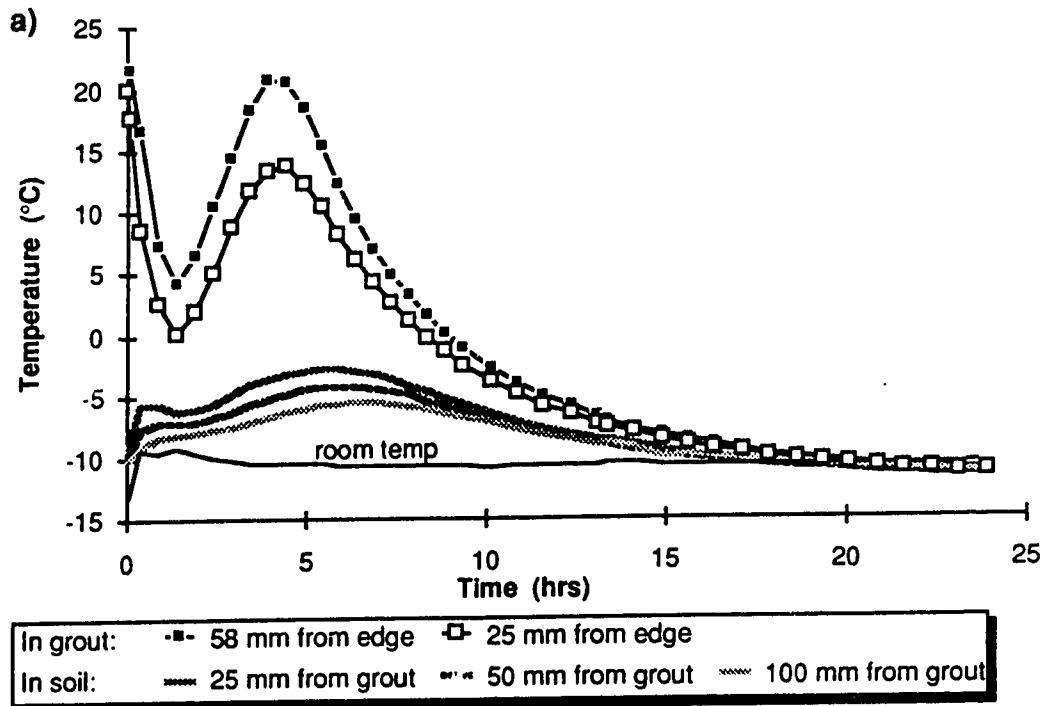


Figure C.8: Mix II-7, grout and soil temperature versus time  
a) 600 mm cell  
b) Constant temperature bath cell (CTBC)

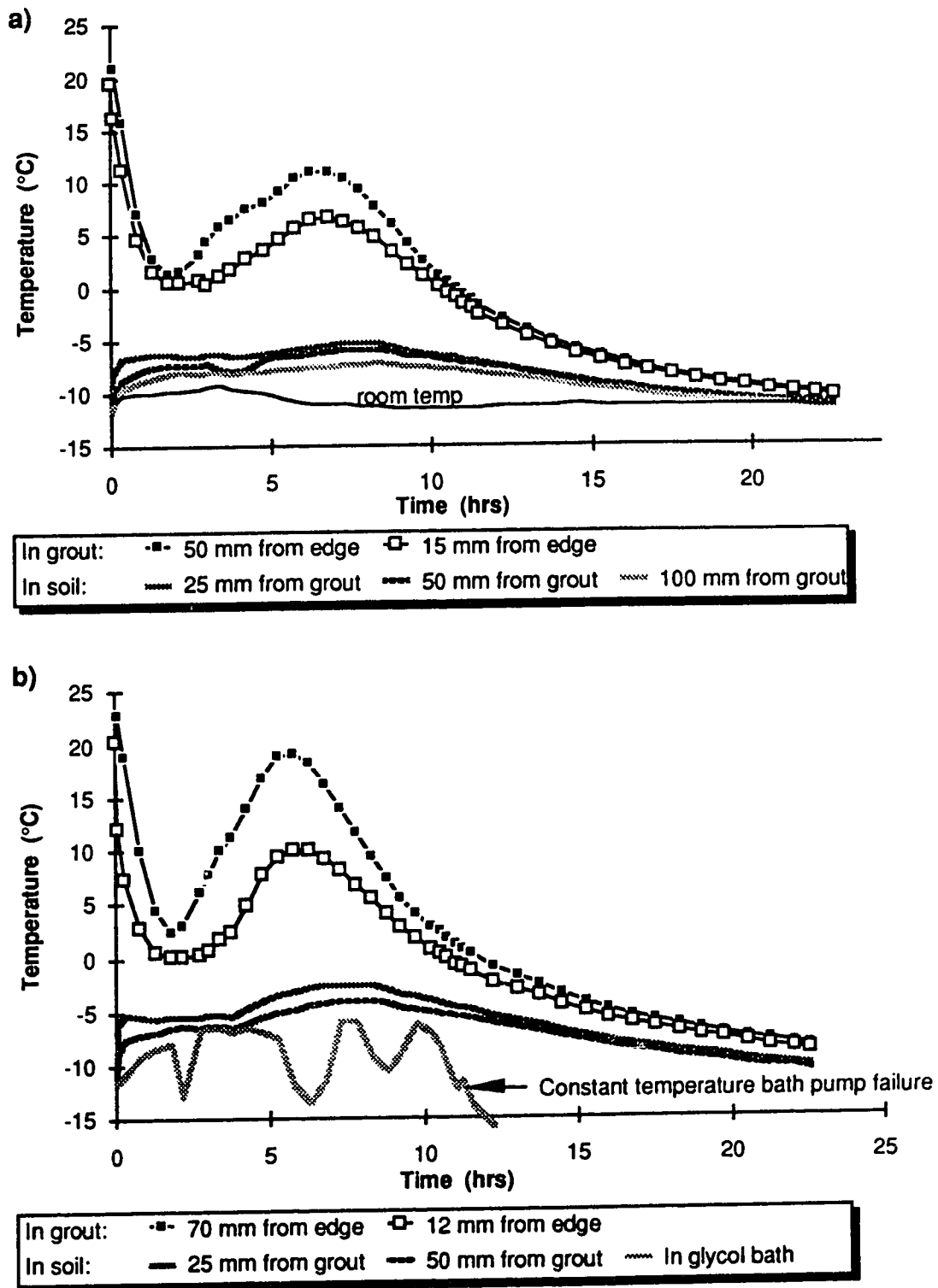


Figure C.9: Mix II-8, grout and soil temperature versus time  
a) 600 mm cell  
b) Constant temperature bath cell (CTBC)

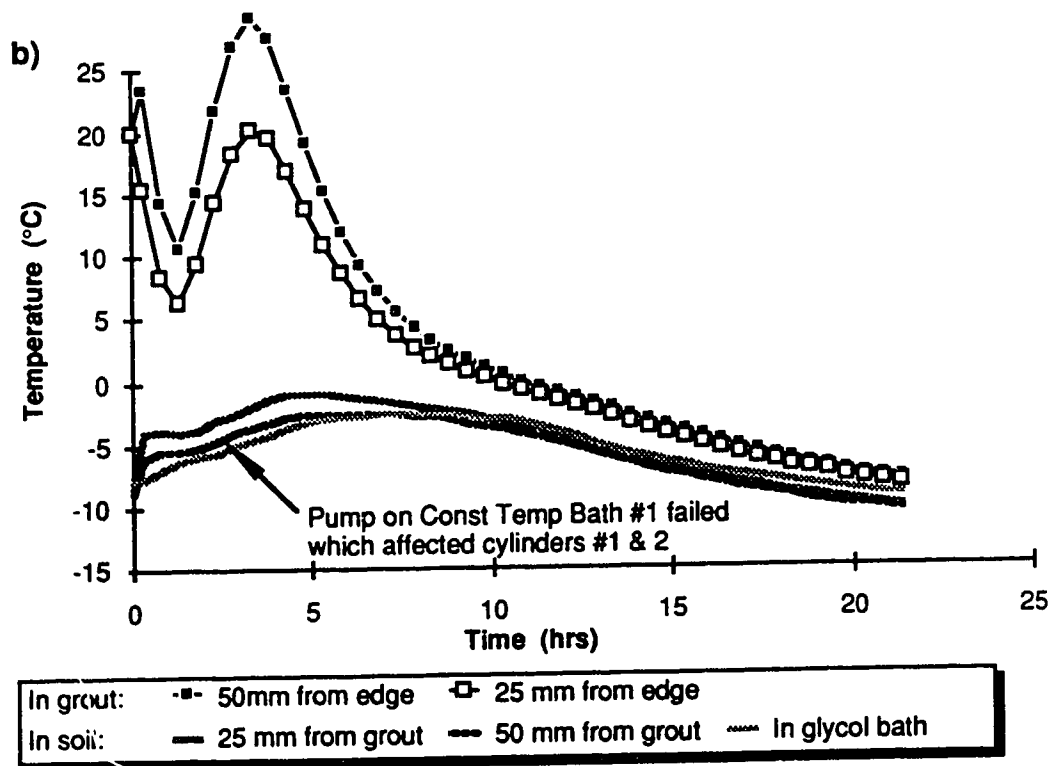
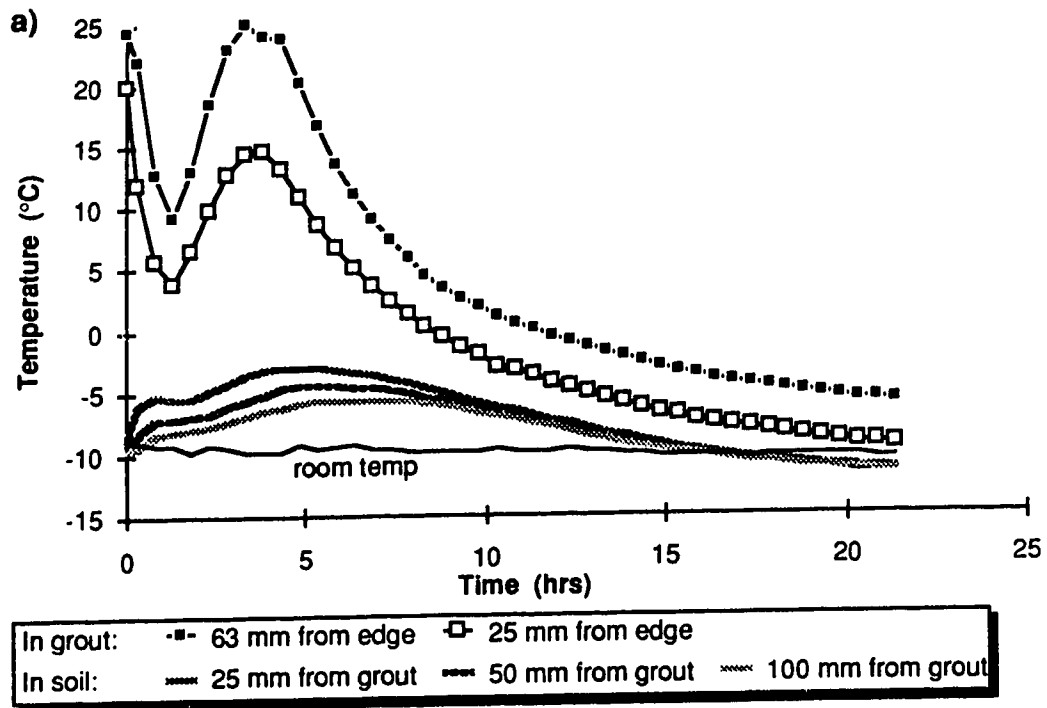


Figure C.10: Mix III-9, grout and soil temperature versus time  
a) 600 mm cell  
b) Constant temperature bath cell (CTBC)

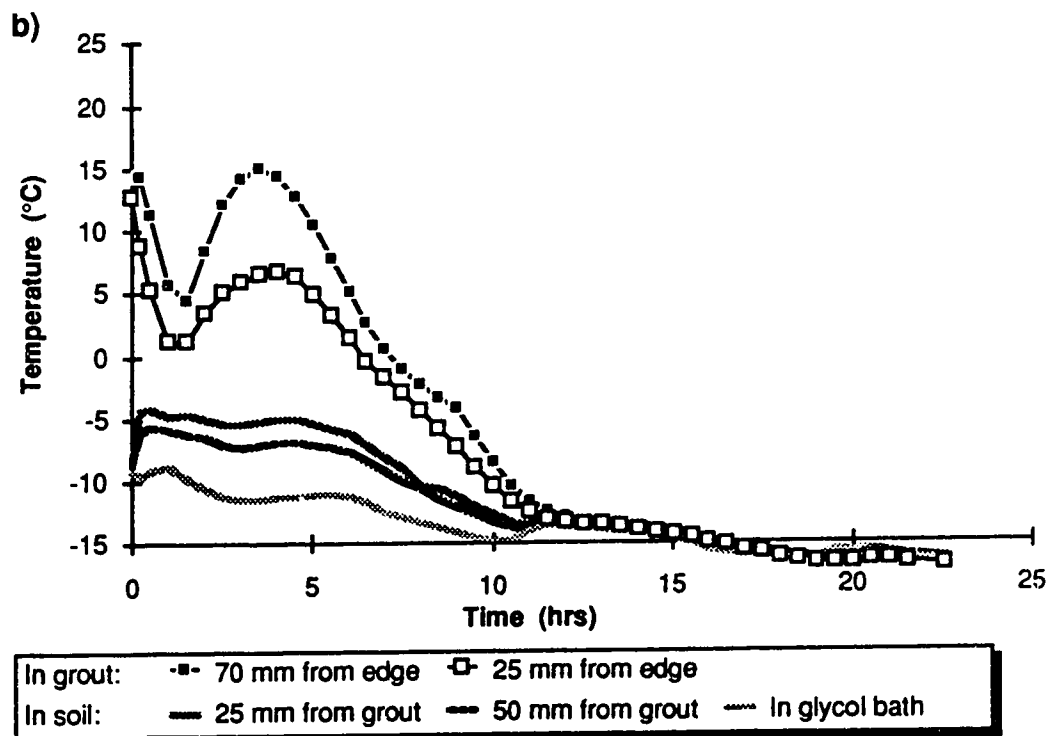
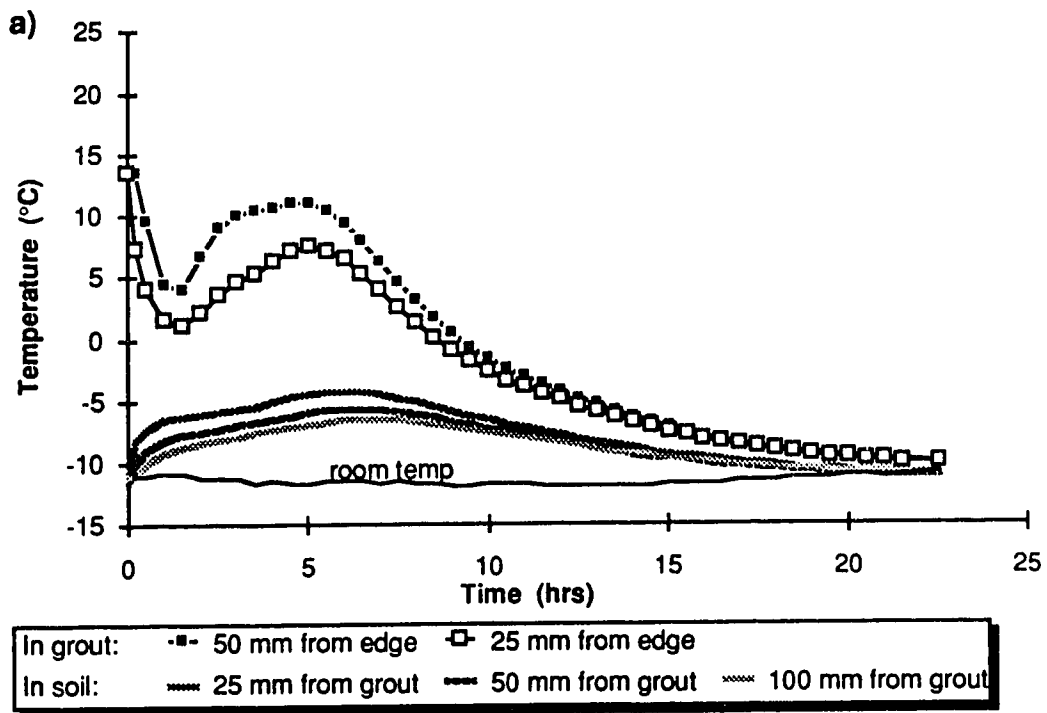


Figure C.11: Mix III-10, grout and soil temperature versus time  
a) 600 mm cell  
b) Constant temperature bath cell (CTBC)

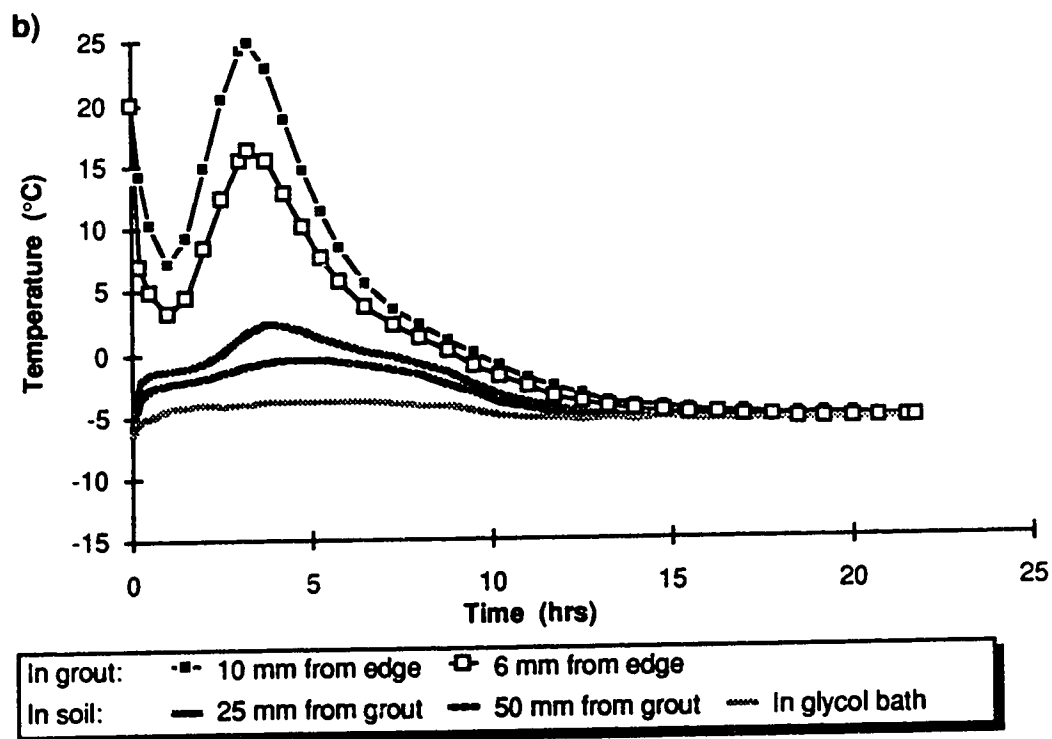
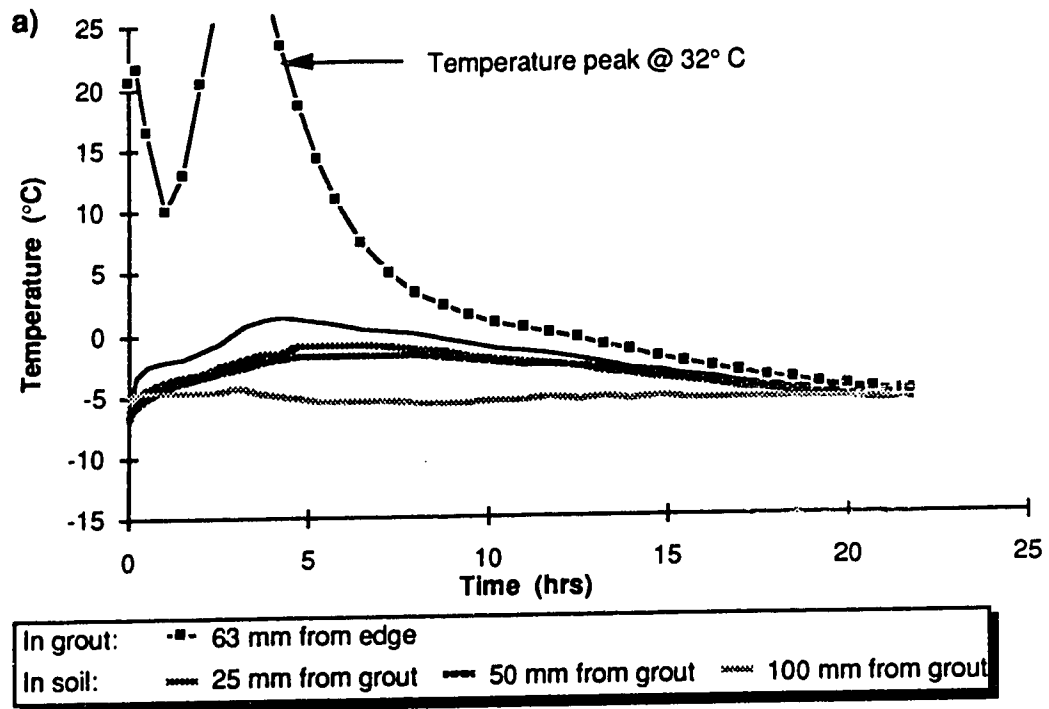


Figure C.12: Mix III-11, grout and soil temperature versus time  
a) 600 mm cell  
b) Constant temperature bath cell (CTBC)

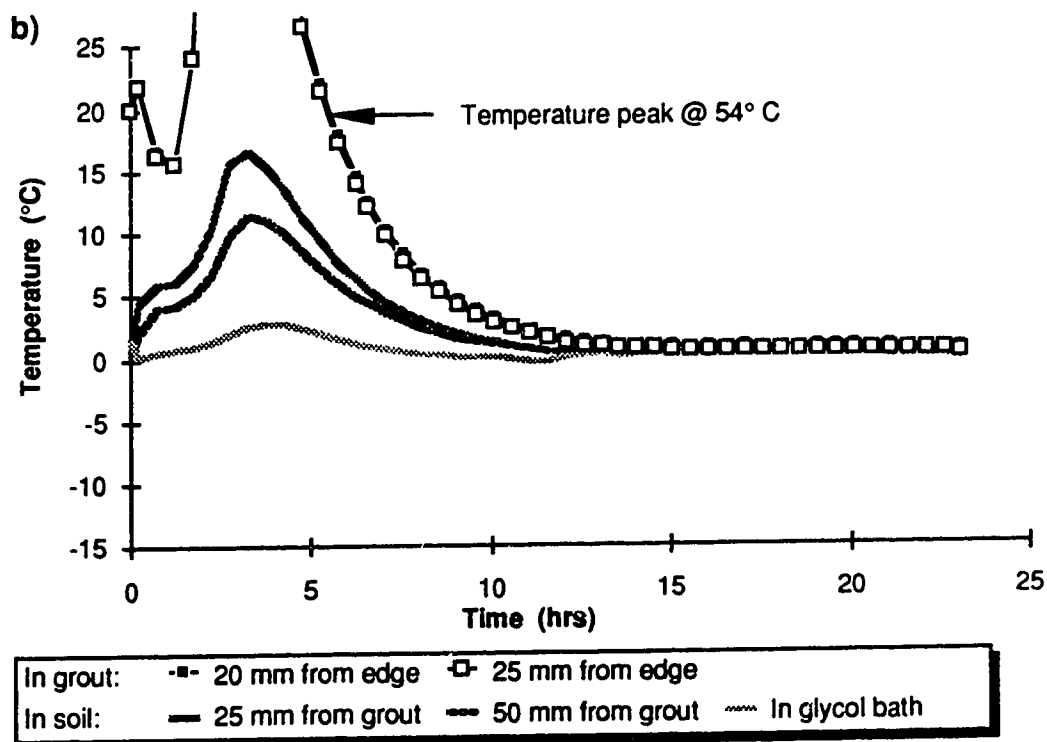
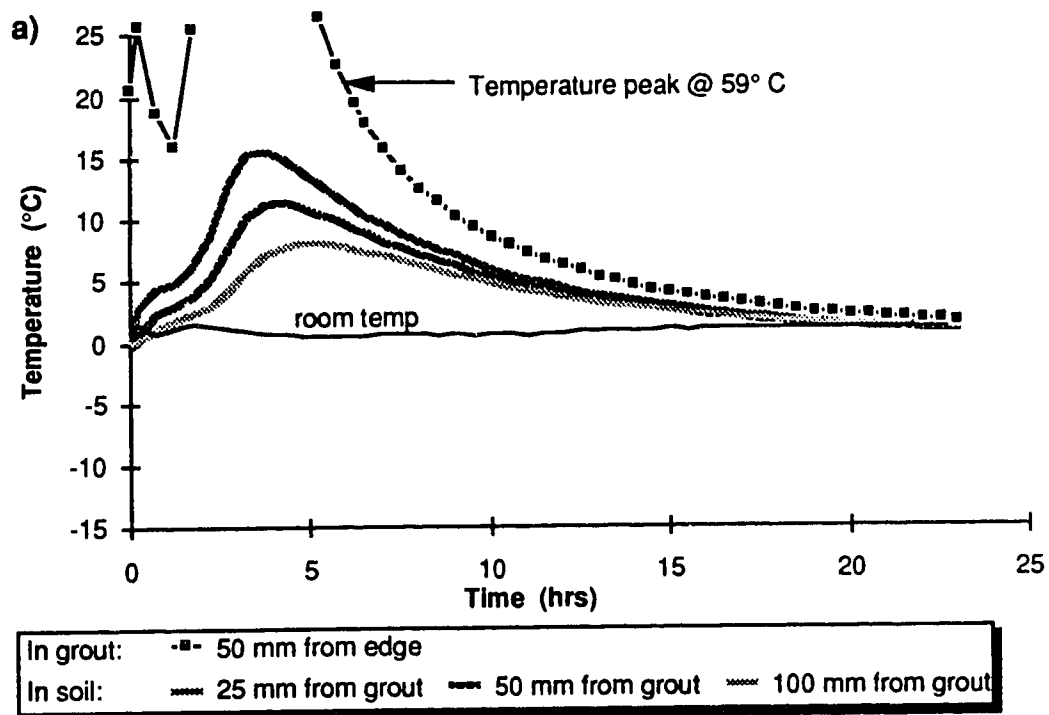


Figure C.13: Mix III-12, grout and soil temperature versus time  
a) 600 mm cell  
b) Constant temperature bath cell (CTBC)

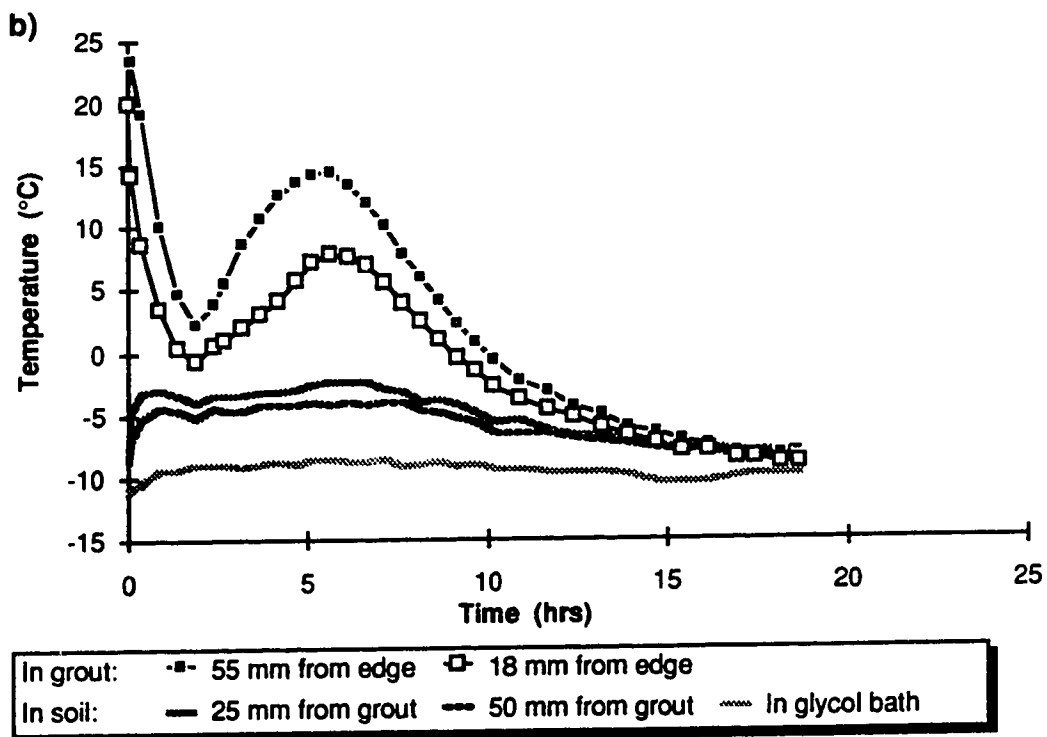
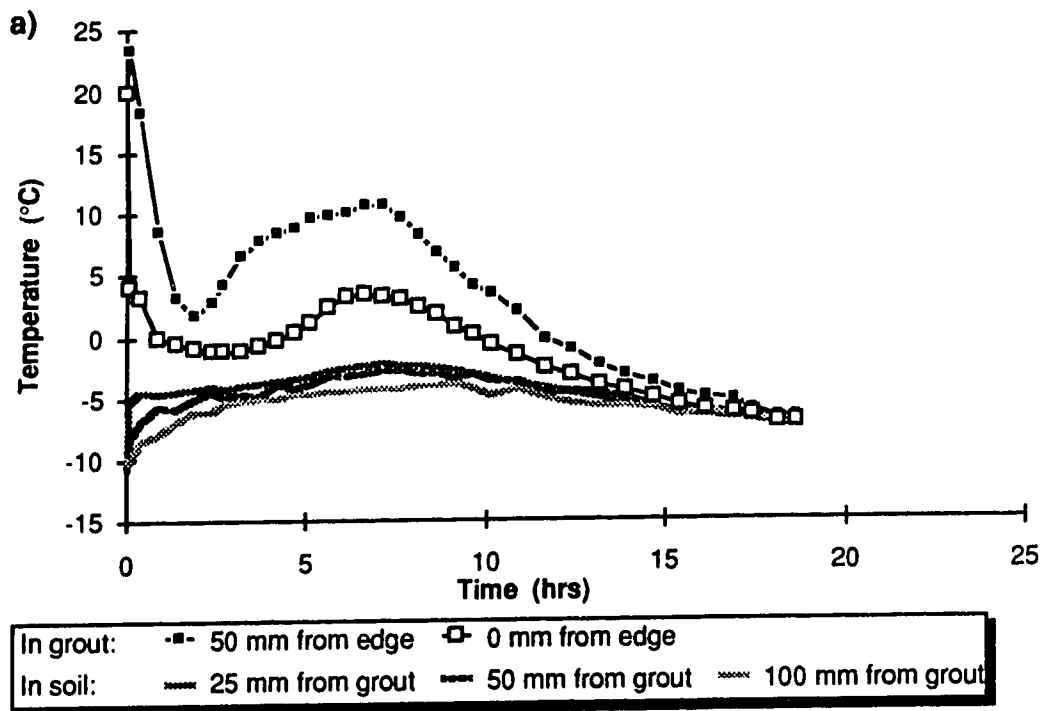


Figure C.14: Repeat of mix II-8, grout and soil temperature versus time  
a) 600 mm cell  
b) Constant temperature bath cell (CTBC)



**APPENDIX D**  
**CONSTANT DISPLACEMENT RATE**  
**MODEL PILE TEST RESULTS**

Shear stress versus displacement

Comparisons of test data relating to

tests with same conditions  
tests in different frames  
effect of salinity  
effect of backfill  
effect of pile surface treatment  
effect of soil temperature

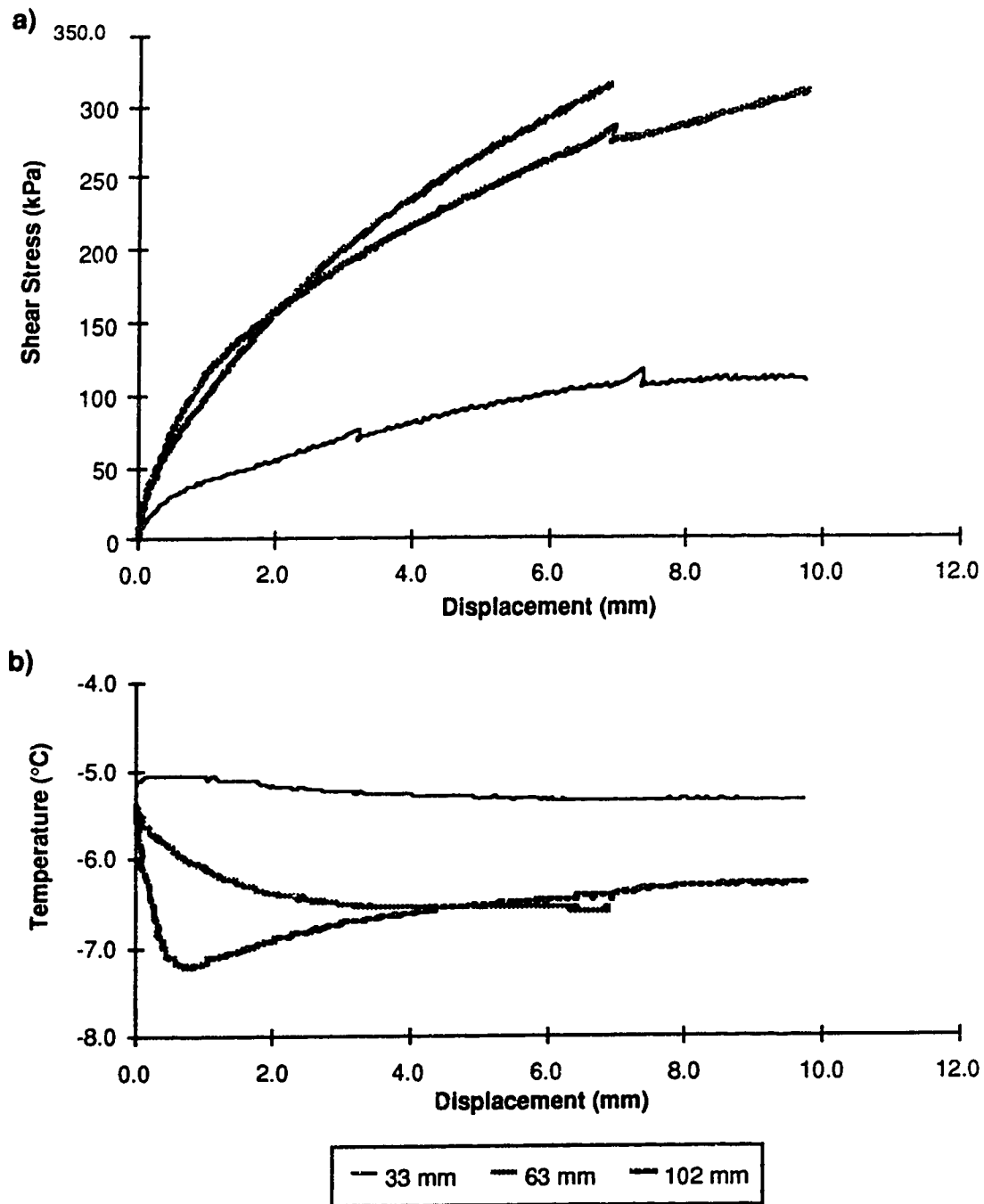


Figure D.1: Test #4, Salinity = 30 ppt, Nominal T = -5° C, Backfill = Sand  
a) Shear stress versus displacement  
b) Temperature versus displacement

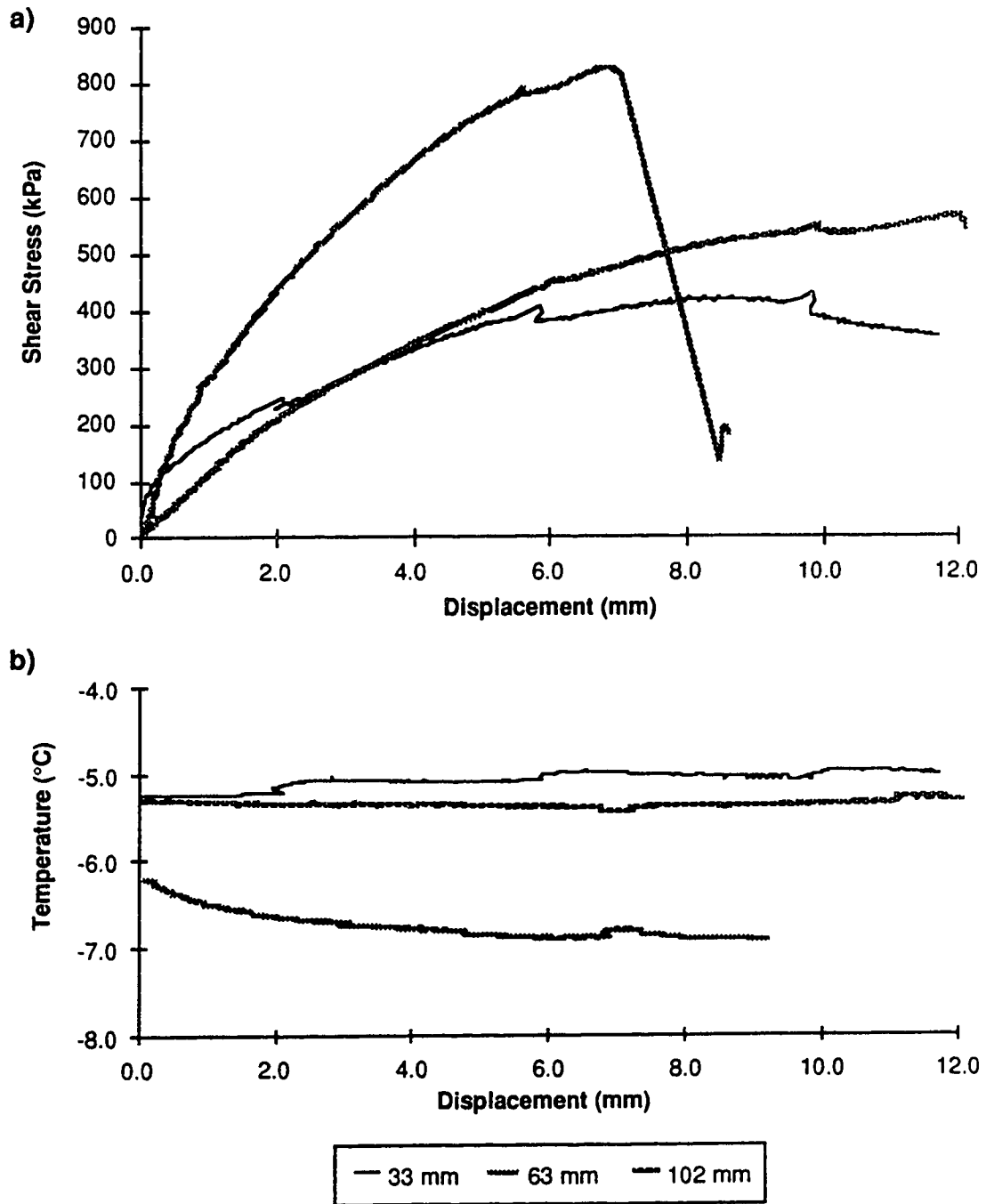


Figure D.2: Test #5, Salinity = 20 ppt, Nominal T = -5° C, Backfill = Sand  
a) Shear stress versus displacement  
b) Temperature versus displacement

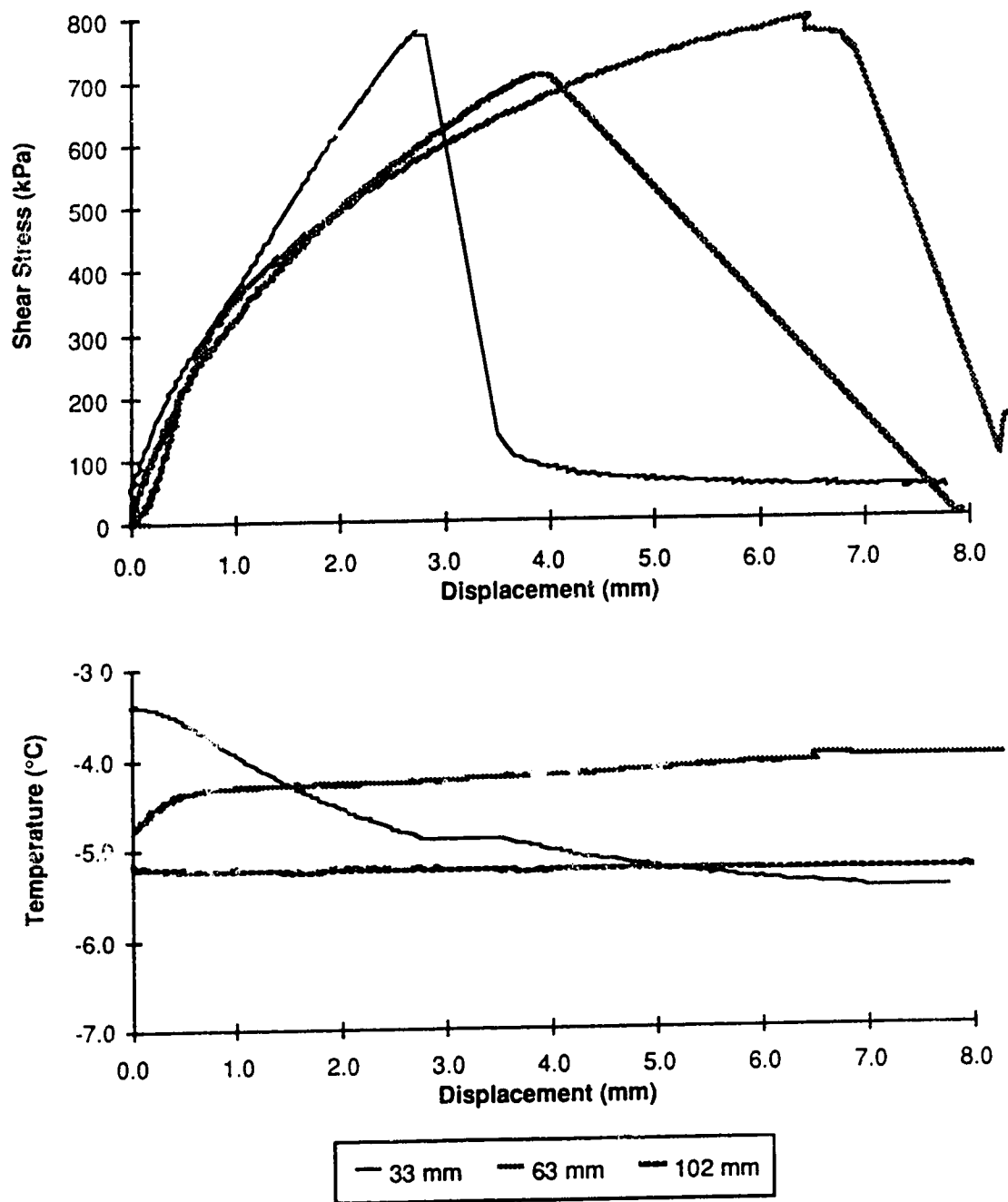


Figure D.3: Test #6, Salinity = 10 ppt, Nominal  $T = -5^{\circ}\text{C}$ , Backfill = Sand  
a) Shear stress versus displacement  
b) Temperature versus displacement

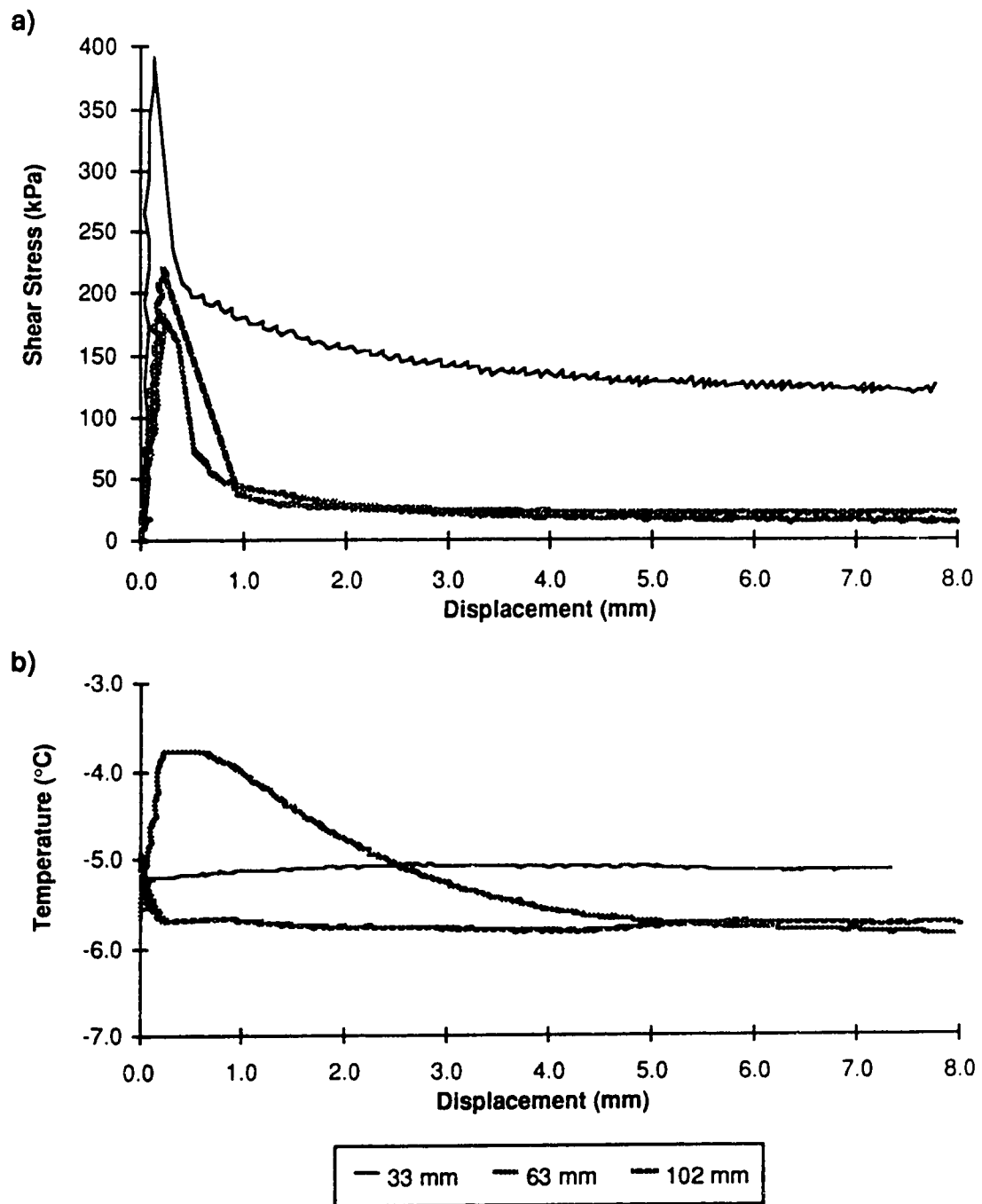


Figure D.4: Test #7, Salinity = 0 ppt, Nominal  $T = -5^{\circ}\text{C}$ , Backfill = Sand,  
 Smooth pipe pile  
 a) Shear stress versus displacement  
 b) Temperature versus displacement

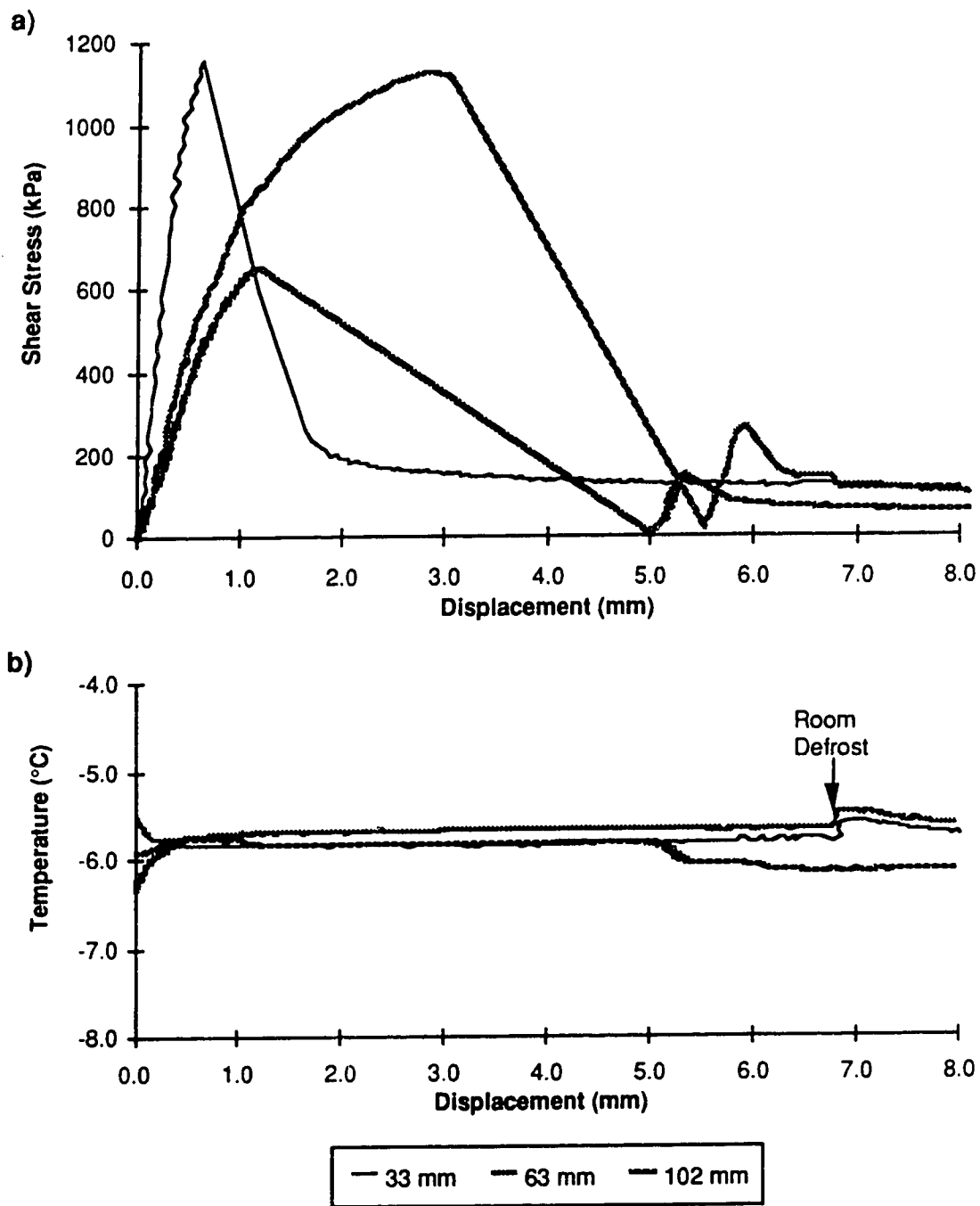


Figure D.5: Test #8, Salinity = 0 ppt, Nominal T = -5° C, Backfill = Sand  
a) Shear stress versus displacement  
b) Temperature versus displacement

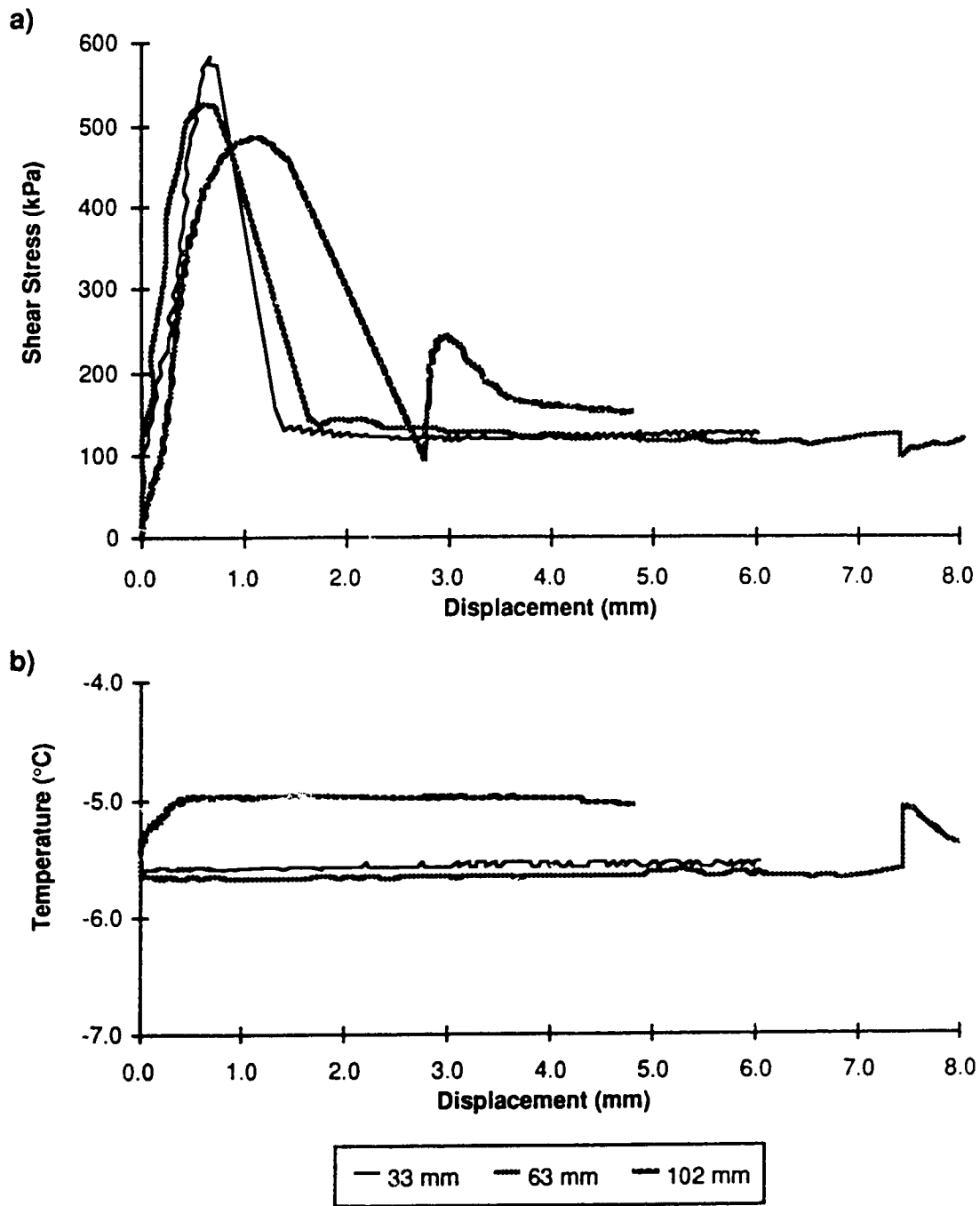


Figure D.6: Test #9, Salinity = 0 ppt, Nominal  $T = -5^{\circ}\text{C}$ , Backfill = Cuttings  
a) Shear stress versus displacement  
b) Temperature versus displacement

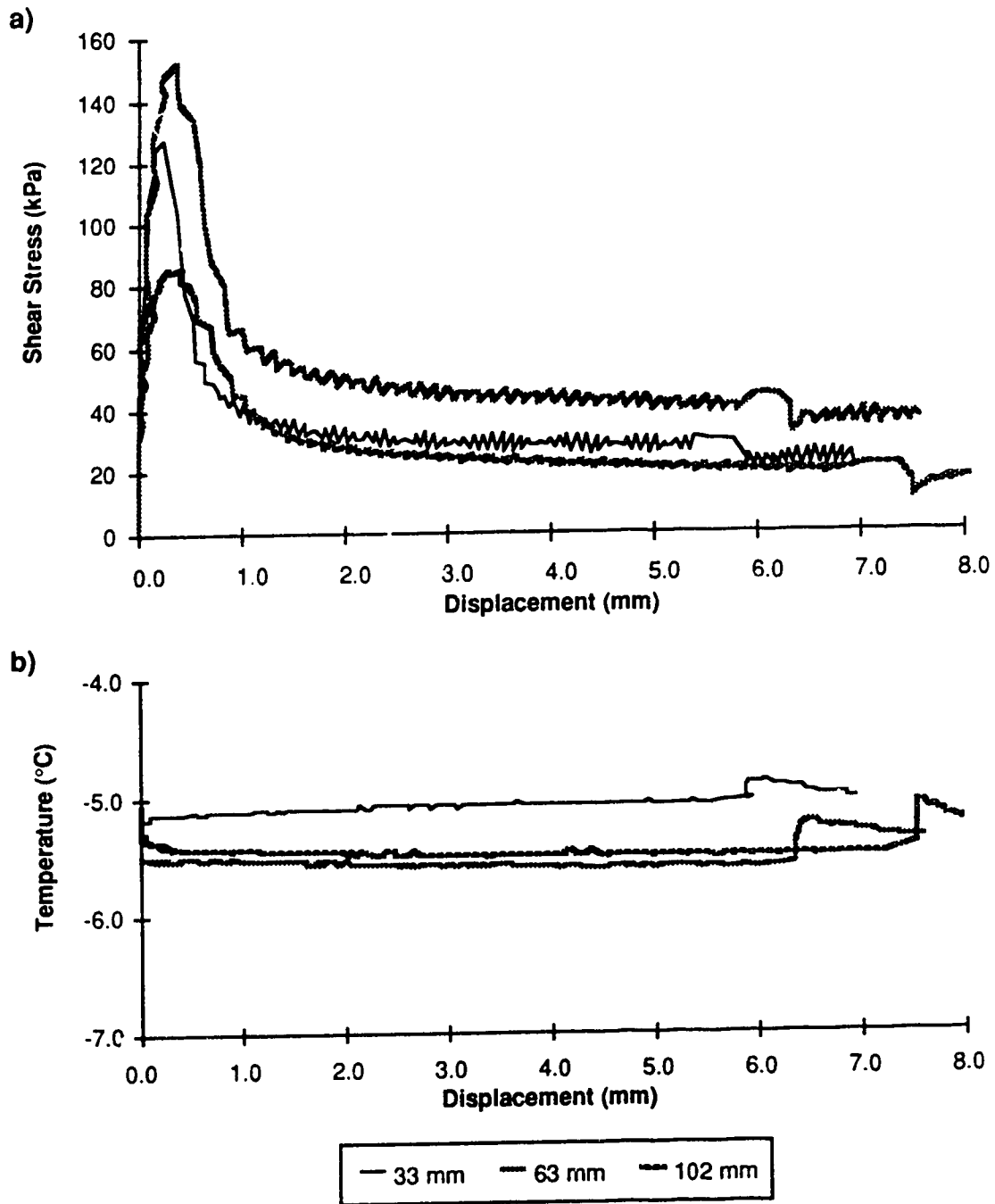


Figure D.7: Test #10, Salinity = 10 ppt, Nominal  $T = -5^{\circ}\text{C}$ , Backfill = Cuttings  
a) Shear stress versus displacement  
b) Temperature versus displacement



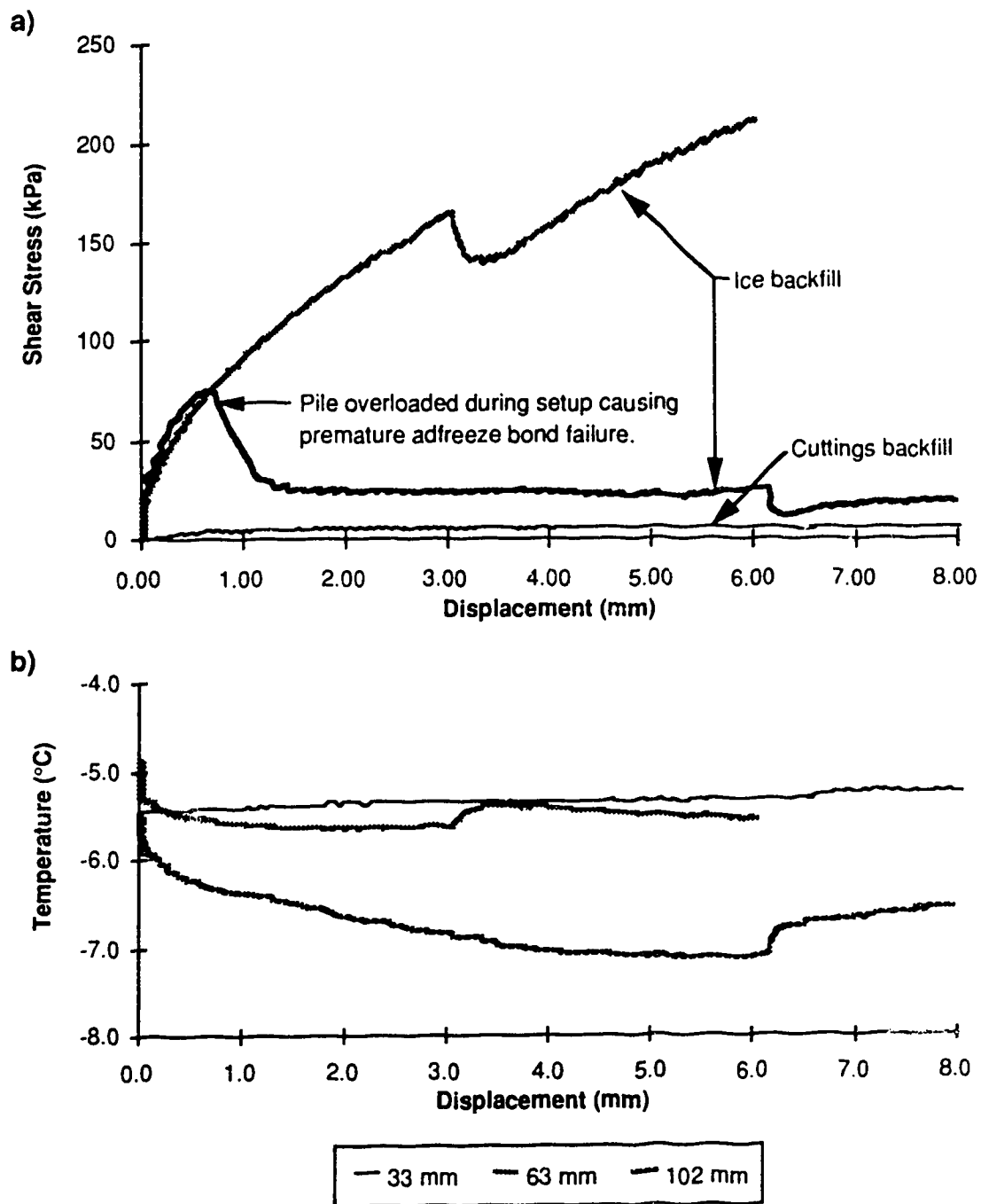


Figure D.8: Test #11, Salinity = 30 ppt, Nominal  $T = -5^{\circ}\text{C}$ , Backfill = Cuttings or Ice  
a) Shear stress versus displacement  
b) Temperature versus displacement

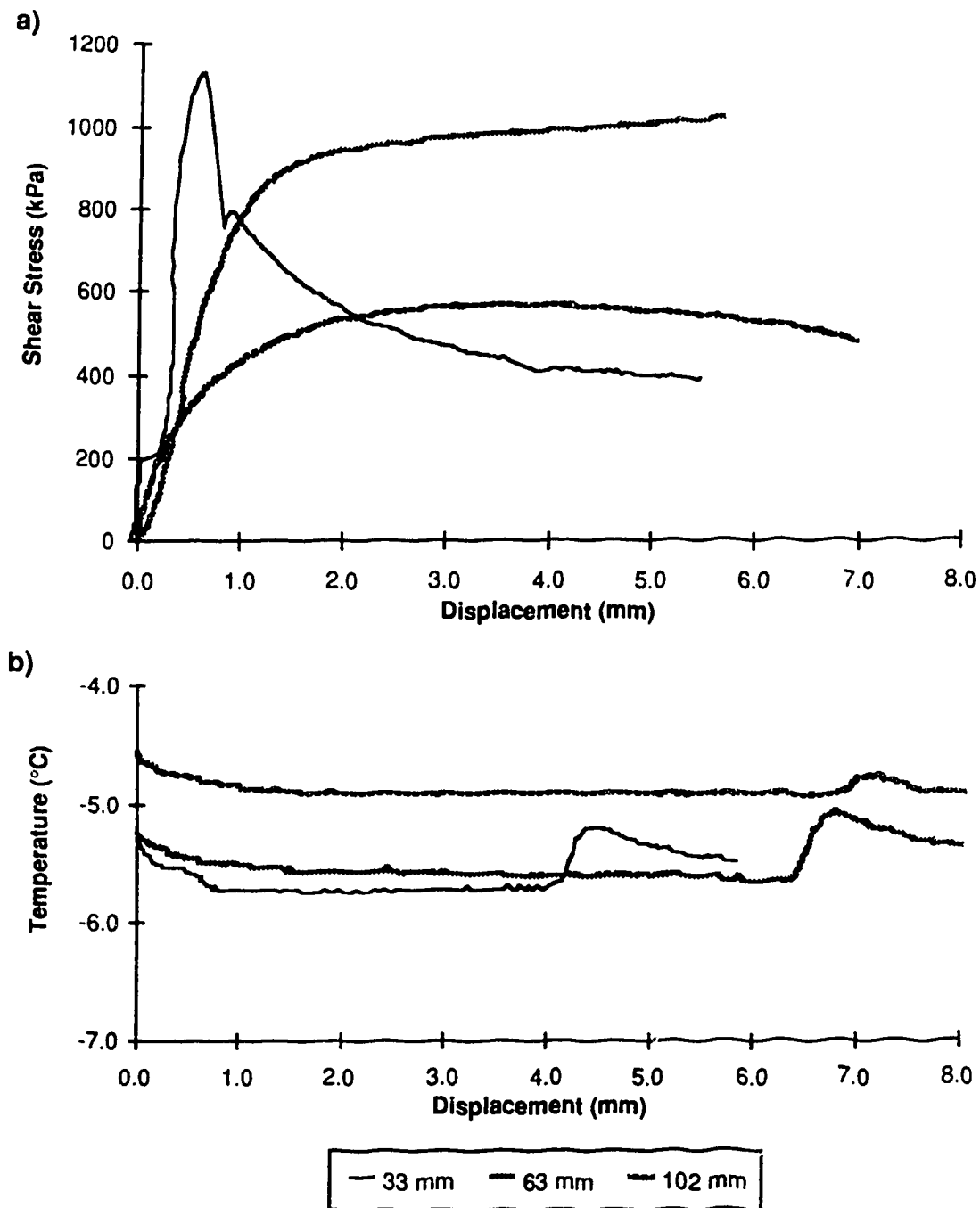


Figure D.9: Test #12, Salinity = 0 ppt, Nominal T =  $-5^{\circ}\text{C}$ , Backfill = Grout in smooth hole

- a) Shear stress versus displacement  
b) Temperature versus displacement

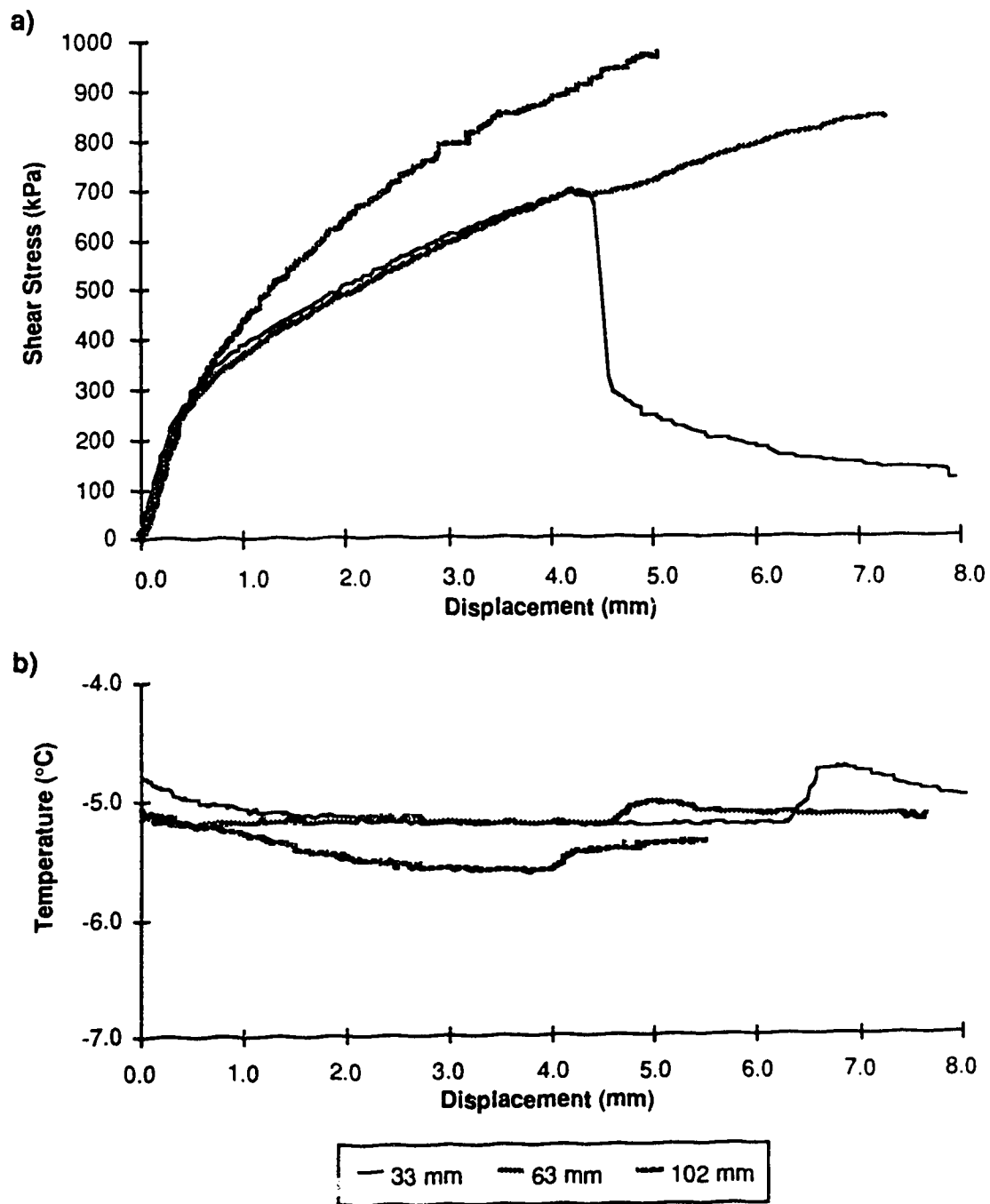


Figure D.10: Test #13, Salinity = 10 ppt, Nominal  $T = -5^{\circ}\text{C}$ , Backfill = Grout in smooth hole

- a) Shear stress versus displacement  
b) Temperature versus displacement

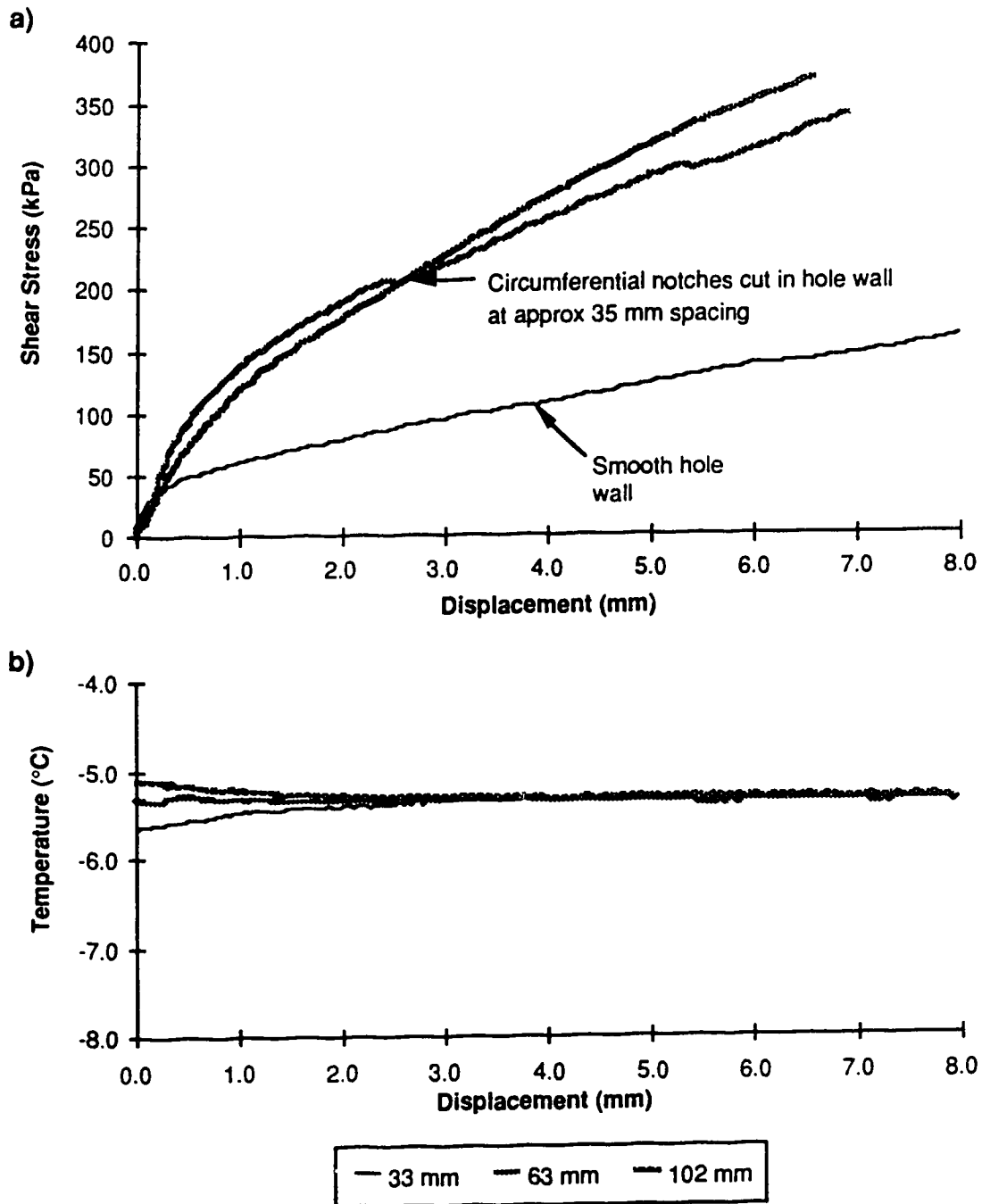


Figure D.11: Test #14, Salinity = 20 ppt, Nominal  $T = -5^{\circ}\text{C}$ , Backfill = Grout  
a) Shear stress versus displacement  
b) Temperature versus displacement

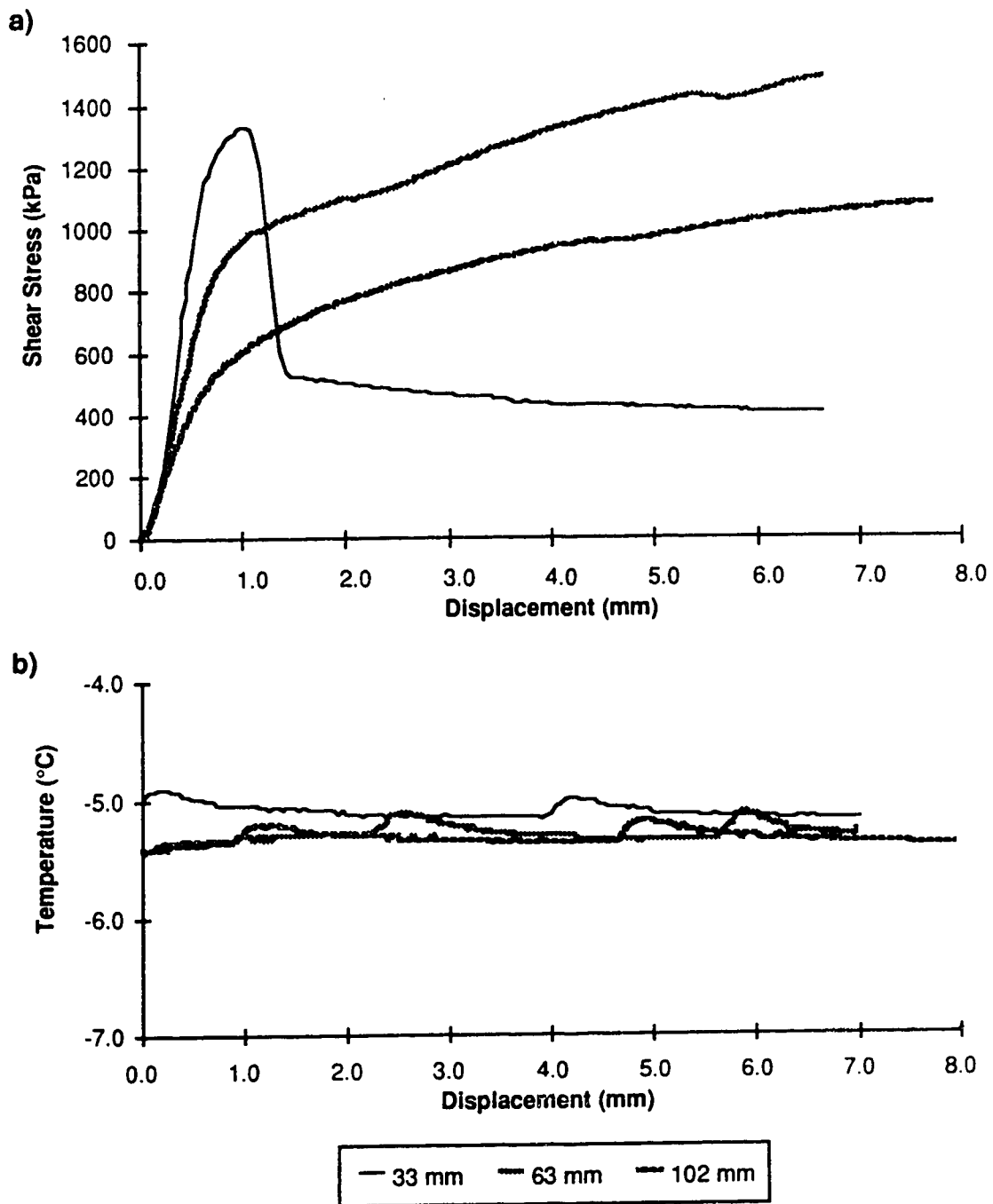


Figure D.12: Test #15, Salinity = 0 ppt, Nominal T = -5°C, Backfill = Grout  
a) Shear stress versus displacement  
b) Temperature versus displacement

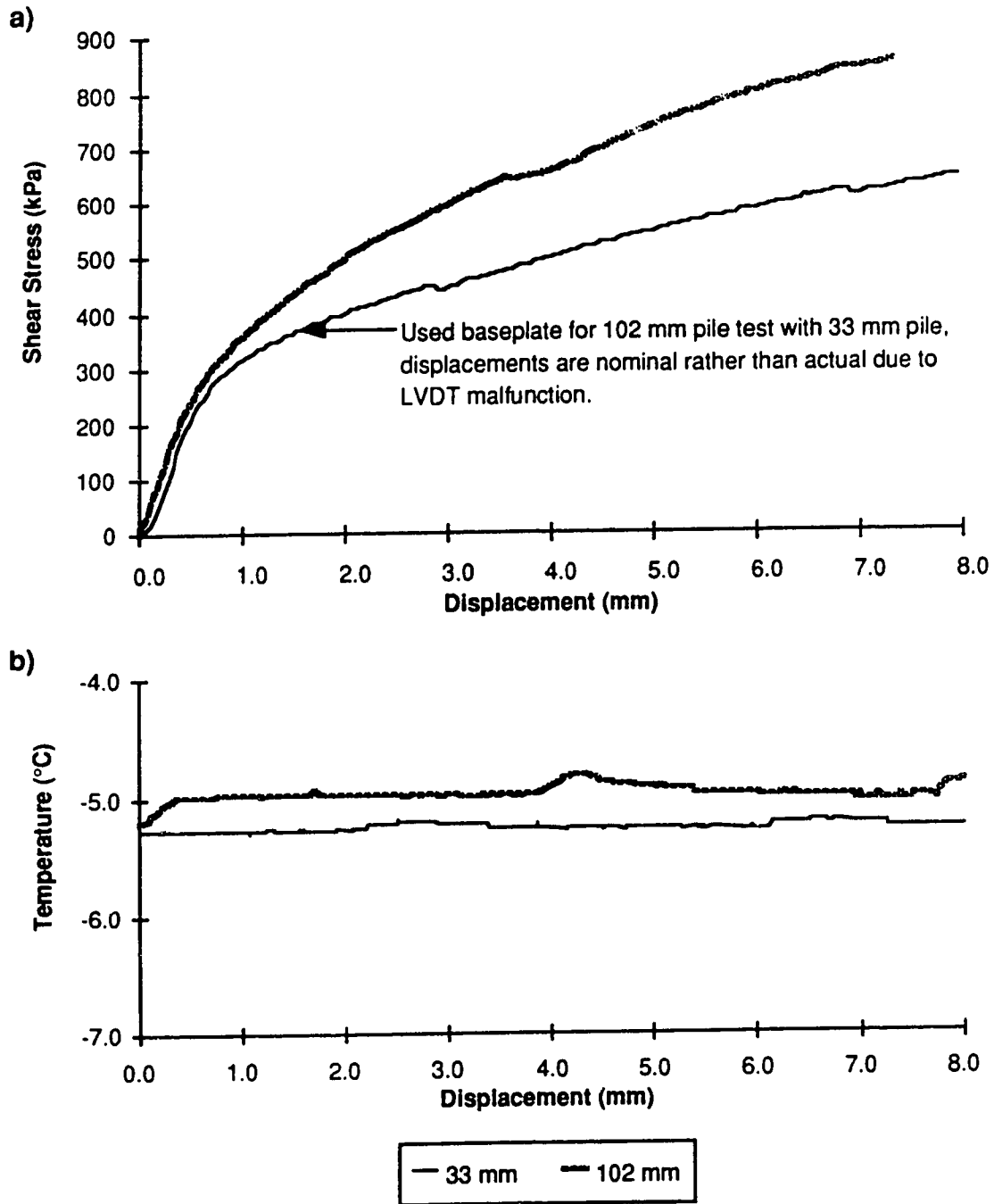


Figure D.13: Test #16, Salinity = 10 ppt, Nominal  $T = -5^{\circ}\text{C}$ , Backfill = Grout  
a) Shear stress versus displacement  
b) Temperature versus displacement

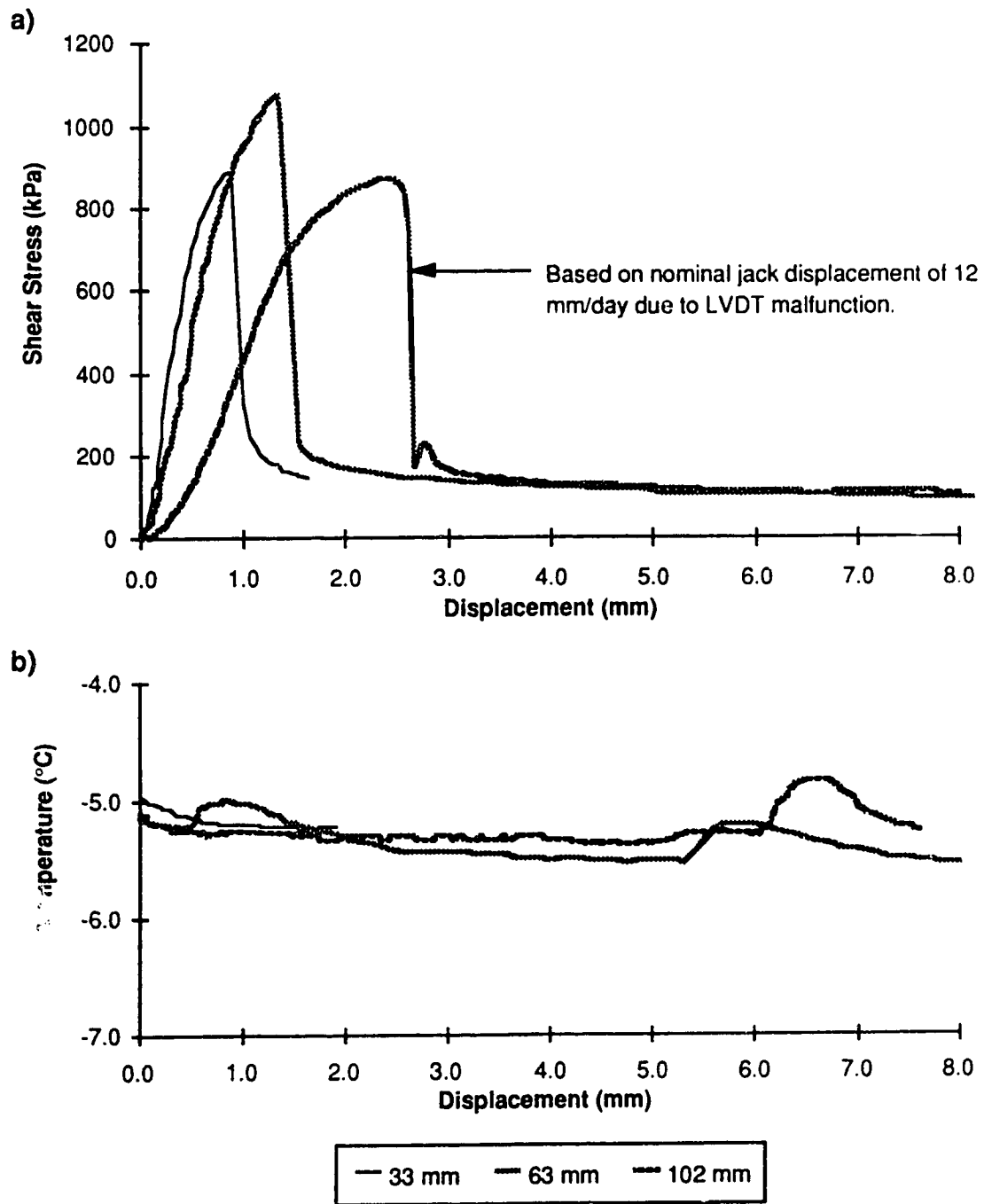


Figure D.14: Test #18, Salinity = 0 ppt, Nominal  $T = -5^{\circ}\text{C}$ , Backfill = Sand  
a) Shear stress versus displacement  
b) Temperature versus displacement

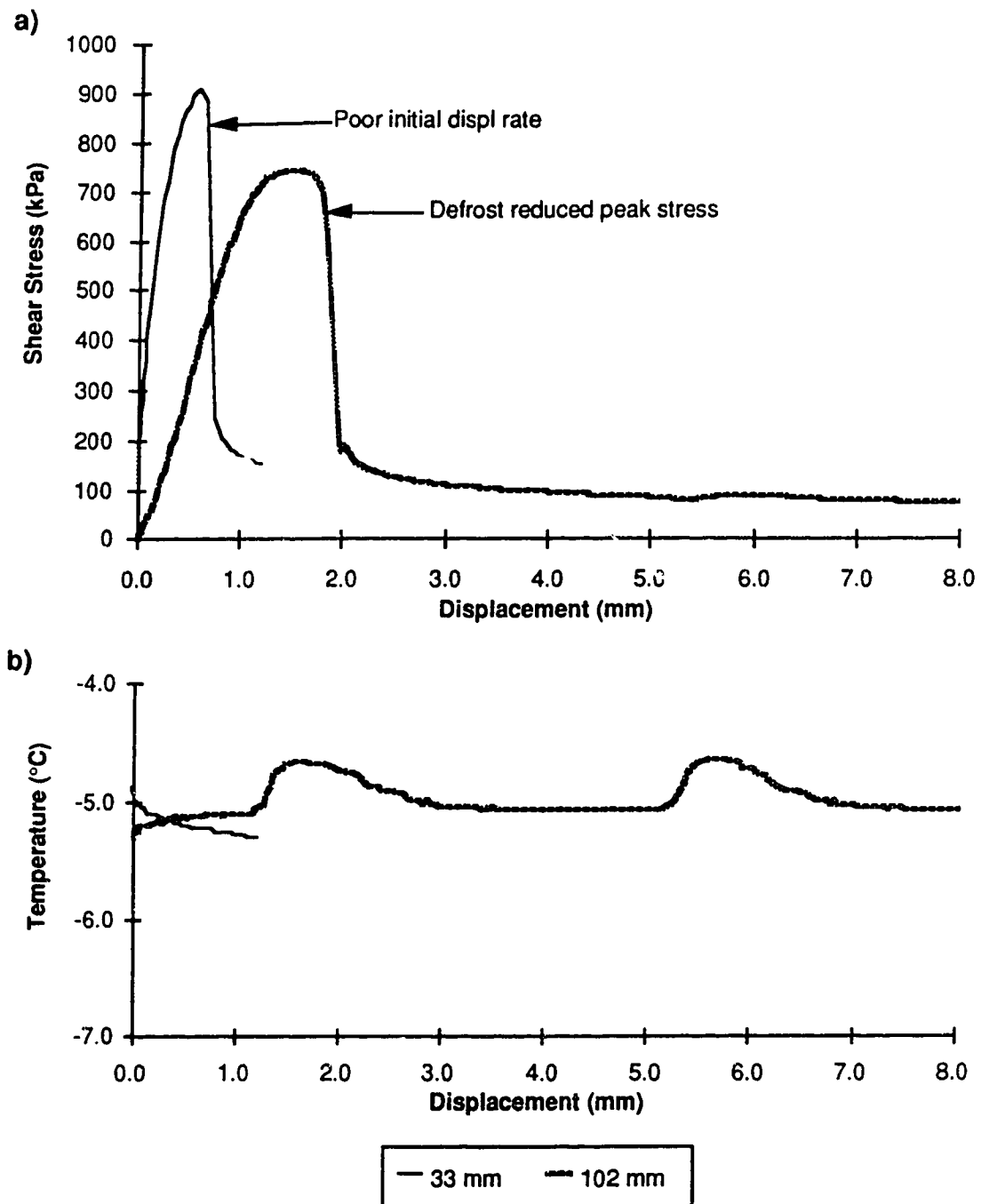


Figure D.15: Test #23, Salinity = 0 ppt, Nominal T = -5° C, Backfill = Sand  
a) Shear stress versus displacement  
b) Temperature versus displacement



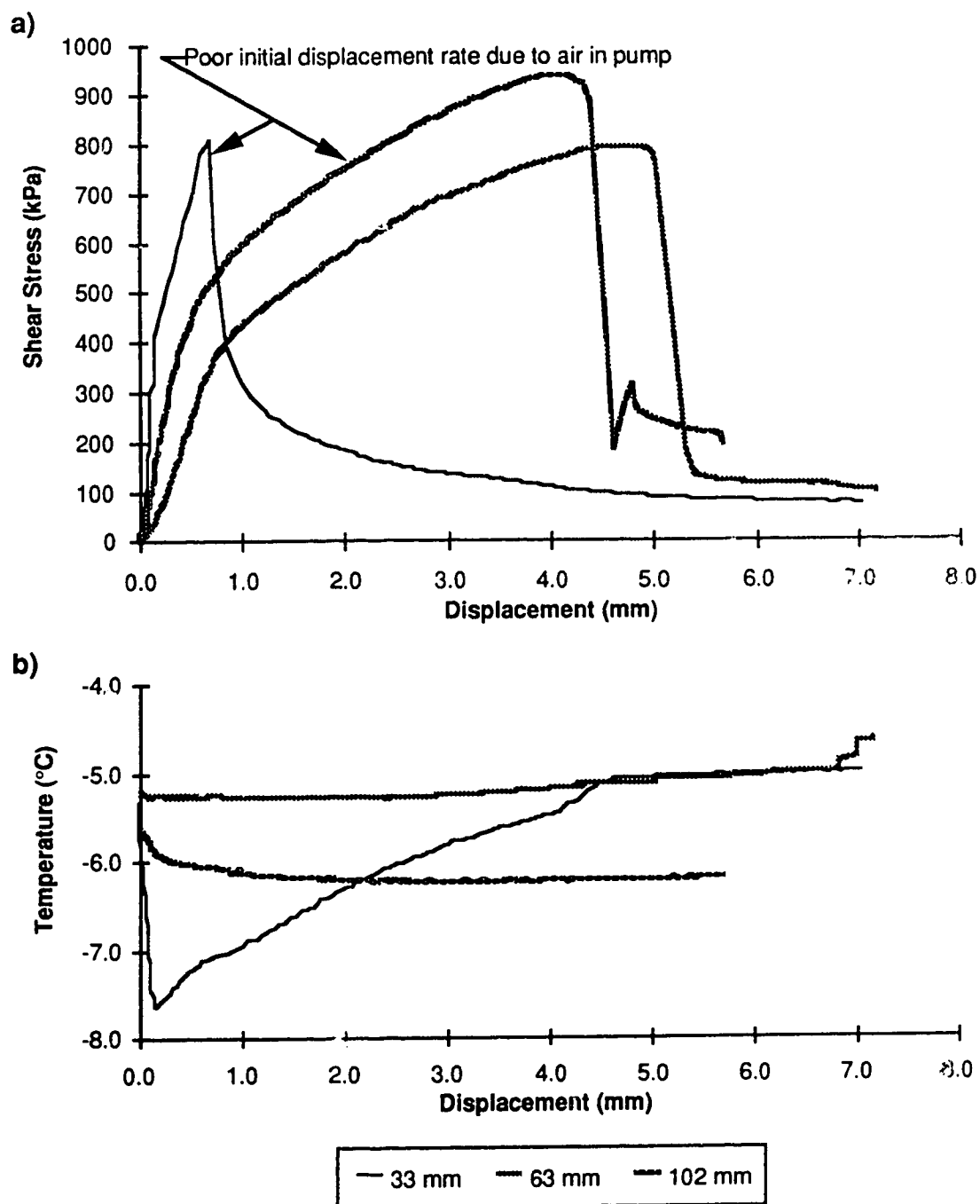


Figure D.16: Test #29, Salinity = 10 ppt, Nominal  $T = -5^{\circ}\text{C}$ , Backfill = Sand  
a) Shear stress versus displacement  
b) Temperature versus displacement

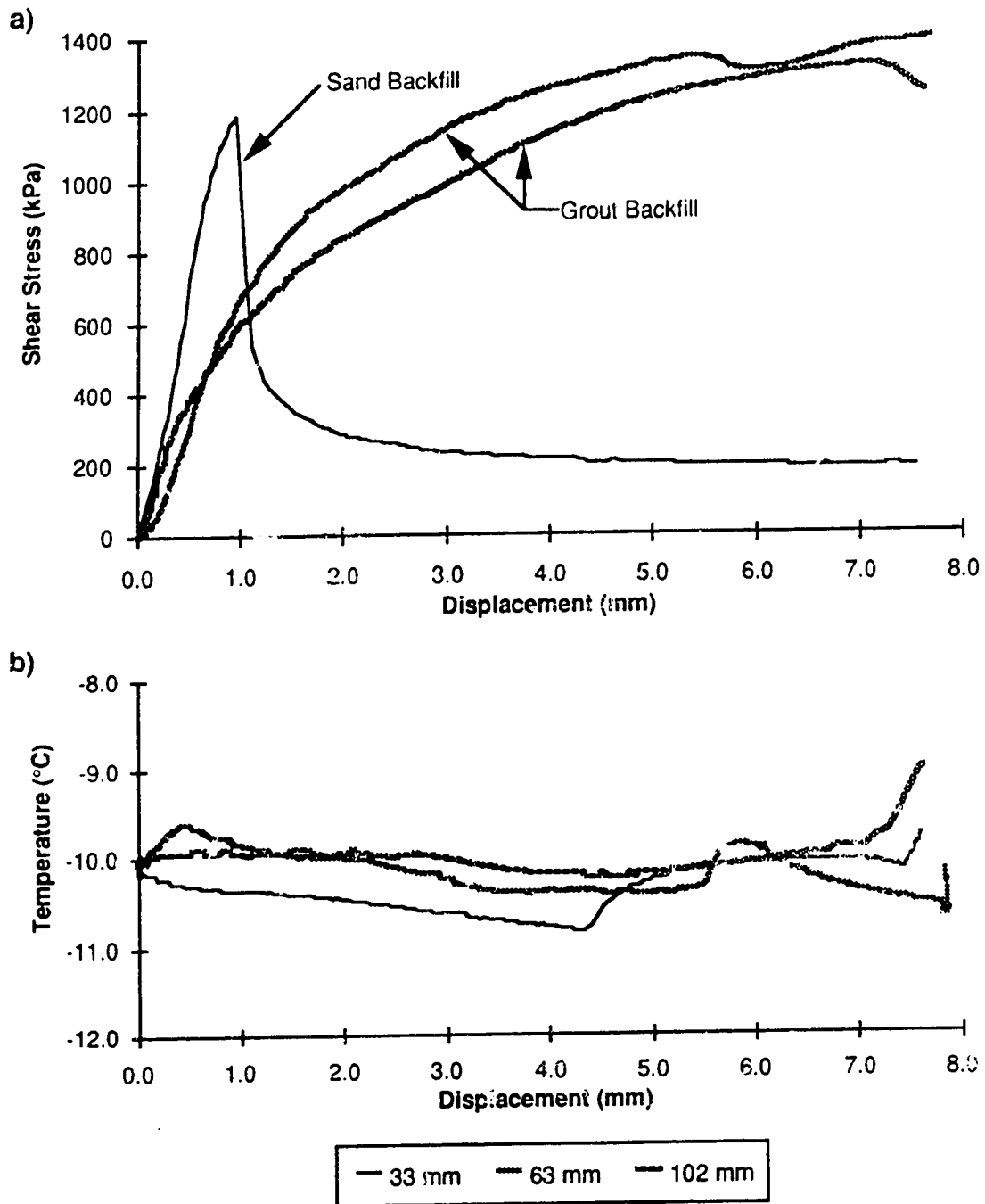


Figure D.17: Test #32, Salinity = 10 ppt, Nominal T = -10° C, Backfill = Sand & Grout  
 a) Shear stress versus displacement  
 b) Temperature versus displacement

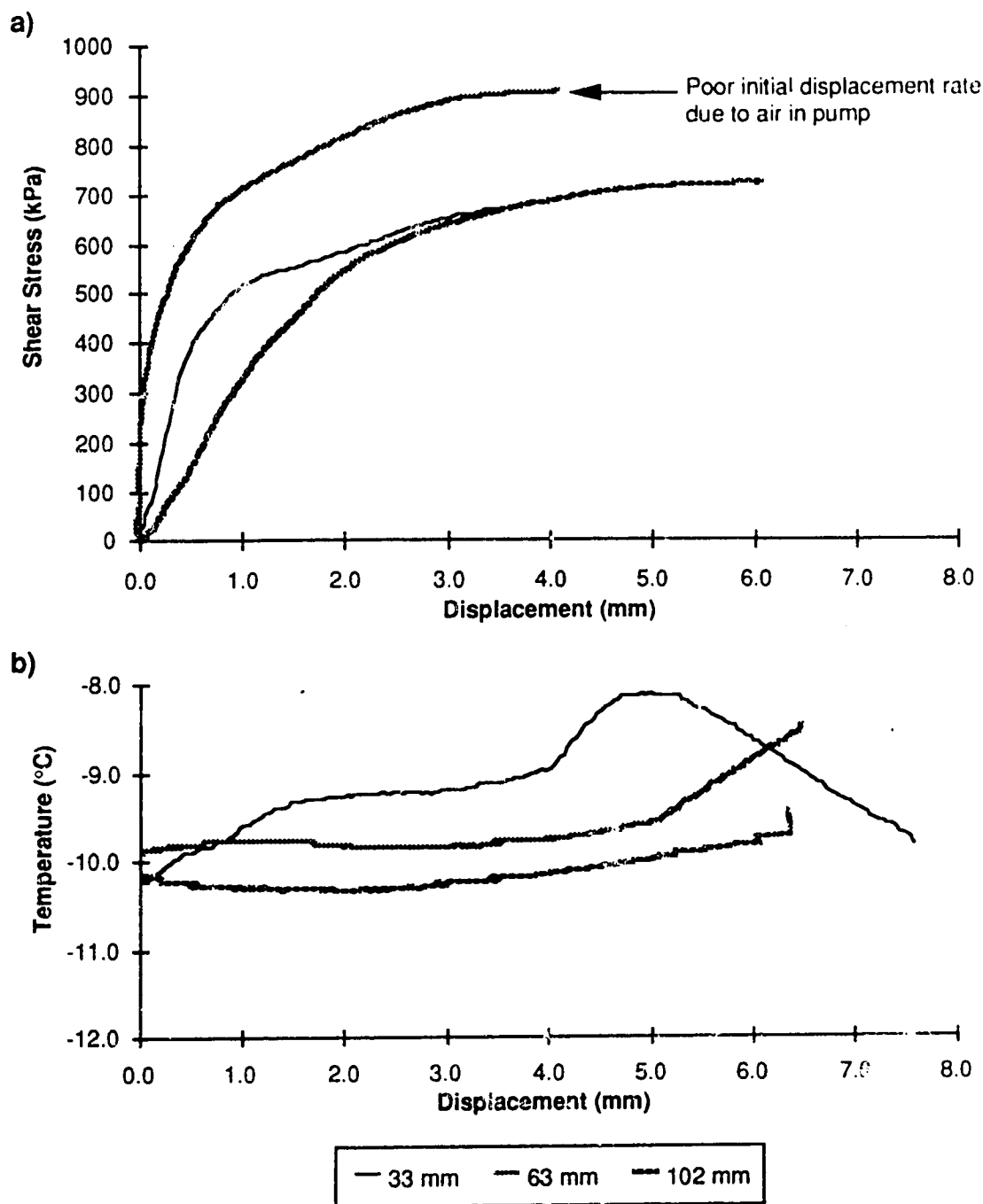


Figure D.18: Test #35, Salinity = 30 ppt, Nominal T =  $-10^{\circ}\text{C}$ , Backfill = Grout

- a) Shear stress versus displacement  
b) Temperature versus displacement

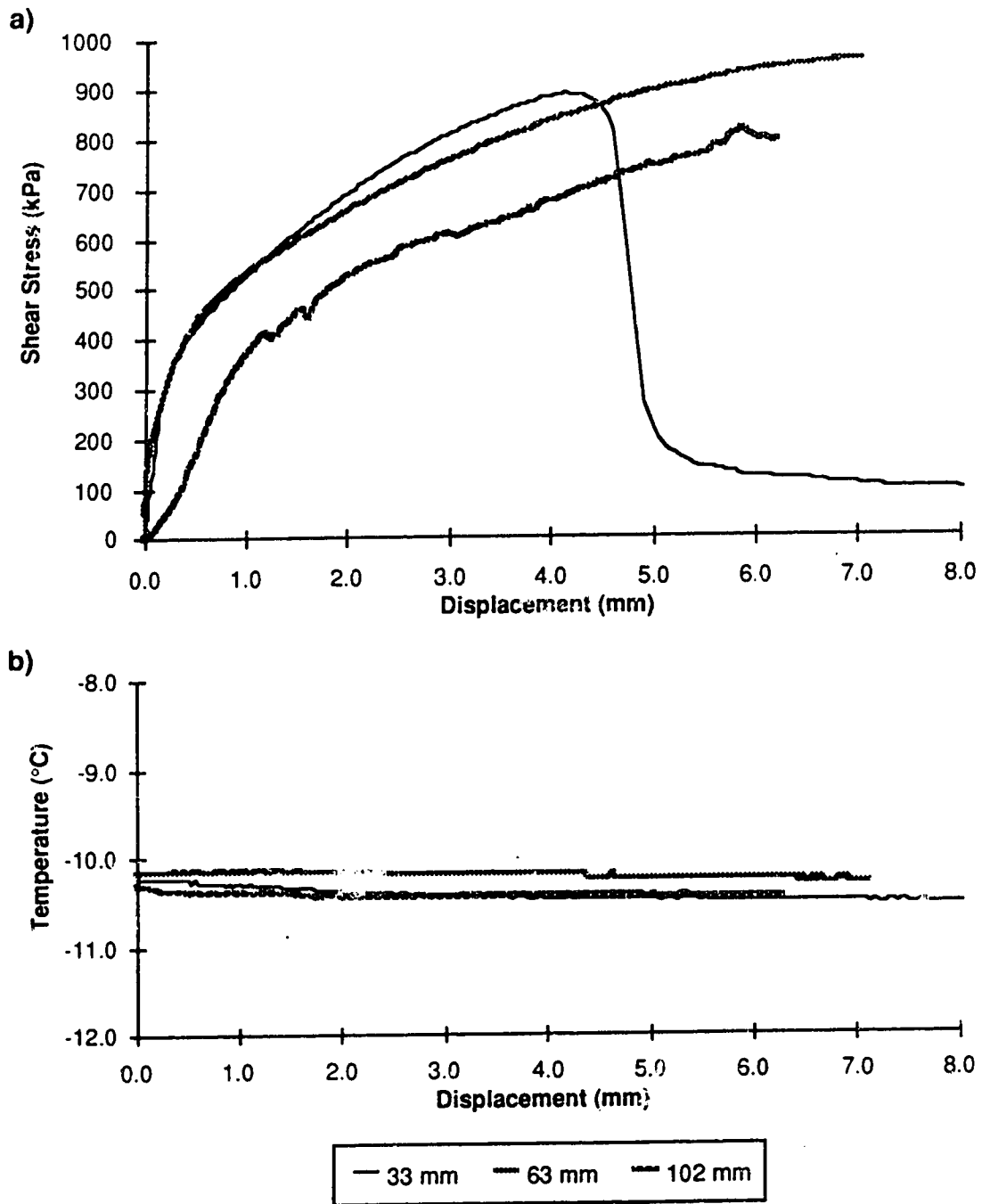


Figure D.19: Test #37, Salinity = 30 ppt, Nominal T =  $-10^{\circ}\text{C}$ , Backfill = Sand  
a) Shear stress versus displacement  
b) Temperature versus displacement

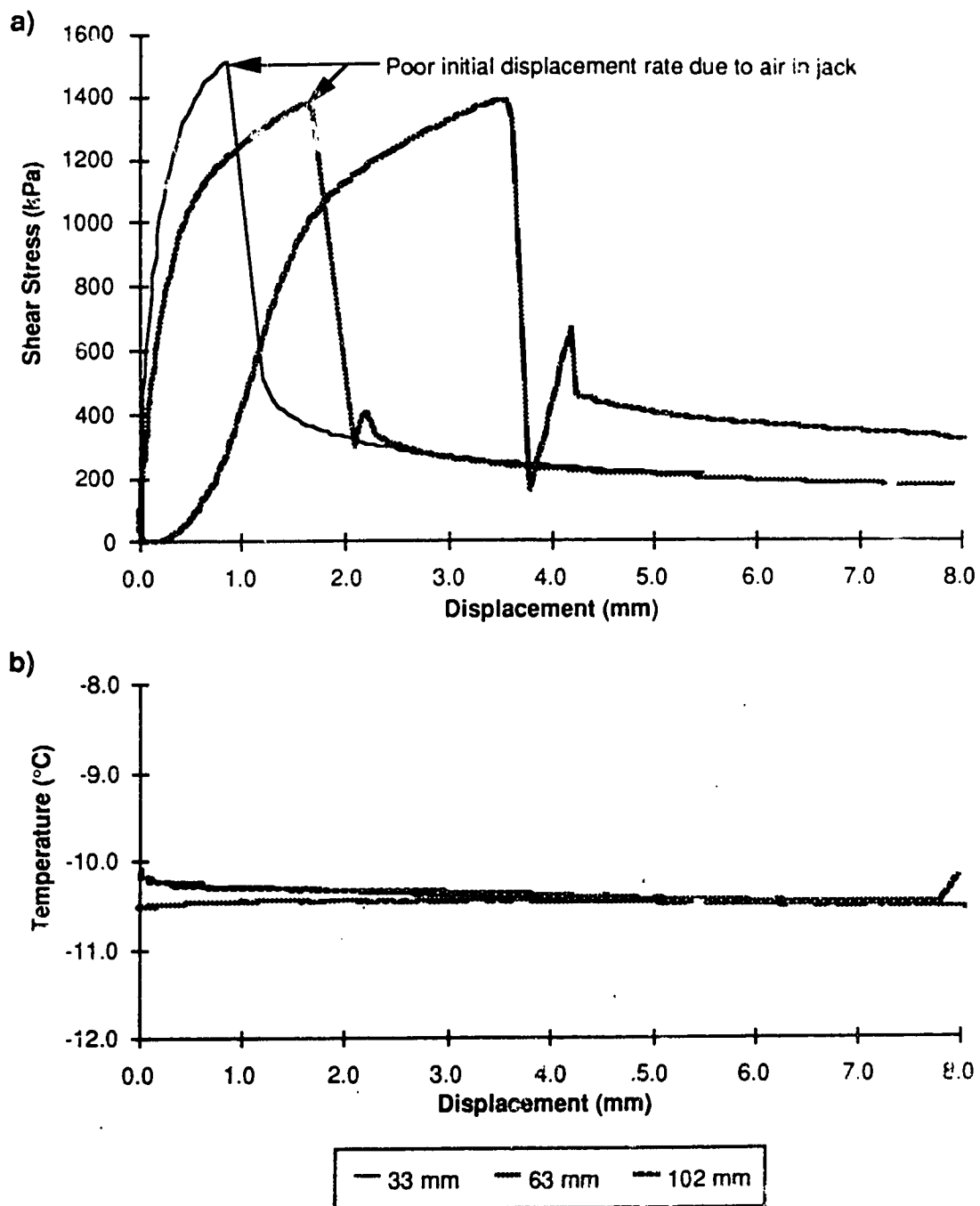


Figure D.20: Test #38, Salinity = 10 ppt, Nominal T = -10° C, Backfill = Sand  
a) Shear stress versus displacement  
b) Temperature versus displacement

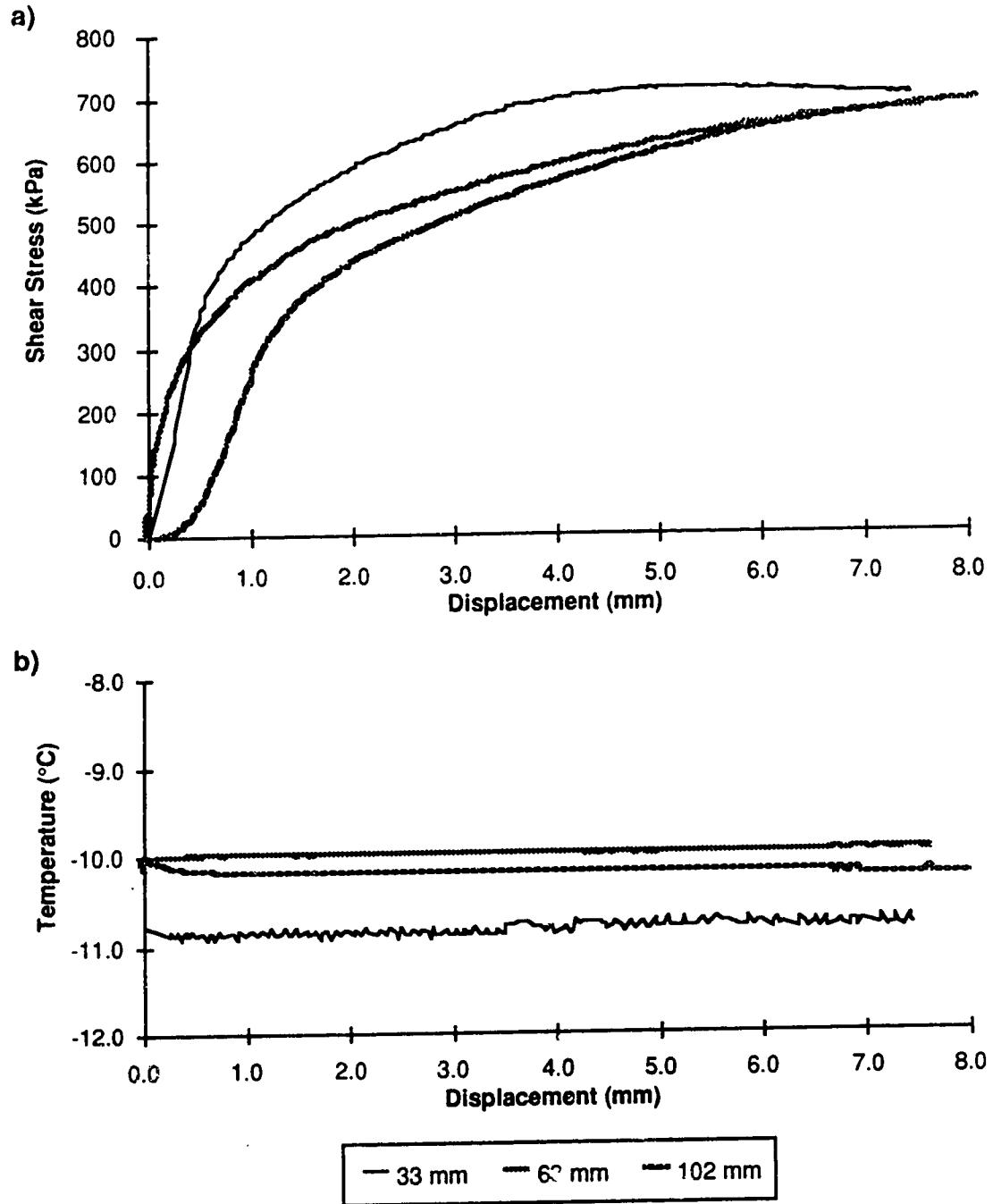


Figure D.21: Test #42, Salinity = 30 ppt, Nominal  $T = -10^{\circ}\text{C}$ , Backfill = Grout  
a) Shear stress versus displacement  
b) Temperature versus displacement

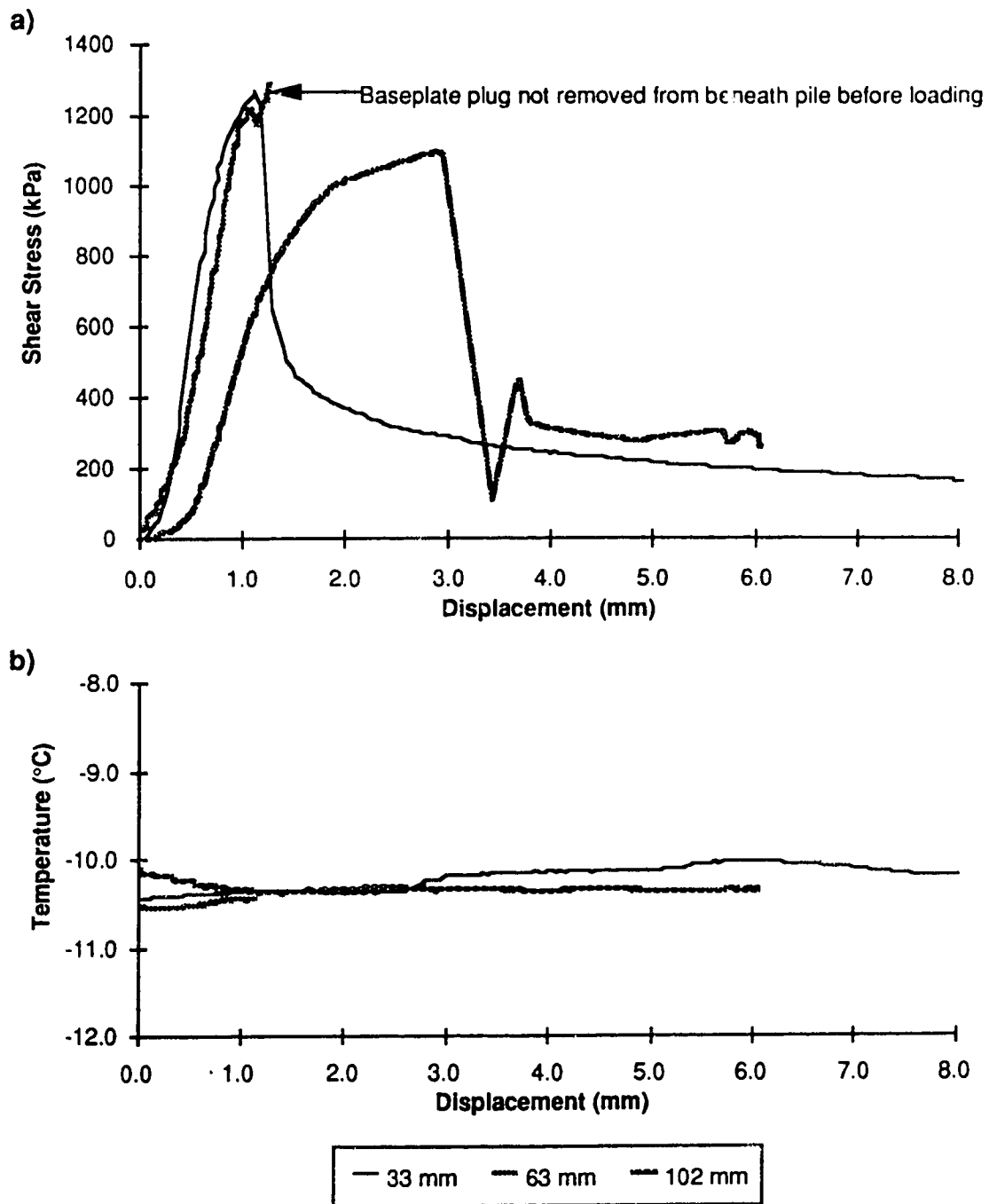


Figure D.22: Test #43, Salinity = 10 ppt, Nominal  $T = -10^{\circ}\text{C}$ , Backfill = Sand.  
 a) Shear stress versus displacement  
 b) Temperature versus displacement

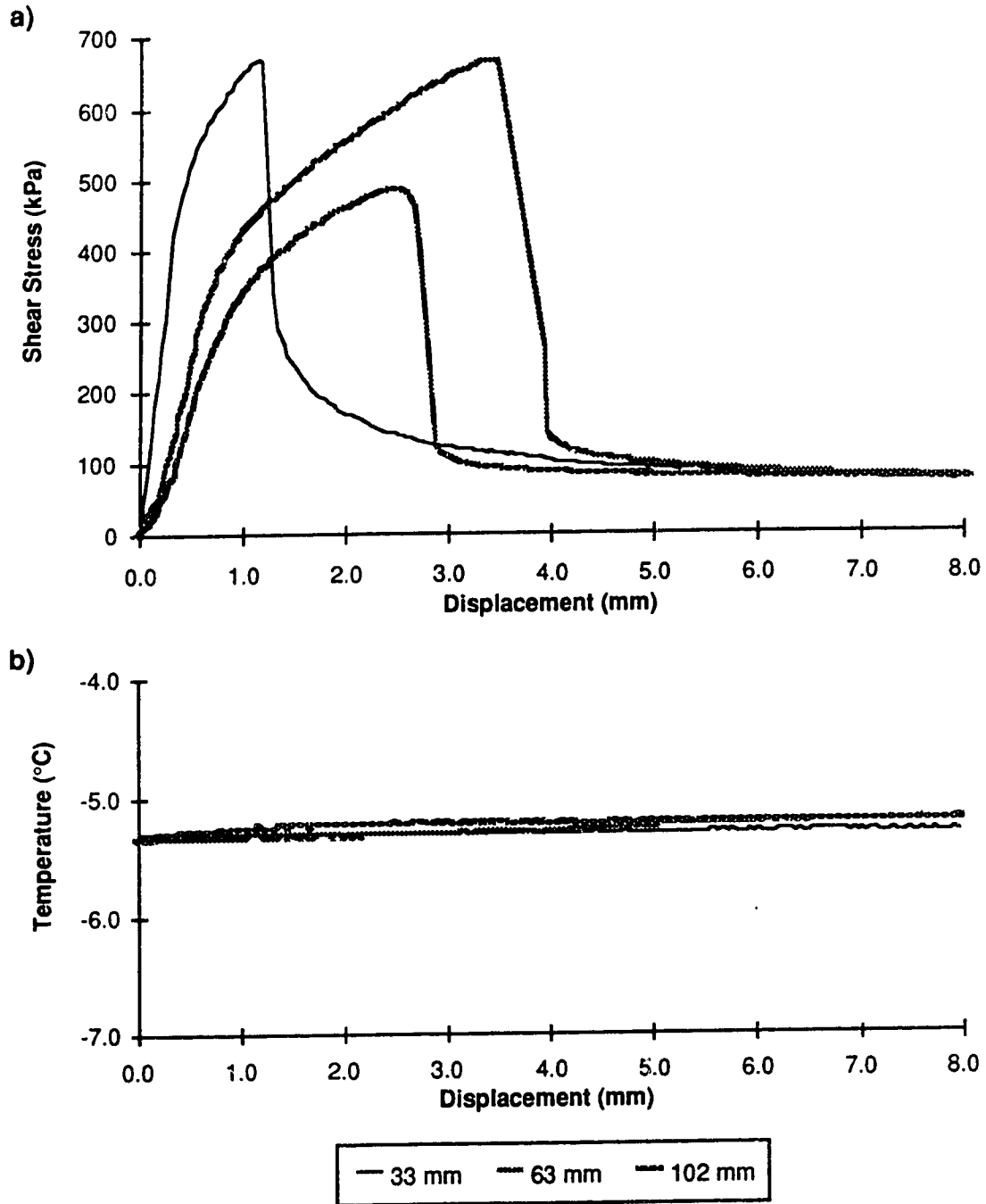


Figure D.23: Test #44, Salinity = 10 ppt, Nominal T =  $-5^{\circ}\text{C}$ , Backfill = Sand  
a) Shear stress versus displacement  
b) Temperature versus displacement



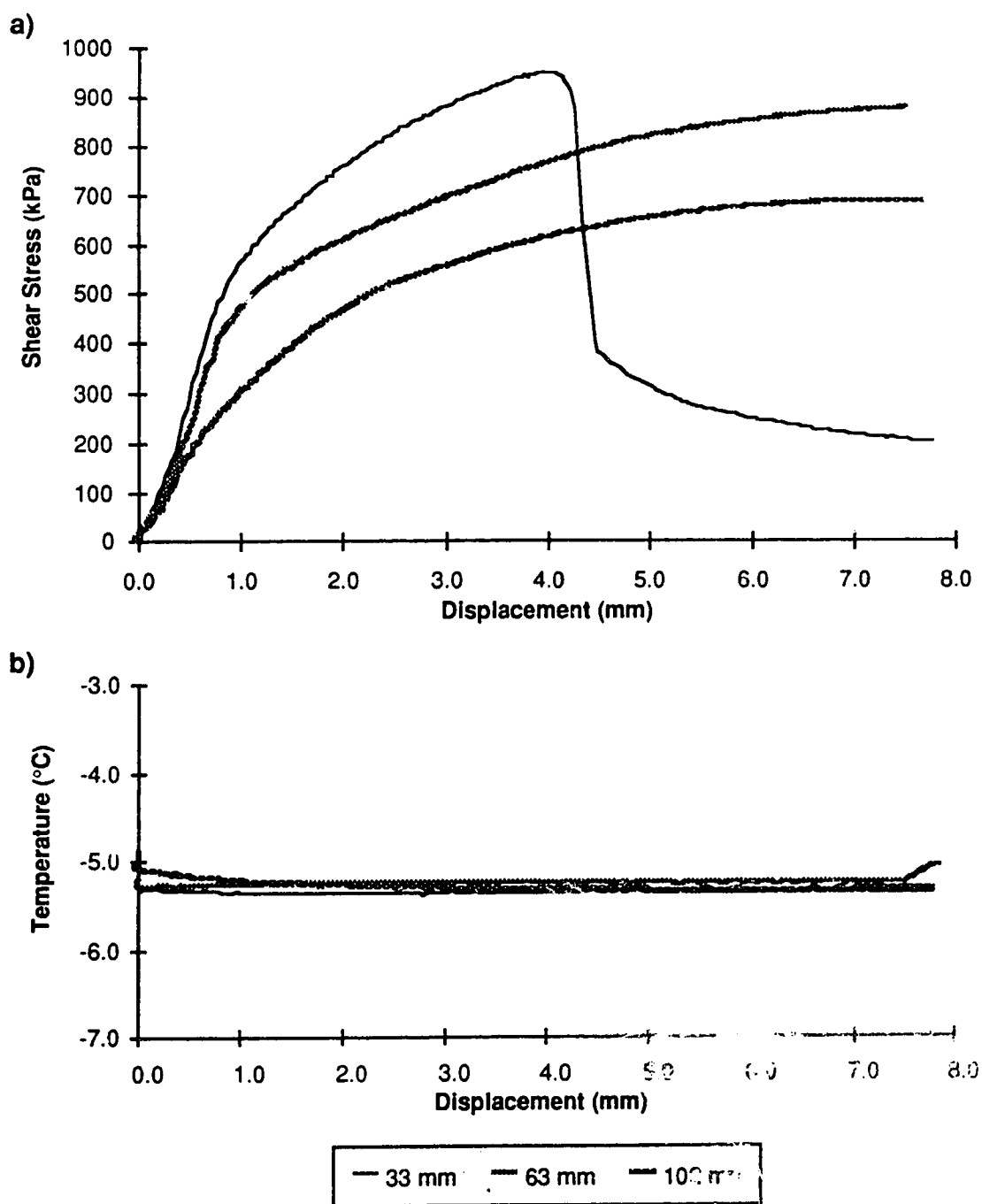


Figure D.24: Test #45, Salinity = 10 ppt, Nominal T = -5° C, Backfill = Grout  
a) Shear stress versus displacement  
b) Temperature versus displacement

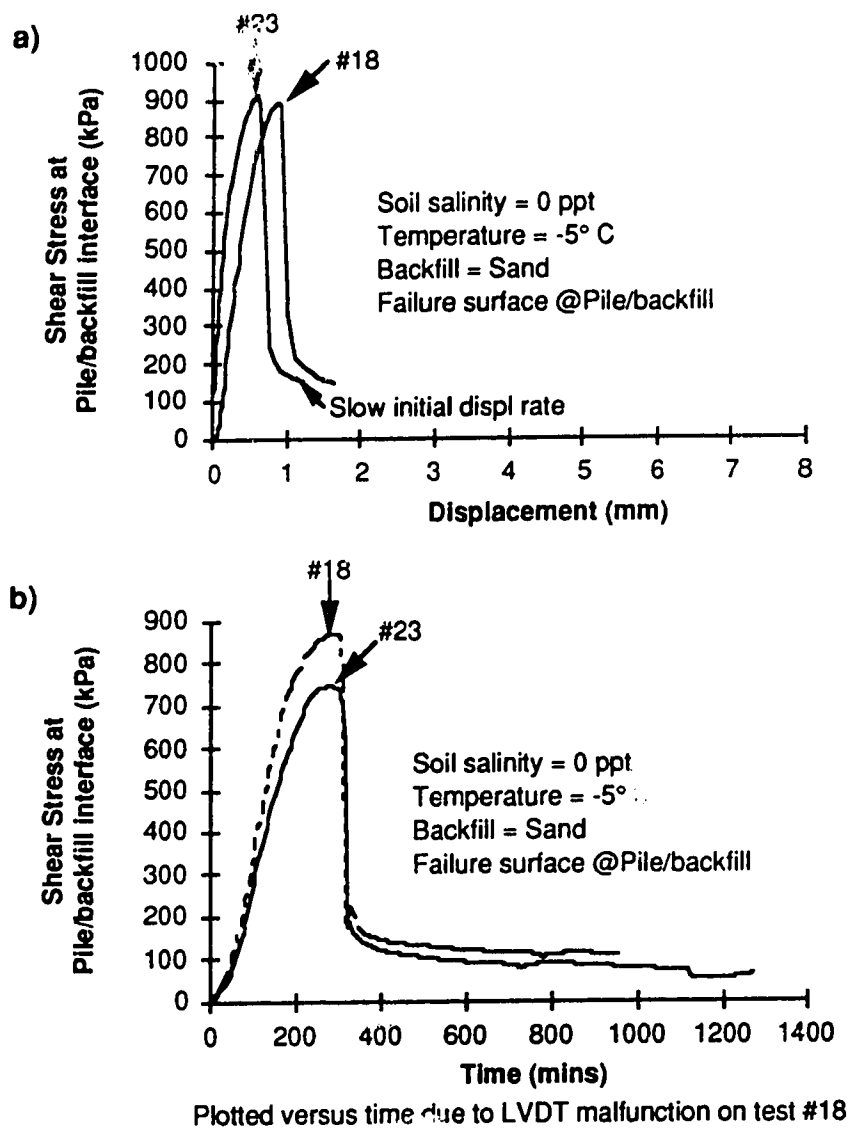


Figure D.23: Comparison of tests with same conditions—#18 & #23  
a) 33 mm pile  
b) 102 mm pile

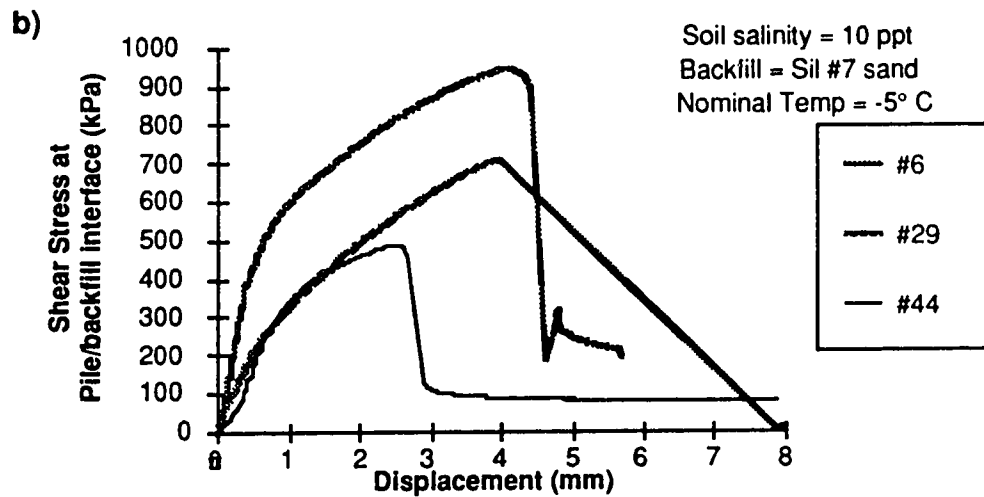
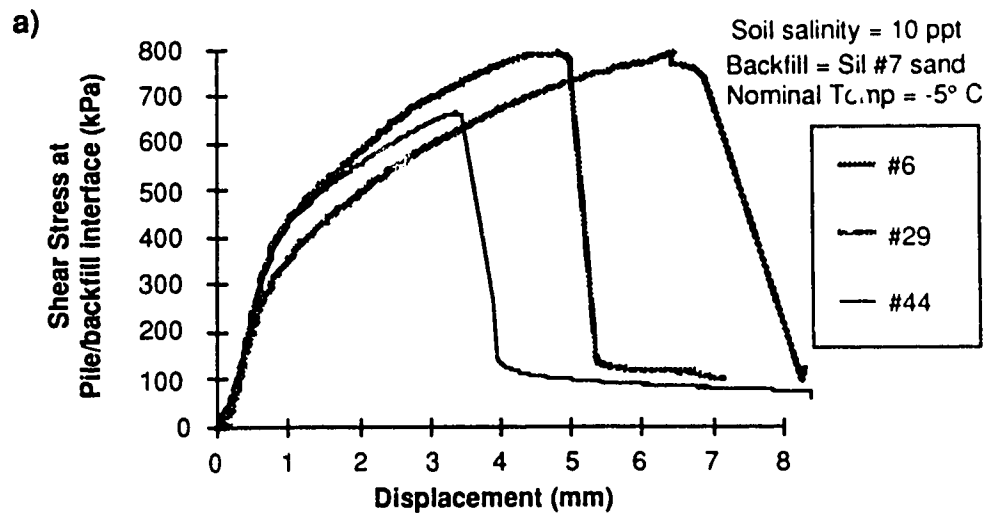


Figure D.26: Comparison of tests with same conditions - #6, #29, and #44  
a) 63 mm pile  
b) 102 mm pile

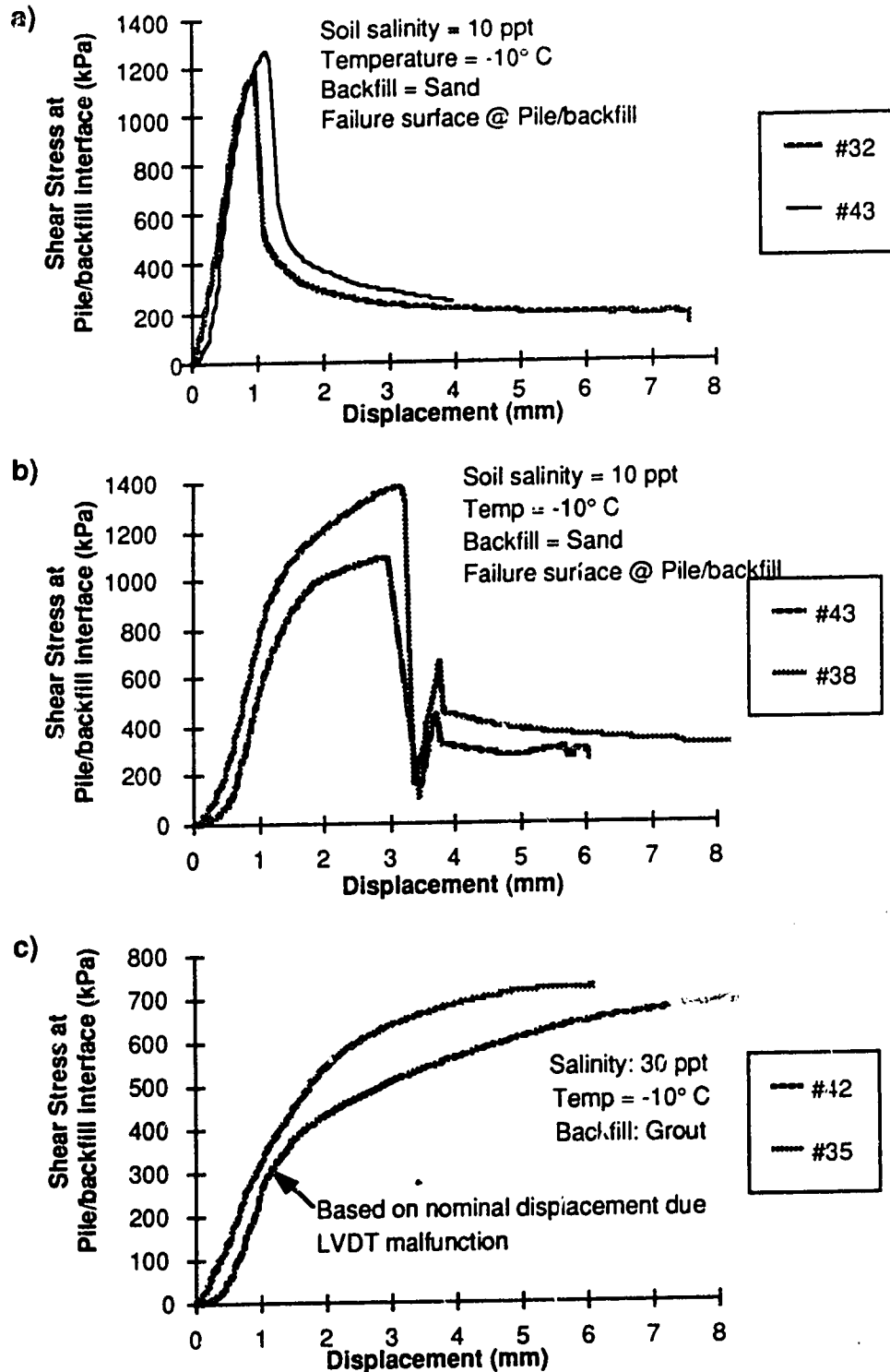


Figure D.27: Comparison of tests with same conditions —  $T = -10^{\circ}\text{C}$

- a) #32 & #43, 33 mm pile
- b) #38 & #43, 102 mm pile
- c) #35 & #42, 102 mm pile

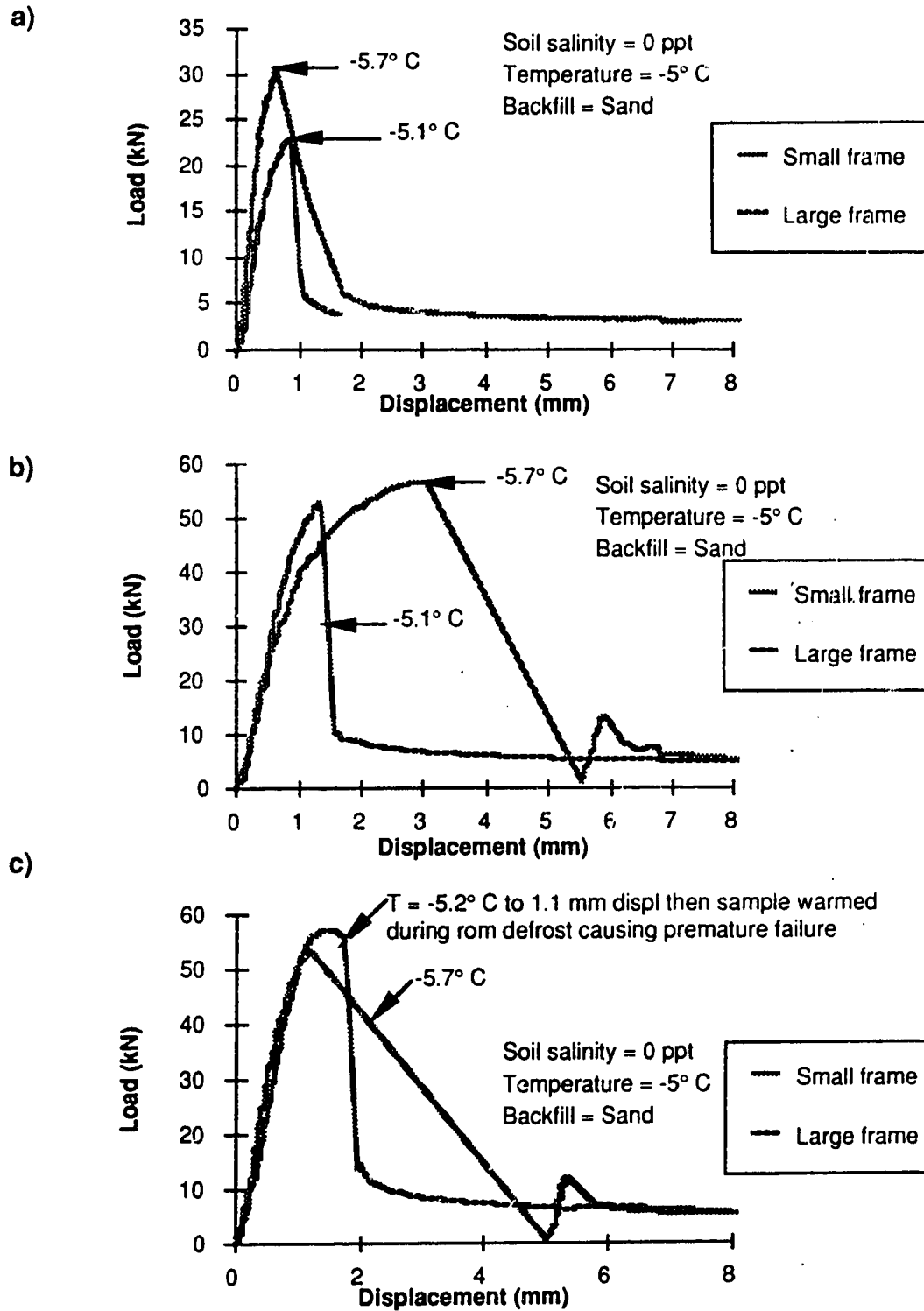


Figure D.28: Comparison of similar tests in different frames, Load versus displacement

- a) 33 mm pile
- b) 63 mm pile
- c) 102 mm pile

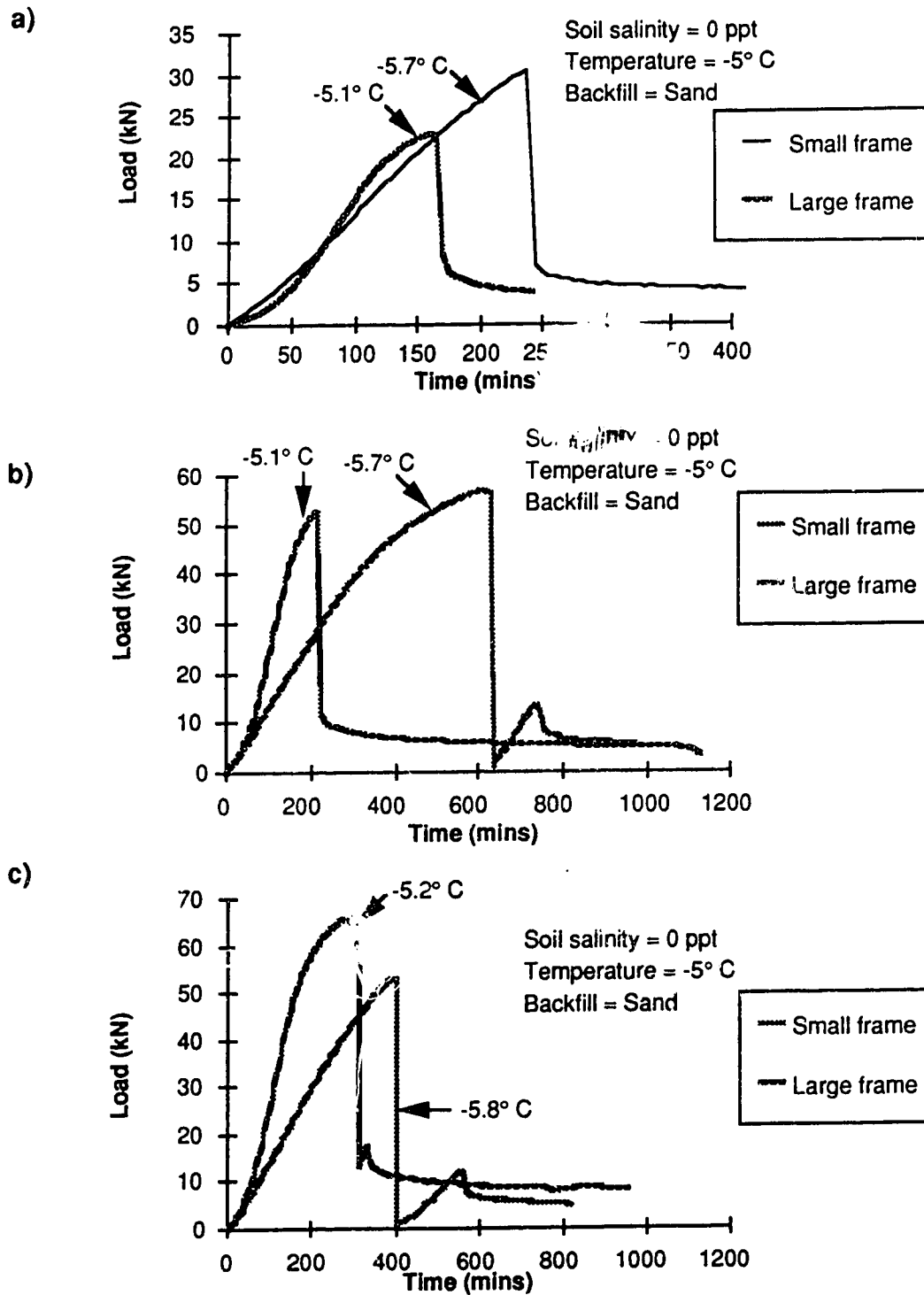


Figure D.29: Comparison of similar tests in different frames, Load versus time

- a) 33 mm pile
- b) 63 mm pile
- c) 102 mm pile

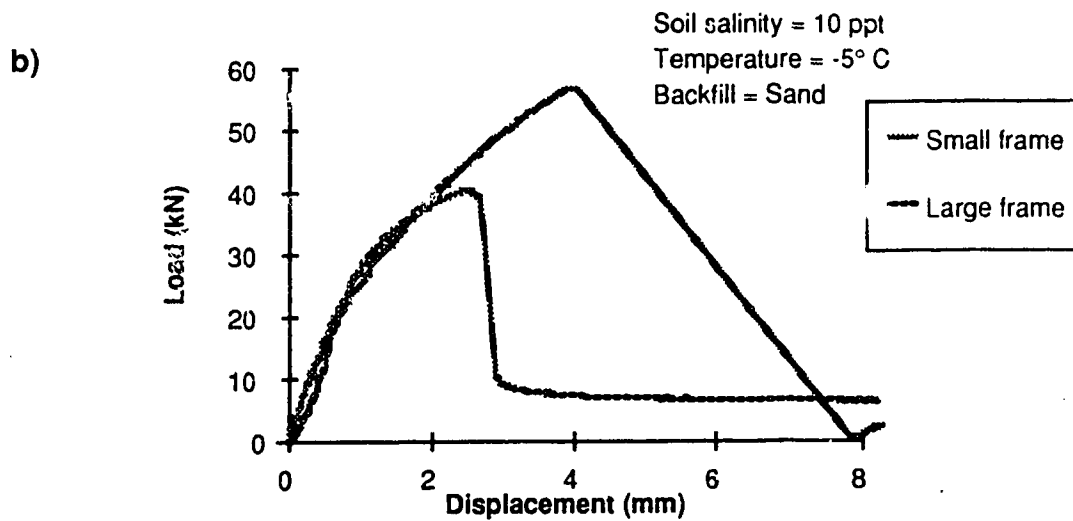
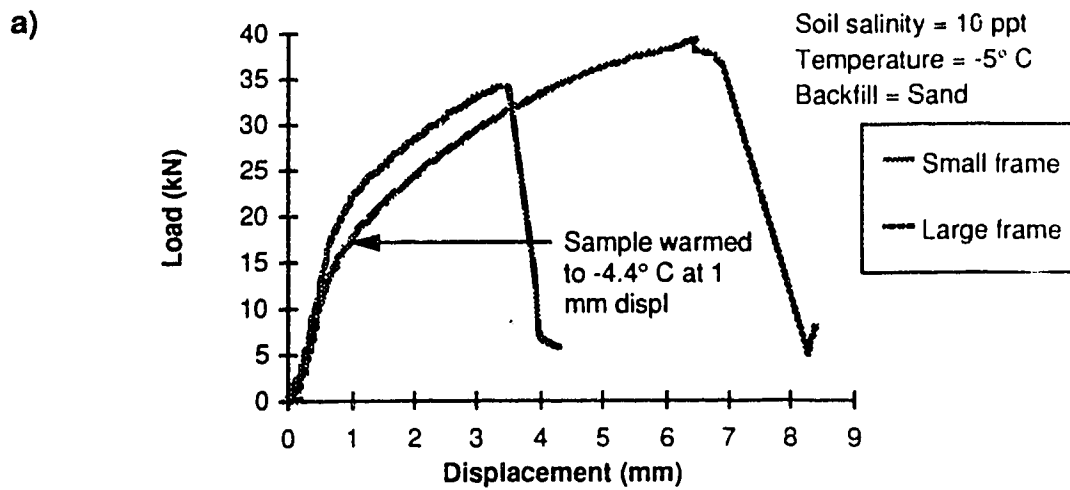


Figure D.30: Comparison of similar tests with different frames-Load vs displacement  
a) 63 mm pile  
b) 102 mm pile

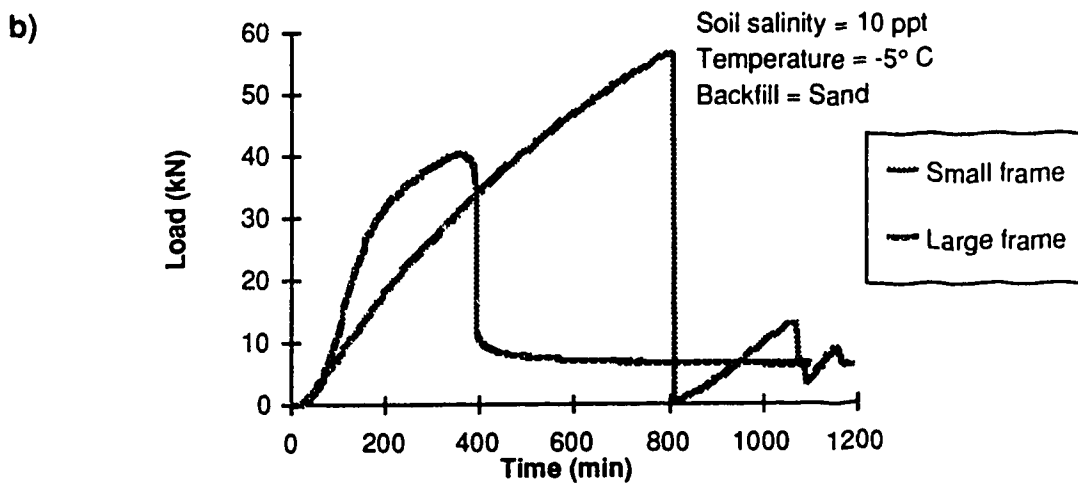
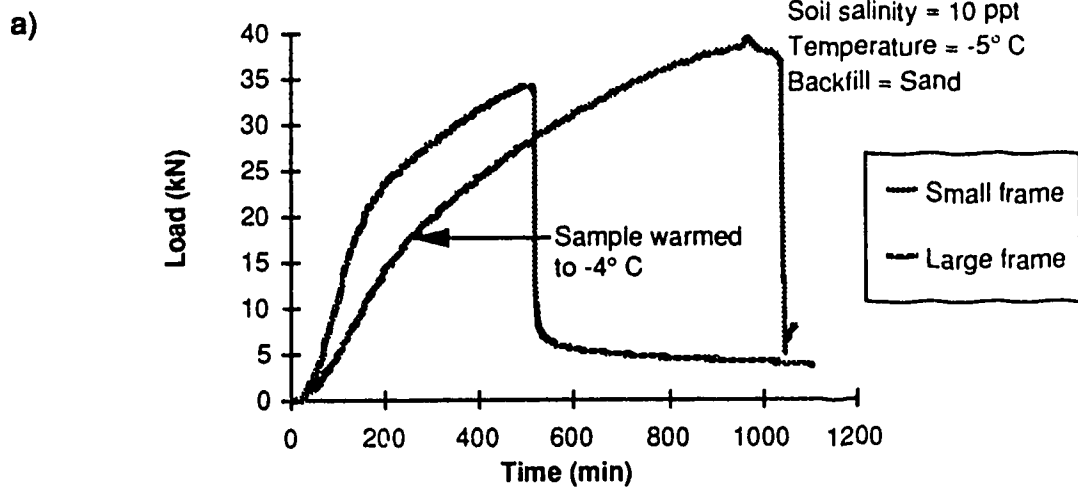


Figure D.31: Comparison of similar tests with different frames-Load vs time  
a) 63 mm pile  
b) 102 mm pile



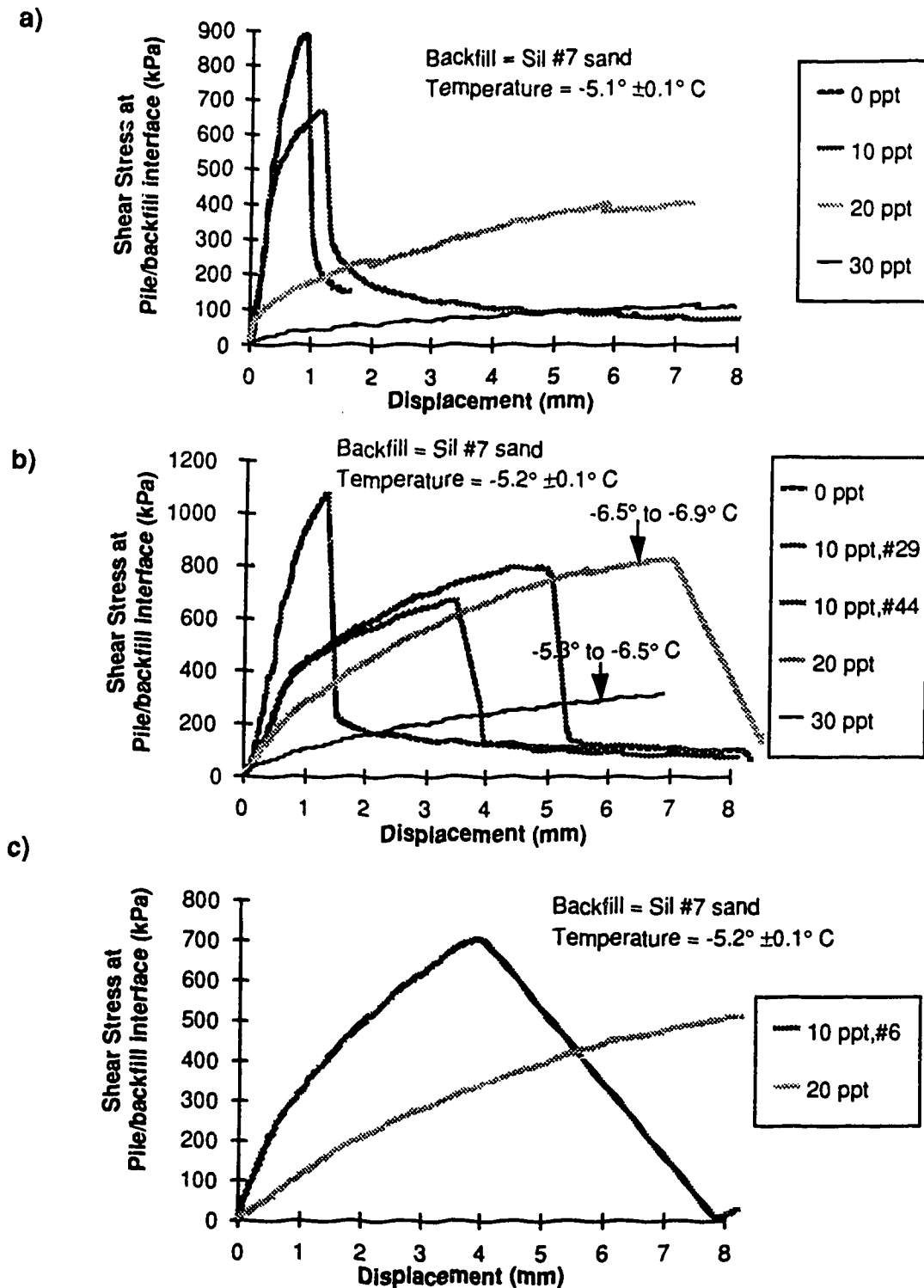


Figure D.32: Effect of variation of salinity on performance of sand backfilled piles

- a) 33 mm pile
- b) 63 mm pile
- c) 102 mm pile

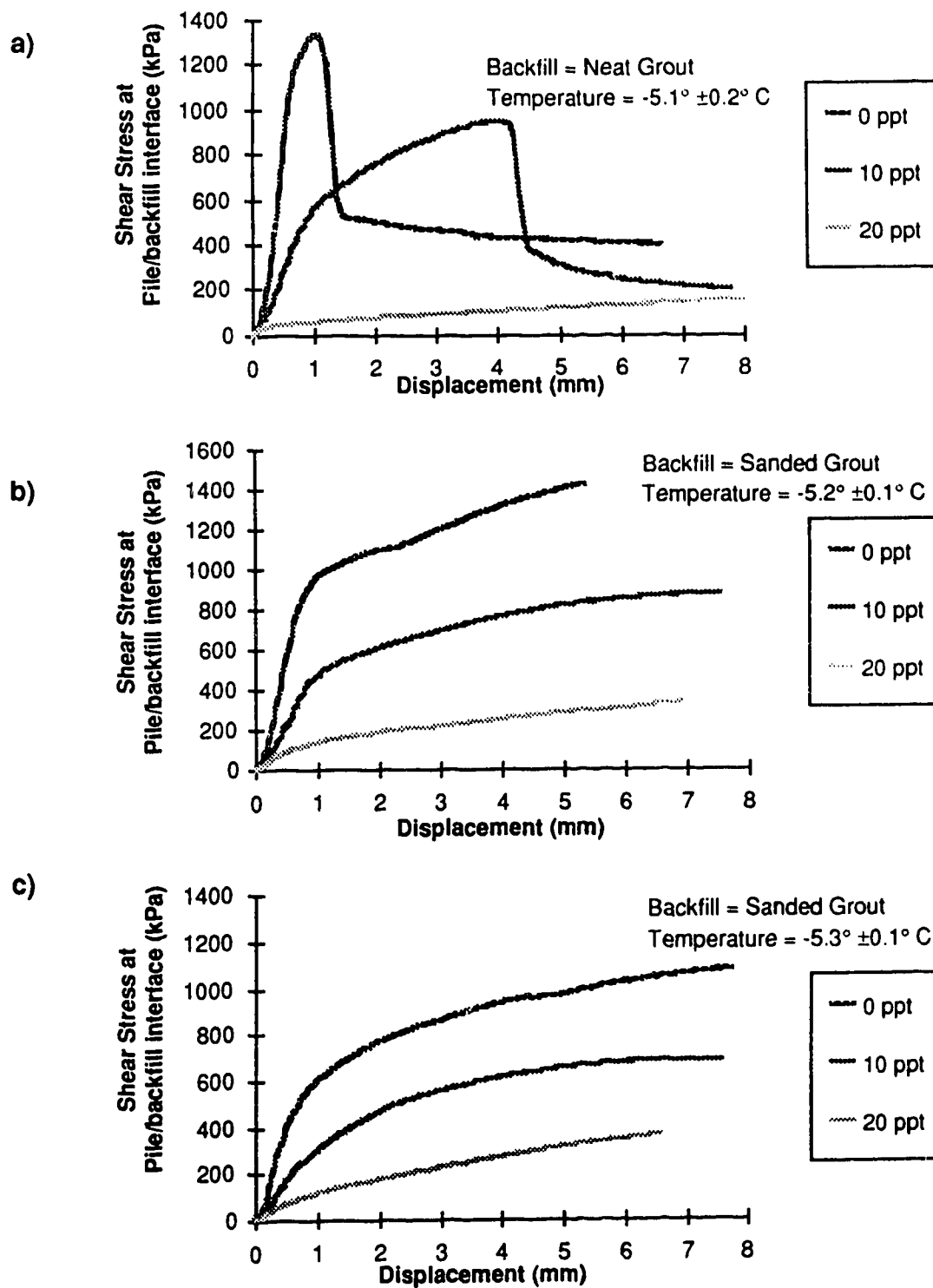


Figure D.33: Effect of variation of salinity on performance of grout backfilled piles

- a) 33 mm pile
- 63 mm pile
- c) 102 mm pile

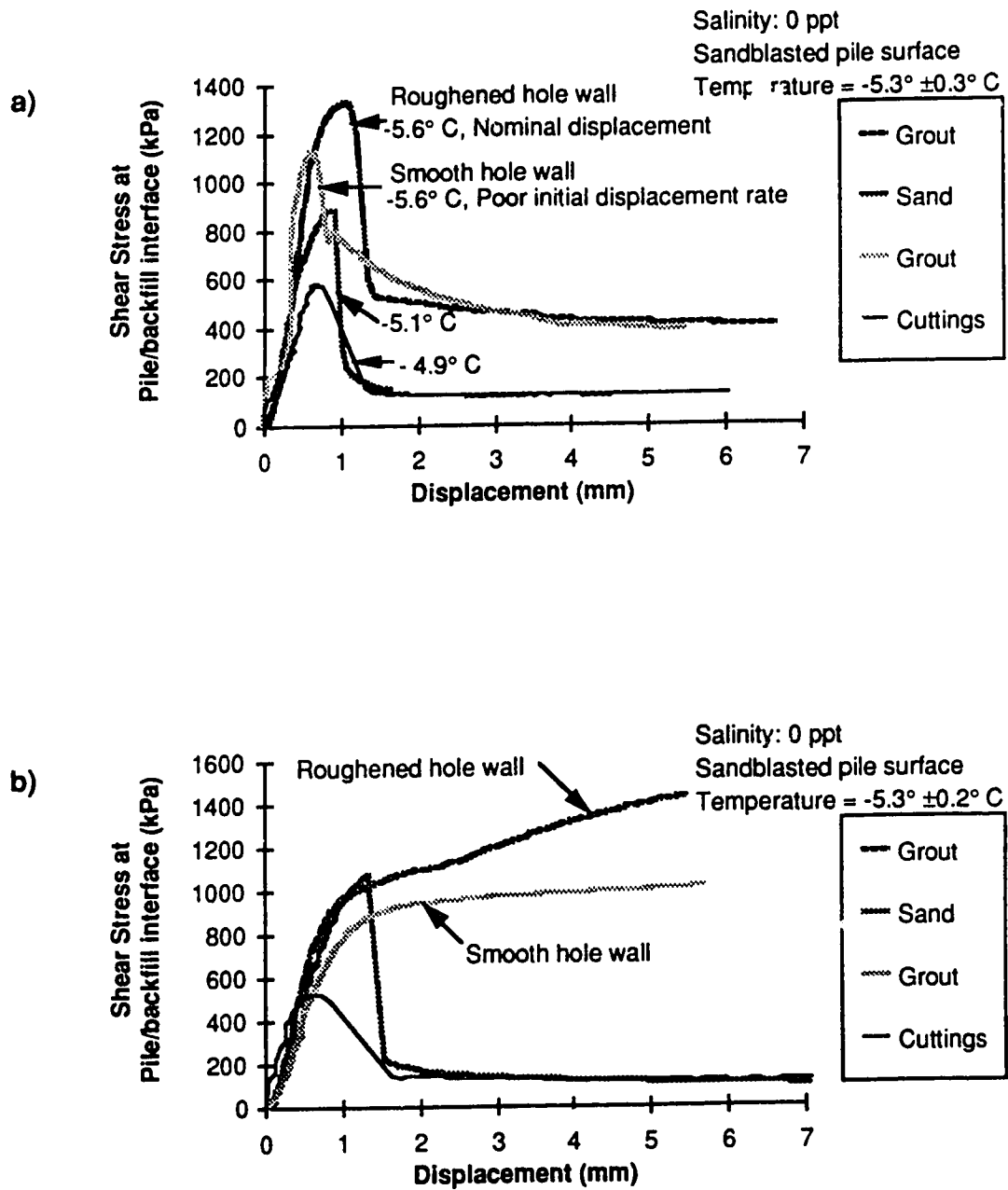


Figure D.34: Comparison of backfill effects on pile performance,  $S = 0$  ppt  
a) 33 mm pile  
b) 63 mm pile

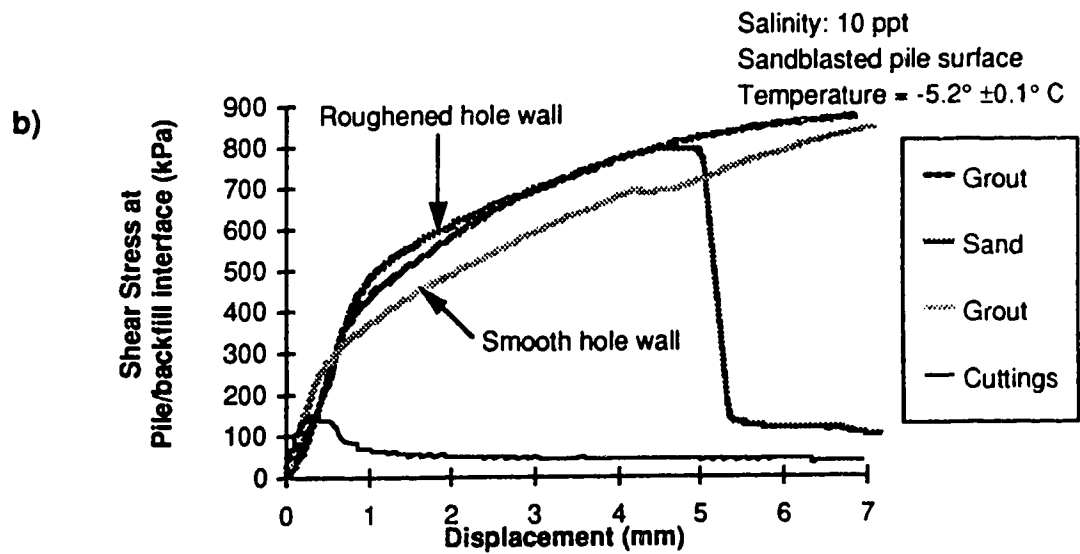
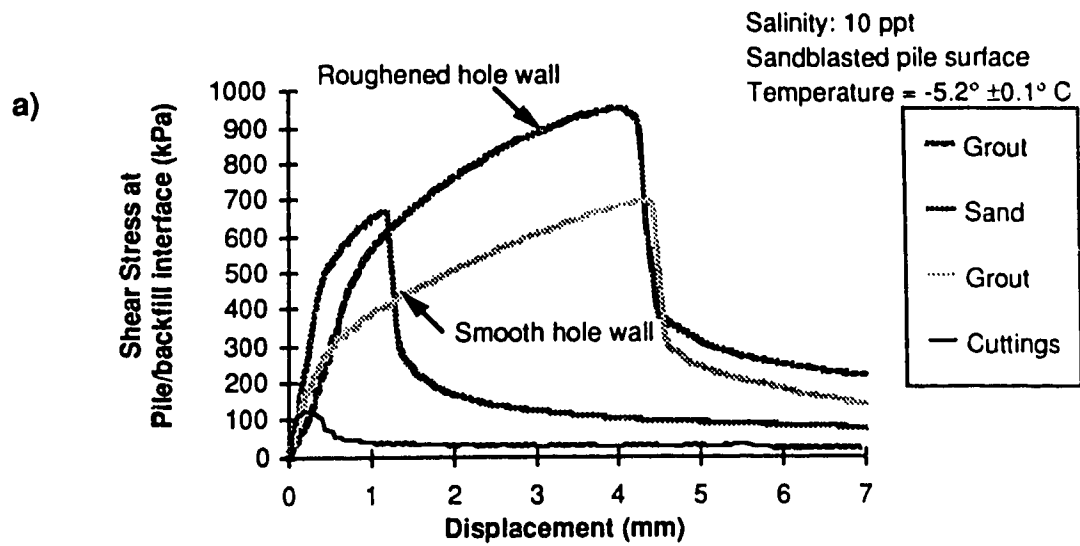


Figure D.35: Comparison of backfill effects on pile performance,  $S = 10$  ppt  
a) 33 mm pile  
b) 63 mm pile

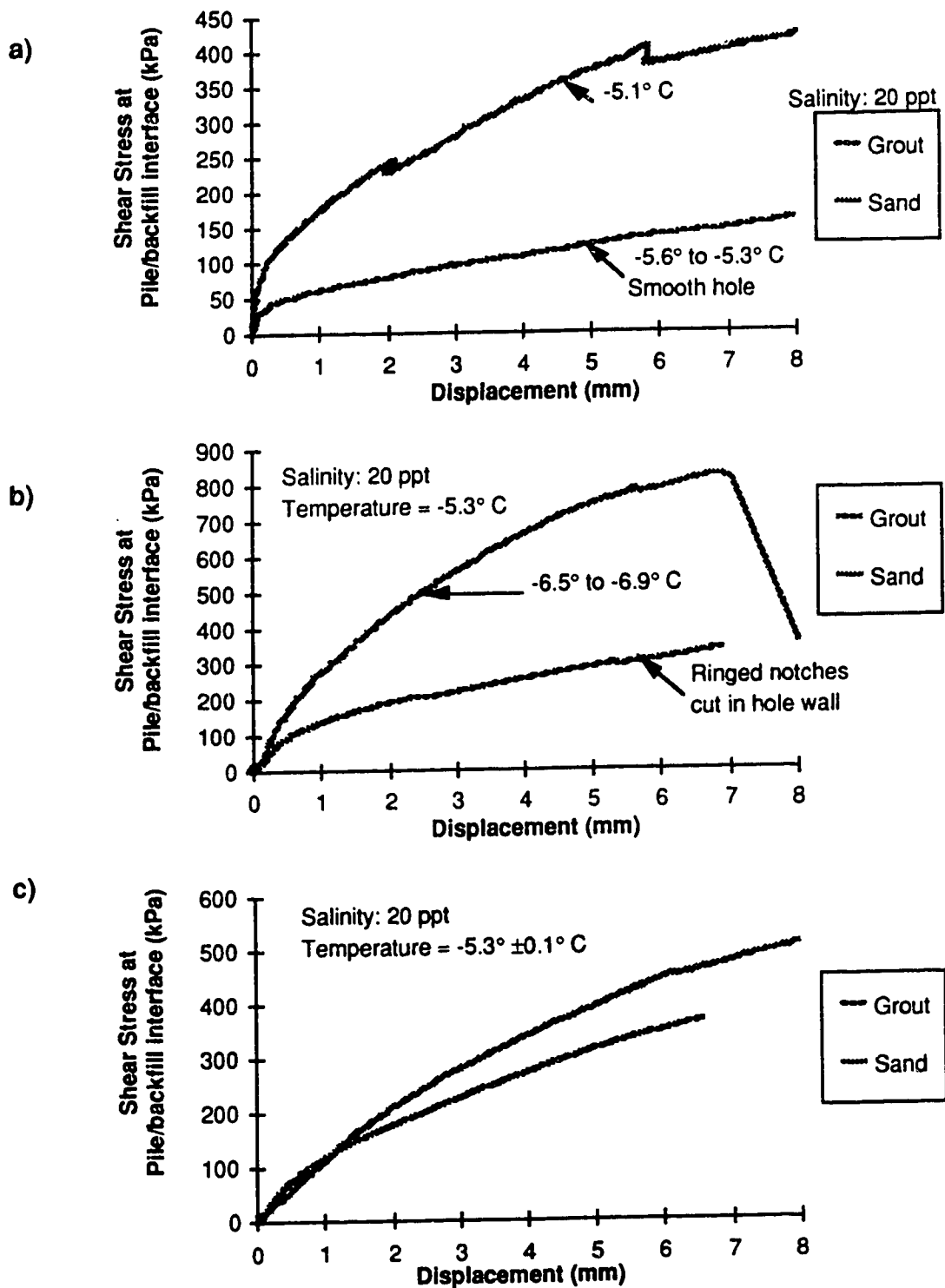


Figure D.36: Comparison of backfill effects on pile performance,  $S = 20$  ppt,  $T = -5^{\circ}\text{C}$   
 a) 33 mm pile  
 b) 63 mm pile  
 c) 102 mm pile

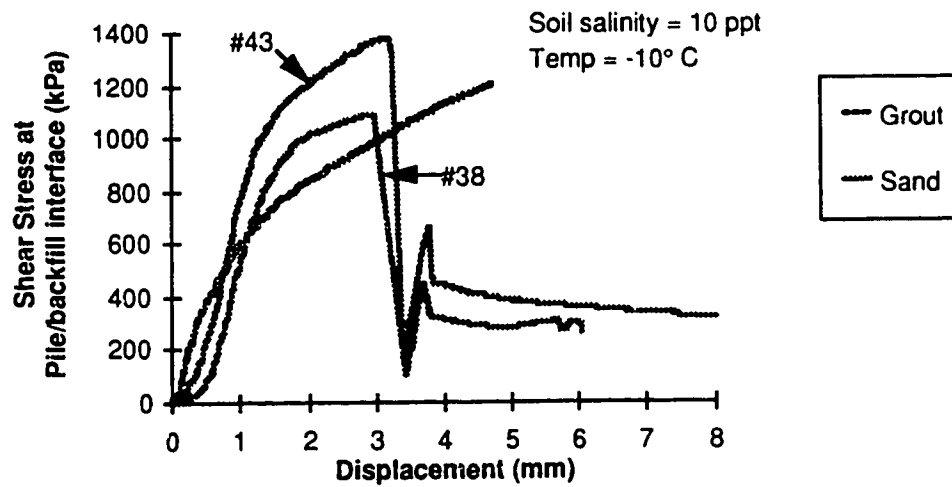


Figure D.37: Comparison of backfill effects on pile performance,  $S = 10$  ppt,  
 $T = -10^{\circ}\text{C}$ , 102 mm pile.

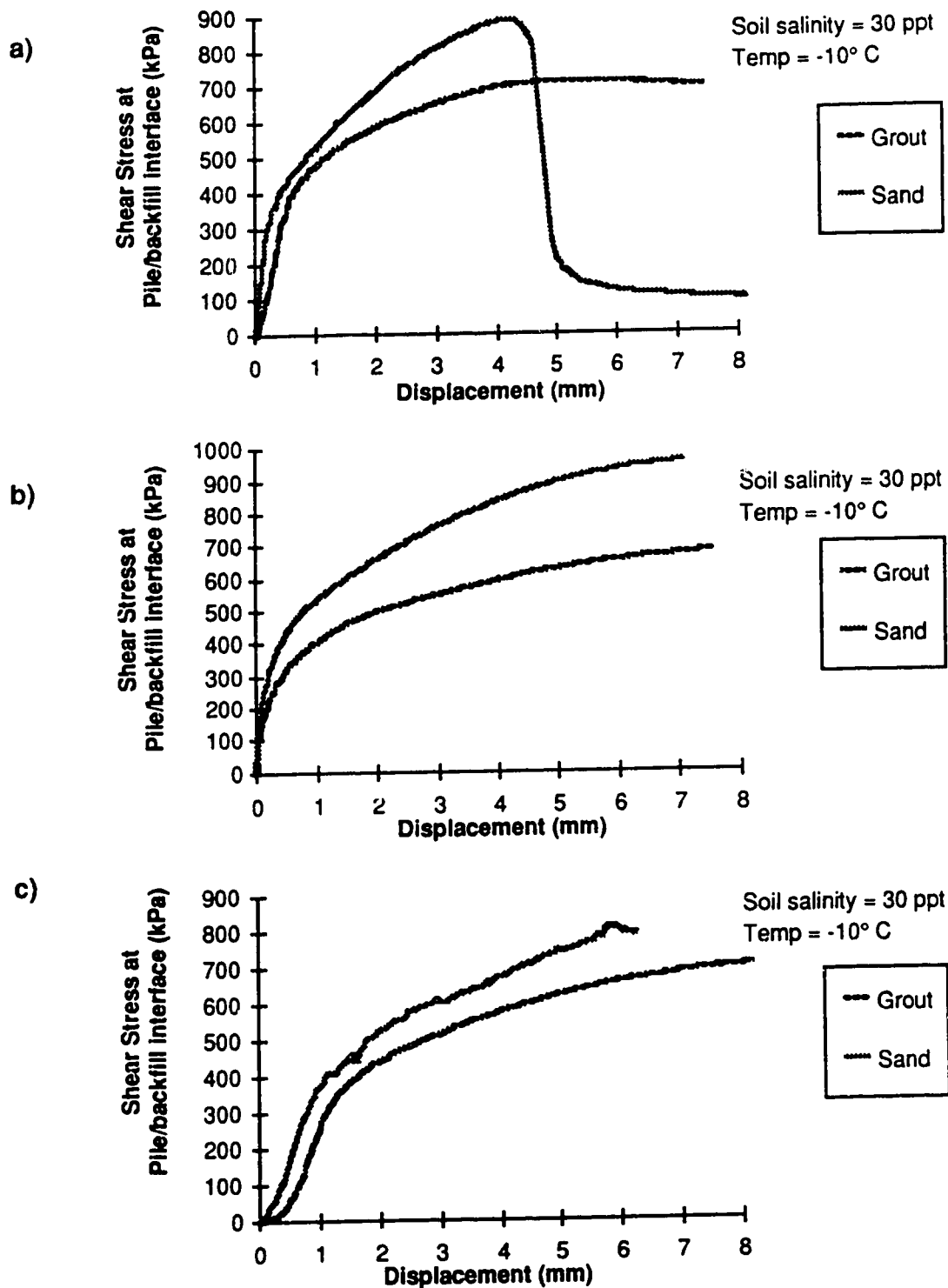


Figure D.38: Comparison of backfill effects on pile performance, S=30 ppt, T = -10° C

- a) 33 mm pile
- b) 63 mm pile
- c) 102 mm pile

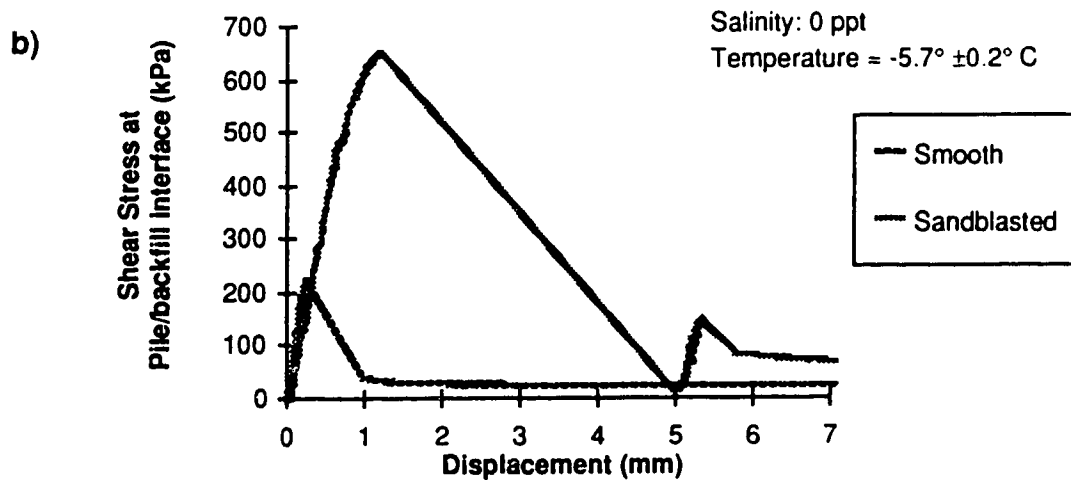
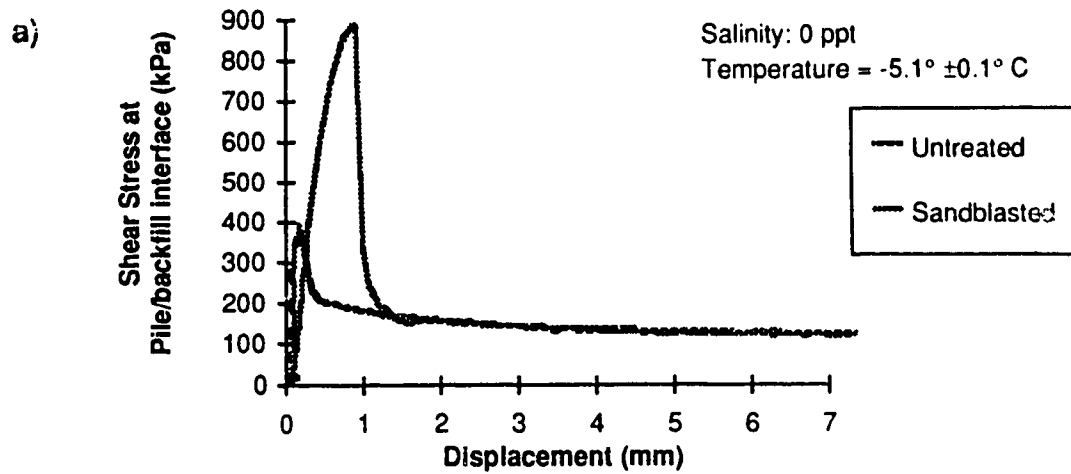


Figure D.39: Comparison of pipe surface treatment effect on pile performance  
a) 33 mm pile  
b) 102 mm pile



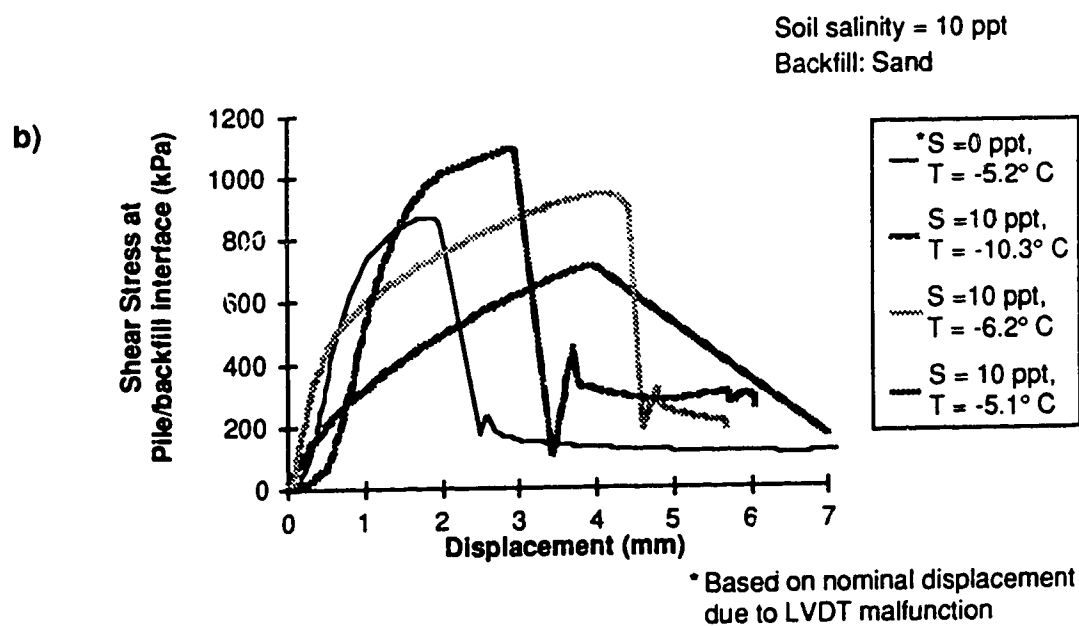
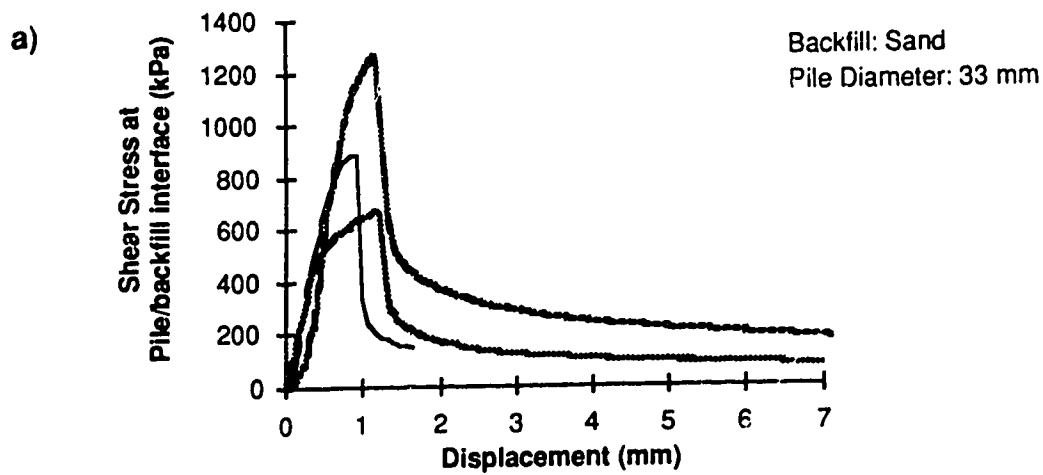


Figure D.40: Comparison of effect of temperature, sand backfilled piles, S = 10 ppt  
a) 33 mm pile  
b) 102 mm pile

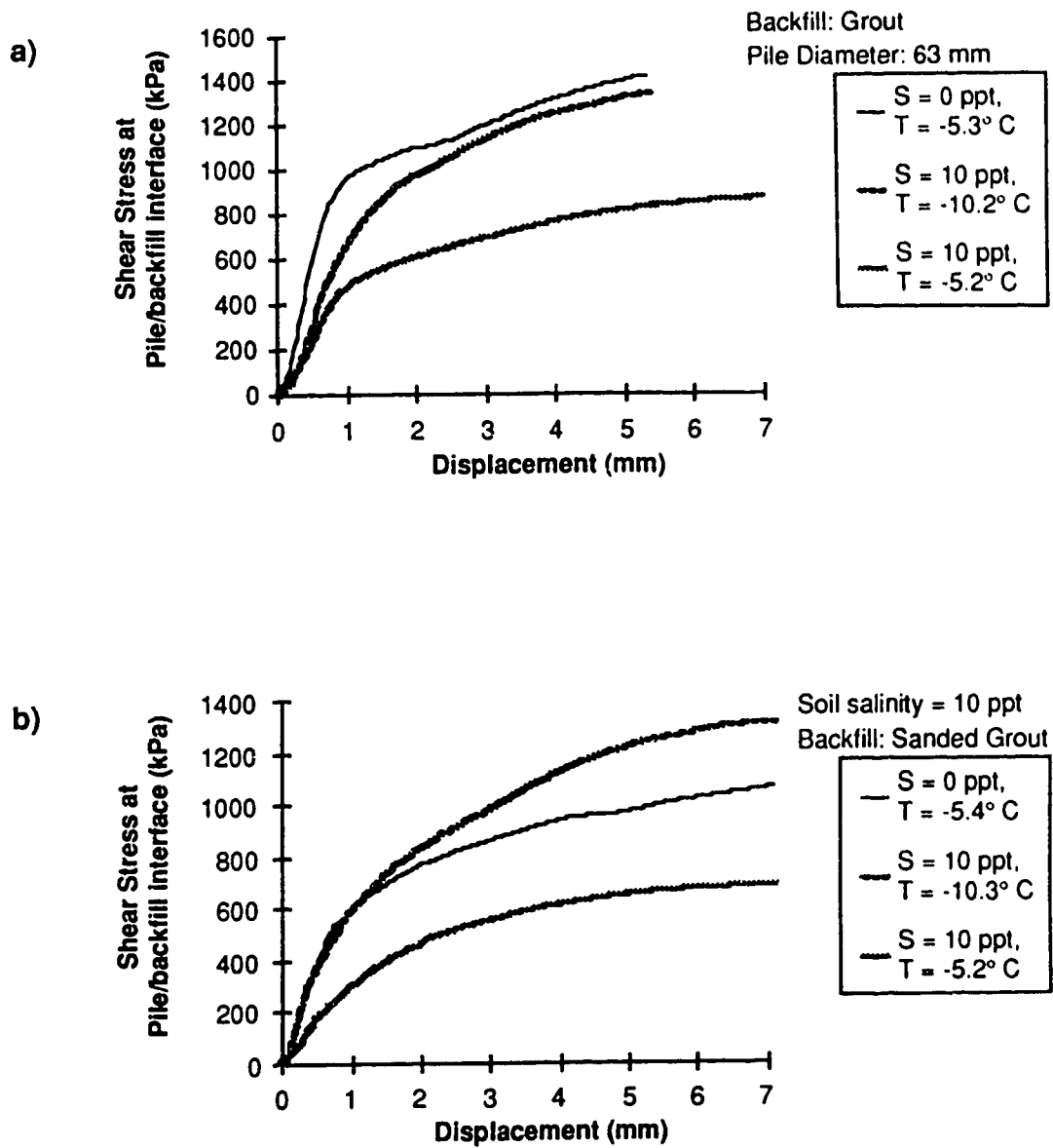


Figure D.41: Comparison of effect of temperature, grout backfilled piles, S = 10 ppt  
a) 63 mm pile  
b) 102 mm pile

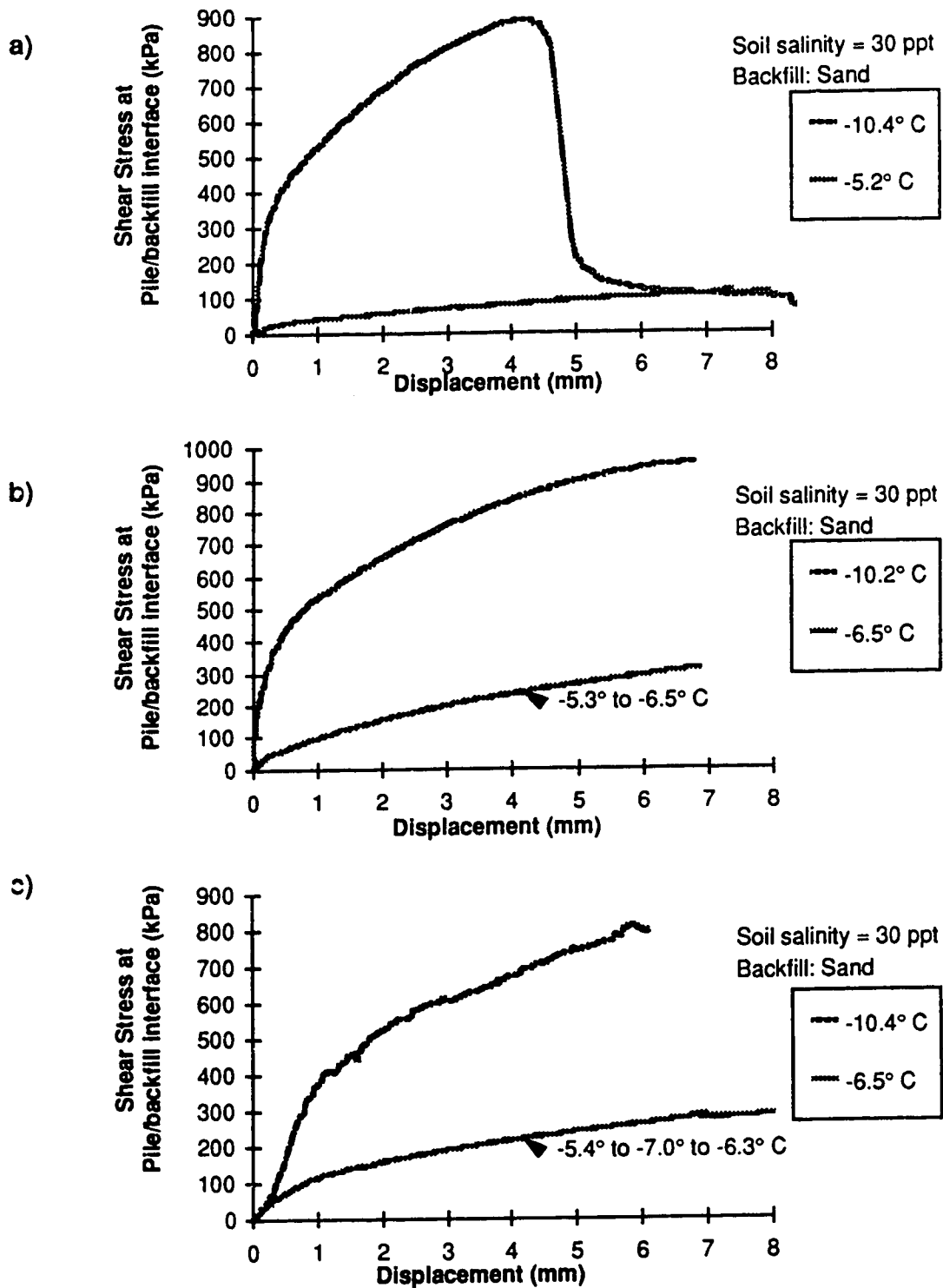


Figure D.42: Comparison of effect of temperature, sand backfilled piles, S = 30 ppt

- a) 33 mm pile
- b) 63 mm pile
- c) 102 mm pile

**APPENDIX E**  
**CONSTANT LOAD**

**MODEL PILE TEST RESULTS**

Load, displacement and temperature versus time

Log displacement rate versus log time

Regression analysis of attenuating displacement rate parameters

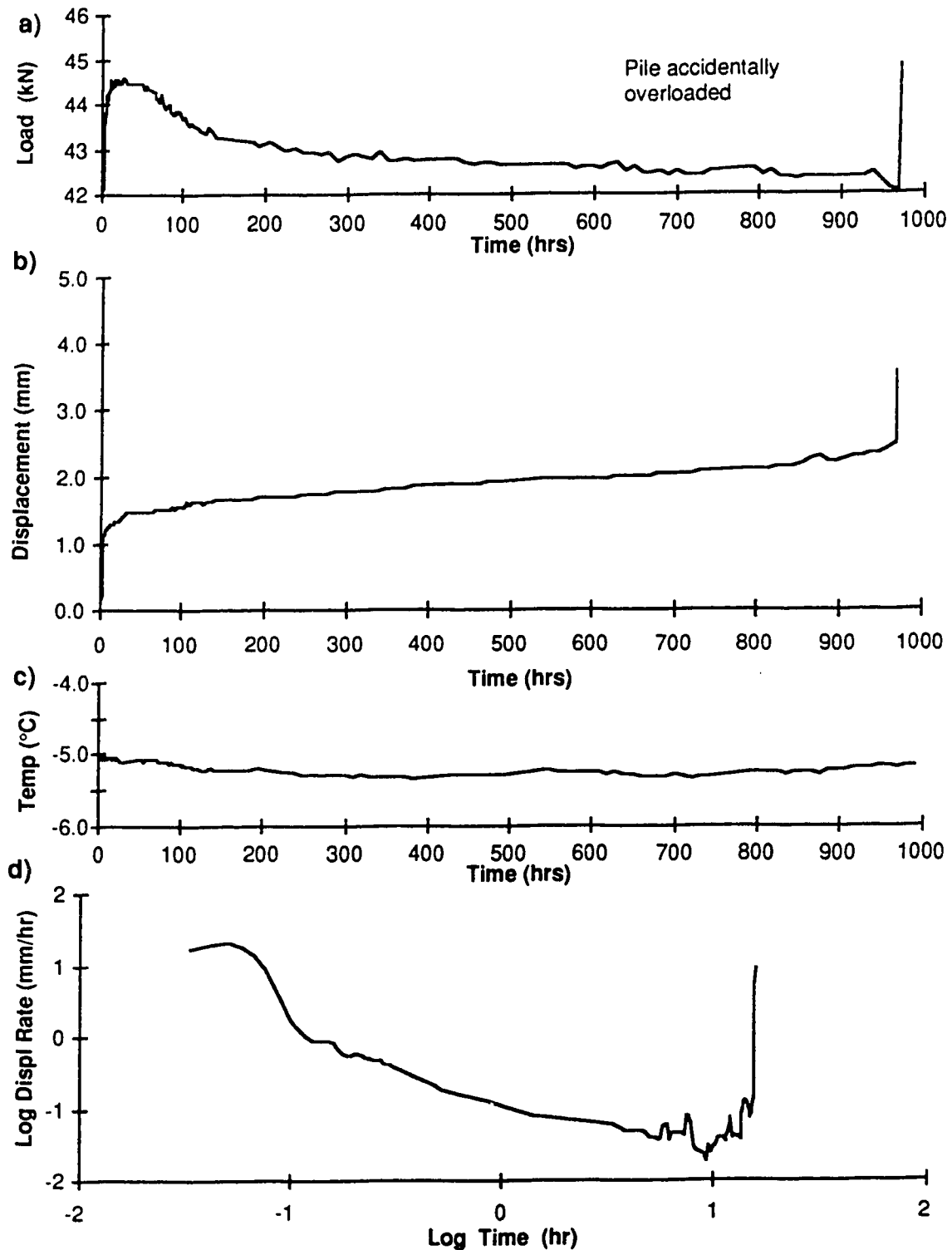


Figure E.1: Test #19-63, 0 ppt, Sand backfill, 537 kPa

- a) load vs time
- b) displacement vs time
- c) temperature vs time
- d) log displacement rate vs log time

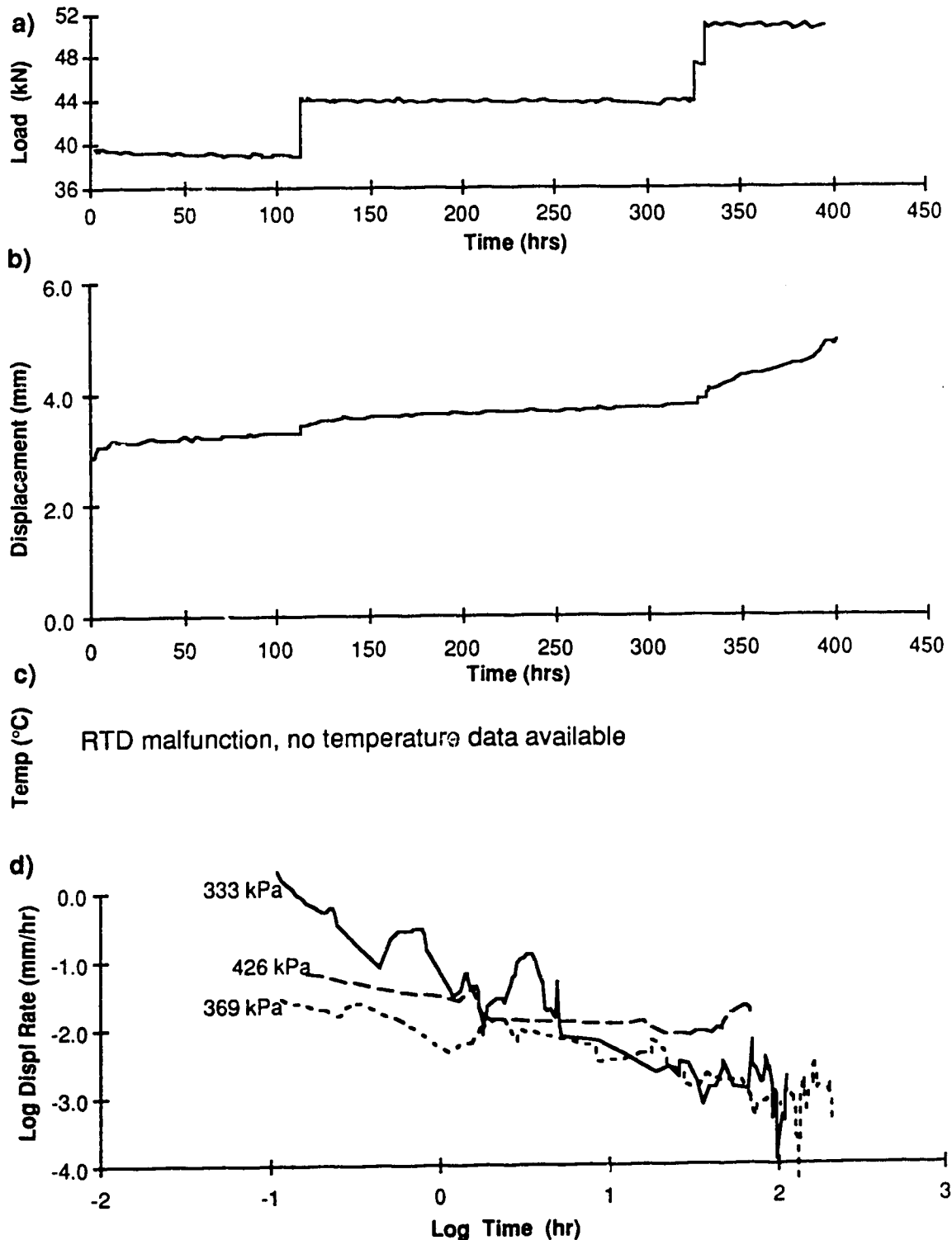


Figure E.2: Test #19-102, 0 ppt, Sand backfill, 333, 369, 426 kPa

- a) load vs time
- b) displacement vs time
- c) temperature vs time
- d) log displacement rate vs log time

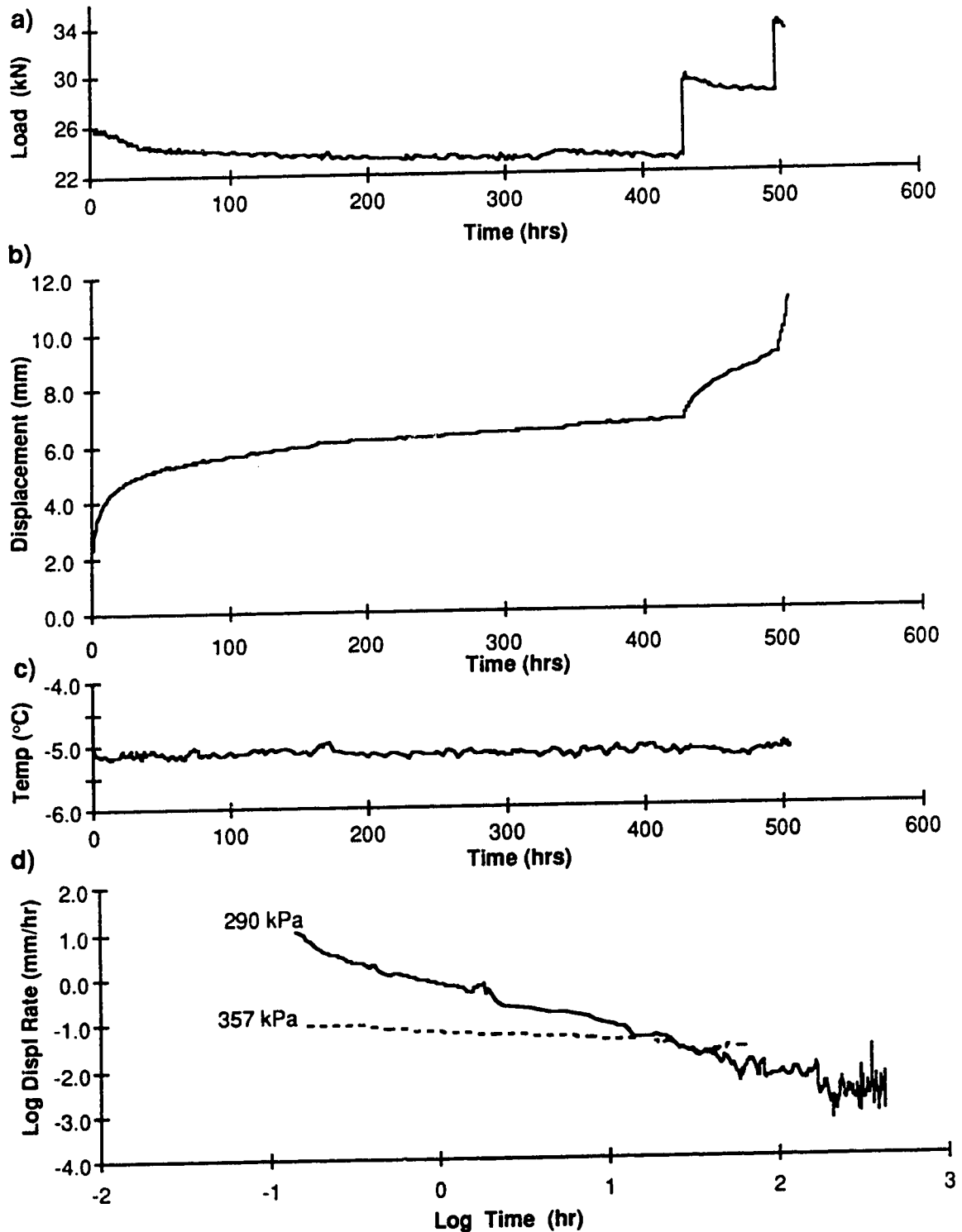


Figure E.3: Test #20-63, 10 ppt, Sand backfill, 290, 357 kPa  
a) load vs time  
b) displacement vs time  
c) temperature vs time  
d) log displacement rate vs log time

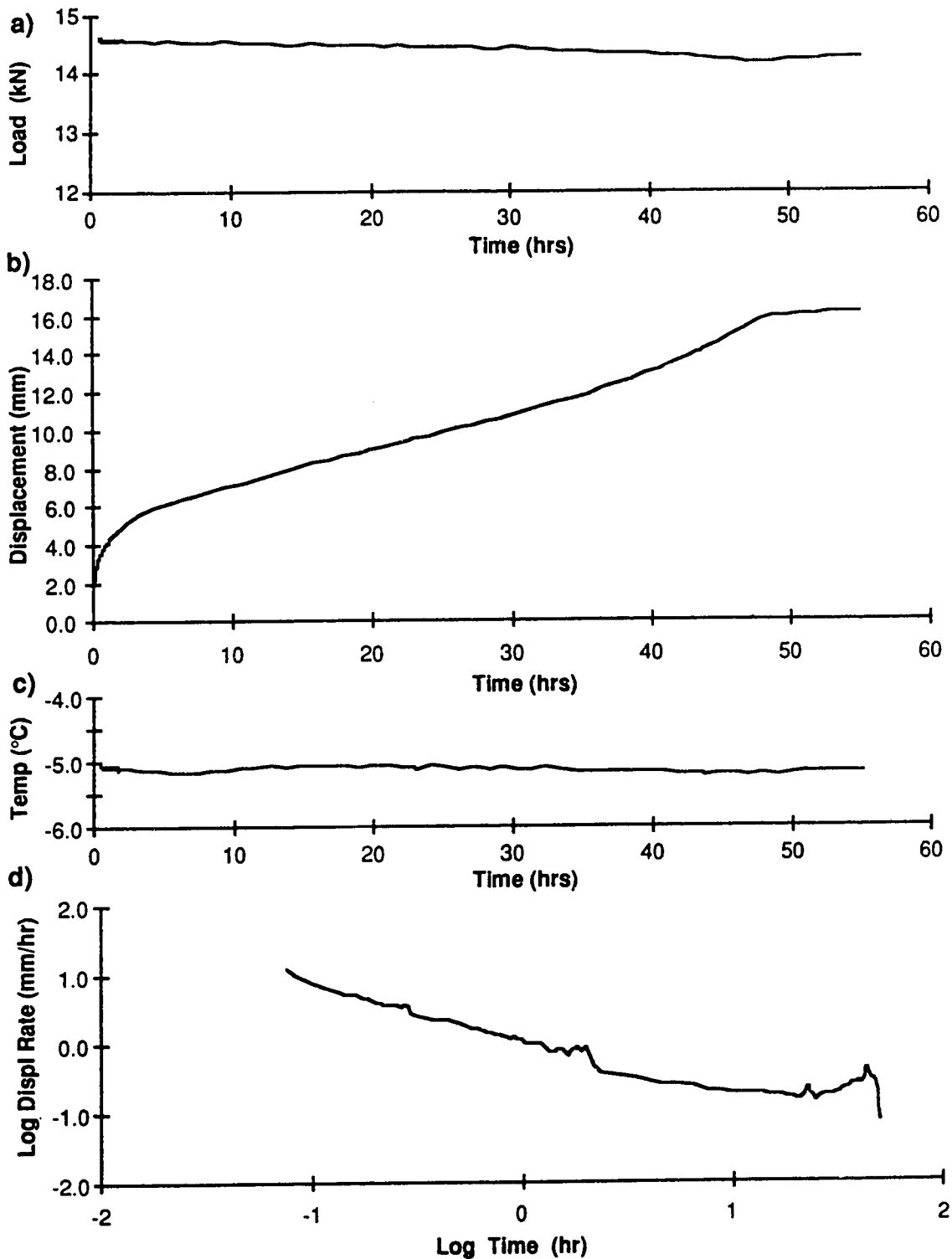


Figure E.4: Test #21-102, 10 ppt, Sand backfill, 195 kPa

- a) load vs time
- b) displacement vs time
- c) temperature vs time
- d) log displacement rate vs log time



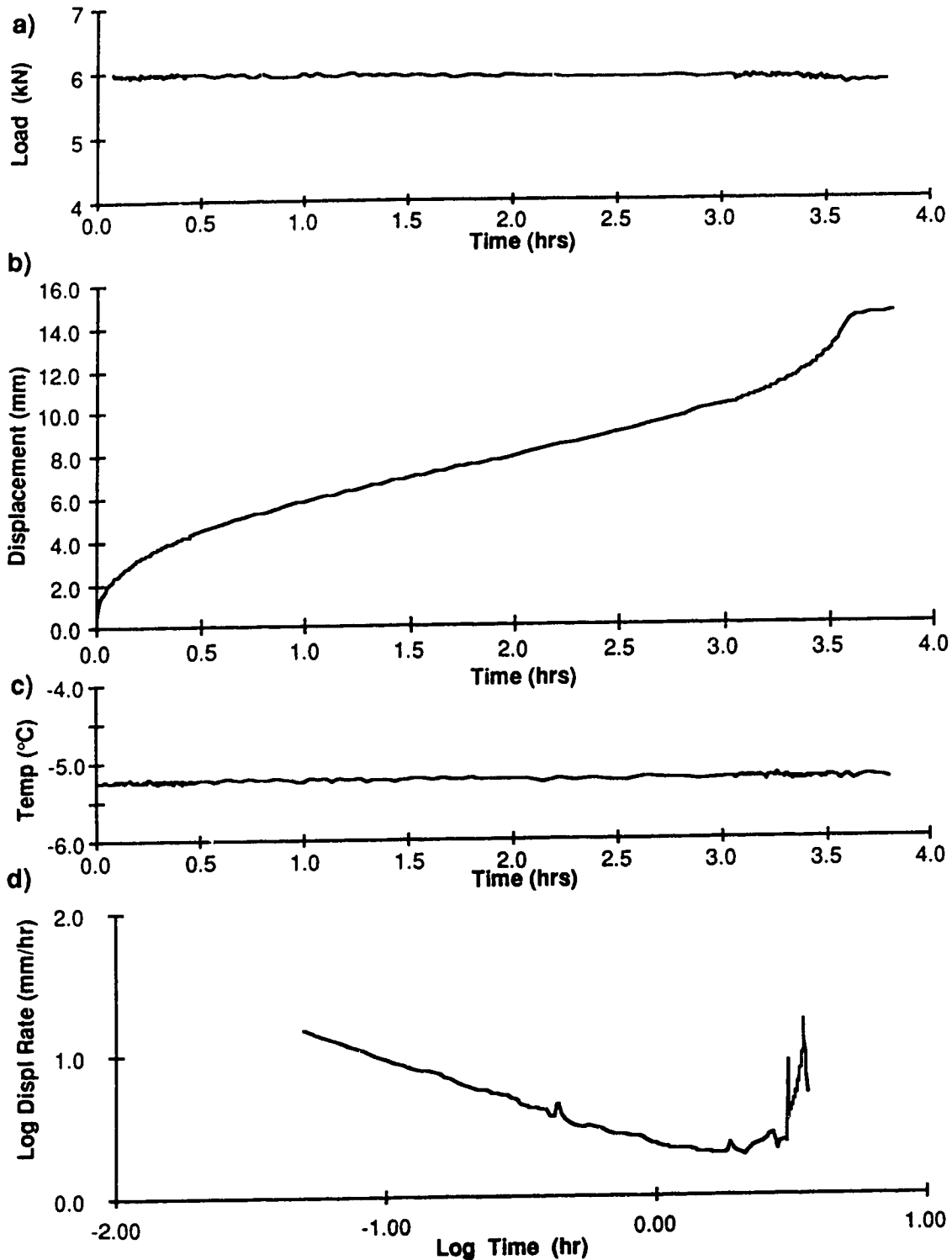


Figure E.5: Test #22-33, 30 ppt, Sand backfill, 147 kPa

- a) load vs time
- b) displacement vs time
- c) temperature vs time
- d) log displacement rate vs log time

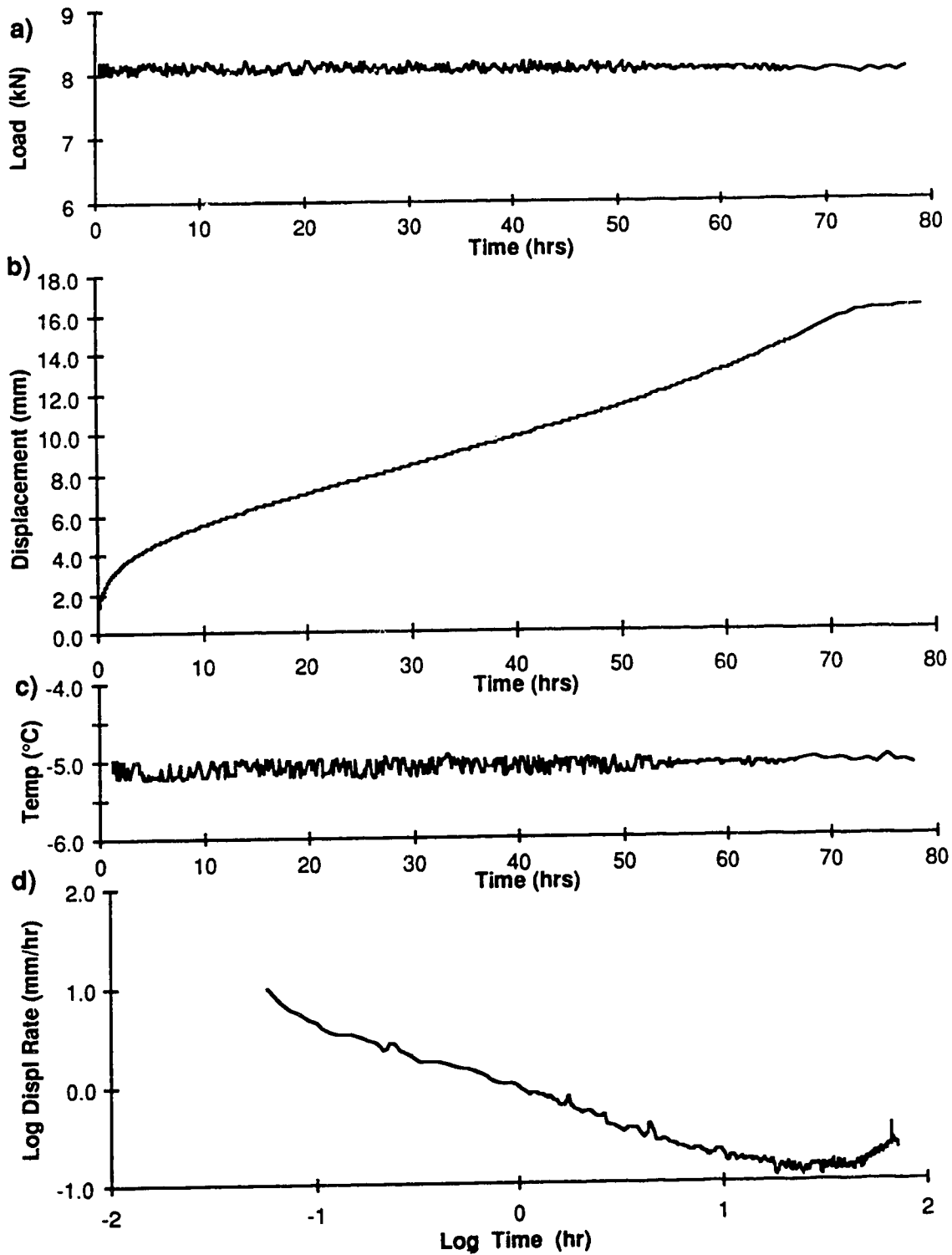


Figure E.6: Test #22-63, 30 ppt, Sand backfill, 101 kPa

- a) load vs time
- b) displacement vs time
- c) temperature vs time
- d) log displacement rate vs log time

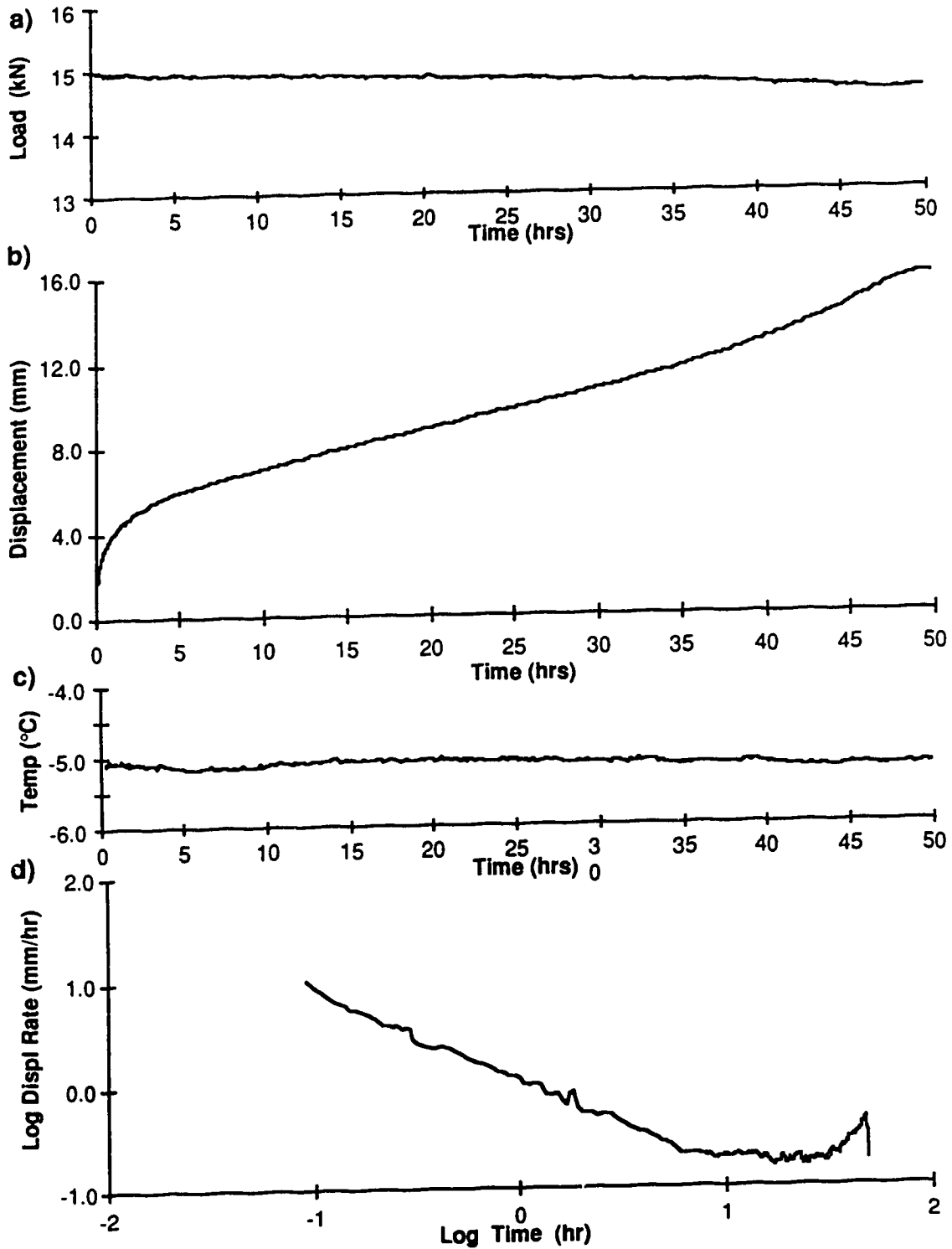


Figure E.7: Test #22-102, 30 ppt, Sand backfill, 124 kPa

- a) load vs time
- b) displacement vs time
- c) temperature vs time
- d) log displacement rate vs log time

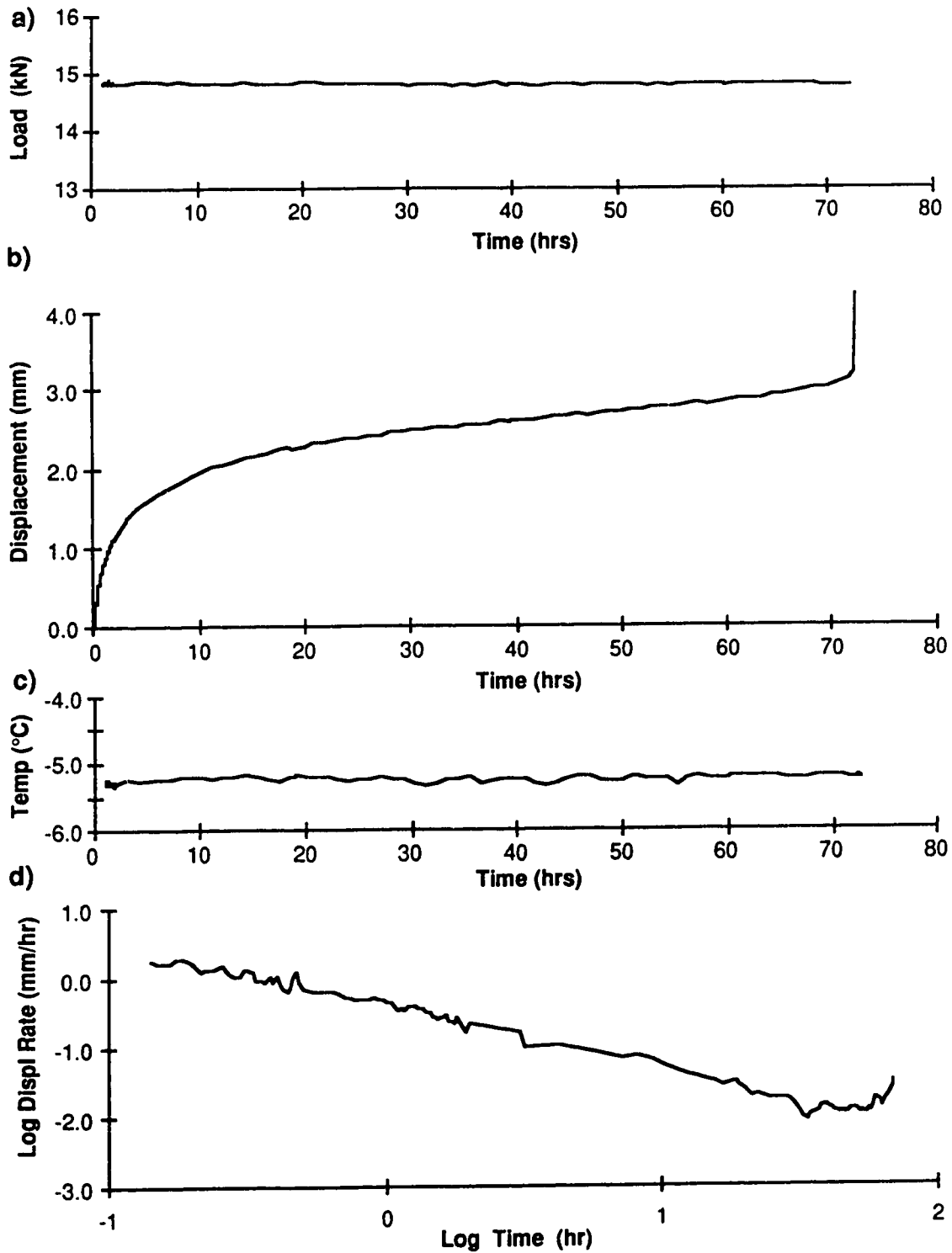


Figure E.8: Test #24-33, 10 ppt, Sand backfill, 362 kPa

- a) load vs time
- b) displacement vs time
- c) temperature vs time
- d) log displacement rate vs log time

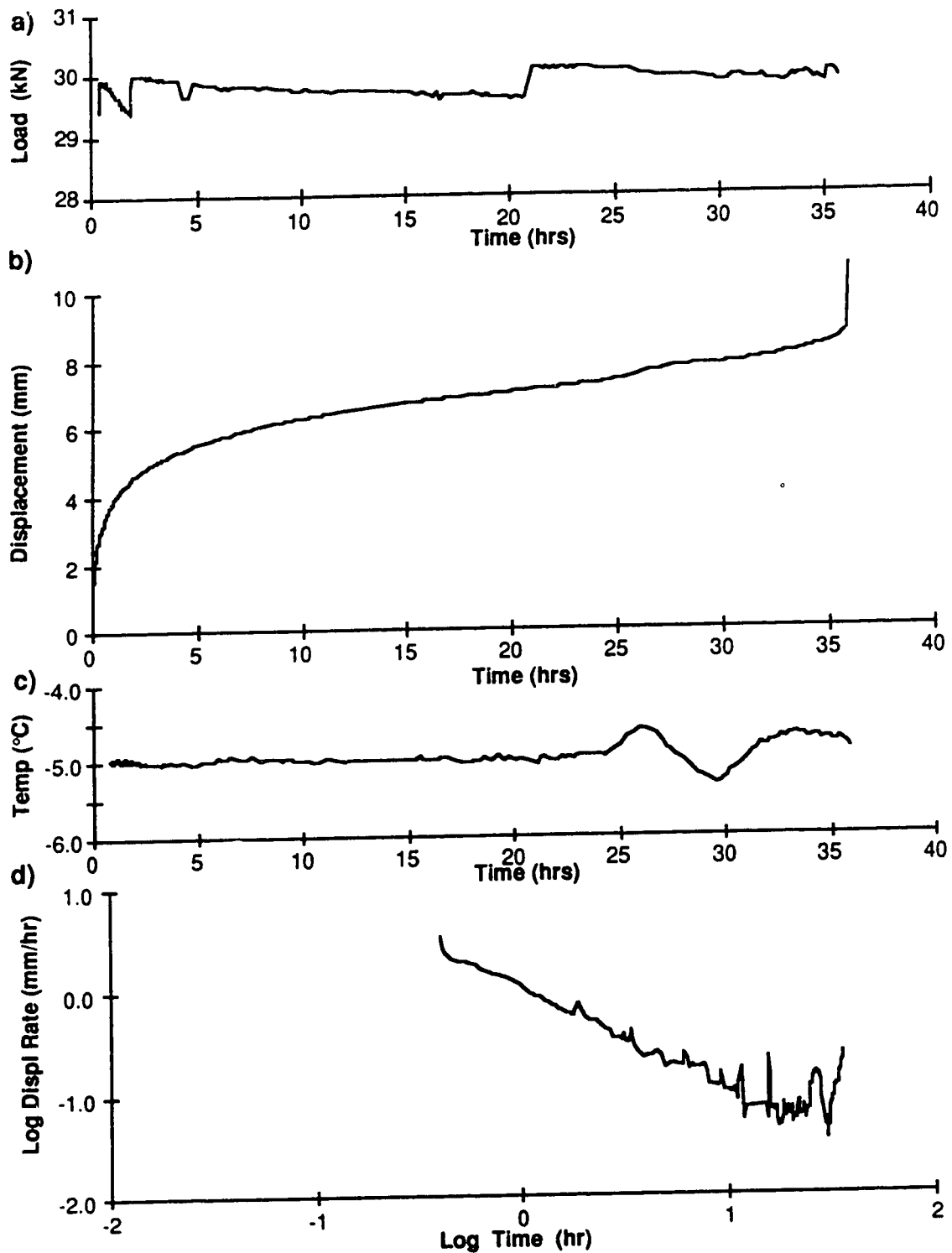


Figure E.9: Test #24-63, 10 ppt, Sand backfill, 365 kPa

- a) load vs time
- b) displacement vs time
- c) temperature vs time
- d) log displacement rate vs log time

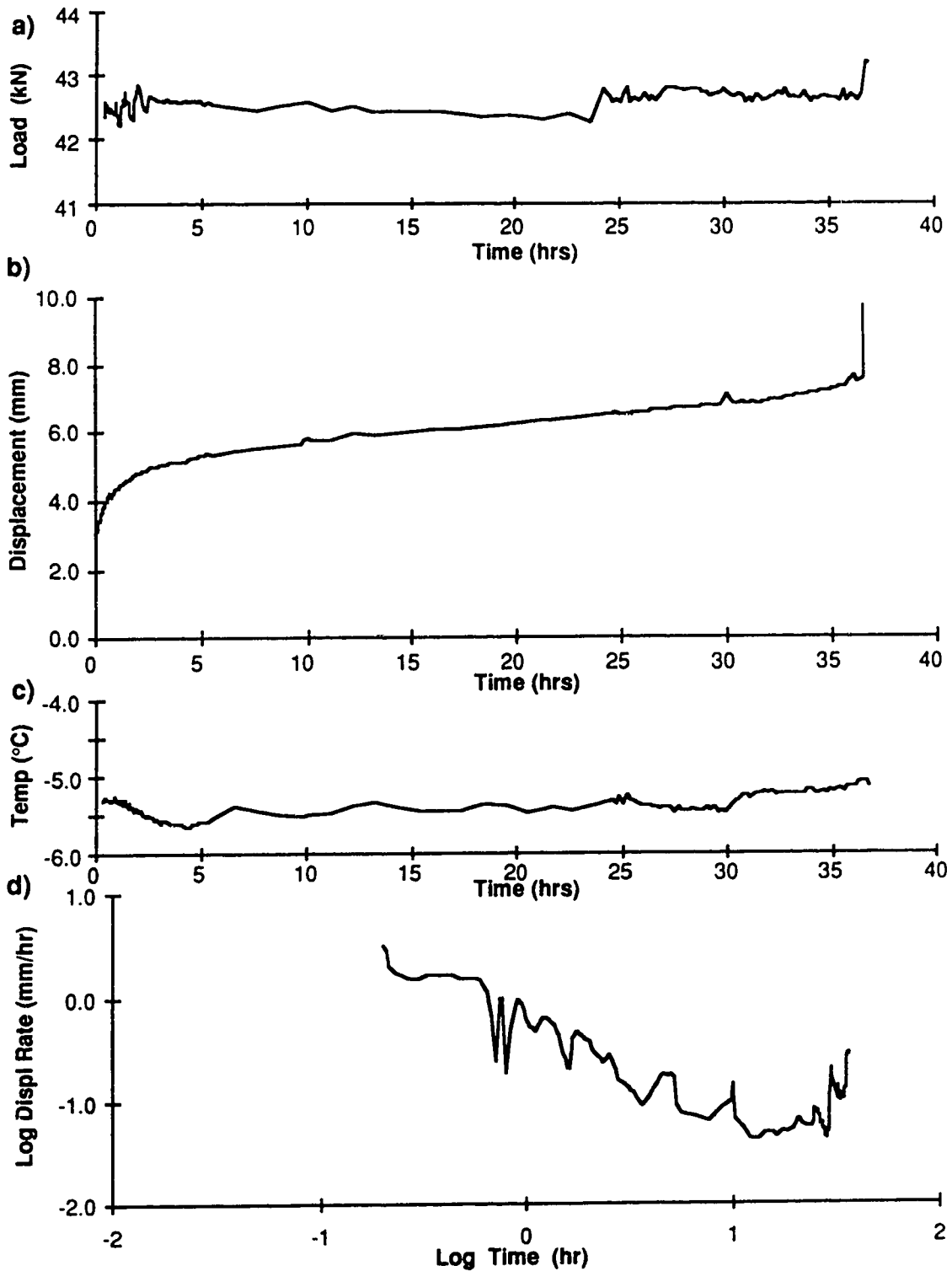


Figure E.10: Test #24-102, 10 ppt, Sand backfill, 356 kPa

- a) load vs time
- b) displacement vs time
- c) temperature vs time
- d) log displacement rate vs log time

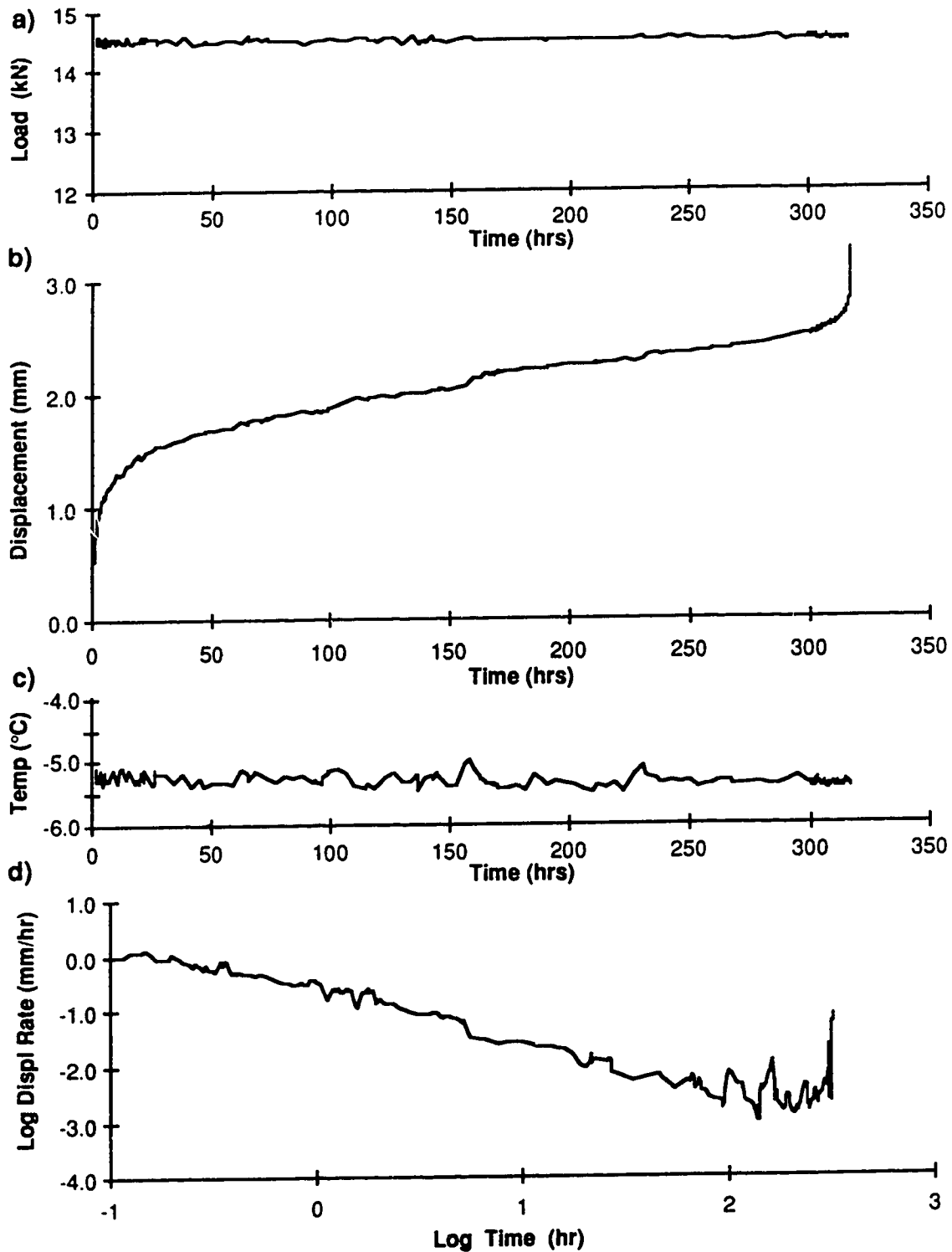


Figure E.11: Test #25-33, 10 ppt, Sand backfill, 355 kPa

- a) load vs time
- b) displacement vs time
- c) temperature vs time
- d) log displacement rate vs log time

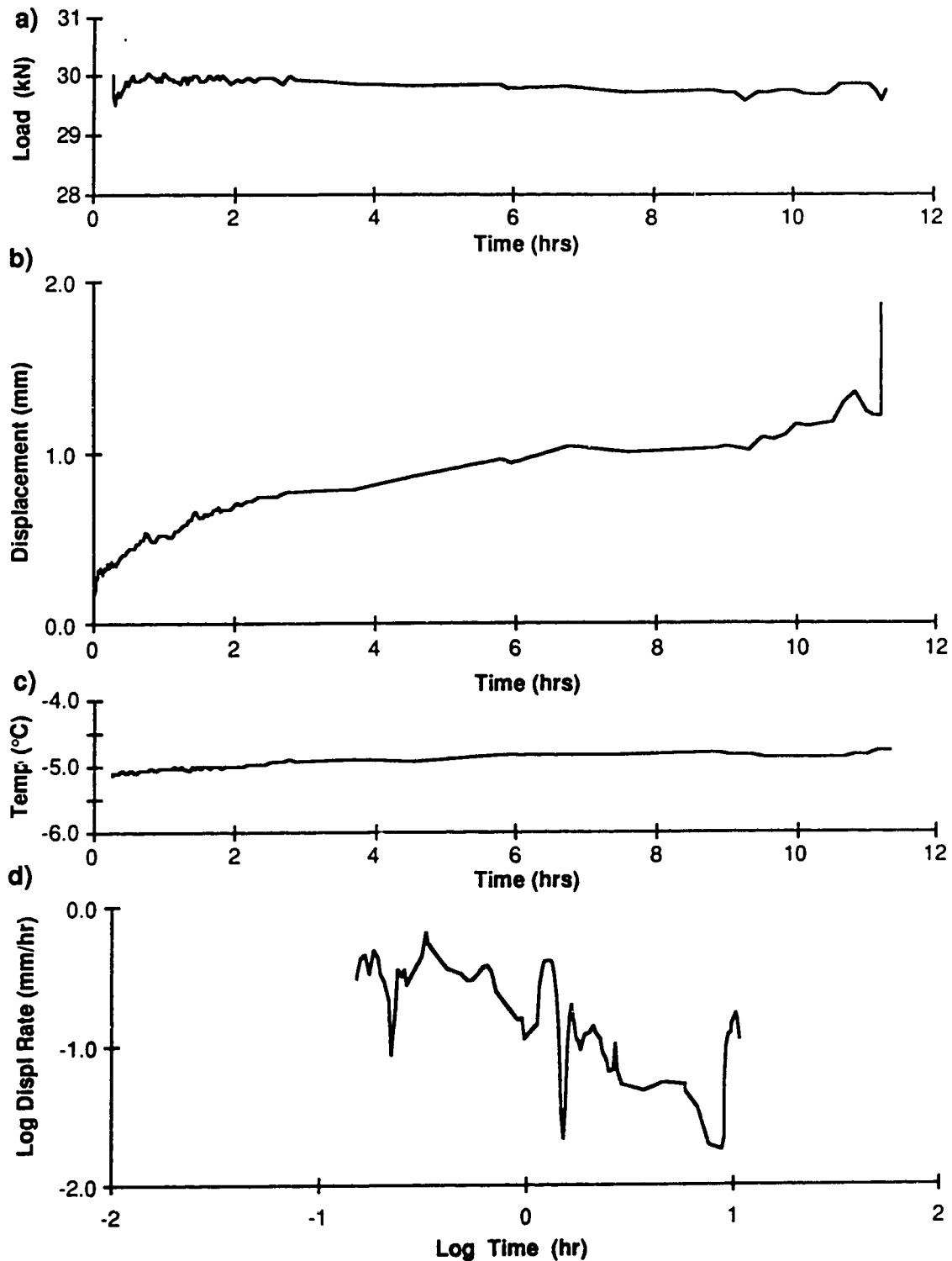


Figure E.12: Test #25-63, 10 ppt, Sand backfill, 373 kPa

- a) load vs time
- b) displacement vs time
- c) temperature vs time
- d) log displacement rate vs log time



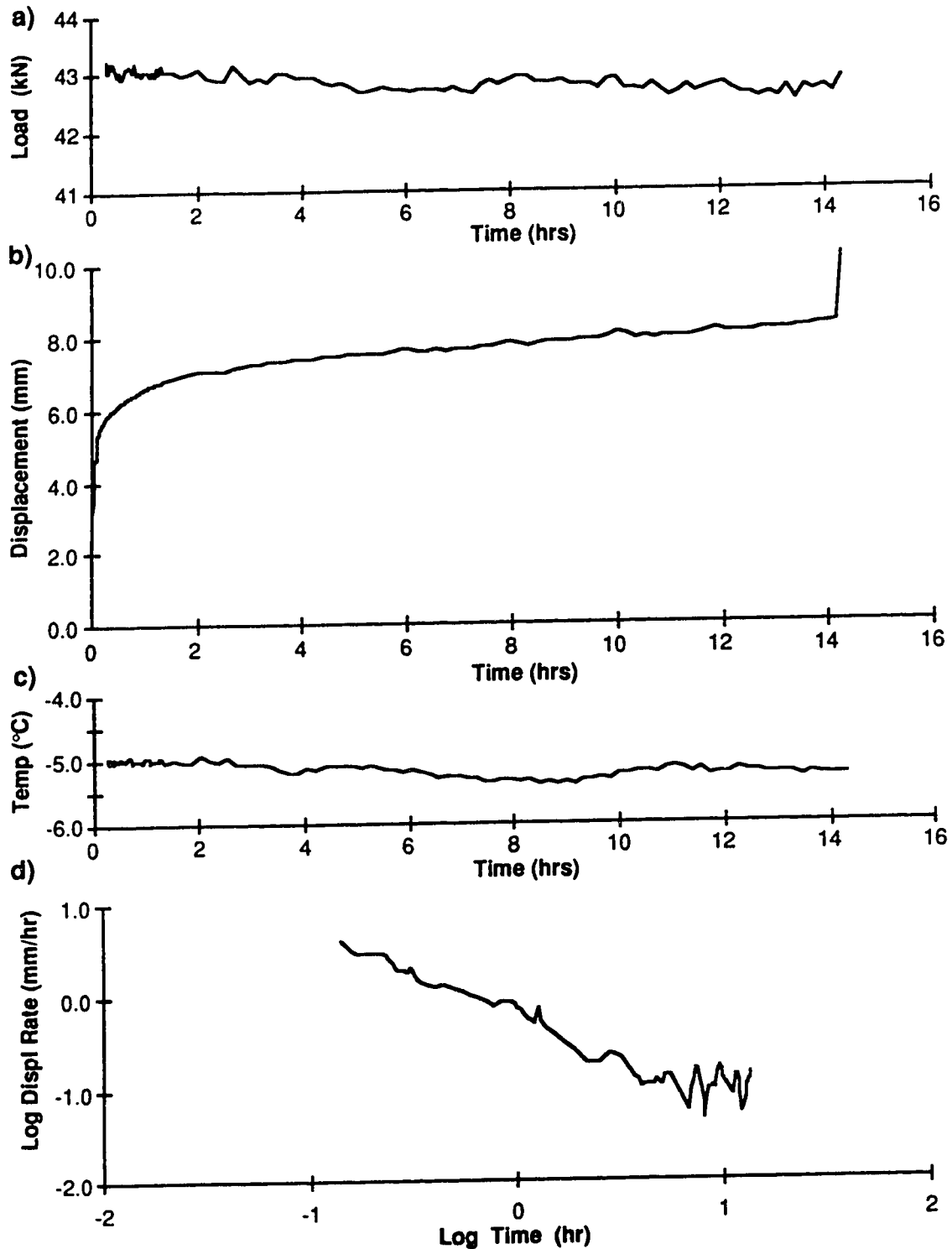


Figure E.13: Test #25-102, 10 ppt, Sand backfill, 359 kPa

- a) load vs time
- b) displacement vs time
- c) temperature vs time
- d) log displacement rate vs log time

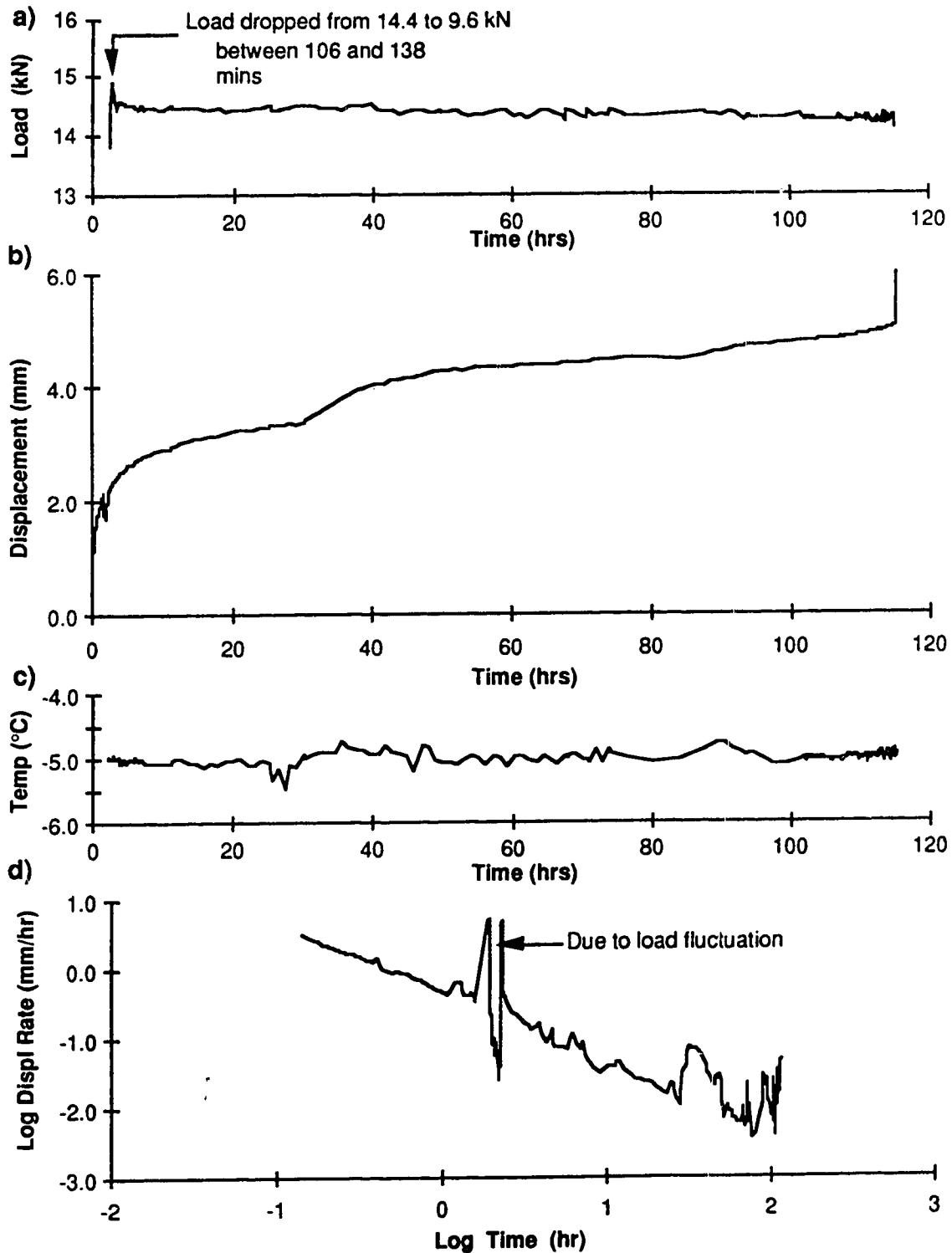


Figure E.14: Test #26-33, 10 ppt, Sand backfill, 353 kPa

- a) load vs time
- b) displacement vs time
- c) temperature vs time
- d) log displacement rate vs log time

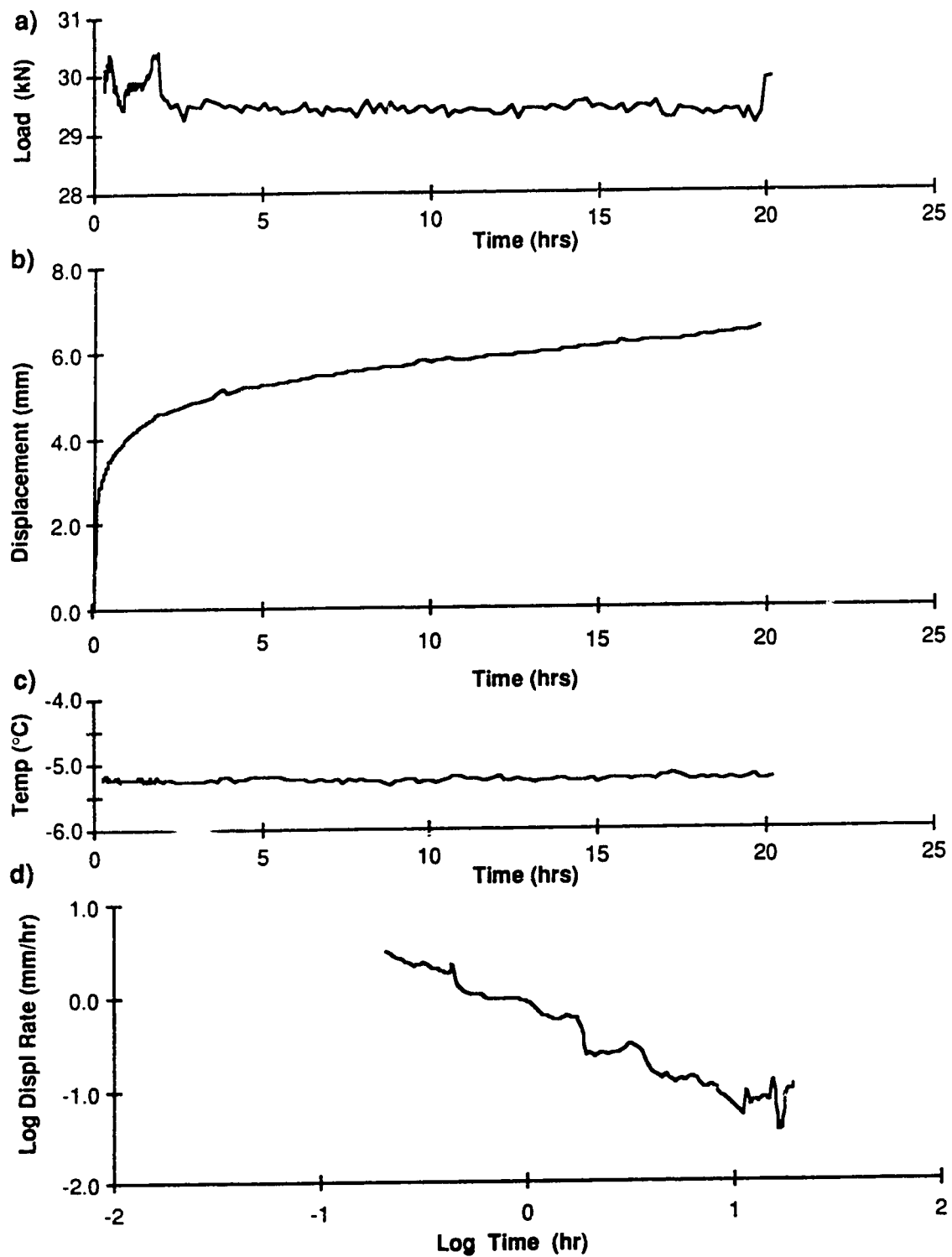


Figure E.15: Test #26-63, 10 ppt, Sand backfill, 367 kPa

- a) load vs time
- b) displacement vs time
- c) temperature vs time
- d) log displacement rate vs log time

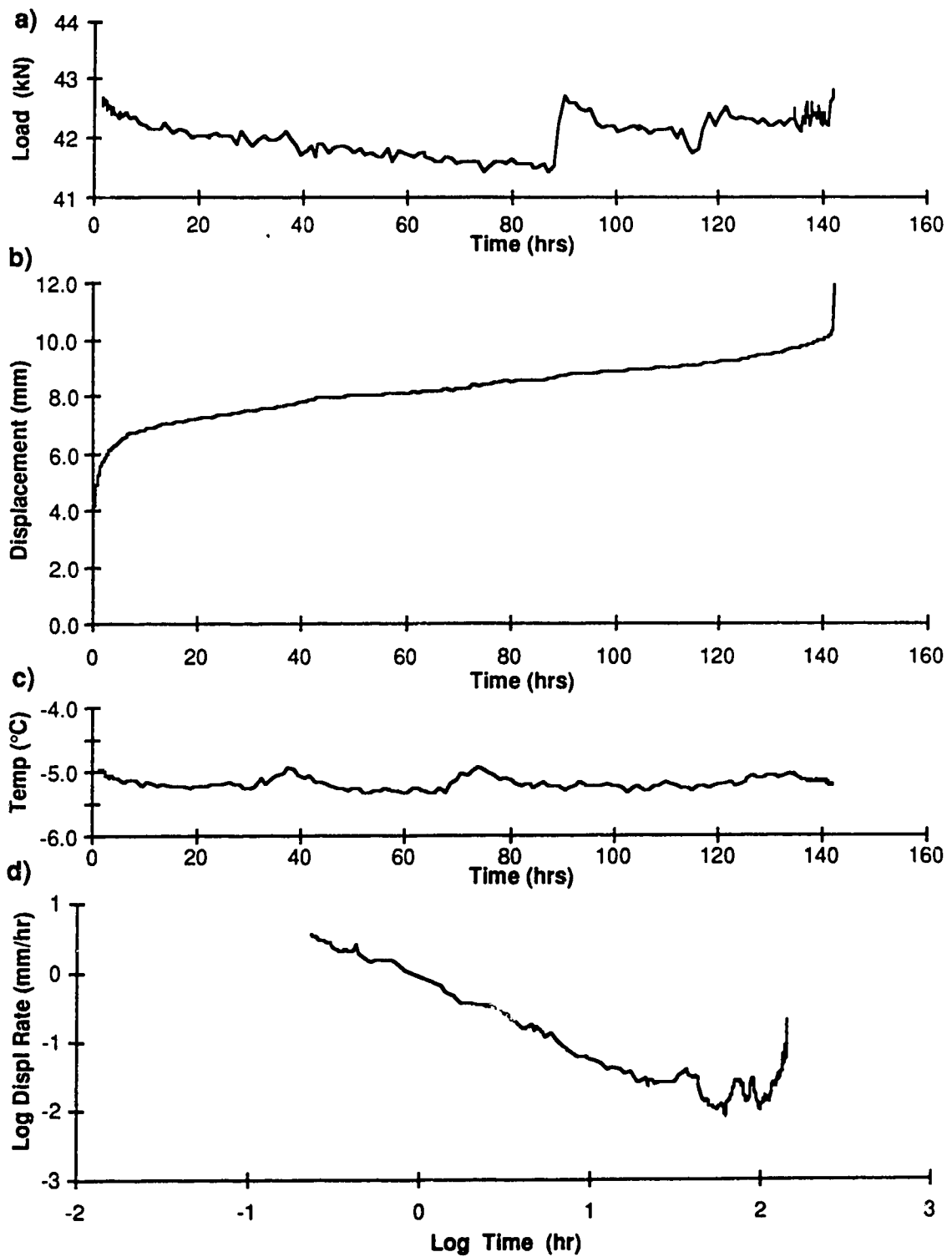


Figure E.16: Test #26-102, 10 ppt, Sand backfill, 355 kPa

- a) load vs time
- b) displacement vs time
- c) temperature vs time
- d) log displacement rate vs log time

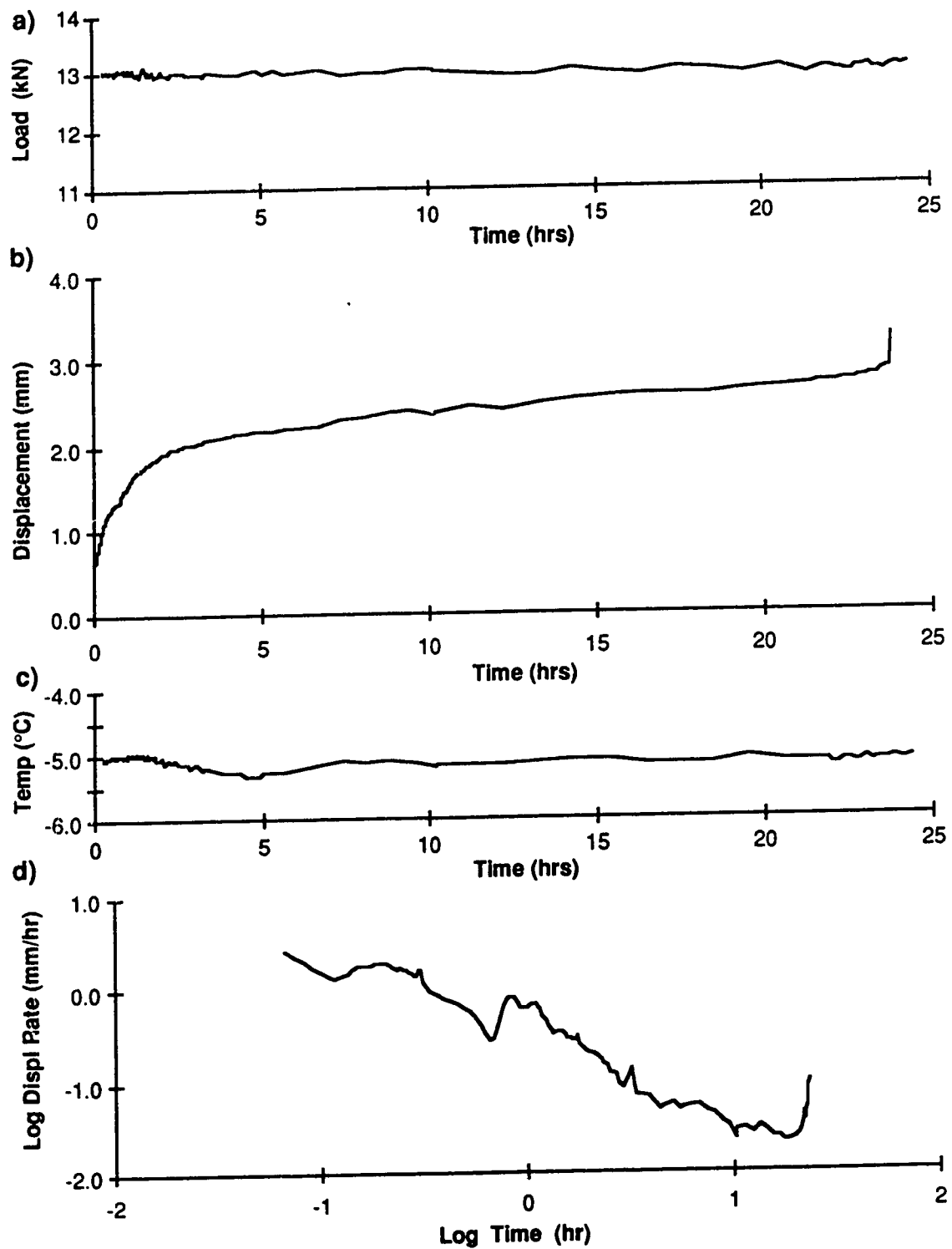


Figure E.17: Test #27-33, 10 ppt, Sand backfill, 318 kPa

- a) load vs time
- b) displacement vs time
- c) temperature vs time
- d) log displacement rate vs log time

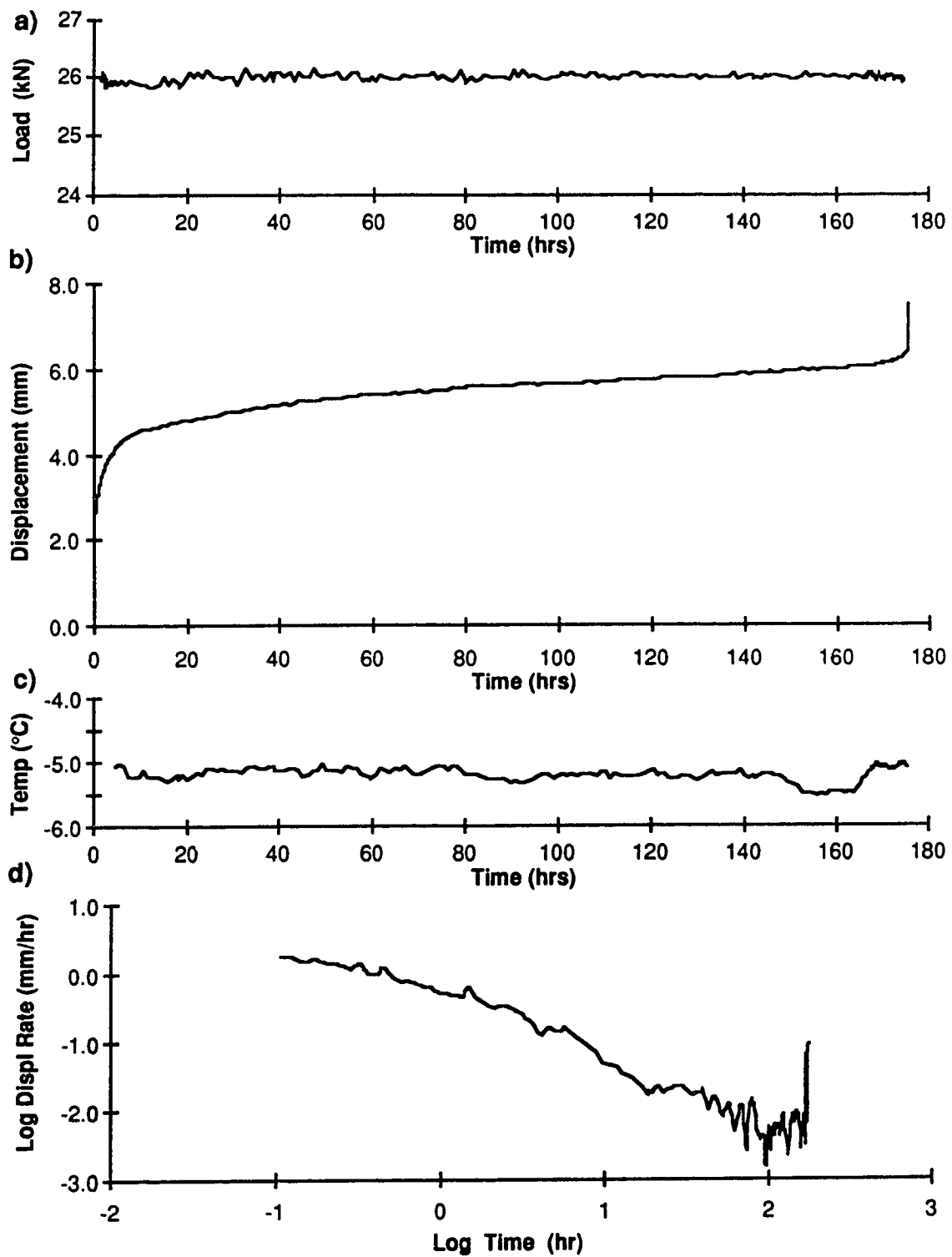


Figure E.18: Test #27-63, 10 ppt, Sand backfill, 325 kPa

- a) load vs time
- b) displacement vs time
- c) temperature vs time
- d) log displacement rate vs log time

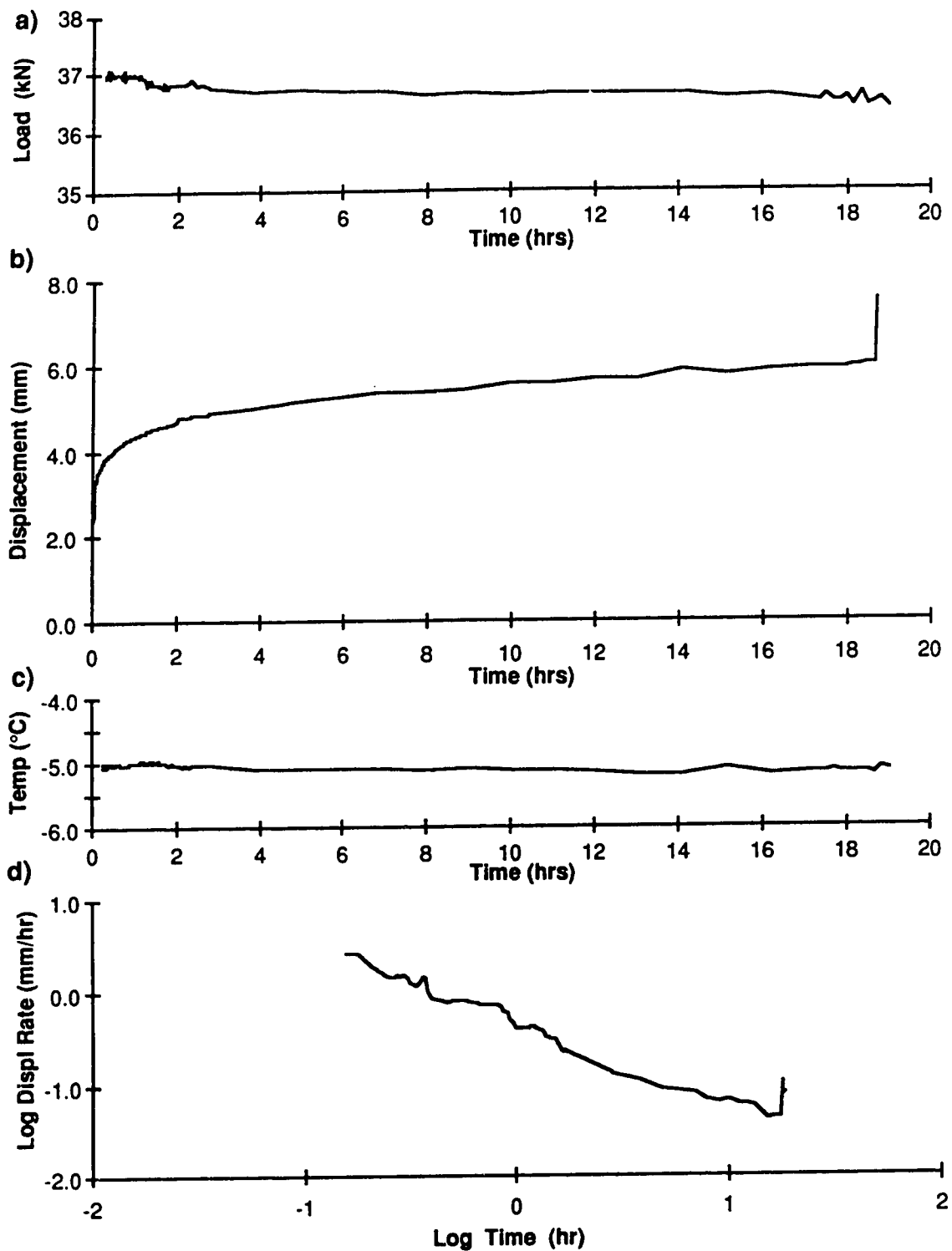


Figure E.19: Test #27-102, 10 ppt, Sand backfill, 307 kPa

- a) load vs time
- b) displacement vs time
- c) temperature vs time
- d) log displacement rate vs log time

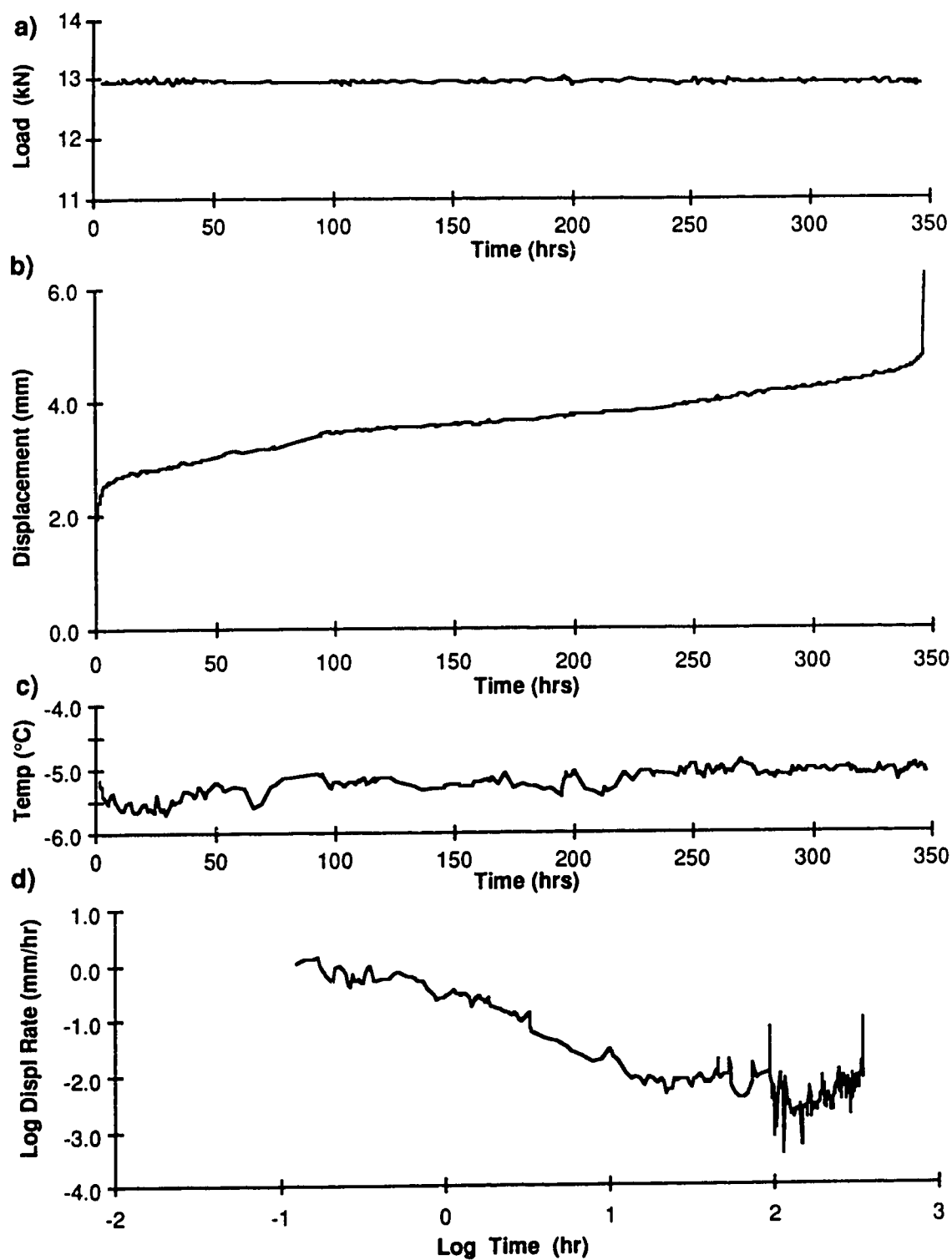


Figure E.20: Test #28-33, 10 ppt, Sand backfill, 312 kPa

- a) load vs time
- b) displacement vs time
- c) temperature vs time
- d) log displacement rate vs log time



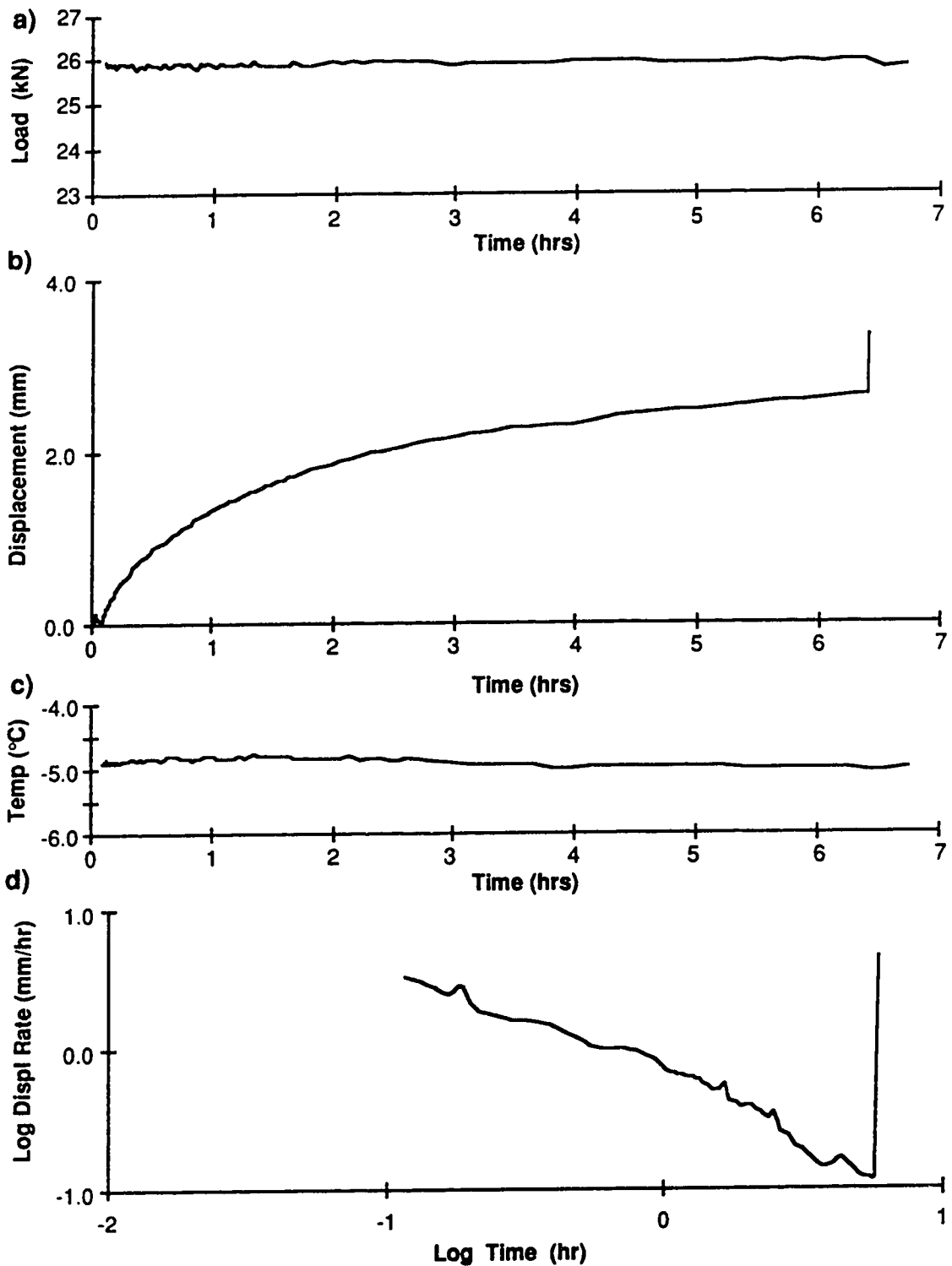


Figure E.21: Test #28-63, 10 ppt, Sand backfill, 317 kPa

- a) load vs time
- b) displacement vs time
- c) temperature vs time
- d) log displacement rate vs log time

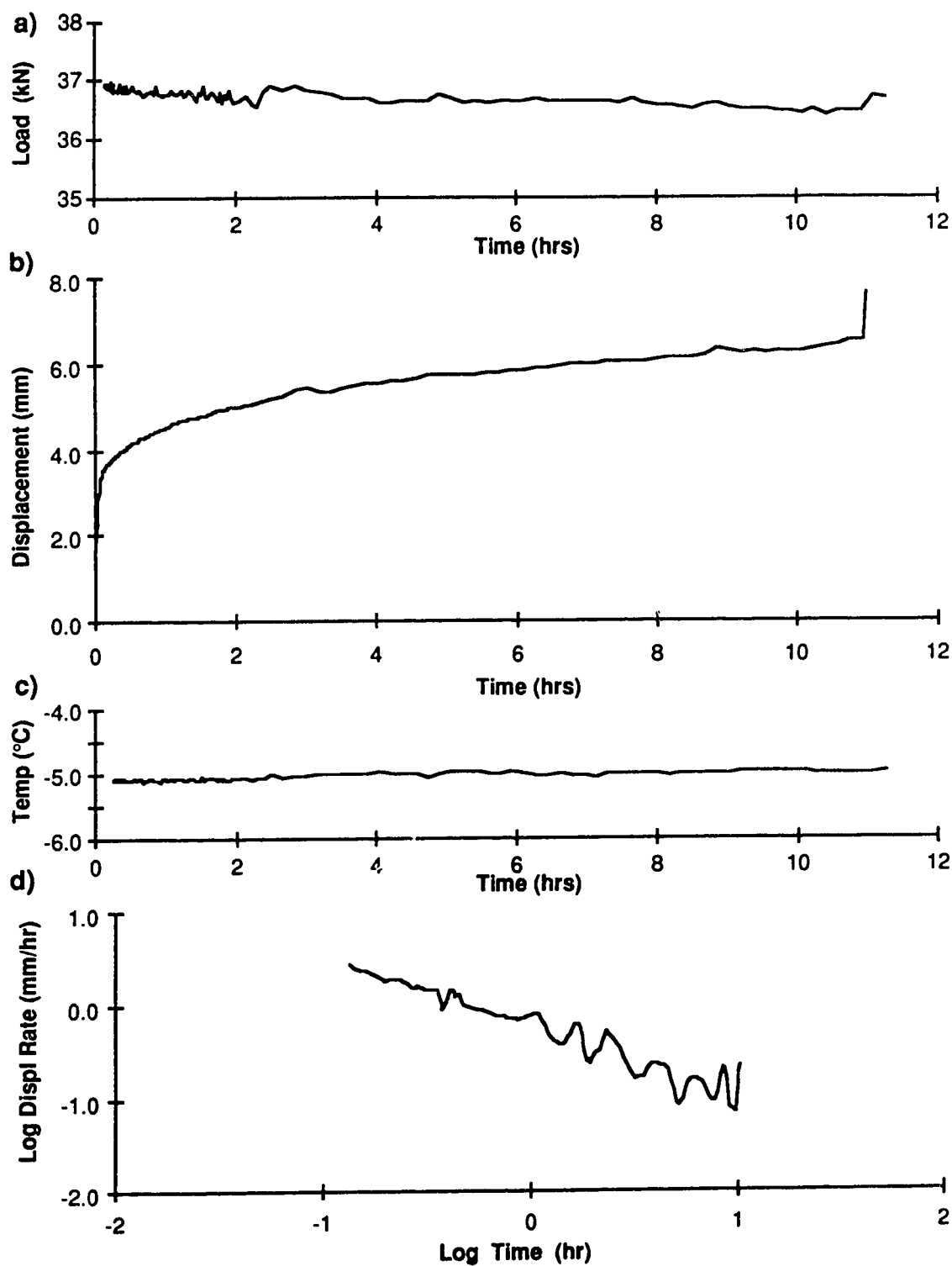


Figure E.22: Test #28-102, 10 ppt, Sand backfill, 301 kPa

- a) load vs time
- b) displacement vs time
- c) temperature vs time
- d) log displacement rate vs log time

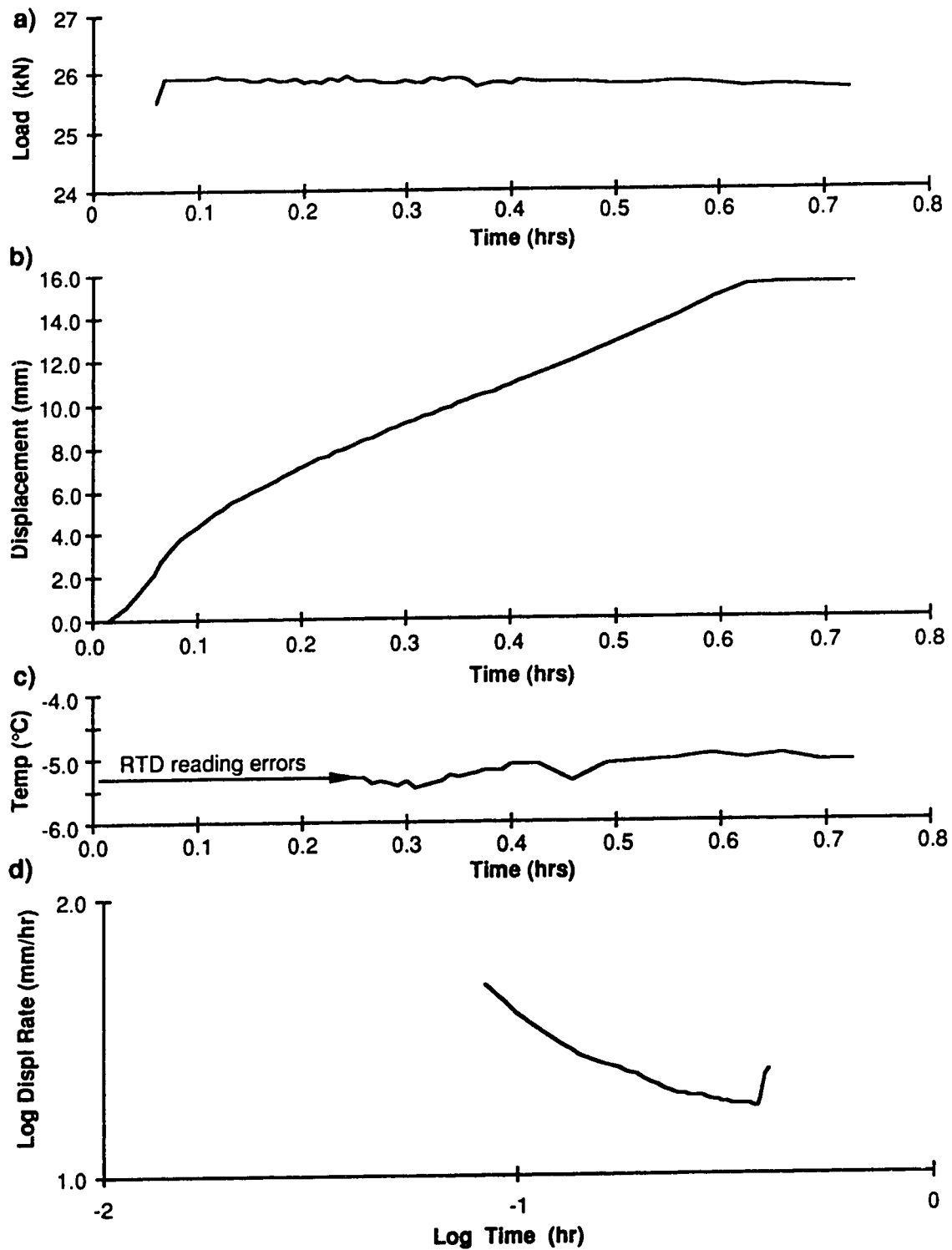


Figure E.23: Test #30-63, 30 ppt, Sand backfill, 323 kPa

- a) load vs time
- b) displacement vs time
- c) temperature vs time
- d) log displacement rate vs log time

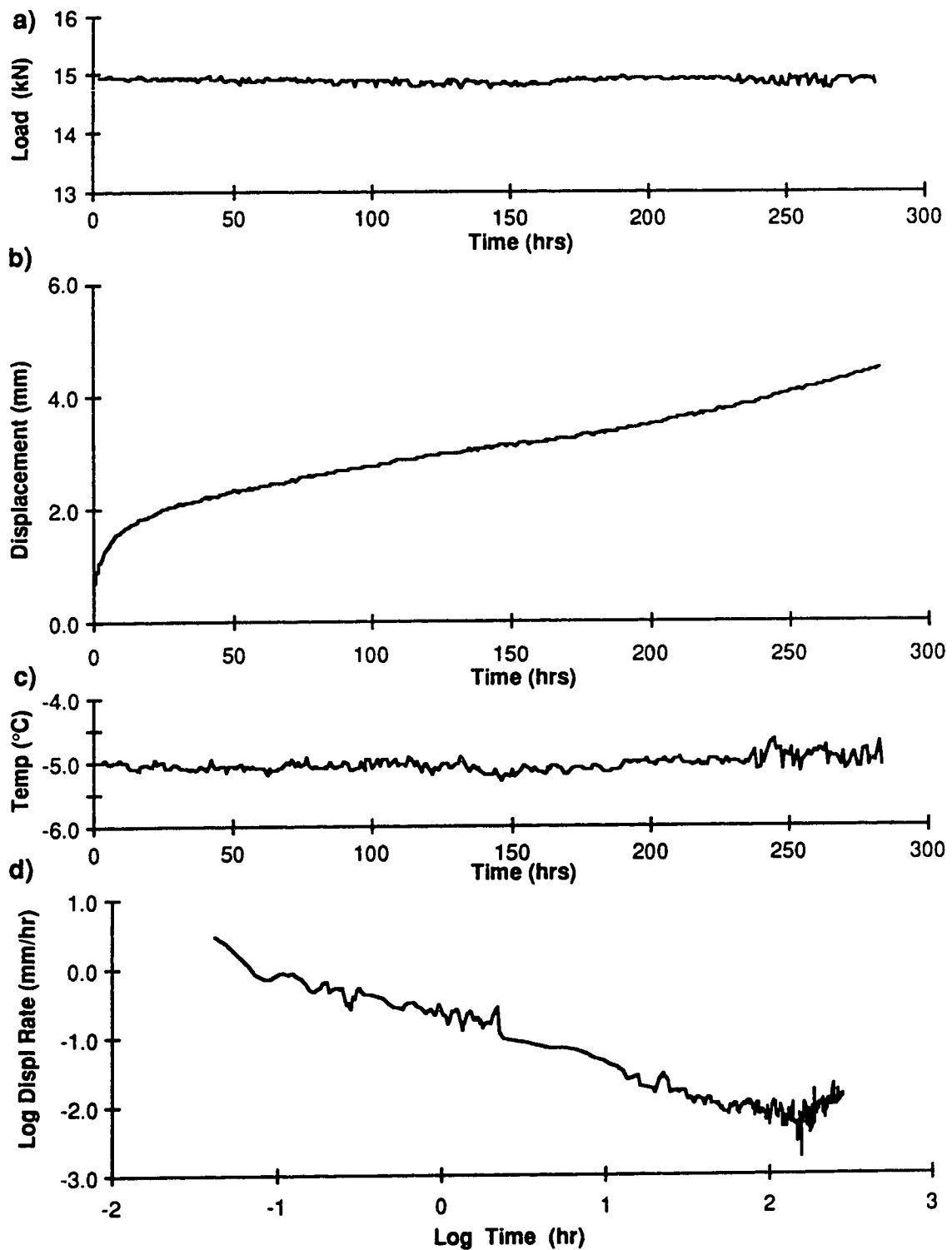


Figure E.24: Test #31-33, 10 ppt, Grout backfill, 365 kPa

- a) load vs time
- b) displacement vs time
- c) temperature vs time
- d) log displacement rate vs log time

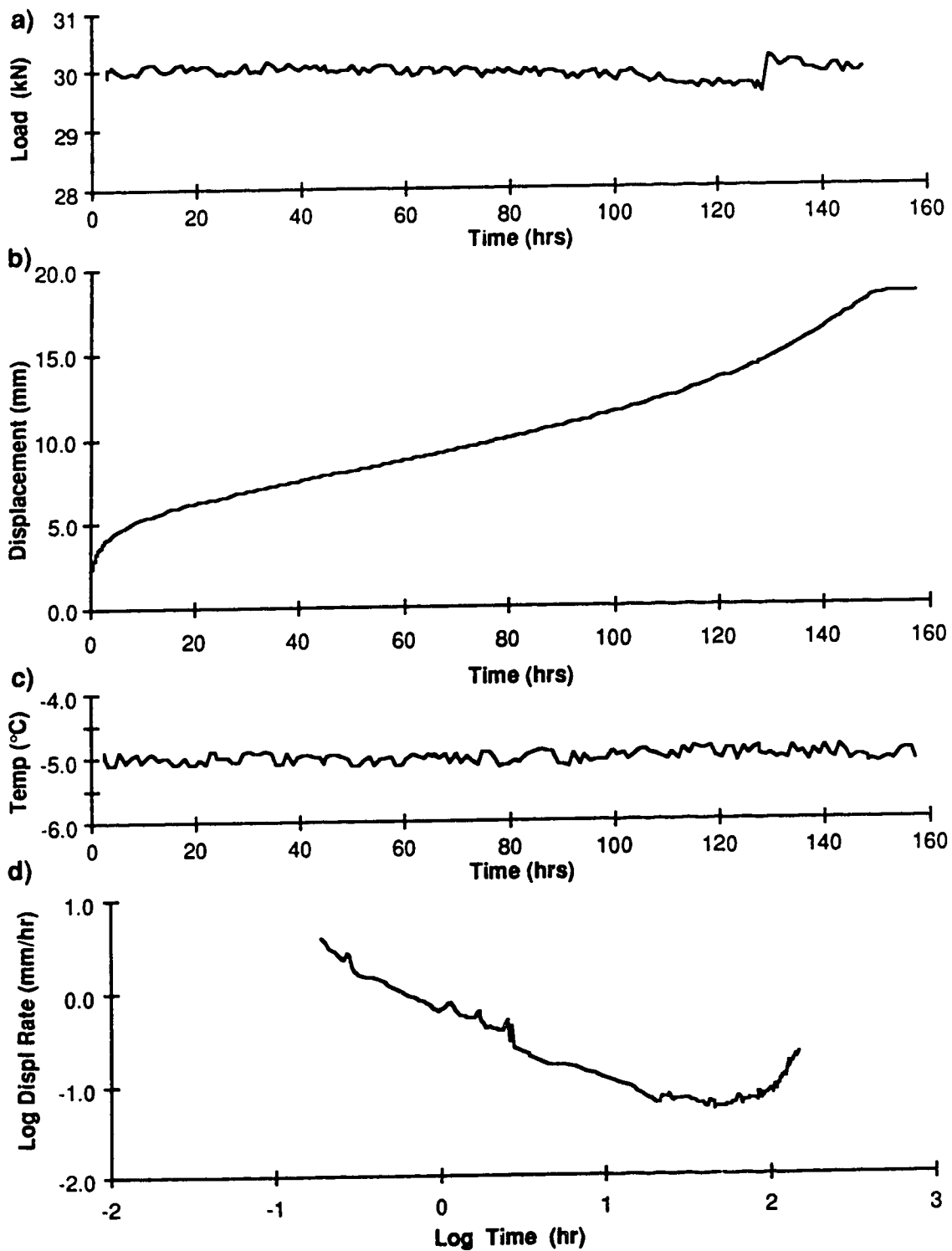


Figure E.25: Test #31-63, 10 ppt, Grout backfill, 374 kPa

- a) load vs time
- b) displacement vs time
- c) temperature vs time
- d) log displacement rate vs log time

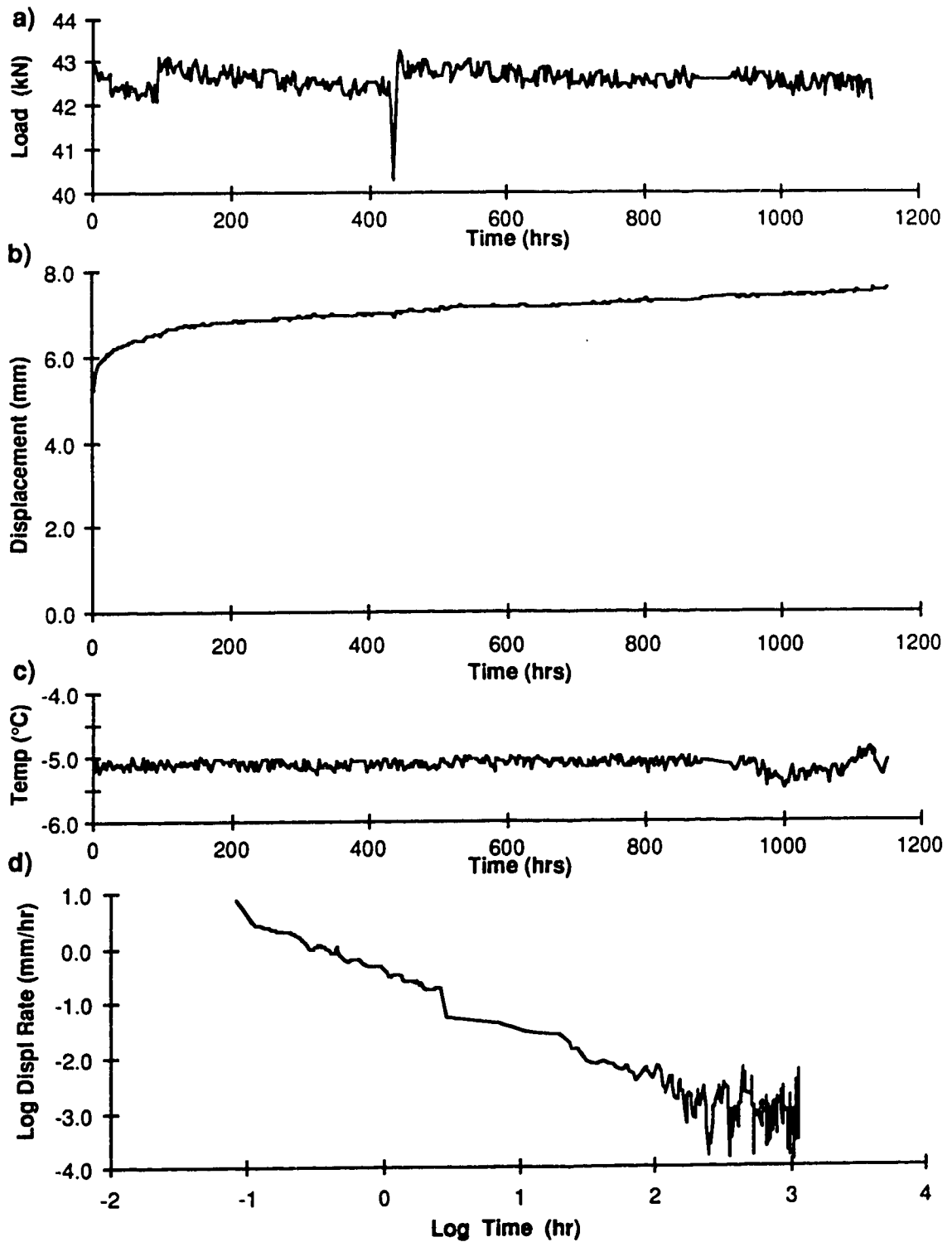


Figure E.26: Test #31-102, 10 ppt, Grout backfill, 359 kPa

- a) load vs time
- b) displacement vs time
- c) temperature vs time
- d) log displacement rate vs log time

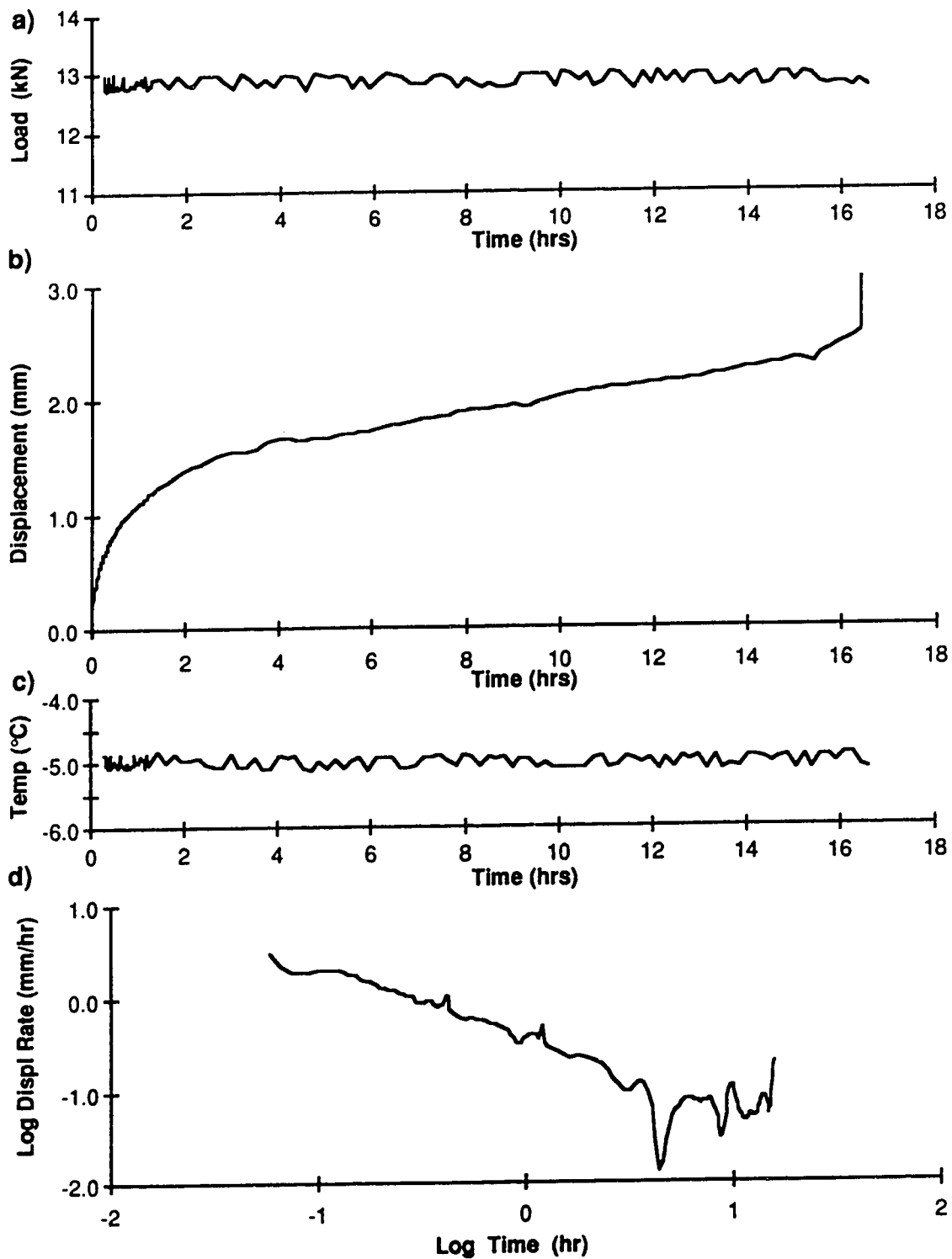


Figure E.27: Test #33-33, 10 ppt, Sand backfill, 316 kPa

- a) load vs time
- b) displacement vs time
- c) temperature vs time
- d) log displacement rate vs log time

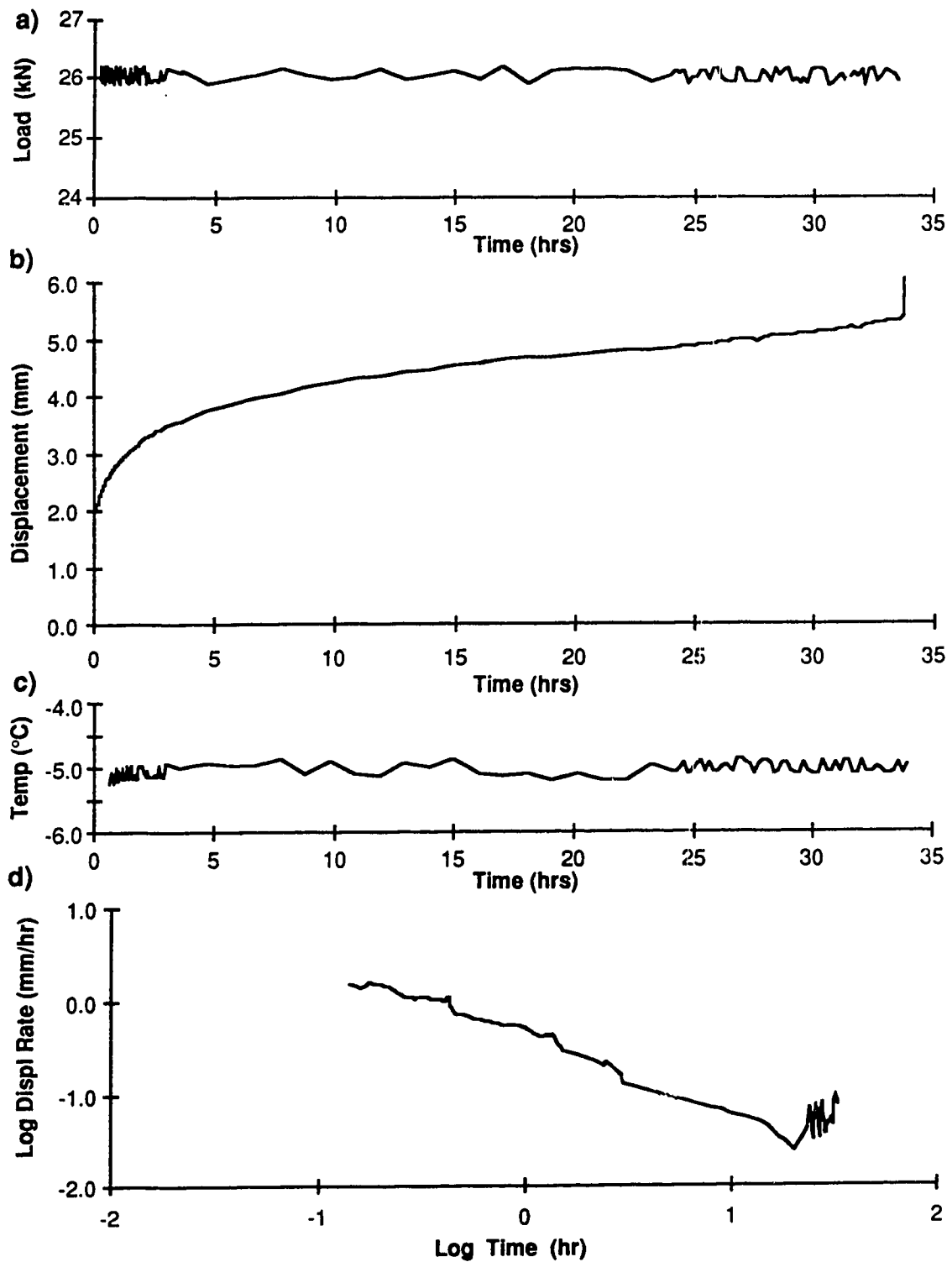


Figure E.28: Test #33-63, 10 ppt, Sand backfill, 325 kPa

- a) load vs time
- b) displacement vs time
- c) temperature vs time
- d) log displacement rate vs log time



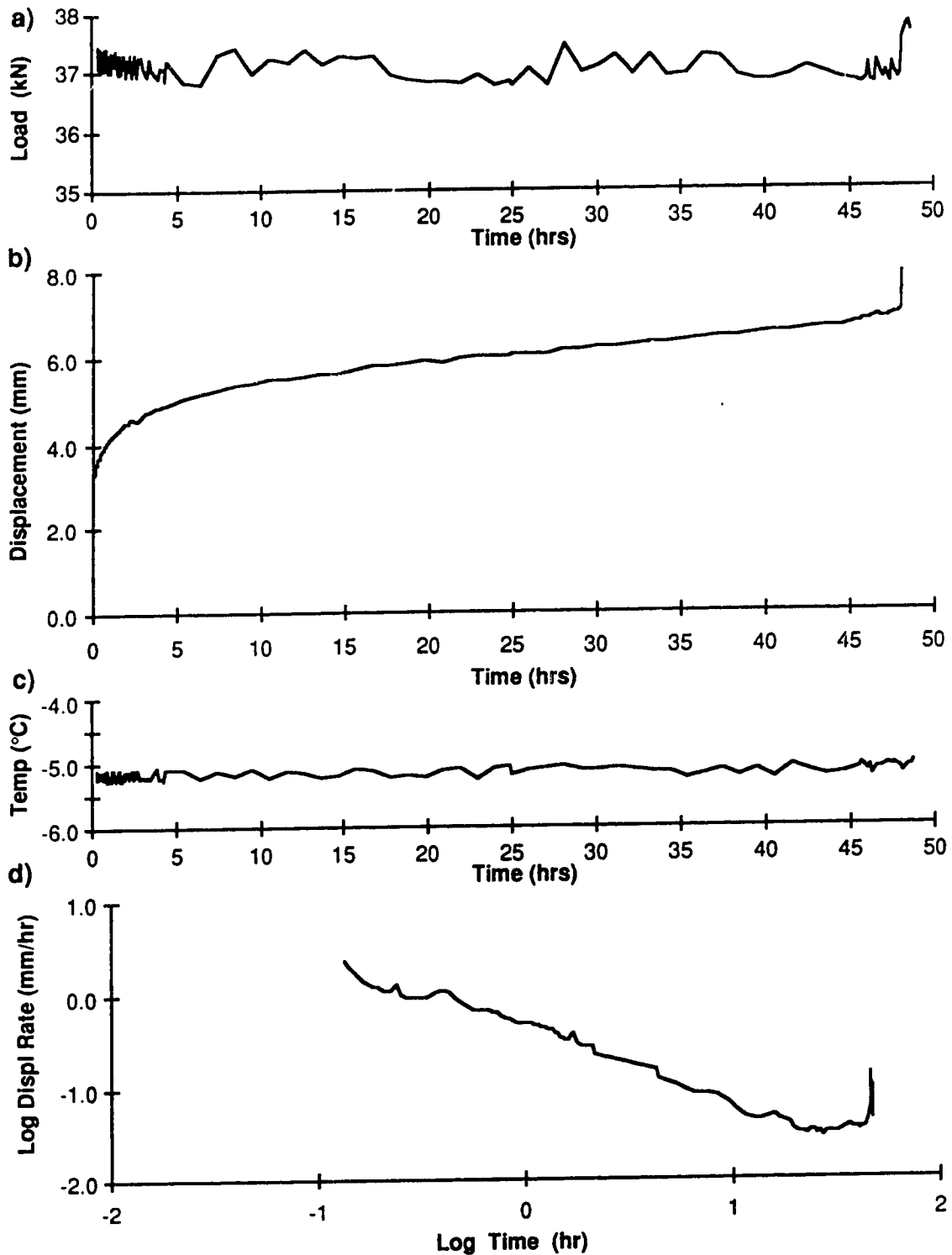


Figure E.29: Test #33-102, 10 ppt, Sand backfill, 310 kPa

- a) load vs time
- b) displacement vs time
- c) temperature vs time
- d) log displacement rate vs log time

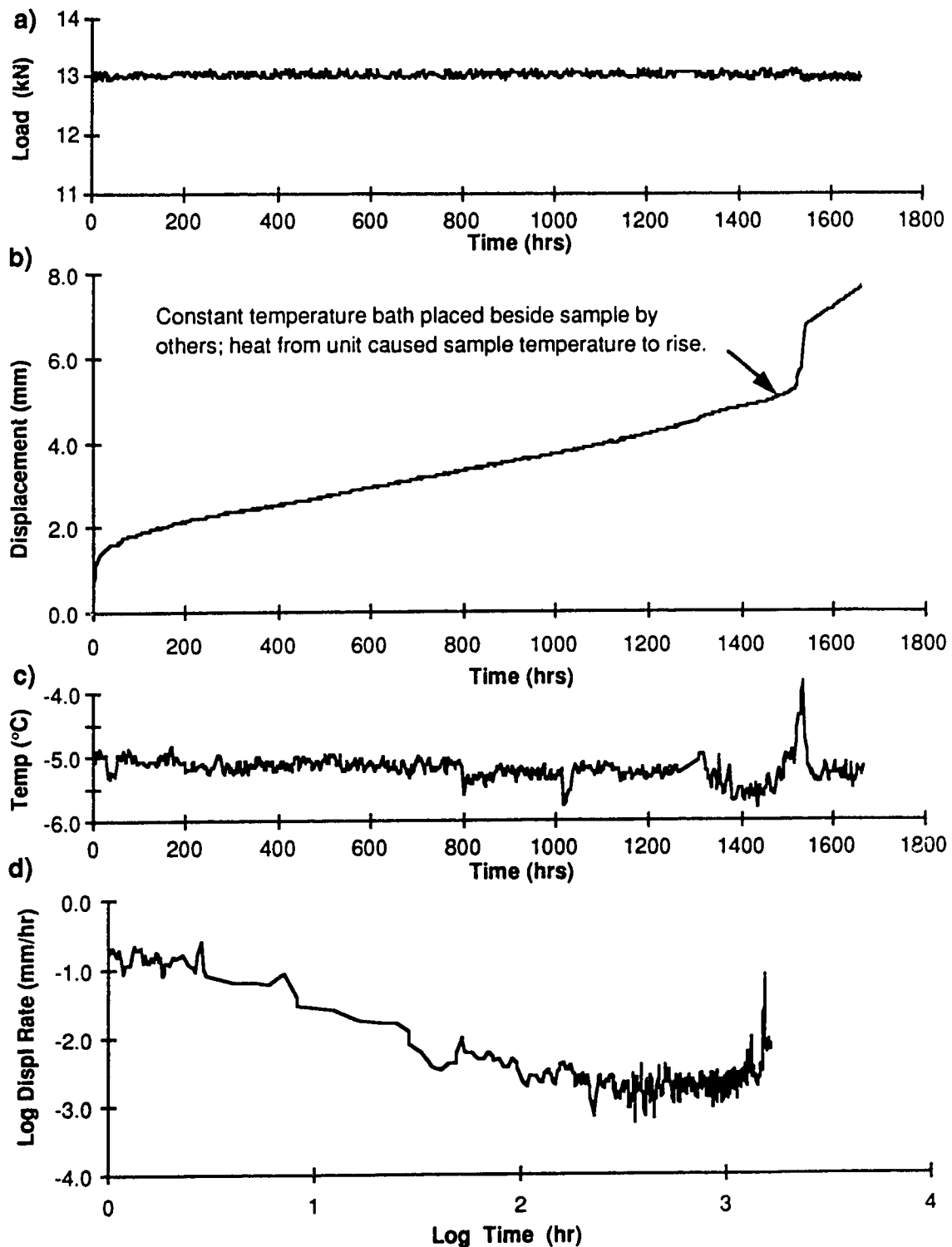


Figure E.30: Test #34-33, 10 ppt, Grout backfill, 318 kPa

- a) load vs time
- b) displacement vs time
- c) temperature vs time
- d) log displacement rate vs log time

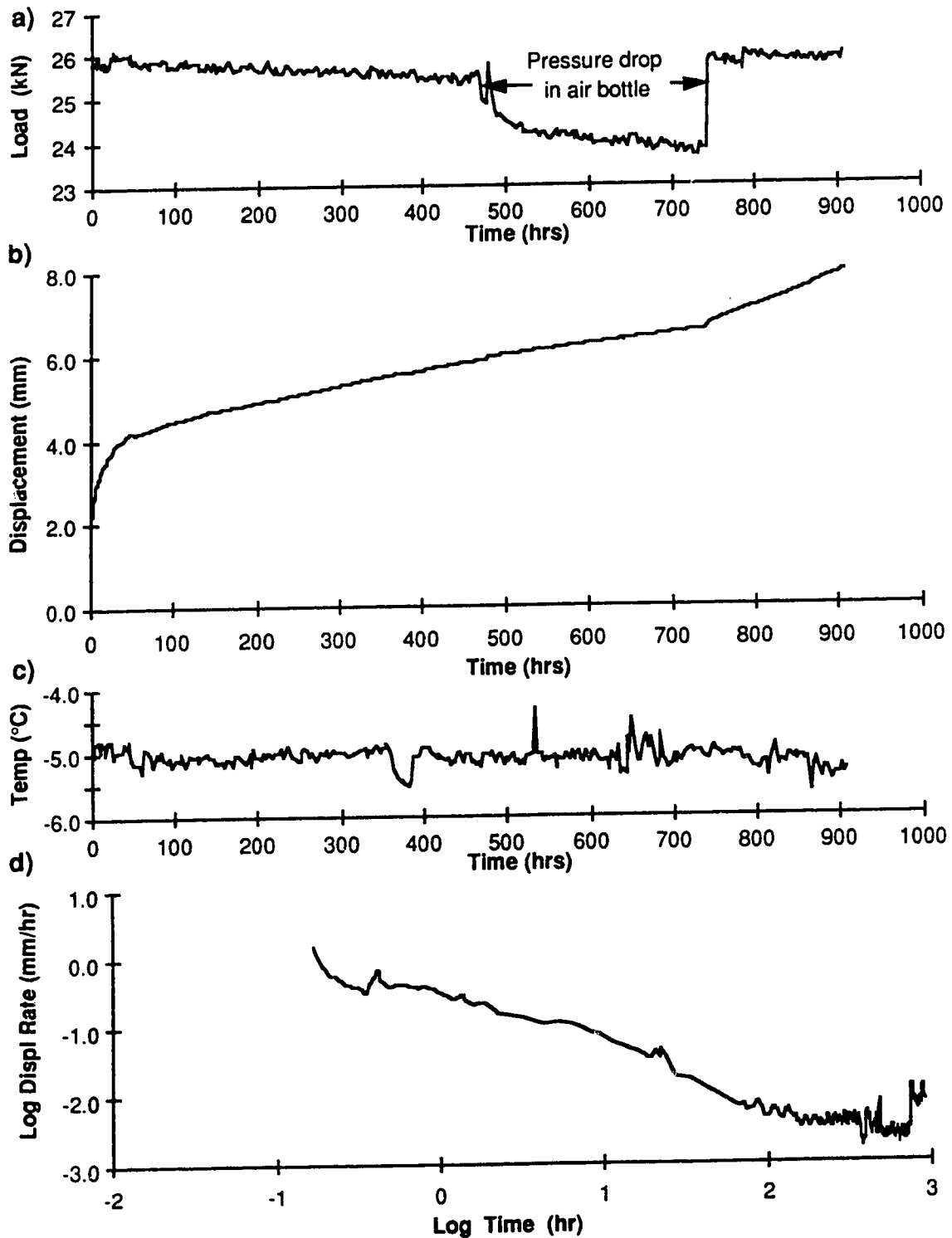


Figure E.31: Test #34-63, 10 ppt, Grout backfill, 322 kPa

- a) load vs time
- b) displacement vs time
- c) temperature vs time
- d) log displacement rate vs log time

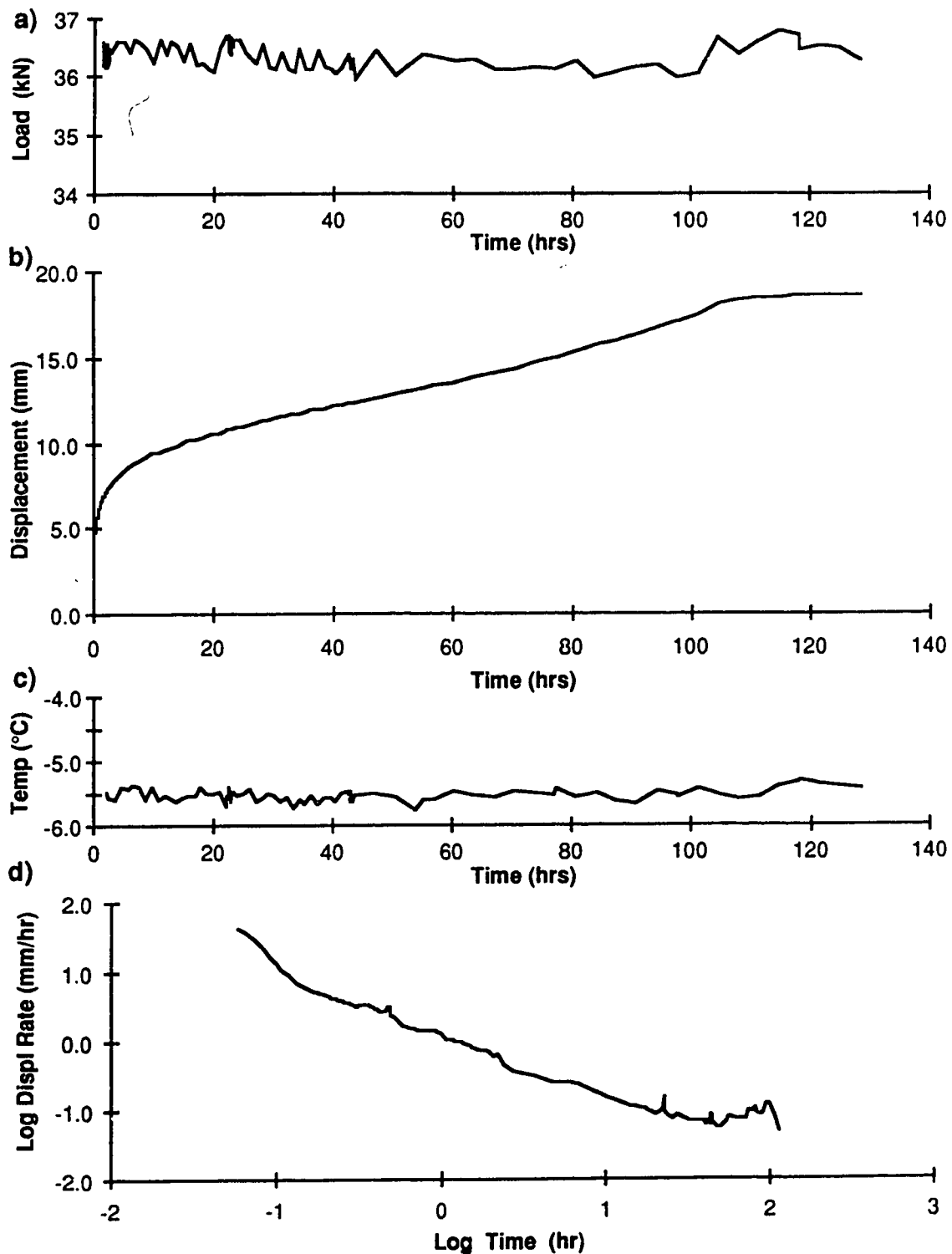


Figure E.32: Test #34-102, 10 ppt, Grout backfill, 305 kPa

- a) load vs time
- b) displacement vs time
- c) temperature vs time
- d) log displacement rate vs log time

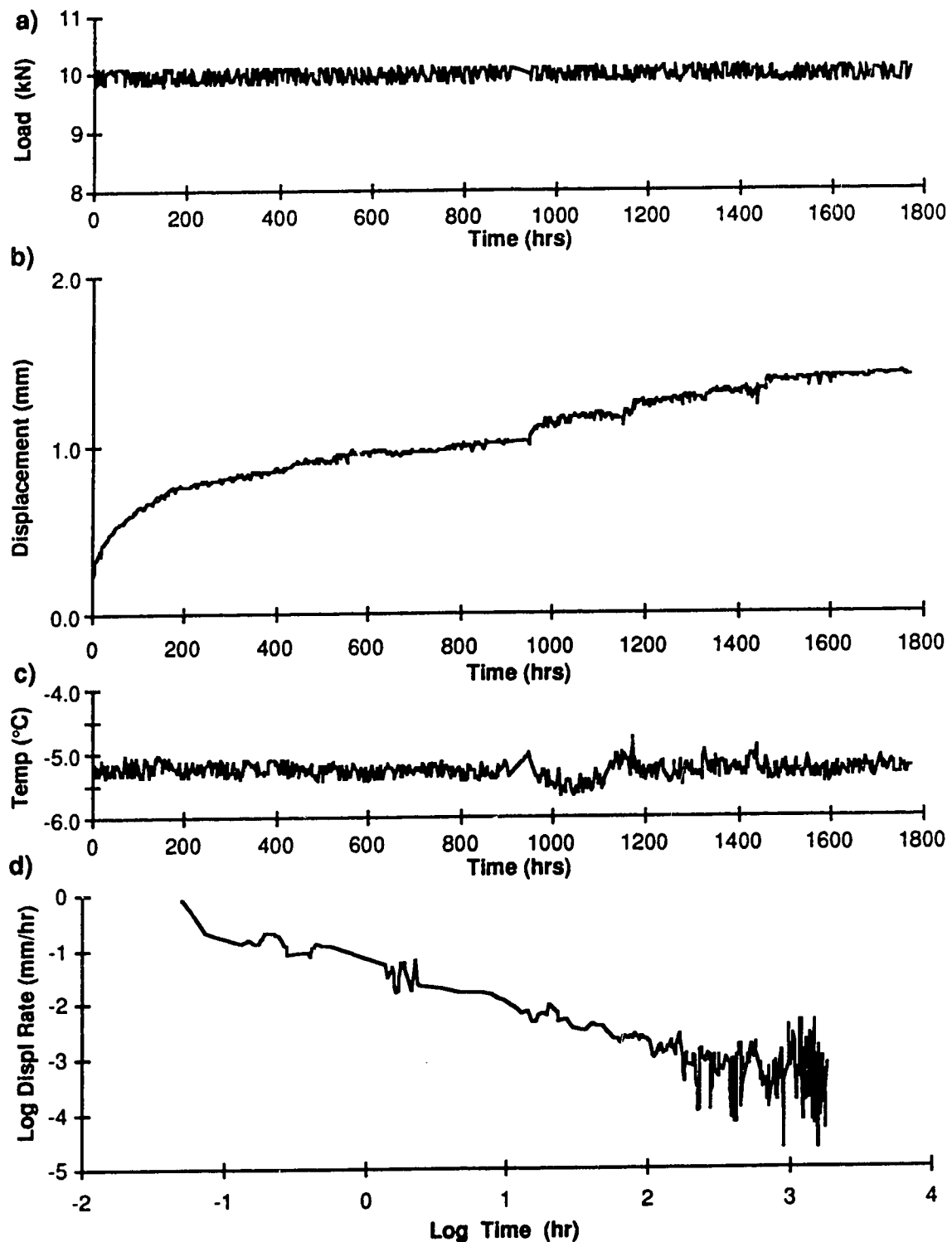


Figure E.33: Test #36-33, 10 ppt, Grout backfill, 245 kPa

- a) load vs time
- b) displacement vs time
- c) temperature vs time
- d) log displacement rate vs log time

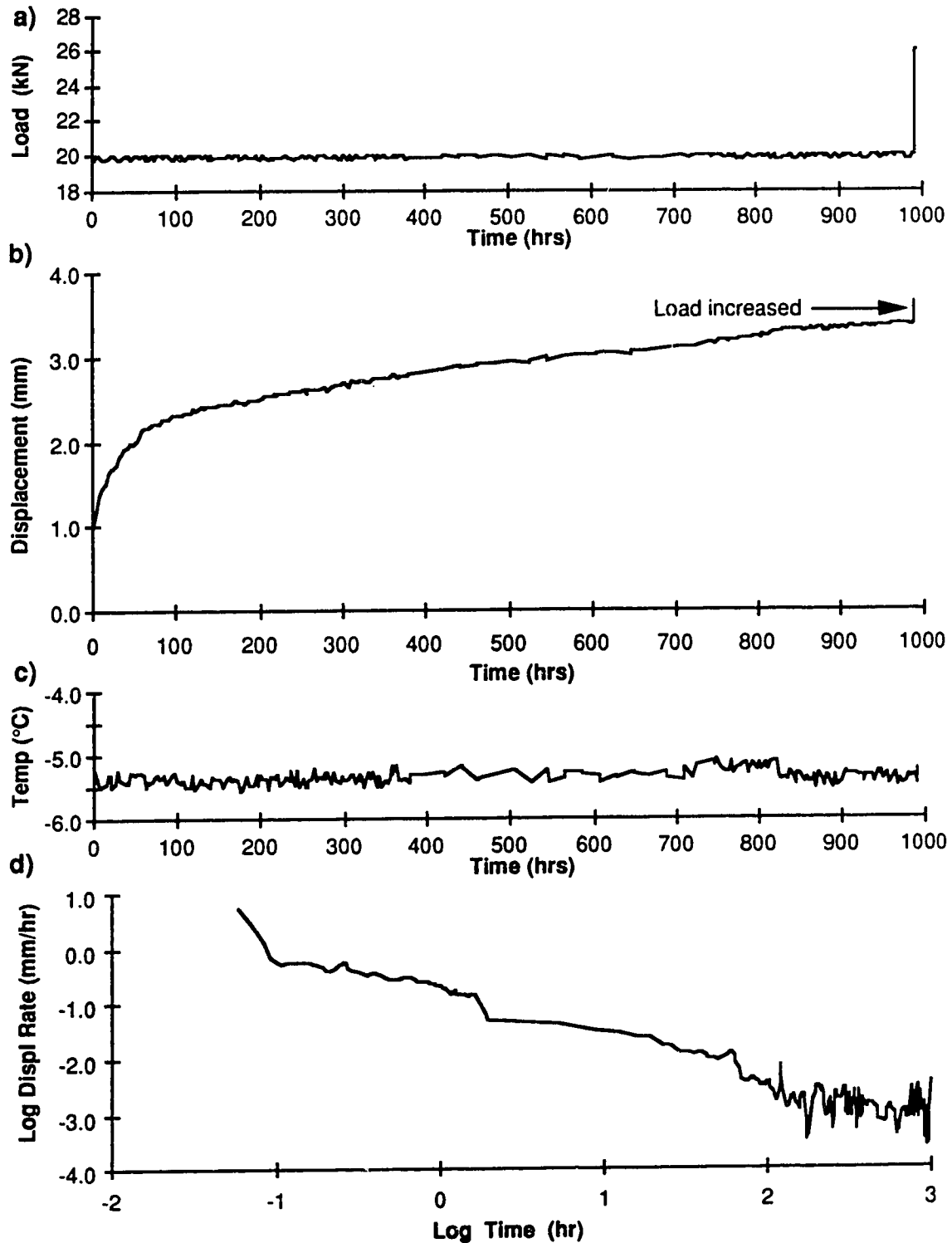


Figure E.34: Test #36-63, 10 ppt, Grout backfill, 248 kPa

- a) load vs time
- b) displacement vs time
- c) temperature vs time
- d) log displacement rate vs log time

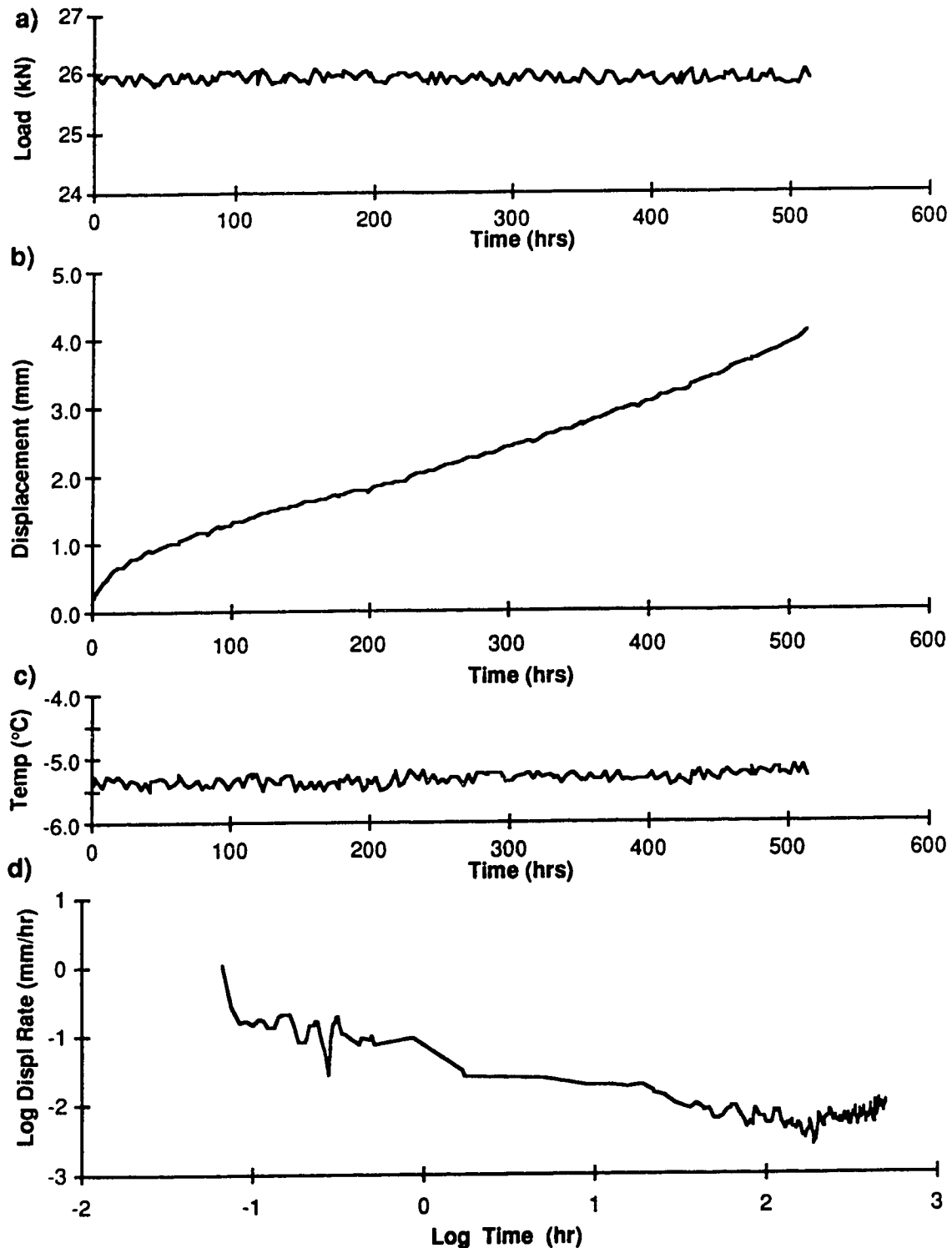


Figure E.35: Test #36-63-2, 10 ppt, Grout backfill, 330 kPa

- a) load vs time
- b) displacement vs time
- c) temperature vs time
- d) log displacement rate vs log time

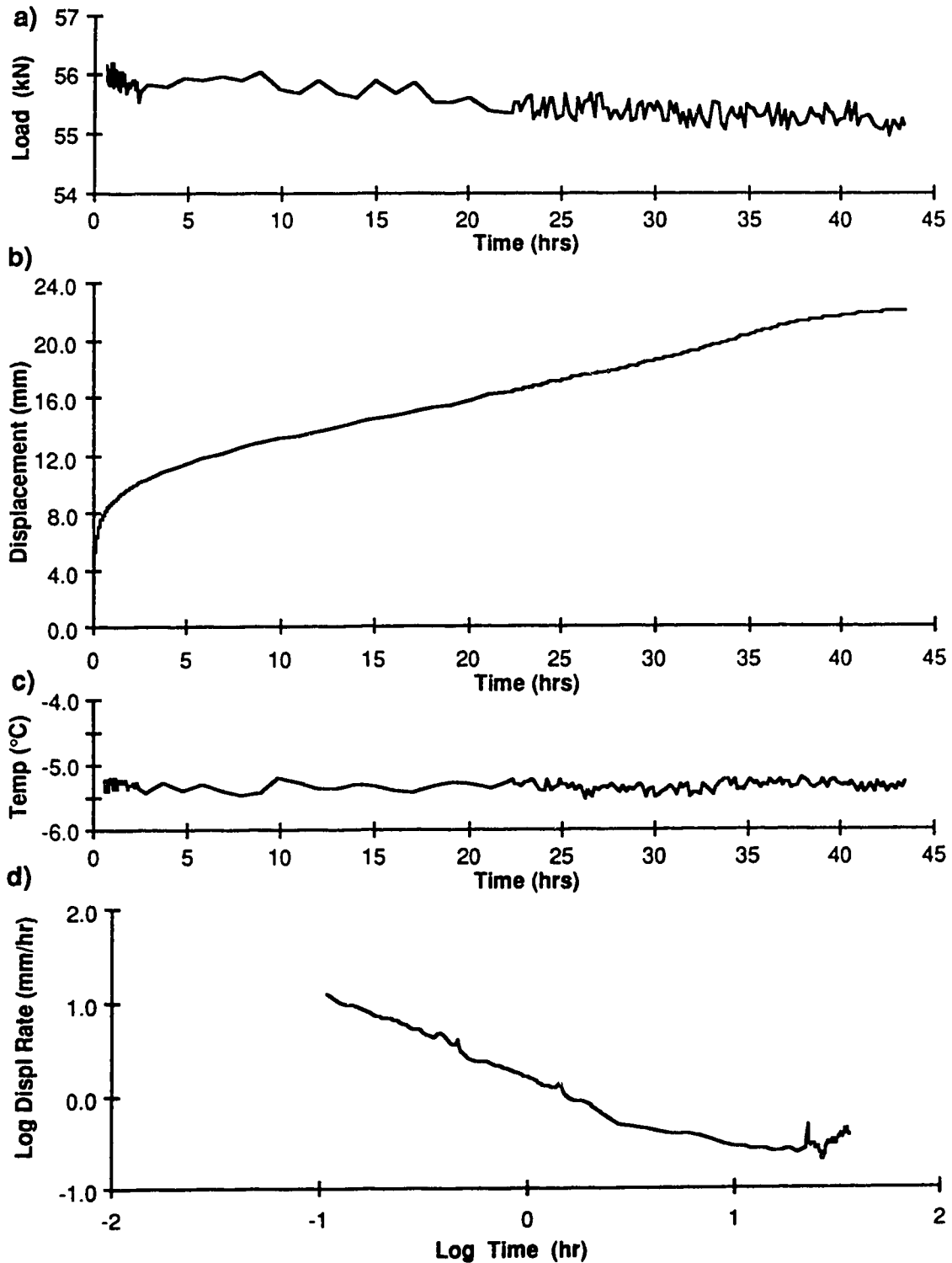


Figure E.36: Test #36-102, 10 ppt, Grout backfill, 495 kPa

- a) load vs time
- b) displacement vs time
- c) temperature vs time
- d) log displacement rate vs log time



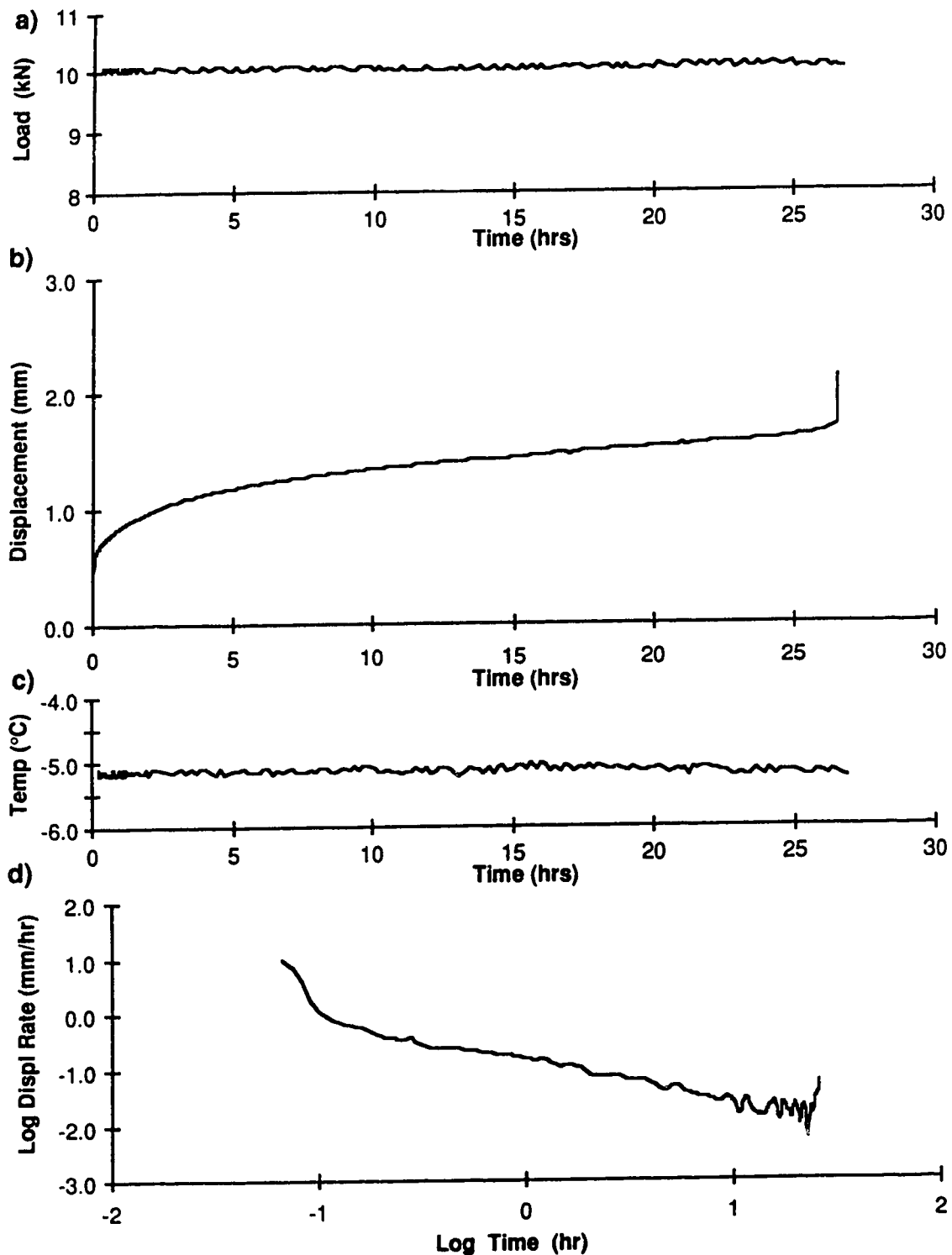


Figure E.37: Test #39-33, 10 ppt, Sand backfill, 252 kPa

- a) load vs time
- b) displacement vs time
- c) temperature vs time
- d) log displacement rate vs log time

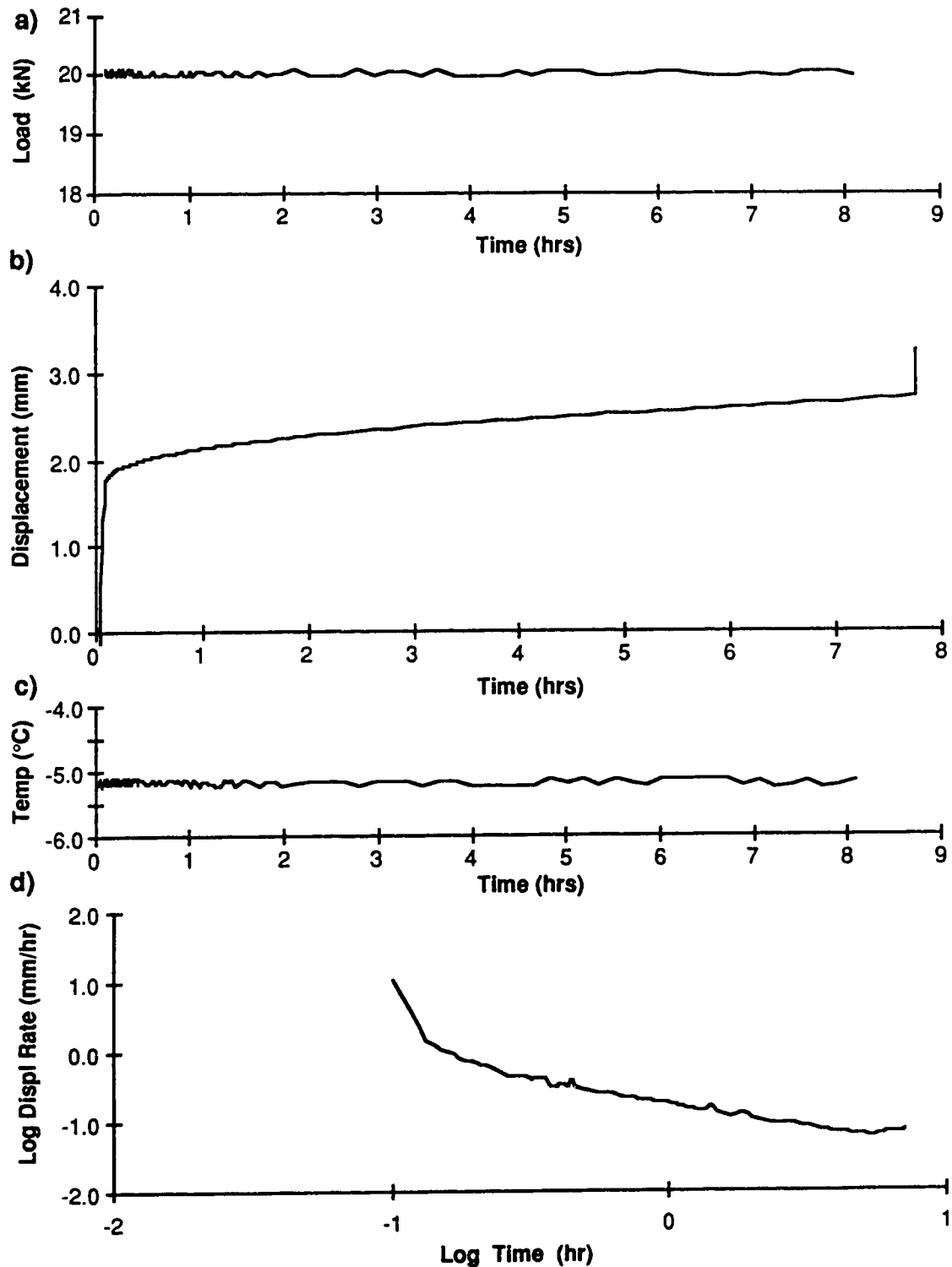


Figure E.38: Test #39-63, 10 ppt, Sand backfill, 255 kPa

- a) load vs time
- b) displacement vs time
- c) temperature vs time
- d) log displacement rate vs log time

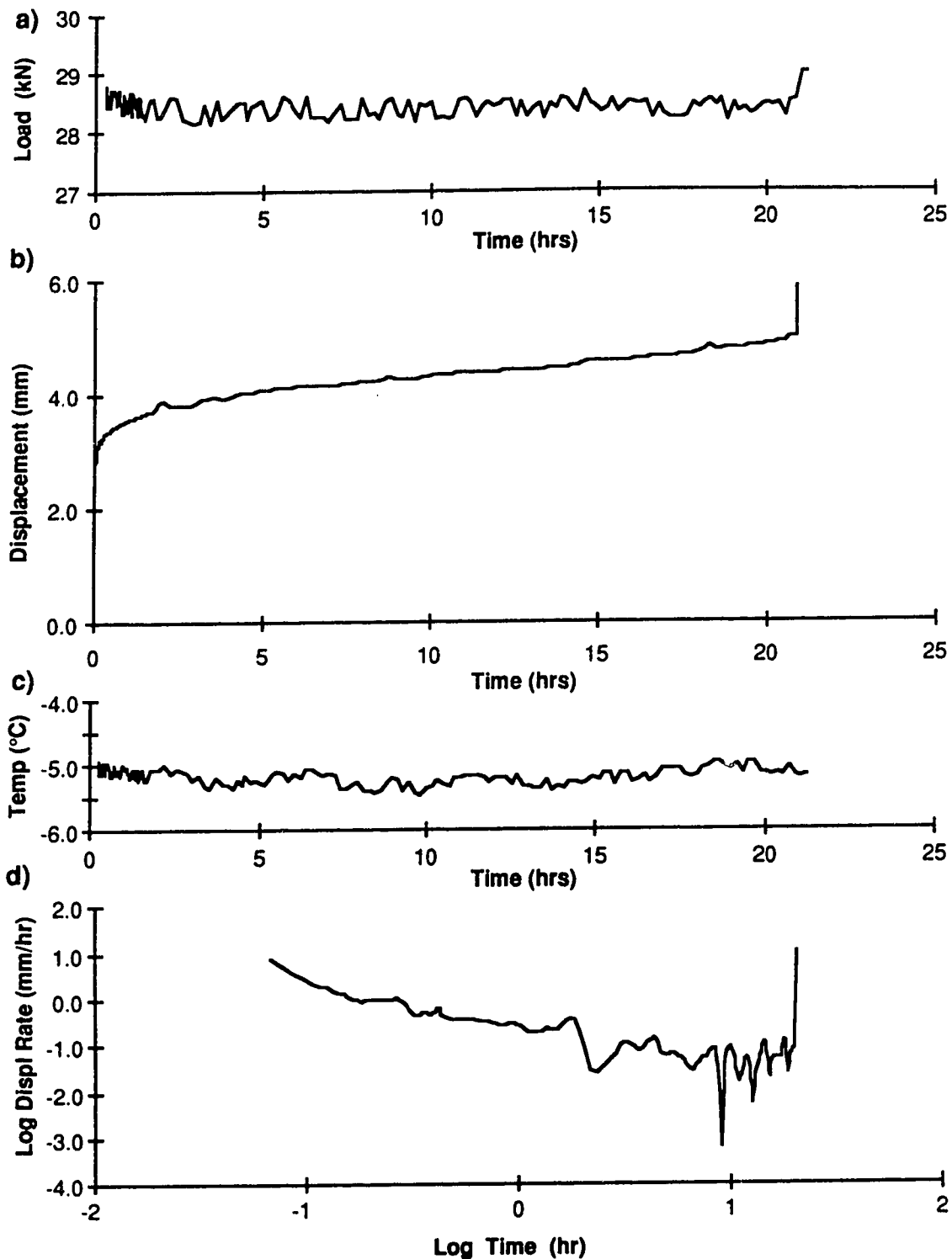


Figure E.39: Test #39-102, 10 ppt, Sand backfill, 243 kPa

- a) load vs time
- b) displacement vs time
- c) temperature vs time
- d) log displacement rate vs log time

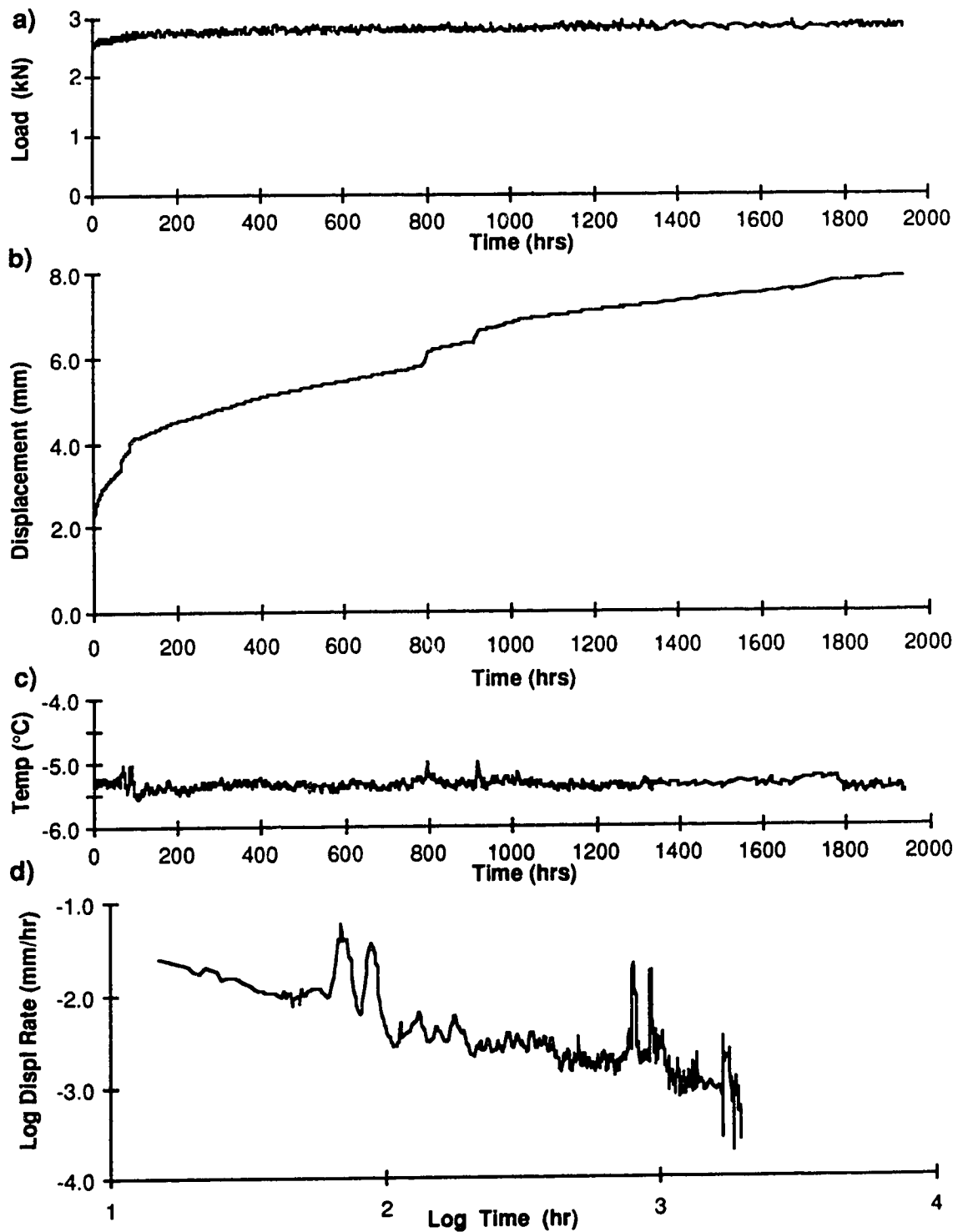


Figure E.40: Test #40-33, 30 ppt, Grout backfill, 69 kPa

- a) load vs time
- b) displacement vs time
- c) temperature vs time
- d) log displacement rate vs log time

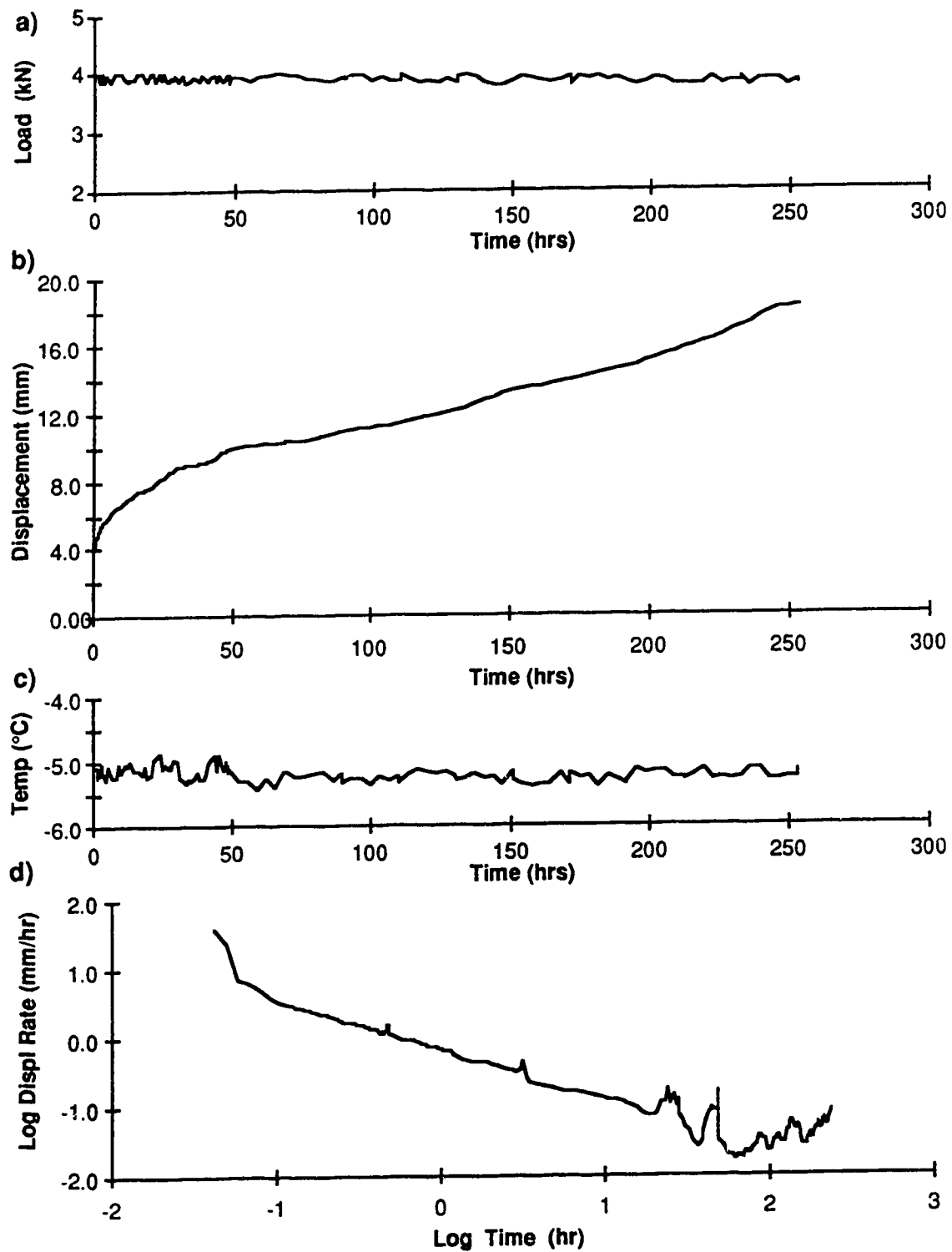


Figure E.41: Test #41-33, 30 ppt, Grout backfill, 97 kPa

- a) load vs time
- b) displacement vs time
- c) temperature vs time
- d) log displacement rate vs log time

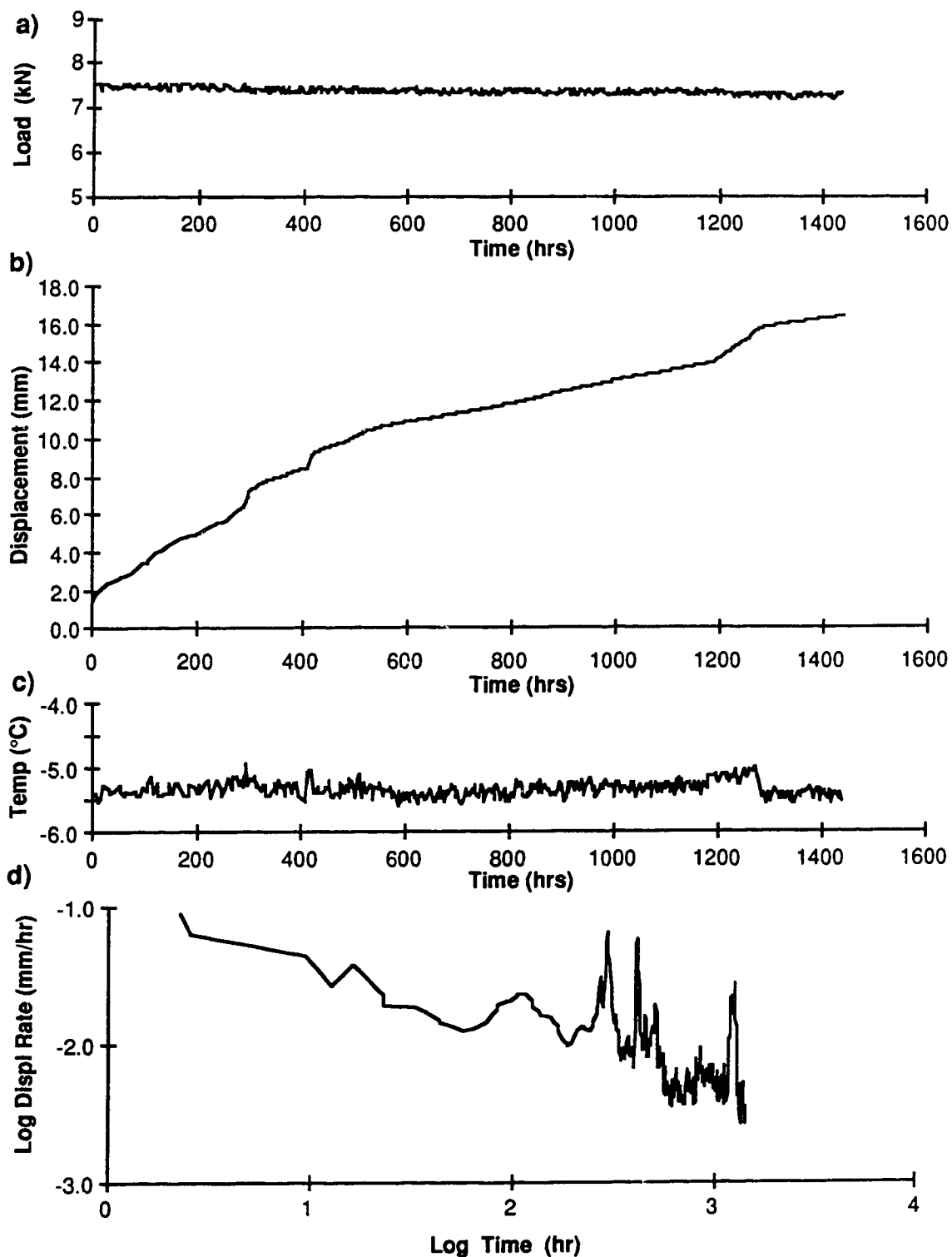


Figure E.42: Test #41-63, 30 ppt, Grout backfill, 92 kPa

- a) load vs time
- b) displacement vs time
- c) temperature vs time
- d) log displacement rate vs log time

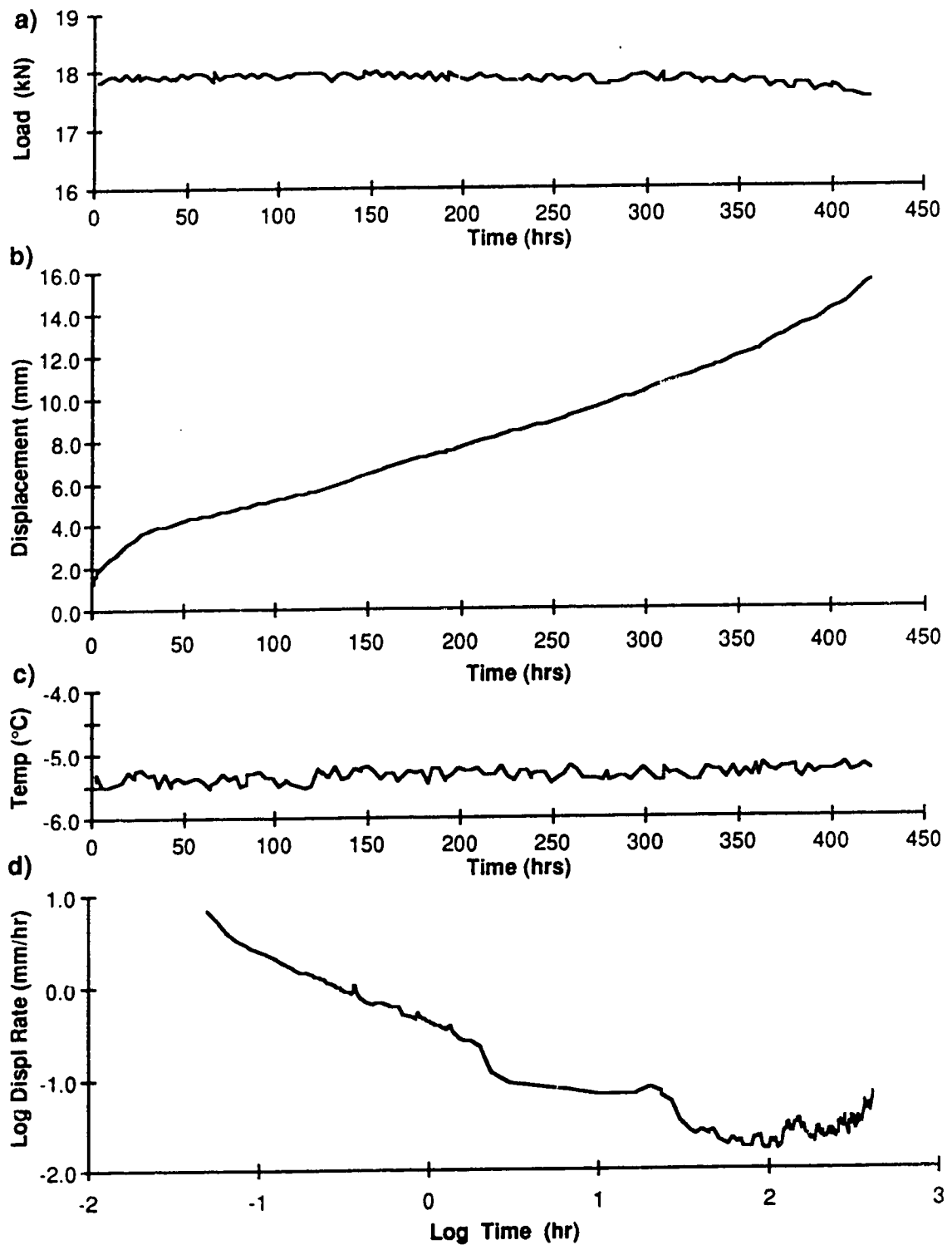


Figure E.43: Test #41-102, 30 ppt, Grout backfill, 163 kPa

- a) load vs time
- b) displacement vs time
- c) temperature vs time
- d) log displacement rate vs log time

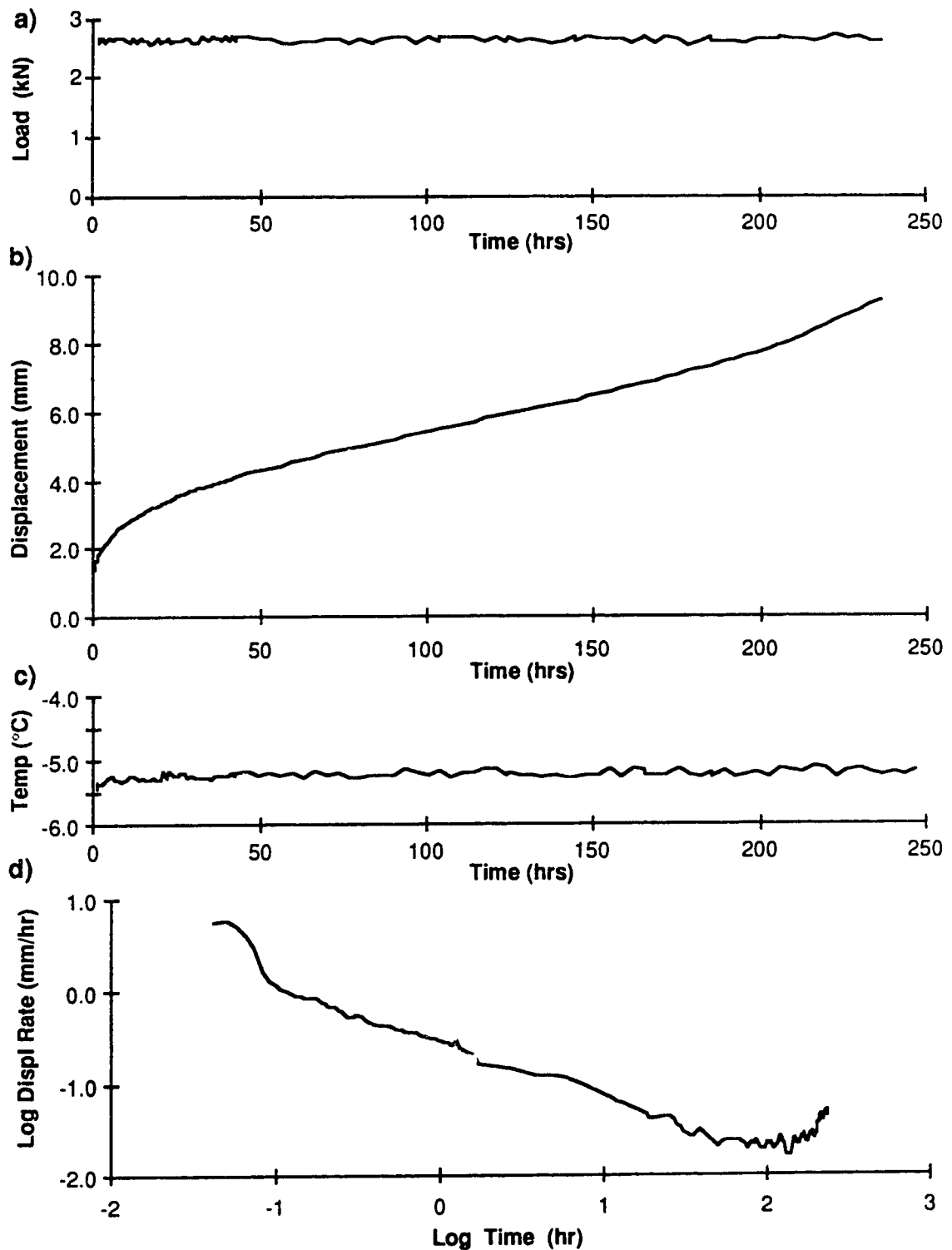


Figure E.44: Test #46-33, 30 ppt, Sand backfill, 68 kPa

- a) load vs time
- b) displacement vs time
- c) temperature vs time
- d) log displacement rate vs log time



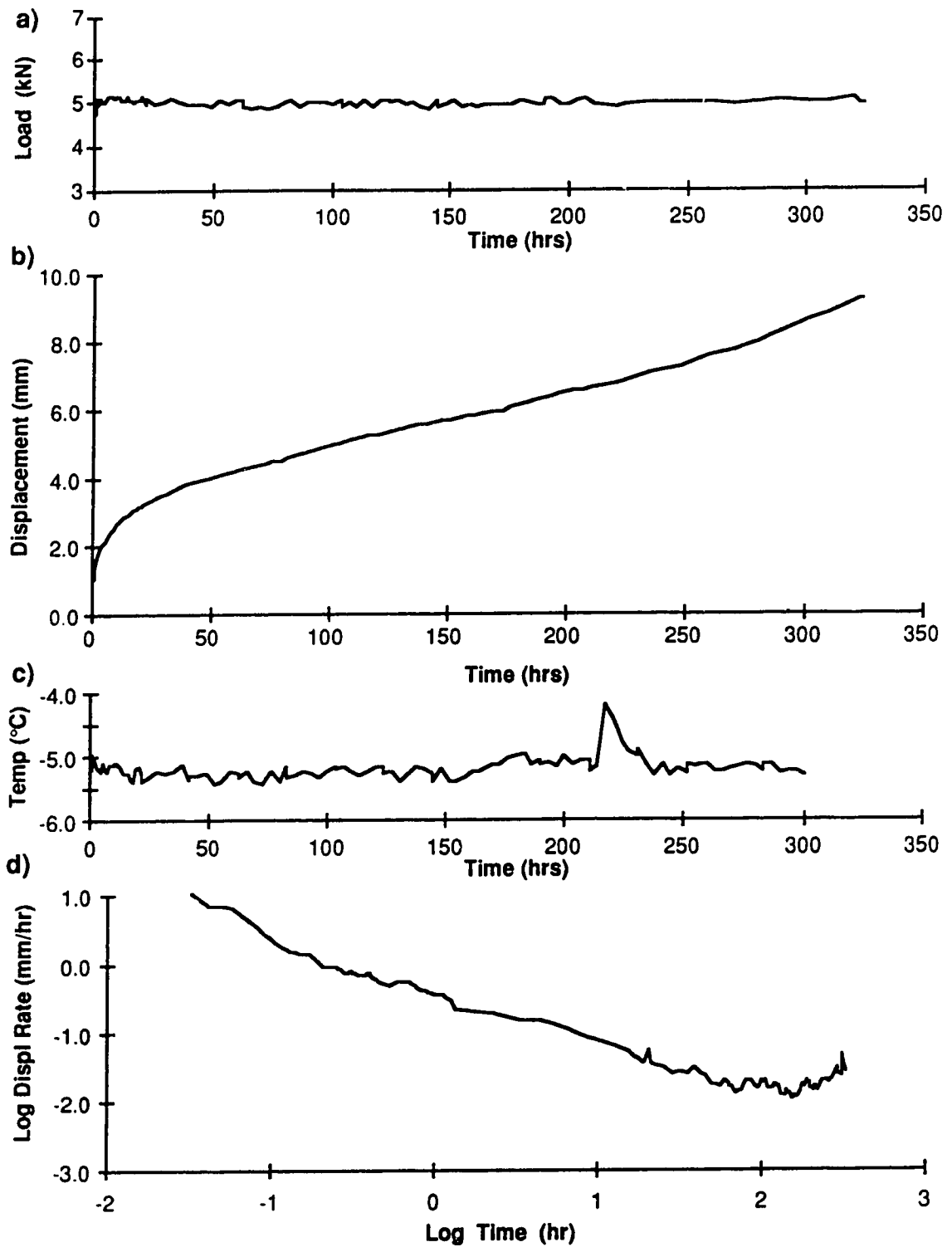


Figure E.45: Test #46-63, 30 ppt, Sand backfill, 66 kPa

- a) load vs time
- b) displacement vs time
- c) temperature vs time
- d) log displacement rate vs log time

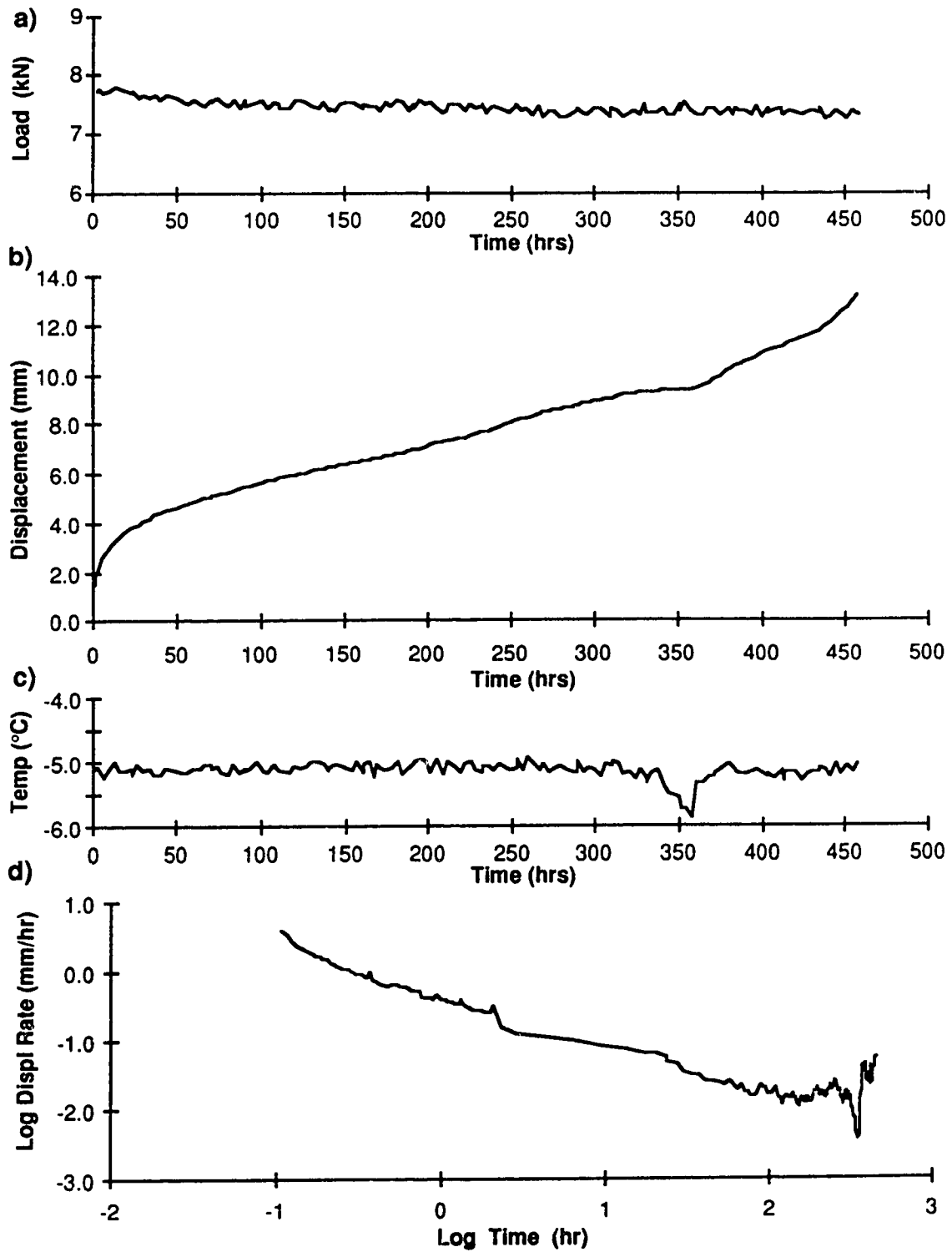


Figure E.46: Test #46-102, 30 ppt, Sand backfill, 65 kPa

- a) load vs time
- b) displacement vs time
- c) temperature vs time
- d) log displacement rate vs log time

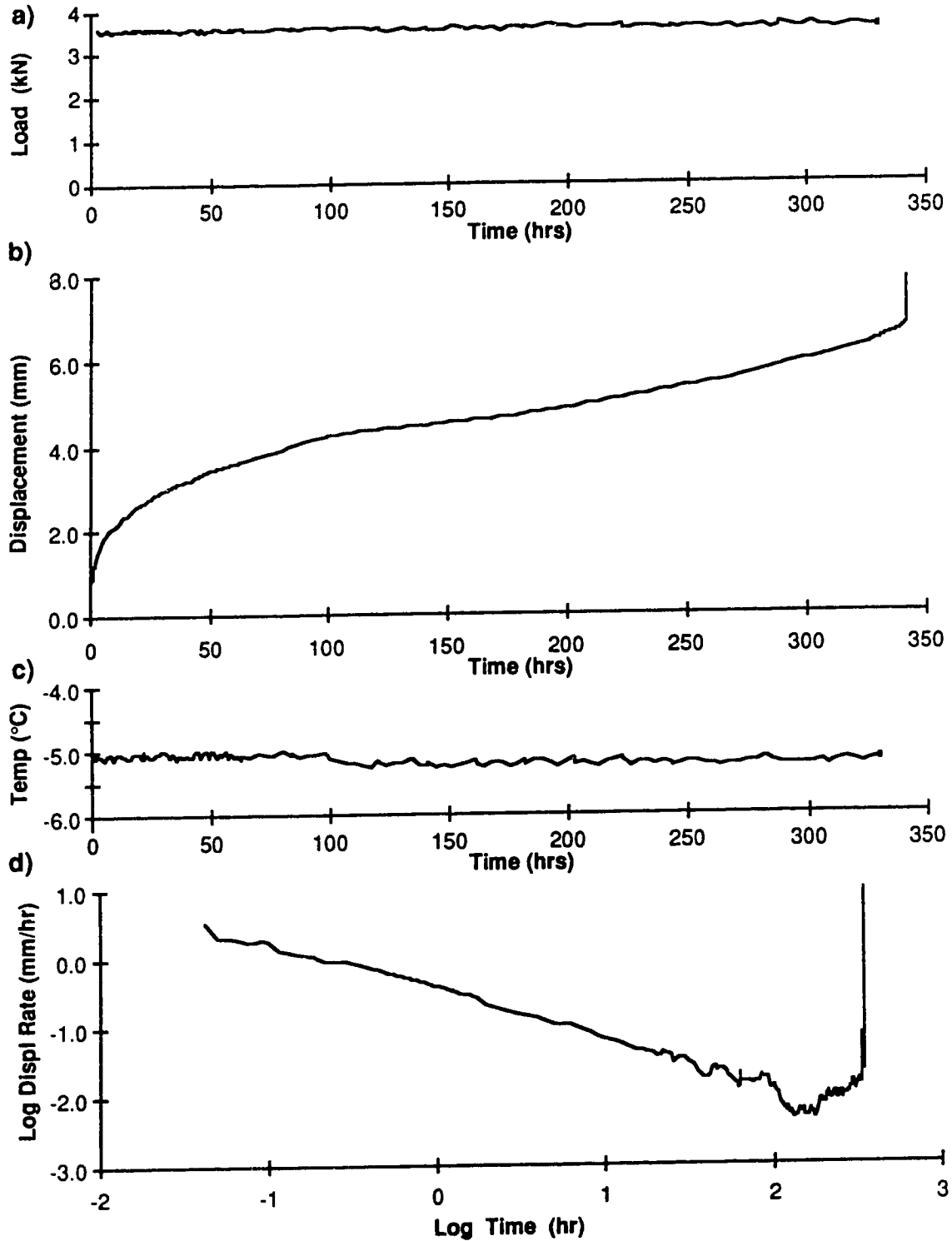


Figure E.47: Test #47-33, 30 ppt, Sand backfill, 89 kPa

- a) load vs time
- b) displacement vs time
- c) temperature vs time
- d) log displacement rate vs log time

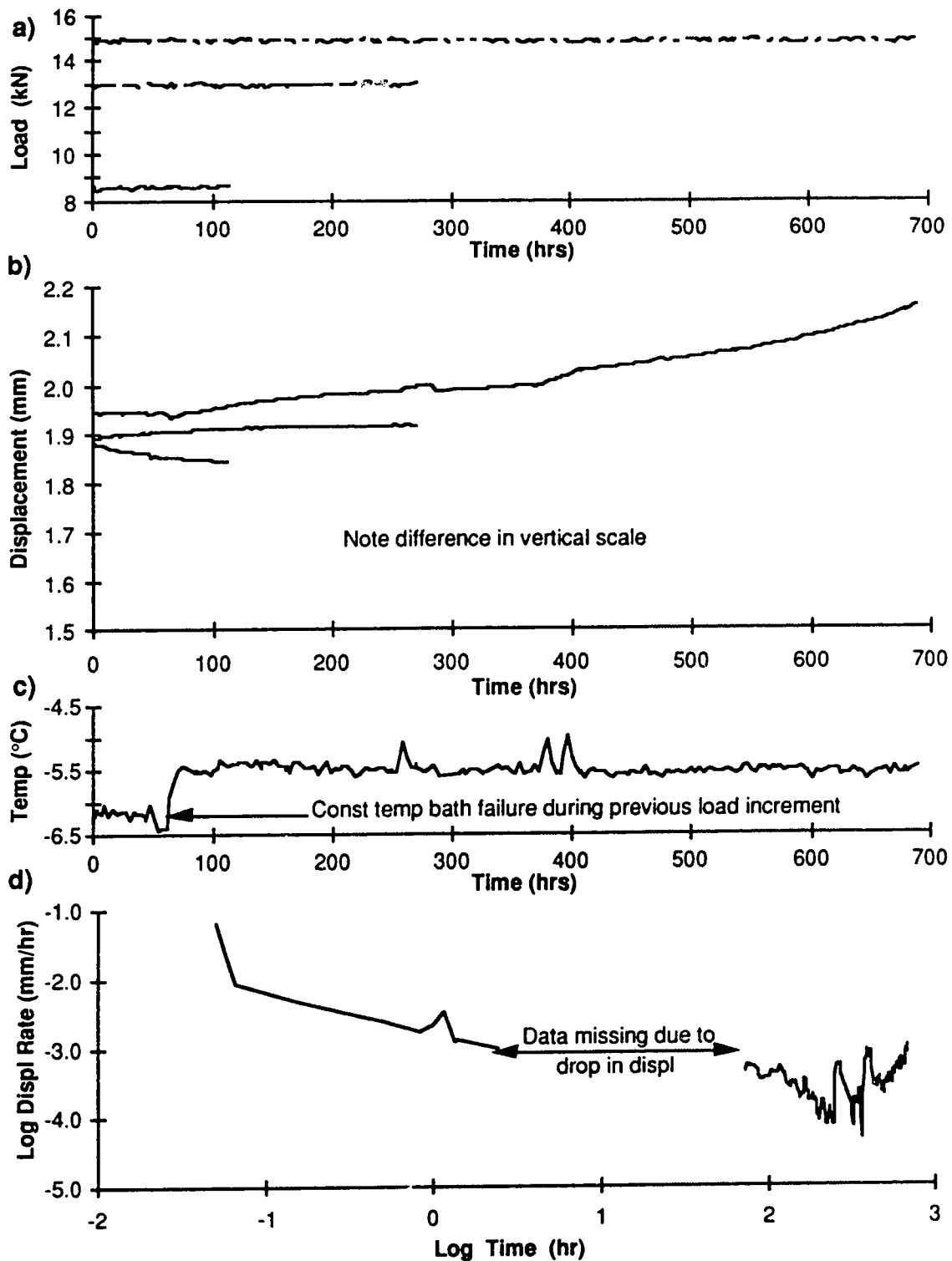


Figure E.48: Test #48-33, 0 ppt, Sand backfill  
a) load vs time (three load increments)  
b) displacement vs time (three load increments)  
c) temperature vs time (last load increment only)  
d) log displacement rate vs log time (last load increment only)

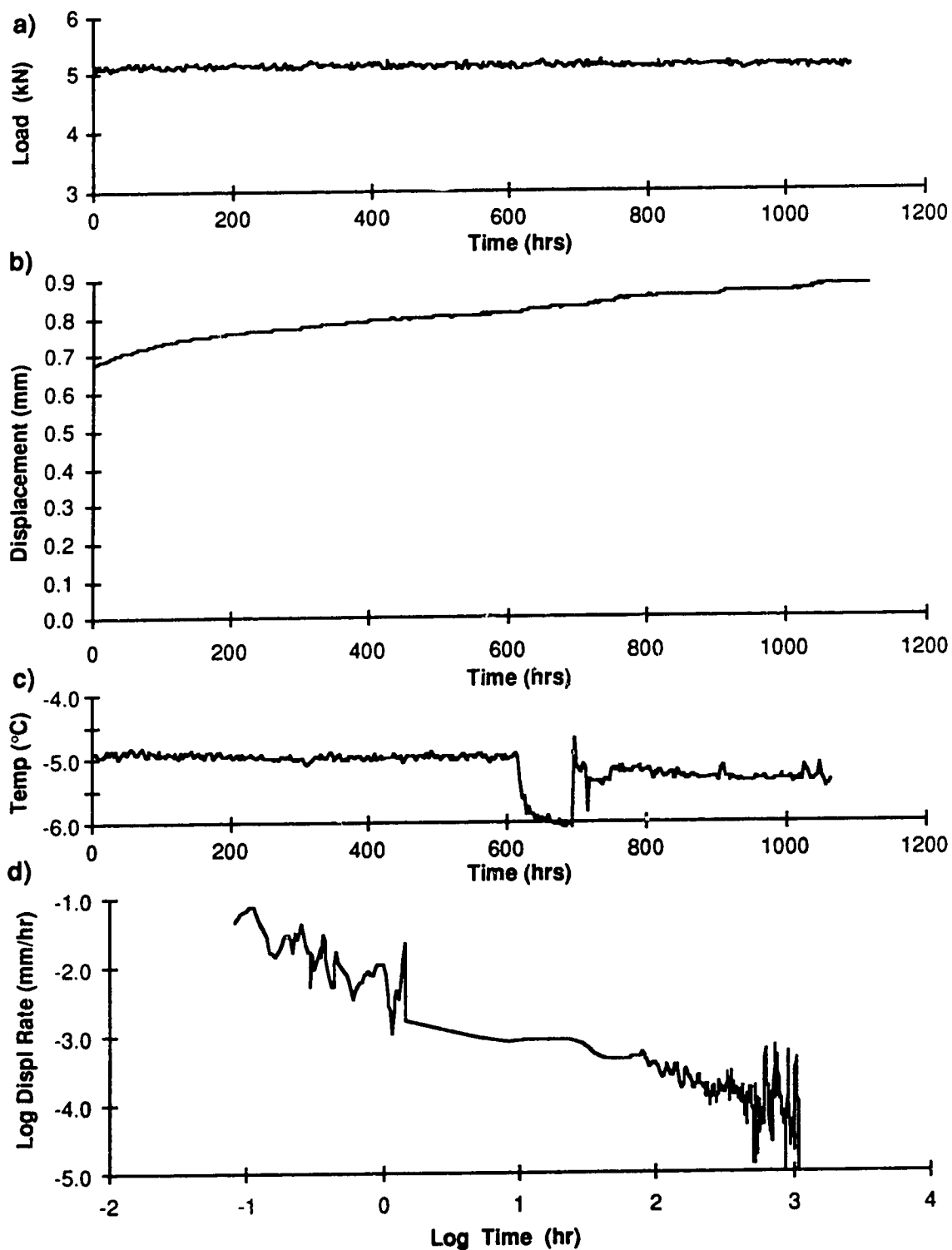


Figure E.49a: Test #49-33, 10 ppt, Sand backfill, 130 kPa

- a) load vs time
- b) displacement vs time
- c) temperature vs time
- d) log displacement rate vs log time

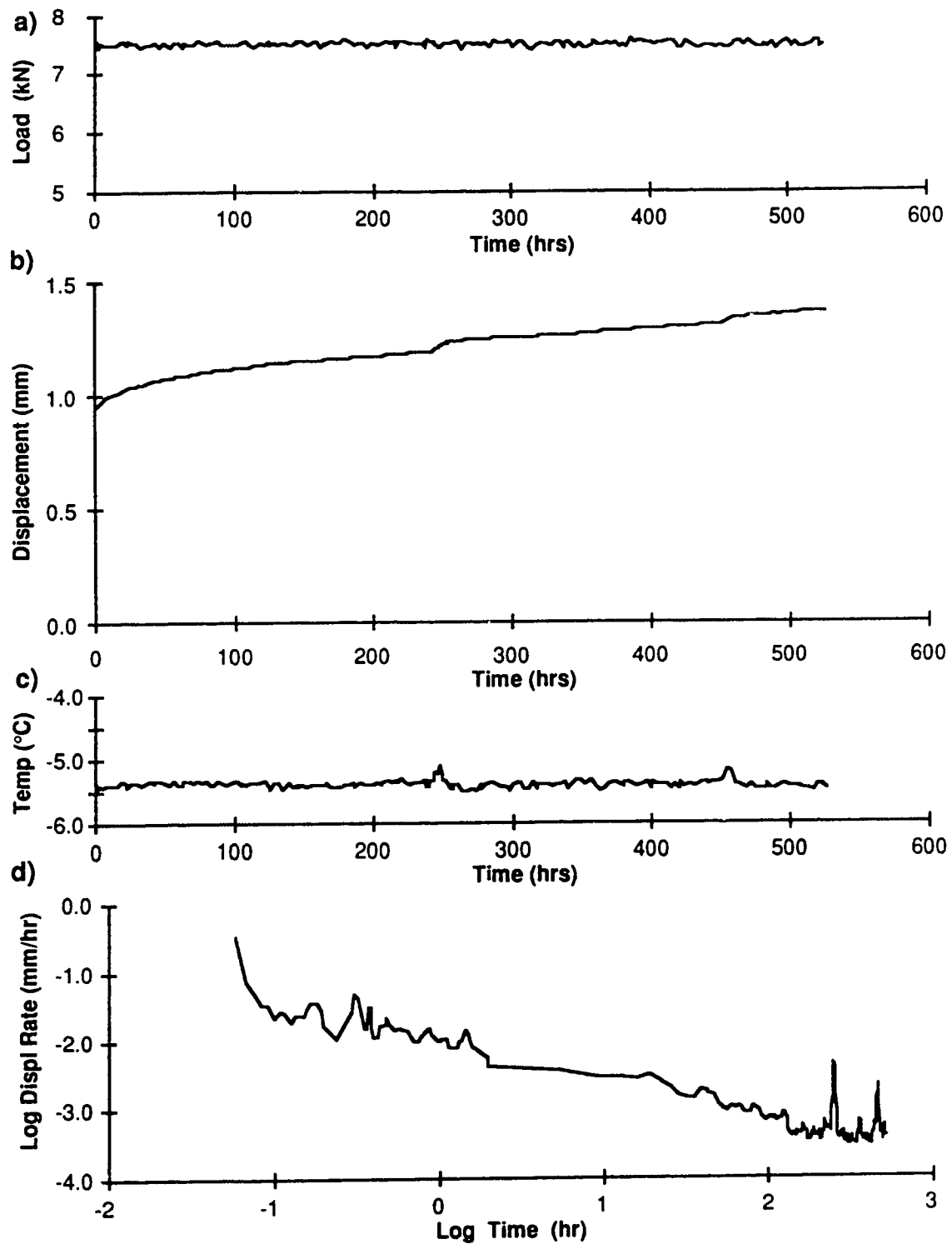


Figure E.49b: Test #49-33, 10 ppt, Sand backfill, 184 kPa

- a) load vs time
- b) displacement vs time
- c) temperature vs time
- d) log displacement rate vs log time

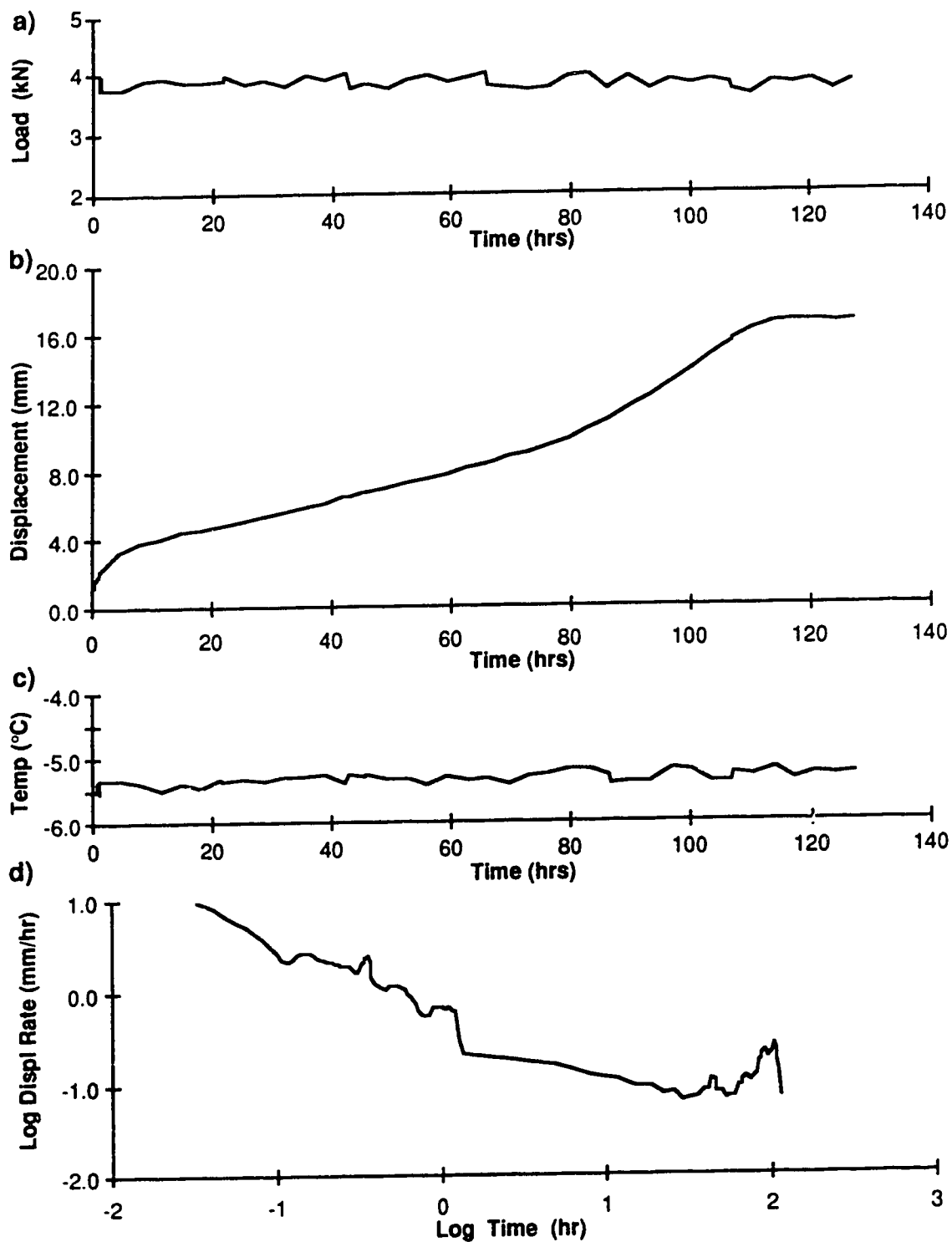


Figure E.50: Test #50-33, 30 ppt, Sand backfill, 95 kPa

- a) load vs time
- b) displacement vs time
- c) temperature vs time
- d) log displacement rate vs log time

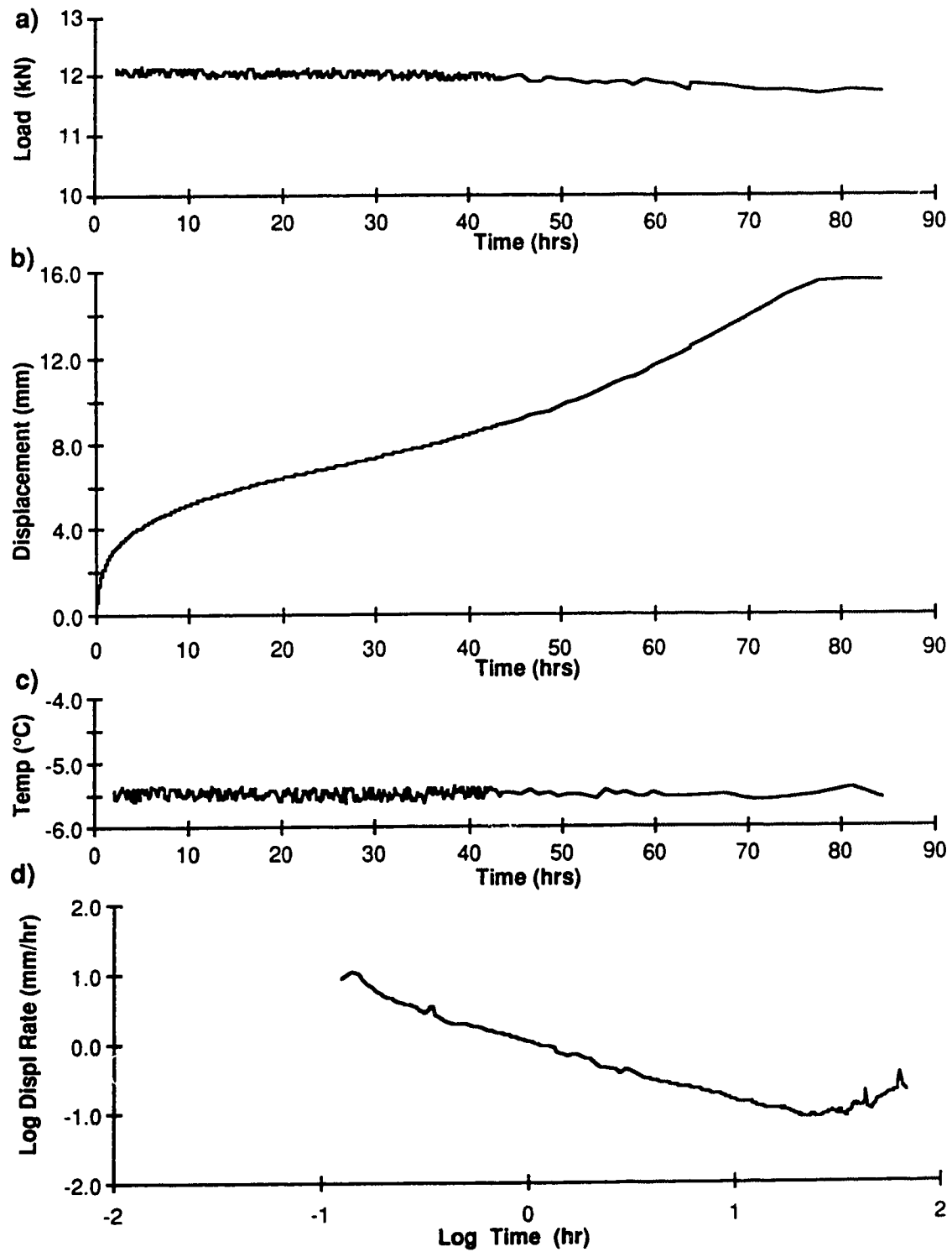


Figure E.51: Test #50-63, 30 ppt, Grout backfill, 150 kPa

- a) load vs time
- b) displacement vs time
- c) temperature vs time
- d) log displacement rate vs log time



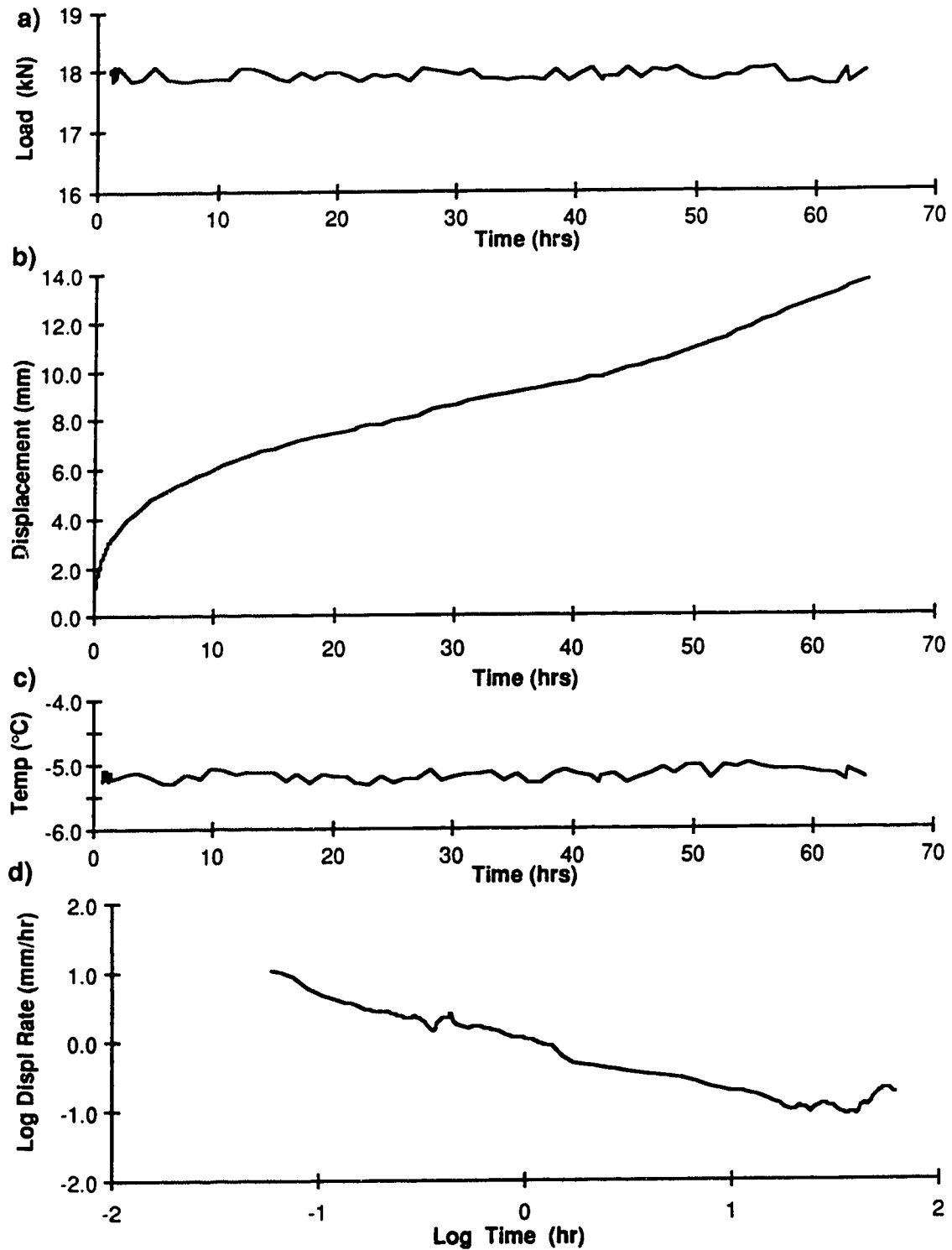


Figure E.52: Test #50-102, 30 ppt, Grout backfill, 150kPa

- a) load vs time
- b) displacement vs time
- c) temperature vs time
- d) log displacement rate vs log time

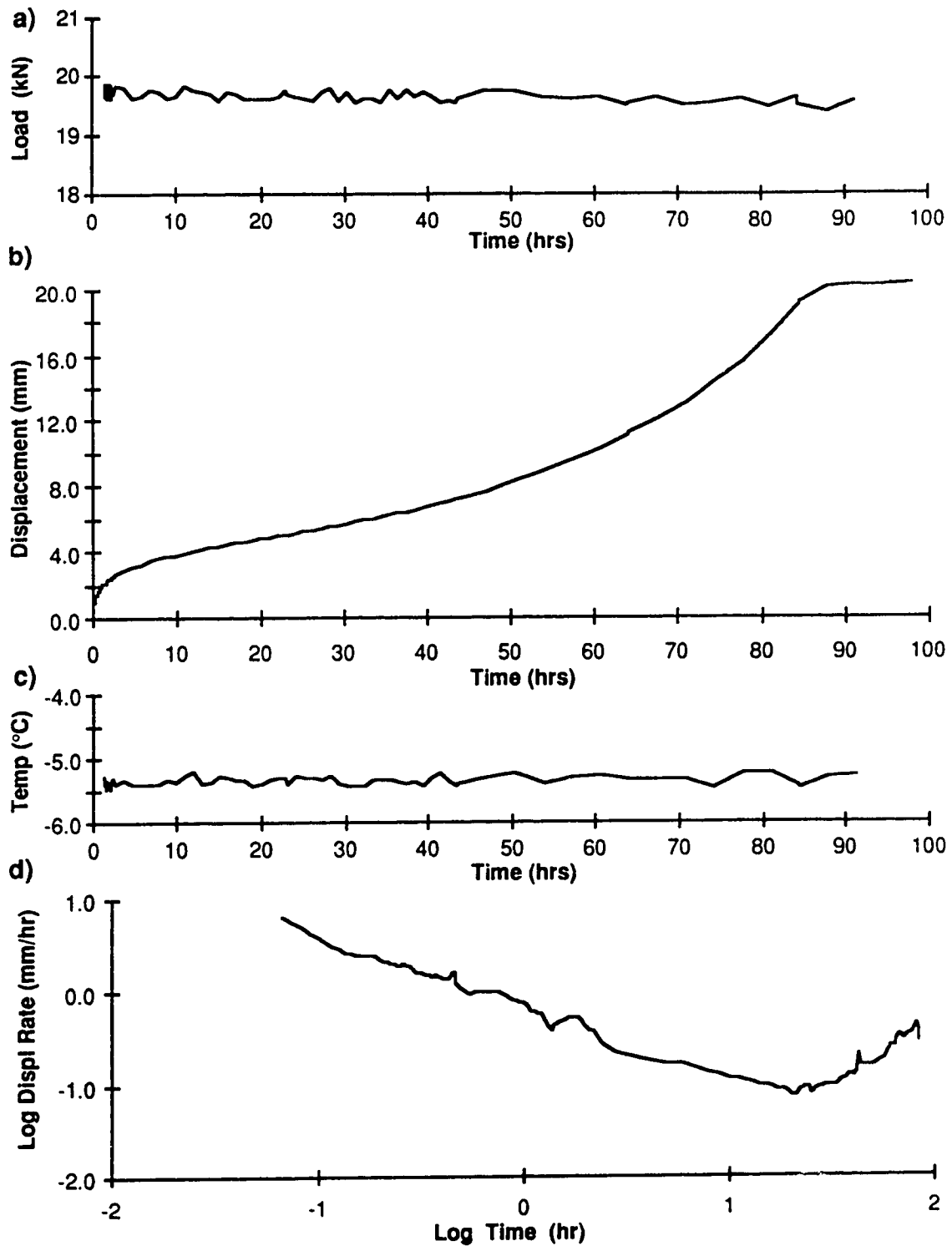


Figure E.53: Test #51-33, 10 ppt, Grout backfill, 482 kPa

- a) load vs time
- b) displacement vs time
- c) temperature vs time
- d) log displacement rate vs log time

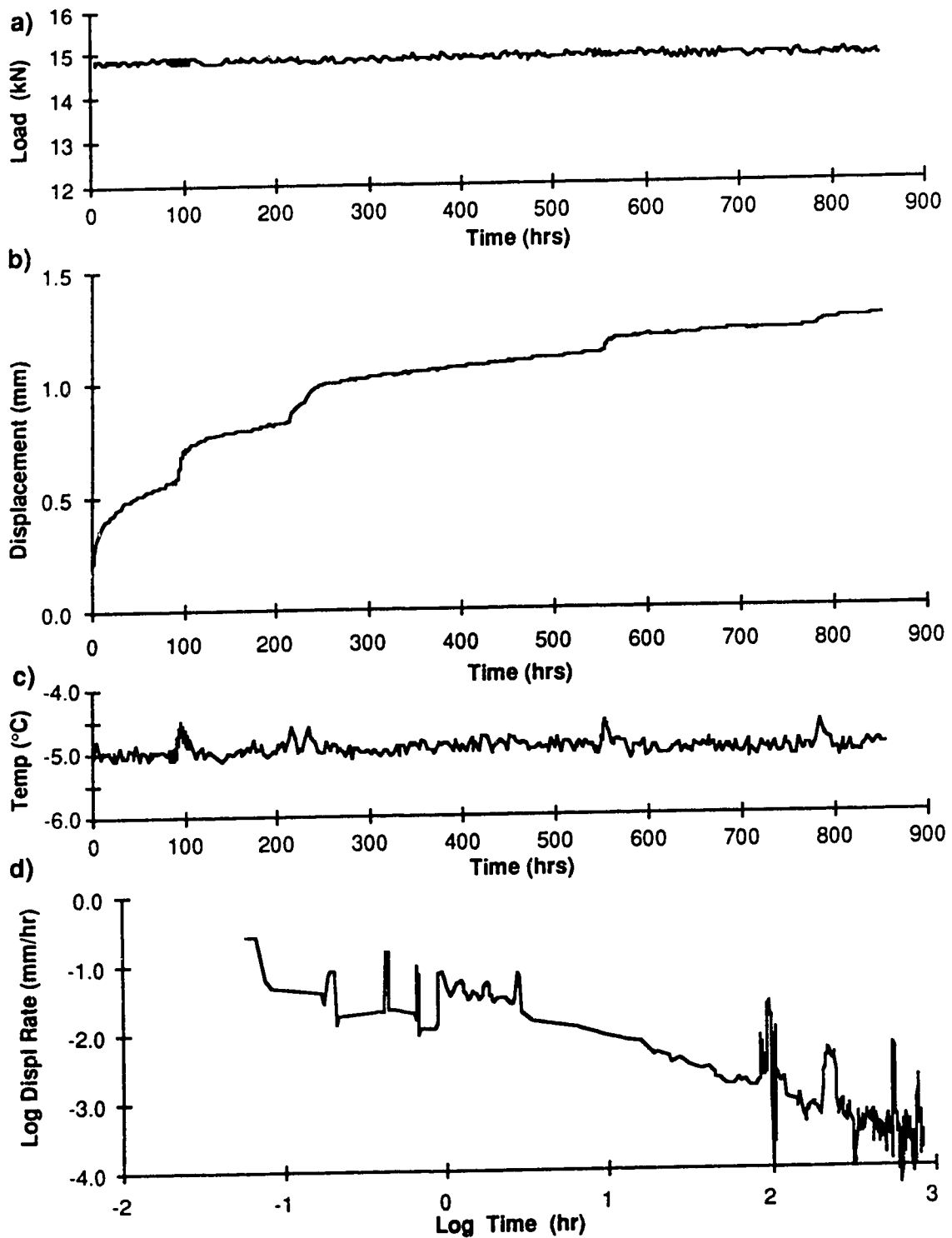


Figure E.54: Test #51-63, 10 ppt, Sand backfill, 186 kPa

- a) load vs time
- b) displacement vs time
- c) temperature vs time
- d) log displacement rate vs log time

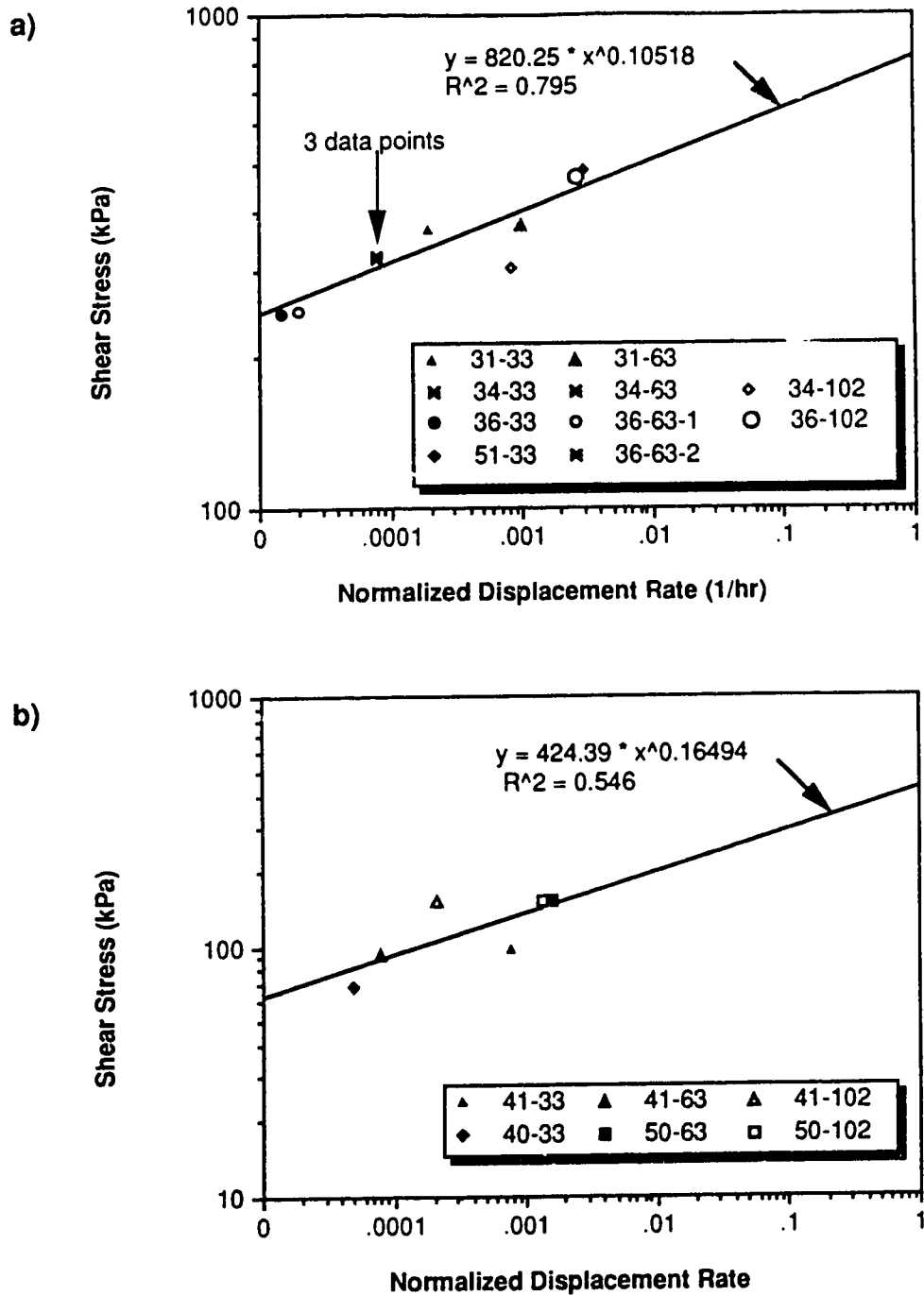


Figure E.55: Regression analysis of constant load test results for grouted piles  
a) salinity = 10 ppt  
b) salinity = 30 ppt

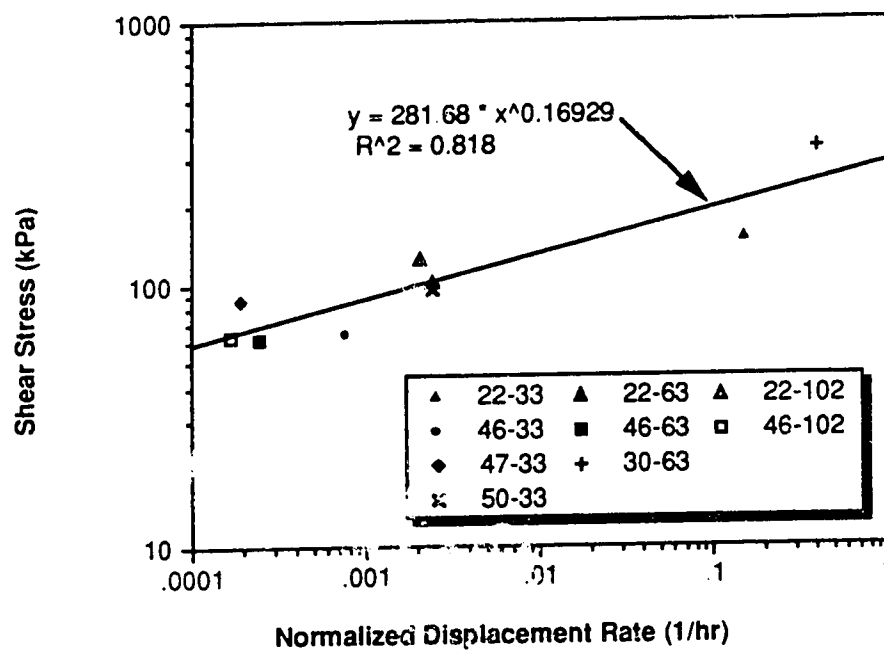


Figure E.56: Regression analysis of constant load test results for sand backfilled piles, salinity = 30 ppt

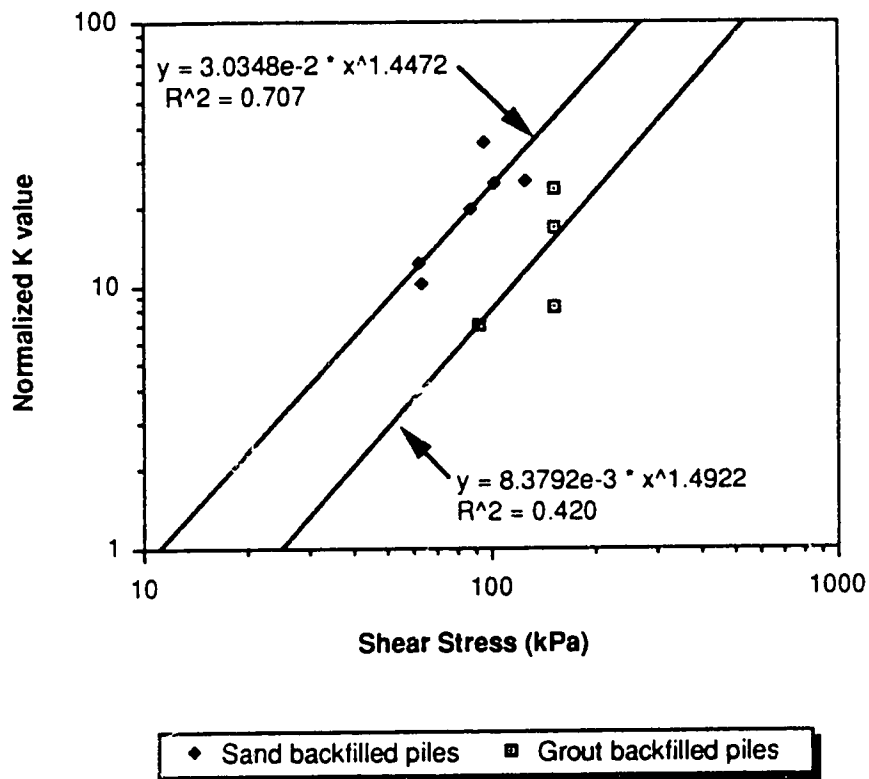


Figure E.57: Regression analysis, Normalized K versus stress for tests in native soil with a salinity of 30 ppt

**APPENDIX F**  
**DERIVATION OF FORMULATION**  
**FOR TIME DEPENDENT DISPLACEMENT OF PILES**

A constitutive relationship to describe the time dependent deformation of frozen soils may be expressed as a simple power law of stress and time (after Ladanyi 1972 and Ladanyi and Johnston 1974), and may be written as

$$\dot{\epsilon}_e = D \sigma_e^c t^b \quad [1]$$

where  $\epsilon_e$  and  $\sigma_e$  denote the von Mises equivalent strain and stress, respectively (after Odquist 1966), defined by

$$\epsilon_e^2 = \frac{4}{3} I'_2 = \frac{2}{9} [(\epsilon_1 - \epsilon_2)^2 + (\epsilon_2 - \epsilon_3)^2 + (\epsilon_3 - \epsilon_1)^2] \quad [2]$$

$$\sigma_e^2 = 3 J'_2 = \frac{1}{2} [(\sigma_1 - \sigma_2)^2 + (\sigma_2 - \sigma_3)^2 + (\sigma_3 - \sigma_1)^2] \quad [3]$$

where  $I'_2$  and  $J'_2$  denote the second invariants of strain and stress deviatoric tensor, respectively,  $D$  is a material and temperature dependent parameter,  $c \geq 1$  is the creep exponent for stress,  $t$  denotes time, and  $b$  is the time exponent  $\leq 1$ .

For a constant strain rate (often referred to as secondary or steady-state creep) which has been observed for polycrystalline ice.  $b = 1$ ,  $c \rightarrow n$ , and  $D \rightarrow B$  and [1] may be written as

$$\dot{\epsilon}_e = B \sigma_e^n \quad [4]$$

For vertically loaded piles in frozen soil, tangential strains around the pile are zero hence each soil element deforms under plane strain conditions, i.e.

$$\epsilon_1, \epsilon_2 = 0, \epsilon_3 = -\epsilon_1 \quad [5]$$

$$\sigma_1, \sigma_2 = \frac{1}{2} (\sigma_1 + \sigma_3), \sigma_3 \quad [6]$$

substituting the terms in [5] into [2] yields

$$\epsilon_e^2 = \frac{4}{3} \epsilon_1^2, \text{ or } \epsilon_1 = \frac{\sqrt{3}}{2} \epsilon_e \quad [7]$$

substituting the terms in [6] into [3] yields

$$\sigma_e^2 = \frac{3}{4} (\sigma_1 - \sigma_3)^2, \text{ or } \sigma_e = \frac{\sqrt{3}}{2} (\sigma_1 - \sigma_3) \quad [8]$$

substituting the terms in [8], into [1] yields



$$\varepsilon_1 = \left(\frac{\sqrt{3}}{2}\right)^{(n+1)} D (\sigma_1 - \sigma_3)^c t^b \quad [9]$$

For the case of simple shear with an incompressible material

$$\tau = \frac{1}{2} (\sigma_1 - \sigma_3) \quad [10]$$

$$\gamma = 2 \varepsilon_1 \quad [11]$$

and [9] becomes

$$\gamma = \sqrt{3}^{(c+1)} D \tau^c t^b \quad [12]$$

Assuming that the pile is much more rigid than the surrounding frozen soil, and that the shear stress is uniformly distributed along the depth of the pile, the shear stress along the pile surface may be expressed as

$$\tau_a = \frac{P}{2 \pi a L} \quad [13]$$

(Nixon and McRoberts 1976) where  $P$  denotes the load applied at the top of the pile,  $a$  denotes the pile radius, and  $L$  denotes the embedded pile length. Assuming that end-bearing stresses are zero, it can be shown (Nixon and McRoberts 1976) that for a weightless soil the applied shear stress,  $\tau_a$ , at  $r = a$  is related to the shear stress,  $\tau$ , at any other radius by the expression

$$\tau = \tau_a (a / r) \quad [14]$$

Substituting [14] into [12]

$$\gamma = \sqrt{3}^{(c+1)} D \left(\frac{\tau_a a}{r}\right)^c t^b \quad [15]$$

It can also be shown (Nixon and McRoberts 1976) that the shear distortion is related to the displacement by the expression

$$\gamma = \frac{-du}{dr} \quad [16]$$

where  $u$  is the displacement at any radius,  $r$ . Substituting [16] into [15] yields

$$\frac{du}{dr} = -\sqrt{3}^{(c+1)} D \left(\frac{\tau_a a}{r}\right)^c t^b \quad [17]$$

Integrating [16] to obtain the pile displacement and introducing the boundary conditions

at  $r = a$ ,  $u = u_a$ , and

at  $r = \infty$ ,  $u = 0$

(Nixon and McRoberts 1976) the following expression is obtained for the pile displacement

$$u_a = \frac{\sqrt{3}^{(c+1)} D \tau_a^c a^b}{(c-1)} \quad [18]$$

To account for the reduction in shear strength with increasing pile diameter, pile displacements are often normalized to the pile radius (Morgenstern et al. 1981; Weaver 1979), thus 18 becomes

$$\frac{u_a}{a} = \frac{\sqrt{3}^{(c+1)} D \tau_a^c a^b}{(c-1)} \quad [19]$$

For an attenuating pile displacement rate  $b < 1$ , and  $c > 1$ . For a constant displacement rate, as described for [4],  $b = 1$ ,  $c \rightarrow n$ , and  $D \rightarrow B$  and [19] may be written as

$$\frac{u_a}{a} = \frac{\sqrt{3}^{(n+1)} B \tau_a^n}{(n-1)} \quad [20]$$

**APPENDIX G**  
**BALLPARK COST ESTIMATE**  
**FOR ADFREEZE AND GROUTED PILES**

In order to examine the economic viability of grouted piles compared to adfreeze, soil slurry backfilled piles, a ballpark estimate has been prepared. The estimate is based upon a large pile foundation (> 100 piles) and has used a typical pile configuration, based upon the author's experience of piling in the Canadian Arctic in Iqaluit and on the Short Range Radar foundations. Costing data is believed to be reasonable in 1991 dollars.

Because individual piling loads and spacing are governed by structural details, it is difficult to compare foundation requirements for different structures in a simple manner. For this reason the cost estimate has been prepared as a cost per kN capacity for one pile configuration. Actual pile requirements and thus costs will vary between projects.

Pile capacities are calculated for a native silty sand soil with salinities of 0, 10, and 30 ppt. Because solute diffusion through a soil slurry backfill may reduce adfreeze bond strengths (see Chapter 6), the adfreeze bond strength values used in the analysis are calculated for piles with a saline backfill. As shown in Chapter 6, grout backfilled piles will fully mobilize the shear strength of the surrounding soil, hence pile capacities are calculated based upon the long-term shear strength of the native soil.

#### **Conditions**

Native soil.....silty sand, ice-poor  
 Native soil temperature .....-5° C  
 Pile type .....sandblasted pipe  
 Backfill .....grout or silty sand  
 Loading type .....compressive

#### **Pile Configuration**

Pile diameter..... 114 mm  
 Hole diameter..... 170 mm  
 Pipe length..... 8 m  
 Effective embedment ... 5 m  
 Pipe above grade ..... 1 m

## PILE CAPACITY CALCULATIONS

	Salinity (ppt)	S = 0	S = 10	S = 30
<b>Design Strengths (kPa)</b>				
Sustained adfreeze bond strengths for saline backfill		200	25	6
Long-term shear strength		300	250	65
<b>Pile Capacity (kN)</b>				
Slurry backfilled		179	22	5
Grout backfilled		401	334	87

## COSTING DATA

<b>*Grout Costs/m (\$)</b>				
Purchase	25 kg bag	30		based on order of 1000 bags
Shipping†	25 kg bag	17		
Total cost/m		27		@ 4 bags/7 m pile
<b>†Shipping costs</b>				
Truck to Hay River	45 kg	15.84		
Barge to Komakuk Beach	45 kg	15.83		
Total	45 kg	31.67		
<b>Estimated total cost/m (\$)</b>				
Item	Unit	Backfill		Comments
		Grout	Slurry	
Backfill material*	m	27	0	
Pipe purchase	m	20	20	
Pipe shipping†	m	11	11	
Pile installation	m	130	108	estimate 20% more expensive to install grout backfilled piles
20% overhead		38	28	
10 % profit		23	17	
Total	m	249	184	

## ESTIMATED PILE COSTS

	Salinity (ppt)	S = 0	S = 10	S = 30
<b>Pile configuration</b>		<b>\$/kN capacity</b>		
Slurry backfilled @ \$184/m		7.21	57.96	240
Grout backfilled @ \$249/m		4.35	5.22	20